DISSERTATION

RHODIUM-CATALYZED CYCLOADDITIONS TO CONSTRUCT NITROGEN HETEROCYCLES AND PROGRESS TOWARDS THE SYNTHESIS OF IONOMYCIN

Submitted by

Kevin Martin Oberg

Department of Chemistry

In partial fulfillment of the requirements

For the Degree of Doctor of Philosophy

Colorado State University

Fort Collins, Colorado

Spring 2014

Doctoral Committee:

Advisor: Tomislav Rovis

Alan J. Kennan
Eric M. Ferreira
James R. Neilson
Shane B. Kanatous

ABSTRACT

RHODIUM-CATALYZED CYCLOADDITIONS TO CONSTRUCT NITROGEN HETEROCYCLES AND PROGRESS TOWARDS THE SYNTHESIS OF IONOMYCIN

The ability to construct molecules in a rapid, atom-economical fashion is a major goal of organic chemistry. This work describes four topics; pyridone synthesis, mechanistic understanding in [2+2+2] cycloadditions, pyrimidinone synthesis, and progress towards ionomycin.

The first chapter describes the synthesis of 4,6-substituted 2-pyridones and 3,5-substituted 4-pyridones from the rhodium-catalyzed [2+2+2] cycloaddition of two alkynes and an isocyanate.

Our group demonstrated that an enantioselective rhodium-catalyzed [2+2+2] cycloaddition of alkenyl isocyanates and alkynes generates indolizidinone and quinolizidinone products. Although trends for product and regioselectivity were established, the underlying mechanism was unclear. The second chapter describes X-ray analysis of rhodium·phosphoramidite complexes in conjunction with other mechanistic work to elucidate a theory that explains product and regioselectivity in this reaction. This system is amazing in that it illuminates the factors contributing to oxidative cycloadditions in a spectacular fashion by delivering two different products.

The third chapter describes the enantioselective synthesis of pyrimidinones from a rhodium-catalyzed [4+2] cycloaddition of α,β-unsaturated imines and isocyanates.

The final chapter describes our group's progress toward the synthesis of ionomycin using rhodium-catalyzed desymmetrization of anhydrides with zinc nucleophiles.

ACKNOWLEDGMENTS

Just as it takes a village to raise a child, it takes a huge investment from numerous people to train a chemistry graduate student and I am indebted to an innumerable amount of people.

I thank my advisor, Tomislav Rovis, for mentoring and guiding me through the first stage of my growth as a scientist. Tom sets a high bar for science and striving towards that level has made me a better researcher. He also encouraged and had the patience for me to explore my own ideas. Sometimes, I can get lost in the details and Tom has helped me see the bigger picture of projects and chemistry in general. Finally, Tom understands that chemistry is done by people and has a human aspect; in this regard, he has been a spectacular boss.

I thank my parents for their tireless support and encouragement. I thank Christine Bergholtz (KCHS) and Brian O'Brien (Gustavus) for getting me excited about science and directing me towards organic chemistry.

During my time in graduate school, I have been blessed with an awesome work environment. The people in the Rovis family, past and present, have given me amazing scientific (and philosophical) discussions, mentorship, and good times. I especially thank my close friends, Dan and Christen, who adopted me and for all the ski trips, happy hours, and barbecues.

A significant part of my graduate work was X-ray crystallography, I thank Oren Anderson and Susie Miller for their training and expertise. For the assembly of the High Throughput Experimentation platform, we thank Merck, Inc., specifically Spencer Dreher, for their expertise and allowing us to model our system on their platform. In order to implement the plans and expertise from Merck, we need to thank Karen Kahler, Ron Costello, Tom Frederick, and James Shorkey for helping in the actual execution.

The cycloaddition chemistry was based on previous work in our group and a large portion of it was a collaborative effort. Not only did Robert Yu start the cycloaddition chemistry, he mentored me

during my first year in lab. Ernest Lee initiated the pyridone project and laid a lot of ground work for our mechanistic understanding. I collaborated with Derek Dalton on X-ray crystallography and the mechanistic understanding of the alkenyl isocyanate and terminal alkyne cycloaddition chemistry. I thank him for countless hours of discussion, swapping .res files, and white board sessions. Additionally, Stepháne Perreault was an invaluable asset in molding our mechanistic understanding. The work on ionomycin was initiated by Matt Cook and pushed a long ways by Brian Cochran and I am indebted to their hard work. On the ionomycin project, I also thank Kerem Ozboya, Claire Filloux, and John Wood for helpful discussions, Dan Henderson and Eric Newcomb for material and suggestions, and Chris Rithner for his NMR expertise.

I thank the National Science Foundation and Japan Society for the Promotion of Science for funding my East Asia and Pacific Summer Institution experience. I thank Professor Keiji Maruoka at Kyoto University for hosting me in his laboratory for the summer. I thank Professor Takuya Hashimoto for directly supervising my research and teaching me new lab techniques. I also thank the entire Maruoka group for their friendliness, taking me around Kyoto, and teaching me chemistry and Japanese. I also thank Garret Miyake and Guy DeLumeau who helped me while living in Japan.

Finally, I thank the people that made this dissertation presentable by proofreading and making constructive suggestions on my chapters; Darrin Flanigan, Claire Filloux, Kerem Ozboya, and Tiffany Piou.

TABLE OF CONTENTS

CHAPTER 1

Metal-Catalyzed [2+2+2] Cycloadditions and Regioselective Rhodium-Catalyzed [2+2+2] Cycloaddition of Alkynes and Isocyanates to Form Pyridones

1.1 Metal Catalyzed [2+2+2] Cycloadditions

Organic chemistry has come a long way in the past two centuries and the basic questions have shifted from "Is it possible for us to make..." to "How can we efficiently and expediently make...". It can be argued that Hendrickson[1] initiated this shift, but the concept of efficiency is now being embraced and espoused. This concept has been refined in the ideas of atom economy,[2] step economy,[3] redox economy,[4] and green chemistry.[5] The time and material required for synthetic endeavors reminds us that, as a field, organic chemistry is still not fully mature and there is room for improvement. Synthesis of natural and non-natural targets challenges current methodology and exposes missing synthetic tools. Methods development is the arena where new synthetic tools are developed that can reinvent the ways that we target molecules.

Cycloaddition reactions are powerful synthetic tools. The rapid generation of complexity in a single step, the incorporation of all the starting material into the product, and the ability to control regio- and enantioselectivity make cycloadditions an attractive method. In [2+2+2] cycloadditions, three new σ bonds are formed, up to three separate π components can be incorporated, and up to six stereocenters can be set in a single step (Figure 1.1.1). In addition to carbocycles, the introduction of a heteroatom into the π component makes this an excellent approach to heterocycles. Although thermal [2+2+2] cycloadditions are possible,[6] extreme temperatures (400 °C) are necessary.[7] Metal catalysis offers a way to overcome

---

[1] (a) Hendrickson, J. B. *J. Am. Chem. Soc.* **1971**, *93*, 6847-6854. (b) Hendrickson, J. B. *J. Am. Chem. Soc.* **1975**, *97*, 5784-5800.
[2] Trost, B. M. *Science* **1991**, *254*, 1471-1477.
[3] Wender, P. A.; Verma, V. A.; Paxton, T. J.; Pillow, T. H. *Acc. Chem. Res.* **2008**, *41*, 40-49.
[4] Burns, N. Z.; Baran, P. S.; Hoffmann, R. W. *Angew. Chem. Int. Ed.* **2009**, *48*, 2854-2867.
[5] Hudlicky, T.; Frey, D. A.; Koroniak, L.; Claeboe, C. D.; Brammer Jr., L. E. *Green Chem.* **1999**, *1*, 57-59.
[6] Woodward, R. B.; Hoffmann, R. *Angew. Chem. Int. Ed., Eng.* **1969**, *8*, 781-853.

these prohibitive conditions. Reppe was the first to demonstrated the promise of metal-catalyzed [2+2+2] cycloadditions in the 1940s by his synthesis of benzene from acetylene using a nickel catalyst.[8]

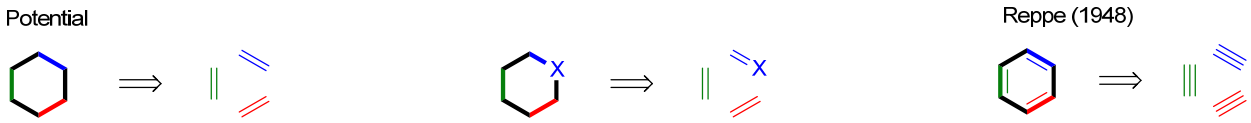

Figure 1.1.1. [2+2+2] Cycloadditions: Potential and Demonstrated Reactivity.

Since Reppe's report, [2+2+2] cycloadditions of alkynes have been greatly expanded.[9] This approach challenged the conventional aromatic substitution approach to construct aromatic compounds. Although cyclizing three different alkynes to make aromatic compounds could render their synthesis trivial, this has proven a difficult task. Chemoselectivity is a major issue as the cyclization of just one or two components tends to predominate over incorporation of all three components. Even with just one or two unsymmetrical π components, regioselectivity is another difficult problem to overcome. These problems are compounded when alkenes are used as enantioselectivity becomes an additional issue. The use of alkenes and π components containing heteroatoms tends to suffer from chemoselectivity problems due to differences in reactivity of the various π components. Ideally, a catalyst could be created that overcomes all these difficulties, but to date this has not been achieved. Many solutions have emerged including the use of stoichiometric metals,[10] tethering strategies,[11] and the use of alkyne surrogates.[12] Treatment of π components with stoichiometric metal generates a metallacycle that is sequentially reacted with the final π component to generate the desired product. This approach can overcome chemoselectivity problems, but regioselectivity can still be problematic and the use of stoichiometric metals is typically undesirable. Tethering two of the π components has proven a very effective strategy and typically solves

---

[7] Berthelot, M. C. R. *Hebd. Seances Acad. Sci.***1866**, *62*, 905.
[8] Reppe, V. W.; Schweckendiek, W. J. *Liebigs Ann.* **1948**, *560*, 104-116.
[9] For reviews on [2+2+2] cycloadditions of alkynes see: (a) Saito, S.; Yamamoto, Y. *Chem. Rev.* **2000**, *100*, 2901-2915. (b) Kotha, S.; Brahmachary, E.; Lahiri, K. *Eur. J. Org. Chem.* **2005**, 4741-4767. (c) Agenet, N.; Busine, O.; Slowinski, F.; Gandon, V.; Aubert, C.; Malacria, M. *Org. React.* **2007**, *68*, 1-302. (d) Galan, B. R.; Rovis, T. *Angew. Chem. Int. Ed.* **2009**, *48*, 2830-2834. (e) Broere, D. J.; Ruijter, E. *Synthesis* **2012**, *44*, 2639-2672.
[10] Suzuki, D.; Urabe, H.; Sato, F. *J. Am. Chem. Soc.* **2001**, *123*, 7925-7926.
[11] Use of in-situ tether: Yamamoto, Y.; Ishii, J.-i.; Nishiyama, H.; Itoh, K. *J. Am. Chem. Soc.* **2004**, *126*, 3712-3713.
[12] Hara, H.; Hirano, M. Tanaka, K. *Org. Lett.* **2008**, *10*, 2537-2540.

regioselectivity and chemoselectivity problems for two of the π components. Although effective, it still suffers from regio- and chemoselectivity of the untethered π component and generates bicycles that are not always desirable. Finally, alkyne surrogates and π components with widely varying sterics and electronics have been used to construct carbocycles with three different π components in an intermolecular fashion. This is the closest to ideal [2+2+2] cycloadditions, but use of special substrates and limited product scope restrict the utility of this approach. In short, cycloadditions are a powerful method for carbo- and heterocycle construction, but still suffer from problems in controlling chemo- and regioselectivities.

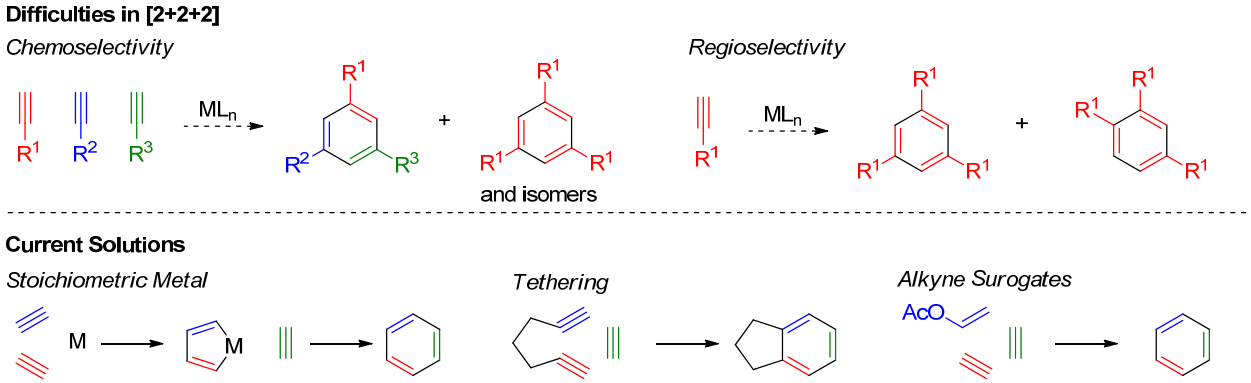

Figure 1.1.2. Difficulties in [2+2+2] cycloadditions and current solutions.

1.2 Nitrogen Heterocycle Synthesis via Metal-Catalyzed [2+2+2] Cycloadditions

Nitrogen containing heterocycles are found in many biologically active compounds, both originating from nature and produced by the pharmaceutical industry. [2+2+2] cycloadditions incorporating a nitrogen π component offer a rapid synthesis of these heterocycles. In this effort nitriles, isocyanates, carbodiimides,[13] and imines[14] have been used in [2+2+2] cycloadditions with alkynes (Figure

[13] (a) Hoberg, H.; Burkhart, G. *Synthesis* **1979**, 525-526. (b) Hong, P.; Yamazaki, H. *Tetrahedron Lett.* **1977**, 1333-1336. (c) Diversi, P.; Ingrosso, G.; Lucherini, A.; Malquori, S. *J. Mol. Catal.***1987**, *40*, 267-280. (d) Young, D. D.; Teske, J. A.; Deiters, A. *Synthesis* **2009**, 3785-3790.
[14] (a) Ogoshi, S.; Ikeda, H.; Kurosawa, H. *Pure Appl. Chem.* **2008**, *80*, 1115-1125. (b) Adak, L.; Chan, W. C.; Yoshikai, N. *Chem. Asian J.* **2011**, *6*, 359-362.

1.2.1). [15] The use of nitriles to make pyridines is a powerful method and is well reviewed.[16] In our work, we have used isocyanates to synthesize pyridones using rhodium as a catalyst.

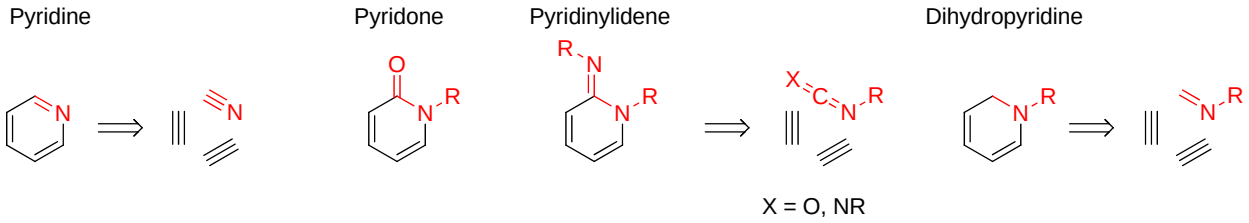

Figure 1.2.1. Nitrogen heterocycles synthesis using [2+2+2].

Pyridone can refer to two constitutional isomers, 2-pyridone **1** or 4-pyridone **2** (Figure 1.2.2). Pyridones display a variety of biological activities, and typical syntheses utilize condensation reactions and transformations from other heterocycles.[17] In addition to potential bioactivity, pyridones can serve as building blocks for other heterocycles. One of the more well known condensations to make 2-pyridone is the Guareschi-Thorpe condensation of a β-diketone **6** and an α-cyanoester **7**.[18] Pyridones are also constructed from other heterocycles. This includes the oxidation of pyridinium salts **9** and condensation of pyranones **10** with ammonium.[19] 4-pyridones are similarly made through condensations[20] and transformations from other heterocycles as seen in the Gould-Jacobs reaction.[21] This is a small sampling of ways to make pyridones. Although classical methods for pyridone synthesis exist, the development of new methods allows for substitution patterns that are difficult or impossible to attain with older methods.

---

[15] Use of isothiocyanates in these reactions leads to sulfur containing heterocycles. For examples, see: (a) Yamazaki, H. *J. Synth. Org. Chem., Jpn.* **1987**, *45*, 244-257. (b) Yamamoto, Y.; Kinpara, K.; Saigoku, T.; Takagishi, H.; Okuda, S.; Nishiyama, H.; Itoh, K. *J. Am. Chem. Soc.* **2005**, *127*, 605-613. (c) Tanaka, K.; Wada, A.; Noguchi, K. *Org. Lett.* **2006**, *8*, 907-909.

[16] (a) Varela, J. A.; Saá, C. *Chem. Rev.* **2003**, *103*, 3787-3801. (b) Chopade, P. R.; Louie, J. *Adv. Syn. Catal.* **2006**, *348*, 2307-2327. (c) Heller, B.; Hapke, M. *Chem. Soc. Rev.* **2007**, *36*, 1085-1094. (d) Varela, J. A.; Saá, C. *Synlett* **2008**, 2571-2578.

[17] (a) Mitscher, L. A. *Chem. Rev.* **2005**, *105*, 559-592. (b) Torres, M.; Gil, S.; Parra, M. *Curr. Org. Chem.* **2005**, *9*, 1757-1779.

[18] Li, J. J. Name Reactions: 2nd edition. *Springer-Verlag Berlin Heidelberg*, New York, **2003**.

[19] (a) Katritzky, A. R.; Patel, R. C.; Shanta, M. *J. Chem. Soc. Perkin Trans. 1* **1980**, 1888-1889. (b) Torres, M.; Gil, S.; Parra, M. *Curr. Org. Chem.* **2005**, *9*, 1757-1779.

[20] Eicher, T.; Hauptmann, S. The Chemistry of Heterocycles: 2nd edition. *Wiley-VCH GmbH & Co.*, Weinheim, **2003**.

[21] Gould, Jr., R. G.; Jacobs, W. A. *J. Am. Chem. Soc.* **1939**, *61*, 2890-2895.

In addition to [2+2+2] cycloadditions that are discussed below, newer methods, such as C-H activation, have been recently been applied to the synthesis of pyridones as well.[22]

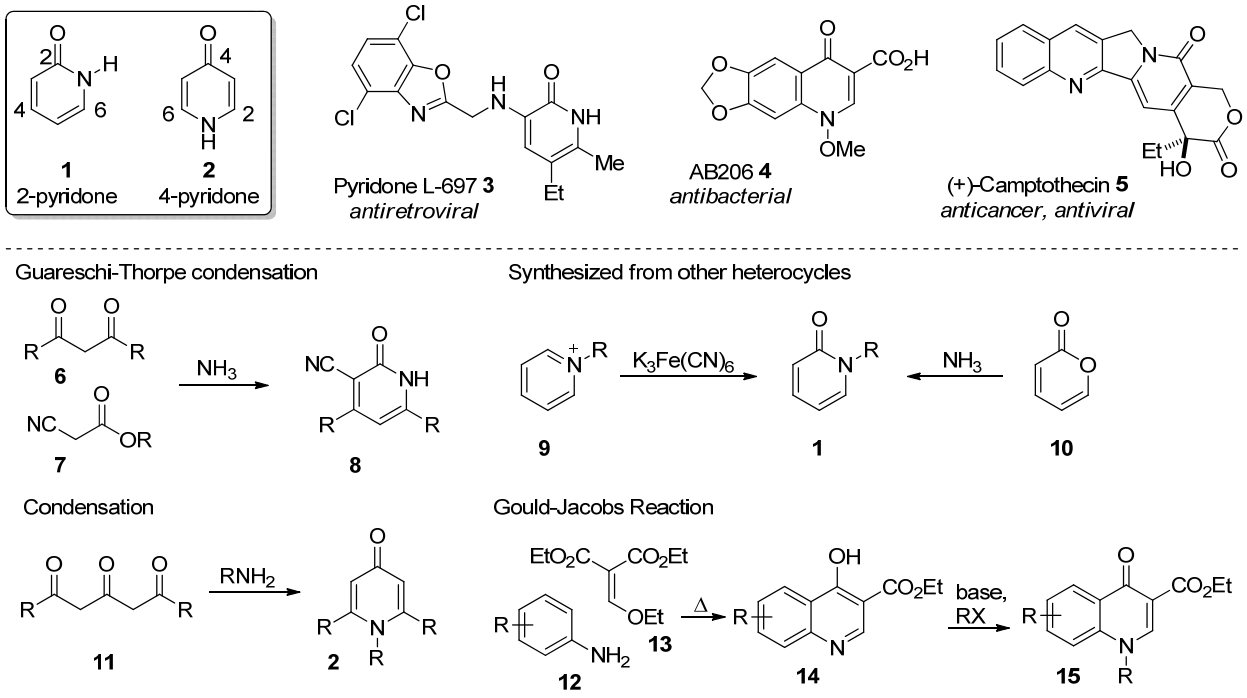

Figure 1.2.2. Pyridone isomers and numbering, biologically active pyridones, and typical pyridone syntheses.

The first reports of pyridone synthesis using [2+2+2] cycloadditions of two equivalents of alkyne and one equivalent of isocyanate were during the 1970s and 1980s. Yamazaki's report of using a cobaltacyclopentadiene catalyst to synthesize pyridones was the first (Eq 1).[23] This catalysts generates two different regioisomers (**1aa** and **1aa'**). Hoberg disclosed that nickel is also a competent catalyst for generating pyridones from alkynes and isocyanates (Eq 2).[24] Hoberg also described the generation of various metallacycles, such as **I** and **II**, using stoichiometric nickel. Flynn reported pyridone synthesis

[22](a) Su, Y.; Zhao, M.; Han, K.; Song, G.; Li, X. *Org. Lett.* **2010**, *12*, 5462-5465. (b) Hyster, T. K.; Rovis, T. *Chem. Sci.* **2011**, *2*, 1606-1610.
[23] (a) Hong, P.; Yamazaki, H. *Synthesis* **1977**, *1*, 50-52. (b) Hong, P.; Yamazaki, H. *Tetrahedron Lett.* **1977**, *15*, 1333-1336.
[24] (a) Hoberg, H.; Oster, B. W. *Synthesis* **1982**, 324-325. (b) Hoberg, H.; Oster, B. W. *J. Organomet. Chem.* **1983**, *234*, C35-C38. (c) Hoberg, H.; Oster, B. W. *J. Organomet. Chem.* **1983**, *252*, 359-364.

using a rhodacyclopentadiene catalyst, but alkyne trimerization was the main product.[25] This demonstrated that rhodium is a competent catalyst for this transformation, but also shows the difficulty in controlling chemoselectivity.

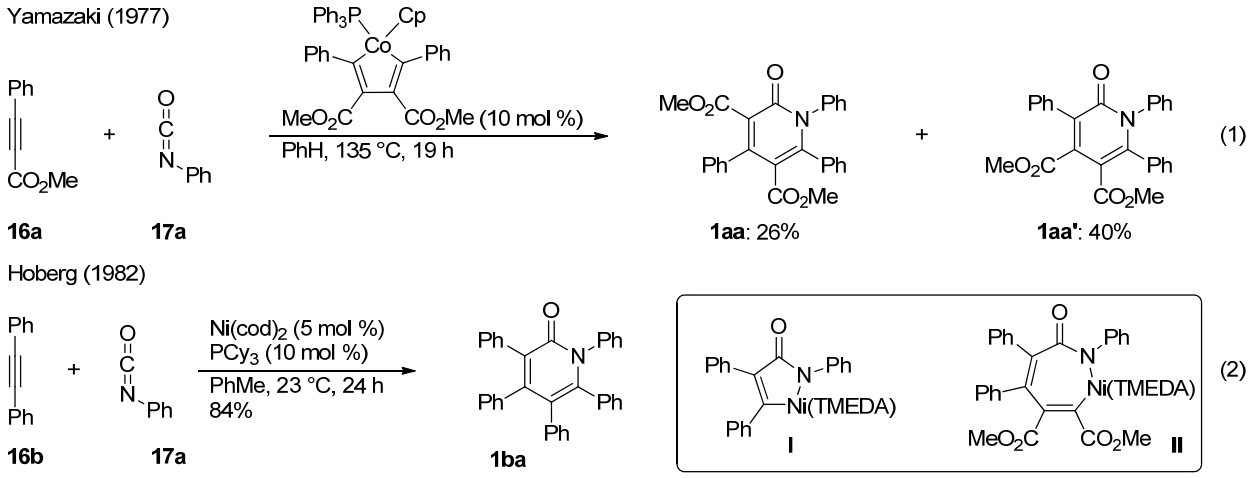

Vollhardt employed a tethering strategy that overcame some of the problems associated with chemo- and regioselectivity by connecting the alkyne to the isocyanate (Eq 3).[26] This methodology was used in the synthesis of camptothecin **5**. Research groups have used similar tethering strategies in developing other catalytic systems including ruthenium,[27] nickel,[28] and rhodium.[29] Tanaka has shown that the use of a chiral cationic rhodium catalyst can generate pyridones **21** that contain axial chirality with high enantioselectivities (Eq 4).[30]

[25] Flynn, S. T.; Hasso-Henderson, S. E.; Parkins, A. W. *J. Mol. Catal.* **1985**, *32*, 101-105.
[26] (a) Earl, R. A.; Vollhardt, K. P. C. *J. Am. Chem. Soc.* **1983**, *105*, 6991-6993. (b) Earl, R. A.; Vollhardt, K. P. C. *J. Org. Chem.* **1984**, *49*, 4786-4800.
[27] (a) Yamamoto, Y.; Takagishi, H.; Itoh, K. *Org. Lett.* **2001**, *3*, 2117-2119. (b)Yamamoto, Y.; Kinpara, K.; Saigoku, T.; Takagishi, H.; Okuda, S.; Nishiyama, H.; Itoh, K. *J. Am. Chem. Soc.* **2005**, *127*, 605-613.
[28] (a) Duong, H. A.; Cross, M. J.; Louie, J. *J. Am. Chem. Soc.* **2004**, *126*, 11438-11439. (b) Duong, H. A.; Louie, J. *J. Organomet. Chem.* **2005**, *690*, 5098-5104. (c) Duong, H. A.; Louie, J. *Tetrahedron* **2006**, *62*, 7552-7559.
[29] Kondo, T.; Nomura, M.; Ura, Y.; Wada, K.; Mitsudo, T. *Tetrahedron Lett.* **2006**, *47*, 7107-7111.
[30] (a) Tanaka, K.; Wada, A.; Noguchi, K. *Org. Lett.* **2005**, *7*, 4737-4739. (b) Tanaka, K. *Synlett* **2007**, 1977-1993. (c) Tanaka, K.; Takahashi, Y.; Suda, T.; Hirano, M. *Synlett* **2008**, 1724-1728.

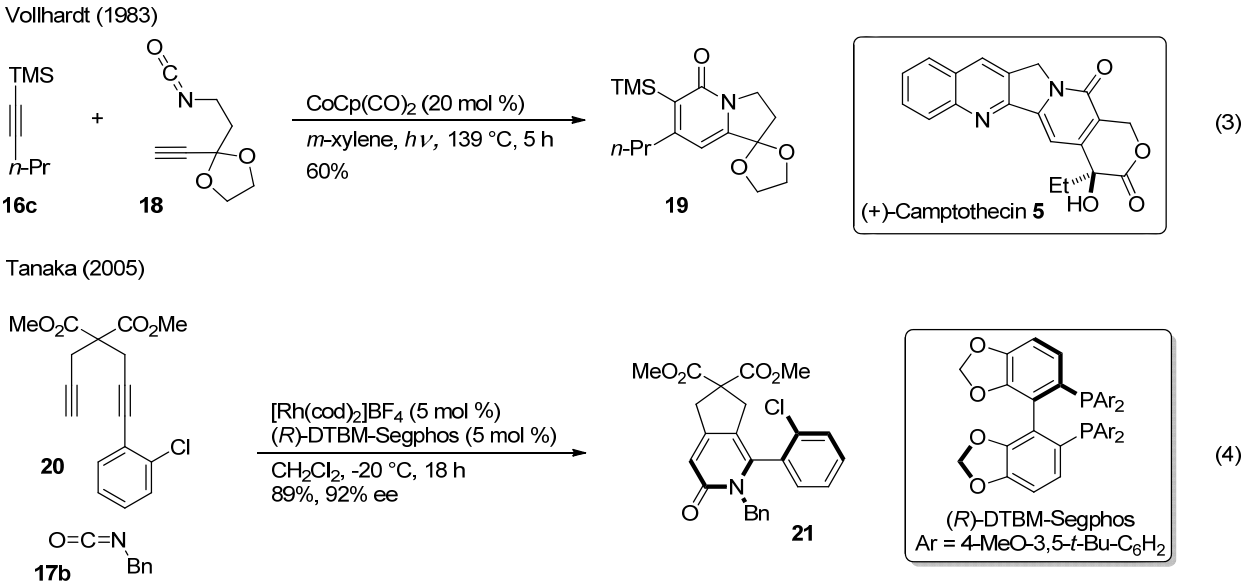

1.3 [2+2+2] Cycloaddition of Alkenyl Isocycanates and Alkynes

Our research group sought to replace one of the alkynes with an alkene to generate a carbon stereocenter. With the exception of Tanaka's example, none of these reports contain chirality. In 2006, Yu and Rovis reported using alkenyl isocyanates **22** and alkynes **16** to generate lactam **23** and vinylogous amide **24** products (Eq 5).[31] This reaction was rendered enantioselective using phosphoramidite ligands (Eq 6).[32] During our lab's investigation of the rhodium-catalyzed cycloaddition of alkenyl isocyanates and alkynes, the errant formation of 2-pyridone **1** was noted. Dr. Robert Yu observed this with longer tether lengths.[33] Dr. Ernest Lee reported 2-pyridone formation with bulky 1,1-disubstituted alkenyl isocyanates and when the reaction is run at higher concentrations using 1,1-disubstituted alkenyl isocyanates (Eq 7).[34]

[31] Yu, R. T.; Rovis, T. *J. Am. Chem. Soc.* **2006**, *128*, 2782-2783.
[32] Yu, R. T.; Rovis, T. *J. Am. Chem. Soc.* **2006**, *128*, 12370-12371.
[33] Yu, R. T. Enantioselective rhodium-catalyzed [2+2+2] and [4+2+2] cycloaddition reactions of alkenyl heterocumulenes: applications to alkaloid synthesis. Ph.D. Dissertation, Colorado State University, Fort Collins, CO, 2009.
[34] (a) Lee, E. E.; Rovis, T. *Org. Lett.* **2008**, *10*, 1231-1234. (b) Lee, E. E. Colorado State University, Fort Collins, CO. Unpublished work, 2007.

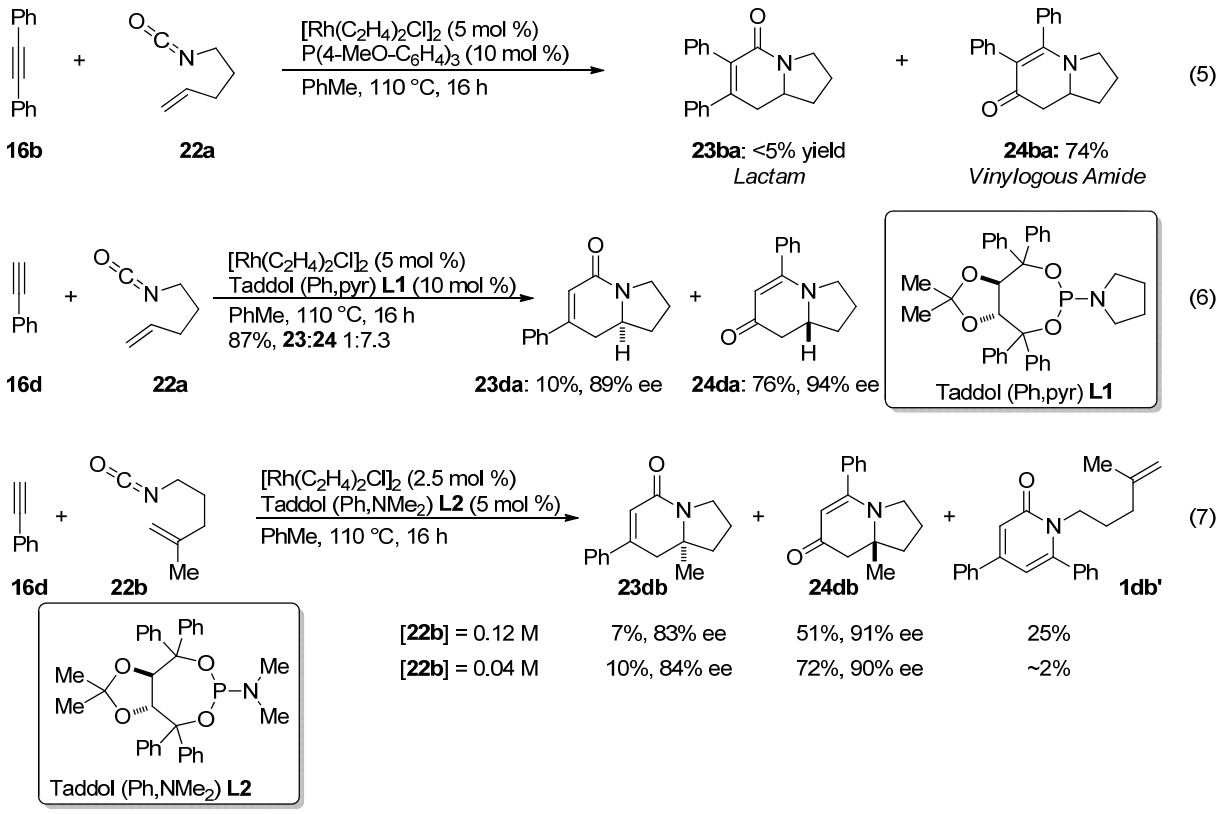

The proposed mechanism for lactam, vinylogous amide, and pyridone formation is below (Figure 1.3.1). Initial coordination of the alkyne and isocyanate to rhodium leads to complex **III**. This complex can oxidatively cyclize in two ways: either with C-N bond formation generating rhodacycle **IV** or C-C bond formation generating rhodacycle **VI**. From rhodacycle **IV**, the alkene coordinates to rhodium and undergoes a 1,2-migratory insertion. Reductive elimination of rhodacycle **V** leads to lactam **23** and regenerates the catalyst. Alternatively, generation of rhodacycle **VI** leads to a metallacycle where the alkene cannot coordinate and instead a CO migration occurs to generate rhodacycle **VIII**. Now the alkene coordinates and undergoes a migratory insertion to make 7-membered rhodacycle **IX** that reductively eliminates forming vinylogous amide **24**. With this proposed mechanism, an exogenous alkyne can bind to rhodacycle **IV** or **VI**. Migratory insertion of the alkyne and reductive elimination generates 2-pyridone **1**. As mentioned earlier, 2-pyridone is observed in the reaction and this mechanism accounts for its formation. From this mechanistic hypothesis, we see that another product could be generated from interception of rhodacycle **VIII** by an alkyne. This would lead to the formation of 4-pyridone **2**, which

had not been reported from this reaction. The isolation of 4-pyridone would provide indirect evidence for rhodacycle **VI**.

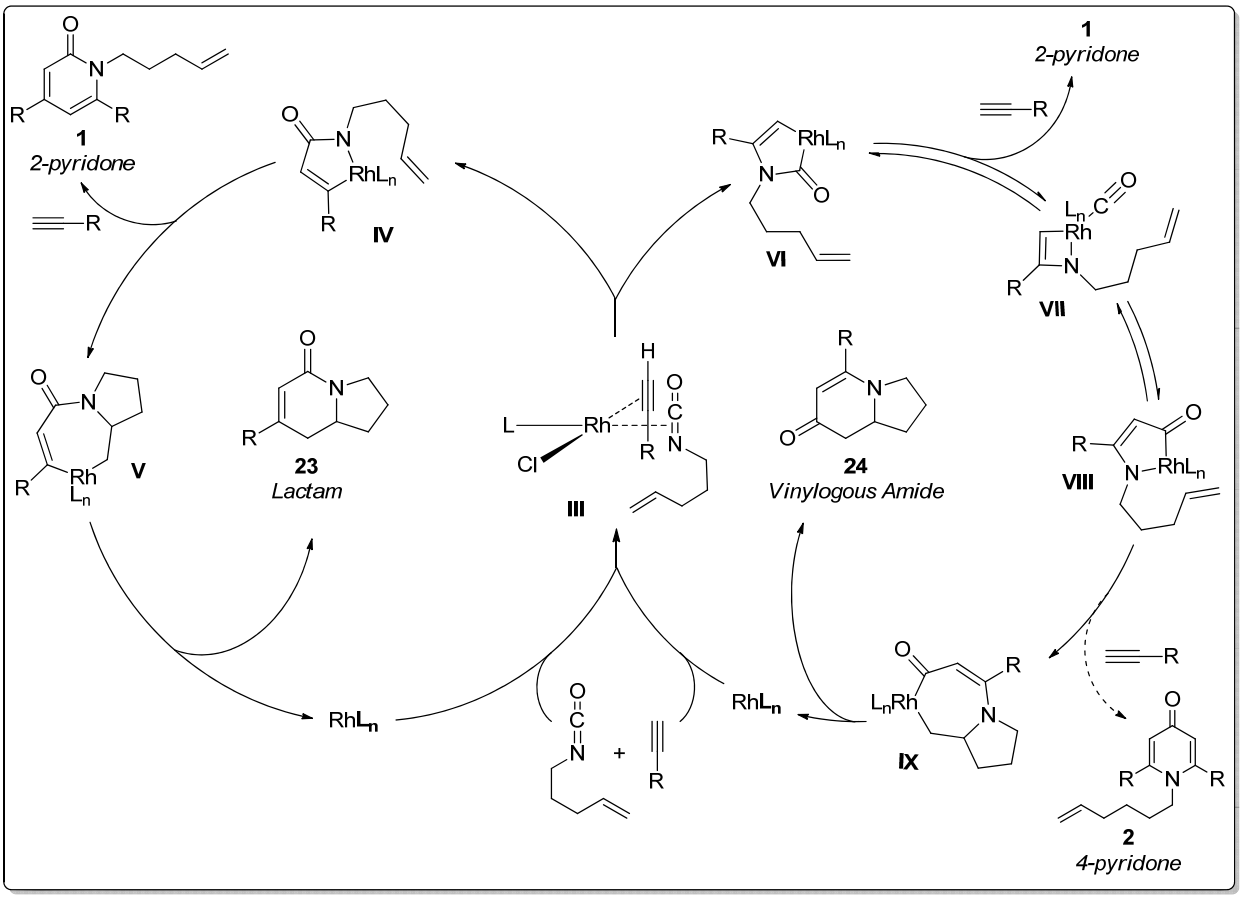

Figure 1.3.1. Proposed mechanism for [2+2+2] cycloaddition of alkyenyl isocyanates and alkynes.

1.4 Development of a Rhodium·Phosphoramidite-Catalyzed [2+2+2] Pyridone Synthesis[35]

We sought to expand the synthesis of pyridones from alkynes and isocyanates using our rhodium·phosphoramidite catalyst system. In addition to developing a useful method for making pyridones, we focused on revealing mechanistic insight into the cycloaddition of alkenyl isocyanates and alkynes. We chose to investigate terminal alkynes initially as these products were observed in our previous work. The use of untethered terminal alkynes presents two problems; metal catalysts are known

[35] Reprinted with permission from *Tetrahedron*, Vol *65*, Kevin M. Oberg, Ernest E. Lee, Tomislav Rovis, "Regioselective rhodium-catalyzed intermolecular [2+2+2] cycloaddition of alkynes and isocyanates to form pyridones", 5056-5061. Copyright (**2009**) Elsevier.

to dimerize terminal alkynes[36] and the regiochemistry of pyridone formation can be substrate and catalyst dependent. Initial results using *rac*-MonoPhos **L3** as a ligand for rhodium shows pyridone yield depends on the electronics of the alkyne (Table 1.4.1). Electron-rich aryl alkynes give higher yields, whereas more electron-deficient alkynes produce lower yields. With these initial results, we chose phenylacetylene **16d** and benzyl isocyanate **17b** to look at the effect ligand had on the reaction. Benzyl isocyanate **17b** was chosen because the reaction was easier to monitor and analyze using ^{1}H NMR, and phenylacetylene **16d** allowed for changes in yield to be more easily detected.

Table 1.4.1. Initial Alkyne Scope.[a]

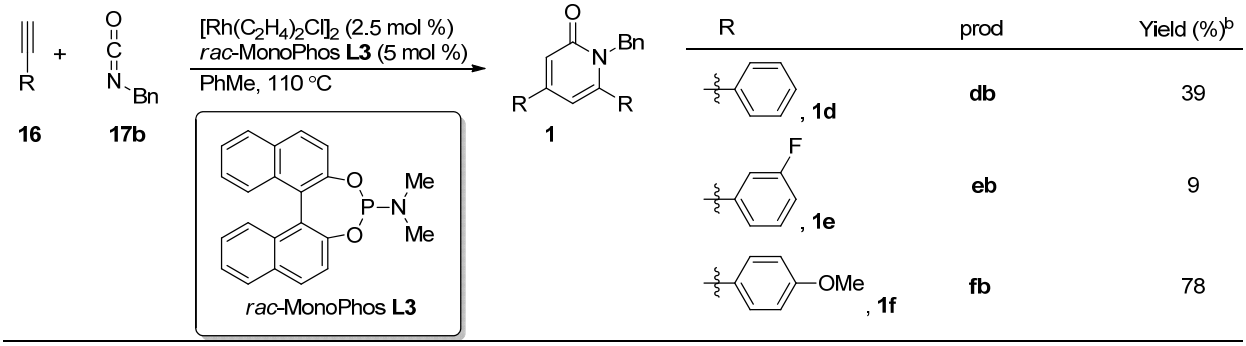

[a] Reaction conditions: **16** (3 equiv), **17b** (0.24 mmol), $[Rh(C_2H_4)_2Cl]_2$ (2.5 mol %), *rac*-**L3** (5 mol %) in PhMe reflux for 12 h.
[b] Isolated yield.

The use of triphenylphosphine as a ligand produces an additional product in this reaction (Eq 8). NMR analysis identified the product as enynamide **25db**.[37] This conjecture was confirmed by ^{1}H NMR comparison of the same compound synthesized by a different route, which was graciously provided by Professor Abarbri.[38]

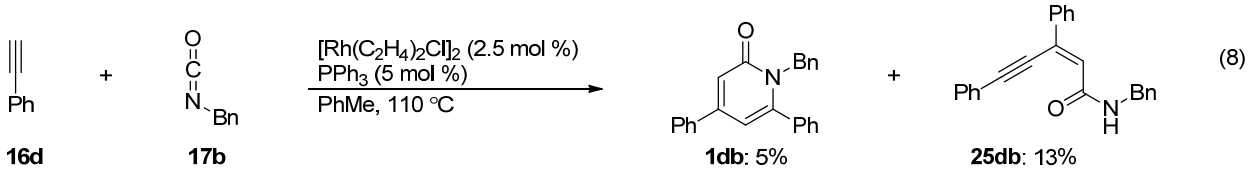

[36] (a) Albano, P.; Aresta, M. *J. Organomet. Chem.* **1980**, *190*, 243-246. (b) Ohshita, J.; Furumori, K.; Matsuguchi, A.; Ishikawa, M. *J. Org. Chem.* **1990**, *55*, 3277-3280.
[37] See also: Hoshhino, Y.; Shibata, Y.; Tanaka, K. *Angew. Chem. Int. Ed.* **2012**, *51*, 9407-9411.
[38] (a) Cherry, K.; Thibonnet, L.; Duchêne, A.; Parrain, J.; Abarbri, M. *Tetrahedron Lett.* **2004**, *45*, 2063-2066. (b) Abarbri, M. Faculté des Sciences de Tours, Tours, France. Personal communication, 2008.

Optimization of pyridone yields by varying the ligand is shown in Table 1.4.2. In general, triaryl phosphine ligands produce poor yields of both products (entries 1-7). Tricyclohexylphosphine as a ligand produces a low yield of the desired pyridone and the highest yield of enynamide (entry 8). The use of an amidophosphite or a phosphite ligand does not produce any detectable product (entries 9, 10). The use of phosphoramidite ligands provide the highest yield of pyridone **1db** with the lowest amount of enynamide **25db** (entries 11-16). The highest yielding is *rac*-**L5**[39] (entry 14). When rhodium bisethylene chloride dimer or MonoPhos **L3** is removed from the reaction, no product is observed, demonstrating the need for both rhodium and ligand to be present for the reaction to proceed.

Table 1.4.2. Investigation of ligand.[a]

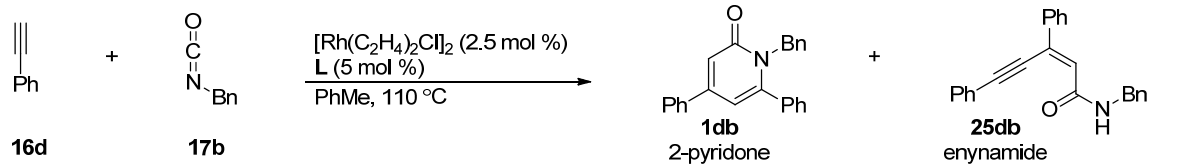

16d **17b** **1db** 2-pyridone **25db** enynamide

entry	L	yield **1db** (%)[b]	yield **25db** (%)[b]	entry	L	yield **1db** (%)[b]	yield **25db** (%)[b]
1	PPh_3	5	13	9	$P(NMe_2)_3$	-	-
2	$P(4\text{-}MeO\text{-}C_6H_4)_3$	11	18	10	$P(OPh)_3$	-	-
3	$P(4\text{-}F_3C\text{-}C_6H_4)_3$	22	12	11	D-**L2**	48	13
4	$P(C_6F_5)_3$	-	-	12	*rac*-**L3**	39	-
5	$P(2\text{-}Me\text{-}C_6H_4)_3$	<5	-	13	**L4**	64	10
6	$P(2\text{-}Fur)_3$	9	9	***14***	*rac*-**L5**	***68***	***6***
7	$AsPh_3$	12	6	15	**L6**	42	8
8	PCy_3	21	27	16	**L7**	59	8

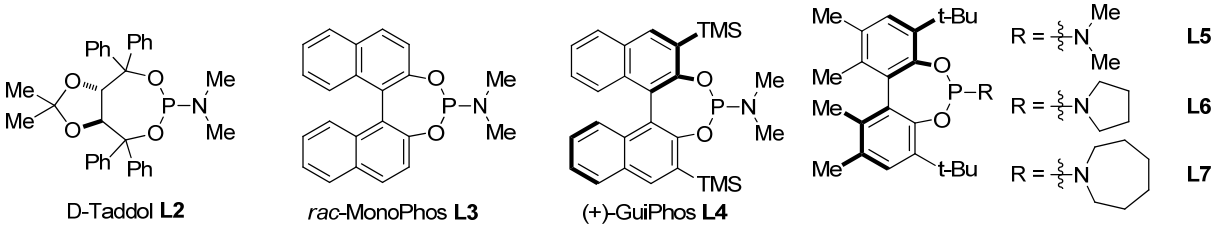

D-Taddol **L2** *rac*-MonoPhos **L3** (+)-GuiPhos **L4**

[a] Reaction conditions: **16d** (3 equiv), **17b** (0.24 mmol), $[Rh(C_2H_4)_2Cl]_2$ (2.5 mol %), **L** (5 mol %) in PhMe reflux for 12 h.
[b] Isolated yield.

[39] Giacomina, F.; Meetsma, A.; Panella, L.; Lefort, L.; de Vries, A. H. M.; de Vries, J. G. *Angew. Chem. Int. Ed.* **2007**, *46*, 1497-1500.

Once we found that GuiPhos **L4** was a good ligand for this reaction, we did some initial exploration with other isocyanates and alkynes. During these initial investigations, we found that three products are produced when hexyl isocyanate **17c** and 1-octyne **1g** are used as reactants (Eq 9). 2-Pyridone **1gc** is produced in moderate yield and enynamide **25gc** is seen in trace yield. The final product is 4-pyridone **2gc**. This product was predicted by our proposed mechanism, but until this point had yet to be isolated. One of the reasons for its elusiveness can be attributed to its high polarity. In order to isolate it, 10:1 EtOAc:MeOH is required as the eluent during column chromatography (typically, 2:1 or 1:1 Hex:EtOAc is used to elute lactam, vinylogous amide, and 2-pyridone).

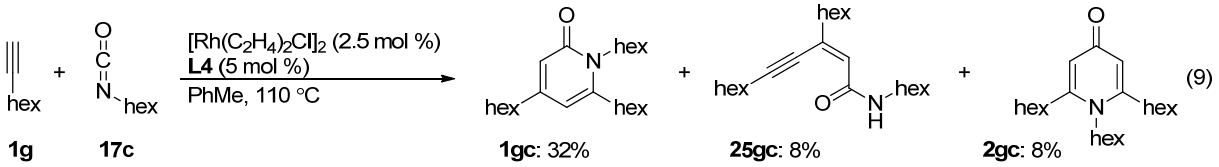

(9)

1.5 Scope and Regiochemistry of Pyridone Synthesis

We investigated the scope of terminal alkynes using benzyl isocyanate **17b** (Table 1.5.1). As *rac*-**L5** generates the most 2-pyridone and least enynamide, we chose it as the ligand. As seen previously, electron-rich aryl alkynes are higher yielding than electron-deficient alkynes (**1db**, **1eb**, **1fb**). Substitution is tolerated at the para (**1fb**), meta (**1hb**), and ortho (**1ib**) positions of arylalkynes, but the yield lowers with ortho subsitution (**1ib**).[40] Other conjugated alkynes, such as 3-ethynylthiophene (**1jb**) and 1-ethynylcyclohexene (**1kb**), produce high yields of 2-pyridone. Aliphatic alkynes give lower yields than conjugated alkynes (**1gb**, **1lb**, **1mb**, **1nb**). Ethoxyacetylene (**1ob**) also produces 2-pyridone in moderate yield. This reaction proceeds with exquisite catalyst control, and only 4,6-substituted 2-pyridone was observed for every alkyne investigated.

[40] Although a decent probe of steric tolerance, methyl substitution would be better than methoxy; methoxy substitution at the meta position is electron-withdrawing and could produce lower yields based on electronics rather than sterics alone.

Table 1.5.1. Alkyne Scope.[a,b]

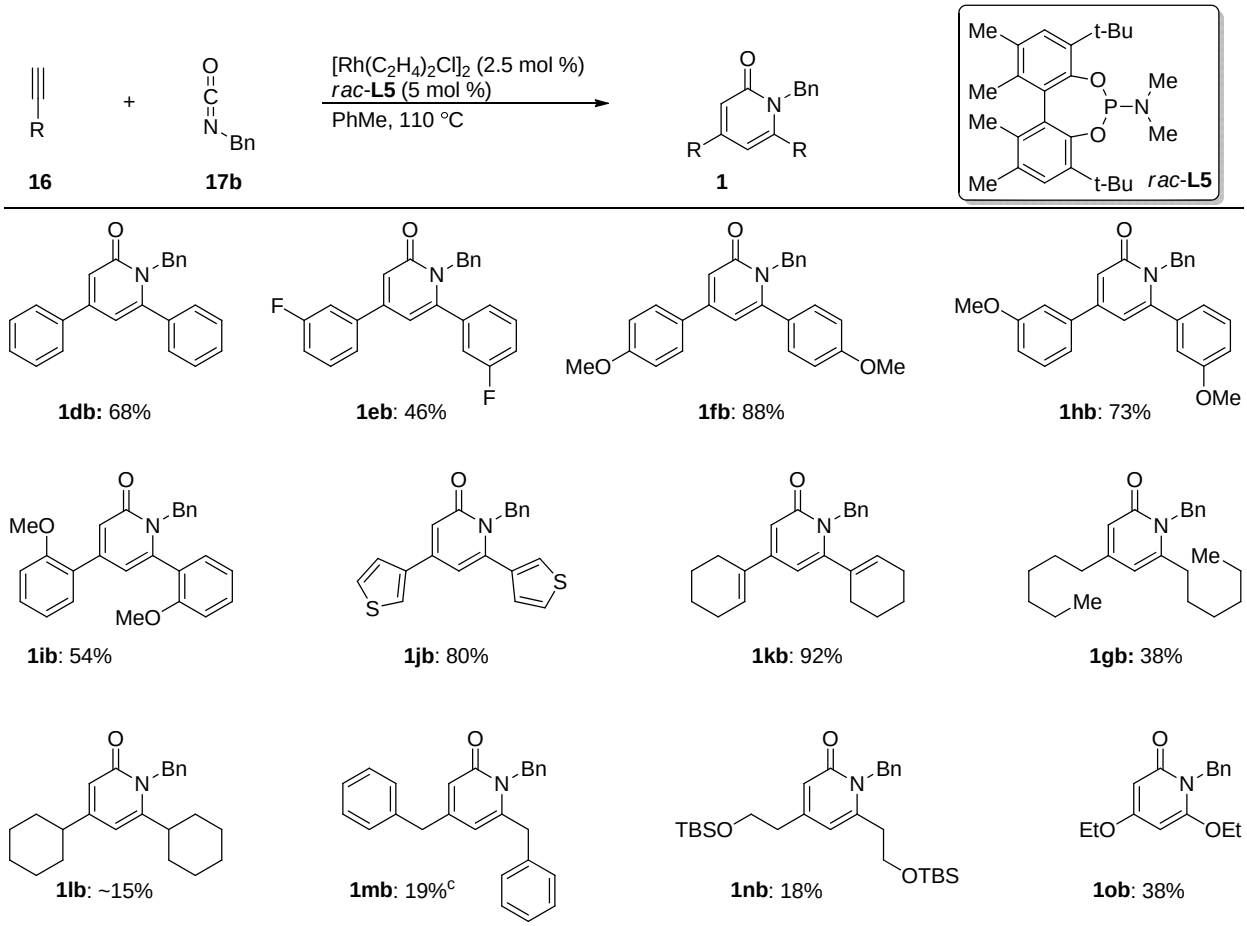

[a] Reaction conditions: **16** (3 equiv), **17b** (0.24 mmol), $[Rh(C_2H_4)_2Cl]_2$ (2.5 mol %), *rac*-**L5** (5 mol %) in PhMe reflux for 12 h.
[b] Isolated yield. [c] Isolated 16% of enynamide **25mb**.

We determined the regioisomer to be 4,6-substituted based on comparisons with similar compounds in the literature (Figure 1.5.1). Our observed coupling constants around 2 Hz are consistent with a 1,3 proton relationship (**26**[41] and **27**[42]). For 2-pyridones, protons in a 1,4 relationship (**28**)[43] are singlets and 1,2 coupled protons (**29**)[44] have coupling constants around 7 Hz. Chemical shifts of similar compounds in the literature suggest 4,6-substitution, because 3,5-substituted pyridones are more

[41] Carles, L.; Narkunam, K.; Penlou, S.; Rousset, L.; Bouchu, D.; Ciufolini, M. A. *J. Org. Chem.* **2002**, *67*, 4304-4308.
[42] Sutherland, A.; Gallagher, T. *J. Org. Chem.* **2003**, *68*, 3352-3355.
[43] Yamamoto, K. Yamazaki, S.; Murata, I. *J. Org. Chem.* **1987**, *52*, 5239-5243.
[44] Overman, L. E.; Tsuboi, S.; Roos, J. P.; Taylor, G. F. *J. Am. Chem. Soc.* **1980**, *102*, 747-754.

deshielded (**27**). This regiochemical assignment was confirmed by X-ray crystallography.[45] Our previous synthesis of lactam and vinylogous amide always generates products with the proton α to the carbonyl. This same trend is seen with pyridone formation and this suggests that pyridones are generated from similar rhodacycles.

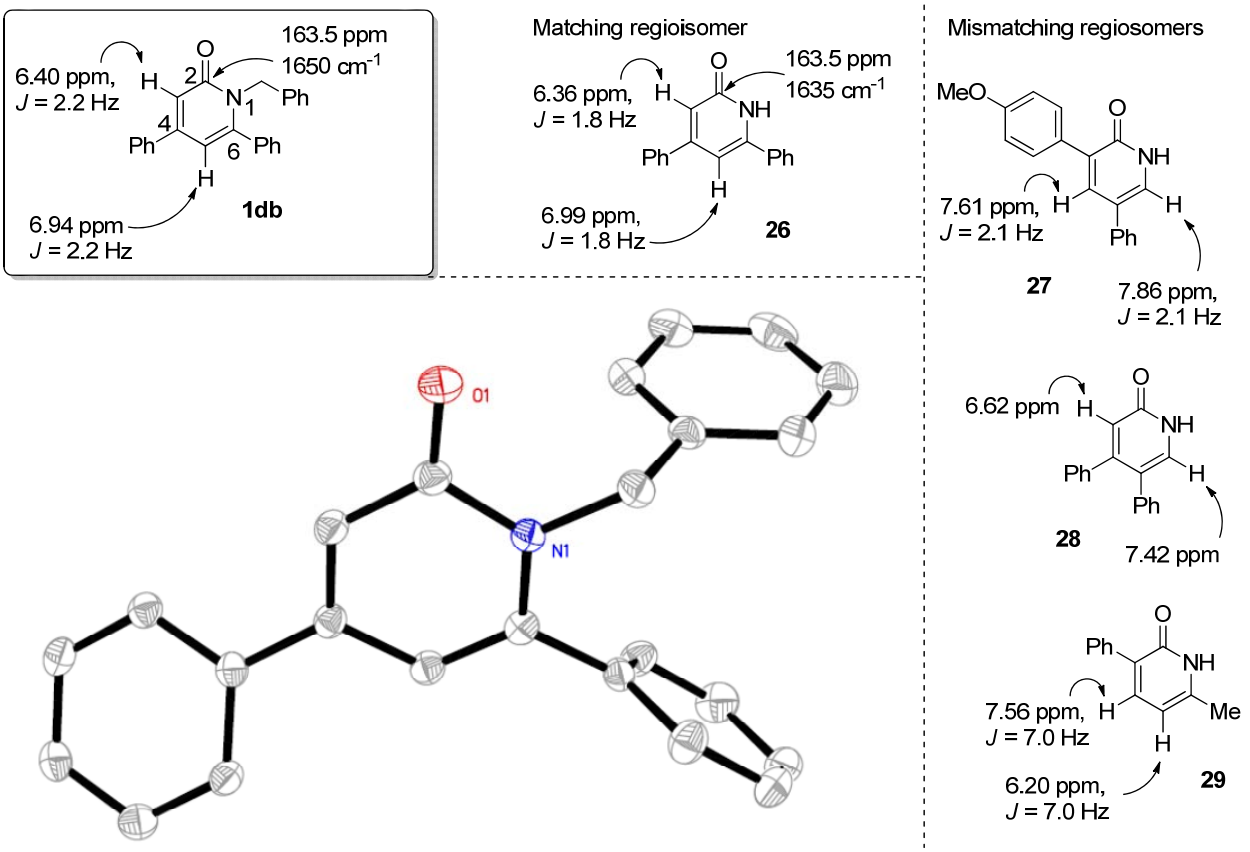

Figure 1.5.1. Regiochemistry determination of 2-pyridone.

Many of the [2+2+2] cycloadditions in the literature for the syntheis of pyridones use internal alkynes or tethered alkynes. A listing of the known reactions using terminal alkynes is shown in Table 1.5.2. The earliest report utilizing terminal alkynes is by Hoberg with a single example using nickel that generates 4,5-substituted pyridone.[46] Diversi and coworkers report the use of a cobalt catalyst and depending on the isocyanate used, either a mixture of regioisomers or a single 3,6-regioisomer is

[45] Oberg, K. M.; Rovis T. (2013) Private communication to the Cambridge Structural Database, deposit number CCDC 917626.
[46] Hoberg, H.; Oster, B. W. *Synthesis* **1982**, 324-325.

generated.[47] Tanaka has reported the most expansive scope of terminal alkynes using cationic rhodium with a bidentate ligand. The regioselectivity is dependent on the alkyne employed in the reaction and a mixture of regioisomers is typically observed.[48] Notable exceptions are the use of silylalkynes and alkynylethers[49] that produce single regioisomers. The rhodium·phosphoramidite catalyst system provides remarkable selectivity for a single regioisomer, independent of the alkyne.

Table 1.5.2. Regiochemistry of [2+2+2] Cycloadditions of Terminal Alkynes and Isocyanates.

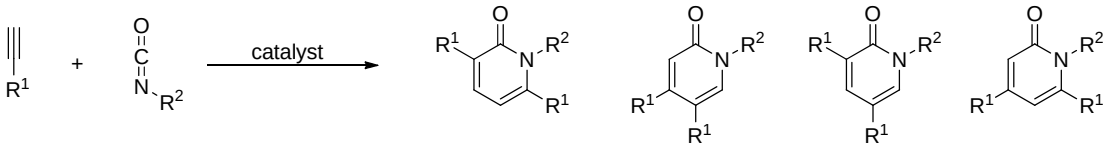

				3,6-substituted	4,5-substituted	3,5-substituted	4,6-substituted
Report	R^1	R^2	catalyst			yield (%)	
Hoberg (46)	Ph	Ph	$Ni(cod)_2$, PCy_3	-	15	-	-
Diversi (47)	*n*-Bu	Cy	$CoCp(C_2H_4)_2$	15	-	-	15
	n-Bu	Ph		19	-	-	-
Tanaka (48)	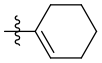	Bn	$[Rh(cod)_2]BF_4$, H8-BINAP	-	47	-	1
	n-dec	Bn		-	31	<5	30
	TMS	*n*-Bu		-	-	65	-
(49)	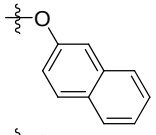	*n*-Bu		-	-	-	53
	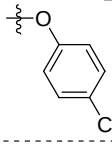	*n*-Bu		-	-	-	33
Rovis (35)	Ph	Bn	$[Rh(C_2H_4)_2Cl]_2$, *rac*-**L5**	-	-	-	68
	n-hex	Bn		-	-	-	38
	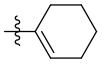	Bn		-	-	-	92

We also sought to use internal alkynes with this rhodium·phosphoramidite system, but they are surprisingly recalcitrant. Internal alkynes such as diphenyl acetylene, 1-phenyl-1-butyne, 1-propynyl-1-cyclohexane, and 5-decyne do not produce product with these phosphoramidite ligands. The use of

[47] Diversi, P.; Giovanni, I.; Lucherini, A.; Malquori, S. *J. Mol. Catal.* **1987**, *40*, 267-280.
[48] Tanaka, K.; Wada, A.; Noguchi, K. *Org. Lett.* **2005**, *7*, 4737-4739.
[49] Komine, Y.; Tanaka, K. *Org. Lett.* **2010**, *12*, 1312-1315.

dimethyl acetylenedicarboxylate generates a low amount (20%) of arene product.[50] The lack of reactivity with internal alkynes is unexpected because Kondo showed that a $RhCl(PPh_3)_x$ system catalyzes pyridone formation with internal symmetrical alkynes.[51] Methyl phenylpropiolate **16a** does provide product with MonoPhos (*rac*-**L3**), but shows no reaction with *rac*-**L5** as a ligand (Eq 10). We assigned the regioisomer of pyridone **1ab** by comparison to a similar pyridone in the literature.[52] Saponification of the ester groups and subsequent decarboxylation of the resulting acid produces pyridone **1db** confirming our original assignment. When a high-yielding alkyne, para-methoxyphenyl acetylene **16f**, is added to a solution of premixed methyl phenylpropiolate **16a**, benzyl isocyanate **17b**, and RhCl·*rac*-**L5**, we observe no product (Eq 11). This suggests that the catalyst is being tied up, potentially in an unproductive metallacycle.

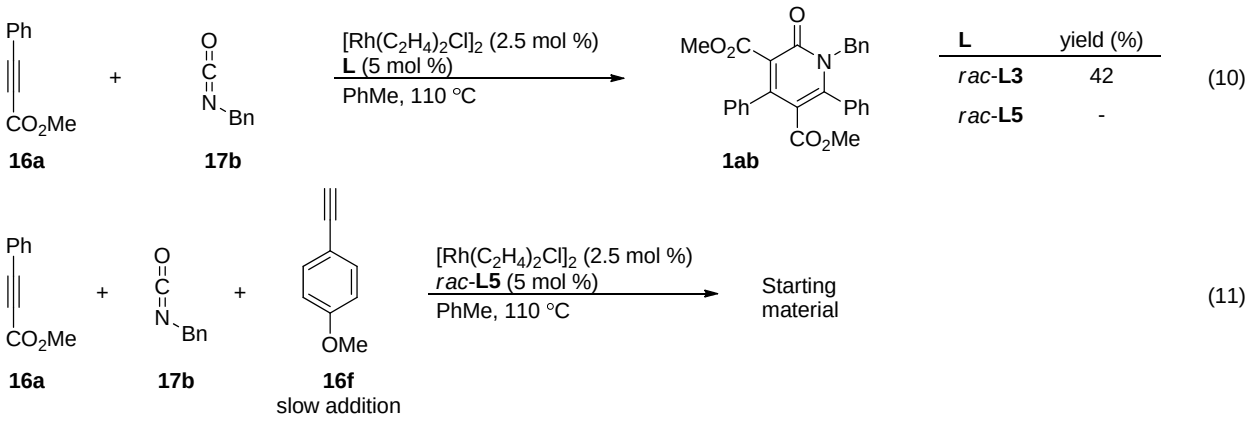

We looked at the scope of isocyanates that participate in the reaction (Table 1.5.3). During the investigation of isocyanates, we observed more 4-pyridone. Benzyl **17b** and para-methoxybenzyl isocyanate **17d** generate 2-pyridone **1** in good yield with trace amounts of 4-pyridone **2** (entries 1,2). Alkyl isocyanates generate moderate yields of 2-pyridone with low amounts of 4-pyridone (entries 3,4). Aryl isocyanates produce a good combined yield of pyridone and the ratio of 2- to 4-pyridone is dependent on the electronics of the isocyanate (entries 5-8). Generally, more electron-deficient

[50] (a) Kotha, S.; Khedkar, P. *Eur. J. Org. Chem.* **2009**, 730-738. (b) Oinen, M. E. The Enantioselective Rhodium Catalyzed [2+2+2] Cycloaddition of Alkenyl Isocyanates with Diaryl Acetylenes and 1,2-Disubstituted Alkenyl Isocyanates. M.S. Thesis, Colorado State University, Fort Collins, CO, 2010.
[51] Kondo, T.; Nomura, M.; Ura, Y.; Wada, K.; Mitsudo, T. *Tetrahedron Lett.* **2006**, *47*, 7107-7111.
[52] Hong, P.; Yamazaki, H. *Synthesis* **1977**, *1*, 50-52.

arylisocyanates produce more 4-pyridone. Vinyl isocyanates work in the reaction, but the ratio of 2- to 4-pyridone is potentially skewed in entry 9 with (E)-(2-isocyanatovinyl)benzene **17j**. This isocyanate is unstable and decomposed as it was being used. The use of *p*-toluenesulfonyl isocyanate leads to an intractable mixture and chlorosulfonyl isocyanate reacts uncatalyzed with alkynes.[53]

Table 1.5.3. Scope of isocyanates.[a]

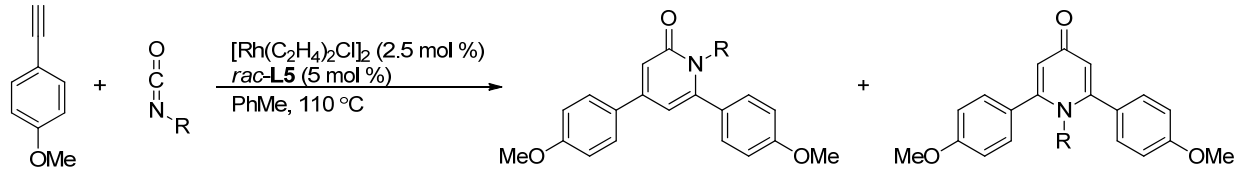

16f **17** **1** **2**

entry	R	product	yield **1** (%)[b]	yield **2** (%)[b]
1	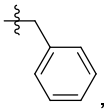 **17b**	**fb**	88	4
2	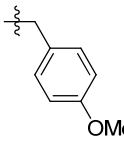 OMe, **17d**	**fd**	79	4
3	*n*-hex, **17c**	**fc**	52	18
4	Cy, **17e**	**fe**	55	12
5	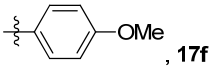 **17f**	**ff**	43	19
6	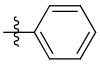 **17g**	**fg**	37	20
7	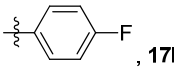 **17h**	**fh**	48	23
8	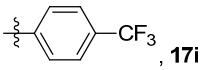 **17i**	**fi**	34	30
9	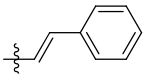 **17j**	**fj**	13	17

[a] Reaction conditions: **16f** (3 equiv), **17** (0.24 mmol), $[Rh(C_2H_4)_2Cl]_2$ (2.5 mol %), *rac*-**L5** (5 mol %) in PhMe reflux for 12 h.
[b] Isolated yield.

The generation of a single 2-pyridone regioisomer remains the same with a variety of isocyanates. Additionally, we only observe 2,6-substituted 4-pyridones. This regiochemical assignment is based on NMR analysis and literature comparisons (Figure 1.5.2). The NMRs for the 4-pyridones are striking in their simplicity suggesting a C2 symmetric molecule. Chemical shifts of the protons suggests 2,6-subsituted 4-pyridones when compared to compounds in the literature.[54] This assignment was confirmed

[53] Moriconi, E. J.; Shimakawa, Y. *J. Org. Chem.* **1972**, *37*, 196-207.
[54] For **30**, see: Barluenga, J.; Lopez Ortiz, F.; Palacios, F.; Gotor, V. *Synth. Commun.***1983**, *13*, 411-417. For **31** and **33**, see: Patonay, T.; Lévai, A.; Rimán, É.; Varma, R. S. *ARKIVOC* **2004**, *7*, 183-195. For **32** and **34**, see: Beak, P.; Bonham, J. *J. Am. Chem. Soc.* **1965**, *87*, 3365-3371.

by X-ray crystallography.[55] Once again, the regiochemistry is the same as the vinylogous amide regiochemistry and supports our proposed mechanism.

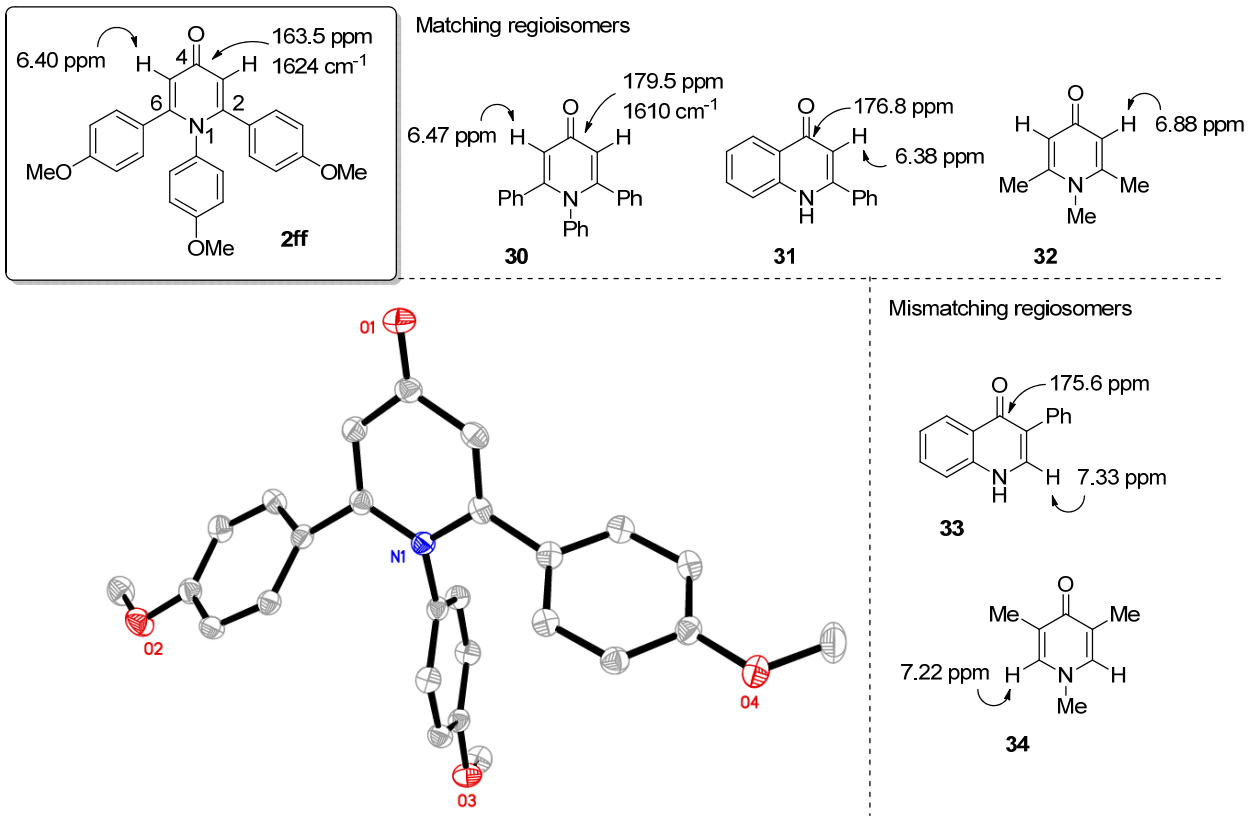

Figure 1.5.2. Regiochemistry determination of 4-pyridone.

Deprotecting the products would make this method more useful as many transformations utilize NH pyridones.[56] Initially, we attempted to deprotect our benzyl protected pyridone **1db** using dissolving metal conditions, ethyl chloroformate, and hydrogenation,[57] but these conditions left the benzyl group intact (Eq 12). Due to the difficulty of removing the benzyl group, we attempted to deprotect the para-methoxy benzyl protecting group on pyridone **1gd** (Eq 13). Once again, hydrogenation did not provide any of the desired product. Treatment with ceric ammonium nitrate deprotected some of the pyridone as evidence by the aldehyde peak in the crude ^{1}H NMR, but this reaction was messy and difficult to purify.

[55] Oberg, K. M.; Rovis T. (2013) Private communication to the Cambridge Structural Database, deposit number CCDC 917625.
[56] Kelly, T. R.; Lang, F. *J. Org. Chem.* **1996**, *61*, 4623-4633.
[57] It should be noted that the hydrogenation was done at 1 atmosphere and higher pressures may give different results.

We found that refluxing pyridone **1gd** in trifluoroacetic acid provided our deprotected pyridone **35** in good yield.[58]

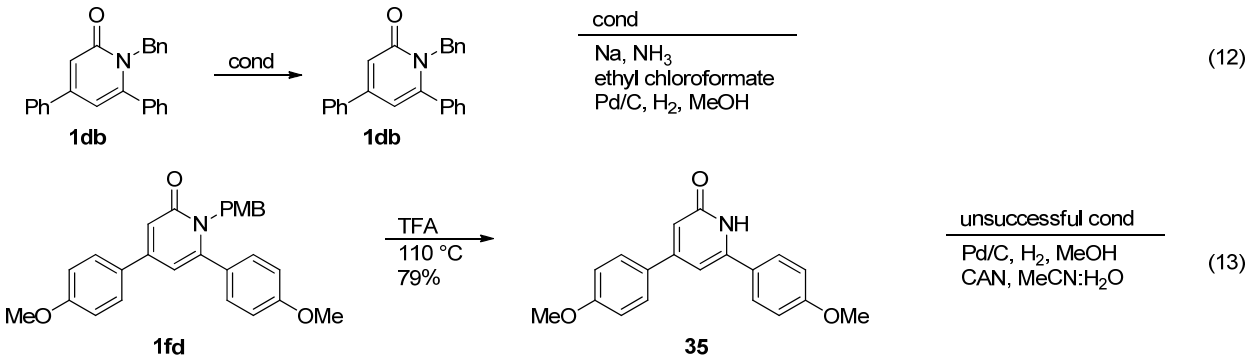

1.6 Proposed Mechanism

We propose the following mechanism for pyridone formation (Figure 1.6.1), which is similar to the mechanism proposed for the [2+2+2] cycloaddition of alkenylisocyanates and alkynes (Figure 1.3.1). The alkyne and isocyanate coordinate to rhodium generating complex **III**. This can undergo oxidative cyclization to form one of two metallacycles. In Pathway A, rhodacycle **X** is formed and C-N bond formation occurs. Insertion of an alkyne into this rhodacycle and reductive elimination generates 2-pyridone **1**. Rhodacycle **X** can also undergo a CO migration to generate rhodacycle **XI**. Insertion of an alkyne into this rhodacycle followed by reductive elimination furnishes 4-pyridone **2**. Alternatively, complex **III** can undergo cyclization leading to rhodacycle **XII**, where C-C bond formation occurs. Alkyne insertion followed by reductive elimination generates 2-pyridone **1**. These metallacycles are similar to the ones we propose for the cyclization of alkenyl isocyanates and alkynes (**X**:**VI**, **XI**:**VIII**, **XII**:**IV**). A discussion of regioselective metallacyle formation will be left for the next chapter that discusses the mechanism of the [2+2+2] cycloaddition of alkenyl isocyanates and terminal alkynes.

[58] Furuta, T.; Kitamura, Y.; Hashimoto, A.; Fujii, S.; Tanaka, K.; Kan, T. *Org. Lett.* **2007**, *9*, 183-186.

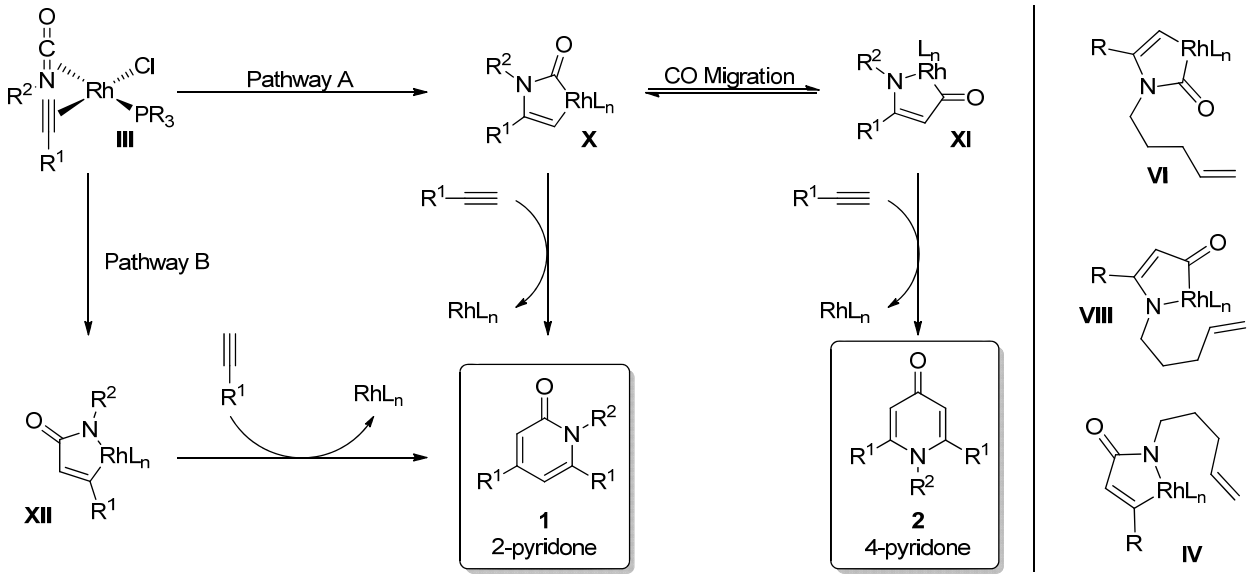

Figure 1.6.1. Proposed mechanism for pyridone formation.

Although it is possible that both pathways are operative in this reaction, we believe that pathway A, via rhodacycle **X**, is predominant. From rhodacycle **XII**, it is not possible to generate 4-pyridone **2**. Rhodacycle **X** can generate 2-pyridone **1** or 4-pyridone **2**. Indirect evidence for this mechanistic hypothesis is seen when the yields of pyridone are compared with product selectivity in the [2+2+2] cycloaddition of alkenyl isocyanates and alkynes (Figure 1.6.2). According to our proposed mechanism, rhodacycle **IV** generates lactam and rhodacycle **VI** generates vinylogous amide. Therefore, a higher ratio of vinylogous amide suggests more formation of rhodacycle **VI**. In the reaction to make pyridones, alkynes that generate more vinylogous amide also produce higher yields of pyridone. This suggests these alkynes generate more **VI** and **X** leading to vinylogous amide and pyridone, respectively. The opposite is seen with alkynes that favor lactam. Metallacycles such as rhodacycle **XII** have been isolated before,[59] but metallacycles with the CO α to the metal, such as rhodacycle **X**, are unprecedented. The generation of 4-pyridone in these reactions implicates this type of metallacycle exists in both this reaction and [2+2+2] cycloadditions of alkenyl isocyanates and alkynes.

[59] Hoberg, H.; Oster, B. W. *J. Organomet. Chem.* **1983**, *234*, C35-C38.

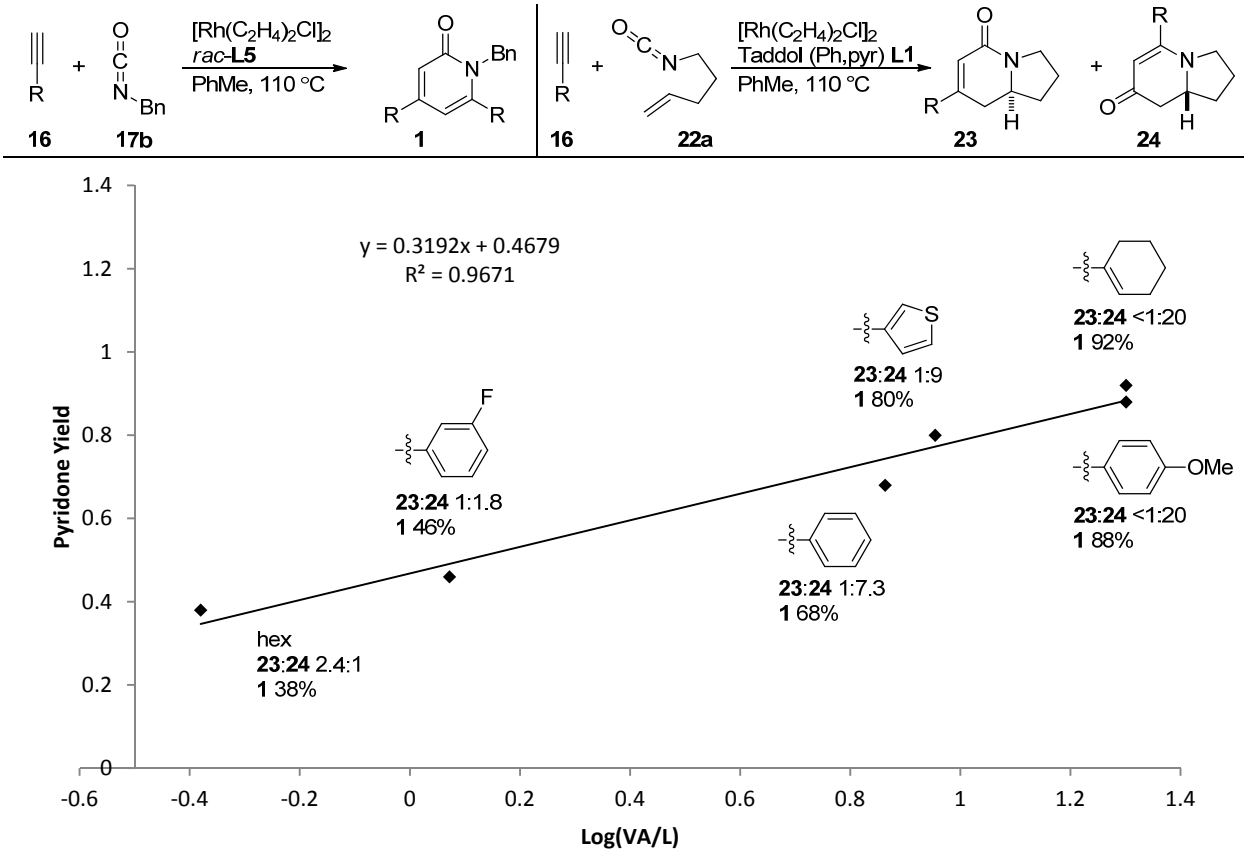

Figure 1.6.2. Correlation of pyridone yield to vinylogous amide selectivity.

The ratio of 2-pyridone to 4-pyridone appears to be independent of alkyne concentration (Eq 14). When the reaction is conducted with high concentration and higher alkyne equivalents, a slightly better yield of pyridone is generated, but the ratio is the same as standard reaction conditions. When the alkyne is slowly added under more dilute conditions, a lower yield of pyridone is seen, but once again the ratio remains the same. This can be explained by two mechanisms that are indistinguishable at this time. One, the equilibration between rhodacycle **X** and **XI** is rapid and dependent on the alkyne and isocyanate that are already bound to the metal via the metallacycle. Two, the exogenous alkyne is bound to the metal and the difference in rates between migratory insertion of the alkyne into rhodacycles **X** or **XI** determines the selectivity that is observed.

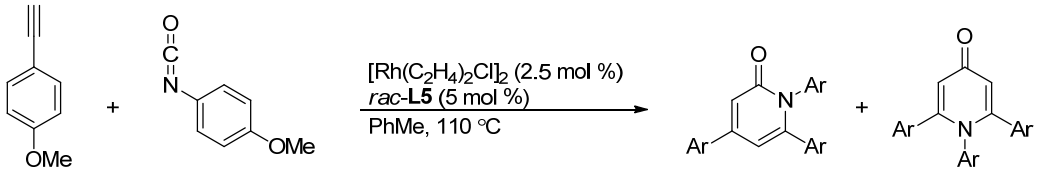

(14)

equiv **16f**	conc **16f**	**1ff** yield (%)	**2ff** yield (%)	ratio **1**:**2**
9 equiv	2.2 M	50	22	2.3:1
3 equiv	0.1 M	43	19	2.3:1
3 equiv (slow add)	0.05 M	18	9	2:1

We attempted to incorporate three different π components using the rhodium·phosphoramidite system with two electronically different alkynes (Eq 15). As mentioned earlier, the incorporation of three different π components in a controlled fashion is a difficult task. A mixture of four products was obtained. Although we did not achieve the goal of selective product formation, we see that different alkynes react at different rates during oxidative cyclization and alkyne insertion. If pyridone is generated from rhodacycle **X**, we see that **1fb** and **36**, which derived from oxidative cyclization of the more electron-rich alkyne, have a higher combined yield than **37** and **1eb**, derived from cyclization of the more electron-deficient alkyne. This gives a ratio of 2.6:1 for cyclization of para-methoxyphenyl acytelene **16g** over meta-fluorophenyl acytelene **16f**. A ratio of ~1.4:1 of the more electron-rich alkyne **16g** to the more electron-deficient alkyne **16f** (1.6:1 and 1.2:1) is observed for the second alkyne insertion. From this, we see that electron-rich aryl alkynes undergo oxidative cyclization faster that electron-deficient aryl alkynes and that the second alkyne insertion is much less selective than the initial oxidative cyclization.

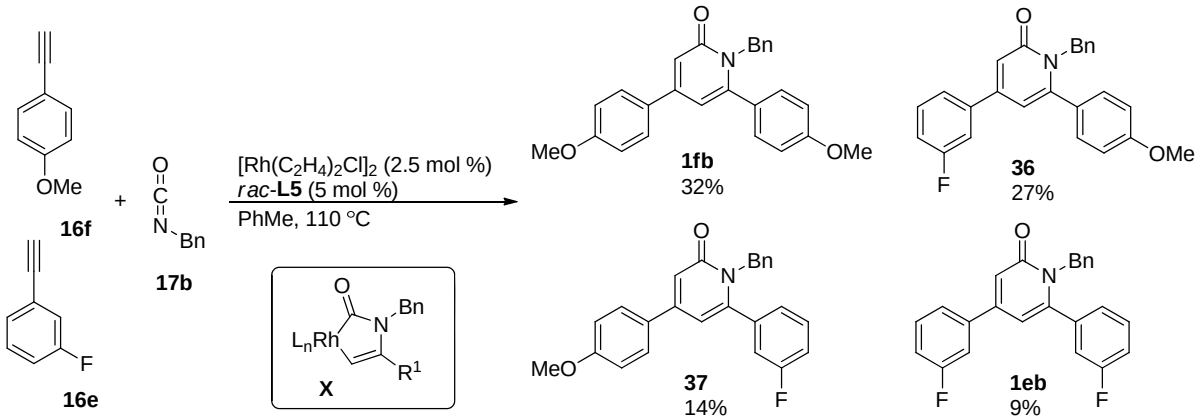

(15)

The generation of pyridone can also be explained by other mechanisms. It is possible that two alkynes undergo oxidative cyclization to form rhodacyclopentadienes such as **XIII**, **XIV**, and **XV** (Figure 1.6.3). Isocyanate insertion into these metallacycles and reductive elimination furnishes pyridone. This mechanism is closely related to the [2+2+2] cyclotrimerization of alkynes and has also been suggested for pyridone formation.[60] Although possible, a number of observations suggest this is not operative in our case. The regiochemistry of metallacyclopentadiene formation tends to be either metallacycle **XIII** or **XIV** or a mixture of one of these metallacycles with metallacyclopentadiene **XV**. The selectivity is typically dependent on the sterics and electronics of the alkyne. Looking back at Table 1.5.2 of other catalyst systems, we see pyridones that would be generated from these types of metallacycles. In our case, we see a single regioisomer independent of the size and electronics of the alkyne. Additionally, the formation of 4-pyridone **2** from any of these metallacycles would not be possible. Finally, we do not see arene formation in our reactions that would be derived from interception of any of these metallacycles with an exogenous alkyne. This has been noted with other catalyst systems. The lack of arene formation also indirectly suggests that the initial oxidative cyclization occurs between the isocyanate and alkyne.

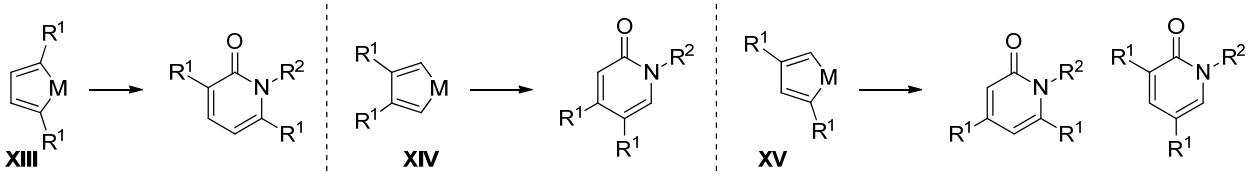

Figure 1.6.3. Metallacyclopentadiene for pyridone formation.

Another mechanistic possibility is that enynamide **25** is an intermediate en route to 2-pyridone **1**. When enynamide **25db** is subjected to the reaction conditions, only enynamide **25db** is recovered and pyridone **1db** is not observed. It would also be impossible to get to 4-pyridone **2** from this intermediate. We propose that enynamide **25** is generated from a similar mechanism that has been proposed for

[60] For reviews, see: (a) Varela, J. A.; Saá, C. *Chem. Rev.* **2003**, *103*, 3787-3801. (b) Chopade, P. R.; Louie, J. *Synlett* **2006**, *348*, 2307-2327. (c) Heller, B.; Hapke, M. *Chem. Soc. Rev.* **2007**, *36*, 1085-1094. (d) Varela, J. A.; Saá, C. *Synlett* **2008**, *17*, 2571-2578. For individual papers, see: (d) Wakatsuki, Y.; Yamazaki, H. *J. Organomet. Chem.* **1977**, *139*, 169-177. (e) Hardesty, J. H.; Koerner, J. B.; Albright, T. A.; Lee, G.-Y. *J. Am. Chem. Soc.* **1999**, *121*, 6055-6067. (f) Kichner, K.; Calhorda, M. J.; Schmid, R.; Veiros, L. F. *J. Am. Chem. Soc.* **2003**, *125*, 11721-11729. (g) Dachs, A.; Torrent, A.; Pla-Quintane, A.; Roglans, A.; Jutand, A. *Organometallics* **2009**, *28*, 6036-6043.

terminal alkyne dimerization by metal catalysts.[61] A C-H insertion into the terminal alkyne generates rhodium hydride **XVI**. This species undergoes a 1,2 migration across another alkyne generating another rhodium hydride **XVII**. This same process occurs with an isocyanate, and reductive elimination of rhodium hydride **XVIII** generates the enynamide **25** and regenerates the catalyst.

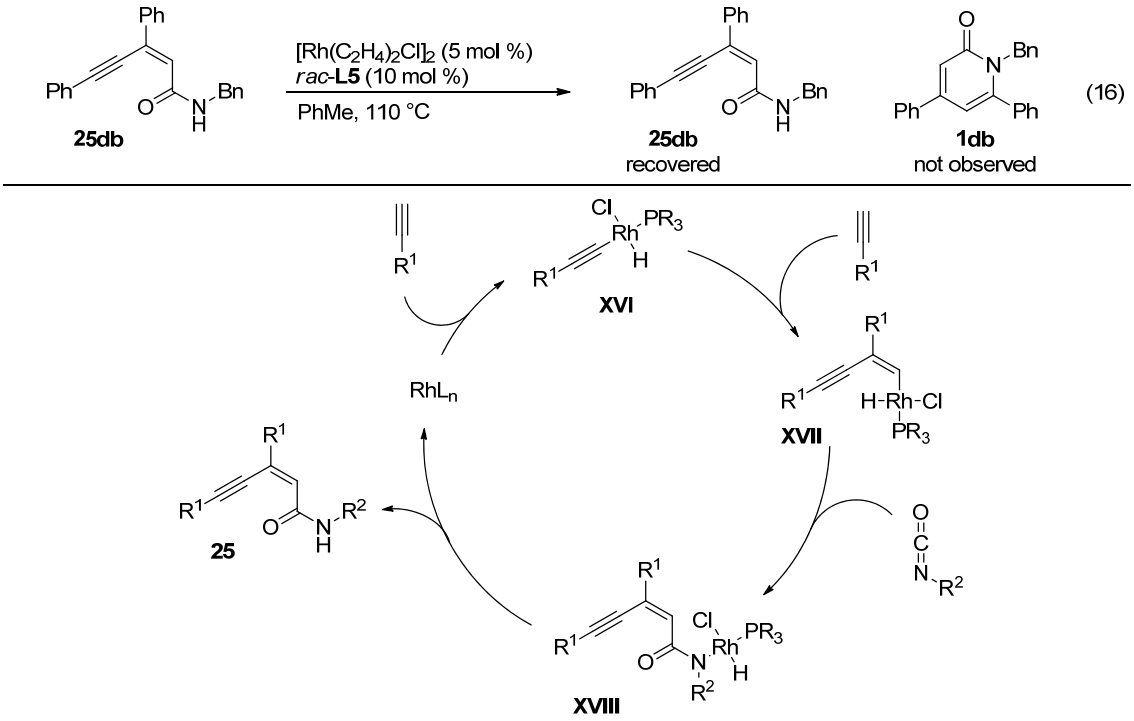

Scheme 1.6.1. Test of enynamide as reaction intermediate and proposed mechanism for enynamide formation.

1.7 Conclusion

In conclusion, we have developed a rhodium·phosphoramidite catalyzed [2+2+2] cylcoaddition of terminal alkynes and isocyanates to generate pyridones. This reaction proceeds with excellent catalyst control generating a single regioisomer of 2-pyridone. Additionally, this reaction works best with terminal alkynes, a substrate that is traditionally difficult. From the same reaction, 4-pyridone is also isolated as a single regiosomer. The isolation of 4-pyridone is the first example of a CO migration for pyridone

[61] Schäfer, H.-A.; Marcy, R.; Rüping, T.; Singer, H. *J. Organomet. Chem.* **1982**, *240*, 17-25.

synthesis using a [2+2+2] cycloaddition of alkynes and isocyanates. We propose that initial oxidative cyclization occurs between an alkyne and isocyanate, an unusual mechanistic feature in [2+2+2] cycloadditions to generate pyridones. More importantly, the generation of 4-pyridone suggests the existence of rhodacycle **X**, where the carbonyl of the isocyanate is α to the metal. This metallacycle has not been reported, and this observation supports our mechanistic proposals in the [2+2+2] cycloaddition of alkenyl isocyanates and alkynes that will be discussed in the next chapter.

CHAPTER 2

Mechanistic Insight into the Enantioselective Rhodium-Catalyzed [2+2+2] Cycloaddition of Terminal Alkynes and Alkenyl Isocyanates[1]

2.1 Introduction

Indolizidines and quinolizidines make up the core of a variety of natural products (Figure 2.1.1).[2] The great variety of approaches to these motifs highlights the difficulty that constructing these cores can pose.[3] In 2006, Yu and Rovis discovered and developed the [2+2+2] cycloaddition between alkenyl isocyanates and alkynes that efficiently constructs these cores.[4] Through the use of phosphoramidite ligands,[5] this reaction was rendered enantioselective (Eq 1).[6]

Isolation of lactam **3** from the [2+2+2] cycloaddition of alkenyl isocyanates and alkynes is expected, but generation of vinylogous amide **4** is surprising. Vinylogous amide **4** is derived from a fragmentation of the isocyanate. The amount of lactam **3** or vinylogous amide **4** produced is dependent on substrate sterics and electronics, as well as the nature of the phosphoramidite ligand. The mechanistic factors that determine product selectivity and product regiochemistry remained elusive and posed an interesting mechanistic problem.

---

[1] Reprinted with permission from *Journal of the American Chemical Society*, Vol *131*, Derek M. Dalton, Kevin M. Oberg, Robert T. Yu, Ernest E. Lee, Stéphane Perreault, Mark Emil Oinen, Melissa L. Pease, Guillaume Malik, Tomislav Rovis, "Enantioselective Rhodium-Catalyzed [2 + 2 + 2] Cycloadditions of Terminal Alkynes and Alkenyl Isocyanates: Mechanistic Insights Lead to a Unified Model that Rationalizes Product Selectivity", 15717-15728. Copyright (**2009**) American Chemical Society.

[2] (a) Daly, J. W. *J. Med. Chem.* **2003**, *46*, 445-452. (b) Daly, J. W.; Spande, T. F.; Garraffo, H. M. *J. Nat. Prod.* **2005**, *68*, 1556-1575.

[3] For reviews of recent syntheses, see: (a) Michael, J. P. *Nat. Prod. Rep.* **2005**, *22*, 603-626. (b) Michael, J. P. *Nat. Prod. Rep.* **2007**, *24*, 191-222. (c) Michael, J. P. *Nat. Prod. Rep.* **2008**, *25*, 139-165.

[4] Yu, R. T.; Rovis, T. *J. Am. Chem. Soc.* **2006**, *128*, 2782-2783.

[5] Teichert, J. F.; Feringa, B. L. *Angew. Chem. Int. Ed.* **2010**, *49*, 2486-2528.

[6] Yu, R. T.; Rovis, T. *J. Am. Chem. Soc.* **2006**, *128*, 12370-12371.

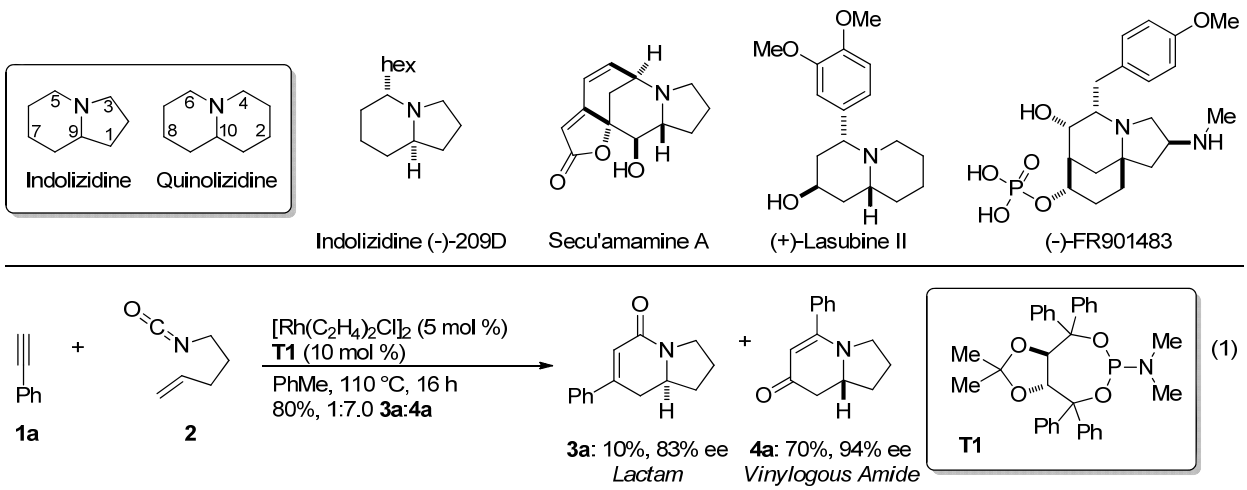

Figure 2.1.1. Indolizidine and quinolizidine structures: natural products and indolizidine synthesis via [2+2+2] cycloaddition of alkenyl isocyanates and alkynes.

The proposed mechanism, mechanism **A**, for the formation of lactam **3**, vinylogous amide **4**, and side products, 2-pyridone **5** and 4-pyridone **6** is depicted in Figure 2.1.2. Initially, the alkenyl isocyanate **2** and alkyne **1** coordinate to rhodium generating coordination complex **I**. From here, conrotatary cyclization can proceed in two ways. Cyclization with C-C bond formation generates rhodacycle **II**.[7] Coordination of the alkene and 1,2-migratory insertion forms rhodacycle **III** that reductively eliminates to furnish lactam **3** and regenerate the catalyst. Alternatively, cyclization with C-N bond formation generates rhodacycle **IV**. Coordination of the alkene is prohibited in this rhodacycle and a CO migration, via **V**, furnishes rhodacycle **VI**. At this point, the alkene can coordinate and insert to make rhodacycle **VII**. Reductive elimination makes vinylogous amide **4**. Coordination and insertion of an exogenous alkyne to rhodacycle **II** or **IV** forms 2-pyridone **5**. In a similiar fashion, coordination and insertion of an alkyne into rhodacycle **VI** generates 4-pyridone **6**.

[7] For selected publications with similar metallacycles involving an isocyanate and alkyne see: (a) Hoberg, H. *J. Organomet. Chem.* **1988**, *358*, 507-517. (b) Duong, H. A.; Louie, J. *J. Organomet. Chem.* **2005**, *690*, 5098-5104. (c) Louie, J. *Curr. Org. Chem.* **2005**, *9*, 605-623 (d) Yamamoto, Y.; Kinpara, K.; Saigoku, T.; Takagishi, H.; Okuda, S.; Nishiyama, H.; Itoh, K. *J. Am. Chem. Soc.* **2005**, *127*, 605-613. (e) Kondo, T.; Nomura, M.; Ura, Y.; Wada, K.; Mitsudo, T. *Tetrahedron Lett.* **2006**, *47*, 7107-7111. (f) Duong, H. A.; Louie, J. *Tetrahedron* **2006**, *62*, 7552-7559. (g) Kondo, T.; Nomura, M.; Ura, Y.; Wada, K.; Mitsudo, T.-a. *J. Am. Chem. Soc.* **2006**, *128*, 14816-14817.

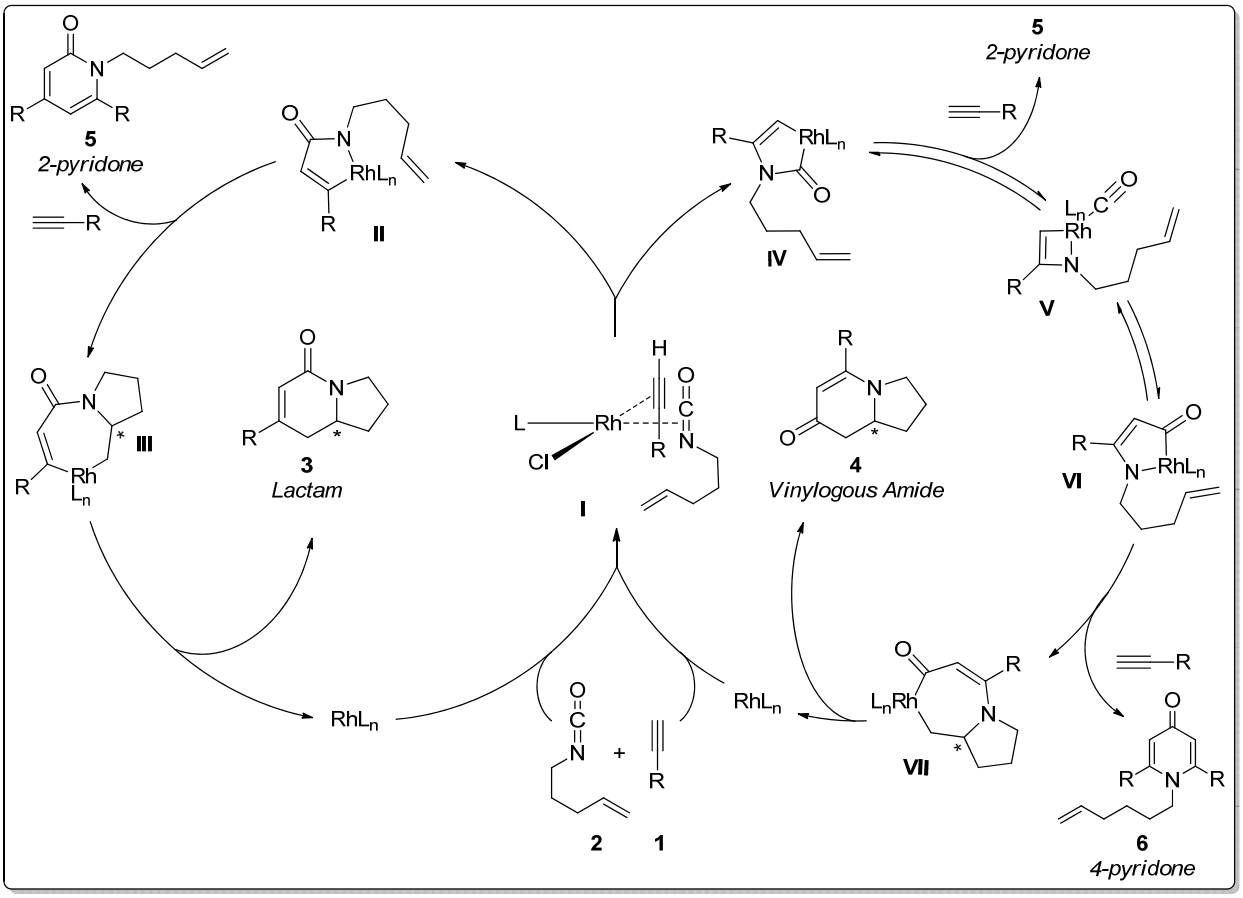

Figure 2.1.2. Proposed mechanism **A** of [2+2+2] cycloaddition of alkenyl isocyanates and alkynes. Coordination of alkyne and isocyanate followed by cyclization generates rhodacycle **II** or **IV** that eventually makes the observed products.

An alternative mechanism, mechanism **B**, can be proposed wherein the alkene and isocyanate cyclize first (Figure 2.1.3). In this mechanism, cyclization of the alkene and isocyanate generates **IX** and sets the sp^3 stereocenter. Coordination of the alkyne to rhodacycle **IX** and insertion generates rhodacycle **III** that reductively eliminates to make lactam **3**. Rhodacycle **IX** is in equilibrium with rhodacycle **XI** via a CO migration. Coordination of an alkyne to rhodacycle **XI** and insertion generates rhodacycle **XII** en route to vinylogous amide **6**. According to this mechanism, the equilibrium between rhodacycles **IX** and **X** and/or the rate of alkyne insertion into either rhodacycle determines product selectivity.

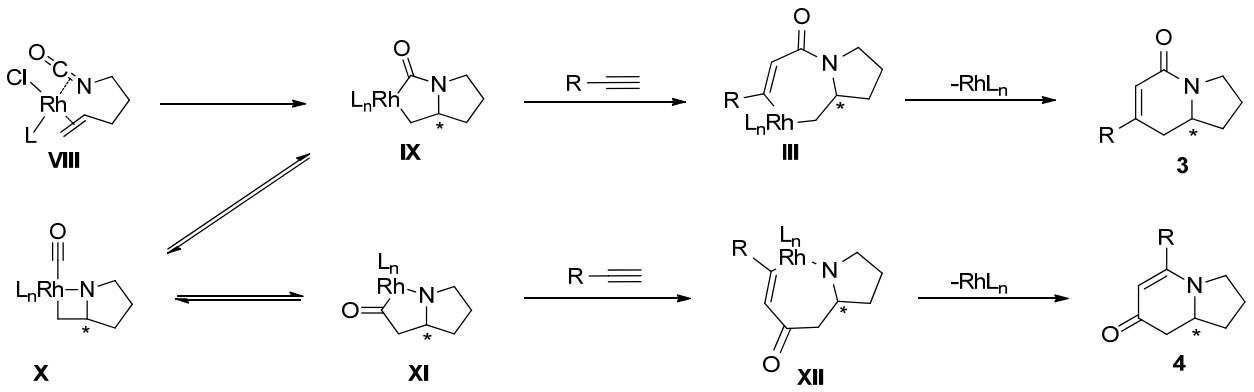

Figure 2.1.3. Alternative mechanism **B**: alkene and isocyanate cyclize to form common rhodacycle **IX**.

Although mechanism **B** is reasonable, a few pieces of data suggests that it is not operative. Mechanism **B** predicts a dependence of the reaction rate on the alkenyl isocyanate, so different alkenyl isocyanates should change the rate. Dr. Ernest Lee tested this hypothesis by performing competition experiments between alkenyl isocyanate **2** and 1,1-disubstituted alkenyl isocyanate **7** with different alkynes (Eq 2 and 3).[8] If the alkenyl isocyanate is involved in the turnover limiting step,[9] isocyanates **2** and **7** are predicted to react at different rates giving an unequal product ratio. Using benzyl acetylene **1b** (selective for lactam), a 1:1 ratio of lactam **3b** to **8b** derived from isocyanates **2** and **7** is observed. The same result occurs with para-methoxyphenyl acetylene **1c** (selective for vinylogous amide), where a 1:1 ratio of vinylogous amide **4c** and **9c** is observed. This suggests that the olefin is not involved in the turnover limiting step. This also suggests that the initial cyclization between the alkyne and alkenyl isocyanate is irreversible and product determining, as depicted in mechanism **A**.

Dr. Lee also found that higher concentrations of alkyne with alkenyl isocyanate **7** generates more 2-pyridone **5a** (Eq 4).[10] Lower alkyne concentration lowers the amount of 2-pyridone **5a**. This indirectly suggests that cyclization occurs between the alkyne and isocyanate, as depicted in mechanism **A**. If cyclization of the alkyne and isocyanate does occur, higher concentrations of alkyne favor intermolecular

[8] Lee, E. E. Colorado State University, Fort Collins, CO. Unpublished work, 2007.
[9] For a study of *thermodynamic* effects of nickel coordination by substituted alkenes, see: Tolman, C. A. *J. Am. Chem. Soc.* **1974**, *96,* 2780-2789.
[10] Lee, E. E.; Rovis, T. *Org. Lett.* **2008**, *10*, 1231-1234.

interception of rhodacycle **II**/**IV** by a second equivalent of alkyne over the intramolecular insertion of the tethered alkene. Additionally, when even bulkier 1,1-disubstituted alkenyl isocyanates are used (such as phenyl), only 2-pyridone **5** is observed.[11] If cyclization is not reversible, the formation of pyridone in the reaction suggests the isocyanate and alkyne cyclize first.

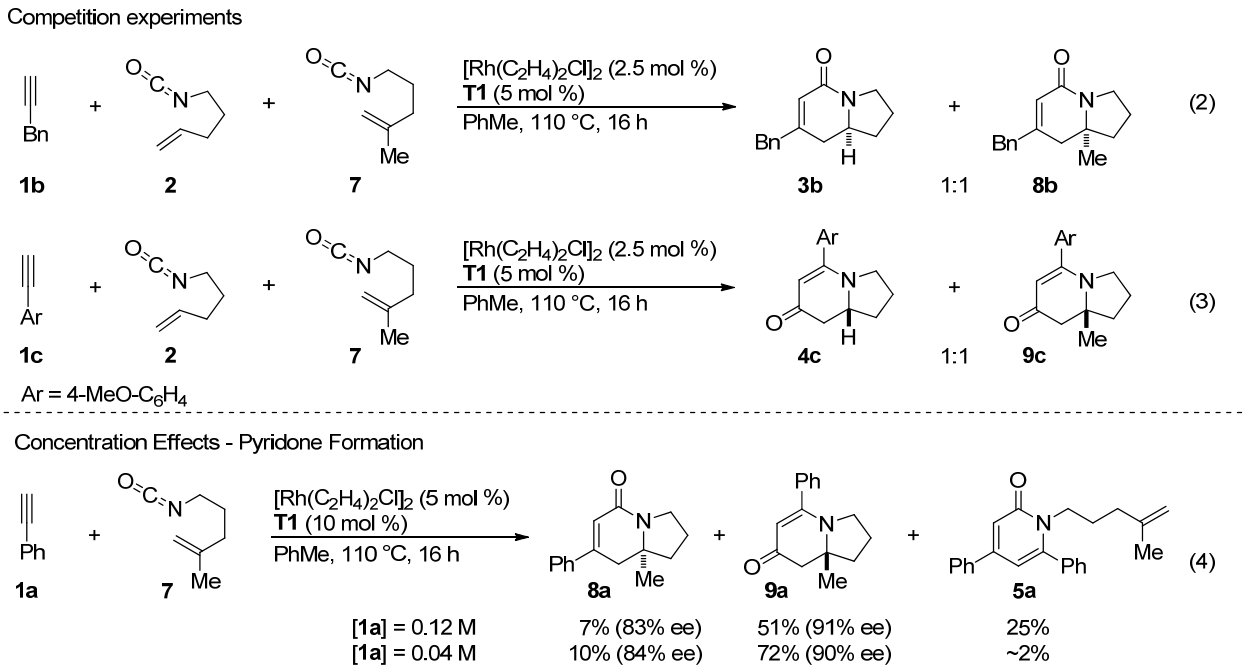

Finally, if mechanism **B** is operative, the enantiodetermining step occurs during formation of rhodacycle **IX**. The formation of common rhodacycle **IX** predicts that lactam **3** and vinylogous amide **4** should both have a stereocenter with the same configuration. With the same Taddol phosphoramidite, the stereochemistry is opposite for both lactam **3** and vinylogous amide **4**. This suggests that mechanism **B** is not operative. With all this indirect evidence, we believe that mechanism **A** is operative.

During our group's work on this transformation, a number of trends in product selectivity have been observed. Dr. Yu documented product selectivity based on the electronics and sterics of terminal alkynes. Electron-rich aryl alkynes provide more vinylogous amide and electron-deficient aryl alkynes

[11] Lee, E. E. Colorado State University, Fort Collins, CO. Unpublished work, 2007.

provide more lactam (Figure 2.1.3).[12] This occurs in a predictable and linear fashion as demonstrated by a Hammett plot.[13]

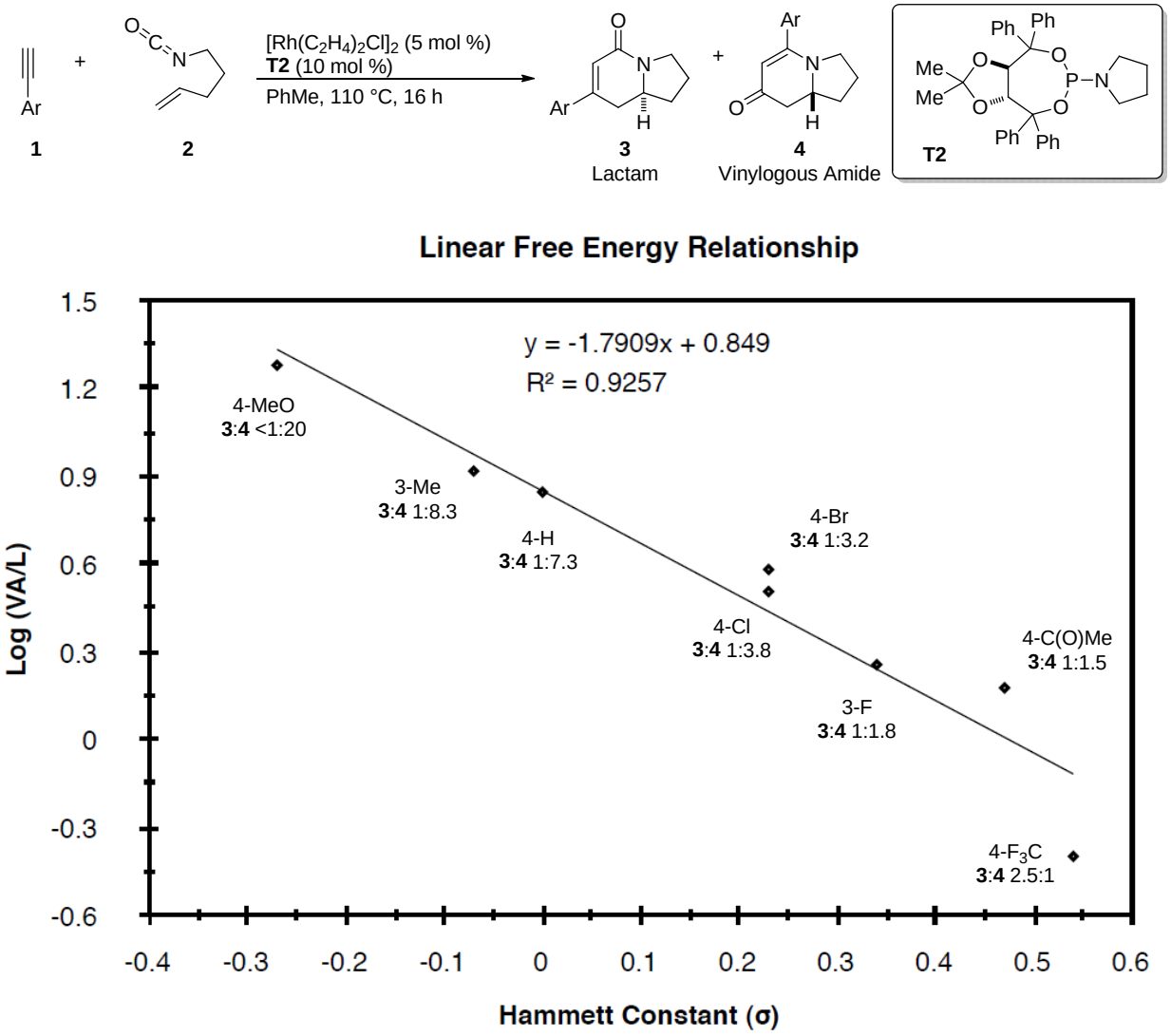

Figure 2.1.3. Hammett plot correlating alkyne electronics with product selectivity.

Dr. Yu also found that the size of the alkyne influences product selectivity. Smaller alkynes favor lactam **3** and larger alkynes favor vinylogous amide **4** (Table 2.1.1).[14]

[12] Yu, R. T.; Rovis, T. *J. Am. Chem. Soc.* **2006**, *128*, 12370-12371.
[13] Hansch, C.; Leo, A.; Taft, R. W. *Chem. Rev.* **1991**, *91*, 165-195.
[14] Yu, R. T.; Lee, E. E.; Malik, G.; Rovis, T. *Angew. Chem. Int. Ed.* **2009**, *48*, 2379-2382.

Table 2.1.1. Correlation of alkyne size with product selectivity.

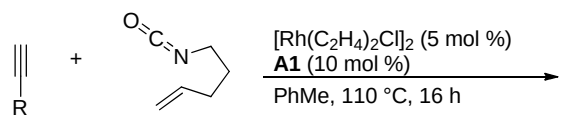

1 **2** **3** **4**

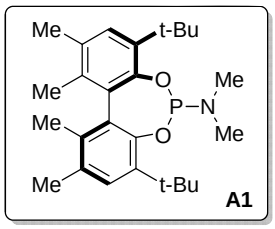

entry	R	**3**:**4**	yield (%)	ee (%) **4**
1	hex	1:6.0	66	91
2	Cy	1:14	86	91
3	*t*-Bu	1:10	67	79
4	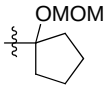	1:>20	60	81

In addition to product selectivity based on the alkyne, the ligand exerts a large influence on product selectivity (Figure 2.1.4). In general, we observe that Taddol ligands slightly favor lactam, whereas BINOL and BiAryl ligands favor vinylogous amide.

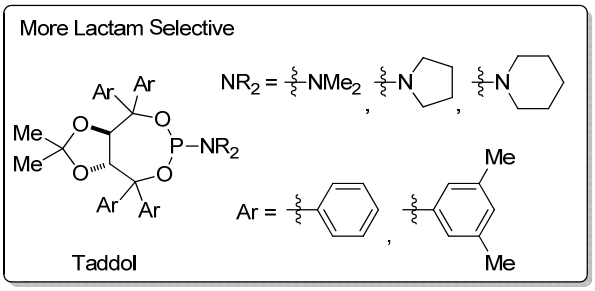

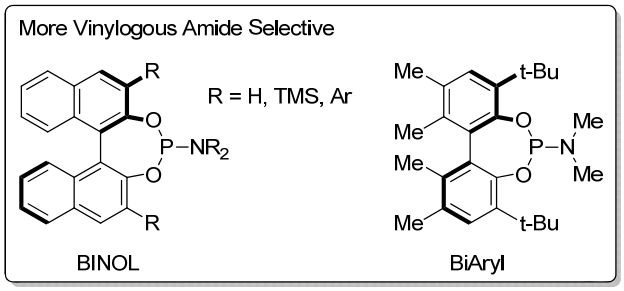

Figure 2.1.4. Phosphoramidite ligands commonly used in the [2+2+2] cycloaddition.

Although we had observed these trends in product selectivity and could use them to make predictions, questions remained about the mechanism (Figure 2.1.5). We observe remarkable regioselectivity in the reaction with terminal alkynes; the hydrogen is α to the carbonyl in the products for both lactam **3** and vinylogous amide **4**. We have never observed the opposite regioisomer despite using a wide range of alkynes and phosphoramidite ligands. In collaboration with my colleague, Derek Dalton, we attempted to answer the questions, "What determines regioselectivity?" and "What controls product selectivity?"

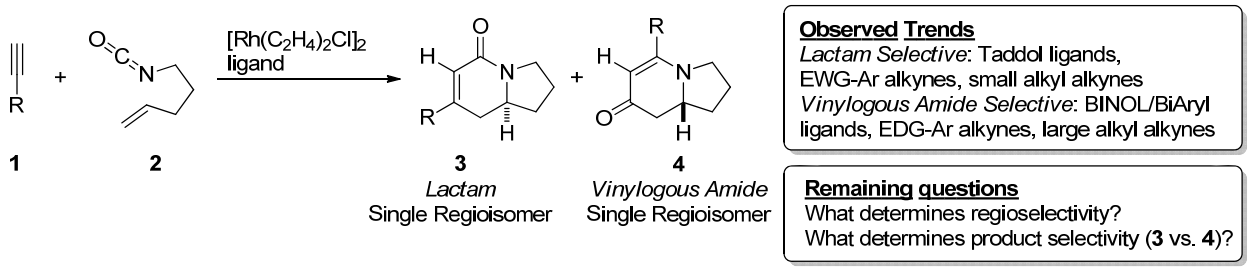

Figure 2.1.5. Observed trends in product selectivity and remaining mechanistic questions.

2.2 Investigation of Phosphoramidite Ligands

Due to the impact of ligand structure on product selectivity, we conducted a structure activity relationship study. Although numerous ligands had been synthesized and employed in the cycloaddition, a systematic comparison was lacking. The effect of ligand structure on product selectivity for both aryl and alkyl terminal alkynes is shown in Table 2.2.1. A number of trends emerge from this data. Overall, Taddol phosphoramidite ligands are more lactam selective than BINOL and BiAryl phosphoramidites. We see that the amine portion of the Taddol phosphoramidite affects product selectivity and enantioselectivity (entries 1-4). The smallest amine (pyrrolidyl) is vinylogous amide selective and is the most enantioselective. As the amine gets larger (N,N-dimethylamine, piperidyl, and N,N-dicyclohexyl), more lactam is generated and lower enantioselectivities is observed. This trend is repeated with various aryl substitutions (entries 5-9). With BINOL and biaryl phosphoramidites, the amine has less of an impact (entries 10-15). Finally, the electronics of the aryl substituent on the Taddol ligands affects product selectivity (entries 2, 5, 7, 8). The most electron-deficient ligand **T7** favors vinylogous amide, and product selectivity shifts to lactam with increasing electron-richness **T2**, **T6**, **T8**.

Table 2.2.1. Structure activity relationship of phosphoramidites with terminal alkynes.

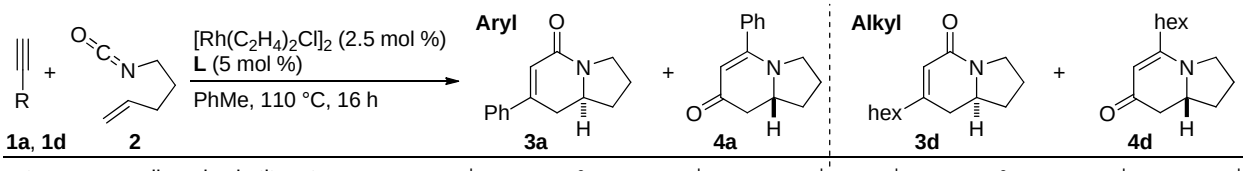

1a, **1d** **2** **3a** **4a** **3d** **4d**

entry		ligand substituent		**3a**:**4a**[b]	yield (%)[c]	ee (%) **3a**[d]	ee (%) **4a**[d]	**3d**:**4d**[b]	yield (%)[c]	ee (%) **3d**[d]	ee (%) **4d**[d]
	L	R^1	R^2								
1	**T1**	Ph	NMe_2	1:7.0	80[f]	83	94	3.2:1	81[f]	81	73
2	**T2**	Ph		1:7.3	87[f]	89	94	2.4:1	80[f]	83	70
3	**T3**	Ph	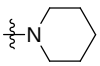	1:3.3	76[f]	90	81	5.0:1	78[f]	80	33
4	**T4**	Ph	NCy_2	1:2.0	14	-	-	>20:1	5	-	-
5	**T5**	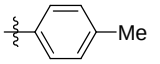		1:6.5	84	91	95	2.5:1	55	87	76
6	**T6**	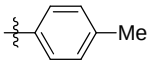	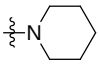	1:2.8	68	87	85	8.3:1	68	83	46
7	**T7**	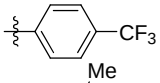	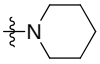	1:>20	67	69	84	1:1	31	79	74
8	**T8**	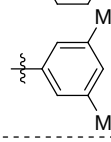		1:5.6	84	96	97	4.0:1	77	90	74
9	**T9**		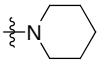	1:1.6	75	94	94	12.5:1	72	82	51
10	**B1**	H	NMe_2	1:2.2	32[f]	5	55[e]	1:1.9	19	14	67[e]
11	**B2**[e]	Me	NMe_2	1:4.5	50[f]	45[e]	8	1:4.2	34	18[e]	59
12	**B3**	TMS	NMe_2	1:7.1	74	36	45[e]	1:3.6	53	32	95[e]
13	**B4**	TMS		1:12.5	77	37	55[e]	1:3.6	51	50	95[e]
14	**B5**	TMS	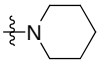	1:12	82	43	55[e]	1:3.2	63	47	92[e]
15	**A1**			1:>20	77	41	3[e]	1:6.2	75	8	91[e]

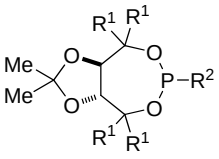
Taddol (**T**)

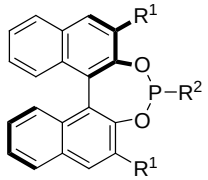
BINOL (**B**)

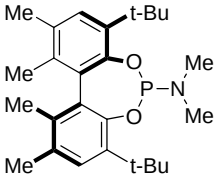
BiAryl **A1**

[a] Reaction conditions: **1** (2 equiv), **2**, $[Rh(C_2H_4)_2Cl]_2$ (2.5 mol %), **L** (5 mol %) in PhMe at 110 °C for 16 h. [b] Ratio determined by ^1H NMR of crude reaction. [c] Combined isolated yield. [d] Determined by HPLC analysis on a chiral stationary phase. [e] Opposite enantiomer. [f] Reaction conditions: **1** (2 equiv), **2**, $[Rh(C_2H_4)_2Cl]_2$ (5 mol %), **L** (10 mol %) in PhMe at 110 °C for 16 h.

2.3 X-Ray Analysis of Rhodium(cod)Cl·Phosphoramidite Complexes

We also obtained crystal structures of some of our phosphoramidites complexed to rhodium. We chose to synthesize complexes using $[Rh(cod)Cl]_2$ based on the existence of ligated cyclooctadiene rhodium complexes in literature.[15] Additionally, we thought that complexes derived from $[Rh(cod)Cl]_2$ would be more stable than those generated from $[Rh(C_2H_4)_2Cl]_2$ because the bisethylene complex decomposes in air. In our first crystallization attempt, we mixed (+)-**T9** with $[Rh(cod)Cl]_2$ in dichloromethane, and this solution was layered with heptanes. The solution slowly evaporated to yield X-ray quality crystals. After collecting data, we solved our first rhodium(I)(cod)chloride·phosphoramidite crystal structure: Rh(cod)Cl·**T9**[16] (Figure 2.3.1). After this initial success, we attempted to crystallize a range of phosphoramidite ligands bound to rhodium. This led to five more structures: Rh(cod)Cl·**T8**,[17] Rh(cod)Cl·**T1**,[18] Rh(cod)Cl·**T2**,[19] Rh(cod)Cl·**A1**,[20] and Rh(cod)Cl·**B4**.[21] Selected bond lengths and product selectivity for each ligand is shown in Figure 2.3.1.

[15] For publications of rhodium and iridium phosphoramidite crystal structures see: (a) Bartels, B.; García-Yebra, C.; Rominger, F.; Helmchen, G. *Eur. J. Inorg. Chem.* **2002**, 2569-2586. (b) Leitner, A.; Shekhar, S.; Pouy, M. J.; Hartwig, J. F. *J. Am. Chem. Soc.* **2005**, *127*, 15506-15514. (c) Faller, J. W.; Milheiro, S. C.; Parr, J. *J. Organomet. Chem.* **2006**, *691*, 4945-4955. (d) Giacomina, F.; Meetsma, A.; Panella, L.; Lefort, L.; de Vries, A. H. M.; de Vries, J. G. *Angew. Chem. Int. Ed.* **2007**, *46*, 1497-1500. (e) Mikhel, I. S.; Ruegger, H.; Butti, P.; Camponovo, F.; Huber, D.; Mezzetti, A. *Organometallics* **2008**, *27*, 2937-2948. (f) Filipuzzi, S.; Maennel, E.; Pregosin, P. S.; Albinati, A.; Rizzato, S.; Veiros, L. F. *Organometallics* **2008**, *27,* 4580-4588.
[16] Deposit number CCDC 739239.
[17] Deposit number CCDC 739238.
[18] Deposit number CCDC 739237.
[19] Deposit number CCDC 757562. For an additional structure, see: Oberg, K. M. ; Dalton, D. M.; Oinen, M. E.; Rovis, T. Private communication to the Cambridge Structural Database, deposit number CCDC 739236.
[20] Deposit number CCDC 739234.
[21] Deposit number CCDC 739235.

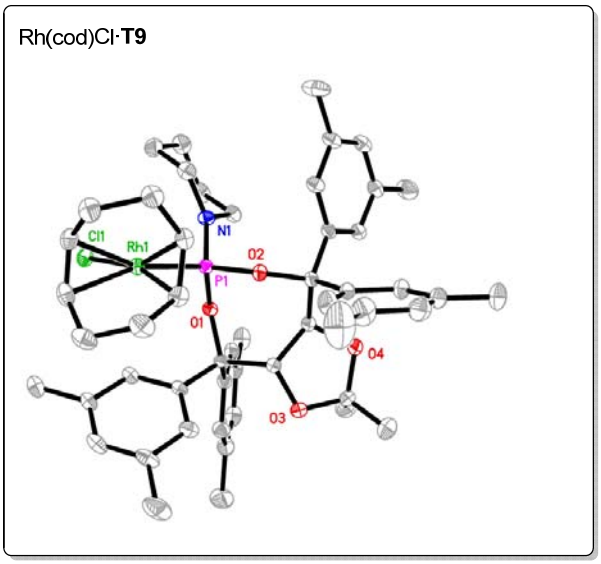

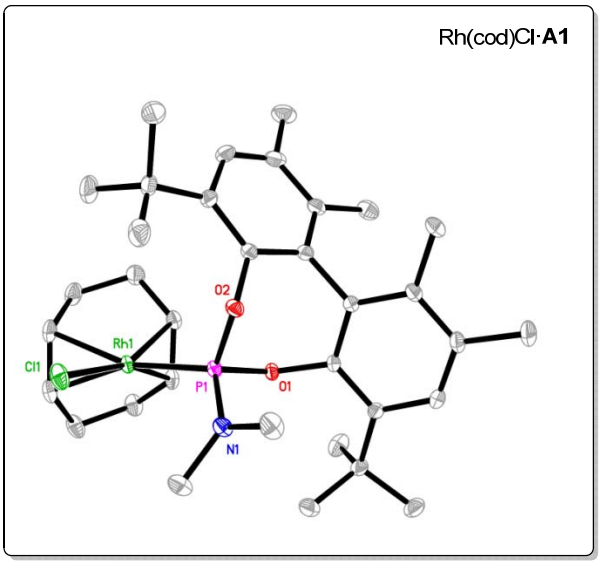

Ligand	T9	T8	T1	T2	A1	B4
Rh–P	2.2703(4)	2.2688(6)	2.2648(6)	2.2547(3)	2.2451(4)	2.2388(9)
Rh–Cl	2.3654(4)	2.3765(6)	2.3777(6)	2.3842(3)	2.3485(4)	2.3455(8)
Trans to P						
Rh–‖	2.132	2.131	2.140	2.152	2.162	2.151
C=C	1.409(2)	1.377(4)	1.376(4)	1.3781(18)	1.369(3)	1.365(5)
Trans to Cl						
Rh–‖	1.994	1.992	1.997	1.995	2.013	2.003
C=C	1.413(3)	1.395(4)	1.417(3)	1.4131(16)	1.409(2)	1.396(5)
Ph L:VA (**3**:**4**)	1:1.6	1:5.6	1:7.0	1:7.3	1:>20	1:7.1
hex L:VA (**3**:**4**)	12.5:1	4.0:1	3.2:1	2.4:1	1:6.2	1:3.6

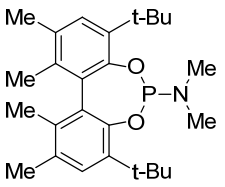

A1

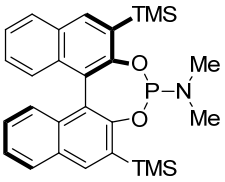

B4

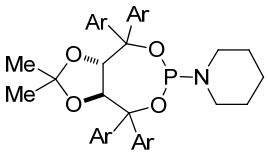

T9 Ar = *m*-xylyl

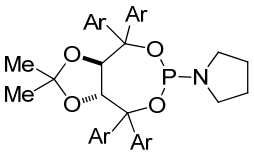

T8 Ar = *m*-xylyl

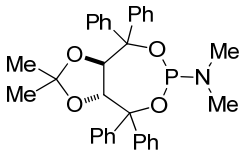

T1

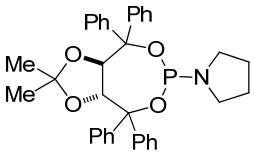

T2

Figure 2.3.1. Crystal structures of Rh(cod)Cl·**T9** and Rh(cod)Cl·**A1**, selected bond lengths from Rh(cod)Cl·**L** structures, and product selectivity for phenyl acetylene (**1a**) and 1-octyne (**1d**) using these ligands.

From this data, we see that rhodium-phosphorous bond length correlates with product selectivity. Longer Rh-P bonds correlate to more lactam **3** and shorter Rh-P bond lengths correlate to more

vinylogous amide **4** (Figure 2.3.2). This is also seen with phosphoramidites **B4** and **A1**, but the trend is more clear in the Taddol series and is not complicated by large structural differences between the different ligand scaffolds.

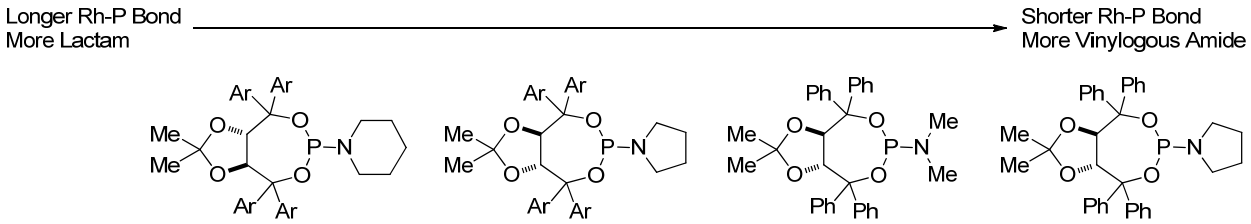

Ligand	**T9** Ar = *m*-xylyl	**T8** Ar = *m*-xylyl	**T1**	**T2**
Rh–P	2.2703(4)	2.2688(6)	2.2648(6)	2.2547(3)
Ph L:VA (**3**:**4**)	1:1.6	1:5.6	1:7.0	1:7.3
hex L:VA (**3**:**4**)	12.5:1	4.0:1	3.2:1	2.4:1

Figure 2.3.2. Correlation of Rh-P bond lengths with product selectivity with phenyl acetylene (**1a**) and 1-octyne (**1d**).

We tested to see if these ligated rhodium complexes are catalytically competent and compared them to *in situ* generated catalysts (Table 2.3.1). Our general conditions utilize catalyst generated *in situ* by mixing $[Rh(C_2H_4)_2Cl]_2$ and the ligand (entry 1). The same reaction with $[Rh(cod)Cl]_2$ as the precatalyst provides similar product selectivity and enantioselectivity but a lower yield (entry 2). This decrease in yield has been observed in previous precatalyst screens.[22] We believe the improved performance with the bisethylene complex is due to the ease in which ethylene dissociates from rhodium and generates the active catalyst. When the preformed Rh(cod)Cl·**T1** complex (even sitting on the bench under ambient air and temperature for a month) is used, the same result is obtained as the *in situ* generated catalyst from mixing $[Rh(cod)Cl]_2$ and **T1** (entry 3).

[22] Yu, R. T. Enantioselective rhodium-catalyzed [2+2+2] and [4+2+2] cycloaddition reactions of alkenyl heterocumulenes: applications to alkaloid synthesis. Ph.D. Dissertation, Colorado State University, Fort Collins, CO, 2009.

Table 2.3.1. Rh(cod)Cl·**T1** exhibits similar reactivity to *in situ* formed catalyst.

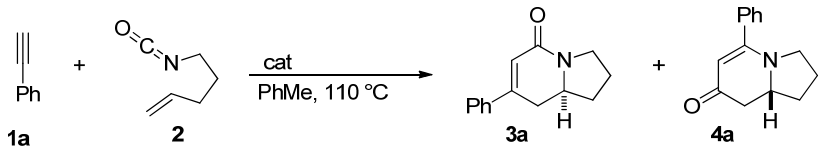

entry	cat (5 mol %)	**3a**:**4a**[b]	yield (%)[c]	ee (%) **3a**[d]	ee (%) **4a**[d]
1	$[Rh(C_2H_4)_2Cl]_2$, **T1**	1:8.3	94	81	91
2	$[Rh(cod)Cl]_2$, **T1**	1:7	66	84	91
3	Rh(cod)Cl·**T1**	1:9	70	82	91

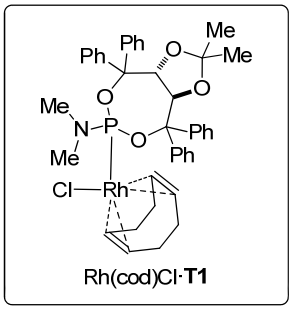

2.4 Model for Regioselectivity

The regioselectivity of the [2+2+2] cycloaddition of alkenyl isocyanate **2** and terminal alkynes **1** is excellent (Eq 5). We observe 7-substituted lactam **3** and 5-substituted vinylogous amide **4**, and the hydrogen is α to the carbonyl (6-H) (Eq 5). To date, we have never observed 6-substituted lactam **3'** or 6-substituted vinylogous amide **4'** using a variety of terminal alkynes and phosphoramidite ligands. A model that explains regioselectivity can be constructed from an analysis of the Rh(cod)Cl·**L** structures.

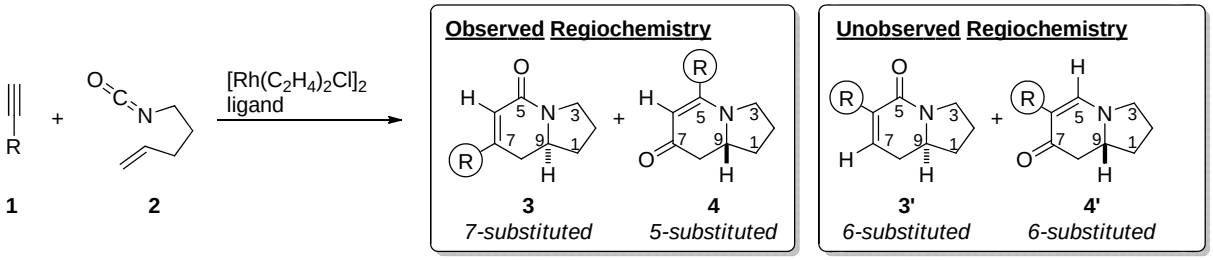

(5)

During our examination of the Rh(cod)Cl·**L** structures, we noticed that one side of the rhodium square planar complex is sterically hindered (Figure 2.4.1). This steric hindrance is imposed by one of the Taddol aryl rings and the aryl ring of the BINOL/BiAryl complexes. We propose this hindrance biases the coordination of the isocyanate and alkyne[23] so that the smaller substituents are facing the more hindered face of rhodium (Complex **I**, Figure 2.4.1). Although it is possible that the alkyne and the isocyanate

[23] We believe the alkynes displace the ethylenes in the reaction before the isocyanate binds. This bis alkyne complex dissociates the alkyne trans to the phosphoramidite, as it has a larger trans influence than the chloride, and the isocyanate coordinates to generate complex **I**.

coordinate to rhodium parallel to the square plane,[24] we believe they bind orthogonal to the square plane as depicted in Figure 2.4.1. This is based on X-ray structures of other d^8 complexes and calculations.[25] This coordination minimizes steric repulsion between the π components and allows them to backbond to the metal.[26]

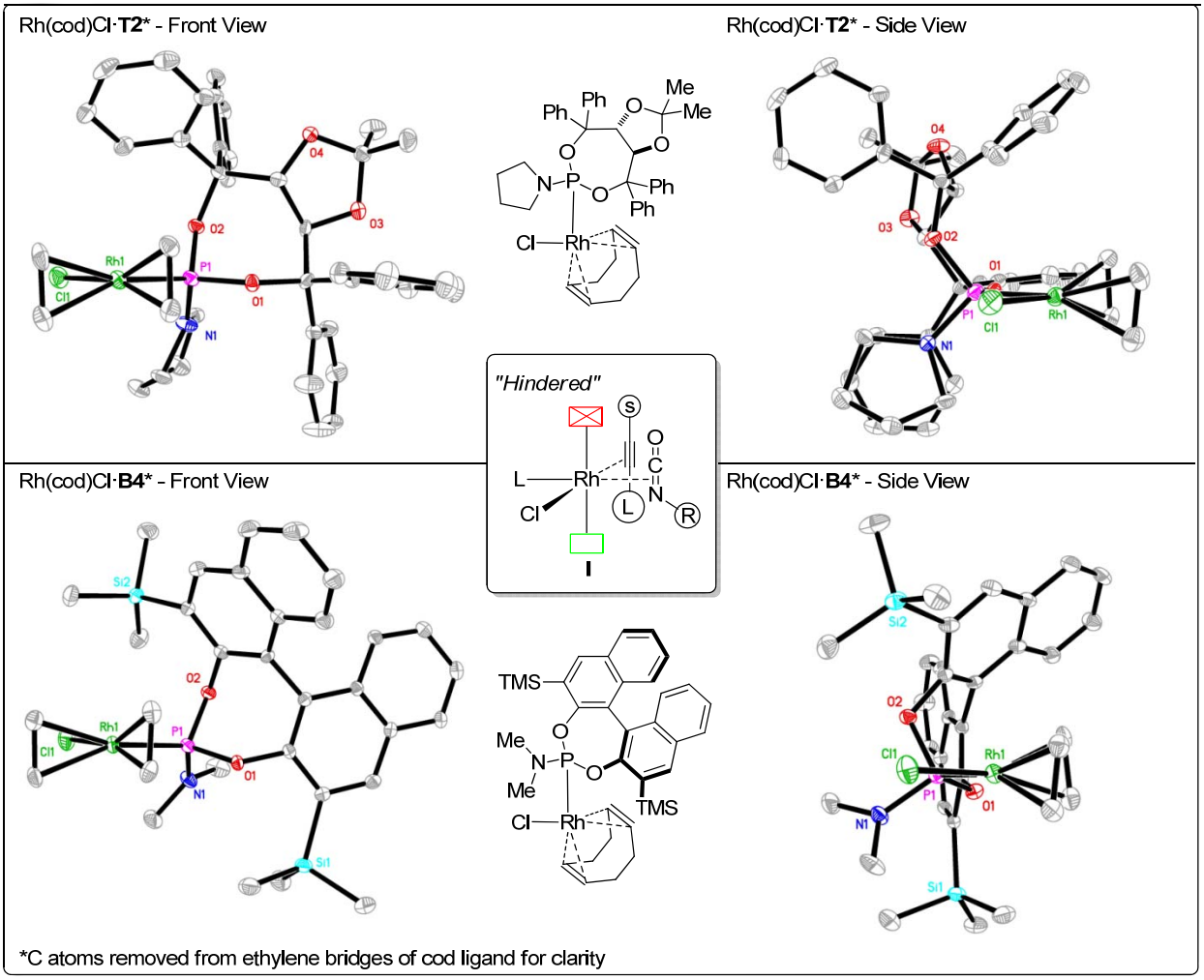

Figure 2.4.1. Steric hindrance of one rhodium face by phosphoramidite ligand.

[24] Imabayashi, T.; Fujiwara, Y.; Nakao, Y.; Sato, H.; Sakaki, S. *Organometallics* **2005**, *24*, 2129-2140.
[25] For crystal structures, see: (a) Davies, G. R.; Hewerston, W. H.; Maise, R. H. B.; Owston, P. G.; Patel, C. G. *J. Chem. Soc.* **1970**, 1873. (b) Beauchamp, A. L.; Rochon, F. R.; Theophanides, T. *Can. J. Chem.* **1973**, *51*, 126. For computational analysis of alkyne coordination to Pd, see: (c) de Vaal, P.; Dedieu, A. *J. Organomet. Chem.* **1994**, *478*, 121-129. For computational analysis of alkyne coordination to Co, see: (d) Wakatsuki, Y.; Nomura, I.; Kitaura, K.; Morokuma, K.; Yamazaki, H. *J. Am. Chem. Soc.* **1983**, *105*, 1907-1912.
[26] Dewar-Chatt-Duncanson model, see: (a) Hartwig, J. *Organotransition Metal Chemistry: From Bonding to Catalysis*; University Science Books: Sausalito, California, 2010. (b) Dewar, M. J. S. *Bull. Soc. Chim. Fr.* **1951**, *18*, 79. (c) Chatt, J.; Duncanson, L. A. *J. Chem. Soc.* **1953**, 2939.

From coordination complex **I**, cyclization can occur in a concerted, conrotatory fashion in one of two ways producing either of the two products (Figure 2.4.2). If the smaller substituents of the two π components fold away from the metal, via **TSI**, rhodacycle **II** is formed. From here, alkene migratory insertion and reductive elimination furnishes 7-subsituted lactam **3** with the proton α to the carbonyl. Alternatively, if the smaller substituents fold toward the metal, via **TSII**, rhodacycle **IV** is generated. After the CO shift, rhodacycle **VI** is made and the proton is now α to the carbonyl. Olefin insertion and reductive elimination forms 5-substituted vinylogous amide **4**. This model is based on the assumption that oxidative cyclization is an irreversible, concerted process.[27]

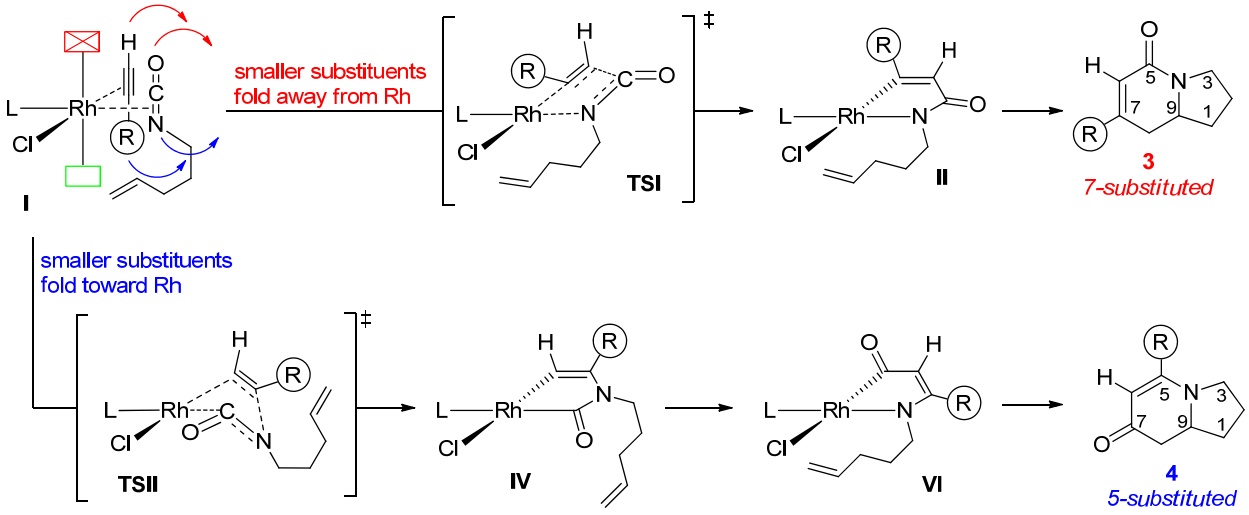

Figure 2.4.2. Regioselectivity model. Small substituents face more hindered face in coordination complex **I** due to the large phosphoramidite ligand. Concerted cyclization relays regiochemistry from complex **I**.

2.5 Model for Product Selectivity

We have seen that product selectivity in this reaction correlates with a number of factors: alkyne sterics, alkyne electronics, and phosphorous-rhodium bond lengths. In developing a model to explain

[27] (a) For calculations on the concerted nature of oxidative cyclization, see: Wakatsuki, Y.; Nomura, I.; Kitaura, K.; Morokuma, K.; Yamazaki, H. *J. Am. Chem. Soc.* **1983**, *105*, 1907-1912. (b) For experiments on the irreversibility of oxidative cyclization of alkynes and isocyanates, see: Eq 2 and 3 reproduced from Lee, E. E. Colorado State University, Fort Collins, CO. Unpublished work, 2007 and Dalton, D. M.; Oberg, K. M.; Yu, R. T.; Lee, E. E.; Perreault, S.; Oinen, M. E.; Pease, M. L.; Malik, G.; Rovis, T. *J. Am. Chem. Soc.* **2009**, *131*, 15717-15728.

product selectivity, we looked at previous models in the literature that explain product selectivity in cycloadditions. The first model explored is an electronic model put forth by Stockis and Hoffmann. The second theory is a steric model developed by Wakatsuki and Yamazaki. A strict application of either model fails to explain product selectivity in the [2+2+2] cycloaddition of alkenyl isocyanates and alkynes, but a model for product selectivity taking into account both electronic and steric contributions does a credible job at describing the factors that contribute to product selectivity.

Stockis and Hoffmann performed computations on metallacycle formation and concluded that orbital overlap between the metal and π components induce the observed regioselectivity.[28] The model system that they explored was the cyclization of a d^8 iron complex with ethylene. They polarized the olefins in their computations and determined which bis-olefin metal complex was the most stable during metallacycle formation. They found that complex **A** is lower in energy during and after metallacyle formation.[29] Complex **A** is lower in energy because the π* of the bound olefins stabilizes the metal d_{xy} orbital during metallacycle formation. This means the largest LUMO coefficient of the π bond prefers to be β to the metal and translates to carbons with electron-withdawing groups or more electronegative heteroatoms prefering to be α to the metal in the metallacyle. The authors note that this model does not apply to metallacycle formation that is reversible, and sterics were not considered in their computations. During these calculations, they found that unsymmetrical complex **B** is intermediate in energy between complexes **A** and **C**. This suggests that the stabilization effects from the π components during oxidative cycloaddition can act independently of one another.

[28] Stockis, A.; Hoffmann, R. *J. Am. Chem. Soc.* **1980**, *102*, 2952-2962.
[29] Complex **C** is initially lower in energy, but is higher in energy than complexes **A** and **B** during and after metallacycle formation.

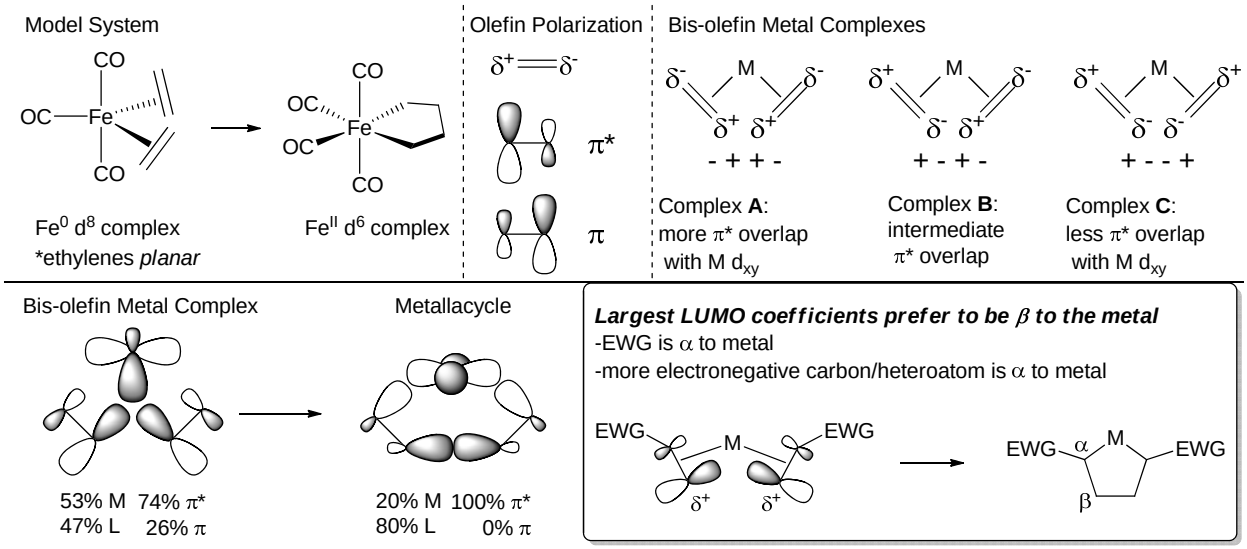

Figure 2.5.1. Stockis-Hoffmann model for regioselectivity in metallacycle formation. The largest LUMO coefficients of the π components prefer to be β to the metal during oxidative cyclization.

Before we apply the Stockis-Hoffmann electronic model to the cyclization of alkenyl isocyanates and alkynes, a discussion of the isocyanate LUMO and reactivity is warranted. The largest LUMO coefficient of the isocyanate is across the C=O double bond (with a small contribution from the C=N double bond), but the largest N-LUMO coefficient is across the C=N double bond (with a small contribution from the C=O double bond).[30] These two energies are almost degenerate. In metal-catalyzed cycloadditions with isocyanates, the C=N bond is typically the reactive bond rather than the C=O bond. This is presumably due to bond strength; the bond strength of a C=N double bond is ~60 kcal/mol whereas the bond strength of a C=O double bond is ~87 kcal/mol.[31] Metal-catalyzed cycloadditions with isothiocyanates are opposite in that the C=S double bond typically reacts (bond strength of C=S double bond is ~58 kcal/mol). In crystal structures of group VIIIB transition metals with isocyanates or

[30] Houk, K. N.; Strozier, R. W.; Hall, J. A. *Tetrahedron Lett.***1974**, *11*, 897-900.

[31] BDE were calculated by subtracting the BDE value of a single bond from the BDE of a double bond to give an approximate BDE of the double bond. Values from: Luo, Y.-R. *Comprehensive Handbook of Chemical Bond Energies*; CRC Press, Taylor & Francis Group, LLC: Boca Raton, Florida, 2007. $O=CH_2$: 180.6 kcal/mol, $HO-C_2H_5$: 93.5 kcal/mol; $^{\bullet}N=CH_2$: 144 kcal/mol, $HN-C_2H_5$: 84.2 kcal/mol; $S=CH_2$: 131.2 kcal/mol, $HS-C_2H_5$: 73.6 kcal/mol; $O=CNCH_3$: 133 kcal/mol, HN=CO: 122 and 86.6 kcal/mol. Despite the use of an imine radical, this crude approximation matches more complex systems (58-66.8 kcal/mol), see; Zhu, X.-Q.; Liu, Q.-Y.; Chen, Q.; Mei, L.-R. *J. Org. Chem.* **2010**, *75,* 789-808.

isothiocycanates bound, C=N binding is more metallacyclopropane-like in isocyanate bound complexes[32] and the C=S binding is more metallacyclopropane-like in isothiocyanate bound structures.[33] This binding mirrors reactivity in metal-catalyzed cycloadditions with isothiocyanates; typically sulfur-heterocycles are generated through reaction of the C=S bond.[34]

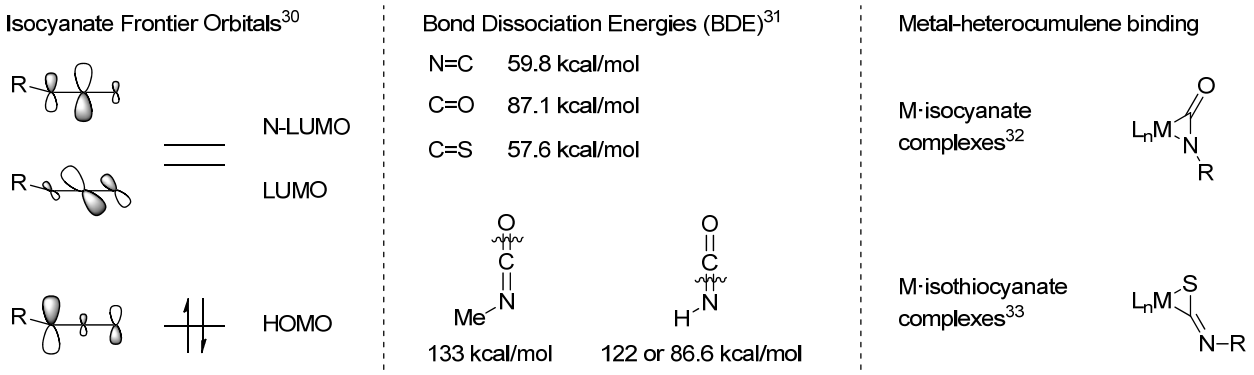

Figure 2.5.2. Reactivity of heterocumulenes with metals: nearly degenerate isocyanate LUMO and N-LUMO, weakness of N=C bond relative to C=O bond explains chemoselectivity, and metal-heterocumulene binding mirrors reactivity.

A strict application of the Stockis-Hoffmann electronic model to the cyclization of alkenyl isocyanates and alkynes does not always predict the correct product (Figure 2.5.2). The largest LUMO coefficient is on the carbon of isocyanates, on the internal carbon of alkyl and electron-donating aryl alkynes, and on the terminal carbon of electron-withdrawing aryl alkynes. For the cyclization of alkyl alkynes with isocyanates, we see that this model predicts 6-subsituted lactam **3'**. This is the observed product but the incorrect regioisomer. The same product is expected for the reaction of electron-donating aryl alkynes and isocyanates. This is both the incorrect product and the incorrect regioisomer. 7-

[32] For metal-isocyanate crystal structures, see: Cobalt; (a) Klein, H. F.; Helwig, M.; Karnop, M.; Koenig, H.; Hammerschmitt, B.; Cordier, G.; Floerke, U.; Haupt, H. J. *Z. Naturforsch., B: Chem Sci.* **1993**, *48*, 785. Nickel; (b) Mindiola, D. J.; Hillhouse, G. L. *Chem. Commun.* **2002**, 1840-1841.
[33] For metal-isothiocyanate crystal structures, see: Nickel; (a) Bianchini, C.; Masi, D.; Mealli, C.; Meli, A. *J. Organomet. Chem.* **1983**, *247*, C29-C31. Nickel and cobalt; (b) Bianchini, C.; Masi, D.; Mealli, C.; Meli, A. *Inorg. Chem.* **1984**, *23*, 2838-2844. Osmium; (c) Flugel, R.; Gevert, O.; Werner, H. *Chem. Ber.* **1996**, *129*, 405.
[34] For examples of isothiocyanate cycloadditions, see: (a) Yamazaki, H. *J. Synth. Org. Chem., Jpn.* **1987**, *45*, 244-257. (b) Yamamoto, Y.; Kinpara, K.; Saigoku, T.; Takagishi, H.; Okuda, S.; Nishiyama, H.; Itoh, K. *J. Am. Chem. Soc.* **2005**, *127*, 605-613. (c) Tanaka, K.; Wada, A.; Noguchi, K. *Org. Lett.* **2006**, *8*, 907-909.

Substituted lactam **3** is predicted for the reaction of electron-withdrawing aryl alkynes and isocyanates. This is both the observed product and correct regioisomer. Although this model does not predict the correct product with every class of alkyne, it predicts the correct product with electron-withdrawing aryl alkynes. Most importantly, it suggests that the isocyanate LUMO always selects for a lactam metallacycle.

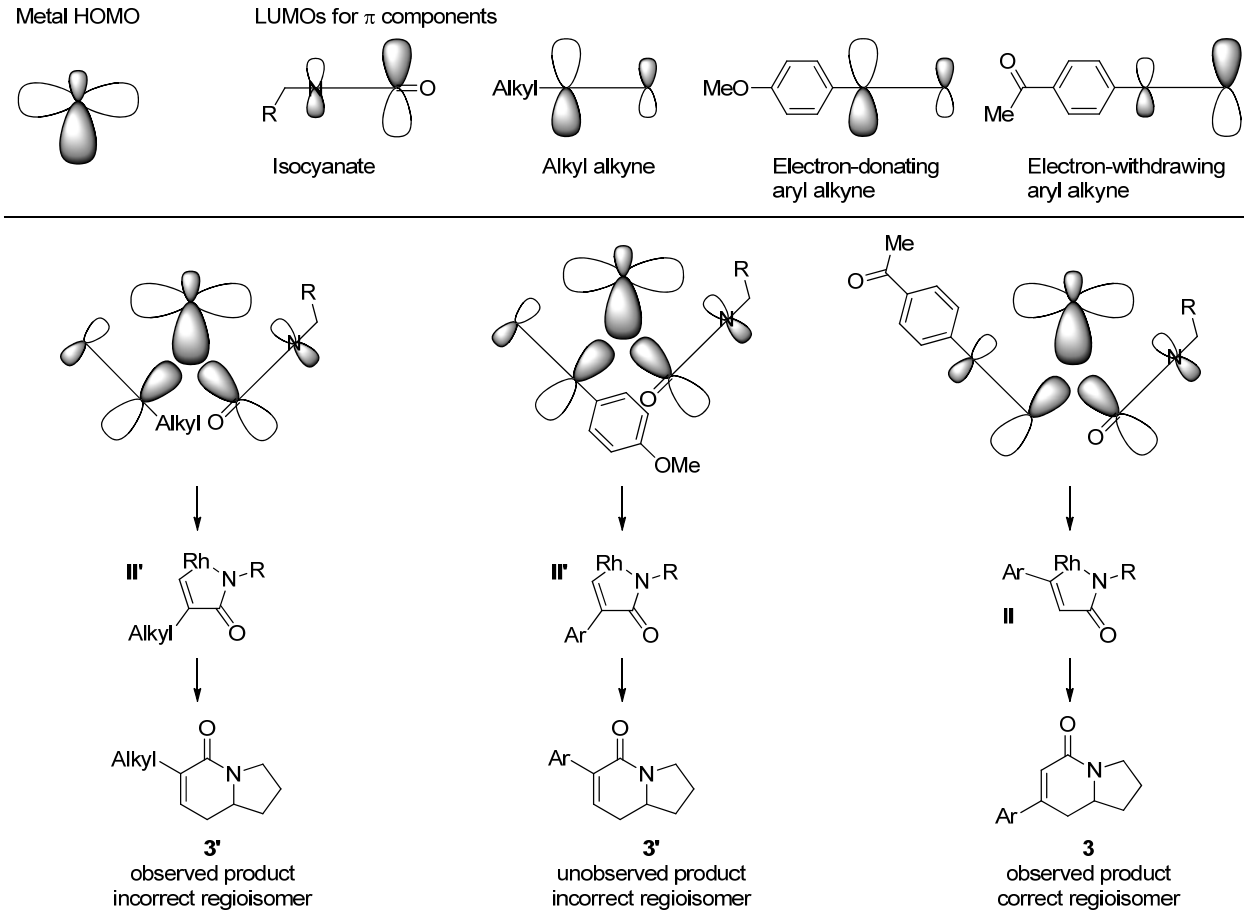

Figure 2.5.2. Strict application of Stockis-Hoffmann model to [2+2+2] cycloaddition of alkenyl isocyanates and alkynes does not always predict observed product.

As the electronic model of Stockis and Hoffmann does not always predict the correct product and regiochemistry, we reasoned that sterics needed to considered. Indeed, we have seen an influence of sterics on product selectivity (Table 2.1.1). We are certainly not the first to consider the effect of sterics

on cycloadditions; Wakatsuki and Yamazaki also noted that application of the Stockis-Hoffmann model to cobaltacyclopentadiene formation did not predict the observed product (Figure 2.5.3). Based on computations and comparisons to experimental results, they established a steric model to explain their observed product selectivity.[35] Based on their computations, they found that cobaltacyclopentadiene formation occurs from a coordination complex where the two π components are aligned orthogonal to the cobalt square plane. From the more stable coordination complex **XIII**, where the small and large substituents of the π components are opposite to one another, cyclization leads to the major isomer **10** they observe. This cyclization goes through a transition state, **TSIII**, where the steric interaction of the alkynes is minimized. If coordination of the π components occurs with the two small substituents on the same side, higher energy coordination complex **XIII'** is generated. Cyclization can proceed with the smaller substituents folding away from the metal (**TSIV**) or towards the metal (**TSV**). Of these two transition states, they calculated that **TSIV** is the lower in energy because there is less alkyne-alkyne steric interaction than in **TSV**. This model based on the sterics of the π components during coordination and cyclization successfully explains their experimental results.

[35] Wakatsuki, Y.; Nomura, I.; Kitaura, K.; Morokuma, K.; Yamazaki, H. *J. Am. Chem. Soc.* **1983**, *105*, 1907-1912.

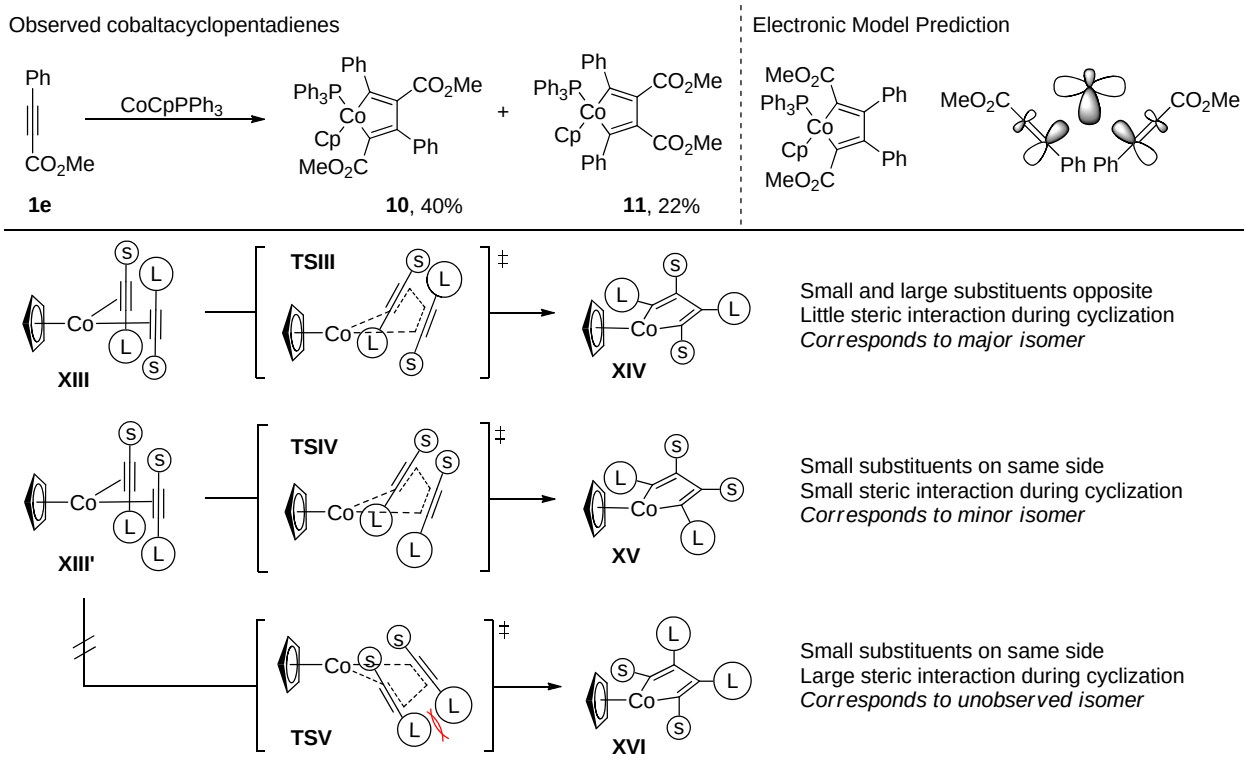

Figure 2.5.3. Wakatsuki and Yamazaki steric model for selectivity. Steric interactions during coordination (**XIII** vs **XIII'**) and cyclization (**TSIV** vs **TSV**) predicts major and minor isomers.

When Wakatsuki and Yamazaki's steric model for selectivity is applied to the cyclization of alkenyl isocyanates and alkynes, we see that it does not predict the observed products. In our case, we can envision two rhodium coordination complexes. Coordination complex **I'**, where the large groups of the π components are opposite one another, corresponds to cobalt complex **XIII**. From complex **I'**, conrotatory cyclization can occur in two ways. Rotation of the isocyanate oxygen and large alkyne substituent away from the metal produces metallacycle **II'** that generates lactam **3'**. Cyclization in the other direction leads to metallacycle **VI'** that generates vinylogous amide **4'**. Coordination complex **I**, where the two larger substituents are on the same side, corresponds to cobalt complex **XIII'**. Cyclization of the two smaller substiuents away from the metal produces metallacyle **II** corresponding to lactam **3**. Alternatively, cyclization the other direction leads to metallacyle **VI** that produces vinylogous amide **4**. According to Wakatsuki and Yamazaki's model, we should see three products; lactam **3'**, vinylogous amide **4'**, and

lactam **3**. The major products are predicted to be lactam **3'** and vinylogous amide **4'**, as these are from the presumably more stable coordination complex **I'**. The minor product is predicted to be lactam **3** that is derived from minor coordination complex **I**. Vinylogous amide **4** should not be observed due to steric interactions between the alkyne and isocyanate during cyclization (Figure 2.5.3, **TSV**). As the observed products are lactam **3** and vinylgous amide **4**, we see that a strict application of the Wakatsuki-Yamazaki steric model does not explain our results.

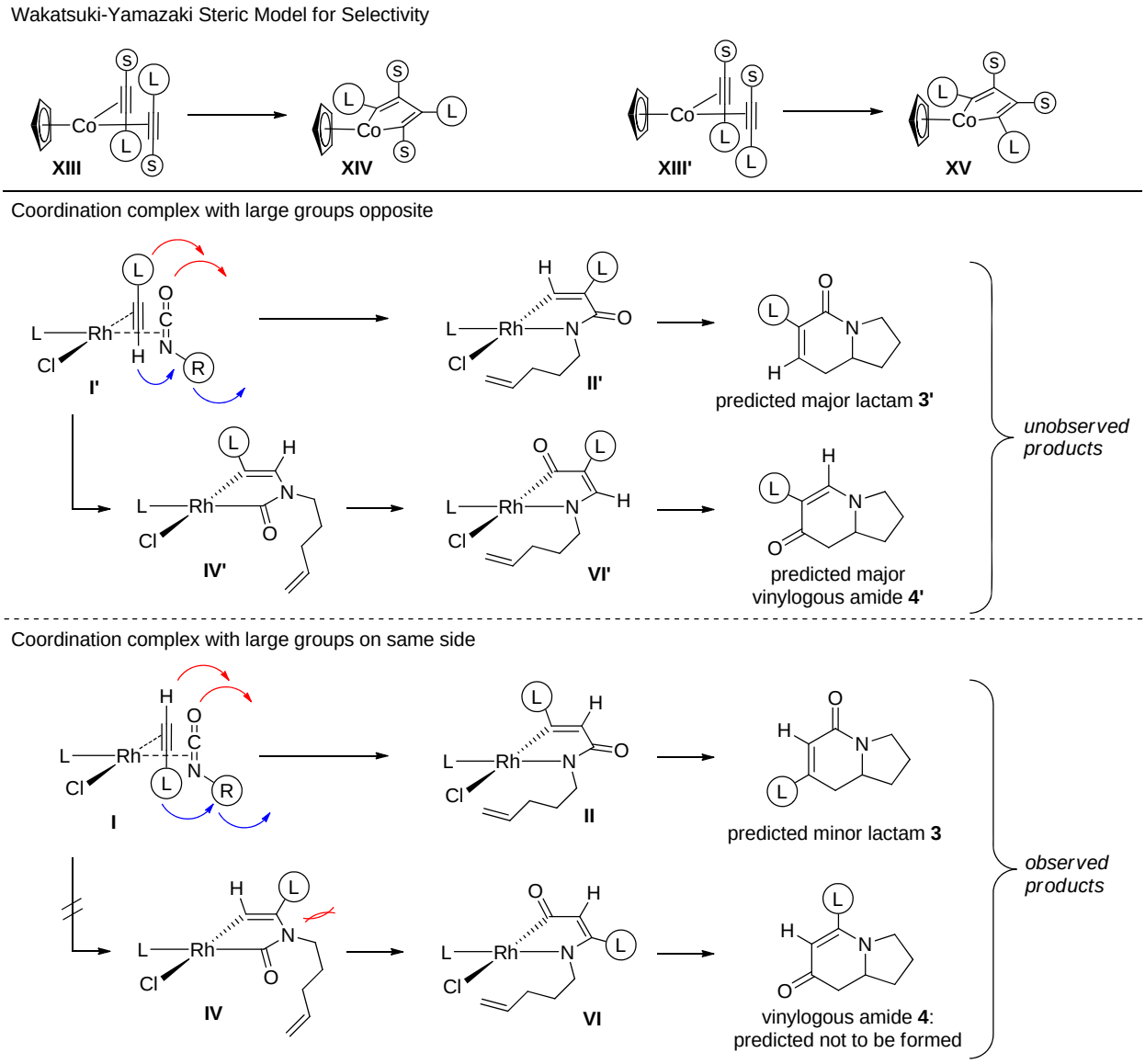

Figure 2.5.4. Strict application of Wakatsuki-Yamazaki does not correctly predict product selectivity for [2+2+2] cylcloadditions of alkenyl isocyanates and alkynes.

By looking at electronic and steric models in isolation to predict product selectivity, we find that neither explains product selectivity alone. However, a combination of both models that accounts for both electronics and sterics does a remarkably good job at predicting product selectivity and explaining many of the trends observed in the [2+2+2] cycloaddition of alkenyl isocyanates and alkynes (Figure 2.5.5) In this revised model, we believe the alkyne and isocyanate bind to generate coordination complex **I** based

on our rhodium·phosphoramidite crystal structures (Figure 2.4.1). Cyclization of the two smaller substituents away from the metal generates rhodacycle **II** via **TSI**, whereas cyclization of the smaller substituents towards rhodium generates rhodacycle **IV** via **TSII**. Based on the previous models, we can lay out the factors that stabilize or destabilize each transition state.

For lactam **3** formation, initial cyclization goes through **TSI**. The isocyanate LUMO always selects for **TSI**, because the largest LUMO coefficient of the isocyanate is β to the metal. Without opposition, this constant electronic preference by the isocyanate would dictate product selectivity and only lactam **3** would be generated. This basal electronic selectivity is reinforced by alkynes that have electron-withdrawing groups, such as electron-deficient aryl alkynes, because the largest LUMO coefficient of the alkyne is also β to the metal. Due to the large size of phosphoramidite ligands, we propose there is steric interaction between the alkyne and ligand during oxidative cyclization that destabilizes **TSI**.

Cyclization through **TSII** leads to vinylogous amide **4** formation. This transition state is stabilized by alkynes that have electron-donating groups, such as electron-rich aryl alkynes, because the largest LUMO coefficient of the alkyne is β to the metal. This transition state also relieves the ligand/alkyne steric interactions that destabilize **TSI**. These stabilizing effects override the inherent selectivity imposed by the isocyanate LUMO, and, as shown by Stockis and Hoffmann (Figure 2.5.1), the π components can work independently of one another.

Proposed transition states

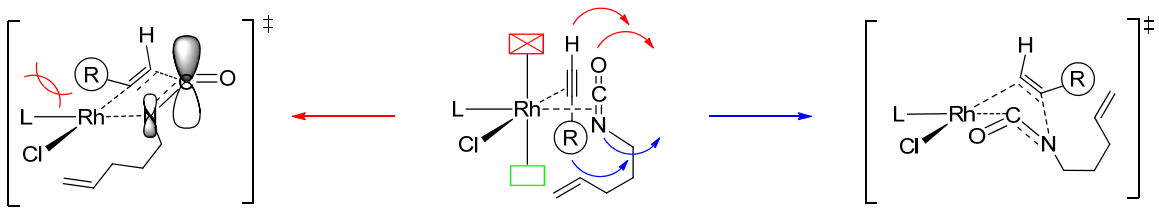

TSI - lactam formation

Factors stablizing **TSI**
-isocyanate LUMO
-alkyne LUMO with EWG
Factors disfavoring **TSI**
-ligand/alkyne steric interactions
-alkyne LUMO with EDG

I

Coordination complex **I**
-top face blocked (Fig 2.4.1)

TSII - vinylogous amide formation

Factors favoring **TSII**
-alkyne LUMO with EDG
-less ligand/alkyne steric interaction
Factors disfavoring **TSII**
-isocyanate LUMO
-alkyne LUMO with EWG

Ligand trends and application of model

Variable	Observed Effect	Speculative Cause
Longer Rh-P bond length	More lactam formation	Less ligand/alkyne interaction favoring **TSI**
Shorter Rh-P bond length	More vinylogous amide formation	More ligand/alkyne interaction destabilizing **TSI**; **TSII** relieves this interaction

Alkyne trends and application of model

Variable	Observed Effect	Speculative Cause
Smaller alkyne	More lactam formation	Less ligand/alkyne interaction favoring **TSI**
Larger alkyne	More vinylogous amide formation	More ligand/alkyne interaction destabilizing **TSI**
EWG on alkyne	More lactam formation	Alkyne LUMO stabilizes **TSI**
EDG on alkyne	More vinylogous amide formation	Alkyne LUMO stabilizes **TSII**

Figure 2.5.5. Transition states for lactam and vinylogous amide products and the factors favoring and destabilizing each. Isocyanate LUMO always selects for **TSI** that generates lactam. Ligand/alkyne steric interactions disfavor **TSI** and therefore select for **TSII** that generates vinylogous amide. Alkyne electronics can favor either transition state and modulate selectivity.

This combined steric and electronic model lays out the factors that control product selectivity and takes into account the observed trends in the cycloaddition of alkenyl isocyanates and terminal alkynes. We have seen that longer Rh-P bond lengths lead to more lactam **3**, whereas shorter Rh-P bond lengths generate more vinylogous amide **4** (Figure 2.3.2). We believe that longer Rh-P bond lengths reduce the steric interaction between the alkyne and ligand in **TSI**. This makes the reaction more lactam selective. Alternatively, shorter Rh-P bond lengths exacerbate the steric interaction between the alkyne and ligand to the point where the electronic selectivity of the isocyanate is overridden, and the reaction goes through **TSII** leading to vinylogous amide. This same steric effect is seen when the size of the alkyne is changed

(Figure 2.1.1); smaller alkynes are more lactam selective and larger alkynes are more vinylogous amide selective. We have also seen a dependable negative Hammett correlation with alkyne electronics when the size of the alkyne remains fairly constant (Figure 2.1.3). Electron-deficient aryl alkynes electronically stabilize **TSI**, electron-rich aryl alkynes electronically stabilize **TSII**, and the other alkynes fall in between these two extremes. This steric and electronic model does a good job of explaining these trends.

This steric/electronic model also takes into account the electronics of the metal (Figure 2.5.6). If the rhodium HOMO is raised, there is better overlap between the rhodium HOMO and the isocyanate LUMO. This stabilizes **TSI** leading to lactam **3**. The rhodium HOMO is raised by electron-rich phosphoramidite ligands and more donating counterions. The opposite effect is seen if the rhodium HOMO is lowered. There is less overlap between the rhodium HOMO and the isocyanate LUMO; this decreases the isocyanate's electronic stabilization of **TSI**. This decrease in electronic stabilization of **TSI** makes steric interactions more important, and the reaction is more vinylogous amide **4** selective. It is difficult to decouple the steric and electronic effects of the phosphoramidite ligand, as more electron-deficient ligands lower the rhodium HOMO *and* shorten the Rh-P bond length. Some experiments by Dr. Catherine Smyth, where she looked at the effects of counterions, shed some light onto the metal electronics.[36] We see that iodide and bromide lead to more lactam formation (entries 1, 2), whereas the more electron-withdrawing cyanide leads to more vinylogous amide formation (entry 5).[37] Although we cannot exclude sterics completely, we see that changing the metal electronics changes product selectivity, and this is accounted for by this combined steric/electronic model.

[36] Dr. Catherine Smyth. Colorado State University, Fort Collins, CO. Unpublished work, 2009.
[37] For review on halide influence on metal catalysis, see: (a) Fagnou, K.; Lautens, M. *Angew. Chem. Int. Ed.* **2002**, *41*, 26-47. For the spectroscopic series, see (b) Tsuchida, R. *Bull. Chem. Soc. Jpn.* **1938**, *13*, 388-400. (c) Miessler, G. L.; Tarr, D. A. Inorganic Chemistry, 3rd ed. Pearson Education, Inc. Upper Saddle River, New Jersey, 2004.

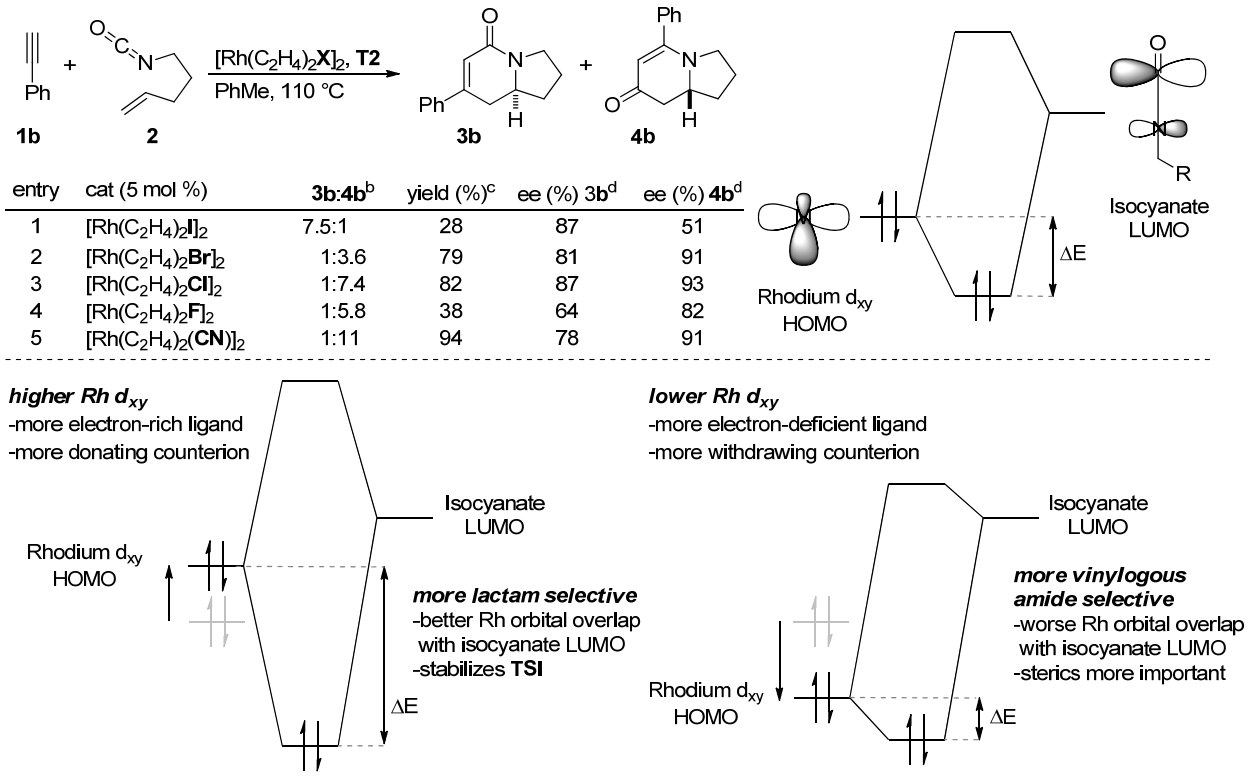

Figure 2.5.6. Influence of metal electronics on product selectivity.

This steric/electronic model has led to the rational design of a new ligand (**T10**) that supports the conclusions of this model (Eq 3).[38] Due to its electron-deficient nature, **T10** displays a short Rh-P bond length and is very selective for vinylogous amide.

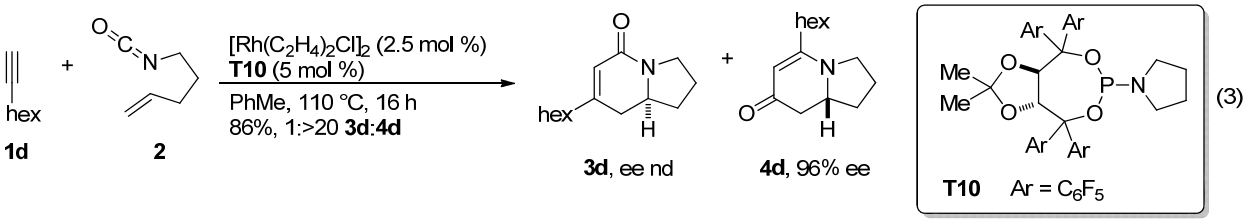

This model provides an excellent framework to rationalize regio- and product selectivity for rhodium-catalyzed [2+2+2] cyclizations of alkenyl isocyanates and *terminal alkynes*. When this model is

[38] (a) Dalton, D. M.; Rappé, A. K.; Rovis, T. *Chem. Sci*. **2013**, *4*, 2062-2070. (b) Dalton, D. M.; Rovis, T. *Org. Lett.* **2013**, *15*, 2346-2349.

applied to similar systems (pyridone formation, internal alkynes, and alkenyl carbodiimides), the results are more ambiguous.

For pyridone formation, we propose the mechanism shown below (Figure 2.5.7). The facets of the mechanism that we hope to address through application of this model is product regioselectiviy (4,6-substituted 2-pyridones **5** and 2,6-substituted 4-pyridones **6**), influence of alkyne electronics on yield, and isocyanate electronic influence on yield. We propose that both 2-pyridone **5** and 4-pyridone **6** are generated from rhodacycle **IV** rather than rhodacycle **II** (Chapter 1.6). Product regioselectivity can be explained by coordination complex **I** and irreversible, conrotatary cyclization. From rhodacycle **IV**, insertion of an alkyne[39] and reductive elimination generates 4,6-substituted 2-pyridone **5**. Rhodacycle **VI** is generated from a CO migration from rhodacycle **IV**; insertion of an alkyne and reductive elimination furnishes 2,6-substituted 4-pyridone **6**. This regioselectivity is the same as lactam **3** and vinylogous amide **4**. Unsurprisingly, the nature of the alkyne influences yield. If products are generated from rhodacycle **IV**, then alkynes that favor **TSII** (large alkynes and electron-rich aryl alkynes) should generate more product. Indeed, we have seen that yields are higher with these alkynes (Table 1.5.1) and yield tracks well with vinylogous amide selectivity (Figure 1.6.1). Based on this model, we predict that more electron-deficient isocyanates should favor **TSI** due to better overlap between the isocyanate LUMO and rhodium HOMO. This should give lower yields as **TSI** leads to rhodacycle **II**, and alkynes that favor lactam are not high yielding for pyridones. Contradictory to this prediction, we observe that electron-deficient aryl isocyanates are just as high yielding as electron-rich aryl isocyanates (Table 1.5.3). In fact, they are more selective for 4-pyridone **6** that is generated from rhodacycle **VI** (itself derived from rhodacycle **IV**). Although product yields based on isocyanate electronics are not fully explained by this steric/electronic model, regioselectivity and yields based on alkyne electronics are what we predict.

[39] The second alkyne insertion is difficult to rationalize. First, π component insertions into metal-nitrogen bonds is not well studied, therefore it is difficult to predict where the alkyne inserts in rhodacycle **II** or **VI**. The factors determining the regiochemistry depend on where the alkyne inserts. For example, insertion into the Rh-N bond of **VI** can be rationalized with steric arguments, while insertion into the Rh-C(O) bond of **VI** can be rationalized with electronic arguments.

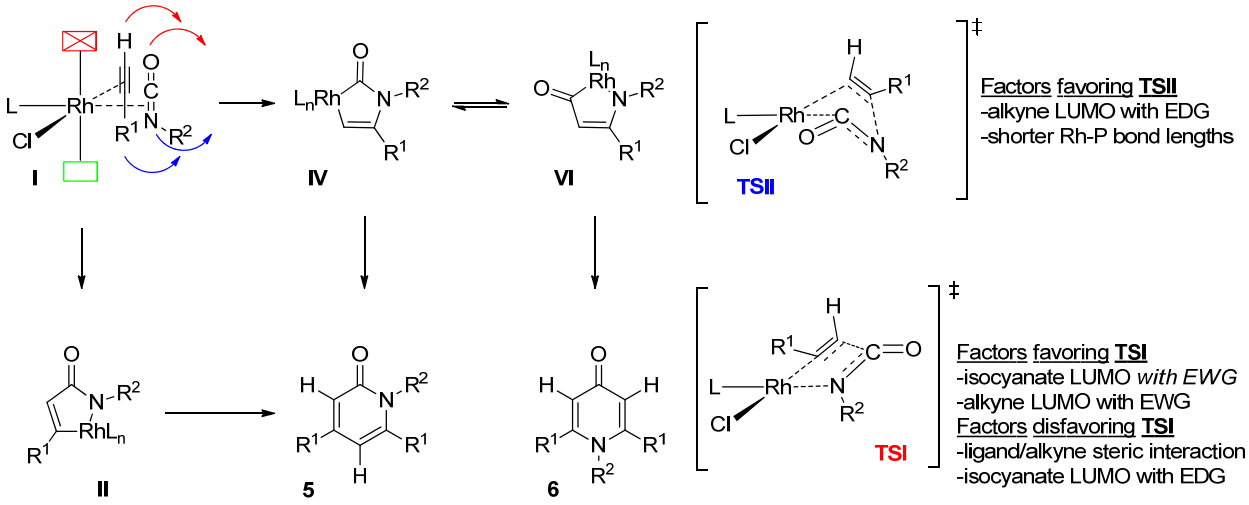

Figure 2.5.7. Coordination complex **I** explains product regioselectivity. Alkyne electronic factors favoring **TSII** give higher yields as expected, but isocyanate electronic factors favoring **TSI** give unexpectedly high yields.

Application of this steric/electronic model to internal alkynes is not perfect (Figures 2.5.8 and 2.5.9). With symmetrical alkynes, we predict that metallacycle formation should be dictated by the electronics of the isocyanate alone, as the electronics and sterics of the alkyne are equal (Figure 2.5.8). The isocyanate LUMO should always select for lactam **3** via **TSI**. We see internal alkyl alkynes are lactam **3** selective, but vinylogous amide **4** selectivity is seen for internal aryl alkynes.[40] This is puzzling.

[40] (a) Yu, R. T.; Rovis, T. *J. Am. Chem. Soc.* **2006**, *128*, 2782-2783. (b) Oinen, M. E.; Yu, R. T.; Rovis, T. *Org. Lett.* **2009**, *11*, 4939-4937.

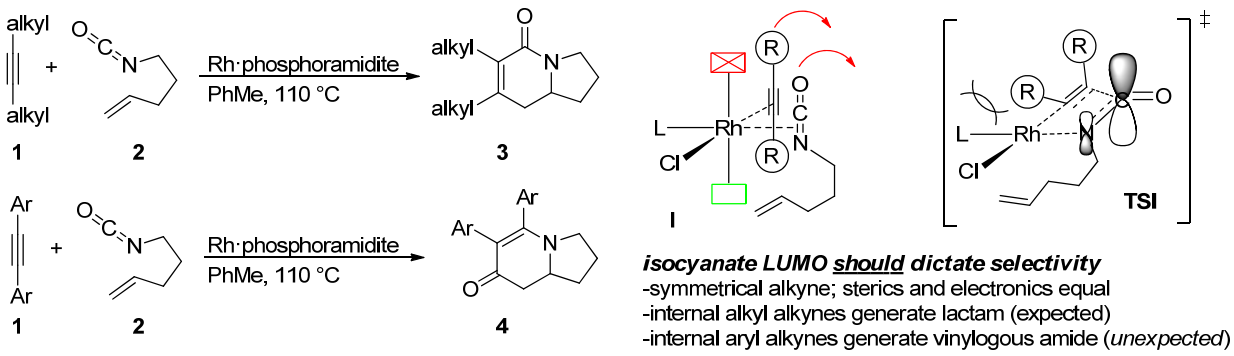

Figure 2.5.8. Symmetrical alkynes have no steric or electronic bias so isocyanate should dictate product selectivity. Internal alkyl alkynes produce lactam **3** as expected, but internal aryl alkynes produce vinylogous amide **4**.

Internal, unsymmetrical alkynes participate in the [2+2+2] cycloaddition in a regioselective fashion.[41] The predicted rhodacycle from this model matches the probable rhodacycle in most cases, but some substrates give a different regioisomer than predicted (Figure 2.5.9). For methyl phenyl propionate **1e**, we predict rhodacycle **IVe** will be formed. This is because the smaller substitutents, isocyanate carbonyl and alkyne ester, are *syn* as predicted from coordination complex **I** and rhodacycle **IVe** is stabilized by the largest alkyne LUMO coefficient β to the metal. This rhodacycle corresponds to vinylogous amide **4e** as the product and this is the observed product when this substrate is used. For 2-methoxyethynylbenzene **1f**, the predicted regioisomer **4f** does not match the observed regioisomer **4f'**. We predict rhodacycle **IVf** will formed as the alkyne ethoxy group and isocyanate should be *syn* in coordination complex **I** based on size.[42] This produces vinylogous amide **4f** with the smaller ethoxy substitution α to the carbonyl group. When alkyne **1f** is subjected to the reaction, the observed product is vinylogous amide **4f'**, where the smaller ethoxy substituent is β to the carbonyl. Although not predicted, rhodacycle **IVf'** is stabilized by the electron-donating group β to the metal. This demonstrates that this

[41] Friedman, R. K.; Rovis, T. *J. Am. Chem. Soc.* **2009**, *131*, 10775-10782.
[42] For A values, see: (a) Anslyn, E. V.; Dougherty, D. A. Modern Physical Organic Chemistry. University Science Books, Sausalito, California, 2006. For cone values (°), see: (b) Tolman, C. A. *Chem. Rev.* **1977**, *77*, 313-348. (c) Wakatsuki, Y.; Nomura, I.; Kitaura, K.; Morokuma, K.; Yamazaki, H. *J. Am. Chem. Soc.* **1983**, *105*, 1907-1912.

steric/electronic model does not always predict the correct product. In this case electronic factors, as described by Stockis and Hoffmann, might be more important.

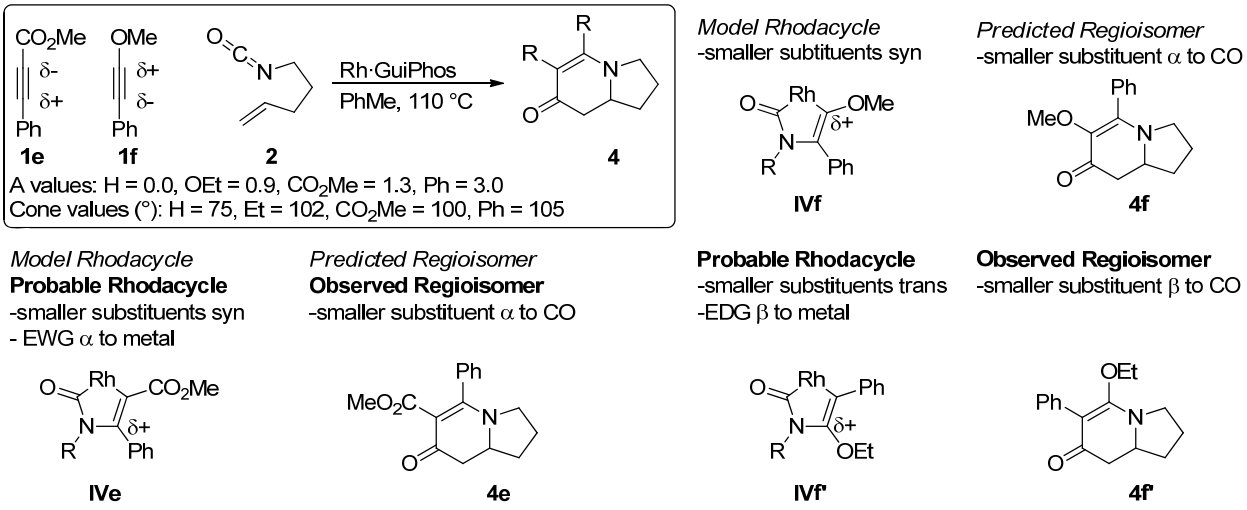

Figure 2.5.9. A combined steric/electronic model predicts the correct product for some internal, unsymmetrical alkynes, but not all.

In an extension of this work, Dr. Yu reported the rhodium-catalyzed [2+2+2] cycloaddition of alkenyl carbodiimides **12** and terminal alkynes (Figure 2.5.10).[43] In this work, alkenyl carbodiimides are selective for lactam type products, bicyclic amidines **13**. Since the same rhodium·phosphoramidite catalyst system is employed, we should be able to apply our model for regio- and product selectivity. If we assume that the N-aryl substituent is larger than the N-alkyl substitutent, we expect coordination complex **I'** to predominate over complex **I**. Contrary to our expectation, exclusive formation of bicyclic products, **13b** and **14b**, is observed, corresponding to products derived from coordination complex **I**. This correlates to the same regiochemistry observed in the cycloaddition of alkyenyl isocyanates and alkynes (**3b** and **4b**). If we presume that the carbodiimide binds in the same fashion as the isocyanate and generates complex **I**, a new steric interaction between the N-aryl imine and ligand is introduced. This interaction will destabilize **TSII**, thus **TSI** will be favored and bicyclic amidines **13** will be generated in

[43] Yu, R. T.; Rovis, T. *J. Am. Chem. Soc.* **2008**, *130*, 3262-3263.

higher yields. As this steric component has such a large effect on product selectivity, it is surprising that only a single regioisomer of product is formed in the reaction.

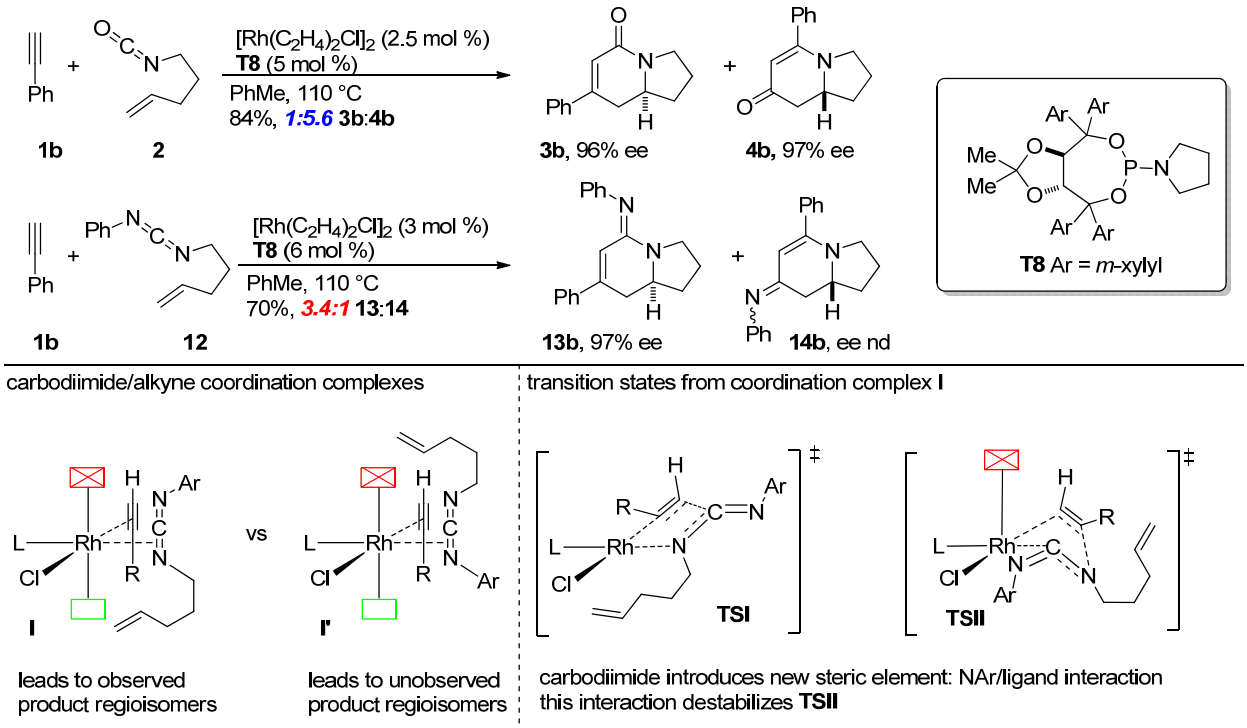

Figure 2.5.10. Use of alkenyl carbodiimides **12** is selective for lactam-like bicyclic amidines **13**. Assuming that N-aryl is larger than N-alkyl, mixtures of regioisomeric products should be observed. Alkenyl carbodiimides introduce new N-aryl/ligand interaction that destabilizes **TSII** leading to more amidine **13**.

Application of this steric/electronic model to pyridone synthesis, internal alkynes, and alkenyl carbodiimides demonstrates that this model does not explain similar reactions using the rhodium·phosphoramidite catalyst with perfect accuracy. Despite these deficiencies, a logical framework to explain product selectivity and regioselectivity has been developed for alkenyl isocyanates and terminal alkynes. This has led to the development of a new ligand, **T10**, that is very selective for vinylogous amide **4**. It must also be kept in mind that small changes in substrate can cause a change in mechanism, and different mechanisms in these other cases have not been ruled out.

2.6 Model for Enantioselectivity

We attempted to explain the enantioselectivity of the reaction using the rhodium(cod)Cl·phosphoramidite crystal structures and the steric/electronic model (Figure 2.6.1). We believe our explanation of lactam **3** stereoinduction is reasonable, but a satisfying explanation for vinylogous amide **4** stereoinduction is still elusive. To predict the correct enantiomer, we must keep three things in mind: for migratory insertion, the alkene must be *syn*-coplanar to the Rh-N bond, one face of the rhodium is hindered by the ligand, and facial selectivity of the alkene is imposed by the tether.

In rhodacycle **II** leading to lactam **3**, alkene coordination in complexes **IIa** and **IIb** are disfavored because the phosphoramidite ligand blocks this face. Complex **IIa** is further disfavored because the alkenyl isocyanate must adopt a high energy twist-boat conformation to coordinate. If coordination to this face is possible, it will be complex **IIb**, in which the alkenyl isocyanate adopts a chair conformation. Complex **IIb** leads to the minor lactam enantiomer. Based on the facial selectivity imparted by the ligand, alkene coordination to rhodium will be favored on the unhindered side and this generates complexes **IIc** and **IId**. Complex **IIc** is disfavored due to the twist chair conformation that needs to be adopted for alkene coordination. The major coordination complex predicted is complex **IId**, as it is in a chair conformation, and this complex leads to the major enantiomer of lactam.

Unlike lactam **3** enantioinduction, a model for vinylogous amide **4** enantioselectivity is much more speculative, as there are probably multiple rearrangements of unobservable Rh(III) intermediates. From rhodacycle **IV**, CO migration probably occurs by amide bond cleavage and amine migration to the open coordination site to generate complex **V**.[44] If the alkenyl carbon migrates to the CO without further rearrangement, complex **VIa** is generated. Migratory insertion of the alkene from this complex leads to the minor enantiomer. Alternatively, from complex **V**, CO migration *onto* the alkenyl carbon generates complex **VIb**. Migratory insertion of the alkene in this complex leads to the major enantiomer, but such a

[44] For selected CO migration references on rhodium(I) species, see: (a) Cavallo, L.; Sola, M. *J. Am. Chem. Soc.* **2001**, *123*, 12294-12302. (b) Gonsalvi, L.; Adams, H.; Sunley, G. J.; Ditzel, E.; Haynes, A. *J. Am. Chem. Soc.* **2002**, *124*, 13597-13612. (c) Gonsalvi, L. *Organometallics* **2003**, *22*, 1047-1054.

CO migration is unprecedented. Mark Oinen has demonstrated that additives can influence vinylogous amide enantioselectivity in the [2+2+2] cycloaddition of alkenyl isocyanates and symmetrical internal alkynes.[45] This suggests the rearrangement(s) from complex **IV** to complex **VI**, where the alkene can coordinate, is not straightforward. Due to the probability of multiple rearrangements, we cannot explain the correct vinylogous amide enantiomer. The difficulty of predicting the correct vinylogous amide enantiomer is further complicated by the fact that Taddol and Binol ligands provide the opposite major enantiomer for vinylogous amide, but both deliver the same major enantiomer for lactam.

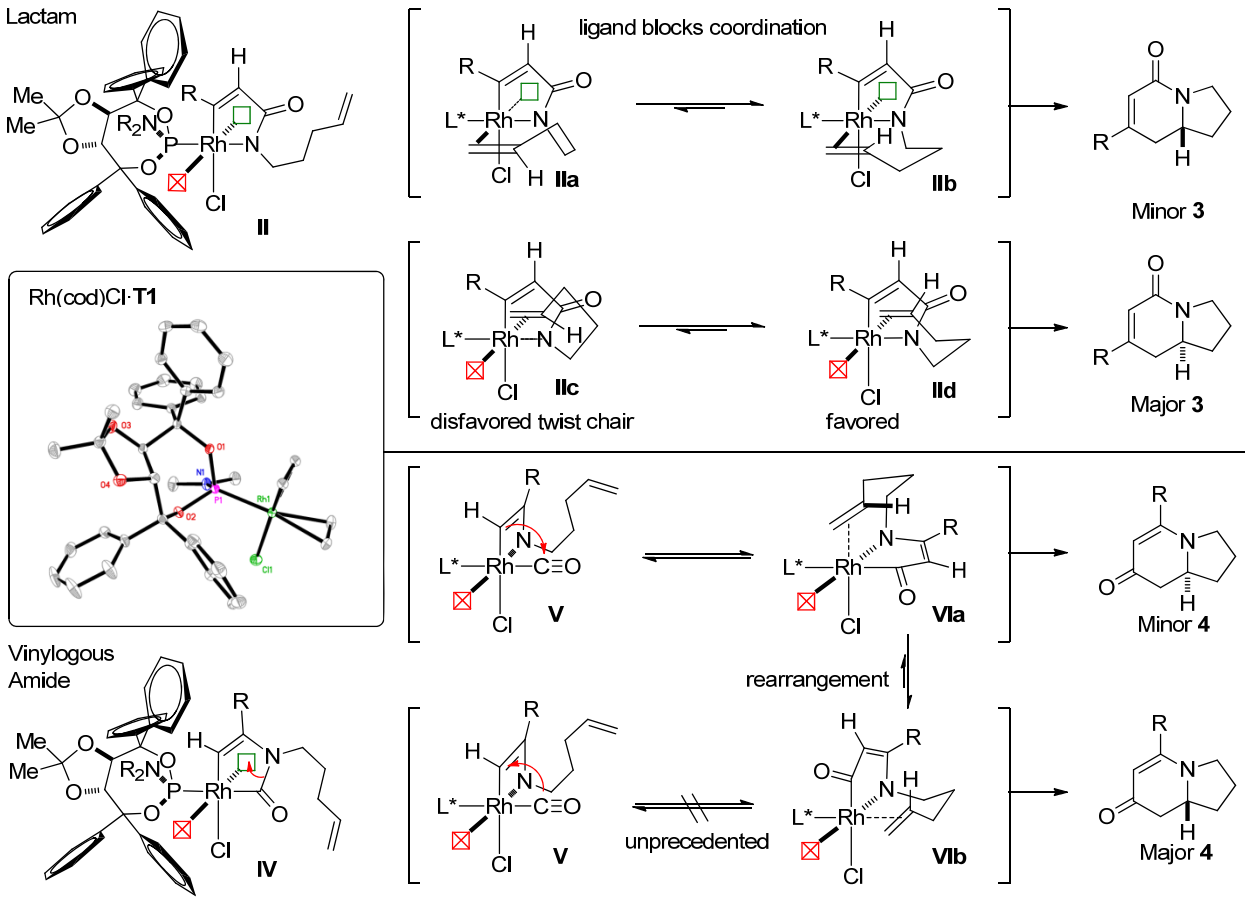

Figure 2.6.1. Major lactam **3** enantiomer derived from complex **IId**, where alkene coordinates to unhindered rhodium face in a chair conformation. Major vinylogous amide **4** enantiomer difficult to

[45] Oinen, M. E.; Yu, R. T.; Rovis, T. *Org. Lett.* **2009**, *11*, 4934-4937.

predict due to multiple rearrangements of rhodium (III) complexes and lack of precedent for CO migration *to* alkenyl carbon.

2.7 Reaction Scalability[46]

In addition to a model that explains the trends in our work on the cycloaddition of alkenyl isocyanates and alkynes, we sought to demonstrate the practicality of the reaction on larger scale. This was realized through the development of a facile, scalable synthesis of phosphoramidite **T2**, a large scale preparation of alkenyl isocyanate **2**, and a [2+2+2] cycloaddition delivering over 5 grams of indolizidinone **4g**.

We have found one of the difficulties in making phosphoramidite ligands is the final conversion of the diol to the phosphoramidite (Eq 4), because it will often be contaminated with oxidized phosphoramidite. Traditionally, we purified our ligands using column chromatography, but we wanted to eliminate this procedure as partially oxidized ligand is occasionally observed. In our efforts to make a scalable synthesis of phosphoramidite **T2**, we initially tried to purify the ligand using an acidic workup, but this leads to oxidized ligand.[47] This sensitivity to acid explains why purification using silica leads to partial oxidation. Our final procedure uses deionized water because the aqueous wash removes most of the phosphorous byproducts.[48] We sought to use recrystallization as our purification method and settled on ethyl acetate as the crystallization solvent (other solvents may be used, such as toluene). This leads to a facile preparation of pure ligand **T2** from diol **15** (Eq 4). Application of this procedure to other ligands generates mixed results. For example, ligands *rac*-**A1** and **T9** are reluctant to crystallize, but ligands **T1** and **T8** have been successfully synthesized using this procedure. One thing to note is that use of an impure diol (indicated by its appearance as a yellow goo or solid instead of a white solid) for ligand

[46] Oberg, K. M.; Martin, T. J.; Oinen, M. E.; Dalton, D. M.; Friedman, R. K.; Neely, J. M.; Rovis, T. *Org. Synth. Submitted.*
[47] ^{31}P NMR shows only product before a 1M HCl wash and then a 1:1 mixture of ligand:oxidized ligand after washing.
[48] ^{31}P NMR initially shows desired product with 5-7 minor peaks and only product after washing.

preparation makes this procedure less likely to succeed. If impure diol is used, column chromatography followed by crystallization is usually necessary.

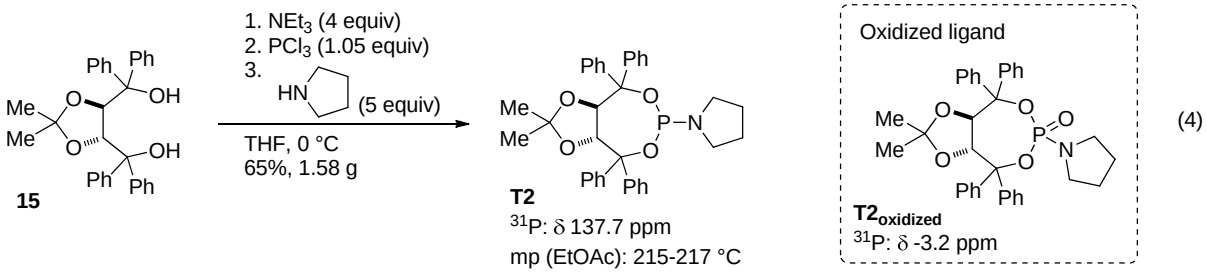

(4)

Preparation of alkenyl isocyanate **2** on large scale is a difficult endeavor. There are many ways to make isocyanates,[49] but our preferred method employs the Curtius rearrangement. We have traditionally synthesized alkenyl isocyanates in one of two ways: conversion of the acyl azide to the isocyanate under reduced pressure[50] and column chromatography of the acyl azide followed by neat conversion of the acyl azide to the isocyanate.[51] These methods work well for small scale, but on larger scale, these approaches can potentially be dangerous if proper precautions are not observed. Our original large scale approach is based on work by Dr. Ernest Lee. After generation of the acyl azide from the carboxylic acid using diphenylphosphoryl azide (DPPA), it can be purified via flash column chromatography and then gently converted to the product (Eq 5). Care must be taken during this procedure! The exothermic conversion from acyl azide to isocyanate happens with heat, releasing nitrogen gas and is therefore autocatalytic. If the acyl azide is purified using column chromatography, the column must be slurry packed and flushed with a lot of solvent to prevent warming of the column. If the column warms with solvent addition, premature conversion of large amounts of acyl azide to isocyanate can cause an explosion. When less than 1.5-2 grams of alkyl azide is isolated, the conversion can be done overnight neat (or overnight with gentle heating <35 °C). If larger amounts (up to 10 g) are isolated after chromatography, the acyl azide needs to be diluted with solvent before the conversion is attempted. We also developed another approach

[49] Ozaki, S. *Chem. Rev.* **1972**, *72*, 457-496.
[50] Yu, R. T.; Rovis, T. *J. Am. Chem. Soc.* **2006**, *128*, 2782-2783.
[51] Lee, E. E.; Rovis, T. *Org. Lett.* **2008**, *10*, 6, 1231-1234.

that avoids column chromatography and handling of the neat acyl azide altogether (Eq 6). We investigated a number of bases in order to make isolation of the alkenyl isocyanate easier. Use of inorganic bases leads to insoluble salts that do not completely convert to the acyl azide. Lighter amine bases distill over with the target isocyanate, so we chose 1,8-diazabicylcoundec-7-ene (DBU) because it is able to convert the acid to the acyl azide but it does not co-distill with the target isocyanate. The hexanes extraction removes most of the DPPA salts and dilutes the acyl azide so that conversion can be done in a controlled fashion at 50 °C. After conversion, a distillation delivers pure isocyanate without purification via flash column chromatography or handling of the neat acyl azide.

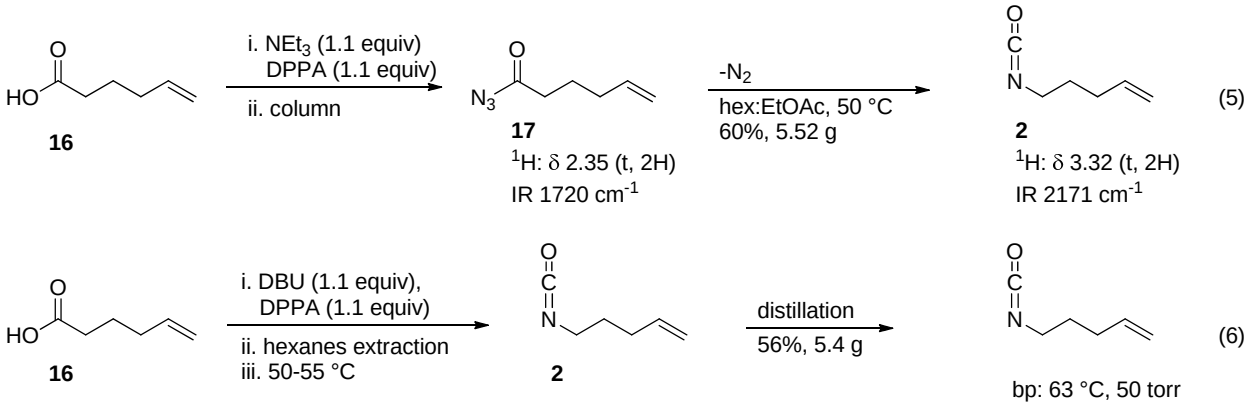

The scale up the [2+2+2] cycloaddition reaction is straightforward, but isolation is more difficult (Eq 7). The catalyst loading can be dropped from the typical 5-10 mol % catalyst loading to 1 mol % without affecting yield or enantioselectivity, but the reaction takes longer (36 h vs 12 h). We attempted to work up the reaction and perform a recrystallization of the product from the crude or worked up reaction. Despite numerous washes, such as NH_4Cl, NH_4OH, Na_2SO_3, or para-toluenesulfonic acid, we could not get a solid that would crystallize. Thus, we purify the reaction via flash column chromatography and isolate the vinylogous amide **4g** in good yield and enantioselectivity.[52] This light brown solid can be recrystallized from EtOAc to increase the enantiopurity and remove some of the color.

[52] On 2.4 mmol scale, lactam **3g** was isolated in trace yield (1:55 ratio of **3**:**4** based on mass). See Appendix 2 for details.

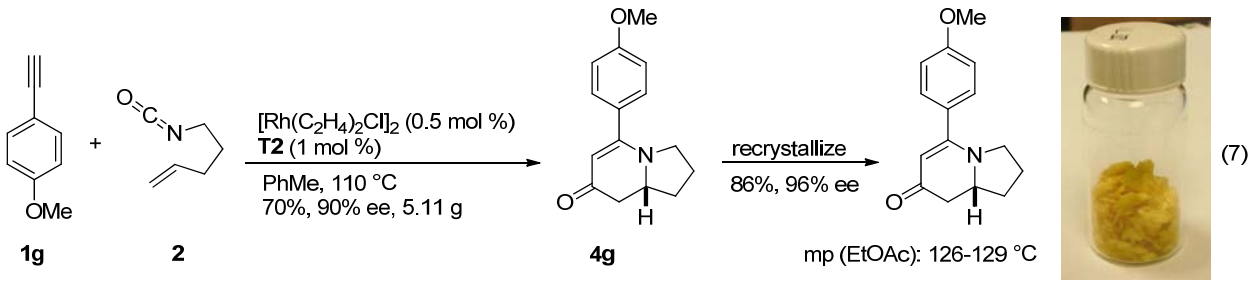

(7)

2.8 Conclusion

We have developed a steric/electronic model that explains regio- and product selectivity for the rhodium-catalyzed [2+2+2] cycloaddition of alkenyl isocyanates and terminal alkynes (Figure 2.8.1). This model is based on previous models developed by Stockis and Hoffmann (electronics) and Wakatsuki and Yamazaki (sterics). This model explains the observed regiochemistry and the product selectivity trends based on Rh-P bond lengths, alkyne sterics, and alkyne electronics. In summary, we believe that regioselectivity is imposed by the ligand that blocks one face of the rhodium center forcing the π components to bind with the smaller substituents facing towards the steric hinderance (coordination complex **I**). Conrotatory cyclization in one direction produces lactam **3**, and cyclization in the opposite direction produces vinylogous amide **4**. In both cases, the original binding in complex **I** leads to the exquisite regiocontrol. Cyclization to either rhodacycle **II** or **IV** depends on the steric and electronic factors that stabilize either **TSI** or **TSII**.

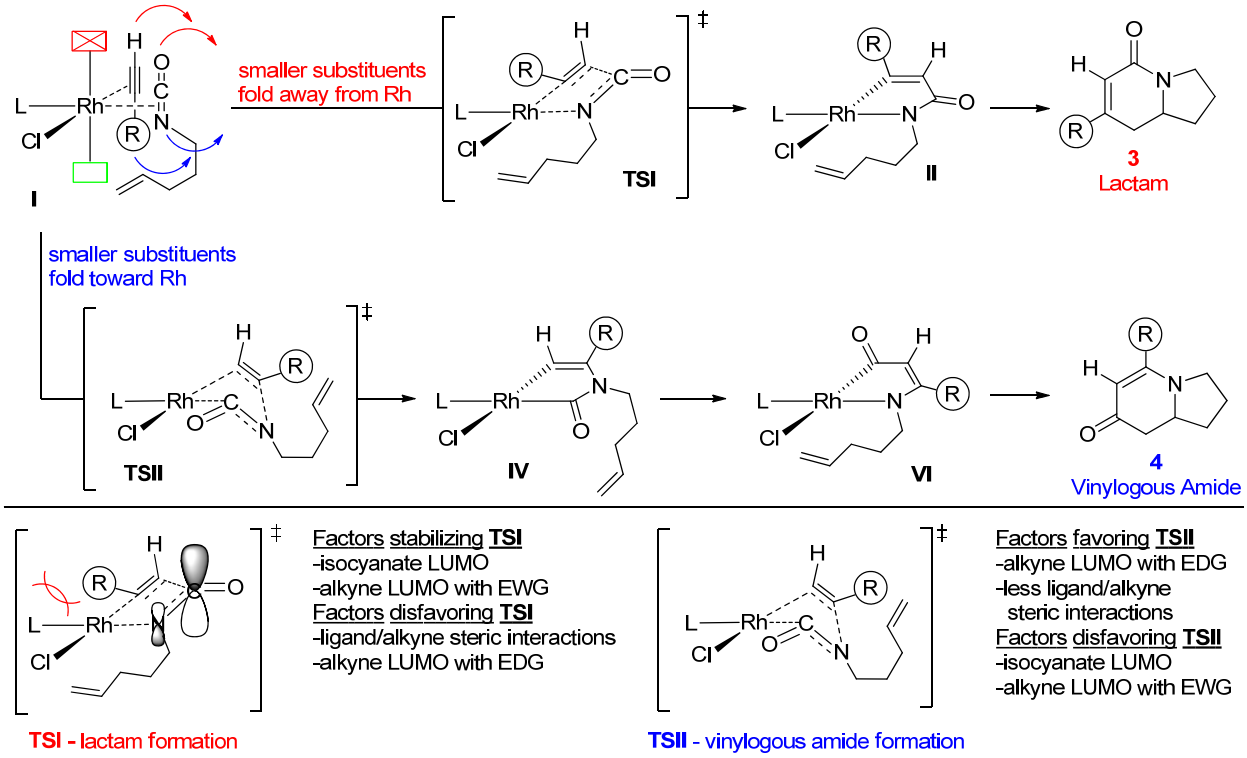

Figure 2.8.1. Model for regio- and product selectivity in the rhodium-catalyzed [2+2+2] cycloaddition of alkenyl isocyanates and alkynes. Coordination complex **I** dicatates regioselectivity of lactam **3** and vinylogous amide **4** products. Electronic and steric factors determine with transition state is more stable and therefore product selectivity.

Additionally, we have developed a scalable synthesis of phosphoramidite **T2** that avoids column chromatography, developed a synthesis of alkenyl isocyanate **2** that avoids column chromatography or neat handling of the intermediate acyl azide, and demonstrated the scalability of the [2+2+2] cycloaddition by synthesizing over 5 grams of indolizidinone **4g** with 1 mol % catalyst loading.

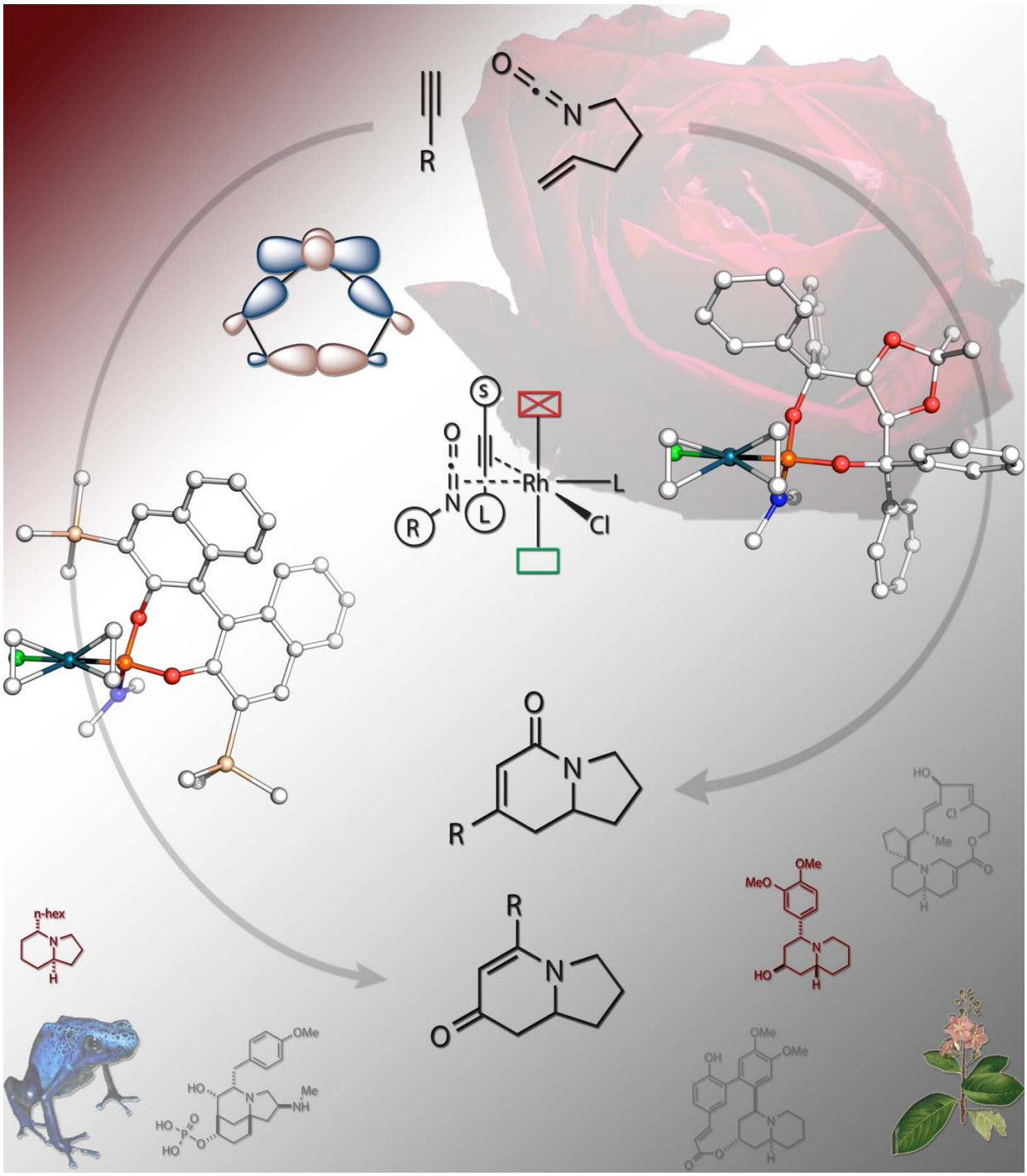
O
N
R
S
O
N
R
L
Rh
L
Cl
O
N
R
R
N
O
n-hex
N
H
OMe
MeO
HO
N
H
HO
Cl
Me
O
H
OMe
HO
HO
P
O
HO
N
Me
NH
OMe
OH
OMe
N
O
O
H

CHAPTER 3

Enantioselective Rhodium-Catalyzed [4+2] Cycloaddition of α,β-Unsaturated Imines and Isocyanates[1]

3.1 Introduction

The Rovis group has a long standing interest in the construction of nitrogen heterocycles, and we sought to expand our repertoire of reactions. We were inspired by Hoberg's report, where he demonstrated that an imine **1** and isocyanate **2** form a metallacyle (**I**) in the presence of nickel cyclooctadiene and tetramethyl ethylene diamine (TMEDA) (Eq 1).[2] We envisioned that replacing the imine with an α,β-unsaturated imine **3** would result in a formal [4+2] cycloaddition, via **I**, to make dihydropyrimidinones **4** (Eq 2).

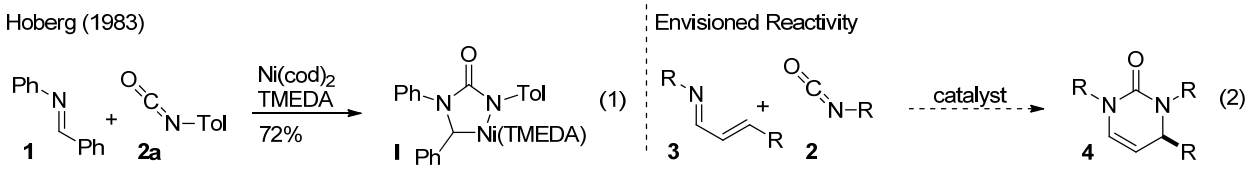

Interest in pyrimidinones[3] stems from their biological activity and modular synthesis via the Biginelli reaction (Figure 3.1.1). Pyrimidinones have structure homology with dihydropyridines, which are calcium channel modulators.[4] In addition to possessing biological activity similar to dihydropyridines (typically antihypertensive), pyrimidinones have been shown to be anticancer agents, antiviral agents, and

[1] Reprinted with permission from *Journal of the American Chemical Society*, Vol *133*, Kevin M. Oberg, Tomislav Rovis, "Enantioselective Rhodium-Catalyzed [4 + 2] Cycloaddition of α,β-Unsaturated Imines and Isocyanates", 4785-4787. Copyright (**2011**) American Chemical Society.

[2] Hoberg, H.; Sümmermann, K. *J. Organomet. Chem.* **1983**, *253*, 383-389.

[3] 3,4-Dihydropyrimidin-2-one is the proper nomenclature based on the Extended Hantzsch-Widman system, but pyrimidinone will be used in its place.

[4] Dihydropyridines are typically synthesized using the Hantzsch dihydropyridine synthesis: (a) Hantzsch, A. *Liebigs Ann. Chem.* **1882**, *215*, 1-82. (b) Stout, D. M.; Meyers, A. I. *Chem. Rev.* **1982**, *82*, 223-243.

a benign prostatic hyperplasic treatment.[5] Pyrimidinones are typically accessed via the Biginelli reaction.[6] As three components (urea **8**, β-ketoester **9**, and aldehyde **10**) are brought together in a single step, this reaction belongs to a class of reactions called multicomponent reactions (MCR).[7] The Biginelli reaction has been made higher yielding using the Atwal modification[8] and rendered enantioselective using chiral acids such as phosphoric acid **11** and hexadentate ligated ytterbium **12**.[9] The use of β-ketoesters **9** as starting material generates pyrimidinones with electron-withdrawing groups at the 5-position, but there are reports of using non-classical starting materials, such as cyclic ketones.[10]

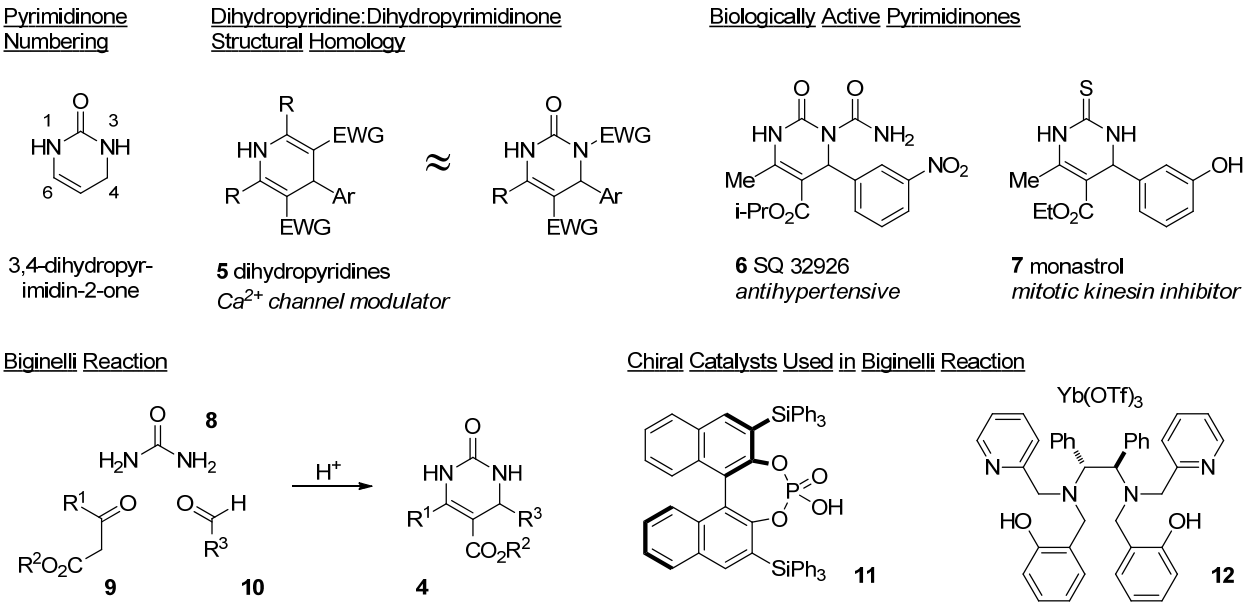

Figure 3.1.1. Pyrimidinone structure, biological activities, and classical synthesis.

An alternative to the Biginelli reaction would be a [4+2] cycloaddition of an α,β-unsaturated imine and an isocyanate. Elliot showed that a thermal reaction of alkenyloxazolines **13** and isocyanates **2**

[5] (a) Kappe, C. O. *Eur. J. Med. Chem.* **2000**, *35*, 1043-1052. (b) Singh, K.; Arora, D.; Singh, K.; Singh, S. *Mini-Rev. Med. Chem.* **2009**, *9*, 95-106.
[6] Biginelli, P. *Gazz. Chim. Ital.* **1893**, *23*, 360-413.
[7] (a) Kappe, C. O. *J. Org. Chem.* **1997**, *62*, 7201-7204. (b) Kappe, C. O. *Acc. Chem. Res.* **2000**, *33*, 879-888.
[8] O'Reilly, B. C.; Atwal, K. S. *Heterocycles* **1987**, *26*, 1185-1188.
[9] (a) Huang, Y.; Yang, F.; Zhu, C. *J. Am. Chem. Soc.* **2005**, *127*, 16386-16387. (b) Li, N.; Chen, X.-H.; Song, J.; Luo, S.-W.; Fan, W.; Gong, L.-Z. *J. Am. Chem. Soc.* **2009**, *131*, 15301-15310. (c) Cai, Y.-F.; Yang, H.-M.; Li, L.; Jiang, K.-Z.; Lai, G.-Q.; Jiang, J.-X.; Xu, L.-W. *Eur. J. Org. Chem.* **2010**, 4986-4990. (d) Saha, S.; Moorthy, J. N. *J. Org. Chem.* **2011**, *76*, 396-402.
[10] (a) Wan, J.-P.; Liu, Y. *Synthesis* **2010**, *23*, 3943-3953. (b) He, Z.-Q.; Zhou, Q.; Wu, L.; Chen, Y.-C. *Adv. Synth. Catal.* **2010**, *352*, 1904-1908.

generates oxazolopyrimidinones[11] diastereoselectively (Eq 4).[12] Orru made α,β-unsaturated imines **3** *in situ* from a Horner-Wadsworth-Emmons reaction of nitriles **14**, aldehydes **10**, and phosphonates **15** and reacted the α,β-unsaturated imines **3** with isocyanates to generate pyrimidinones in a multi-step, one-pot reaction (Eq 5).[13] We sought to develop a metal-catalyzed [4+2] cycloaddition between α,β-unsaturated imines and isocyanates.[14]

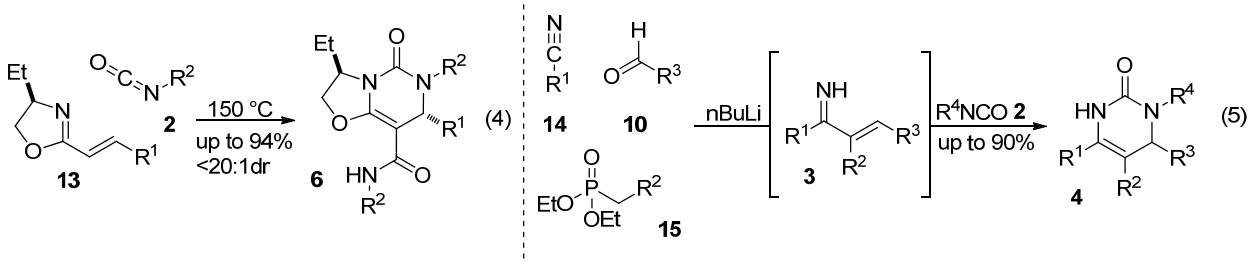

3.2 Initial Studies and Optimization

Our initial efforts centered around nickel catalysts based on Hoberg's metallacycle report. When we mixed α,β-unsaturated imine **3a** and phenyl isocyanate **2a** together in the presence of nickel, the ^{1}H NMR of the unpurified mixture did not show any target material (Eq 6). We then mixed diphenyl imine **1** and alkenyl isocyanate **2b** in the hopes of observing a product derived from trapping of the nickelacycle with the tethered alkene (**17** or **18**). Instead, we observed that the alkenyl isocyanate had trimerized to make isocyanurate **16b** (Eq 7). Upon reinvestigation of our original reactions with phenyl isocyanate **2a**, IR spectroscopy confirmed that isocyanurate **16a** was being generated.[15] Slow addition of the isocyanate did not remedy the problem.

[11] The intermediate pyrimidinones reacts with an additional isocyanate to install the amide at the 5 position.
[12] (a) Elliott, M. C.; Kruiswijk, E. *J. Chem. Soc., Perkin Trans. 1*, **1999**, 3157-3166. (b) Elliott, M. C.; Kruiswijk, E.; Willock, D. J. *Tetrahedron* **2001**, *57*, 10139-10146.
[13] Vugts, D. J.; Koningstein, M. M.; Schmitz, R. F.; de Kanter, F. J. J.; Groen, M. B.; Orru, R. V. A. *Chem. Eur. J.* **2006**, *12*, 7178-7189.
[14] For a similar reaction of α, β-unsaturated imines with ketenes, see; Jian, T.-Y.; Shao, P.-L.; Ye, S. *Chem. Commun.* **2011**, *47*, 2381-2383.
[15] (a) Zhou, A.; Cao, L.; Li, H.; Liu, Z.; Cho, H.; Henry, W. P.; Pittman, Jr., C. U. *Tetrahedron* **2006**, *62*, 4188-4200. (b) National Institute of Advanced Industrial Science and Technology. SDBSWeb. http://sdbs.riodb.aist.go.jp (Accessed April 2010).

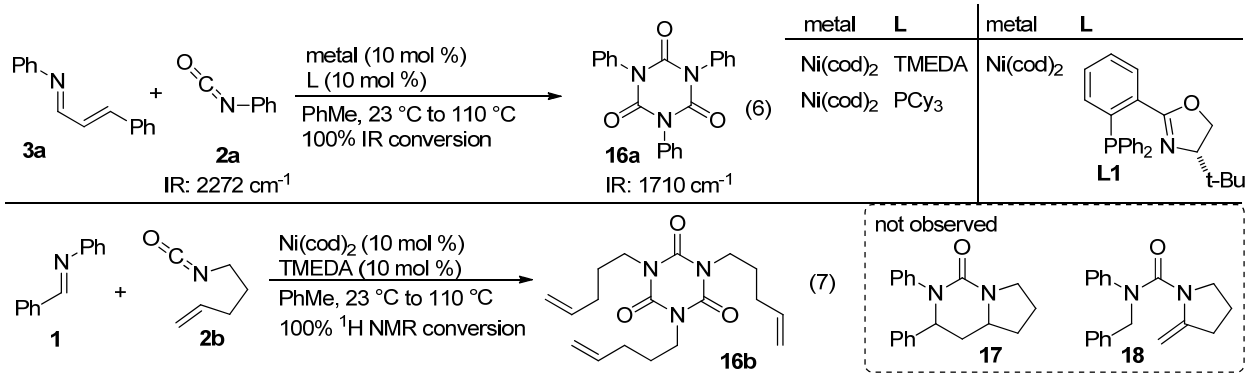

With trimerization of the isocyanate plaguing us when we used nickel catalysts, we investigated other metal catalyst systems (Table 3.2.1). We also chose to use hexyl isocyanate **2c** so trimerization would be detectable by ^{1}H NMR. After some screening, we found that the rhodium·Taddol phosphoramidite catalyst system provides product in moderate yields and good enantioselectivities (entries 3, 4, and 6-8). We found that phosphoramidite scaffolds other than Taddol, such as BINOL, BiAryl, and VAPOL provide high yields, but enantioselectivities are lower (entries 10, 11, and 13). Use of a bidentate ligand (BINAP, **L12**) does not provide any product. The importance of phosphoramidite ligands is demonstrated by the lack of reactivity when $Rh(PPh_3)_3Cl$[16] is used (entry 2). The use of $[Rh(cod)Cl]_2$·**L3** as a catalyst does not yield any product (entry 17). The difference in reactivity from cyclooctadiene to bisethylene is staggering. We have seen lower yields of product when using cyclooctadiene as a ligand on rhodium in previous work (Chapter 2), but the complete lack of product in this reaction with the cyclooctadiene precatalyst is surprising. We settled on **L3** as our optimal ligand as it provides product with the highest enantioselectivitiy and in good yield (entry 4).[17]

[16] In situ generation of $Rh(C_2H_2)_2Cl·PPh_3$ from 1 equivalent of $[Rh(C_2H_4)_2Cl]_2$ and 2 equivalents of PPh_3 yields <2% product.

[17] Solvent and temperature effects with $[Rh(C_2H_4)_2Cl]_2$·**L3** as the catalyst; MeCN at 80 °C yields no product, DCE at 85 °C gives 45% yield with 94% ee, dioxane at 100 °C gives 47% yield with 92% ee, and PhMe at 80 °C yields trace product.

Table 3.2.1. Catalyst optimization.[a]

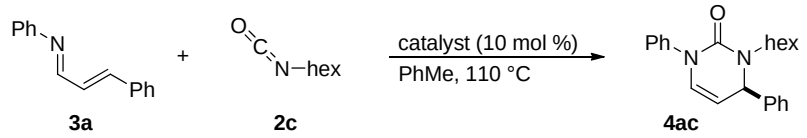

3a **2c** **4ac**

entry	catalyst	yield (%)[b]	ee (%)[c,d]	entry	catalyst	yield (%)[b]	ee (%)[c,d]
1	none	0	-	10	$[Rh(C_2H_4)_2Cl]_2$, **L8**	92	33
2	$Rh(PPh_3)_3Cl$	<5	-	11	$[Rh(C_2H_4)_2Cl]_2$, rac-**L9**	76	-
3	$[Rh(C_2H_4)_2Cl]_2$, **L2**	29	81	12	$[Rh(C_2H_4)_2Cl]_2$, **L10**	21	-52
4	$[Rh(C_2H_4)_2Cl]_2$, **L3**	***56***	***90***	13	$[Rh(C_2H_4)_2Cl]_2$, **L11**	79	74
5	**L3**	0	-	14	$[Rh(C_2H_4)_2Cl]_2$, **L12**	0	-
6	$[Rh(C_2H_4)_2Cl]_2$, **L4**	22	79	15	$Pd(P(tBu)_3)_2$	0	-
7	$[Rh(C_2H_4)_2Cl]_2$, **L5**	29	84	16	$Pd(dba)_2$, TMEDA	0	-
8	$[Rh(C_2H_4)_2Cl]_2$, **L6**	12	68	17	$[Ir(cod)Cl]_2$, **L3**	0	-
9	$[Rh(C_2H_4)_2Cl]_2$, **L7**	<5	nd	18	$[Rh(cod)Cl]_2$, **L3**	0	-

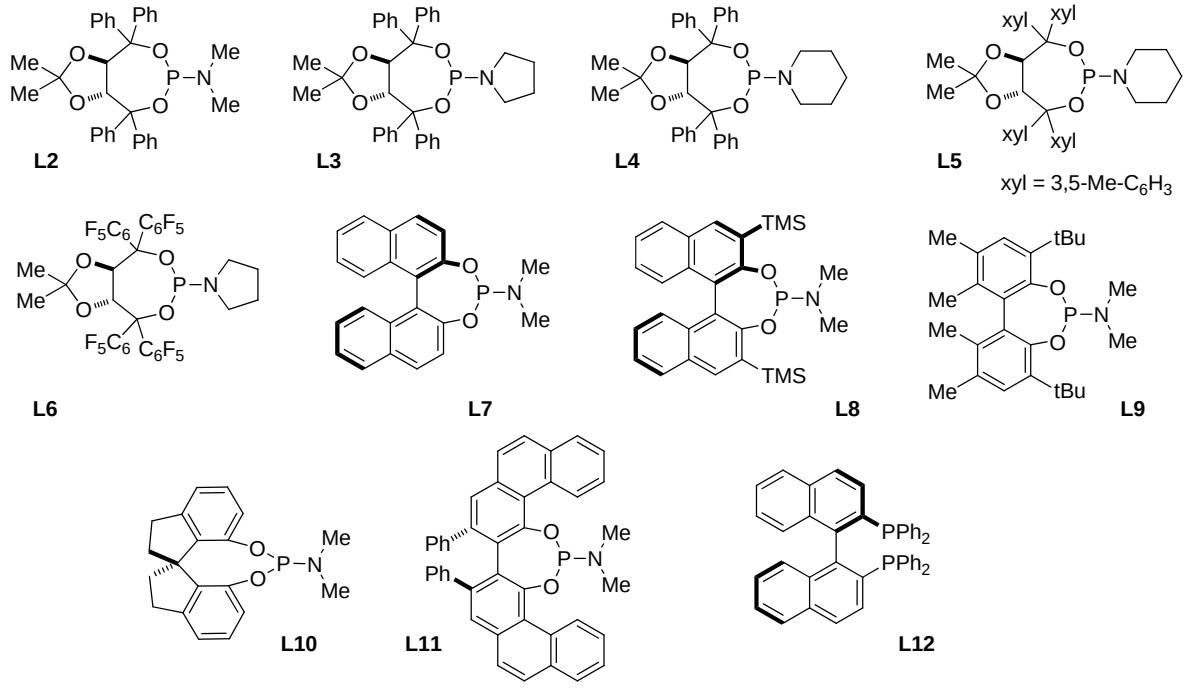

L2 **L3** **L4** **L5**

xyl = 3,5-Me-C_6H_3

L6 **L7** **L8** **L9**

L10 **L11** **L12**

[a] Conditions: **3a** (0.3 mmol), **2c** (1.25 equiv), and catalyst in PhMe at 110 °C for 12 h. [b] Isolated yield. [c] Enantiomeric excess determined by HPLC using a chiral stationary phase. [d] Absolute configuration assigned by analogy to (*R*)-**4ag** (established by X-ray analysis).

3.3 Scope of Pyrimidinone Synthesis and Product Derivatization

We investigated the scope of the reaction using $[Rh(C_2H_4)_2Cl]_2$·**L3** as the catalyst. We found that primary aliphatic *N*-substituted imines provide the highest yields and enantioselectivities, but *N*-aryl

imines[18] also work quite well (Table 3.3.1). Electron-deficient aryl *N*-substituted imines provide slightly higher yields and enantioselectivities (**4cc**) than electron-rich aryl *N*-substituted imines (**4bc**). Although we see this trend in isolated yields, this could be an artifact of isolation[19] because the products are acid sensitive.[20] Primary aliphatic *N*-substituted imines (**4ec**, **4fc**, **4gc**, and **4hc**) provide the highest enantioselectivities, whereas secondary aliphatic *N*-substituted imines (**4dc**) provide high yields with moderate enantioselectivities.[21]

Table 3.3.1. Scope of nitrogen substitution on α,β-unsaturated imine.[a-d]

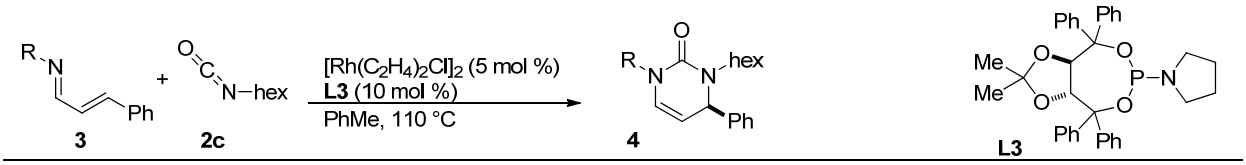

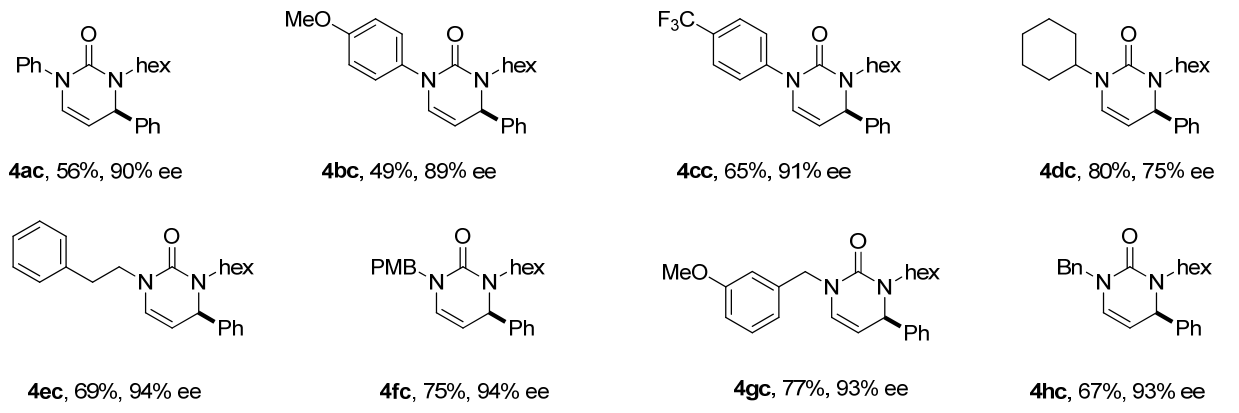

[a-d] See Table 3.2.1

A variety of substituents at the β-position were examined (Table 3.3.2). Ortho aryl β-substitution is tolerated quite well in the reaction providing the desired product in good yield and enantioselectivity (**4ic**). Electron-rich aromatic β-substitution provides higher yields (**4jc**), but lower enantioselectivities than electron-deficient aromatic β-substitution (**4kc**). Heterocycles (**4lc**) and vinyl groups (**4mc**) provide

[18] 4-iodoarylimine does not provide any product.
[19] A comparison of yield for **3a**, **3b**, and **3c**, using 1,3,5-trimethoxybenzene as an internal standard, shows the same conversion for all three substrates (~73%). Isolated yields may be lower for **4bc** as the enamine is more electron-rich and more reactive.
[20] If the pyrimidinones are stirred in DCM/SiO_2 for extended amounts of time, we see minor decomposition by ^1H NMR. After exposure to $CDCl_3$, we observe slight decomposition after a few days. Exposure to 3M HCl causes almost complete destruction of the products.
[21] Allyl *N*-substituted imine yields trace product. α,β-Unsaturated O-methyloxime and α,β-unsaturated *N*,*N*-dimethylhydrazone does not produce any product.

product in good yields and enantioselectivities. Aliphatic β-substitution provides products in lower yields and moderate enantioselectivities (**4nc** and **4oc**). The β-aliphatic α,β-unsaturated imines are unstable so the low yields could be partially due to decomposition of the starting materials.

Table 3.3.2. Scope of β-substitution on α,β-unsaturated imines.[a-d]

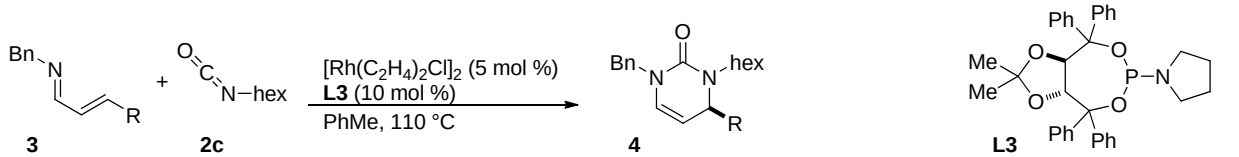

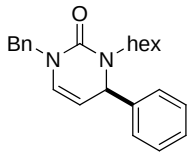
4hc, 67%, 93% ee

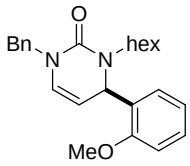

4ic, 67%, 94% ee

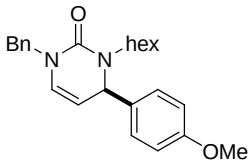

4jc, 69%, 92% ee

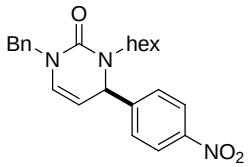

4kc, 36%, 95% ee

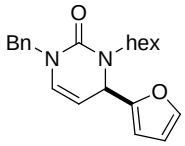
4lc, 82%, 94% ee

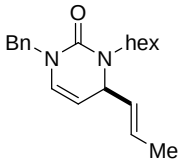

4mc, 60%, 89% ee

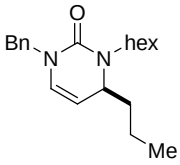

4nc, 38%, 77% ee

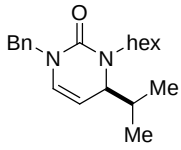

4oc, 53%, 83% ee

[a-d] See Table 2.5.1

When we attempted subjecting β-ester **3p** to the reaction, we isolated a different product, pyrrolone **19p**.[22] Presumably, this product is derived from rhodium acting as a Lewis acid. Intramolecular attack of the imine on the ester releases the alcohol. Quenching of the iminium by the alcohol would generate pyrrolone **19**.[23] This happens with or without isocyanate, but is catalyzed by rhodium (Eq 8). This is suggested by the enantioenduction and absence of product when the reaction was run without catalyst or with only ligand. The use of electron-rich imines is necessary for the reaction; N-phenyl substituted imine **3q** does not provide pyrrolone, but N-alkyl substituted imine **3r** does.

[22] Stereochemistry was arbitrarily assigned based on optical rotation of a *similar* compound: Cuiper, A. D.; Kellogg, R. M.; Feringa, B. L. *Chem. Commun.* **1998**, 655-656.
[23] Similar reactions have been reported: (a) Heaney, H.; Shuhaibar, K. F. *Tetrahedron Lett.* **1994**, *35*, 2751-2752. (b) Lübbers, T.; Angehrn, P.; Gmünder, H.; Herzig, S. *Bioorg. Med. Chem. lett.* **2007**, *17*, 4708-4714.

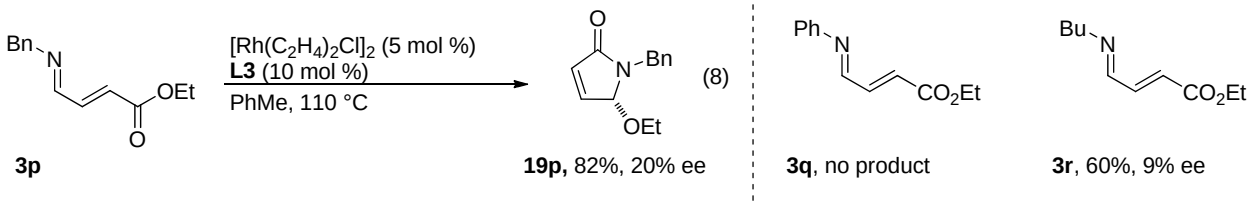

3p **19p,** 82%, 20% ee **3q**, no product **3r**, 60%, 9% ee

We explored which isocyanates participate in the reaction and found that primary alkyl isocyanates work best in this transformation (Table 3.3.3). Interestingly, alkenyl isocyanate provides pyrimidinone **4hb** as the only observable product, and no intramolecular trapping by the tethered alkene is detected. Benzyl and paramethoxybenzyl isocyanate provide product in good yields and enantioselectivities (**4hd** and **4he**). Aromatic isocyanates generate product in lower yields and enantioselectivities (**4hf**). Increasing the size of the isocyanate from primary to secondary causes a sharp decrease in yield and enantioselecitivity (**4hi**), and further increases in size leads to no observable product.[24] We demonstrated that the reaction is scalable by making pyrimidinone **4hd** on a 4.5 mmol scale, and the catalyst loading was lowered to 2 mol % without compromising yield or enantioselectivity.

Table 3.3.3. Isocyanate scope.[a-d]

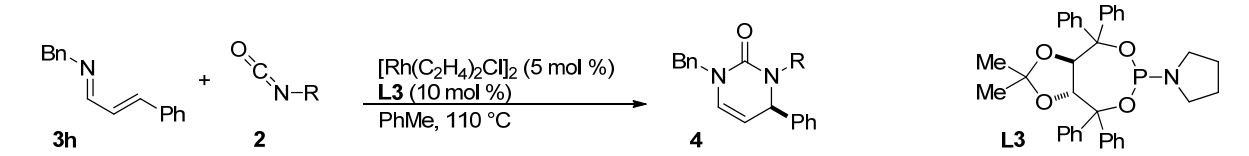

3h **2** **4** **L3**

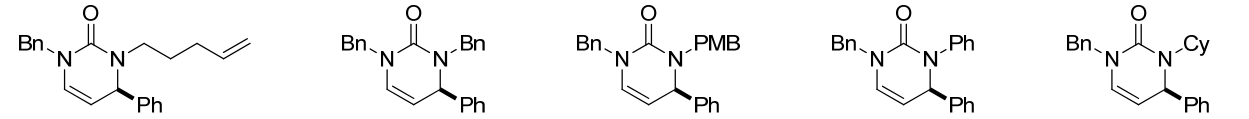

4hb, 53%, 91% ee **4hd**,[e] 65%, 94% ee **4he**, 75%, 93% ee **4ha**, 42%, 84% ee **4hf**,[f] 4%, 81% ee

[a-d] See Table 2.5.1 [e] On 4.5 mmol scale with $[Rh(C_2H_4)_2Cl]_2$ (1 mol %) and **L2** (2 mol %): 71% yield and 94% ee. [f] With **L8** as the ligand: 58% yield and 18% ee.

In order to determine the absolute configuration, diphenyl α,β-unsaturated imine **3a** and 4-bromophenyl isocyanate **2g** were cyclized to yield **4ag** as a solid. After recrystallization to 99% ee, we

[24] Tert-butyl isocyanate and trimethylsilyl isocyanate do not produce any observable product.

obtained a crystal structure[25] to establish the absolute configuration as (*R*), and the other products were assigned by analogy.

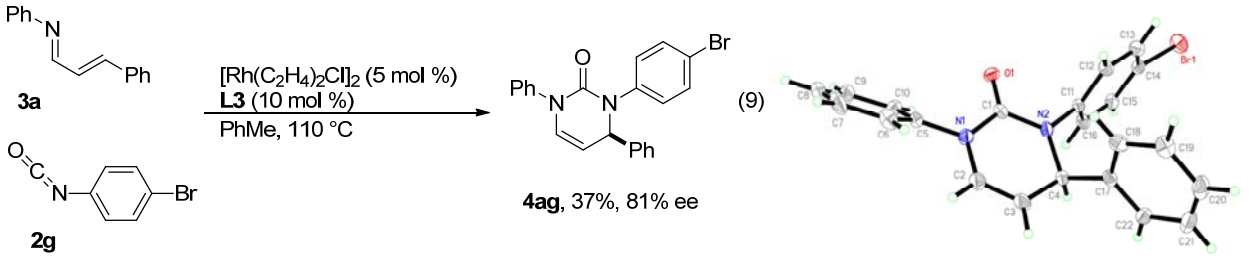

To expand the types of α,β-unsaturated imines that participate in this reaction, we sought to use doubly substituted α,β-unsaturated imines. We found that β,β-methyl α,β-unsaturated imine **3s** provides a small amount of product in the reaction (Eq 10). Other substitutions are not tolerated. For example, β,β-methyl,phenyl α,β-unsaturated imine (**3t**) and α-methyl α,β-unsaturated imine (**3u**) does not yield any product.

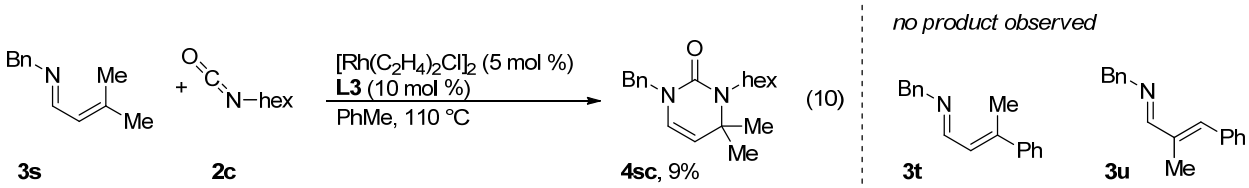

In order to optimize the reaction for α,β-unsaturated imine **3sc**, we used the High-Throughput Experimentation (HTE) [26] platform (Figure 3.3.1) at CSU. We found that $[Rh(C_2H_4)_2Cl]_2$ was the only precatalyst of the metals screened that provides any product. We found **L8** provides the highest yield of pyrimidinone **4sc**. This mirrors the earlier results during our initial catalyst screen (Table 3.2.1) and corresponds to a ~25% yield of pyrimidinone **4sc**.

[25] Deposit number CCDC 837910.
[26] Based on the HTE platform developed by Merck and Co. Inc. (a) Dreher, S. D.; Dormer, P. G.; Sandrock, D. L.; Molander, G. A. *J. Am. Chem. Soc.* **2008**, *130*, 9257-9259. (b) Spencer D. Dreher, Merck and Co. Inc., Rahway, New Jersey, USA. Personal Communication, 2011.

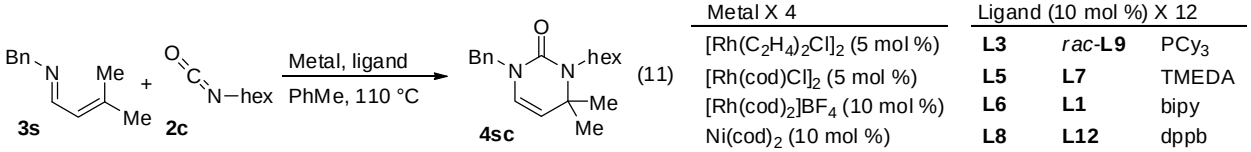

Metal X 4	Ligand (10 mol %) X 12		
$[Rh(C_2H_4)_2Cl]_2$ (5 mol %)	**L3**	*rac*-**L9**	PCy_3
$[Rh(cod)Cl]_2$ (5 mol %)	**L5**	**L7**	TMEDA
$[Rh(cod)_2]BF_4$ (10 mol %)	**L6**	**L1**	bipy
$Ni(cod)_2$ (10 mol %)	**L8**	**L12**	dppb

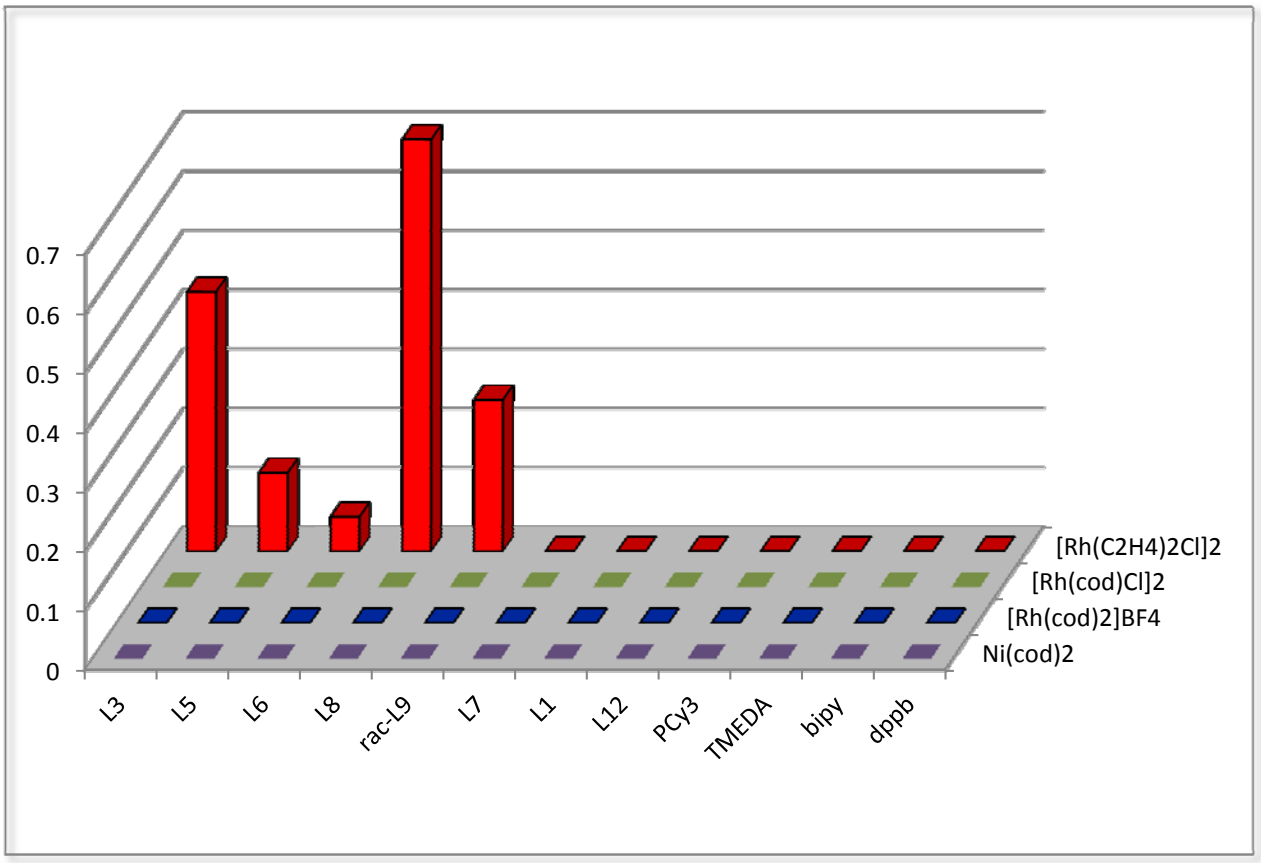

Figure 3.3.1. HTE screen of precatalyst and ligands shows $[Rh(C_2H_4)_2Cl]_2$ and **L8** are best of screened conditions for α,β-unsaturated imine **3sc**.

To improve the utility of this reaction, we sought to deprotect the urea and derivatize the products. Initially, we attempted to deprotect dibenzyl protected pyrimidinone **4hb** via hydrogenation, but only saw reduction of the enamine to generate tetrahydropyrimidinone **20hb** (Eq 12). We thought that making di(para-methoxybenzyl) protected pyrimidinone **4fe** would allow for other deprotection strategies to be investigated and synthesized pyrimidinone **4fe** in good yield and enantioselectivity. Hydrogenation of the enamine followed by heating in trifluoroacetic acid leads to deprotected tetrahydropyrimidinone **21**

(Eq 13). The enantiomer of tetrahydropyrimidinone **21** was synthesized by another group,[27] and comparison of the optical rotations confirmed our assignment of absolute configuration.

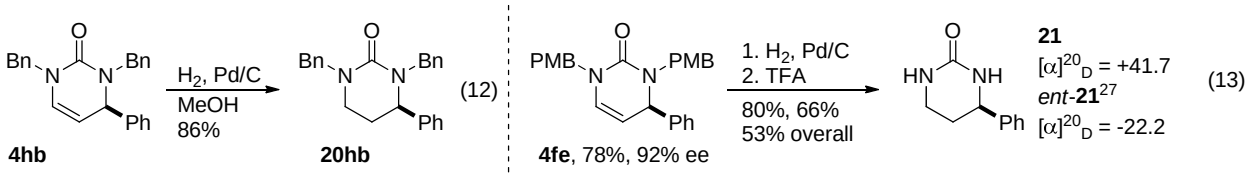

With a tempered nucleophilic enamine as a synthetic handle, we thought derivatization using electrophilic reagents should be possible. Exposure of pyrimidinone **4hb** to *meta*-chloroperoxybenzoic acid provides epoxide **22** in low yield (Eq 13), and treatment with osmium and *N*-methylmorpholine *N*-oxide yields dihydroxydihydropyrimidinone **23** (Eq 15). These products are unstable and decomposition is observed. Treatment of pyrimidinone **4hc** with *N*-bromosuccinimide in wet *N*,*N*-dimethylformamide yields bromohydrin **24hc** (Eq 16). *In situ* generation of the iminium and trapping with an allyl nucleophile yields bromotetrahydropyrimidinone **25**. These transformations proceed with excellent diastereoselectivity (>20:1) and the relative configuration was established by nOe.

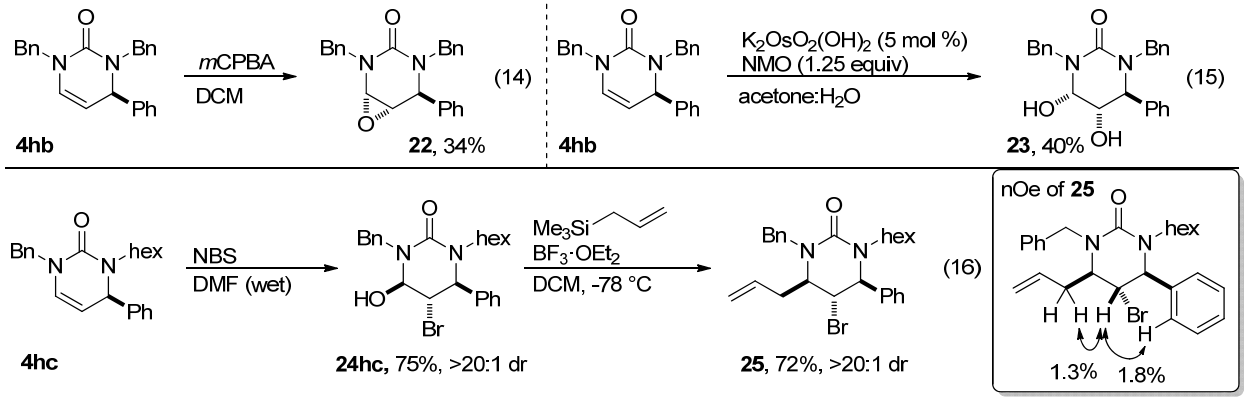

3.4 Proposed Mechanism

The proposed mechanism for this reaction is shown in Figure 3.4.1. Coordination of the α,β-unsaturated imine **3** and isocyanate **2** to rhodium and oxidative cyclization generates rhodacycle **II**. This rhodacycle undergoes an η^1-η^3-η^1 shift, via **III**, to yield 7-membered rhodacycle **IV**. Reductive elimination furnishes pyrimidinone **4** and regenerates the catalyst. The existence of rhodacycle **II** is

[27] He, Z.-Q.; Zhou, Q.; Wu, L.; Chen, Y.-C. *Adv. Synth. Catal.* **2010**, *352*, 1904-1908.

supported by the isolation of nickallacycle **I** by Hoberg.[28] An alternative mechanism can be envisioned that involves an initial [4+1] between rhodium and the α,β-unsaturated imine **3** to generate **V**.[29] Coordination and insertion of the isocyanate forms rhodacycle **IV** that undergoes reductive elimination to furnish product **4** and catalyst. We believe this is not the operative mechanism because different isocyanates give varying enantioselectivity with the same α,β-unsaturated imine. This suggests that the isocyanate is involved in the enantiodetermining step. In the proposed mechanism this is during the oxidative cyclization involving both the α,β-unsaturated imine and isocyanate so the isocyanate affects the enantioselectivity. In the alternative mechanism, only the α,β-unsaturated imine is involved in the first cyclization where the stereocenter is established. As the isocyanate has an effect on the enantioselectivity, we believe that the mechanism involving oxidative cyclization of the imine and isocyanate is operative, but other mechanisms have not been rigorously ruled out.

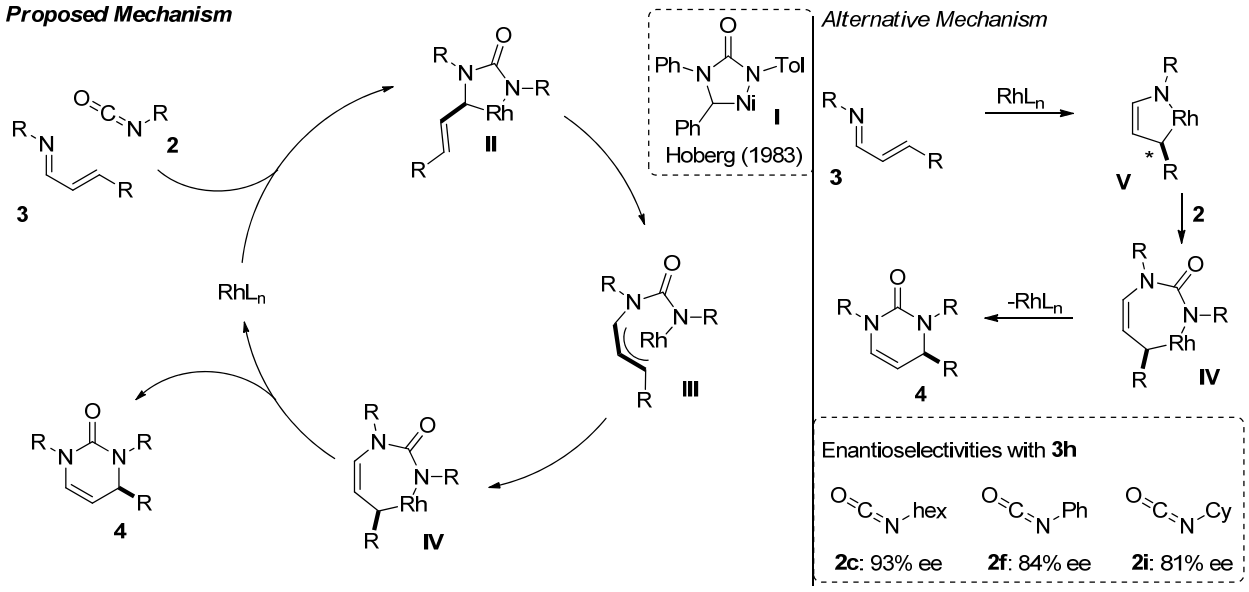

Figure 3.4.1. Proposed mechanism.

[28] Hoberg, H.; Sümmermann, K. *J. Organomet. Chem.* **1983**, *253*, 383-389.
[29] Koyama, I.; Kurahashi, T.; Matsubara, S. *J. Am. Chem. Soc.* **2009**, *131*, 1350-1351.

3.5 Conclusion

In conclusion, we have developed an enantioselective synthesis of pyrimidinones via a rhodium-catalyzed [4+2] cycloaddition of α,β-unsaturated imines and isocyanates. The use of a $[Rh(C_2H_4)_2Cl]_2$·phopshoramidite catalyst proves important; use of $[Rh(cod)Cl]_2$ or phosphine ligands other than phosphoramidite ligands do not provide product. For substrates, primary aliphatic *N*-substituted imines deliver product with the highest yields and enantioselectivities, numerous substitutions at the β position (aryl, heterocyclic, vinyl, and aliphatic) are tolerated, and primary aliphatic isocyanates provide the highest yields and enantioselectivities. Substitution at the α position is not tolerated, and disubstitution at the β position is low yielding with only the dimethyl substrate working in our hands. The products can be derivatized and deprotected, demonstrating the possibility of these compounds to serve as chiral heterocycle building blocks. Finally, we believe the mechanism proceeds through an oxidative cyclization of the α,β-unsaturated imine and isocyanate on rhodium, followed by an η^1-η^3-η^1 shift and reductive elimination to furnish product.

CHAPTER 4

Progress towards the Synthesis of Ionomycin

4.1 Anhydride Desymmetrization and Previous Syntheses of Ionomycin

One of the flagship projects in the Rovis group was the desymmetrization of anhydrides.[1] In an extension of this work, Dr. Matthew Cook developed the desymmetrization of glutaric anhydrides with alkyl zinc reagents using a rhodium·Phox ligand system (Scheme 4.1.1).[2] Desymmetrization of dimethyl glutaric anhydride **1** offers an efficient route to deoxypolypropionate synthons **2**. Since then, the desymmetrization of trisubstituted glutaric anhydrides **3** has been achieved by Dr. Brian Cochran and offers a synthesis of polypropionate synthons **4**.[3] The synthesis of these motifs has garnered well deserved attention due to its ubiquity in natural products having interesting biological properties.[4] Nature uses an iterative linear assembly process to create a wide range of motifs found in thousands of natural products using hundreds of polyketide synthase enzymes and a few simple building blocks.[5] Traditionally, these motifs are chemically synthesized using aldol technology[6] or synthons from chiral pool.[7] In a testament to the importance of polypropionate synthesis, a number of methodologies that access these motifs have

[1] (a) Bercot, E. A.; Rovis, T. *J. Am. Chem. Soc.* **2002**, *124*, 174-175. (b) O'Brien, E. M.; Bercot, E. A.; Rovis, T. *J. Am. Chem. Soc.* **2003**, *125*, 10498-10499. (c) Bercot, E. A.; Rovis, T. *J. Am. Chem. Soc.* **2004**, *126*, 10248-10249. (d) Bercot, E. A.; Rovis, T. *J. Am. Chem. Soc.* **2005**, *127*, 247-254. (e) Johnson, J. B.; Yu, R. T.; Fink, P.; Bercot, E. A.; Rovis, T. *Org. Lett.* **2006**, *8*, 4307-4310. (f) Rogers, R. L.; Moore, J. L.; Rovis, T. *Angew. Chem. Int. Ed.* **2007**, *46*, 9301-9304. (f) Johnson, J. B.; Bercot, E. A.; Williams, C. M.; Rovis, T. *Angew. Chem. Int. Ed.* **2007**, *46*, 4514-4518. (g) Johnson, J. B.; Bercot, E. A.; Rowley, J. M.; Coates, G. W.; Rovis, T. *J. Am. Chem. Soc.* **2007**, *129*, 2718-2725.

[2] (a) Cook, M. J.; Rovis, T. *J. Am. Chem. Soc.* **2007**, *129*, 9302-9303. (b) Cook, M. J.; Rovis, T. *Synthesis* **2009**, 335-338. (c) Johnson, J. B.; Cook, M. J.; Rovis, T. *Tetrahedron* **2009**, *65*, 3202-3210. (d) Cook, M. J. Colorado State University, Fort Collins, CO. Unpublished work, 2008.

[3] Henderson, D. D.; Cochran, B. M.; Filloux, C. M.; Rovis, T. *Submitted*.

[4] Koskinen, A. M. P.; Karisalmi, K. *Chem. Soc. Rev.* **2005**, *34*, 677-690.

[5] For reviews of polypropionate synthesis by nature, see: (a) Staunton, J.; Weissman, K. J. *Nat. Prod. Rep.* **2001**, *18*, 380-416. (b) Fischbach, M. A.; Walsh, C. T. *Chem. Rev.* **2006**, *106*, 3468-3496.

[6] (a) Evans, D. A.; Nelson, J. V.; Taber, T. R. *Top. in Stereochem.* **1982**, *13*, 1-115. (b) Palomo, C.; Oiarbide, M.; García, J. M. *Chem. Soc. Rev.* **2004**, *33*, 65-75.

[7] Hanessian, S. *J. Org. Chem.* **2012**, *77*, 6657-6688.

been developed.[8] A number of these methods share an iterative approach with nature in constructing these motifs. We believe the strength in our approach, the desymmetrization of anhydrides, is that it forges a carbon-carbon bond to deliver enantioenriched (deoxy)polypropionate synthons that are five or more carbons in length in a single step.

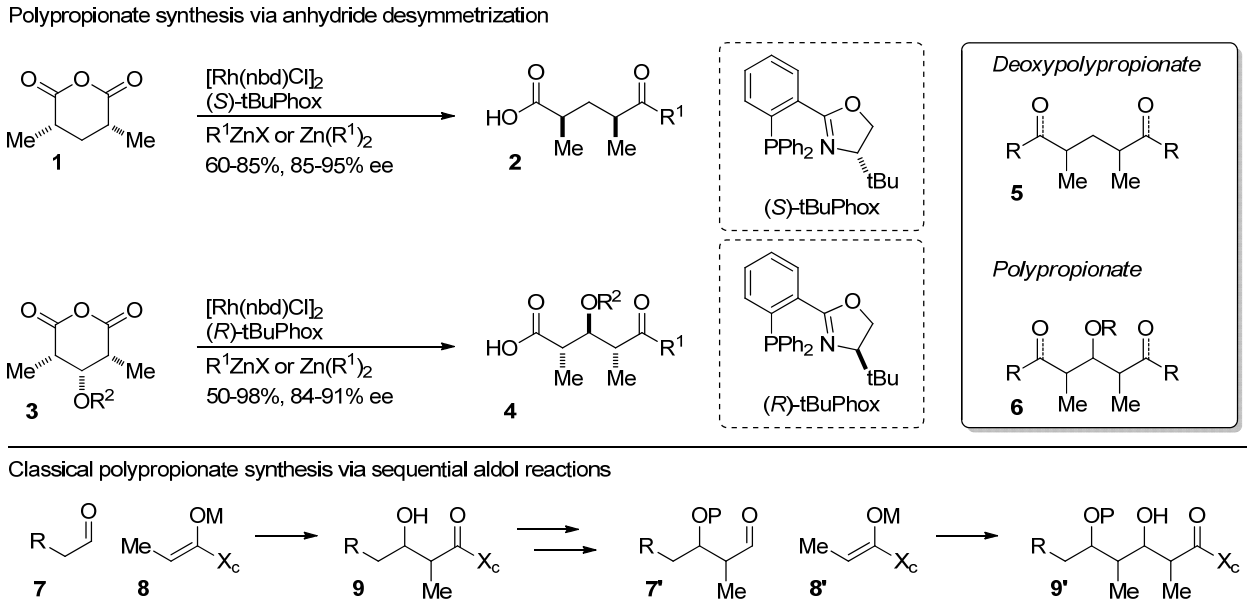

Scheme 4.1.1. Synthesis of deoxypolypropionates and polypropionates via anhydride desymmetrization and gold standard aldol synthesis of polypropionates.

In an effort to demonstrate the synthetic utility of anhydride desymmetrization for the synthesis of natural compounds containing deoxypolypropionate and polypropionate motifs, Dr. Cook devised a route to ionomycin **10** based on anhydride desymmetrization.[9] Ionomycin was isolated from *Streptomyces congoblatus* fermentation broths in 1978 (Figure 4.1.1).[10] Although it demonstrated some antibiotic properties, its affinity for calcium is the more interesting feature and ionomycin is used as a tool in

[8] For selected examples, see: (a) Negishi, E.-i.; Kondakov, D. Y. *Chem. Soc. Rev.* **1996**, *25*, 417-426. (b) Li, J.; Menche, D. *Synthesis* **2009**, *14*, 2293-2315. (c) Bower, J. F.; Kim, I. S.; Patman, R. L.; Krische, M. J. *Angew. Chem. Int. Ed.* **2009**, *48*, 34-46.

[9] Cook, M. J. Colorado State University, Fort Collins, CO. Unpublished work, 2008.

[10] For activity and isolation: (a) Liu, C.-m.; Hermann, T. E. *J. Biol. Chem.* **1978**, *253*, 5892-5894. (b) Liu, W.-c.; Slusarchyk, D. S.; Astle, G.; Trejo, W. H.; Brown, W. E.; Meyers, E. *J. Antibiot.* **1978**, *31*, 815-819. For structure elucidation, see: (c) Toeplitz, B. K.; Cohen, A. I.; Funke, P. T.; Parker, W. L.; Gougoutas, J. Z. *J. Am. Chem. Soc.* **1979**, *101*, 3344-3353.

neuroscience.[11] Since its isolation, there have been four total syntheses of ionomycin by Hanessian, Evans, Lautens, and Kocienski. In addition to these completed syntheses, a number of fragment syntheses and approaches have been reported.[12]

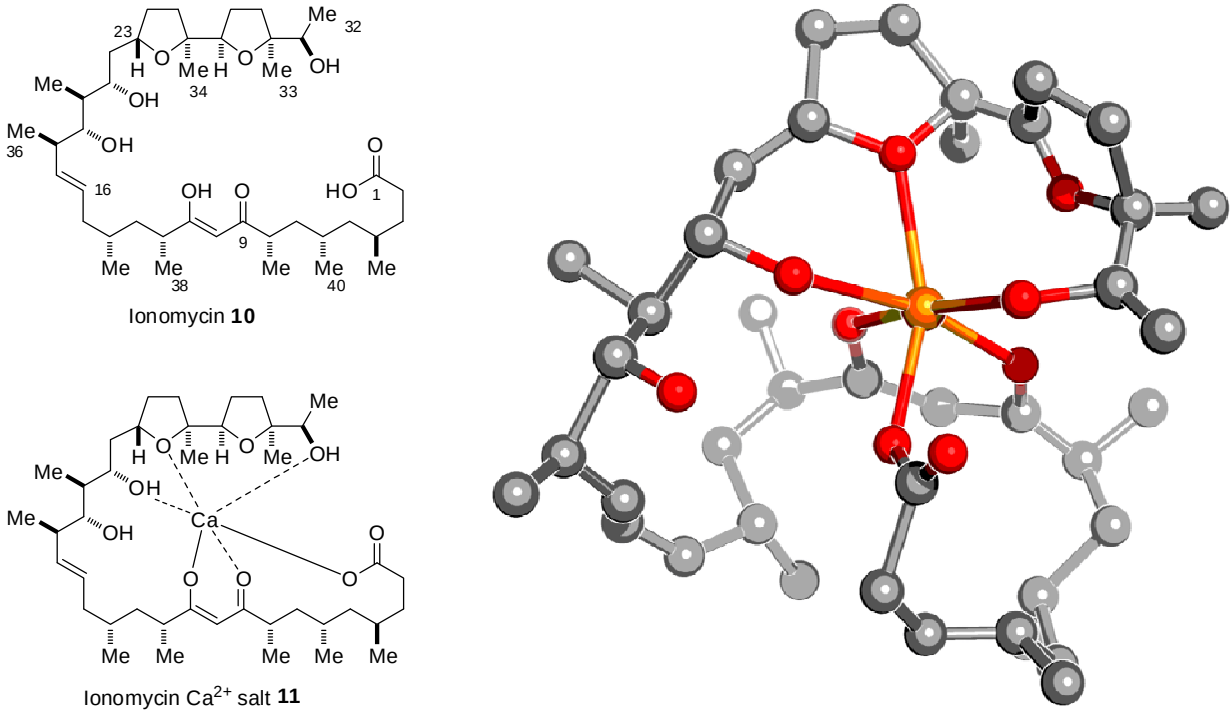

Figure 4.1.1. Structure of ionomycin.

Hanessian's synthesis[13] of ionomycin was a beautiful demonstration of the chiron approach and cyclic strategy for the synthesis of enantiopure, complex natural products (Figure 4.1.2). The butenolide

[11] (a) Liu, C.-m.; Hermann, T. E. *J. Biol. Chem.* **1978**, *253*, 5892-5894. (b) Kauffman, R. F.; Taylor, R. W.; Pfeiffer, D. R. *J. Biol. Chem.* **1980**, *255*, 2735-2739.

[12] (a) Wuts, P. G. M.; D'Costa, R.; Butler, W. *J. Org. Chem.* **1984**, *49*, 2582-2588. (b) Nicoll-Griffith, D.; Weiler, L. *J. Chem. Soc., Chem. Commun.* **1984**, 659-661. (c) Schreiber, S. L.; Wang, S. *J. Am. Chem. Soc.* **1985**, *107*, 5303-5305. (d) Spino, C.; Weiler, L. *Tetrahedron Lett.* **1987**, *28*, 731-734. (e) Shelly, K. P.; Weiler, L. *Can. J. Chem.* **1988**, *66*, 1359-1365. (f) Nicoll-Griffith, D. A.; Weiler, L. *Tetrahedron* **1991**, *47*, 2733-2750. (g) Taschner, M. J.; Chen, Q.-Z. *Bioorg. Med. Chem. Lett.* **1991**, *1*, 535-538. (h) Guidon, Y.; Yoakin, C.; Gorys, V.; Ogilvie, W. W.; Delorme, D.; Renaud, J.; Robinson, G.; Lavallée, J.-F.; Slassi, A.; Jung, G.; Rancourt, J.; Durkin, K.; Liotta, D. *J. Org. Chem.* **1994**, *59*, 1166-1178. (i) Hu, T. Q.; Weiler, L. *Can. J. Chem.* **1994**, *72*, 1500-1511. (j) von der Emde, H.; Langels, A.; Noltemeyer, M.; Brüchner, R. *Tetrahedron Lett.* **1994**, *35*, 7609-7612. (k) Montaña, A. M.; García, F.; Grima, P. M. *Tetrahedron* **1999**, *55*, 5483-5504. (l) Montaña, A. M.; García, F.; Grima, P. M. *Tetrahedron Lett.* **1999**, *40*, 1375-1378. (m) Spino, C.; Allan, M. *Can. J. Chem.* **2004**, *82*, 177184. (n) Novak, T.; Tan, Z.; Liang, B.; Negishi, E.-i. *J. Am. Chem. Soc.* **2005**, *127*, 2838-2839. (o) Marshall, J. A.; Mikowski, A. M. *Org. Lett.* **2006**, *8*, 4375-4378.

chiron **13** serves as an excellent way to build polypropionate fragments with desired *syn* or *anti* stereochemistry. Despite its strength, the butenolide building block failed to provide a straightforward route to the deoxypolypropionate motif and the synthesis was lengthy. This shortcoming was overcome through the deployment of γ-butyrolactones **14**. Both of these chirons were derived from L-glutamic acid **12**. The major disconnections in Hannessian's synthesis were a Wittig olefination (C22-C23), Julia-Lythgoe olefination (C16-C17), and an aldol reaction (C10-C11).

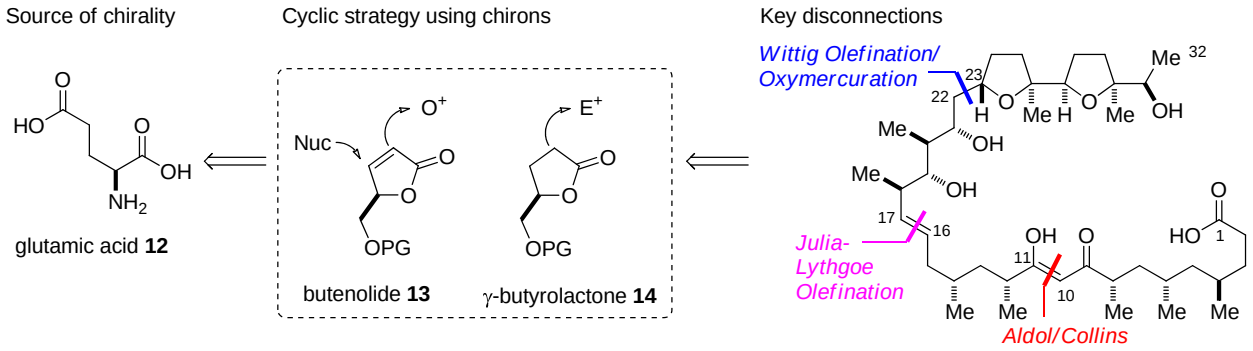

Figure 4.1.2. Outline of Hannessian's approach to ionomycin.

Through the use of γ-butyrolactones, Hanessian was able to construct both the C1-C10 fragment **20** and the C11-C16 fragment **17** (Scheme 4.1.2). Through the synthesis of γ-butyrolactone **14a**, the installment of the C6 and C8 stereocenters were controlled. The key C8 methyl substituent was installed using a sulfur-assisted S_N2 cuprate addition (**16** to **17**). This completed the synthesis of the C11-C16 fragment **17** and the same material was used to construct the C1-C10 fragment. Once again, stereocontrol was enforced through the use of a γ-butyrolactone, **14b**.

[13] Fragment syntheses: (a) Hanessian, S.; Murray, P. J.; Sahoo, S. P. *Tetrahedron Lett.* **1985**, *26*, 5627-5630. (b) Hanessian, S.; Murray, P. J. *Can. J. Chem.* **1986**, *64*, 2231-2234. (c) Hanessian, S.; Murray, P. J. *Tetrahedron* **1987**, *43*, 5055-5072. Total synthesis: (d) Hanessian, S.; Cooke, N. G.; DeHoff, B.; Sakito, Y. *J. Am. Chem. Soc.* **1990**, *112*, 5276-5290.

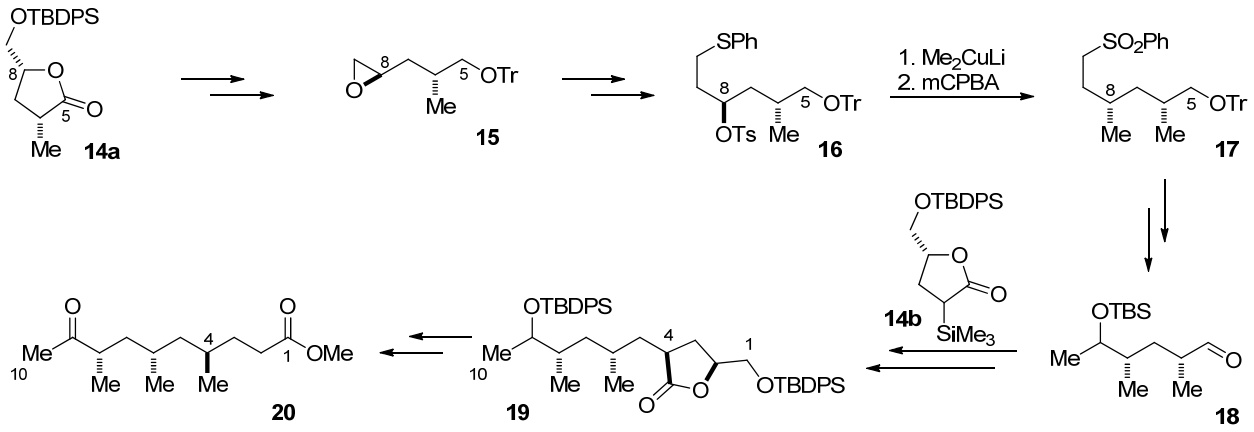

Scheme 4.1.2. Synthesis of C1-C10 fragment **20** and C11-C16 fragment **17** using γ-butyrolactones.

The synthesis of C17-C22 fragment **25** was accomplished through cyclic stereocontrol by installing the methyl and hydroxyl substituents on butenolide chirons **13** (Scheme 4.1.3). Starting with butenolide **13a**, the C19 stereocenter was used to install the C17 and C18 stereocenters. After conversion of lactone **21** to another butenolide **13b**, the same strategy was used to install the C20 and C21 stereocenters. In this case, diastereoselectivity was not as good, but the undesired epi-**23** compound could undergo the same synthetic sequence and be epimerized to generate the more thermodynamically stable aldehyde **25**.

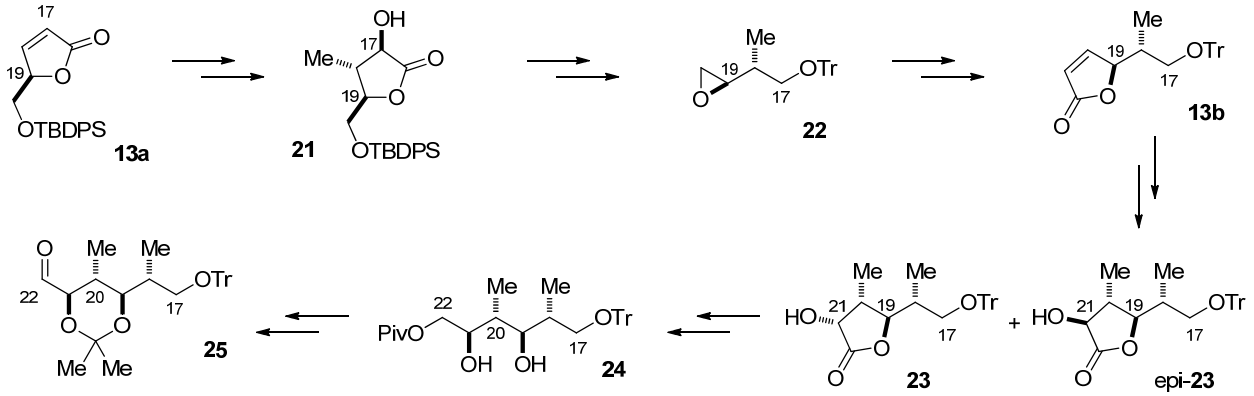

Scheme 4.1.3. Synthesis of C17-C22 fragment using butenolide chirons **13**.

The initial stereoinduction in the synthesis of the C23-C32 fragment **32** came from a Sharpless asymmetric epoxidation of racemic alcohol **26** (Scheme 4.1.4). This chirality was transferred using a vanadium-catalyzed epoxidation to synthesize tetrahydrofuran **31**, setting the both C26 and C27 stereocenters correctly. Elaboration to coupling partner **32** was done through functional group manipulation at C23.

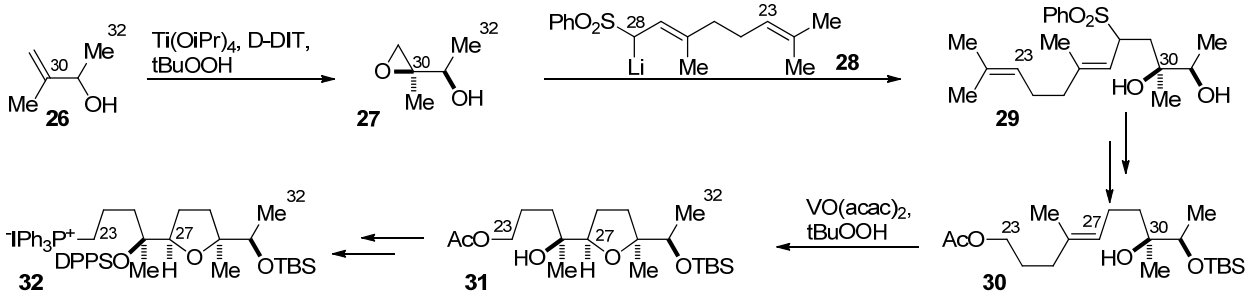

Scheme 4.1.4. Synthesis of northern fragment.

With all the fragments in hand, the task of coupling and elaboration to ionomycin remained. The C23-C32 fragment **32** was coupled with C17-C22 fragment **25** using a Wittig olefination, and the C23 stereocenter was established using an oxymercuration of olefin **33**. The trans-double bond and connection of the C17-C32 fragment with the C11-C16 fragment was done using a Julia-Lythgoe olefination. The final C1-C10 fragment was attached through an aldol/Collins oxidation sequence to generate protected ionomycin **36**. Removal of the protecting groups and conversion to the calcium salt following precedent[14] generated the ionomycin calcium complex **11**.

[14] Dow, R. L. The total synthesis of ionomycin. Ph.D. Dissertation, Harvard University, Cambridge, MA, 1985.

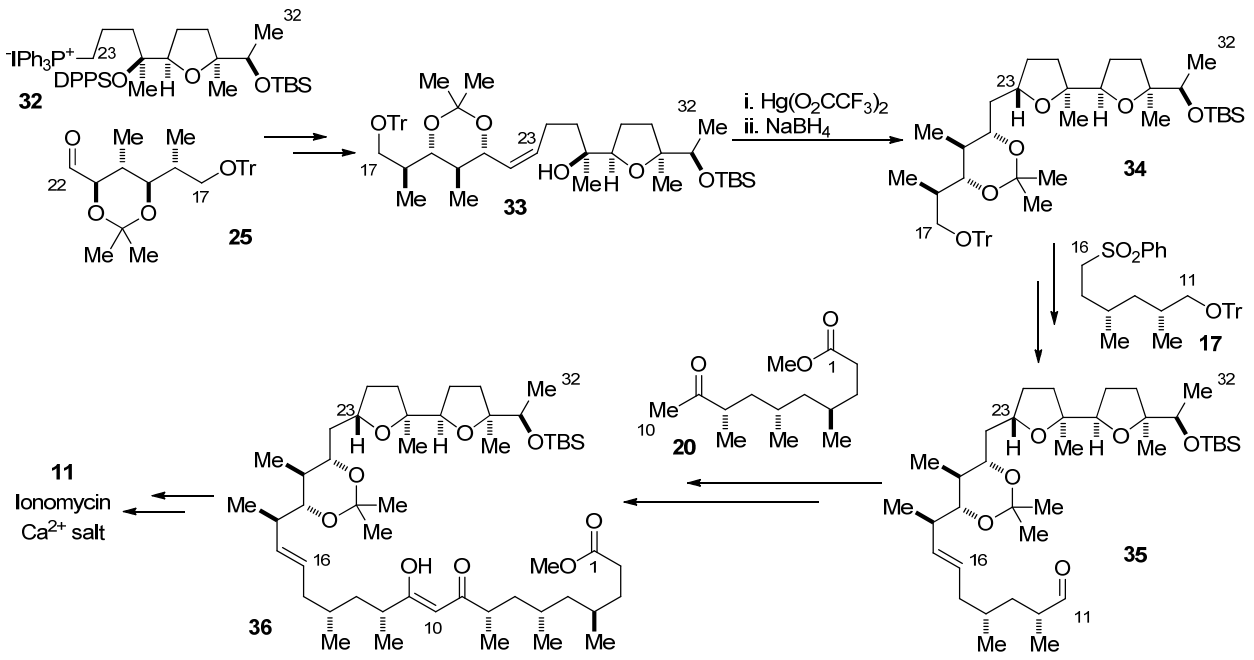

Scheme 4.1.5. Completion of ionomycin calcium salt.

It is suiting that Hanessian's and Evans' syntheses were published back to back as they serve as excellent foils to one another: Hanessian showcases a cyclic strategy using chiral pool material and Evans demonstrates the utility of acyclic control by using recyclable chiral auxiliaries.[15] All the stereocenters in Evans' synthesis were installed directly or derived from stereocenters installed through the addition of oxazolidinone imides **40** or prolinol amides **41** into electrophiles. The key disconnections of ionomycin into four large fragments were the same in Hanessian's and Evans' syntheses.

[15] Fragment syntheses (a) Evans, D. A.; Morrissey, M. M.; Dow, R. L. *Tetrahedron Lett.* **1985**, *26*, 6005-6008. (b) Evans, D. A.; Dow, R. L. *Tetrahedron Lett.* **1986**, *27*, 1007-1010. Total synthesis: (c) Evans, D. A.; Dow, R. L.; Shih, T. L.; Takacs, J. M.; Zahler, R. *J. Am. Chem. Soc.* **1990**, *112*, 5290-5313.

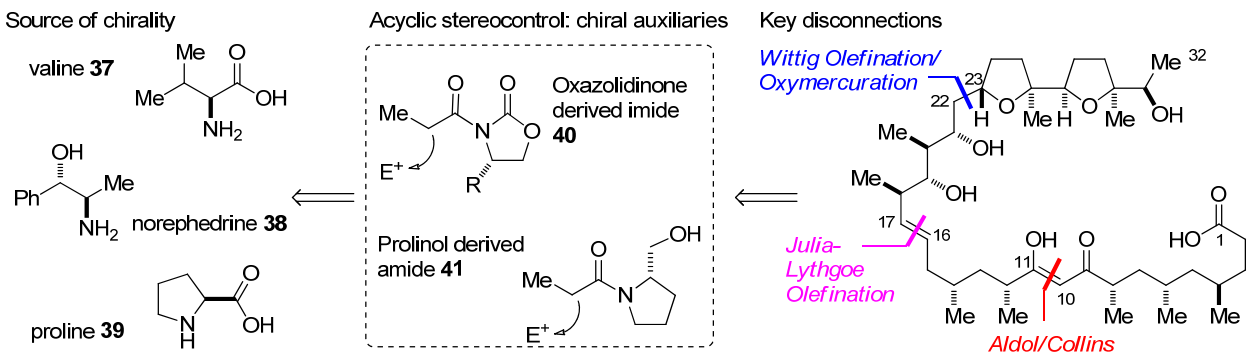

Figure 4.1.3. Outline of Evans' approach to ionomycin.

Evans' synthesis of the C1-C10 fragment **20** used oxazolidinones **40** to directly install the C8 and C4 methyl substituents and indirectly set the C6 stereocenter. An aldol reaction established the C8 methyl stereocenter and a C9 alcohol stereocenter that would be used to direct the C6 methyl stereocenter. The C4 methyl stereocenter was installed using an alkylation of an oxazolidinone with allylic iodide **44**. The final methyl stereocenter was installed using a directed hydrogenation of diene **47** using a cationic rhodium catalyst.

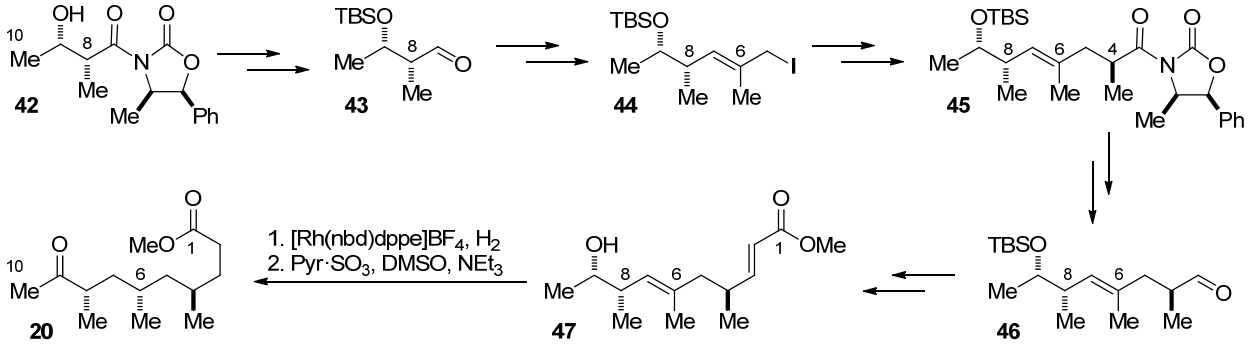

Scheme 4.1.6. Synthesis of C1-C10 fragment **20**.

In the synthesis of the C11-C16 fragment **51**, both methyl stereocenters were installed using alkylation of enolates attached to chiral auxiliaries. The second alkylation in this sequence required the more nucleophilic prolinol-derived amide **41** to install the C12 methyl stereocenter. With both methyl substituents installed, elaboration to sulfone **51** completed the C11-C16 fragment.

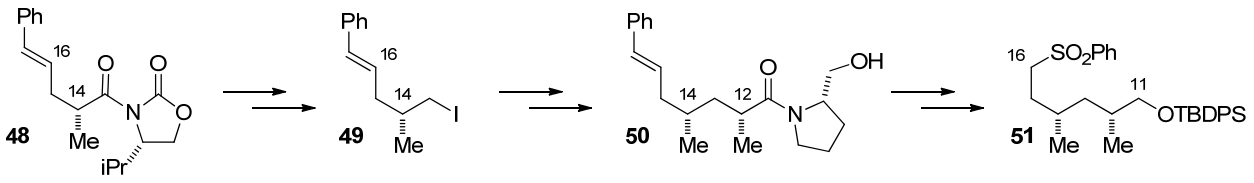

Scheme 4.1.7. Synthesis of C11-C16 fragment **51** using alkylation of valine derived imide and prolinol derived amide to install C12 and C14 stereocenters.

In the synthesis of the C17-C22 synthon **59**, Evans showcased a synthesis of Roche aldehyde **53** and utilized his recently developed crotonimide **54**. Initial efforts to crotylate Roche aldehyde **53** gave disappointing diastereoselectivity, but the aldol reaction of aldehyde **53** and crotonimide **54** yielded aldol adduct **55** that could be elaborated to crotylation product **57** with complete control of stereochemistry. The terminal alkene was dihydroxylated to generate diol **58** with some of the undesired C21 isomer. Both diastereomers were converted to acetonide **59**, and the unwanted C21 diastereomer could be epimerized to the desired isomer.

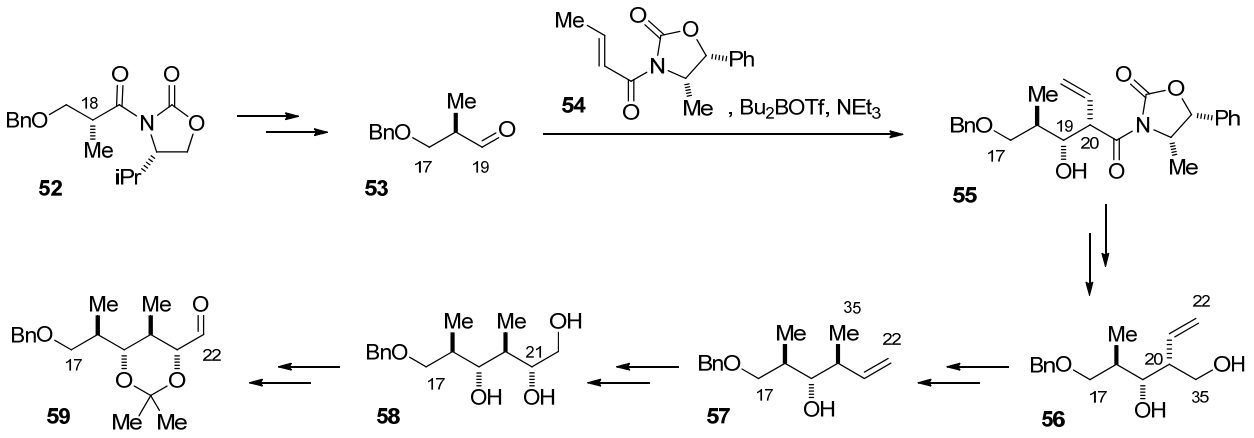

Scheme 4.1.8. The synthesis of aldehyde **59** included a synthesis of Roche aldehyde **53** and the use of crotonimide **54** aldol reaction.

The northern fragment started with an aldol reaction of geraniol derived aldehyde **60** with imide **40c**. An unselective epoxidation/ring closing cascade generated tetrahydrofuran **62** that was lactonized

under basic conditions. Ozonolysis of bicyclic enol **63** generated ketone **64** that underwent a diastereoselective Grignard addition. Derivatization at C23 delivered tetrahydrofuran **65**.

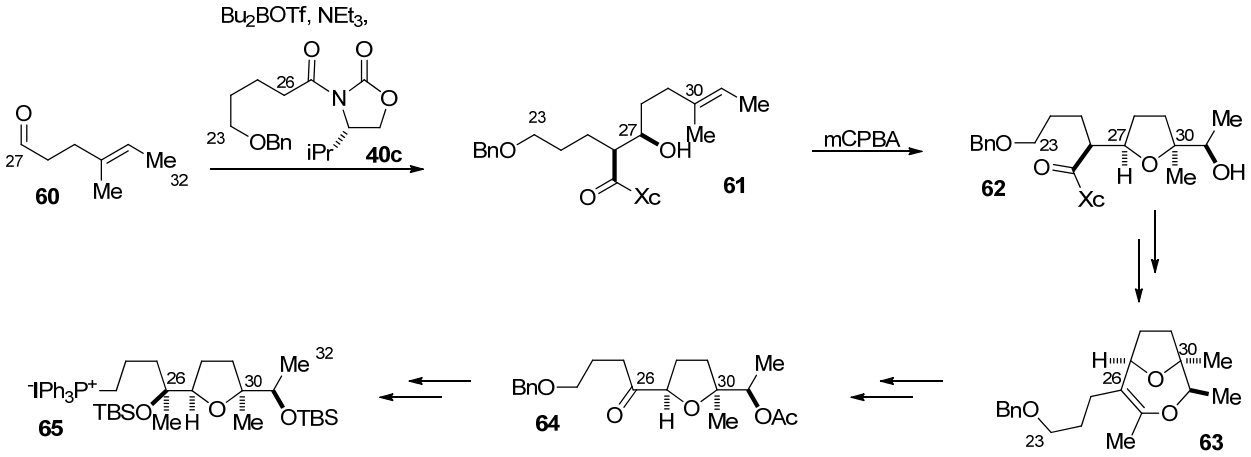

Scheme 4.1.9. An aldol reaction set the initial stereocenter for the C23-C32 fragment **65**.

Evans' and Hannessian's coupling sequences were very similiar. A Wittig olefination joined the C23-C32 fragment **65** and C17-C22 fragment **59** and the C23 stereocenter was established through oxymercuration. The C16-C17 bond was formed with a Julia-Lythgoe olefination to install the trans-double bond. After the aldol/Collins oxidation sequence, protected ionomycin **36** was converted to the calcium salt following earlier group precedent.[16]

[16] Dow, R. L. The total synthesis of ionomycin. Ph.D. Dissertation, Harvard University, Cambridge, MA, 1985.

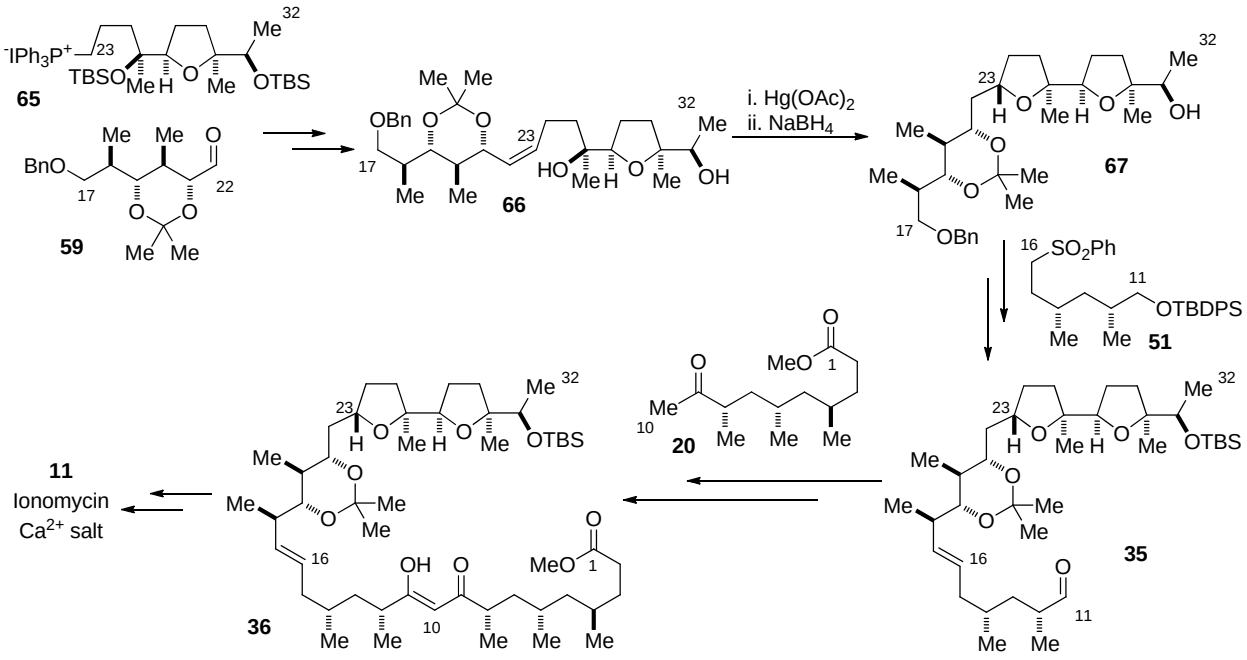

Scheme 4.1.10. Assembling fragments to make ionomycin calcium salt.

Over a decade later, Lautens published his synthesis[17] of ionomycin highlighting the utility of desymmetrization of oxabicyclic alkenes for polypropionate synthesis.[18] This methodology does an excellent job synthesizing polypropionates. However, this approach requires a deoxygenation sequence for deoxypolypropionate generation. The C16-C17 trans-double bond and β-diketone were constructed in the same way as Hanessian and Evans. The top two fragments were joined using a sulfone addition and the C23 stereocenter was generated from an S_N2 displacement of a tosylate.

[17] Fragment synthesis: (a) Lautens, M.; Chiu, P.; Colucci, J. T. *Angew. Chem. Int. Ed.* **1993**, *32*, 281-283. Total synthesis: (b) Lautens, M.; Colucci, J. T.; Hiebert, S.; Smith, N. D.; Bouchain, G. *Org. Lett.* **2002**, *4*, 1879-1882.
[18] Lautens, M.; Fagnou, K.; Hiebert, S. *Acc. Chem. Res.* **2003**, *36*, 48-58.

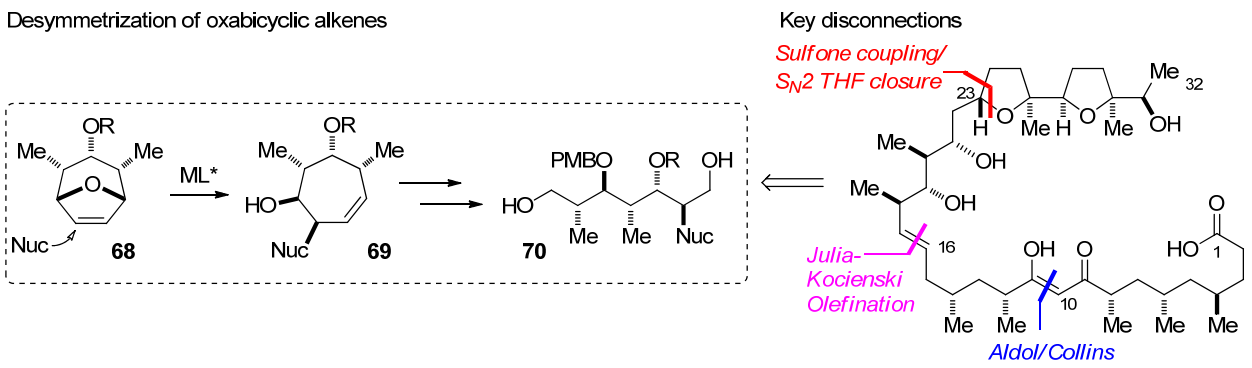

Figure 4.1.4. Lautens' employment of oxabicyclic alkene desymmetrization to synthesize ionomycin.

The C1-C10 fragment synthesis showcases the palladium-catalyzed dialkylzinc opening of oxabicycle alkene **68a**.[19] This single transformation sets every methyl stereocenter for this fragment; C4, C6, and C8. After ozonolysis of the alkene, the alcohols at C5 and C7 were removed through sequential Barton-McCombie deoxygenations.

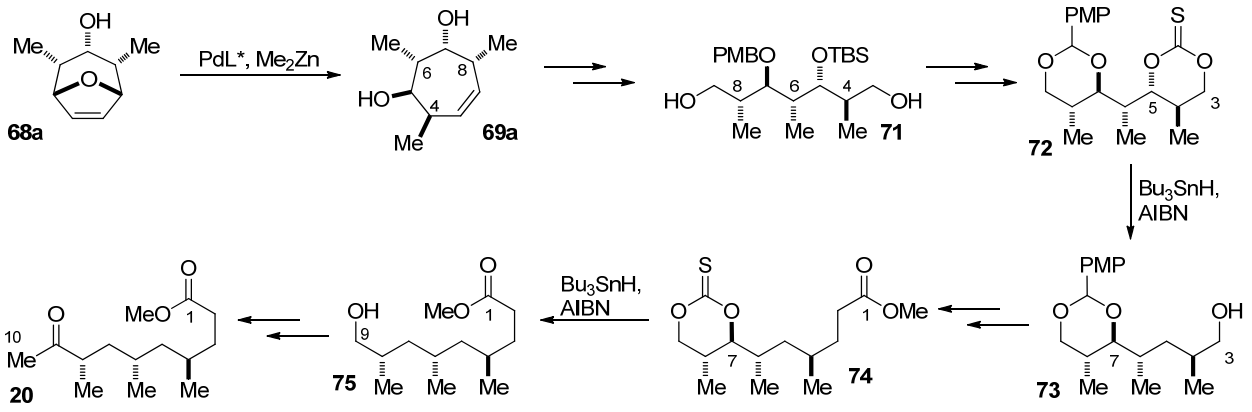

Scheme 4.1.11. C1-C10 fragment synthesis showcasing oxabicyclic alkene desymmetrization.

The synthesis of the C11-C16 fragment **78** used dimethyl glutaric anhydride **1** for the installation of the *syn* dimethyl substituents. The anhydride **1** was converted to the diester, which underwent a desymmetrization with α-chymotrypsin to deliver carboxylester **76**. Conversion of carboxylester **76** to sulfone **78** was straightforward.

[19] (a) Lautens, M.; Renaud, J.-L.; Hiebert, S. *J. Am. Chem. Soc.* **2000**, *122*, 1804-1805. (b) Lautens, M.; Hiebert, S.; Renaud, J.-L. *Org. Lett.* **2000**, *2*, 1971-1973.

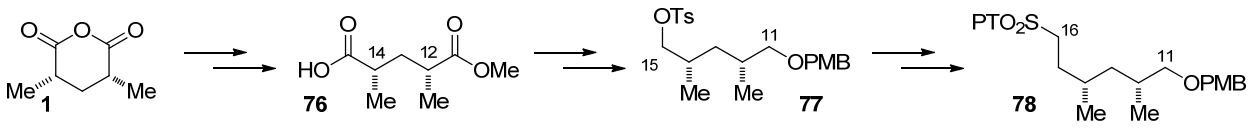

Scheme 4.1.12. The synthesis of the C11-C16 fragment **78** employed enzymatic desymmetrization.

The synthesis of the C17-C23 fragment **80** demonstrated the power of oxabicyclic alkenes desymmetrization to synthesize polypropionates.[20] Desymmetrization of oxabicycle **68b** with diisobutylaluminum hydride (DIBAL) generates alkene **69b** that contains the correct C18-C20 stereotriad. The inversion of the C21 alcohol was necessary before ozonolysis generated diol **79** that now contains the correct stereochemistry of the ionomycin polypropionate. The two alcohols were elaborated to generate aldehyde **80**.

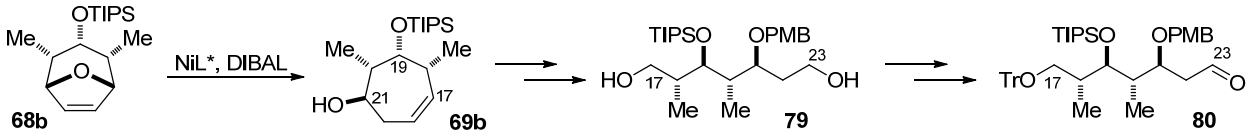

Scheme 4.1.13. The expedient synthesis of the C17-C23 fragment showcases the utility of the oxabicyclic alkene desymmetrization for the synthesis of polypropionates.

Starting from geranyl acetate **81**, the C24-C32 fragment **86** was synthesized. Initial stereoinduction was done with a Sharpless asymmetric epoxidation. After an acid-catalyzed epoxide opening, this stereochemistry was translated using a vanadium-catalyzed epoxidation and cyclization sequence to generate tetrahydrofuran **85**. The C32 oxygen was removed and the C26 alcohol protected to generate C24-C32 coupling partner **86**.

[20] (a) Lautens, M.; Chiu, P.; Ma, S.; Rovis, T. *J. Am. Chem. Soc.* **1995**, *117*, 532-533. (b) Lautens, M.; Rovis, T. *J. Am. Chem. Soc.* **1997**, *119*, 11090-11091.

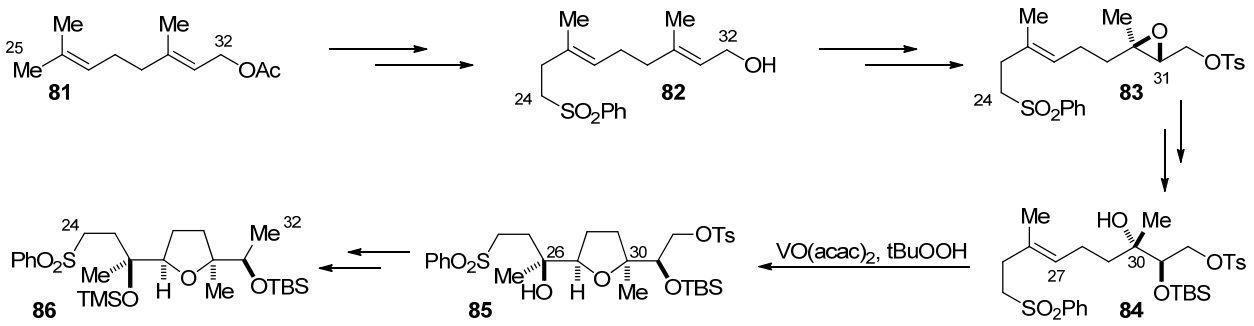

Scheme 4.1.14. C24-C32 fragment synthesis from geranyl acetate **81** using a Sharpless asymmetric epoxidation to install stereochemistry and a vanadium-catalyzed epoxidation to translate the initial stereoinduction.

At this point, the fragments were completed and ready to be coupled. The top fragments were joined by addition of the sulfone anion of **86** into aldehyde **80** and elaboration of the resultant alcohol delivered ketone **87**. The C23 ketone was diastereoselectively reduced and tosylated; S_N2 displacement by the C27 alcohol generated bistetrahydrofuran fragment **88** with the correct C23 stereocenter. The coupling of the C17-C32 fragment with the C11-C16 fragment **78** was done with a Julia-Kocienski coupling. The C1-C10 fragment was installed using an aldol/Collins oxidation sequence. Using a similar deprotection sequence, ionomycin calcium salt **11** was synthesized.

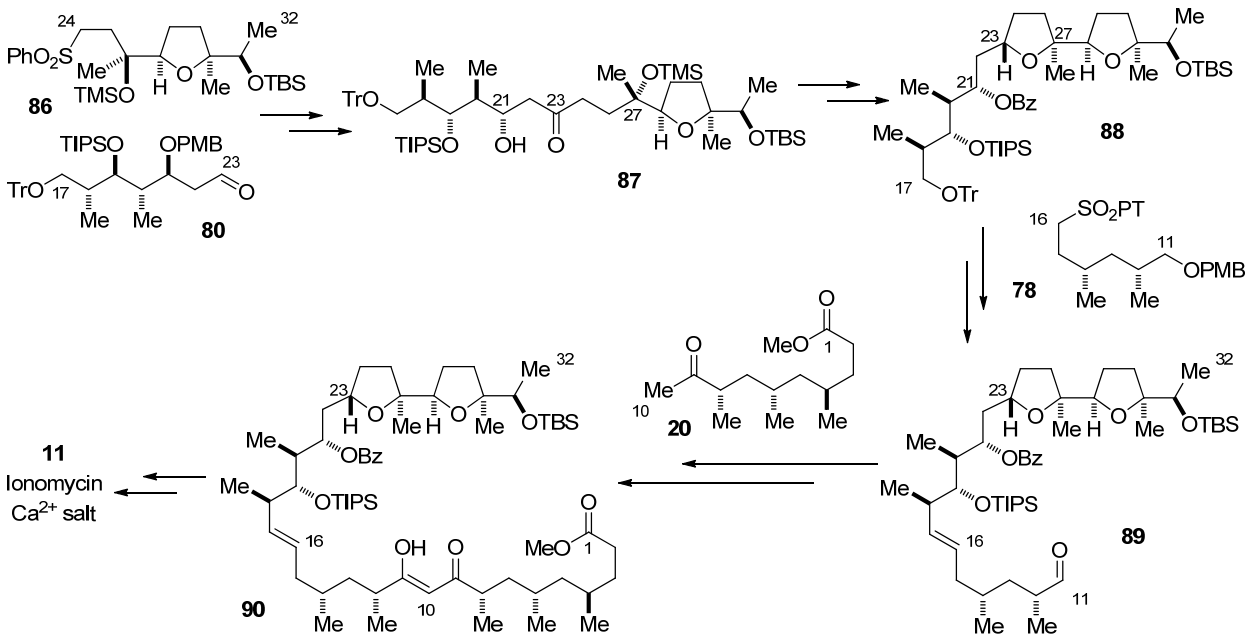

Scheme 4.1.15. Lautens' completion of ionomycin calcium complex **11**.

Kocienski's synthesis[21] of ionomycin featured non-classical disconnections of ionomycin that highlights the utility of newer chemistry to unite and manipulate larger, late stage material. This includes a gold-catalyzed cycloisomerization, the utilization of iron complex **91** to install the C4 methyl stereocenter, a platinum-catalyzed hydrosilylation to install the C21 alcohol, and rhodium-catalyzed rearrangement to install the β-diketone.

[21] Fragment syntheses: (a) Cooksey, J.; Kocienski, P.; Li, Y.-F. *Collect. Czech. Chem. Commun.* **2005**, *70*, 1653-1668. (b) Cooksey, J. P.; Kocienski, P. J.; Li, Y.-f.; Schunk, S.; Snaddon, T. N. *Org. Biomol. Chem.* **2006**, *4*, 3325-3336. (c) Li, Y.; Cooksey, J. P.; Gao, Z.; Kocienski, P. J.; McAteer, S. M.; Snaddon, T. N. *Synthesis*, **2011**, 104-108. Total synthesis: (d) Gao, Z.; Li, Y.; Cooksey, J. P.; Snaddon, T. N.; Schunk, S.; Viseux, E. M. E.; McAteer, S. M.; Kocienski, P. J. *Angew. Chem. Int. Ed.* **2009**, *48*, 5022-5025.

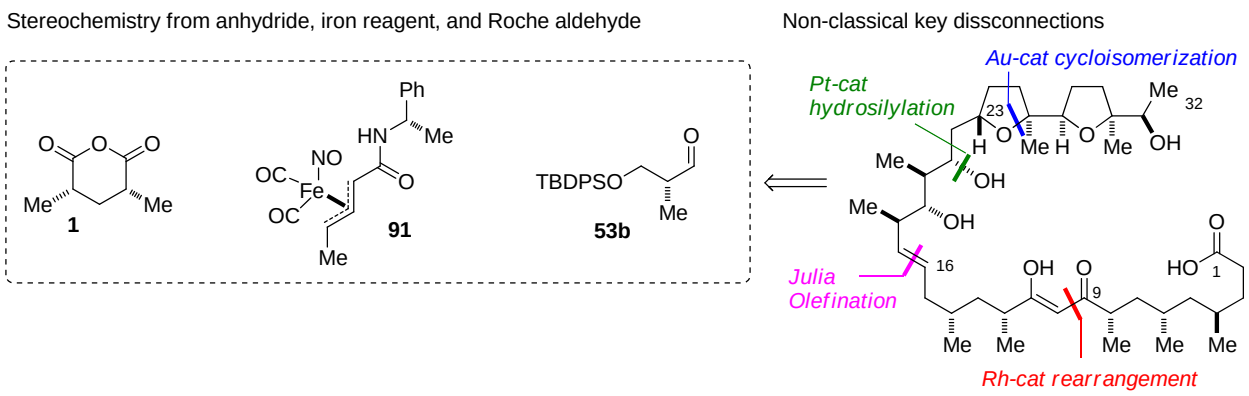

Figure 4.1.5. Kocienski's synthesis that employed newer chemistry to manipulate large fragments.

The assembly of the C1-C9 fragment **97** used anhydride **1** to generate the *syn*-C6 and C8 methyl stereocenters and iron complex **91** to install the C4 methyl stereocenter. After methanolysis of anhydride **1**, resolution using (S)-(-)-1-phenylethylamine generated carboxylester *ent*-**76**. This was converted to cuprate **95** that was added into iron complex **91** generating the C4 methyl substituent stereoselectively. Amide **96** was then elaborated to C1-C9 fragment **97**.

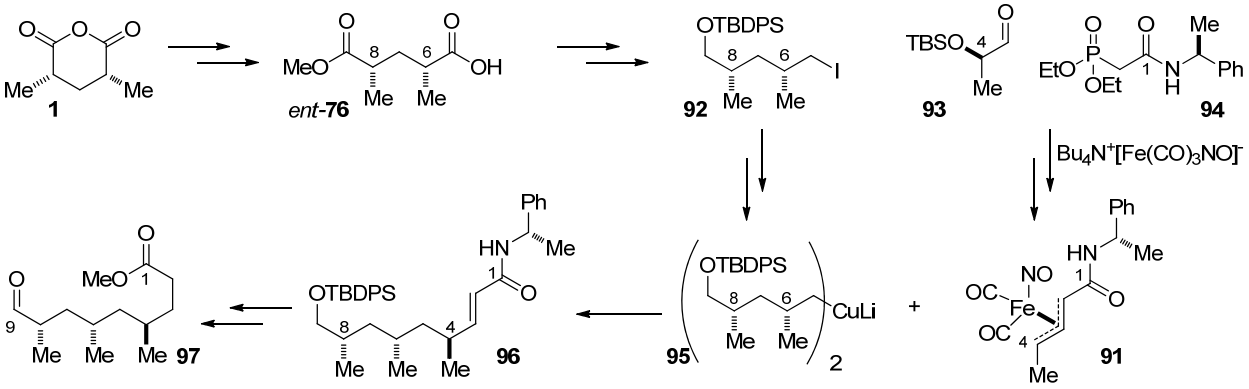

Scheme 4.1.16. Synthesis of C1-C9 fragment from anhydride **1** and iron complex **91**.

After methanolysis of anhydride **1**, resolution using (R)-(+)-1-phenylethylamine generated carboxylester **76**. Homologation using the Arndt-Eistert reaction delivered carboxylic acid **98** that was converted to sulfone **99**.

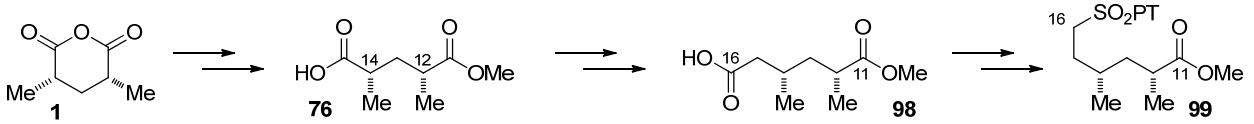

Scheme 4.1.17. C11-C16 fragment synthesis.

Using the stereocenter in Roche aldehyde **53b**, the C19 alcohol and C18 methyl substituent were installed diastereoselectively.[22] Diol differentiation and elaboration furnished aldehyde **102**.

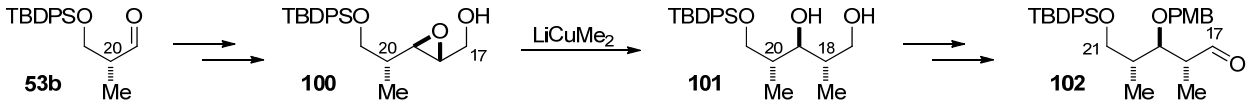

Scheme 4.1.18. C17-C21 fragment synthesis from Roche aldehyde **53b**.

Although geranyl acetate **81** was the starting material, Kocienski's synthesis of bistetrahydrofuran **109** is unique from the other syntheses and features a gold-catalyzed cycloisomerization. Reduction of ynone **103** using Noyori asymmetric transfer hydrogenation generated propargylic alchol **104** with the C27 stereocenter in place. Sharpless asymmetric epoxidation of the allylic alcohol and spontaneous cyclization generated tetrahydrofuran **105**. After manipulation of the alcohols, the alkyne was added into (-)-glyceraldehyde acetal; mesylation of the resultant alcohol generated mesylate **106**. A S_N2' addition of methyl cuprate generated allene **107** that was used in the key gold-catalyzed cycloisomerization to generate bistetrahydrofuran **108**. Reduction of the alkene and alcohol elaboration generated sulfone **109**.

[22] Johnson, M. R.; Nakata, T.; Kishi, Y. *Tetrahedron Lett.* **1979**, *20*, 4343-4346.

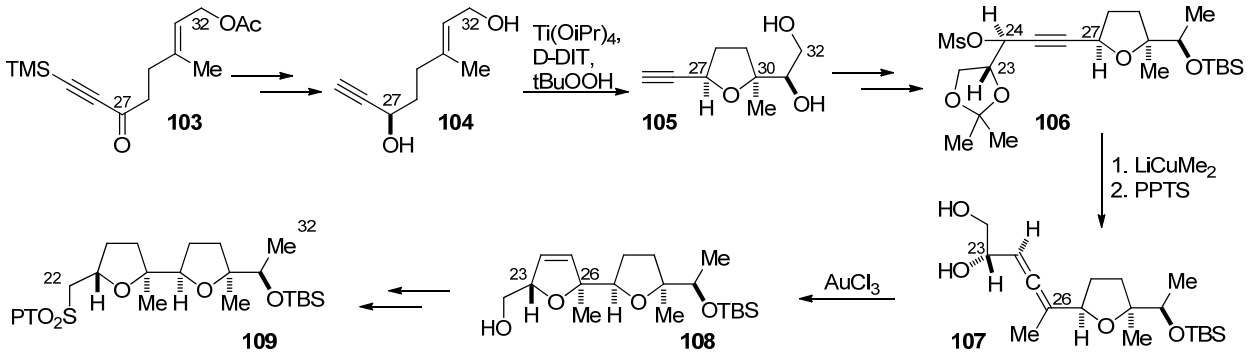

Scheme 4.1.19. The synthesis of the C22-C32 fragment **109** featured a gold-catalyzed cycloisomerization of allene **107**.

Kocienski's synthesis is quite different in the coupling of the northern and southern fragments from the previous syntheses. A Julia-Kocienski olefination coupled bistetrahydrofuran **109** with aldehyde **102**. The C19 alcohol stereocenter was used in an intramolecular hydrosilylation of the alkene to install the C21 alcohol. The C16-C17 bond was installed with another Julia-Kocienski olefination and the C11 ester was converted to an α-diazoketone (**112**). Addition of the α-diazoketone into aldehyde **97** was followed by a rhodium-catalyzed rearrangement to construct β-diketone **36**. This protected ionomycin was converted to the calcium complex **11** as described before.

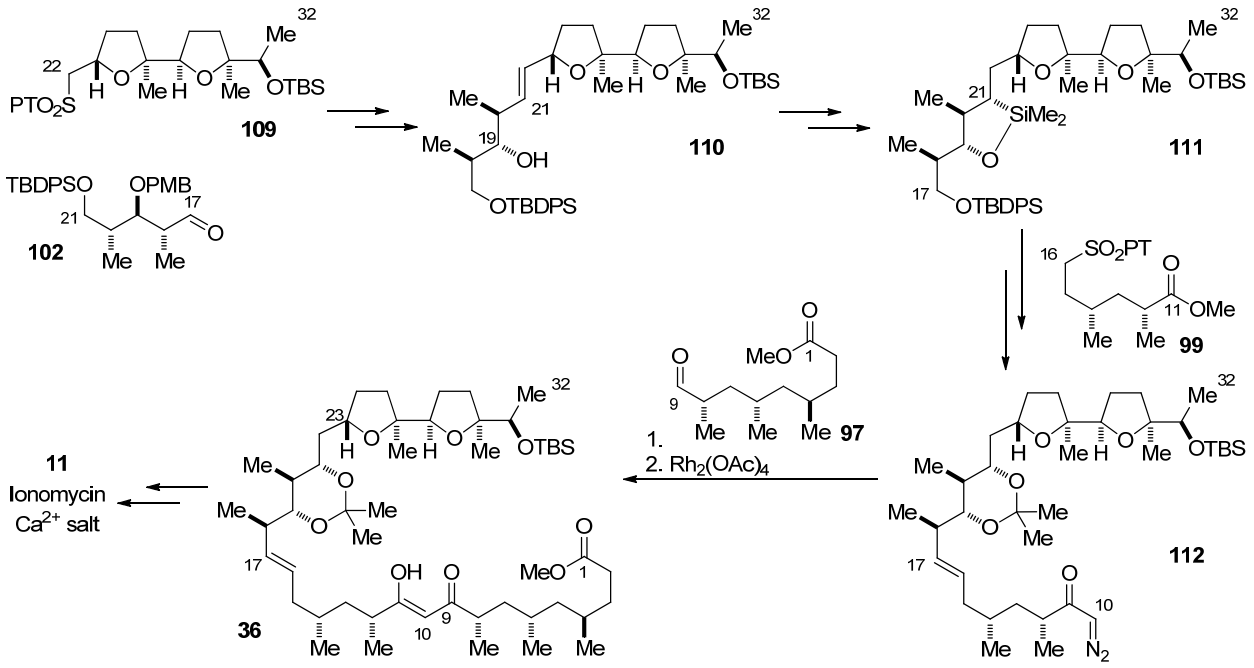

Scheme 4.1.20. The coupling sequence was a departure from the classical disconnections and showcased a late stage rhodium-catalyzed rearrangement to install the β-diketone.

4.2. Previous Work towards Ionomycin in the Rovis Group

The route to ionomycin **10** undertaken in our lab was to showcase the desymmetrization methodology developed in the group (Figure 4.2.1). We sought to employ this methodology in the synthesis of three of the four fragments. The C1-C9 and C10-C16 deoxypolypropionate fragments would be derived from ketoacids **2** generated from the desymmetrization of dimethyl glutaric anhydride **1**. The C17-C22 polypropionate fragment would come from ketoacid **4** by the desymmetrization of trisubstituted anhydride **3**. This approach mimics previous syntheses in that the molecule is divided into four fragments with slightly different disconnects. Our first generation synthesis disconnected the β-diketone using an aldol between methyl ketone **116** and aldehyde **115**; previous aldol disconnections were between C10 and C11, whereas this plan was between C9 and C10. The initial Julia olefination to install the trans-double bond initially put the aldehyde on C16 (**115**) and the sulfone on C17 (**114**). An enol silane addition (**114**) into an oxocarbenium generated from lactol **113** was to connect C22 and C23 and establish the C23

stereocenter. Due to difficulties with the Julia-Kocienski olefination in our first generation approach, the coupling partners were switched in our second generation. This placed the sulfone on C16 (**119**) and the aldehyde on C17 (**118**). Finally, a third generation synthesis was needed due to difficulties in establishing the correct C23 stereocenter using the oxocarbenium enol silane addition. We joined the northern fragments through a palladium cross coupling of thioester **120** and alkyne **121**. The C23 stereocenter was installed through two approaches, a reductive cyclization and ketone reduction/S_N2 displacement sequence. During our initial route exploration towards the synthesis of ionomycin, we used (*S*)-tBuPhox, as this was the cheaper antipode of ligand. Towards the end of the second generation synthesis, we switched to (*R*)-tBuPhox for material that we hoped would be incorporated into our synthetic ionomycin.

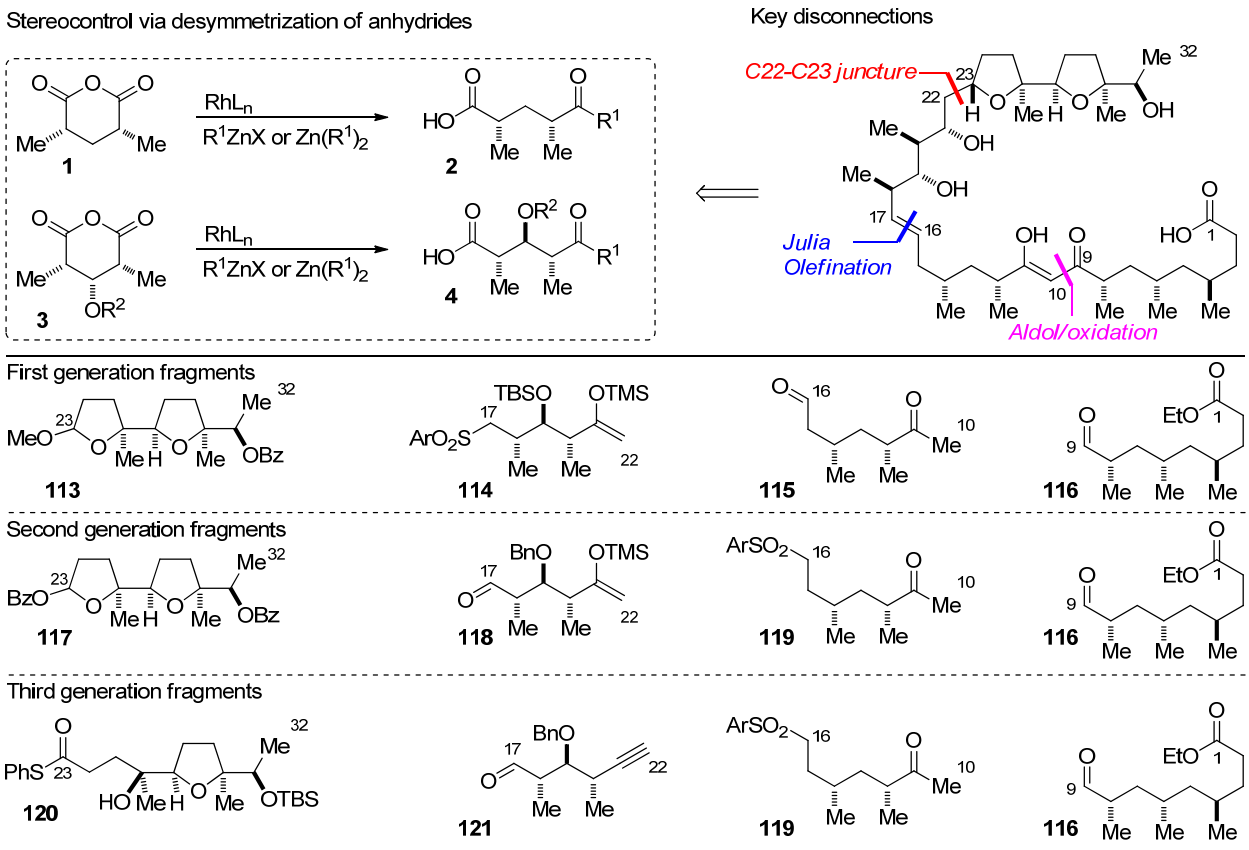

Figure 4.2.1. Rovis group's approach to ionomycin **10** utilizing desymmetrization of anhydrides to construct polypropionate and deoxypolypropionate fragments.

By employing the desymmetrization methodology, Dr. Cook synthesized the carbon skeleton of the C1-C9 fragment. Desymmetrization of anhydride **1** with dialkyl zinc reagent **122**[23] provides ketoacid **2a** in good yield and enantioselectivity. This installs the *syn* dimethyl substituents and the carbon backbone in a single step. Alkylation of unprotected ketoacid **2a** installs the C4 methyl substituent diastereoselectively. We believe this alkylation goes through a chelate of the potassium counterion (**I**) by the carboxylate and enolate. When methyl ester **127** is subjected to the reaction conditions, a 1:1 mixture of C4 diastereomers of ketoester **128** is generated. The ketone was protected as the dithiolane to make carboxylic acid **124**. Chemoselective reduction of the carboxylic acid followed by reoxidation generates aldehyde **126**.

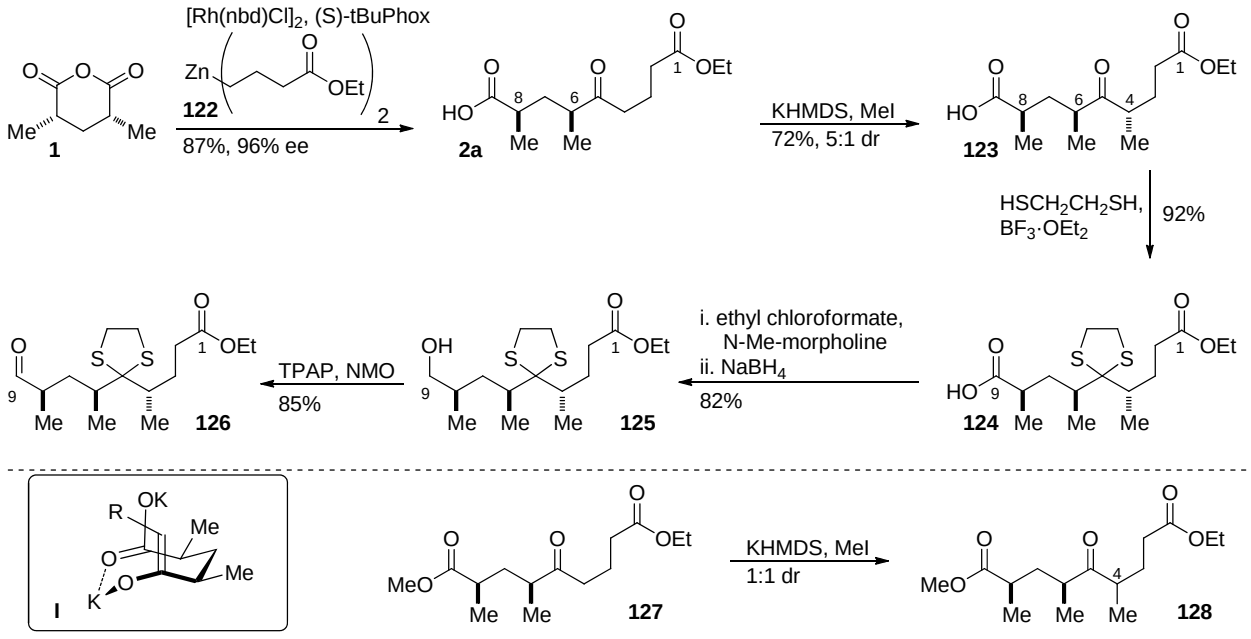

Scheme 4.2.1. Synthesis of C1-C9 fragment using desymmetrization chemistry.

Using the same starting material, the penultimate piece of the C10-C16 fragment was synthesized. Desymmetrization of anhydride **1** with methyl zinc bromide generates ketoacid **2b** in good yield and enantioselectivity with the requisite *syn* dimethyl substituents on C12 and C14. Global

[23] For organozinc reagents, see; (a) Rozema, M. J.; Sidduri, A.; Knochel, P. *J. Org. Chem.* **1992**, 57, 1956-1958. (b) Knochel, P.; Singer, R. D. *Chem. Rev.* **1993**, *93*, 2117.

reduction, iodination of the primary alcohol, and oxidation of the secondary alcohol generates iodoketone **129**. Displacement of the iodide generates cyanoketone **130** that is poised to be used in the aldol coupling, where the cyano group serves as a protected aldehyde.

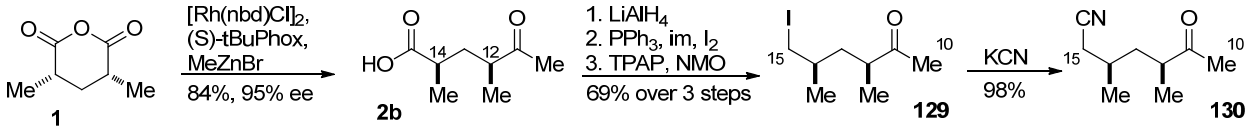

Scheme 4.2.2. Synthesis of C10-C16 fragment using anhydride desymmetrization methodology.

Attempts to make the C17-C22 fragment via anhydride desymmetrization were thwarted by difficulties in substrate synthesis. Utilizing the approach devised by Harada and Oku,[24] diol **133a** was synthesized, but direct oxidation was not successful. Instead, an approach based on crotylation of Roche ester **134** was utilized.[25] Crotylation of aldehyde **135** generates alkene **136**. Wacker oxidation of the alkene and sulfone oxidation makes methyl ketone **137**, completing the synthesis of enol silane precursor **137**.

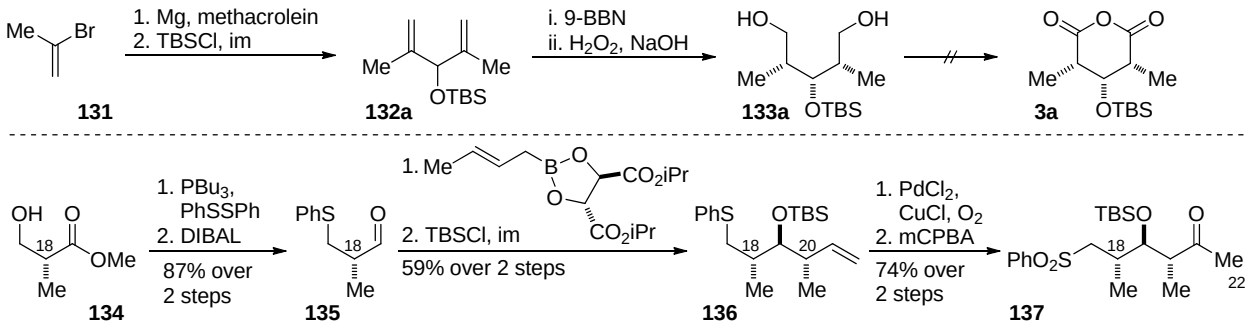

Scheme 4.2.3. Oxidation of diol **133** was unsuccessful. Synthesis of C17-C22 fragment **137** from Roche ester **134** was successful.

[24] Harada, T.; Matsuda, Y.; Uchimura, J.; Oku, A. *J. Chem. Soc., Chem. Commun.* **1990**, 21-22.
[25] Roush, W. R.; Palkowitz, A. D.; Palmer, M. A. J. *J. Org. Chem.* **1987**, *52*, 316-318.

Using a modified procedure developed by Paterson,[26] the synthesis of the C23-C32 fragment **113** was achieved (Scheme 4.1.3). Allylic oxidation of geranyl acetate **81** generates allylic alcohol **138**.[27] Stereoinduction is accomplished using Sharpless asymmetric epoxidation.[28] Conversion of the alcohol to an alkyl iodide and acetate hydrolysis delivers epoxyalcohol **139**. Two carbon homologation using the enolate of tert-butyl acetate followed by Sharpless epoxidation generates diepoxide **140**. Cyclization of the diepoxide was done using camphorsulfonic acid as outlined by Paterson. Conversion of the primary alcohol to the bromide enables its removal via hydrogenolysis.[29] Reduction using DIBAL generates the lactol that can be converted to acetal **113**.

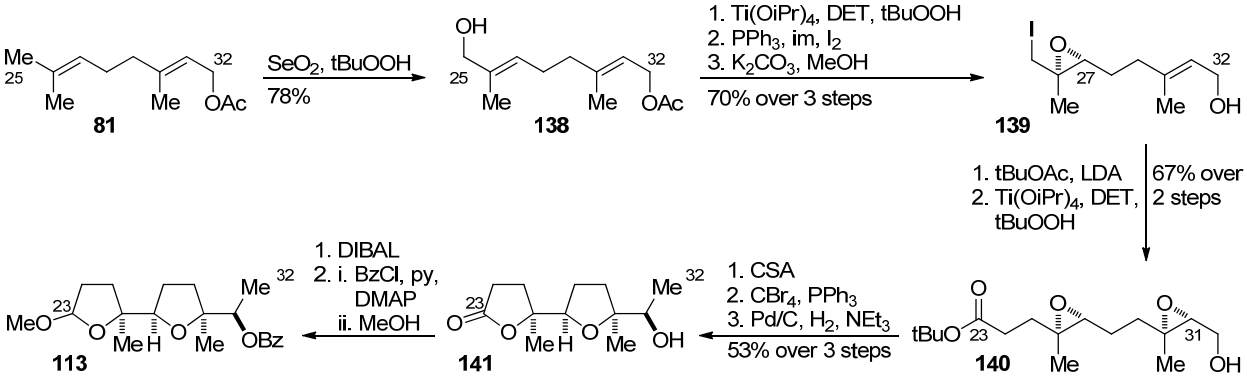

Scheme 4.2.4. Initial synthesis of bistetrahydrofuran fragment.

Dr. Cook showed that the coupling of northern fragments and the southern fragments are possible. The aldol reaction of cyanoketone **130** with aldehyde **126** generates β-hydroxyketone **142**. After generation of the oxocarbenium from acetal **113**, addition of enol silane **143** generates bistetrahydrofuran **144** in modest diastereoselectivity. This selectivity was expected to improve with the use of the larger enol silane in the real coupling.

[26] Paterson, I.; Boddy, I.; Mason, I. *Tetrahedron Lett.* **1987**, *28*, 5205-5208.
[27] Umbreit, M. A.; Sharpless, K. B. *J. Am. Chem. Soc.* **1977**, *99*, 5526-5528.
[28] Katsuki, T.; Sharpless, K. B. *J. Am. Chem. Soc.* **1980**, *102*, 5974-5976.
[29] Pinder, A. R. *Synthesis* **1980**, 425-452.

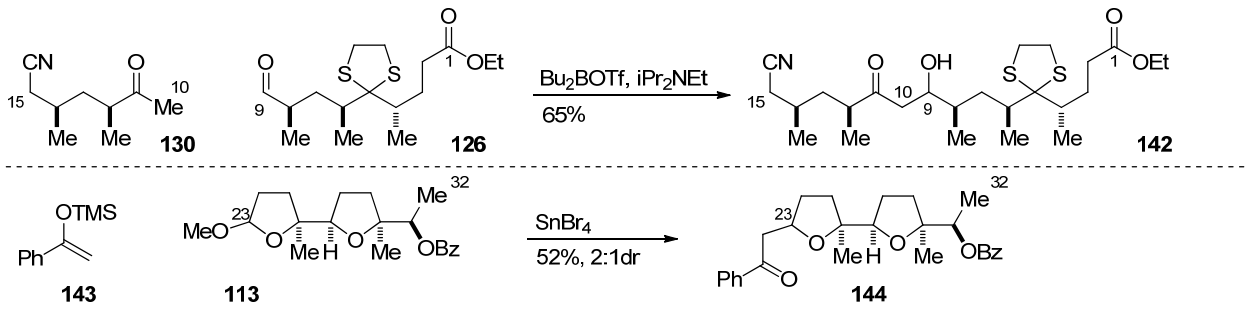

Scheme 4.2.5. Demonstration that initial fragment couplings are possible.

At this point, Dr. Cook left and a new postdoctoral associate, Dr. Brian Cochran, picked up the project.[30] Dr. Cochran's synthesis of the C1-C9 fragment **116** was accomplished with some modifications to the original approach. The chemoselective reduction of the carboxylic acid over the ester is done with borane and recalcitrant dithiolane is removed with Raney® nickel.

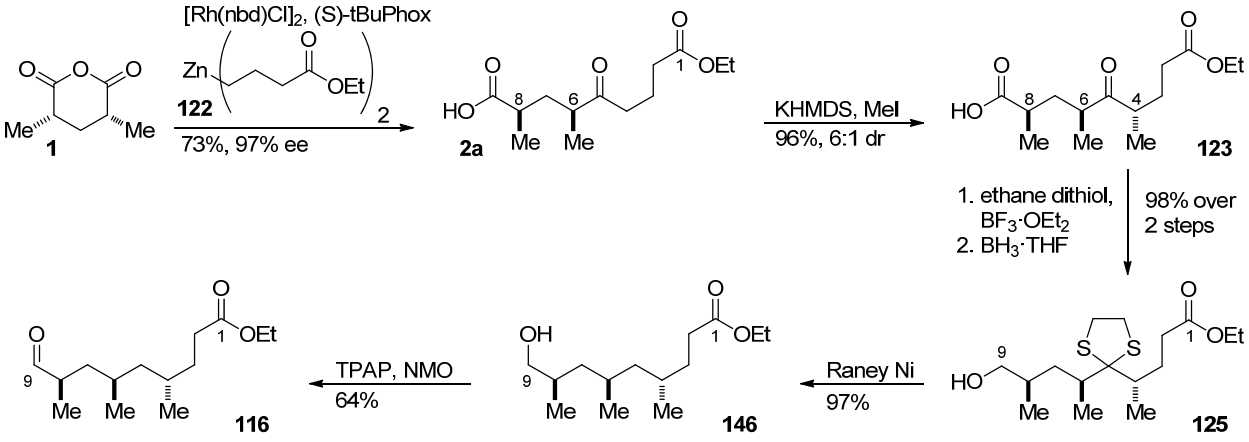

Scheme 4.2.6. Revised route to C1-C9 fragment including removal of the dithiolane protecting group.

The first generation Julia coupling partner **147** was synthesized from previously made cyanoketone **130**. Protection of the ketone as the acetal and reduction of the cyanide using DIBAL generates aldehyde **147**.

[30] Cochran, B. M. Colorado State University, Fort Collins, CO. Unpublished work, 2012.

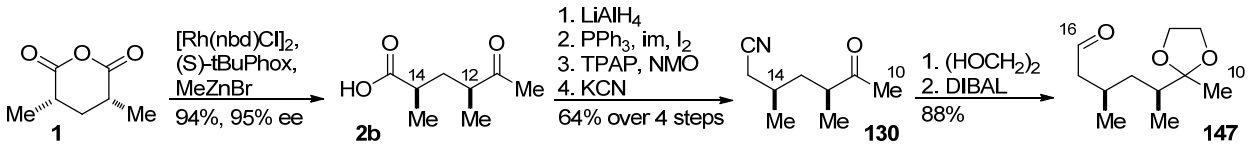

Scheme 4.2.7. Synthesis of C10-C16 fragment with the aldehyde on C16.

One of Dr. Cochran's key breakthroughs was the synthesis the trisubstituted anhydride **3**. Attempts towards a one step oxidation of diol **133** to the diacid produced lactone **148**. Through the use of a Swern oxidation, dialdehyde **149** is generated.[31] Pinnick-Lindgren oxidation makes the desired diacid that is cyclized using trifluoroacetic anhydride to generate trisubstituted anhydride **3**.

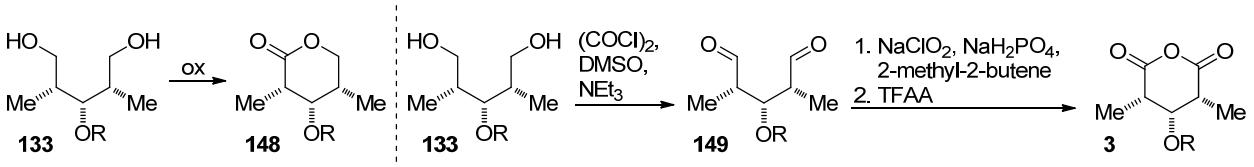

Scheme 4.2.8. Trisubstituted anhydride synthesis: problematic one step oxidation and solution via dialdehyde synthesis.

After synthesis of trisubstituted anhydride **3**, its desymmetrization worked efficiently. Using the same catalyst and zinc reagents, a range of protected (methyl, benzoate, acetate, and benzyl) trisubstituted anhydrides deliver ketoacids **4** with a *trans*, *trans* stereotriad. Benzyl was chosen as the protecting group in the total synthesis of ionomycin due to its stability to a range of reaction conditions and its efficiency in the desymmetrization reaction. Despite the benefits of the benzyl protecting group in the desymmetrization and subsequent reactions, the hydroboration step proceeds in lower diastereoselectivity (3.5:1).

[31] (a) Harada, T.; Kagamihara, Y.; Tanaka, S.; Sakamoto, K.; Oku, A. *J. Org. Chem.* **1992**, *57*, 1637-1639. (b) Kann, N.; Rein, T. *J. Org. Chem.* **1993**, *58*, 3802-3804. (c) Tullis, J. S.; Vares, L.; Kann, N.; Norrby, P.-O.; Rein, T. *J. Org. Chem.* **1998**, *63*, 8284-8294.

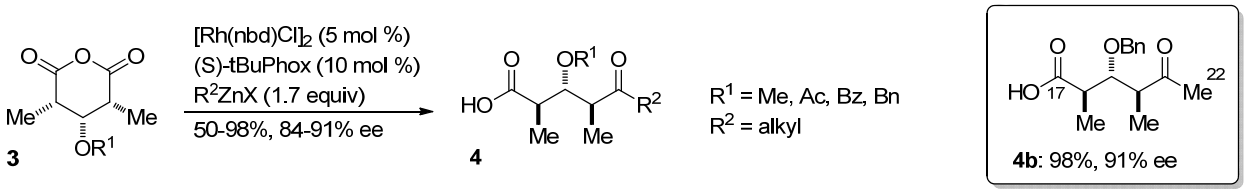

Scheme 4.2.9. Desymmetrization of trisubstituted anhydrides **3** delivering ketoacids with *trans*, *trans* stereotriads.

With the desymmetrization of the trisubstituted fragment established, elaboration to fragments used in the synthesis of ionomycin was undertaken. Global reduction of ketoacid **4b**, selective tosylation of the primary alcohol, and oxidation of the secondary alcohol generates methyl ketone **150**. Displacement of the tosylate with benzothiazole (BT) or phenyl tetrazole (PT) generates the thioether that is oxidized using *meta*-chloroperbenzoic acid (*m*CPBA). Conversion of the methyl ketone to the enol silane generates the enol silane fragment (**114**) to be added into the C23 oxocarbenium.

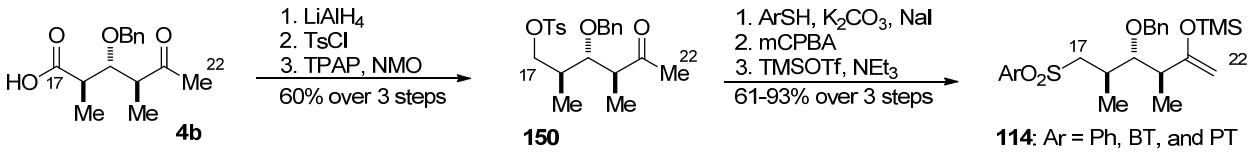

Scheme 4.2.10. C17-C22 fragment synthesis using anhydride desymmetrization methodology.

The C23-C32 fragment was synthesized in the same fashion with minor procedural changes. The iodination and acetate hydrolysis were telescoped in the synthesis of iodoepoxide **139**. Better results are achieved when the bromination and epoxide cyclization reaction order are swapped. Finally, a basic wash allows for the successful isolation of benzoyl acetal **117**.

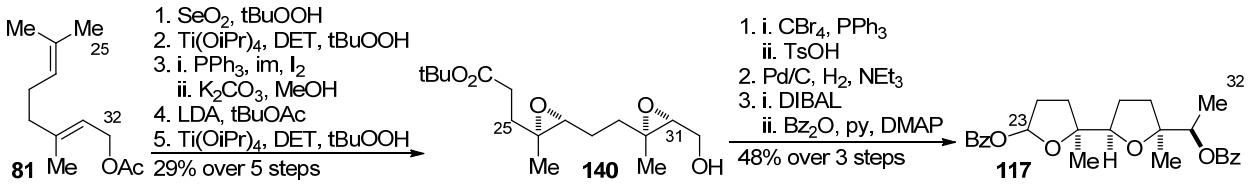

Scheme 4.2.11. Revised synthesis of C23-C32 fragment **117**.

With the C17-C22 and C23-C32 fragments in hand, the enol silane addition was attempted. Addition of enol ether **114a** into the oxocarbenium generated from acetal **117** synthesized the entire C17-C32 carbon framework (**153**).[32] The proposed stereochemical model (**II**) for the addition suggested that steric hinderance of the second tetrahydrofuran would prevent attack of the enol silane from top face of the oxocarbenium and favor bottom side attack to provide the desired C23 diastereomer.

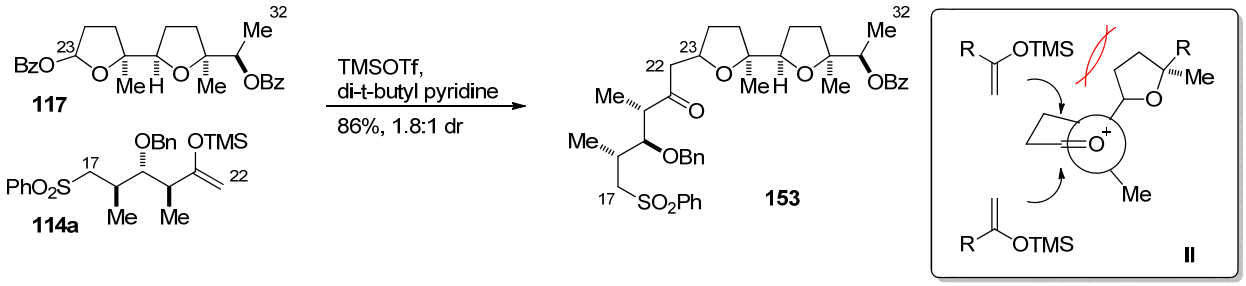

Scheme 4.2.12. Enol silane addition into oxocarbenium: reaction and proposed selectivity model.

Elaboration of the C17-C32 fragment **153** generated Julia coupling partner **154a**. Removal of the benzyl protecting group revealed the free C19 alcohol that was used to do a directed reduction of the C21 ketone.[33] Protection of the 1,3-diol as the acetal generated coupling partner **154a**.

[32] This coupling was also done with the tosylalcohol in place of the sulfone (Scheme 4.2.15); 94%, 3.5:1 dr.
[33] Evans, D. A.; Hoveyda, A. H. *J. Org. Chem.* **1990**, *55*, 5190-5192.

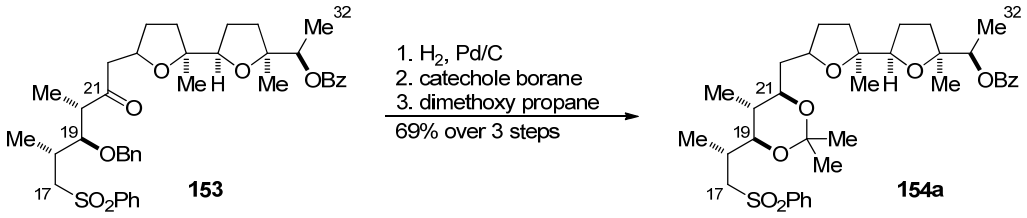

Scheme 4.2.13. Elaboration to Julia coupling partner **154a**.

With C17-C32 sulfone **154** and C10-C16 aldehyde **147** synthesized, the Julia-Kocienski coupling was attempted. Despite the sulfones and conditions tried in the coupling,[34] no desired product was observed.

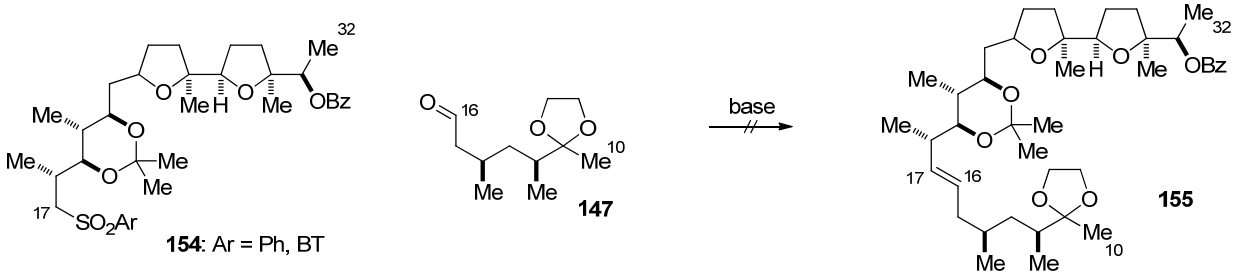

Scheme 4.2.14. Attempts to couple C17 sulfone **154** failed.

The previous syntheses of ionomycin joined these fragments via a Julia olefination, but the coupling partners were reversed: the sulfone was on C16 and the aldehyde was on C17. After these unsuccessful coupling attempts, it was decided to switch the coupling partners and a revised second generation route was drafted and pursued (Figure 4.2.1).

The top fragment was constructed using a modification of the first generation approach. Methyl ketone **151** was converted to enol silane **156**, which can be coupled in the same fashion to acetal **117**. The same sequence from ketone **157** generates tosyl protected alcohol **158**. A number of conditions were

[34] BT derivative was synthesized through displacement of tosylate **150** (Scheme 4.1.10) followed by oxidation with $(NH_4)_6Mo_7O_{24}\cdot 4H_2O$.

attempted to remove the tosylate before a light induced deprotection was shown to work.[35] After oxidation, this sequence generated targeted aldehyde **159**.

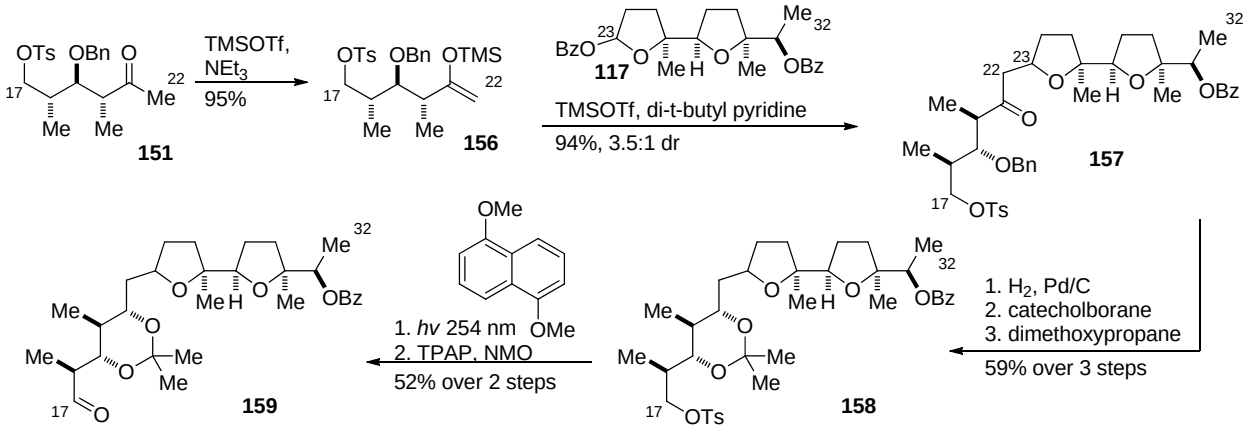

Scheme 4.2.15. Revised route to C17-C32 fragment.

The synthesis of C10-C16 fragment **119** was accomplished with two different approaches using common intermediate **129**. Starting from iodoketone **129**, homologation and elaboration to aldehyde **147** can be achieved by using either cyanide or dithiane. Reduction of the aldehyde and iodination generates alkyl iodide **160**. Displacement of the iodide with phenyl tetrazole and oxidation generates the sulfone. The ketal was deprotected during workup to generate ketosulfone **119**.

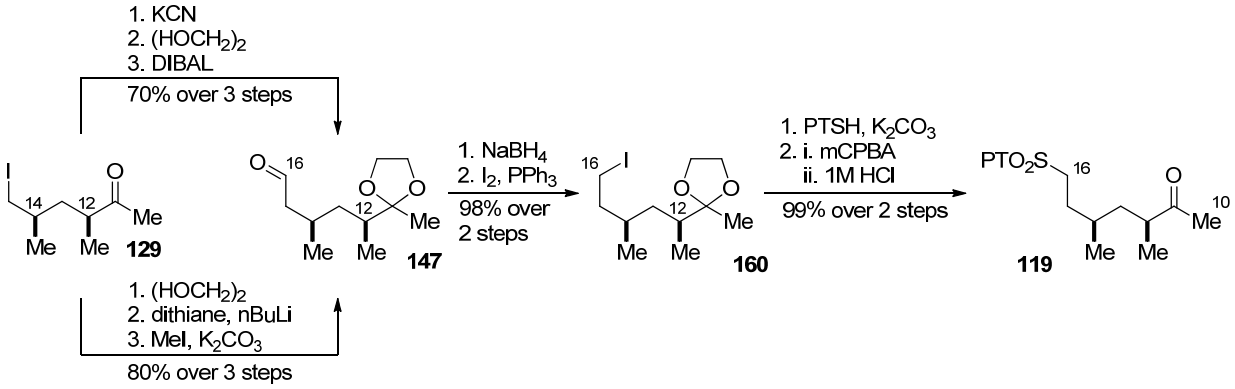

Scheme 4.2.16. Revised route to C10-C16 fragment.

[35] Nishida, A.; Hamada, T.; Yonemitsu, O. *J. Org. Chem.* **1988**, *53*, 3386-3387.

The aldol coupling of the bottom fragment was further optimized. The aldol reaction is accomplished using 9-iodo-9-borabicyclo[3.3.1]nonane, a commercially available boron reagent, that makes the reaction higher yielding and more consistent. Oxidation of β-hydroxyketone **161** is accomplished using 2-iodoxybenzoic acid to generate the β-diketone **162**.[36]

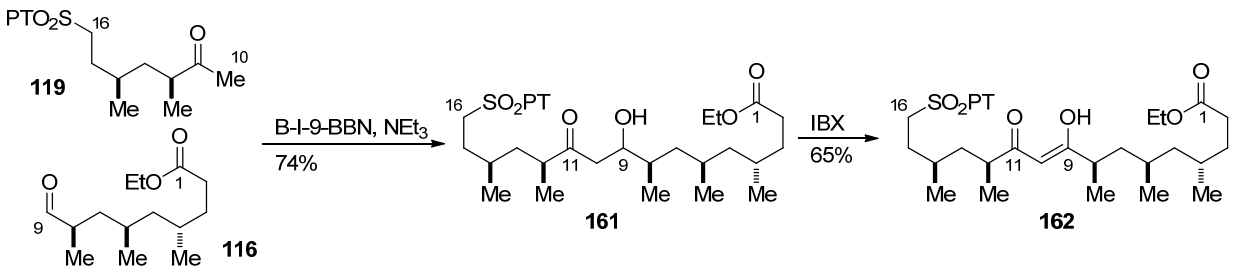

Scheme 4.2.17. Coupling and oxidation of C1-C16 fragment.

At this point, the entire northern and southern fragments were ready for coupling. Julia-Kocienski coupling of aldehyde **159** and unprotected β-diketone **162** was successful. This reaction generates the entire carbon skeleton of ionomycin. Acetal removal is accomplished using trifluoroacetic acid to generate diol **164**,[37] but removal of the benzoate and cleavage of the ethyl ester were sluggish. This demonstrated that an aggressive coupling of protected aldehyde **159** with the unprotected β-diketone **162** was a viable route; the synthesis of the entire skeleton was accomplished in a convergent fashion.

[36] Bartlett, S. L.; Beaudry, C. M. *J. Org. Chem.* **2011**, *76*, 9852-9855.
[37] This reaction was done on *epi*-C18-21 of **163** as drawn in Scheme 4.2.18.

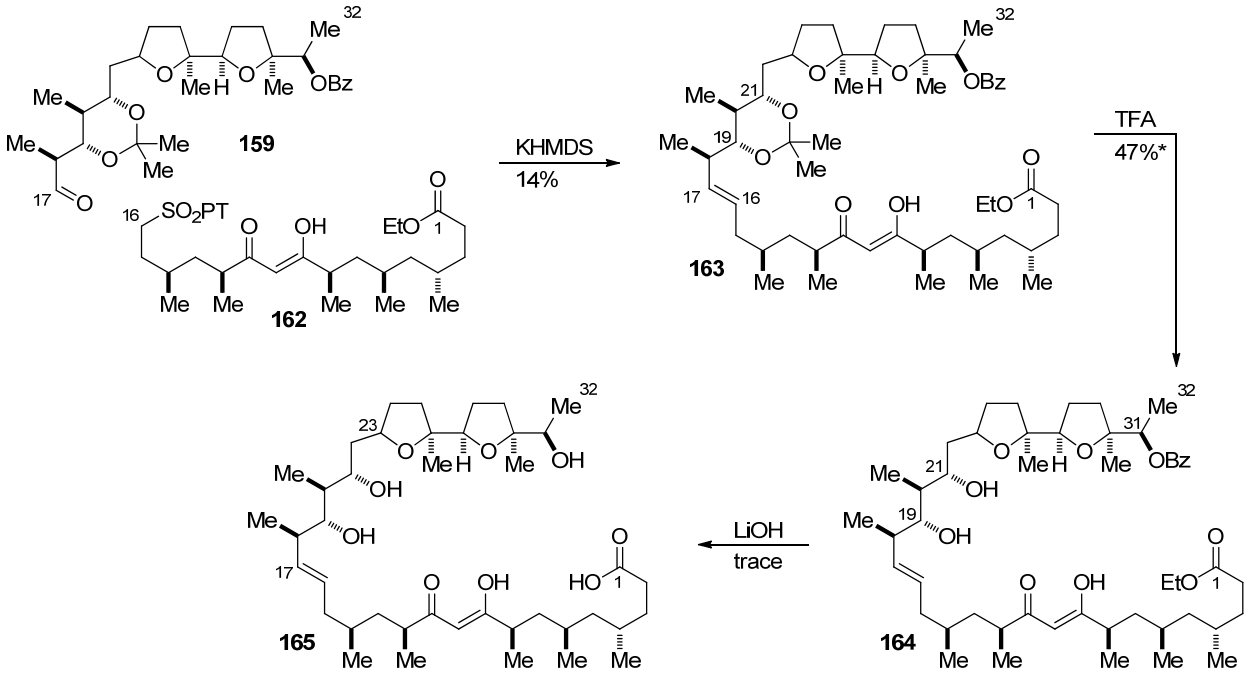

Scheme 4.2.18. Successful Julia-Kocienski coupling and elaboration to acid **165**.

4.3 Synthesis of C1-C16 Fragment

When I initially joined the project, I was tasked with synthesizing the C1-C16 fragment. The C1-C9 fragment was synthesized as before with some minor optimization. In my hands, the use of $[Rh(nbd)OAc]_2$ as the precatalyst[38] in place of $[Rh(nbd)Cl]_2$ provides higher yields[39] in the desymmetrization of dimethyl glutaric anhydride **1**[40] with dialkylzinc reagent **122**. The conversion of the

[38] For the synthesis and chemistry of $[Rh(nbd)OAc]_2$, see: (a) Henderson, D. D.; Cochran, B. M.; Filloux, C. M.; Rovis, T. *Submitted*. For review on halide influence on metal catalysis, see: (b) Fagnou, K.; Lautens, M. *Angew. Chem. Int. Ed.* **2002**, *41*, 26-47.

[39] In a side by side comparison using the same zinc reagent (**122**)and trimethoxybenzene as the internal standard, $[Rh(nbd)Cl]_2$ showed 60% conversion and $[Rh(nbd)OAc]_2$ showed 80% conversion by ^1H NMR of the unpurified reactions. Additionally, the $[Rh(nbd)OAc]_2$ reaction was cleaner as well.

[40] Crystal structure: Oberg, K. M.; Rovis T. (2013) Private communication to the Cambridge Structural Database, deposit number CCDC 946678.

ketone to the dithiolane can only be run for a short amount of time as epimerization is observed. The Raney® nickel reduction is capricious. Yields are variable and sometimes decomposition is observed.[41]

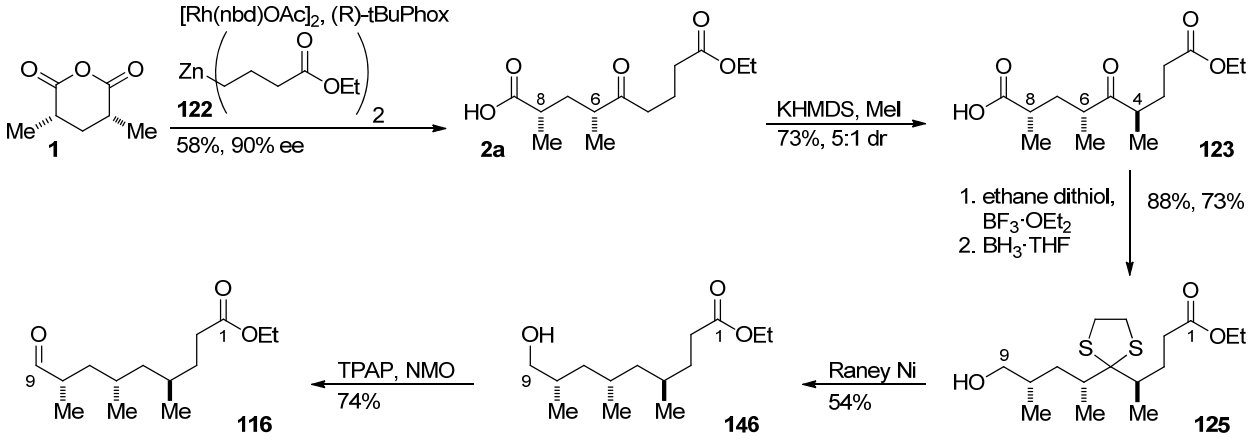

Scheme 4.3.1. Route to C1-C9 fragment.

The route to sulfone **119** is similar to the previously outlined route in Scheme 4.2.16. The desymmetrization of dimethyl glutaric anhydride **1** with methyl zinc bromide generates ketoacid **2b** (Scheme 4.3.2).[42] Generation of thiol **168** is done using a two step process, conversion to the iodide and displacement with thiophenyl tetrazole. An alternative way to access this compound is through use of the Mitsunobu reaction to generate thiol ether **65** in one step.[43] Oxidation of thiol ether **168** to sulfone **169a** is done using meta-chloroperbenzoic acid. Epimerization at C12 is problematic during acetal deprotection. Removal the acetal with 1M HCl overnight results in a 4:1 mixture of C12 diastereomers. Increasing the

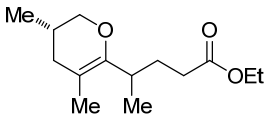

[41] Dihydropyran **166** was isolated as a 1:1 mixture of diastereomers (*possibly* alkene isomers). See; Rainier, J. D.; Allwein, S. P. *Tetrahedron Lett.* **1998**, *39*, 9601-9604.

[42] Using alkyl iodide **129** from the desymmetrization using (S)-tBuPhox, triazole **170** was synthesized and a crystal structure was obtained that confirmed absolute stereochemistry. Oberg, K. M.; Rovis T. (2014) Private communication to the Cambridge Structural Database, deposit number CCDC 991677.

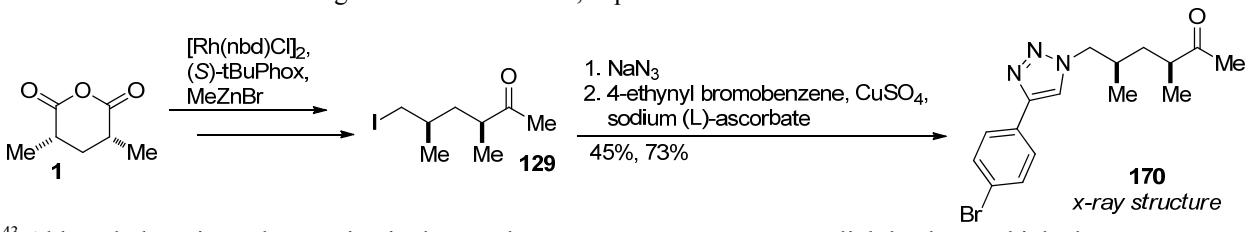

[43] Although the Mitsunobu reaction is shorter, the two step process generates slightly cleaner thiol ether **65**.

concentration improves reaction times, but results in even more epimerization. Lowering the concentration leads to longer reaction times and epimerization still occurs. Working up the *m*CPBA oxidation with sodium metabisulfite ($Na_2S_2O_5$) to remove excess peracid results in loss of the acetal and a 10:1 mixture of C12 diastereomers. Finally, we have found treatment with cerium trichloride heptahydrate and sodium iodide[44] results in complete removal of the ketal without any epimerization.

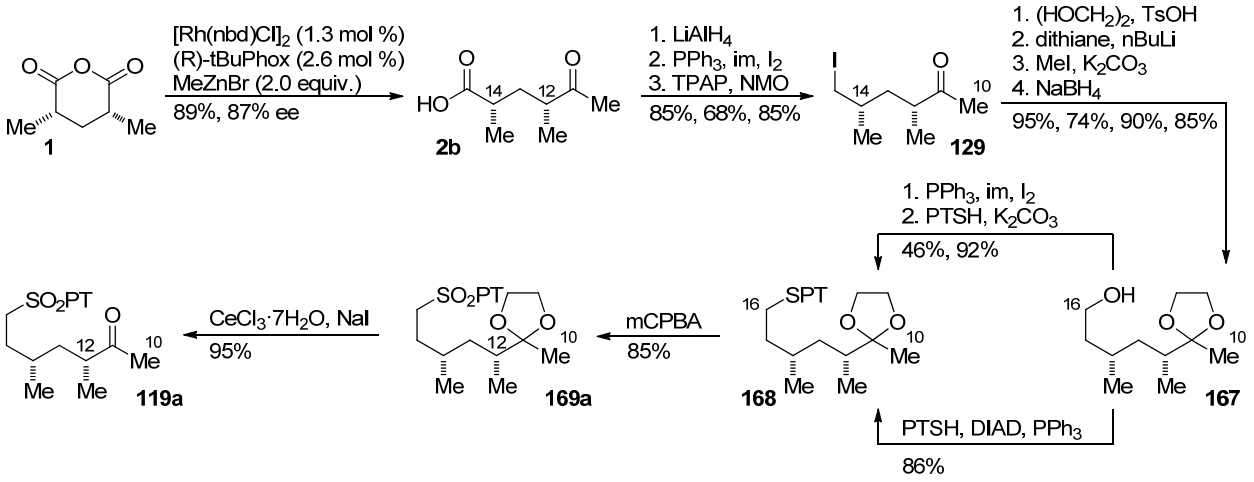

Scheme 4.3.2. Synthesis C10-C16 fragment.

My early attempts performing the desymmetrization reaction were plagued by contamination of carboxylester *rac*-**76**. As the reaction was scaled up, the amounts of carboxylester decreased. Presumably, zinc alkoxides are generated from small amounts of oxygen in the reaction and these open the anhydride uncatalyzed to form carboxylesters. Formation of zinc alkoxides from alkyl zincs and oxygen is a known and well documented process.[45] Larger scale reactions generate more product with less carboxylester presumably due to smaller molar ratios of oxygen.

[44] (a) Marcantoni, E.; Nobili, F. *J. Org. Chem.* **1997**, *62*, 4183-4184. (b) Arjona, O.; Menchaca, R.; Plumet, J. *Org. Lett.* **2001**, *3*, 107-109.
[45] (a) Lewinski, J.; Marciniak, W.; Lipkowski, J.; Justyniak, I. *J. Am. Chem. Soc*. **2003**, *125*, 12698-12699. (b) Lewinski, J.; Sliwinski, D.; Dranka, M.; Justyniak, I.; Lipkowski, J. *Angew. Chem. Int. Ed*. **2006**, *45*, 4826-4829. (c) Jana, S.; Berger, R. J. F.; Frohlich, R.; Pape, T.; Mitzel, N. W. *Inorg. Chem*. **2007**, *46*, 4293-4297.

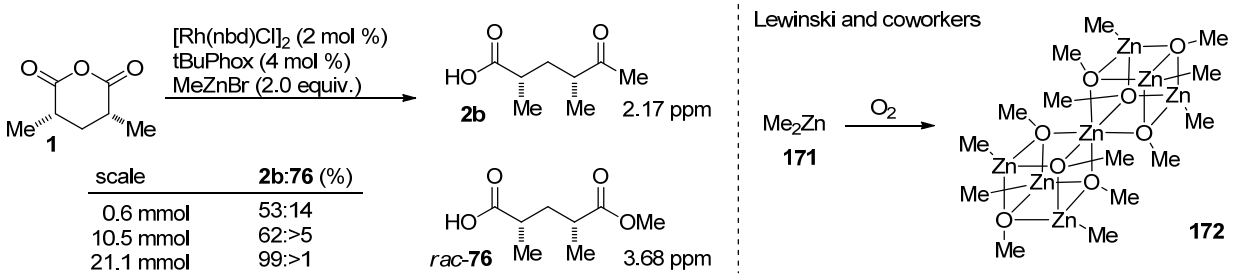

Scheme 4.3.3. Influence of scale on side product formation and presumable cause.

An approach that was investigated to expedite the synthesis of the C10-C16 fragment was alkylation of a methyl sulfone **174** with alkyl iodide **173** (Scheme 4.3.4). The inherent problem with this approach is that the deprotonated sulfone will do S_NAr chemistry to generate "dimer" **175**. Despite this obstacle, we were inspired by reports that fluororomethyl tert-butyltetrazole sulfones had been alkylated[46] and both phenyltetrazole and benzothiazole sulfones had been added into acid chlorides.[47] We also had promising results alkylating phenylsulfone **174d** with alkyl iodide **173**. The deprotection of the acetal **169d** without epimerization proved problematic, but if this could be overcome, then a route utilizing a classical Julia-Lythgoe coupling could be done just as Hanessian and Evans did in their synthesis. Although "dimerization" was not observed with tert-butyltetrazole methyl sulfone **174c**, subjecting it to a range of bases and isobutyl methanesulfonate **176** or 1-iodo-2-methylpropane **177** did not provide any of the targeted alkylated sulfone **178**. Additionally, we attempted to alkylate phenyltetrazole methyl sulfone **174a** and used High Throughput Experimentation (HTE)[48] to screen conditions,[49] but we only observed either starting material or "dimer". Based on a patent report,[50] we also envisioned cross coupling

[46] Zhu, L.; Ni, C.; Zhao, Y.; Hu, J. *Tetrahedron* **2010**, *66,* 5089-5100.
[47] Pospisil, J.; Sato, H. *J. Org. Chem.* **2011**, *76*, 2269-2272.
[48] Based on the HTE platform developed by Merck and Co. Inc. (a) Dreher, S. D.; Dormer, P. G.; Sandrock, D. L.; Molander, G. A. *J. Am. Chem. Soc.* **2008**, *130*, 9257-9259. (b) Spencer D. Dreher, Merck and Co. Inc., Rahway, New Jersey, USA. Personal Communication, 2011.
[49] **174a** was subjected to HTE with following variables: substrate: **176** or **177**; base/acid: LiHMDS, cesium carbonate, 2,2,6,6-tetramethylpiperidine, imidazole, DBU, Amberlyst® 15, sodium acetate, para-toluenesulfonic acid monohydrate; solvent: THF, DMF, PhMe, EtOH, acetone, MeCN.
[50] Ting, P. C.; Aslanian, R. G.; Cao, J.; Kim, D. W.-S.; Kuang, R.; Zhou, G.; Herr, R. J.; Zych, A. J.; Yang, J.; Wu, H.; Zorn, N. Pyridazinone Derivatives Useful as Glucan Synthase Inhibitors. W O 2008/115381 A1. March 12, 2008.

bromomethyl tertbutyltetrazole sulfone[51] **179** with boron reagents. Sp^3-sp^3 cross coupling is a difficult transformation, but it is not without precedent.[52] We screened a number of conditions using HTE, but only recovered starting material or debrominated starting material. Although frustrating, debromination implies that the oxidative addition step may be working, but the transmetallation is not occurring. The use of other cross coupling reagents might be able to solve this problem.

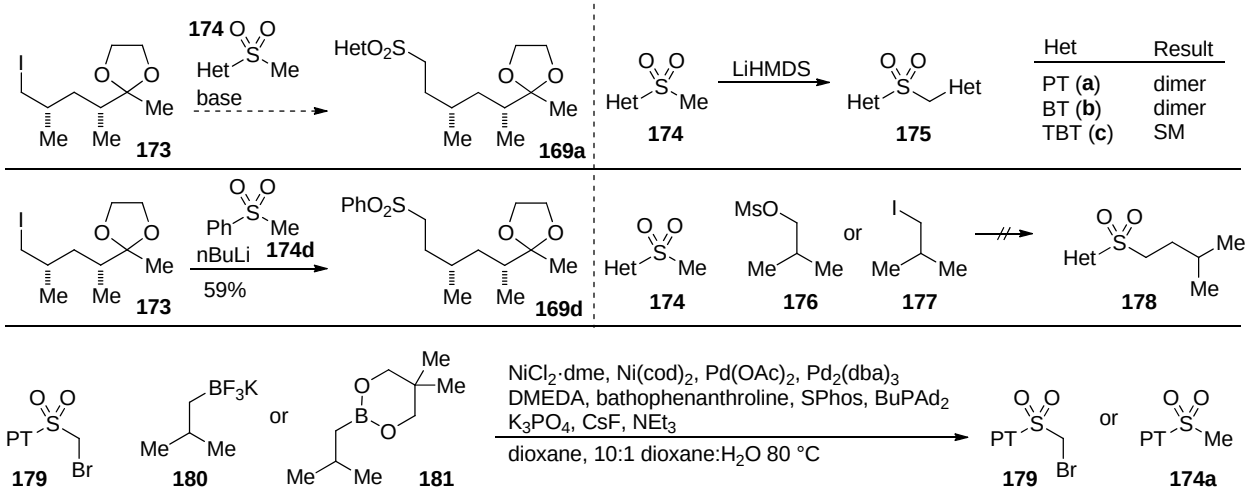

Scheme 4.3.4. Attempted alkylation approach to sulfone **169a**.

The aldol coupling of the C1-C9 and C10-C16 fragments to form β-hydroxyketone **161** and oxidation to β-diketone **162** were done as before.

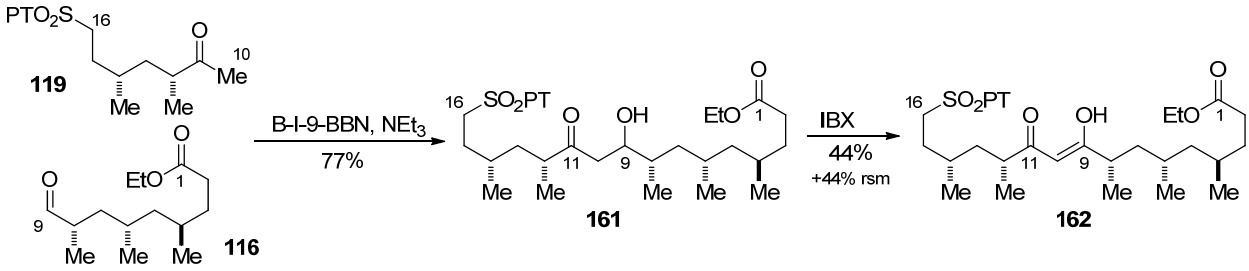

Scheme 4.3.5. Aldol coupling and oxidation to generate C1-C16 fragment.

[51] Lebrun, M.-E.; Marquand, P. L.; Berthelette, C. *J. Org. Chem.* **2006**, *71*, 2009-2013.
[52] (a) Kirchhoff, J. H.; Netherton, M. R.; Hills, I. D.; Fu, G. C. *J. Am. Chem. Soc.* 2002, 124, 13662-13663. (b) Saito, B.; Fu, G. C. *J. Am. Chem. Soc.* **2007**, *129*, 9602-9603.

4.4 C17-C32 Fragment Synthesis via Enol Silane Addition into Oxocarbenium

The synthesis of the C17-C22 fragment included a change in protecting group but otherwise remained the same. Desymmetrization of trisubstituted anhydride **3b**[53] with methyl zinc bromide generates ketoacid **4b**.[54] This was converted to methyl ketone **182** and then enol silane **183**. The switch in protecting groups was to avoid the use of the tosylate "protecting" group due to its vestigial use from the first generation approach.

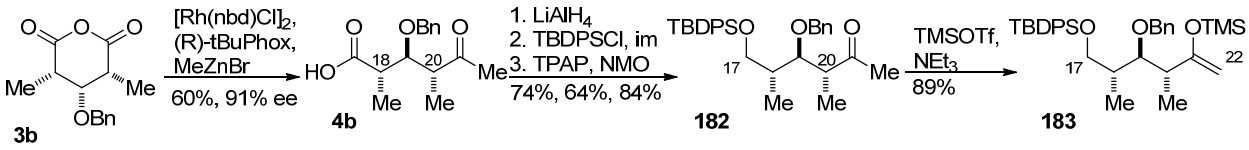

Scheme 4.4.1. Synthesis of the enol silane precursor **183**.

The synthesis of the C23-C32 fragment also included some protecting group changes. With some minor procedural changes, diepoxide **140** was synthesized. After bromination, the cyclization should be done using dry para-toluenesulfonic acid, as the hydrate leads to inconsistent results. The C31 alcohol was protected as the tert-butyldimethylsilyl (TBS) ether because hydrolysis of the benzoyl group at this position was problematic in Dr. Cochran's initial studies. Reduction of the lactone and benzoylation delivered acetal **185**.

[53] Oberg, K. M.; Rovis T. (2014) Private communication to the Cambridge Structural Database, deposit number CCDC 991874.

[54] Desymmetrization of the trisubstituted anhydride **3a** using (*S*)-tBuPhox and its elaboration to sulfone **137b** was accomplished by Dr. Cochran. After Dr. Cochran left, this compound was spotted by Darrin Flanigan and brought to my attention. This compound had crystallized out and the sulfurs gave enough anomalous dispersion for absolute stereochemistry determination. Cochran, B. M.; Oberg, K. M.; Rovis T. (2014) Private communication to the Cambridge Structural Database, deposit number CCDC 991686.

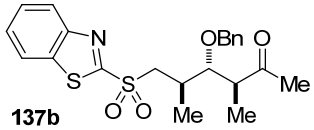

137b
x-ray structure

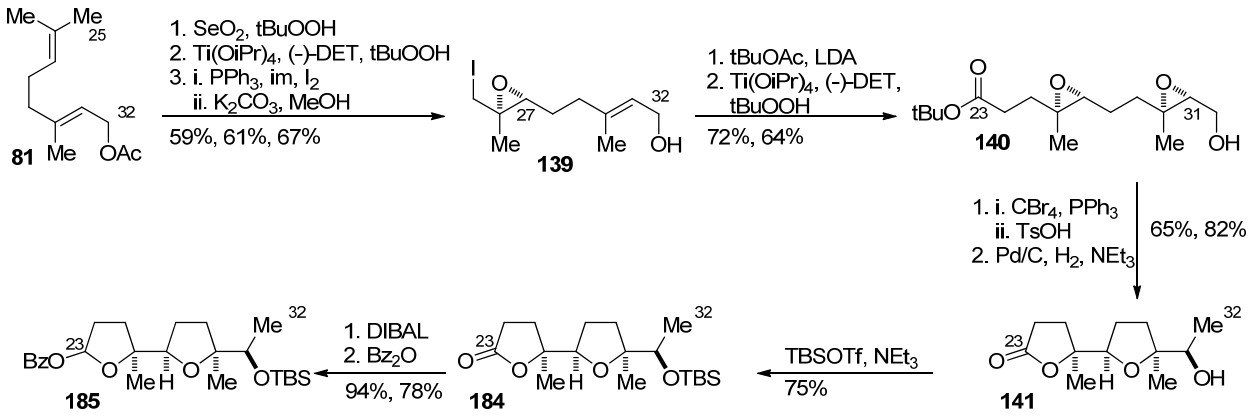

Scheme 4.4.2. C23-C32 acetal synthesis.

The enol silane addition into the oxocarbenium is a high yielding coupling with good diastereoselectivity. After the route was initially devised, a paper on the formal synthesis of ionomycin was published by Kocienski.[55] In their report, they essentially add the same enol silane (**156** vs **188**) into the same oxocarbenium generated from sulfone **189** through a Ley α-heteroalkylation. They found that the major diastereomer **190** corresponded to the undesired stereochemistry at C23 and the minor diastereomer **191** was the desired stereochemistry. Comparison of the ^{1}H NMRs showed that we are also generating the undesired C23 diastereomer as the major product during this reaction.

[55] Li, Y.; Cooksey, J. P.; Gao, Z.; Kocienski, P. J.; McAteer, S. M.; Snaddon, T. N. *Synthesis*, **2011**, 104-108.

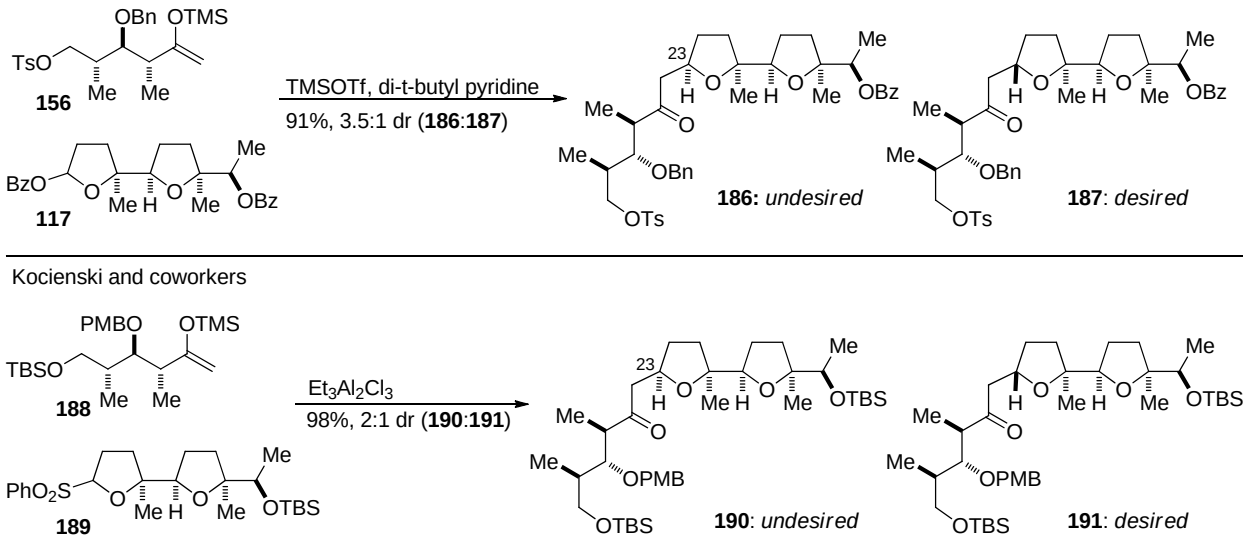

Scheme 4.4.3. Establishment of diastereomer generated from enol silane oxocarbenium addition through comparison to Kocienski and coworkers.

The preference for the undesired diastereomer can be explained by two models (Figure 4.1.1). Woerpel describes a general model for nucleophilic attack of five-membered-ring oxocarbenium ions based on transition state energies.[56] Approach of the nucleophile from the "inside" of the envelope generates a staggered transition state **III** leading to *cis*-tetrahydrofuran **186**. Alternatively, approach of the nucleophile from the "outside" of the envelope generates an eclipsed transition state **IV** leading to the *trans*-tetrahydrofuran **187**. Due to eclipsing interactions generated during the "outside" envelope attack **IV**, this transition state is disfavored and attack from the "inside" of the envelope **III** is lower in energy. This leads to the preference for the undesired C23 diastereomer **186**. An alternative model proposed by Reißig is based on Felkin-Ahn attack on an equilibrating mixture of conformers.[57] In this model, conformer **V** is more prevalent in solution due to the pseudoequatorial placement of the larger THF ring. Attack of this conformer by the enol silane generates the *cis*-tetrahydrofuran **186**. The generation of trans-tetrahydrofuran **187** is lower because conformer **VI** is in lower concentration in solution. This model also

[56] Larsen, H. C.; Ridgway, B. H.; Shaw, J. T.; Woerpel, K. A. *J. Am. Chem. Soc.* **1999**, *121*, 12208-12209.
[57] (a) Schmitt, A.; Reissig, H.-U.; *Synlett* **1990**, 40-42. (b) Schmitt, A.; Reißig, H.-U. *Eur. J. Org. Chem.* **2000**, 3893-3901.

explains the preference for the undesired C23 diastereomer **186**. Although both models suggest a preference for the undesired diastereomer, alkyl enol silanes are *relatively* poor nucleophiles[58] and a weaker nucleophile will lead to a latter transition state so the eclipsing interactions found in transition state **IV** should be more important than an equilibrium between **V** and **VI**.[59]

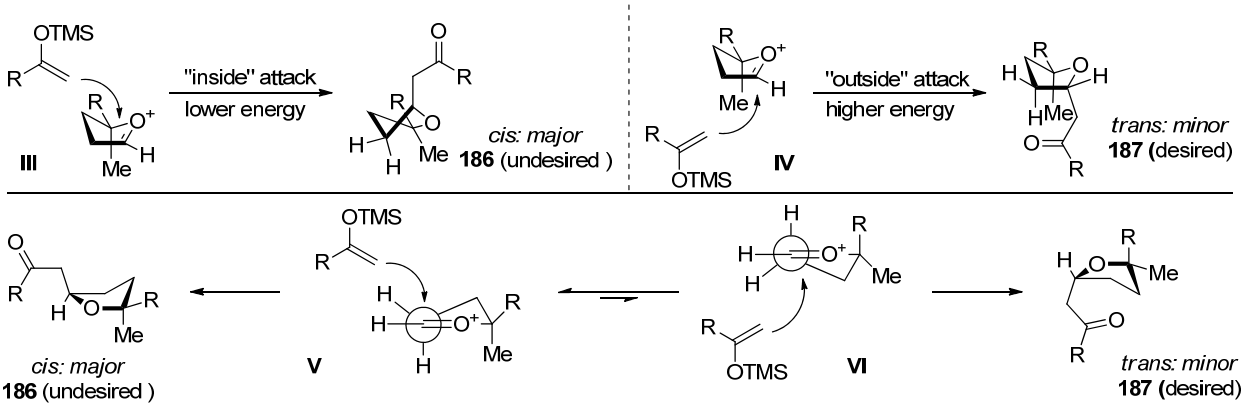

Figure 4.4.1. Models for diastereoselectivity in oxocarbenium addition.

Despite the apparent uphill battle, we attempted to remedy this problem through the use of different enol silanes and reaction conditions. Increasing the size of the silyl group on the enol silane does provide slightly better diastereoselectivity, but at the expense of yield (Scheme 4.4.4). Other conditions using titanium tetrachloride[60] or dibutylboron trifluoromethanesulfonate[61] to generate the enolate in the hopes of having an effect on selectivity through chelation of the benzyl alcohol did not produce any desired product. We also considered an epimerization of the C23 carbon through a retro-Michael/Michael addition. Kocienski and coworkers attempted the same epimerization after getting poor diastereoselectivity in their reaction, but they were unsuccessful. Calculations done by my coworker, Dan

[58] Mayr, H.; Bug, T.; Gotta, M. F.; Hering, N.; Irrgang, B.; Janker, B.; Kempf, B.; Loos, R; Ofial, A. R.; Remennikov, G.; Schimmel, H. *J. Am. Chem. Soc.* **2001**, *123*, 9500-9512.
[59] Anslyn, E. V.; Dougherty, D. A. Modern Physical Organic Chemistry. University Science Books, Sausalito, California, 2006.
[60] Jalce, G.; Seckk, M.; Franck, X.; Hocquemiller, R.; Figadère, B. *J. Org. Chem.* **2004**, *69*, 3240-3241.
[61] (a) Paterson, I.; Gibson, K. R.; Oballa, R. M. *Tetrahedron Lett.* **1996**, *37*, 8585-8588. (b) Evans, D. A.; Coleman, P. J.; Côté, B. *J. Org. Chem.* **1997**, *62*, 788-789.

Henderson, also show that an epimerization approach will be difficult as both of these diastereomers are very similar in energy; the undesired *cis* diastereomer is slightly lower in energy.

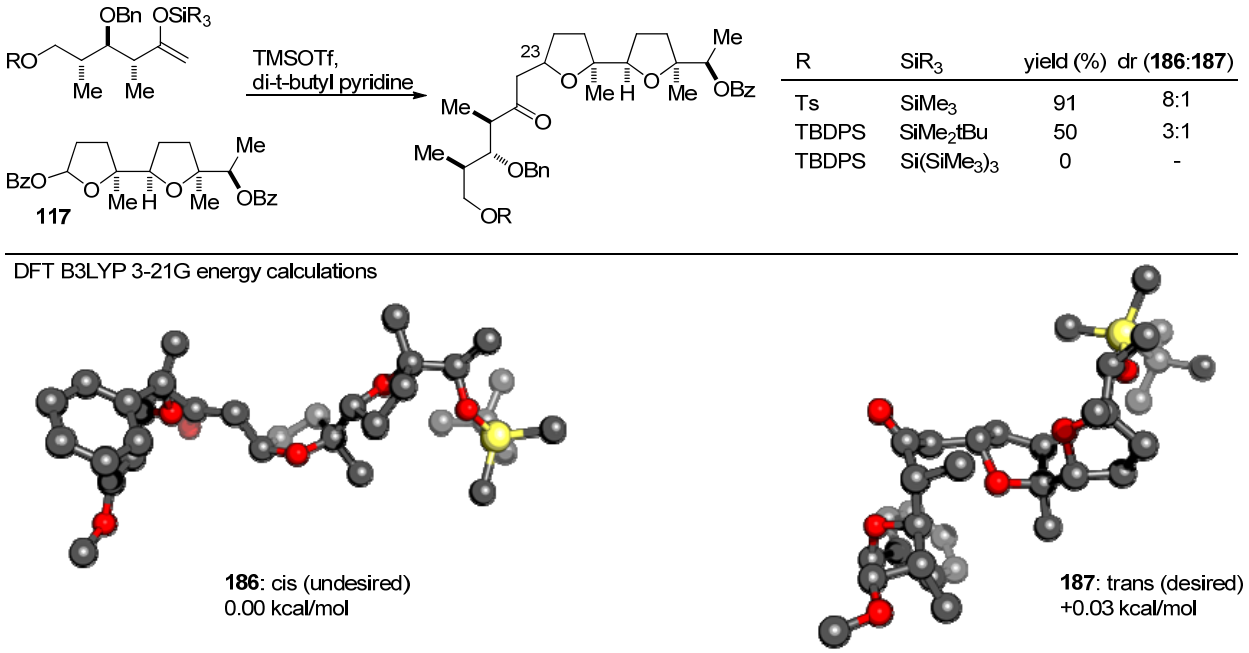

R	SiR_3	yield (%)	dr (**186**:**187**)
Ts	$SiMe_3$	91	8:1
TBDPS	$SiMe_2tBu$	50	3:1
TBDPS	$Si(SiMe_3)_3$	0	-

Scheme 4.4.4. Influence of silane in fragment coupling. Energy calculations showing difficulty in epimerization approach.

At this point, we thought use of a chiral counterion might be able to change the diastereoselectivity of the enol silane addition (Scheme 4.4.5). List has developed disulfonimide **194** that serves as a chiral version of trifluoromethanesulfonimide ($HNTf_2$).[62] The utility of this catalyst was demonstrated in Mukaiyama aldol reaction of naphthaldehyde **192** and silyl ketene acetal **193** to furnish aldol adduct **195** in good yield and enantioselectivity. Based on this report and reports that $HNTf_2$ has generated cyclic oxocarbeniums from methacryloyl and methoxy acetals,[63] we attempted to override the inherent selectivity in our system. Initial investigations of a model system, using enol silane **143** and acetal **196**, showed promising reactivity with $HNTf_2$. When we used disulfonimide **194** in our real system,

[62] (a) García-García, P.; Lay, F.; García-García, P.; Rabalakos, C.; List, B. *Angew. Chem. Int. Ed.* **2009**, *48*, 4363-4366. (b) Ratjen, L.; García-García, P.; Lay, F.; Beck, M. E.; List, B. *Angew. Chem. Int. Ed.* **2011**, *50*, 754-758.
[63] For methacryloyl, see; (a) Zandanel, C.; Dehuyser, L.; Wagner, A.; Baati, R. *Tetrahedron* **2010**, **66**, 3365-3369. For methoxy, see; (b) Midtkandal, R. R.; Macdonald, S. J. F.; Migaud, M. E. *Chem. Commun.* **2010**, *46*, 4538-4540.

we only saw hydrolysis of the enol silane.[64] List has seen such hydrolysis of silyl ketene acetals, and despite our use of solvents from a solvent system and drying the reagents using a benzene azeotrope, we could not avoid this hydrolysis. An additional problem with this approach is that silyl ketene acetals are much more nucleophilic than enol silanes.[65] Despite the initial success using a model system, we chose to investigate other approaches to make the C22-C23 bond and set the C23 stereocenter due to a lack of reactivity in the real system with both the chiral and achiral catalyst.

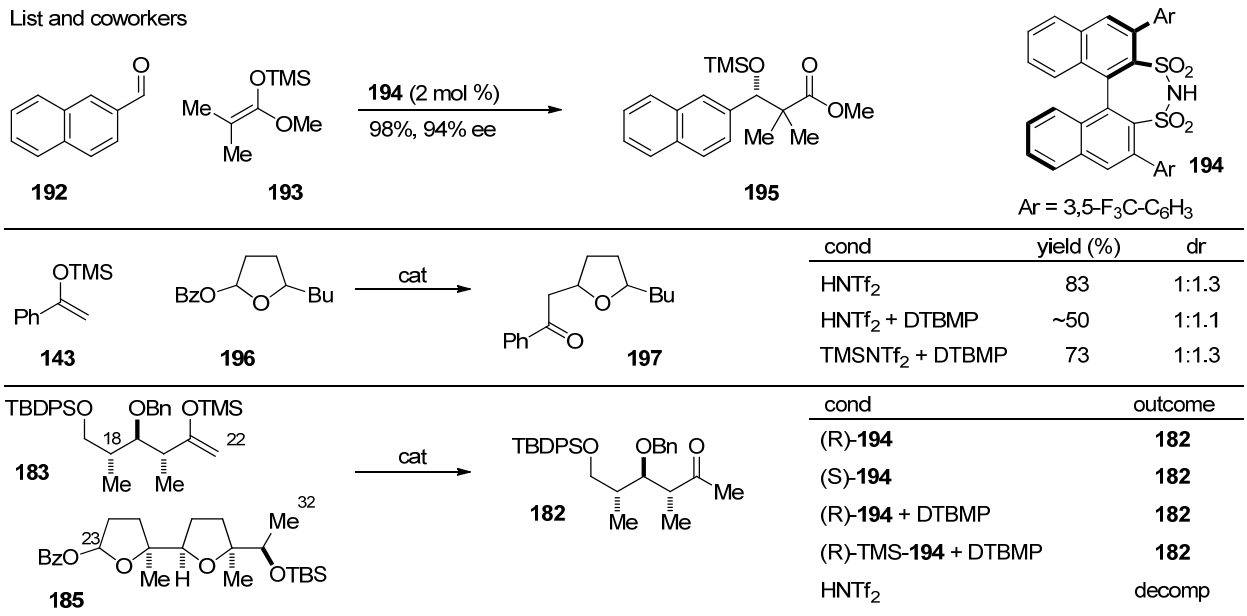

Scheme 4.4.5. Sulfonimides did not catalyze the enol silane addition of enol silane **183** into lactol **185**.

4.5 Attempted C17-C32 Fragment Synthesis via HWE/Michael Cascade

The first alternative bond disconnection was a Horner-Wadsworth-Emmons/Michael addition cascade. This had been used in natural product synthesis before[66] and we thought this could work here as well. The typical ways that β-keto phosphonates are made is through methyl phosphonate addition into

[64] We thank Benjamin List for a sample of (*R*) and (*S*)-**194** and for helpful discussions.
[65] Mayr, H.; Bug, T.; Gotta, M. F.; Hering, N.; Irrgang, B.; Janker, B.; Kempf, B.; Loos, R; Ofial, A. R.; Remennikov, G.; Schimmel, H. *J. Am. Chem. Soc.* **2001**, *123*, 9500-9512.
[66] (a) Zhou, X.-T.; Carter, R. G. *Angew. Chem. Int. Ed.* **2006**, *45*, 1787-1790. (b) Giannis, A.; Heretsch, P.; Sarli, V.; Stößel, A. *Angew. Chem. Int. Ed.* **2009**, *48*, 7911-7914.

aldehydes followed by oxidation, the Arbuzov reaction, and, less frequently, enolate trapping using an electrophilic source of phosphonate.

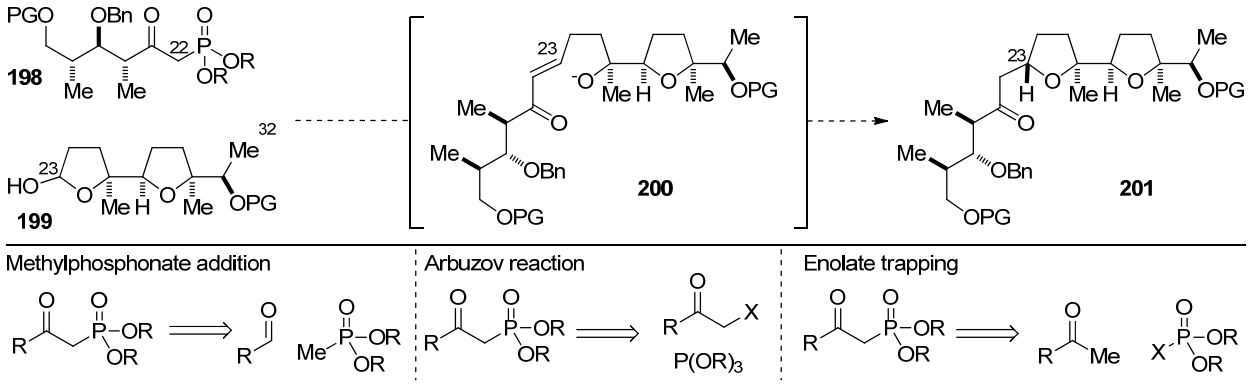

Figure 4.5.1. HWE/Michael cascade approach to set the C23 stereocenter and typical approaches to β-keto phosphonates.

Due to our desymmetrization, the addition of methyl phosphonate into an aldehyde was not a viable route. The desymmetrization of anhydrides with a hydride has not been accomplished in our group. Another approach would be the desymmetrization of the anhydride using a Reformatsky reagent, but we have not been able to achieve this type of desymmetrization either. Although it is possible to convert a methyl ketone into an aldehyde, this is a five to six step process, and the synthesis of such a fragment should be done using different methodology so we did not investigate the methylphosphonate addition approach.

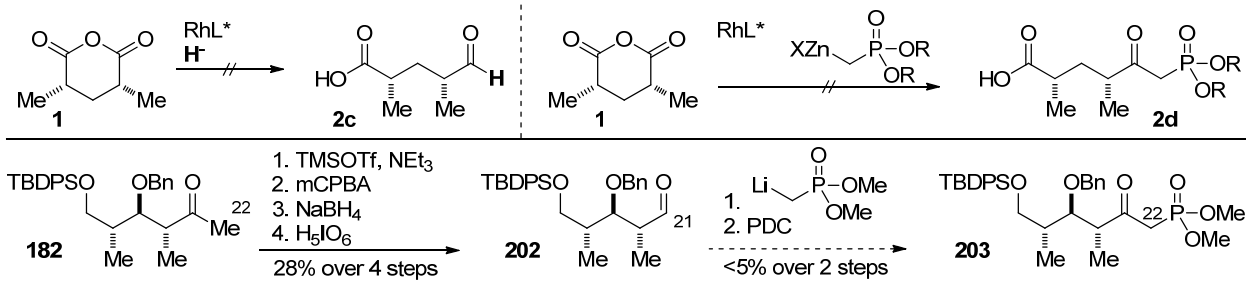

Scheme 4.5.1. Desymmetrizations with hydride sources or zinc phosphonates have not been accomplished in our group. Converting a methyl ketone to a β-keto phosphonate is lengthy.

Our initial efforts focused on the Arbuzov reaction[67] of an α-bromoketone. This route suffered from two flaws; the Perkow reaction is a competing pathway[68] and we observed elimination of benzyl alcohol from our substrate. The first flaw can be fixed through the use of different leaving groups[69] or reaction conditions. The second problem has been a decomposition problem for some time and is a common problem in manipulating aldol adducts. Although there are conditions to facilitate the Arbuzov reaction at lower temperatures,[70] these failed. In combination with the elimination problems at higher temperatures we looked into other approaches to convert our methyl ketone to a β-ketophosphonate.

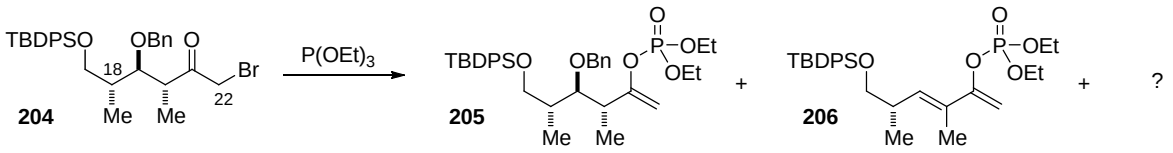

Scheme 4.5.2. Attempts at the Arbuzov reaction lead to a messy reaction with some elimination and possibly Perkow reaction side products.

The other approach that we considered was enolate trapping of an electophilic source of phosphonate. The difficulty with this approach is controlling carbon versus oxygen phosphorylation; phosphorylation typically occurs on oxygen. The use of cerium enolates[71] did not circumvent this problem, and attempts to add into a phosphonite and do air oxidation led to a mess.[72]

Rather than waste more precious material, we turned to model systems. We attempted to protect the ketone as a hydrazone. With the dimethylhydrazone, we were able to achieve carbon phosphorylation, but then deprotection problems precluded this route. We observed starting material with most of the

[67] Bhattacharya, A. K.; Thyagarajan, G. *Chem. Rev.* **1981**, *81*, 415-430.
[68] Borowitz, I. J.; Firstenberg, S.; Borowitz, G. B.; Schuessler, D. *J. Am. Chem. Soc.* **1972**, *94*, 1623-1628. Model substrate:

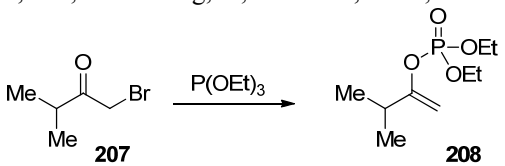

[69] Jacobson, H. I.; Griffin, M. J.; Preis, S.; Jensen, E. V. *J. Am. Chem. Soc.* **1957**, *79*, 2608-2612.
[70] Johnson, A.-L.; Slätt, J.; Janosik, T.; Bergman, J. *Heterocycles* **2006**, *68*, 2165-2170.
[71] Dalpozzo, R.; De Nino, A.; Miele, D.; Tagarelli, A.; Bartoli, G. *Eur. J. Org. Chem.* **1999**, 2299-2301.
[72] Lee, K.; Wiemer, D. F. *J. Org. Chem.* 1991, 56, 5556-5560.

conditions we tried, but some (methyl iodide and trimethylsilyl chloride) gave hydrazine/phosphine adducts by mass. Due to the difficulty in deprotecting the dimethyl hydrazone, we looked at protecting groups that were easier to remove. In this case, the phosphorylation was more difficult.

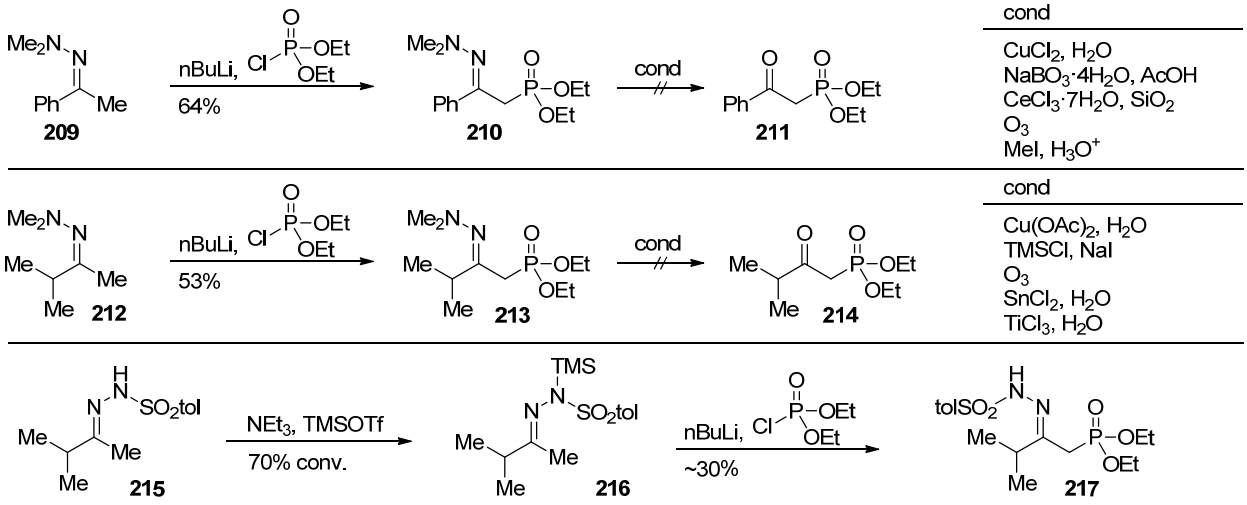

Scheme 4.5.3. Carbon phosphorylation of methyl hydrazones feasible, but deprotection was not achievable.

4.6 C17-C32 Fragment Synthesis via Reduction of Oxocarbenium and Reduction/S_N2 Sequence

Since the addition of a carbon nucleophile into an oxocarbenium gives the wrong diastereomer, we hypothesized that we could switch nucleophile to a hydride and get the correct diastereomer (Figure 4.6.1).

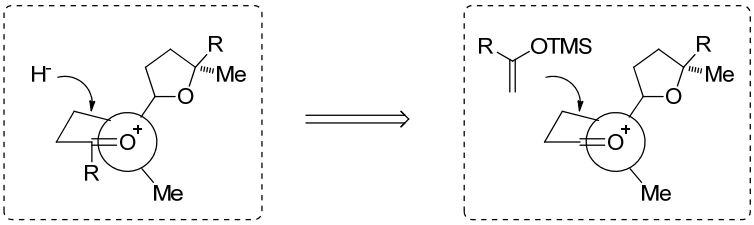

Figure 4.6.1. Switching the nucleophile from carbon to hydrogen should flip the C23 stereocenter.

Changing the order of carbon-carbon bond formation and reduction to change stereochemistry is not without precedence; Kishi and coworkers demonstrated that either diastereomer of C-glycopyranosides can be synthesized by this approach (Scheme 4.6.1).[73] After activating lactol **218**, addition of allyl silane into the oxocarbenium generated from acetal **219** generates C-glycopyranoside **220**. Alternatively, switching the order by allyl Grignard addition to lactone **221** and subsequent acidic reduction, the other diastereomer **223** is generated. They also used the ester enolate from ethyl acetate to do the same transformation.

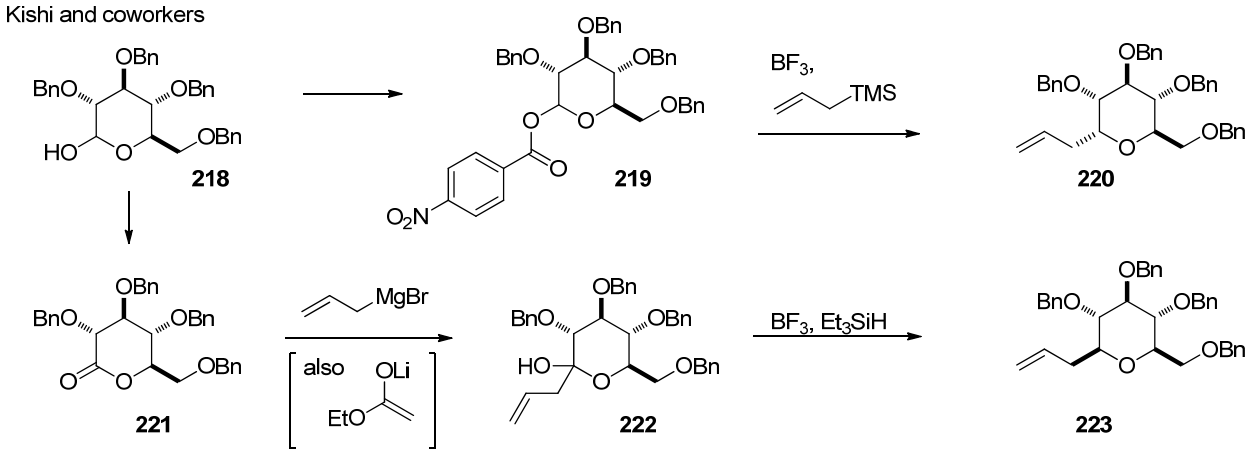

Scheme 4.6.1. Precedent by Kishi and coworkers that switching the nucleophile from carbon to hydrogen switches the major diastereomer.

Ideally, we would like to add an enolate into lactone **184** and reduce the resulting lactol to quickly access our desired tetrahydrofuran diastereomer **201** (Scheme 4.6.2). Our attempts to get this approach to work were thwarted by the inability to make the carbon-carbon bond. Enolates from aliphatic ketones are not as nucleophilic as enolates from esters, and we did not see precedence for ketone enolates adding into lactones. Therefore, we attempted to increase the electrophilicity of the lactone through the generation of

[73] Lewis, M. D.; Cha, J. K.; Kishi, Y. *J. Am. Chem. Soc.* **1982**, *104*, 4976-4978.

dioxocarbeniums with Meerwein's salt[74] or alkylation of a thiolactone,[75] but we did not observe our desired products. We also tried to increase the nucleophilicity of the enolate through the use of dimethyl hydrazone **209**, and even the combination of these approaches did not give usable amounts of product. Finally, we attempted some model studies to couple Weinreb amide **232** and hydrazone **209**,[76] but these reactions were not reproducible in my hands.

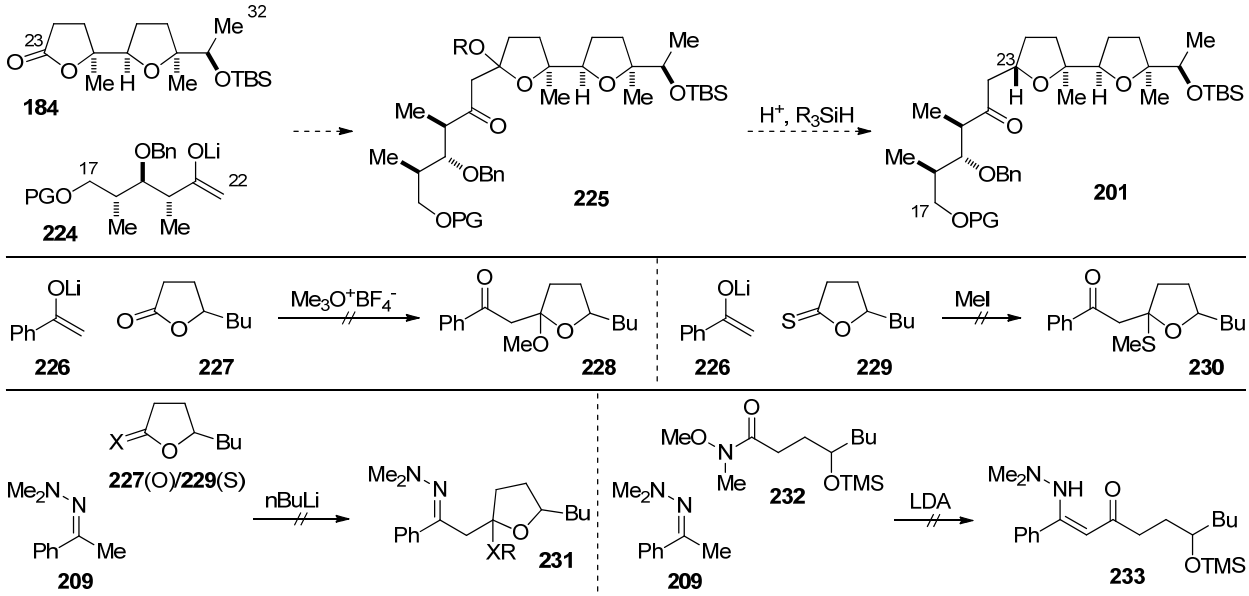

Scheme 4.6.2. Ideal approach to bistetrahydrofuran **201** via an enolate addition and acidic reduction sequence. The inability to form the carbon-carbon bond frustrated this route.

As carbon-carbon bond formation with enolates and enolate derivatives was stumbling, we turned to an alkyne as an alternative nucleophile. This nucleophile has been employed in the synthesis of C-glycopyranosides, giving this approach precedence.[77] Although conditions with the lithium acetylide did

[74] (a) Deslongchamps, P.; Lessard, J.; Nadeau, Y. *Can. J. Chem.* **1985**, *63*, 2485-2492. (b) Velázquez, F.; Olivo, H. F. *Org. Lett.* **2002**, *4*, 3175-3178. (c) Chamberland, S.; Ziller, J. W.; Woerpel, K. A. *J. Am. Chem. Soc.* **2005**, *127*, 5322-5323.
[75] Filippi, J.-J.; Fernandez, X.; Lizzani-Cuvelier, L.; Loiseau, A.-M. *Flavour Fragr. J.* **2006**, *21*, 175-184.
[76] Evans, D. A.; Kaldor, S. W.; Jones, T. K.; Clardy, J.; Stout, T. J. *J. Am. Chem. Soc.* **1990**, *112*, 7001-7031.
[77] Sánchez, M. E. L.; Michelet, V.; Besnier, I.; Genêt, J. P. *Synlett* **1994**, 705-708.

not work, the use of boron trifluoride (BF_3)[78] or cerium(III) chloride[79] facilitated the addition of the alkyne **234** into lactone **227**. The reduction of model ynone **235** using BF_3 and triethylsilane (Et_3SiH) worked (with deprotection of the primary TBS protecting group). After getting the model system to work in our hands, we pushed towards attempting it with the real system.

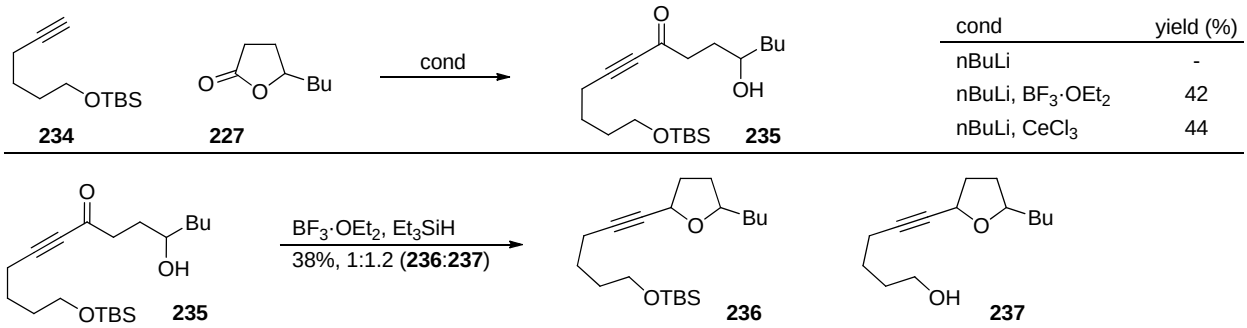

Scheme 4.6.3. Synthesis and reduction of model ynone **235**.

We were able to synthesize our targeted alkyne **239** via elimination of both a vinyl phosphonate **205** and vinyl triflate **238**, but chose the vinyl phosphonate route due to purification reasons. Deprotonation of methyl ketone **182** with lithium bis(trimethylsilyl)amide (LiHMDS) and phosphorylation generates vinyl phosphonate **205**. Traditional elimination conditions using LiHMDS or lithium diisopropylamide failed to generate the targeted alkyne, but elimination was achieved by using tertbutyl lithium. A similar route through vinyl triflate **238** could deliver alkyne **239**, but the polarities of the vinyl triflate and alkyne are the same, making the isolation of alkyne **239** more difficult.

[78] (a) Yamaguchi, M.; Shibato, K.; Fujiwara, S.; Hirao, I. *Synthesis* **1986**, 421-422. (b) Doubský, J.; Streinz, L.; Lešetický, L.; Koutek, B. *Synlett* **2003**, 937-942.
[79] Imamoto, T.; Sugiura, Y.; Takiyama, N. *Tetrahedron Lett.* **1984**, *25*, 4233-4236.

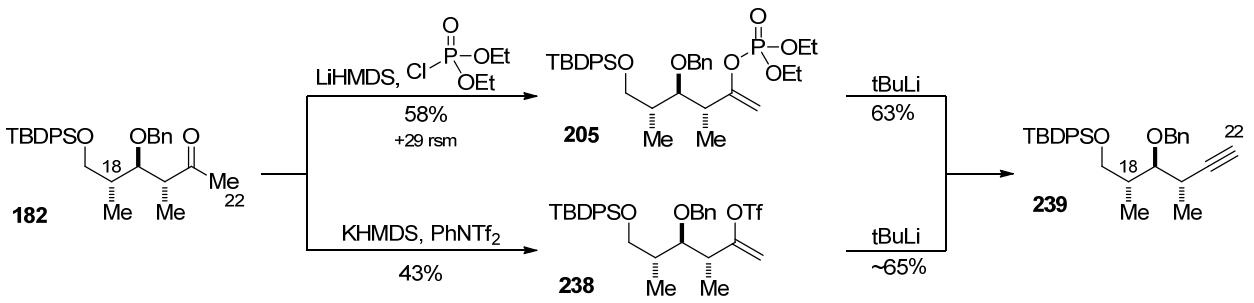

Scheme 4.6.4. Synthesis of alkyne **239**. The route through phosphonate **205** is preferred due to isolation issues with vinyl triflate substrate.

With alkyne **239** and lactone **184** in hand, we attempted the addition. Despite our success in making model ynone **235**, the synthesis of ynone **240** using this approach eluded us. Some control experiments shed some light which substrate is problematic. The addition of dichlorophenylcerium into lactone **184** works, but alkyne **239** does not add into simple lactone **227**.

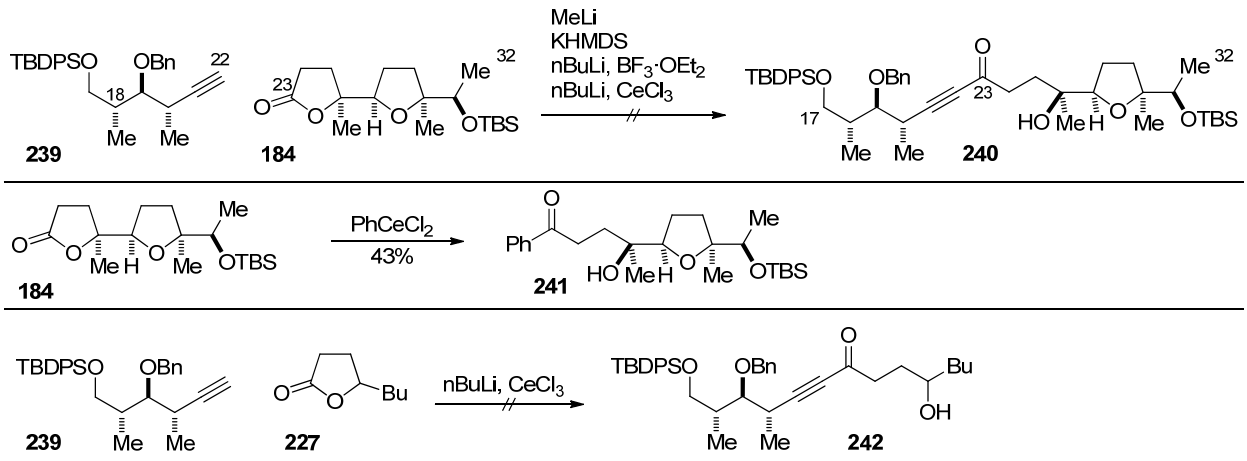

Scheme 4.6.5. Synthesis of ynone **240** fails due to alkyne **239** being unable to add to a lactone.

At this point, forming the carbon-carbon bond was still preventing us from testing our idea. With alkyne **239** in hand, we sought to activate the lactone as a thioester and use a palladium-catalyzed coupling to generate our targeted ynone.[80] Although thioesters from lactones have been synthesized

[80] Tokuyama, H.; Miyazaki, T.; Yokoshima, S.; Fukuyama, T. *Synlett* **2003**, 1512-1545.

before, the synthesis and handling of these compounds is difficult. The yields are low and the compounds are prone to recyclizing to starting material. After finding conditions to make thioester **243**,[81] we were concerned about the viability of the cross coupling due to the free alcohol γ to the thioester as there was no precedence. The reaction is under basic conditions with potentially Lewis acidic metals making recyclization of the lactone a concern.[82] Additionally, it is known that palladium can catalyze the formation of esters from aryl halides with carbon monoxide and alcohols.[83] From the reaction of model thioester **243** and alkyne **234**, we were able to isolate ynone **235** in moderate yield. We were still concerned about the use of alkyne **239** as it had failed to react when model systems had worked in the past, but it also couples with model thioester **243** in low yield. Excited by this result, we attempted the cross coupling of thioester **120** and alkyne **239** and achieved the synthesis of ynone **240**.

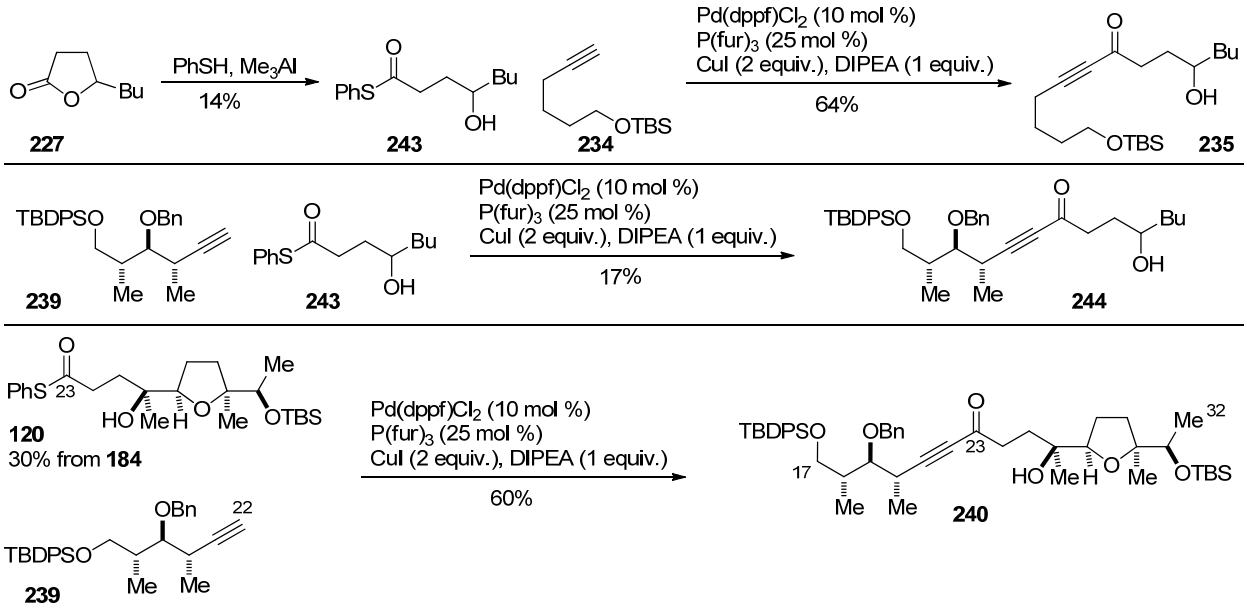

Scheme 4.6.6. Alternate synthesis of ynone **240** via palladium-catalyzed coupling of thioester **120** and alkyne **239**.

[81] Gierasch, T. M.; Shi, Z.; Verdine, G. L. *Org. Lett.* **2003**, *5*, 621-624.
[82] After the reaction, lactone is observed and no thioester remains.
[83] Presumably by alcoholysis of a palladium acyl species, which we seek to form in the reaction. See: (a) Milstein, D. *Acc. Chem. Res.* **1988**, *21*, 428-434. (b) Moser, W. R.; Wang, A. W.; Kildahl, N. K. *J. Am. Chem. Soc.* **1988**, *110*, 2816-2820. (c) Lindsell, W. E.; Palmer, D. D.; Preston, P. N.; Rosair, G. M. *Organometallics* **2005**, *24*, 1119-1133.

After finally forming our targeted carbon-carbon bond, we could investigate reductive cyclization of ynone **240**. Prototypical conditions using BF_3/Et_3SiH and trimethylsilyl trifluoromethanesulfonate/ Et_3SiH[84] did not bring about the desired transformation. We were excited to find that tin tetrachloride and Et_3SiH[85] induces cyclization, but it also removes the secondary TBS protecting group. Reduction with tetramethylammonium triacetoxyborohydride[86] also gives a small amount of product. We found sodium cyanoborohdride[87] and dichloroacetic acid in trifluoroethanol effects the reductive cyclization in 19:1 dr to furnish bistetrahydrofuran **245** in good yield. We were excited to get the reaction to work and suspected, based on our own work and Kishi's, that we had made the correct C23 stereocenter, but we wanted to confirm our stereochemistry before moving on with the synthesis.

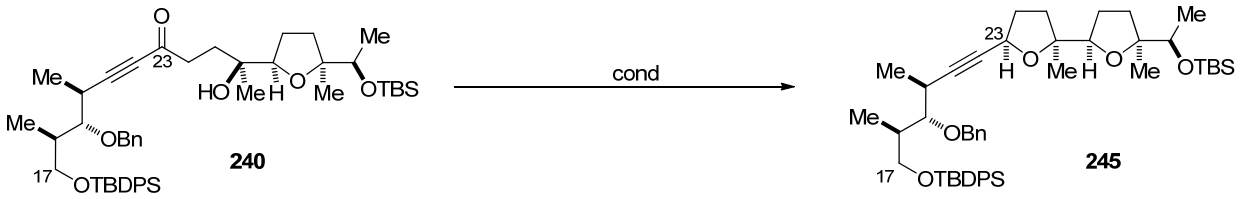

cond	yield (%)	cond	yield (%)
$BF_3{\cdot}OEt_2$, Et_3SiH	SM	$Me_4N[HB(OAc)_3]$, AcOH	>5
TMSOTf, Et_3SiH	decomp	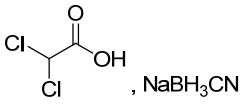	68
$SnCl_4$, Et_3SiH	17 (-TBS)		

Scheme 4.6.7. Reductive cyclization of ynone **240** proceeds in good yields under surprising conditions.

In order to establish the C23 stereocenter that we formed using the acidic reduction condition in making bistetrahydrofuran **245**, we reduced the ynone and performed an S_N2 cyclization. Using Noyori transfer hydrogenation conditions[88] we made both C23 alcoholic stereocenters. While tosylation failed,

[84](a) Nicolaou, K. C.; Hwang, C. K.; Nugiel, D. A. *J. Am. Chem. Soc.* **1989**, *111*, 4136-4137. (b) González, I. C.; Forsyth, C. J. *J. Am. Chem. Soc.* **2000**, *122*, 9099-9108.
[85] Zhang, Z.; Ding, Y.; Xu, J.; Chen, Y.; Forsyth, C. J. *Org. Lett.* **2013**, *15*, 2338-2341.
[86] Enders, D.; Hieronymi, A.; Raabe, G. *Synthesis* **2008**, *10*, 1545-1558.
[87] Wilcox, C. S.; Cowart, M. D. *Carbohydrate Research* **1987**, *171*, 141-160.
[88] (a) Matsumura, K.; Hashiguchi, S.; Ikariya, T.; Noyori, R. *J. Am. Chem. Soc.* **1997**, *119*, 8738-8739. (b) Newcomb, E. T.; Ferreira, E. M. *Org. Lett.* **2013**, *15*, 1772-1775.

mesylation using methanesulfonic anhydride[89] generated bistetrahydrofurans **248** and **245** upon workup. By comparing the ^{1}H NMRs of these compounds, we found that the reductive cyclization surprisingly delivers the wrong C23 stereocenter. Although disappointing, this news was delivered through the synthesis of the correct C23 diastereomer.

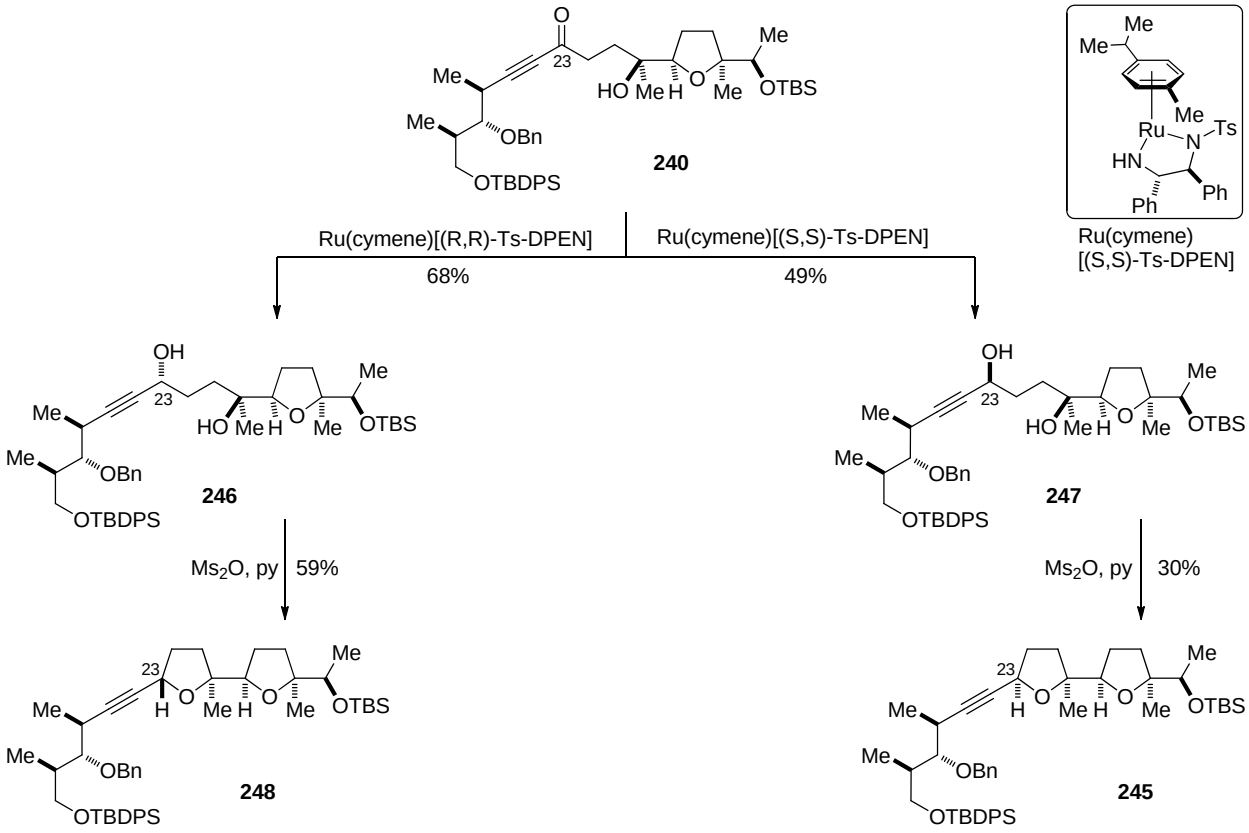

Scheme 4.6.8. Ynone reduction and cyclization to synthesize both C23 diastereomers. ^{1}H NMR showed that we are making the incorrect C23 stereocenter with reductive cyclization conditions.

With bistetrahydrofuran **248** in hand, we attempted to elaborate it to known aldehyde **252**. Dissolving metal conditions effected the reduction of the alkyne down to the alkene and removed the benzyl protecting group as expected, but it also partially reduced the tertbutyldiphenyl silyl (TBDPS)

[89] Ogawa, K.; Koyama, Y.; Ohashi, I.; Sato, I.; Hirama, M. *Angew. Chem. Int. Ed.* **2009**, *48*, 1110-1113.

protecting group. This has been observed before.[90] Tetrabutylammonium fluoride deprotection of alcohol **249** generates diol **250** in good yield. Reconstitution of the TBDPS protecting group[91] constitutes a formal synthesis of aldehyde **252** via Kocienski's synthesis of ionomycin.[92]

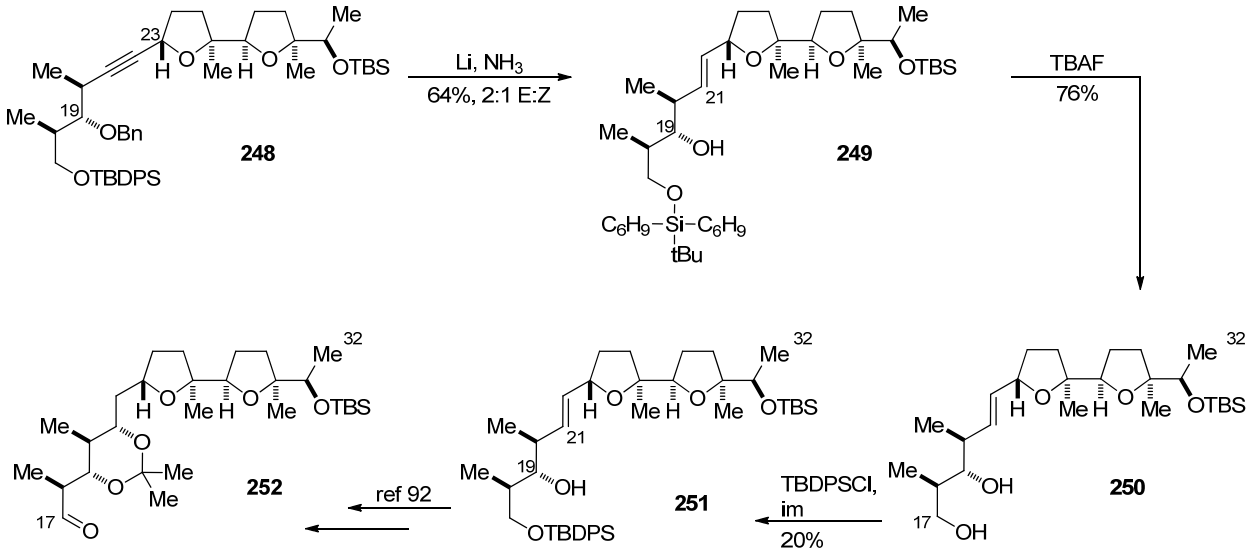

Scheme 4.6.9. Elaboration of alkyne **248**.

At this point, we had a route to homoallylic alcohol **251** and knew that aldehyde **252** could be made in seven steps using known chemistry, but we sought a more expedient route using oxymercuration of *in situ* formed hemiketals developed by Leighton.[93] Although Leighton only reported terminal alkenes, Bonini did the same transformation on simple electron-deficient 1,2-substituted alkenes.[94] When we tried the reaction with homoallylic alcohol **251**,[95] the transformation takes place, but it looks like there might be diastereomers (Scheme 4.6.10). Based on Leighton's work, we *suspect* that the acetonide is *syn* and the

[90] Observed reduction; (a) Kögl, M.; Brecker, L.; Warrass, R.; Mulzer, J. *Eur. J. Org. Chem.* **2008**, 2714-2730. Did not observe reduction; (b) Swindell, C. S.; Patel, B. P. *Tetrahedron Lett.* **1987**, *28*, 5275-5278. (c) VanderRoest, J. M.; Grieco, P. A. *J. Am. Chem. Soc.* **1993**, *115*, 5841-5842. (d) Naidu, S. V.; Kumar, P. *Tetrahedron Lett.* **2007**, *48*, 2279-2282.

[91] Benzylation of the primary alcohol yields 41% monoprotected diol, see Appendix 4 for details.

[92] Gao, Z.; Li, Y.; Cooksey, J. P.; Snaddon, T. N.; Schunk, S.; Viseux, E. M. E.; McAteer, S. M.; Kocienski, P. J. *Angew. Chem. Int. Ed.* **2009**, *48*, 5022-5025.

[93] Dreher, S. D.; Hornberger, K. R.; Sarraf, S. T.; Leighton, J. L. *Org. Lett.* **2000**, *2*, 3197-3199.

[94] (a) Bonini, C.; Campaniello, M.; Chiummiento, L.; Videtta, V. *Tetrahedron* **2008**, *64*, 8766-8772. (b) Bonini, C.; Chiummiento, L.; Funicello, M.; Lupattelli, P.; Videtta, V. *Tetrahedron Lett.* **2008**, *49*, 5455-5457.

[95] This reaction also worked with a benzyl protecting group in 17% yield, see Appendix 4 for details.

diastereomers are from the mercury, but this has not been confirmed. If the stereochemistry is what we suspect, then removal of the mercury, removal of the protecting group, and oxidation would generate targeted aldehyde **252**.

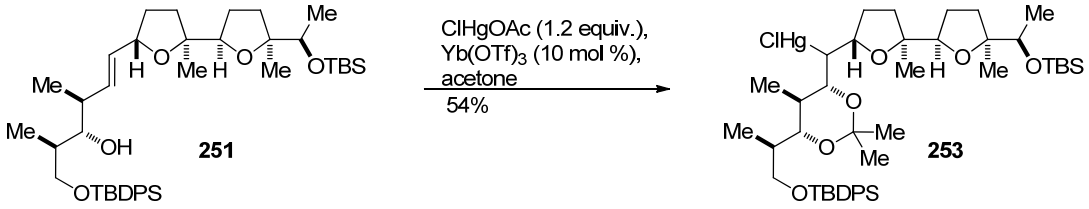

Scheme 4.6.10. Oxymercuration of the hemiketal derived from homoallylic alcohol **251** generates acetal **253**.

4.7 Conclusion

In conclusion, we have demonstrated the utility of catalytic desymmetrization of anhydrides with zinc nucleophiles by synthesizing large portions of ionomycin **10**. Despite the ability of the desymmetrizations to make complex synthons with the correct stereocenters, other parts of the synthesis prevented us from completing ionomycin in the time we had.

We found that the Julia-Kocienski olefination required the sulfone to be on C16 and the olefination could be done to make the entire ionomycin skeleton in the presence of an unprotected β-diketone. We had difficulties in making the desired C23 stereocenter. Initial efforts adding a carbon nucleophile into an oxocarbenium generated the undesired stereocenter. Despite switching the carbon-carbon bond forming and reduction steps, we still generated the undesired stereocenter. We were able to generate the targeted stereocenter using a reduction and S_N2 displacement sequence. We were able to elaborate this material to an intermediate that intercepted Kocienski's synthesis of the top fragment of ionomycin and demonstrated that an oxymercuration approach to install the C21 alcohol is possible.

APPENDIX 1: CHAPTER 1 EXPERIMENTAL

General Methods. All reactions were carried out under an atmosphere of argon in oven-dried glassware with magnetic stirring. Toluene was degassed with argon and passed through one column of neutral alumina and one column of Q5 reactant. Column chromatography was performed on Silicycle Inc. silica gel 60 (230-400 mesh). Thin layer chromatography was performed on Silicycle Inc. 0.25 mm silica gel 60-F plates. Visualization was accomplished with UV light (254 nm), potassium permanganate, and/or cerric ammonium nitrate.

^{1}H NMR and ^{13}C NMR spectra were obtained in $CDCl_3$ at ambient temperature and chemical shifts are expressed in parts per million (δ, ppm). Proton chemical shifts are referenced to 7.26 ppm ($CHCl_3$) and carbon chemical shifts are referenced to 77.0 ppm ($CDCl_3$). Data reporting uses the following abbreviations: s, singlet; bs, broad singlet; d, doublet; dd, doublet of doublets; t, triplet; m, multiplet; and *J*, coupling constant in Hz.

Alkynes **16a**, **16b**, **16d - 16o,** isocyanates **17a - 17c**, **17e - 17i**, triphenylphosphine, tris(4-methoxyphenyl)phosphine, and trifluoroacetic acid were purchased from Aldrich Chemicals Co. and used without further purification. $[Rh(C_2H_4)_2Cl]_2$ and tris(4-trifluoromethylphenyl)phosphine were purchased from Strem Chemical, Inc. and used without further purification. Isocyanate **17d** and **17j** were synthesized by converting the corresponding acid to the acyl azide with diphenylphosphoryl azide and gentle heating of the acyl azide neat to afford the isocyanate as described in previous work.[1] *rac*-**L5** was synthesized as described in the literature.[2]

General procedure for cycloaddition. To an oven-dried round bottom flask, $[Rh(C_2H_4)_2Cl]_2$ (2.3 mg, 0.006 mmol, 2.5 mol %) and *rac*-**L5** (5.1 mg, 0.012 mmol, 5 mol %) were added and an oven-dried reflux condenser was fitted in an inert atmosphere (N_2) glove box. After removal from the glove box, 1 ml of toluene was added via syringe and allowed to stir for 15 min at 23 °C under Ar. A solution of alkyne **16** (0.720 mmol, 3 equiv.) and isocyanate **17** (0.240 mmol) in 1 ml toluene was added via syringe. After rinsing the condenser with additional 6 ml toluene, the reaction was heated to 110 °C in an oil bath and maintained at reflux for 12 h. The reaction mixture was allowed to cool to 23 °C, concentrated *in vacuo*, and purified by flash chromatography (gradient elution typically 1:1 Hex:EtOAc, difficult separations used 95:5 CH_2Cl_2:EtOAc, and 4-pyridones required elution with 10:1 EtOAc:MeOH). Evaporation of solvent afforded the analytically pure compounds.

[1] Lee, E. E.; Rovis, T. *Org. Lett.* **2008**, *10*, 1231-1234.
[2] Giacomina, F.; Meetsma, A.; Panella, L.; Lefort, L.; de Vries, A. H. M.; de Vries, J. G. *Angew. Chem. Int. Ed.* **2007**, *46*, 1497-1500.

Characterization Data for New Compounds.

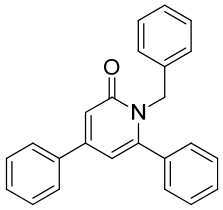

1-benzyl-4,6-diphenyl-2-pyridone (1db). General procedure yielded 68.3 mg (68%) of 2-pyridone. ^{1}H NMR (400 MHz, $CDCl_3$) δ 7.62 (m, 2H), 7.43 (m, 4H), 7.34 (m, 2H), 7.19 (m, 5H), 6.94 (m, 3H), 6.40 (d, J = 2.1 Hz, 1H), 5.22 (s, 2H). ^{13}C NMR (100 MHz, $CDCl_3$) δ 163.5, 150.6, 149.8, 137.2, 137.1, 135.2, 129.4, 129.1, 128.8, 128.6, 128.2, 127.0, 126.8, 126.7, 115.6, 107.8, 48.4. R_f = 0.24 (2:1 Hex:EtOAc). IR (NaCl, $CHCl_3$) 3053, 3027, 2996, 1650, 1603, 1583, 1532, 1486, 748, 723, 697. HRMS (ESI) $[C_{24}H_{20}NO]^+$ calcd 338.15002, found 338.15438.

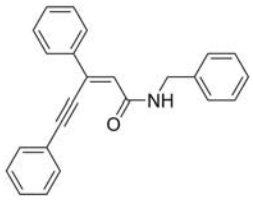

(Z)-N-benzyl-3,5-diphenylpent-2-en-4-ynamide (25db). General procedure yielded 6.2 mg (6%) of enynamide from reaction above. ^{1}H NMR (400 MHz, $CDCl_3$) δ 7.73 (m, 2H), 7.64 (s, 1H), 7.44 - 7.24 (m, 11H), 7.13 (m, 2H), 6.69 (s, 1H), 4.64 (d, J = 5.3 Hz, 2H). ^{13}C NMR (100 MHz, $CDCl_3$) δ 165.0, 137.8, 137.0, 131.6, 129.5, 129.0, 128.8, 128.7, 128.5, 128.3, 128.1, 127.6, 126.9, 121.2, 101.6, 85.8, 44.1. R_f = 0.31 (95:5 CH_2Cl_2:EtOAc). IR (NaCl, $CHCl_3$) 3247, 3058, 3022, 2914, 1639, 1526, 1230, 989. HRMS (ESI) $[C_{24}H_{20}NO]^+$ calcd 338.15002, found 338.15405.

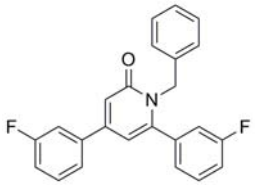

1-benzyl-4,6-bis(3-fluorophenyl)-2-pyridone (1eb). General procedure yielded 41.5 mg (46%) of 2-pyridone. ^{1}H NMR (400 MHz, $CDCl_3$) δ 7.41 (m, 2H), 7.31 (m, 2H), 7.21 (m, 3H), 7.13 (m, 2H), 6.96 (m, 1H), 6.91 (m, 3H), 6.86 (m, 1H), 6.33 (d, J = 2.1 Hz, 1H), 5.20 (s, 2H). ^{13}C NMR (100 MHz, $CDCl_3$) δ 164.2, 163.4, 163.3, 161.8, 160.9, 149.4, 148.7, 139.4, 139.4, 136.9, 136.8, 130.6, 130.5, 130.1, 130.0, 128.4, 127.2, 126.8, 124.5, 122.4, 116.5, 116.3, 116.2, 116.0, 113.9, 113.6, 107.5, 48.5. R_f = 0.24 (2:1 Hex:EtOAc). IR (NaCl, $CHCl_3$) 3063, 3027, 3001, 2955, 1660, 1588, 1537, 1475, 1265, 784, 692. HRMS (ESI) $[C_{24}H_{18}F_2NO]^+$ calcd 374.13118, found 374.13546.

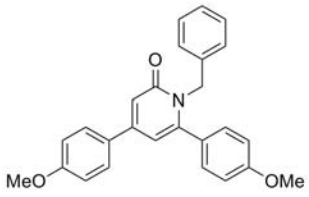

1-benzyl-4,6-bis(4-methoxyphenyl)-2-pyridone (1fb). General procedure yielded 84.8 mg (88%) of 2-pyridone. ^{1}H NMR (400 MHz, $CDCl_3$) δ 7.58 (m, 2H), 7.21 (m, 3H), 7.10 (m, 2H), 6.96 (m, 4H), 6.87 (d, J = 2.1 Hz, 1H), 6.85 (m, 2H), 6.38 (d, J = 2.1 Hz, 1H), 5.21 (s, 2H), 3.84 (s, 3H), 3.82 (s, 3H). ^{13}C NMR (100 MHz, $CDCl_3$) δ 163.7, 160.7, 160.0, 150.0, 149.6, 137.3, 130.0, 129.4, 128.2, 128.0, 127.7, 126.9, 126.7, 114.2, 114.1, 113.6, 107.8, 55.2, 48.4. R_f = 0.23 (1:1 Hex:EtOAc). IR (NaCl, $CHCl_3$) 3063, 3032, 2960, 2838, 1650, 1608, 1511, 1250, 1030, 830, 728. HRMS (ESI) $[C_{26}H_{24}NO_3]^+$ calcd 398.17115, found 398.17577.

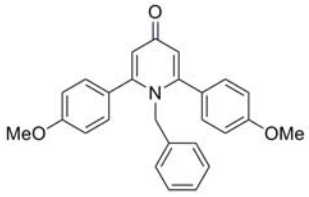

1-benzyl-2,6-bis(4-methoxyphenyl)-4-pyridone (2fb). General procedure yielded 3.4 mg (4%) of 4-pyridone from reaction above. ^{1}H NMR (400 MHz, $CDCl_3$) δ 7.17 (m, 4H), 7.11 (m, 3H), 6.85 (m, 4H), 6.49 (m, 2H), 6.41 (s, 2H), 4.93 (s, 2H), 3.81 (s, 6H). ^{13}C NMR (100 MHz, $CDCl_3$) δ 179.0, 160.3, 153.7, 137.0, 130.0, 128.4, 127.5, 125.7, 120.6, 113.9, 55.3, 53.8. R_f = 0.12 (10:1 EtOAc:MeOH). IR (NaCl, $CHCl_3$) 3068, 3001, 2925, 2838, 1619, 1496, 1250, 1173, 1020, 830. HRMS (ESI) $[C_{26}H_{24}NO_3]^+$ calcd 398.17115, found 398.17478.

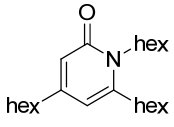

1,4,6-trihexyl-2-pyridone (1gc). General procedure yielded 26.6 mg (32%) of 2-pyridone. ^{1}H NMR (300 MHz, $CDCl_3$) δ 6.22 (d, J = 1.6 Hz, 1H), 5.83 (d, J = 1.9 Hz, 1H), 3.93 (t, J = 7.9 Hz, 2H), 2.54 (t, J = 7.6 Hz, 2H), 2.34 (t, J = 7.3 Hz, 2H), 1.69-1.47 (m, 6H), 1.40-1.26 (m, 18H), 0.91-0.84 (m, 9H). ^{13}C NMR (75 MHz, $CDCl_3$) δ 163.8,

154.2, 148.5, 115.5, 107.4, 43.6, 35.2, 32.9, 31.6, 31.5, 31.4, 29.2, 29.0, 29.0, 28.9, 28.8, 26.7, 22.5, 22.5, 14.0, 14.0, 14.0. R_f = 0.38 (2:1 Hex:EtOAc). IR (NaCl, $CHCl_3$) 2956, 2928, 2858, 1665, 1590, 1546, 1459. LRMS (ESI) $[C_{23}H_{42}NO]^+$ calcd 348.3, found 348.3.

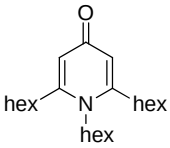

1,2,6-trihexyl-4-pyridone (2gc). General procedure yielded 6.7 mg (8%) of 4-pyridone from reaction above. ^{1}H NMR (400 MHz, $CDCl_3$) δ 6.24 (s, 2H), 3.76 (t, *J* = 8.3 Hz, 2H), 2.53 (t, *J* = 7.6 Hz, 4H), 1.65-1.57 (m, 6H), 1.43-1.29 (m, 18H), 0.92-0.87 (m, 9H). ^{13}C NMR (100 MHz, $CDCl_3$) δ 178.9, 152.4, 117.6, 46.6, 32.8, 31.4, 31.2, 31.0, 29.0, 28.9, 26.7, 22.5, 14.0, 13.9. R_f = 0.11 (4:1 EtOAc:MeOH). IR (NaCl, $CHCl_3$) 2956, 2929, 2858, 1632, 1568, 1459, 1182. LRMS (ESI) $[C_{23}H_{42}NO]^+$ calcd 348.3, found 348.3.

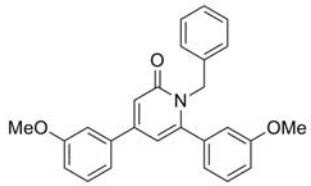

1-benzyl-4,6-bis(3-methoxyphenyl)-2-pyridone (1hb). General procedure yielded 71.4 mg (73%) of 2-pyridone. ^{1}H NMR (400 MHz, $CDCl_3$) δ 7.36 (t, *J* = 8.0 Hz, 1H), 7.29 - 7.14 (m, 6H), 6.96 (m, 4H), 6.92 (d, *J* = 2.1 Hz, 1H), 6.81 (m, 1H), 6.60 (m, 1H), 6.40 (d, *J* = 2.1 Hz, 1H), 5.20 (s, 2H), 3.85 (s, 3H), 3.56 (s, 3H). ^{13}C NMR (100 MHz, $CDCl_3$) δ 163.6, 160.0, 159.1, 150.6, 149.8, 138.8, 137.4, 136.4, 130.0, 129.5, 128.4, 127.0, 126.8, 120.8, 119.1, 115.8, 115.7, 115.1, 113.6, 112.1, 107.6, 55.3, 55.0, 48.7. R_f = 0.26 (95:5 CH_2Cl_2:EtOAc). IR (NaCl, $CHCl_3$) 3063, 3027, 3001, 2955, 2827, 1654, 1588, 1532, 1491, 1286, 1030, 733, 702. HRMS (ESI) $[C_{26}H_{24}NO_3]^+$ calcd 398.17115, found 398.17625.

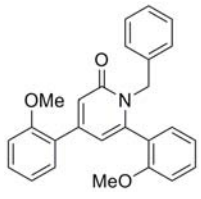

1-benzyl-4,6-bis(2-methoxyphenyl)-2-pyridone (1ib). General procedure yielded 55.0 mg (54%) of 2-pyridone. ^{1}H NMR (400 MHz, $CDCl_3$) δ 7.33 (m, 3H), 7.10 (m, 3H), 6.95 (m, 3H), 6.86 (m, 5H), 6.29 (d, *J* = 2.0 Hz, 1H), 5.44 (d, *J* = 14.8 Hz, 1H), 4.71 (d, *J* = 14.8 Hz, 1H), 3.78 (s, 3H), 3.60 (s, 3H). ^{13}C NMR (100 MHz, $CDCl_3$) δ 163.7, 156.6, 156.4, 149.0, 145.5, 137.4, 131.0, 130.8, 130.2, 130.1, 127.9, 127.5, 127.0, 126.7, 124.5, 120.7, 120.3, 118.7, 111.2, 110.5, 55.5, 55.1, 48.2. R_f = 0.28 (1:1 Hex:EtOAc). IR (NaCl, $CHCl_3$) 3063, 3006, 2966, 2827, 1650, 1603, 1573, 1245, 1020. HRMS (ESI) $[C_{26}H_{24}NO_3]^+$ calcd 398.17115, found 398.17582.

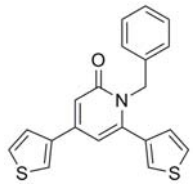

1-benzyl-4,6-di(thiophen-3-yl)-2-pyridone (1jb). General procedure yielded 68.2 mg (80%) of 2-pyridone. ^{1}H NMR (400 MHz, $CDCl_3$) δ 7.61 (dd, *J* = 2.7, 1.6 Hz, 1H), 7.39 (m, 2H), 7.32 (dd, *J* = 5.0, 3.0 Hz, 1H), 7.22 (m, 3H), 7.16 (dd, *J* = 3.0, 1.3 Hz, 1H), 6.98 (m, 2H), 6.91 (dd, *J* = 5.0, 1.3 Hz, 1H), 6.89 (d, *J* = 2.0 Hz, 1H), 6.45 (d, *J* = 2.1 Hz, 1H), 5.22 (s, 2H). ^{13}C NMR (100 MHz, $CDCl_3$) δ 163.7, 145.1, 144.6, 138.6, 137.2, 135.4, 128.4, 127.8, 127.0, 126.9, 126.5, 126.2, 125.9, 125.6, 123.9, 114.6, 107.6, 48.5. R_f = 0.13 (2:1 Hex:EtOAc). IR (NaCl, $CHCl_3$) 3104, 3083, 3022, 3001, 2950, 1660, 1578, 1552, 851, 789, 728. HRMS (ESI) $[C_{20}H_{15}NOS_2]^+$ calcd 350.06286, found 350.06775.

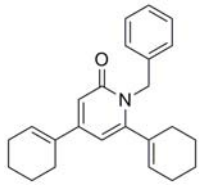

1-benzyl-4,6-dicyclohexenyl-2-pyridone (1kb). General procedure yielded 79.9 mg (92%) of 2-pyridone. ^{1}H NMR (400 MHz, $CDCl_3$) δ 7.21 (m, 2H), 7.14 (m, 1H), 7.07 (m, 2H), 6.44 (d, *J* = 2.0 Hz, 1H), 6.33 (m, 1H), 6.07 (d, *J* = 2.1 Hz, 1H), 5.54 (m, 1H), 5.15 (s, 2H), 2.26 (m, 2H), 2.16 (m, 2H), 1.98 (m, 2H), 1.89 (m, 2H), 1.69 (m, 2H), 1.57 (m, 6H). ^{13}C NMR (100 MHz, $CDCl_3$) δ 164.1, 151.4, 150.8, 137.9, 133.9, 133.6, 130.5, 129.4, 128.2, 126.8, 126.6, 112.6, 103.7, 47.9, 29.6, 26.0, 25.9, 24.9, 22.6, 22.3, 21.8, 21.4. R_f = 0.17 (2:1 Hex:EtOAc). IR (NaCl, $CHCl_3$) 3068, 3022, 2930, 2853, 2827, 1644, 1568, 1521, 1429. 748, 687. HRMS (ESI) $[C_{24}H_{28}NO]^+$ calcd 346.21262, found 346.21702.

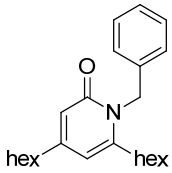

1-benzyl-4,6-dihexyl-2-pyridone (1gb). General procedure yielded 39.8 mg (38%) of 2-pyridone. ^{1}H NMR (400 MHz, $CDCl_3$) δ 7.28 (m, 2H), 7.21 (m, 1H), 7.10 (m, 2H), 6.38 (s, 1H), 5.91 (d, *J* = 1.7 Hz, 1H), 5.32 (s, 2H), 2.47 (t, *J* = 7.8 Hz, 2H), 2.41 (t, *J* = 7.6 Hz, 2H), 1.58 (m, 2H), 1.51 (m, 2H), 1.27 (m, 12H), 0.88 (t, *J* = 6.8 Hz, 3H), 0.86 (t, *J* = 6.9 Hz, 3H). ^{13}C NMR (100 MHz, $CDCl_3$) δ 164.0, 155.0, 149.3, 136.9, 128.6, 127.1, 126.2, 115.4, 107.8, 46.2, 35.3, 32.8, 31.5, 31.4, 29.1, 28.8, 28.5, 22.5, 22.4, 14.0, 13.9. R_f = 0.22 (4:1 Hex:EtOAc). IR (NaCl, $CHCl_3$) 3063, 3027, 2960, 2930, 2853, 1665, 1588, 1547, 1450, 728. HRMS (ESI) $[C_{24}H_{36}NO]^+$ calcd 354.27522, found 354.27904.

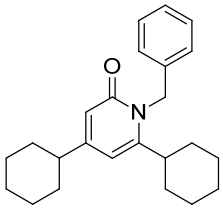

1-benzyl-4,6-dicyclohexyl-2-pyridone (1lb). General procedure yielded 12.6 mg (15%) of 2-pyridone. ^{1}H NMR (300 MHz, $CDCl_3$) δ 7.31-7.19 (m, 3H), 7.13-7.10 (m, 2H), 6.35 (d, *J* = 1.3 Hz, 1H), 5.96 (d, *J* = 1.7 Hz, 1H), 5.37 (s, 2H), 2.54 (m, 1H), 2.29 (m, 1H), 1.86- 1.67 (m, 10H), 1.42-1.15 (m, 10H). ^{13}C NMR (75 MHz, $CDCl_3$) δ 164.3, 159.3, 154.4, 137.5, 128.6, 127.0, 126.3, 113.5, 104.4, 45.8, 43.9, 40.6, 33.5, 32.6, 26.5, 26.4, 25.9, 25.8. R_f = 0.12 (2:1 Hex:EtOAc). IR (NaCl, $CHCl_3$) 2927, 2853, 1661, 1583, 1544, 1496, 1450. LRMS (ESI) $[C_{24}H_{32}NO]^+$ calcd 350.2, found 350.3.

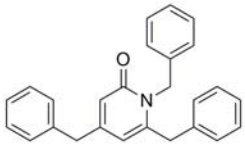

1,4,6-tribenzyl-2-pyridone (1mb). General procedure yielded 17.3 mg (19%) of 2-pyridone. ^{1}H NMR (400 MHz, $CDCl_3$) δ 7.35 - 7.20 (m, 11H), 7.11 (m, 2H), 7.04 (m, 2H), 6.42 (s, 1H), 5.87 (d, *J* = 1.8 Hz, 1H), 5.18 (s, 2H), 3.78 (s, 2H), 3.77 (s, 2H). ^{13}C NMR (100 MHz, $CDCl_3$) δ 164.1, 153.0, 147.1, 137.9, 136.7, 136.2, 129.1, 129.0, 128.8, 128.7, 128.1, 127.2, 127.1, 126.7, 126.1, 117.1, 110.1, 46.2, 41.3, 39.2. R_f = 0.12 (95:5 CH_2Cl_2:EtOAc). IR (NaCl, $CHCl_3$) 3058, 3022, 2996, 1660, 1588, 1542, 1486, 723, 692. HRMS (ESI) $[C_{26}H_{24}NO]^+$ calcd 366.18132, found 366.18559.

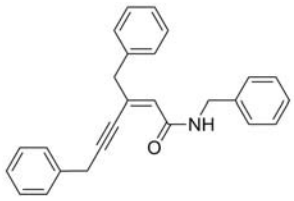

(Z)-N,3-dibenzyl-6-phenylhex-2-en-4-ynamide (25mb). General procedure yielded 14.8 mg (16%) of enynamide from reaction above. ^{1}H NMR (400 MHz, $CDCl_3$) δ 7.40 (s, 1H), 7.37 - 7.14 (m, 13H), 7.05 (m, 2H), 6.09 (s, 1H), 4.42 (d, *J* = 5.5 Hz, 2H), 3.57 (s, 2H), 3.53 (s, 2H). ^{13}C NMR (100 MHz, $CDCl_3$) δ 164.8, 138.0, 137.0, 135.2, 130.4, 129.6, 129.2, 128.7, 128.6, 128.5, 127.8, 127.4, 126.9, 100.5, 80.3, 44.9, 43.6, 25.7. R_f = 0.28 (95:5 CH_2Cl_2:EtOAc). IR (NaCl, $CHCl_3$) 3283, 3058, 3022, 2996, 2914, 1644, 1485, 1450, 697. HRMS (ESI) $[C_{26}H_{24}NO]^+$ calcd 366.18132, found 366.18552.

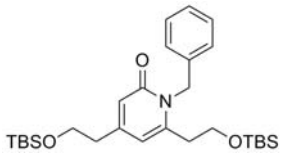

1-benzyl-4,6-bis(2-(tert-butyldimethylsilyloxy)ethyl)-2-pyridone (1nb). General procedure yielded 22.3 mg (18%) of 2-pyridone. ^{1}H NMR (400 MHz, $CDCl_3$) δ 7.28 (m, 2H), 7.21 (m, 1H), 7.09 (m, 2H), 6.40 (s, 1H), 6.00 (s, 1H), 5.43 (s, 2H), 3.82 (t, J = 6.7 Hz, 2H), 3.76 (d, J = 6.3 Hz, 2H), 2.71 (t, J = 6.3 Hz, 2H), 2.62 (t, J = 6.7 Hz, 2H), 0.87 (d, J = 0.8 Hz, 9H), 0.84 (d, J = 0.8 Hz, 9H), 0.03 (d, J = 0.8 Hz, 6H), -0.04 (d, J = 0.8 Hz, 6H). ^{13}C NMR (100 MHz, $CDCl_3$) δ 163.8, 151.5, 146.8, 136.9, 128.7, 127.1, 126.2, 116.9, 109.3, 62.6, 62.3, 46.5, 38.8, 36.0, 25.9, 25.8, 18.3, 18.2, -5.4, -5.6. R_f = 0.22 (95:5 CH_2Cl_2:EtOAc). IR (NaCl, $CHCl_3$) 3063, 3027, 2955, 2925, 2883, 2853, 1660, 1588, 1542, 1255, 1096, 835, 723. HRMS (ESI) $[C_{28}H_{48}NO_3Si_2]^+$ calcd 502.31280, found 502.31729.

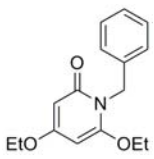

1-benzyl-4,6-diethoxy-2-pyridone (1ob). General procedure yielded 24.2 mg (38%) of 2-pyridone. ^{1}H NMR (400 MHz, $CDCl_3$) δ 7.26 (m, 5H), 5.69 (d, *J* = 2.0 Hz, 1H), 5.21 (bs, 3H), 3.97 (m, 4H), 1.36 (m, 6H). ^{13}C NMR (100 MHz, $CDCl_3$) δ 168.3, 163.6, 156.8, 137.5, 128.2, 128.0, 127.1, 89.9, 79.6, 65.3, 63.9, 43.8, 14.3, 14.0. R_f = 0.24 (1:1 Hex:EtOAc). IR (NaCl, $CHCl_3$) 3063, 3032, 2976, 2935, 2894, 1660, 1593, 1547, 1255,

1189, 1112, 738. HRMS (ESI) $[C_{16}H_{20}NO_3]^+$ calcd 274.13985, found 274.14439.

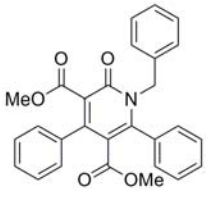

Dimethyl 1-benzyl-2-oxo-4,6-diphenyl-1,2-dihydropyridine-3,5-dicarboxylate (1ab). General procedure using *rac*-**L1** yielded 60.3 mg (42%) of 2-pyridone. ^{1}H NMR (400 MHz, $CDCl_3$) δ 7.44 - 7.31 (m, 8H), 7.21 (m, 3H), 7.11 (m, 2H), 6.90 (m, 2H), 5.15 (s, 2H), 3.64 (s, 3H), 3.05 (s, 3H). ^{13}C NMR (100 MHz, $CDCl_3$) δ 166.1, 165.9, 159.3, 149.4, 148.4, 136.0, 135.5, 132.0, 129.8, 128.8, 128.8, 128.3, 128.2, 128.1, 127.4, 127.3, 127.2, 124.3, 116.0, 52.3, 51.8, 49.3. R_f = 0.38 (2:1 Hex:EtOAc). IR (NaCl, $CHCl_3$) 3063, 3032, 2950, 1736, 1644, 1532, 1486, 1429, 1250, 1214, 1132, 764, 697. HRMS (ESI) $[C_{28}H_{24}NO_5]^+$ calcd 454.16098, found 454.16491.

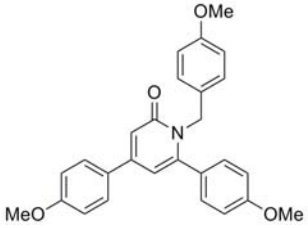

1-(4-methoxybenzyl)-4,6-(4-methoxyphenyl)-2-pyridone (1fd). General procedure yielded 80.8 mg (79%) of 2-pyridone. ^{1}H NMR (400 MHz, $CDCl_3$) δ 7.57 (m, 2H), 7.11 (m, 2H), 6.96 (m, 2H), 6.88 (m, 4H), 6.83 (d, *J* = 2.1 Hz, 1H), 6.74 (m, 2H), 6.34 (d, *J* = 2.1 Hz, 1H), 5.14 (s, 2H), 3.84 (s, 6H), 3.75 (s, 3H). ^{13}C NMR (100 MHz, $CDCl_3$) δ 163.7, 160.6, 160.0, 158.4, 149.8, 149.5, 130.0, 129.5, 128.3, 127.9, 127.8, 114.2, 113.5, 107.6, 55.2, 55.0, 47.7. R_f = 0.18 (1:1 Hex:EtOAc). IR (NaCl, $CHCl_3$) 3063, 3001, 2955, 2832, 1650, 1608, 1506, 1245, 1030, 820, 748. HRMS (ESI) $[C_{27}H_{26}NO_4]^+$ calcd 428.18171, found 428.18407.

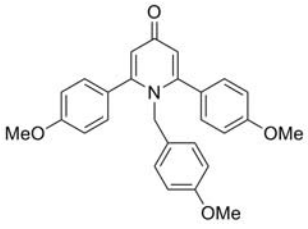

1-(4-methoxybenzyl)-2,6-bis(4-methoxyphenyl)-4-pyridone (2fd). General procedure yielded 4.0 mg (4%) of 4-pyridone from reaction above. ^{1}H NMR (400 MHz, $CDCl_3$) δ 7.18 (m, 4H), 6.86 (m, 4H), 6.62 (m, 2H), 6.41 (s, 2H), 6.38 (m, 2H), 4.87 (s, 2H), 3.81 (s, 6H), 3.72 (s, 3H). ^{13}C NMR (100 MHz, $CDCl_3$) δ 178.9, 160.3, 158.8, 153.8, 130.0, 128.8, 127.5, 127.0, 120.5, 113.9, 113.8, 55.3, 55.2, 53.4. R_f = 0.33 (10:1 EtOAc:MeOH). IR (NaCl, $CHCl_3$) 3006, 2925, 2832, 1619, 1496, 1245, 1173, 1020, 835. HRMS (ESI) $[C_{27}H_{26}NO_4]^+$ calcd 428.18171, found 428.18501.

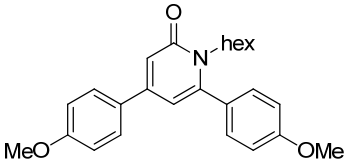

1-hexyl-4,6-bis(4-methoxyphenyl)-2-pyridone (1fc). General procedure yielded 49.9 mg (52%) of 2-pyridone. ^{1}H NMR (400 MHz, $CDCl_3$) δ 7.53 (m, 2H), 7.29 (m, 2H), 6.95 (m, 4H), 6.74 (d, *J* = 2.0 Hz, 1H), 6.29 (d, *J* = 2.0 Hz, 1H), 3.88 (t, *J* = 7.9 Hz, 2H), 3.86 (s, 3H), 3.82 (s, 3H), 1.56 (m, 2H), 1.14 (m, 6H), 0.79 (t, *J* = 7.0 Hz, 3H). ^{13}C NMR (100 MHz, $CDCl_3$) δ 163.5, 160.6, 160.0, 149.5, 149.2, 129.9, 129.7, 128.1, 127.9, 114.2, 113.8, 107.4, 55.3, 55.2, 45.4, 31.0, 28.6, 26.3, 22.3, 13.9. R_f = 0.12 (2:1 Hex:EtOAc). IR (NaCl, $CHCl_3$) 3037, 3001, 2955, 2925, 2853, 2827, 1660, 1614, 1592, 1511, 1301, 1245, 1178, 1030, 825, 723. HRMS (ESI) $[C_{25}H_{30}NO_3]^+$ calcd 392.21810, found 392.22287.

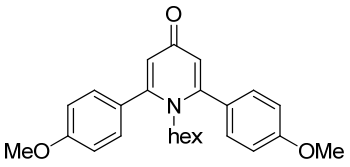

1-hexyl-2,6-bis(4-methoxyphenyl)-4-pyridone (2fc). General procedure yielded 16.8 mg (18%) of 4-pyridone from reaction above. ^{1}H NMR (400 MHz, $CDCl_3$) δ 7.33 (m, 4H), 6.98 (m, 4H), 6.34 (s, 2H), 3.86 (s, 6H), 3.70 (t, *J* = 7.8 Hz, 2H), 1.13 (m, 2H), 0.98 (m, 2H), 0.77 (m, 4H), 0.68 (t, *J* = 7.3 Hz, 3H). ^{13}C NMR (100 MHz, $CDCl_3$) δ 178.7, 160.3, 153.0, 130.0, 127.8, 120.5, 114.0, 55.4, 50.2, 30.6, 29.8, 25.5, 22.0, 13.7. R_f = 0.16 (10:1 EtOAc:MeOH). IR (NaCl, $CHCl_3$) 3001, 2955, 2935, 2853, 1619, 1552, 1501, 1250, 1178, 1035, 830. HRMS (ESI) $[C_{25}H_{30}NO_3]^+$ calcd 392.21810, found 392.22238.

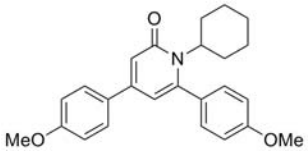

1-cyclohexyl-4,6-bis(4-methoxyphenyl)-2-pyridone (1fe). General procedure yielded 53.5 mg (55%) of 2-pyridone. ^{1}H NMR (400 MHz, $CDCl_3$) δ 7.52 (m, 2H), 7.27 (m, 2H), 6.97 (m, 2H), 6.93 (m, 2H), 6.65 (d, *J* = 2.2 Hz, 1H), 6.23 (d, *J* = 2.2 Hz, 1H), 3.87 (s, 3H), 3.82 (s, 3H), 3.80 (m, 1H), 2.79 (m, 2H), 1.74 (m, 2H), 1.61 (m, 2H), 1.50 (m, 1H), 1.22 (m, 1H), 0.96 (m, 2H). ^{13}C NMR (100 MHz, $CDCl_3$) δ 164.4, 160.5, 159.9, 149.8, 148.8, 129.6, 129.4, 129.2, 127.9, 116.1, 114.2, 113.8, 107.6, 61.8, 55.3, 28.6, 26.1, 24.9. R_f = 0.22 (2:1 Hex:EtOAc). IR (NaCl, $CHCl_3$) 3042, 2996, 2925, 2848, 1650, 1603, 1511, 1245, 1168, 1025, 820, 743. HRMS (ESI) $[C_{25}H_{28}NO_3]^+$ calcd 390.20245, found 390.20656.

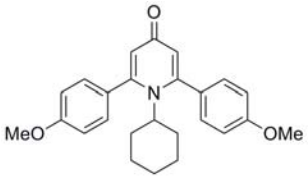

1-cyclohexyl-2,6-bis(4-methoxyphenyl)-4-pyridone (2fe). General procedure yielded 11.5 mg (12%) of 4-pyridone from reaction above. ^{1}H NMR (400 MHz, $CDCl_3$) δ 7.33 (m, 4H), 6.95 (m, 4H), 6.27 (s, 2H), 3.87 (s, 6H), 3.85 (m, 1H), 1.67 (m, 2H), 1.50 (m, 2H), 1.29 (m, 3H), 0.74 (m, 2H), 0.58 (m, 1H). ^{13}C NMR (100 MHz, $CDCl_3$) δ 178.4, 160.2, 154.2, 130.4, 129.1, 121.6, 113.6, 66.1, 55.3, 33.9, 26.6, 24.8. R_f = 0.09 (10:1 EtOAc:MeOH). IR (NaCl, $CHCl_3$) 3001, 2930, 2858, 1624, 1501, 1245, 1025, 830, 733. HRMS (ESI) $[C_{25}H_{28}NO_3]^+$ calcd 390.20245, found 390.20633.

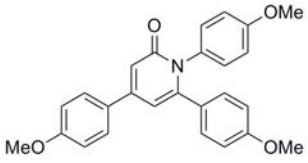

1,4,6-tris(4-methoxyphenyl)-2-pyridone (1ff). General procedure yielded 42.1 mg (43%) of 2-pyridone. ^{1}H NMR (400 MHz, $CDCl_3$) δ 7.62 (m, 2H), 7.07 (m, 2H), 7.02 (m, 2H), 6.98 (m, 2H), 6.84 (d, *J* = 2.0 Hz, 1H), 6.79 (m, 2H), 6.71 (m, 2H), 6.48 (d, *J* = 2.0 Hz, 1H), 3.86 (s, 3H), 3.75 (s, 3H), 3.74 (s, 3H). ^{13}C NMR (100 MHz, $CDCl_3$) δ 164.0, 160.7, 159.3, 158.6, 150.5, 149.4, 131.3, 130.3, 129.9, 129.7, 128.3, 128.0, 114.4, 114.3, 114.0, 113.3, 107.1, 55.3, 55.2, 55.1. R_f = 0.40 (EtOAc). IR (NaCl, $CHCl_3$) 3037, 2996, 2960, 2838, 1650, 1608, 1506, 1250, 1030, 825, 723. HRMS (ESI) $[C_{26}H_{24}NO_4]^+$ calcd 414.16606, found 414.17046.

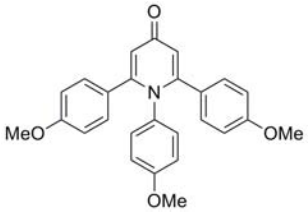

1,2,6-tris(4-methoxyphenyl)-4-pyridone (2ff). General procedure yielded 18.6 mg (19%) of 4-pyridone from reaction above. ^{1}H NMR (400 MHz, $CDCl_3$) δ 6.98 (m, 4H), 6.68 (m, 6H), 6.51 (m, 2H), 6.48 (s, 2H), 3.74 (s, 6H), 3.65 (s, 3H). ^{13}C NMR (100 MHz, $CDCl_3$) δ 178.9, 169.7, 159.4, 158.5, 152.7, 132.7, 130.6, 130.5, 127.9, 119.5, 113.4, 113.3, 55.2, 55.2. R_f = 0.11 (10:1 EtOAc:MeOH). IR (NaCl, $CHCl_3$) 3053, 3001, 2930, 2832, 1624, 1501, 1557, 1434, 1255, 1030, 825, 733. HRMS (ESI) $[C_{26}H_{24}NO_4]^+$ calcd 414.16606, found 414.17067.

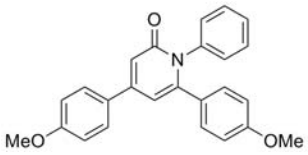

4,6-bis(4-methoxyphenyl)-1-phenyl-2-pyridone (1fg). General procedure yielded 34.7 mg (37%) of 2-pyridone. ^{1}H NMR (400 MHz, $CDCl_3$) δ 7.62 (m, 2H), 7.26 (m, 3H), 7.11 (m, 2H), 7.05 (m, 2H), 6.99 (m, 2H), 6.85 (d, *J* = 2.0 Hz, 1H), 6.69 (m, 2H), 6.50 (d, *J* = 2.0 Hz, 1H), 3.86 (s, 3H), 3.73 (s, 3H). ^{13}C NMR (100 MHz, $CDCl_3$) δ 163.8, 160.8, 159.4, 150.7, 149.1, 138.7, 130.3, 129.7, 129.0, 128.7, 128.2, 128.1, 127.8, 114.6, 114.4, 113.3, 107.2, 55.4, 55.1. R_f = 0.68 (2:1 Hex:EtOAc). IR (NaCl, $CHCl_3$) 3063, 3037, 2960, 2935, 2838, 1655, 1603, 1506, 1250, 1025, 820, 728. HRMS (ESI) $[C_{25}H_{22}NO_3]^+$ calcd 384.15550, found 384.16035.

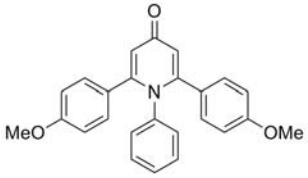

2,6-bis(4-methoxyphenyl)-1-phenyl-4-pyridone (2fg). General procedure yielded 18.2 mg (20%) of 4-pyridone from reaction above. ^{1}H NMR (400 MHz, $CDCl_3$) δ 7.03 (m, 3H), 6.98 (m, 4H), 6.80 (m, 2H), 6.66 (m, 4H), 6.49 (s, 2H), 3.72 (s, 6H). ^{13}C NMR (100 MHz, $CDCl_3$) δ 179.0, 159.4, 152.4, 139.9, 130.5, 129.8, 128.4, 127.9, 127.7, 119.6, 113.3, 55.1. R_f = 0.14 (10:1 EtOAc:MeOH). IR (NaCl, $CHCl_3$) 3058, 3001, 2925, 2832, 1629, 1501,

1296, 1250, 1173, 1025, 830, 728. HRMS (ESI) $[C_{25}H_{22}NO_3]^+$ calcd 384.15550, found 384.16090.

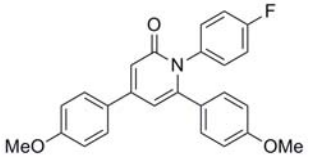

1-(4-fluorophenyl)-4,6-bis(4-methoxyphenyl)-2-pyridone (1fh). General procedure yielded 44.7 mg (48%) of 2-pyridone. ^{1}H NMR (400 MHz, $CDCl_3$) δ 7.62 (m, 2H), 7.07 (m, 4H), 6.97 (m, 4H), 6.84 (d, J = 1.8 Hz, 1H), 6.72 (m, 2H), 6.50 (d, J = 1.8 Hz, 1H), 3.86 (s, 3H), 3.75 (s, 3H). ^{13}C NMR (100 MHz, $CDCl_3$) δ 163.8, 162.8, 160.9, 160.4, 159.5, 150.8, 149.0, 134.6, 130.7, 130.6, 130.3, 129.5, 128.0, 127.9, 115.9, 115.6, 114.4, 114.3, 113.4, 107.3, 55.3, 55.2. R_f = 0.21 (1:1 Hex:EtOAc). IR (NaCl, $CHCl_3$) 3068, 3006, 2930, 2838, 1660, 1608, 1506, 1250, 1030, 820, 728. HRMS (ESI) $[C_{25}H_{21}FNO_3]^+$ calcd 402.14608, found 402.15125.

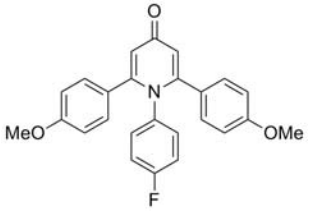

1-(4-fluorophenyl)-2,6-bis(4-methoxyphenyl)-4-pyridone (2fh). General procedure yielded 21.6 mg (23%) of 4-pyridone from reaction above. ^{1}H NMR (400 MHz, $CDCl_3$) δ 6.97 (m, 4H), 6.77 (m, 2H), 6.72 (m, 2H), 6.68 (m, 4H), 6.47 (s, 2H), 3.73 (s, 6H). ^{13}C NMR (100 MHz, $CDCl_3$) δ 178.9, 162.5, 160.0, 159.5, 152.4, 136.0, 131.4, 131.3, 130.5, 127.4, 119.6, 115.6, 115.3, 113.4, 55.1. R_f = 0.19 (10:1 EtOAc:MeOH). IR (NaCl, $CHCl_3$) 3063, 3001, 2930, 2832, 1624, 1573, 1506, 1255, 1178, 835, 728. HRMS (ESI) $[C_{25}H_{21}FNO_3]^+$ calcd 402.14608, found 402.15103.

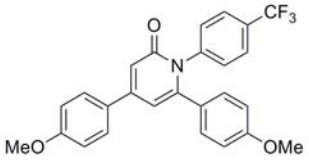

4,6-bis(4-methoxyphenyl)-1-(4-(trifluoromethyl) phenyl)-2-pyridone (1fi). General procedure yielded 35.8 mg (34%) of 2-pyridone. ^{1}H NMR (400 MHz, $CDCl_3$) δ 7.62 (m, 2H), 7.55 (m, 2H), 7.25 (m, 2H), 7.01 (m, 4H), 6.84 (d, *J* = 1.9 Hz, 1H), 6.71 (m, 2H), 6.54 (d, *J* = 1.9 Hz, 1H), 3.86 (s, 3H), 3.75 (s, 3H). ^{13}C NMR (100 MHz, $CDCl_3$) δ 163.8, 161.2, 159.9, 151.4, 148.8, 142.1, 130.5, 130.2, 129.9, 129.6, 128.4, 127.8, 126.1, 126.0, 114.7, 114.6, 113.8, 108.0, 55.6, 55.4. R_f = 0.19 (2:1 Hex:EtOAc). IR (NaCl, $CHCl_3$) 3063, 3001, 2955, 2832, 1660, 1598, 1501, 1250, 1117, 825, 723. HRMS (ESI) $[C_{26}H_{21}F_3NO_3]^+$ calcd 452.14288, found 452.14608.

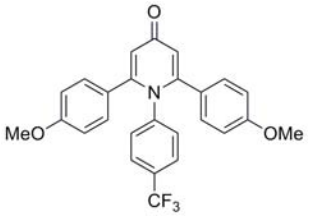

2,6-bis(4-methoxyphenyl)-1-(4-(trifluoromethyl) phenyl)-4-pyridone (2fi). General procedure yielded 31.7 mg (30%) of 4-pyridone from reaction above. ^{1}H NMR (400 MHz, $CDCl_3$) δ 7.30 (m, 2H), 6.94 (m, 6H), 6.67 (m, 4H), 6.52 (s, 2H), 3.72 (s, 6H). ^{13}C NMR (100 MHz, $CDCl_3$) δ 179.1, 160.0, 152.3, 143.2, 130.7, 130.5, 127.2, 125.8, 125.7, 120.0, 113.8, 55.4. R_f = 0.28 (10:1 EtOAc:MeOH). IR (NaCl, $CHCl_3$) 3058, 3001, 2935, 2832, 1629, 1501, 1245, 1178, 1020, 835, 723. HRMS (ESI) $[C_{26}H_{21}F_3NO_3]^+$ calcd 452.14288, found 452.14620.

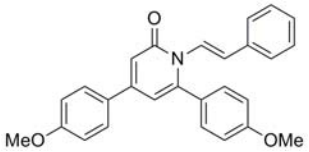

(E)-4,6-bis(4-methoxyphenyl)-1-styryl-2-pyridone (1fj). General procedure yielded 12.8 mg (13%) of 2-pyridone. ^{1}H NMR (400 MHz, $CDCl_3$) δ 7.61 (m, 2H), 7.37 (m, 2H), 7.24 (m, 5H), 7.06 (d, J = 14.7 Hz, 1H), 6.98 (m, 2H), 6.92 (m, 2H), 6.85 (d, J = 1.9 Hz, 1H), 6.66 (d, J = 14.7 Hz, 1H), 6.50 (d, J = 2.0 Hz, 1H), 3.86 (s, 3H), 3.82 (s, 3H). ^{13}C NMR (100 MHz, $CDCl_3$) δ 163.9, 161.0, 160.0, 150.3, 148.2, 134.9, 130.8, 130.4, 129.3, 128.5, 128.1, 128.0, 126.5, 125.4, 114.4, 113.9, 108.4, 55.4, 55.3. R_f = 0.31 (1:1 Hex:EtOAc). IR (NaCl, $CHCl_3$) 3063, 3022, 2955, 2930, 2832, 1655, 1603, 1506, 1250, 1168, 1035, 825, 748. HRMS (ESI) $[C_{27}H_{24}NO_3]^+$ calcd 410.17115, found 410.17465.

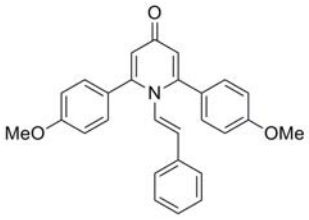

(E)-2,6-bis(4-methoxyphenyl)-1-styryl-4-pyridone (2fj). General procedure yielded 16.8 mg (17%) of 4-pyridone from reaction above. ^{1}H NMR (400 MHz, $CDCl_3$) δ 7.39 (m, 4H), 7.19 (m, 3H), 6.90 (m, 6H), 6.80 (s, 2H), 6.75 (d, J = 14.5 Hz, 1H), 6.01 (d, J = 14.5 Hz, 1H), 3.80 (s, 6H). ^{13}C NMR (100 MHz, $CDCl_3$) δ 176.6, 160.4, 153.8, 134.4, 133.2, 130.8, 128.8, 128.7, 127.7, 126.6, 126.4, 118.2, 114.0, 55.3. R_f = 0.24 (10:1 EtOAc:MeOH). IR (NaCl, $CHCl_3$) 3058, 3007, 2960, 2930, 1619, 1496, 1250, 1178, 1025, 835, 748. HRMS (ESI) $[C_{27}H_{24}NO_3]^+$ calcd 410.17115, found 410.17575.

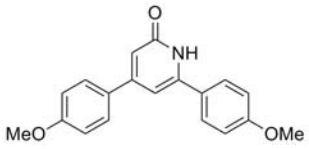

4,6-bis(4-methoxyphenyl)-2-pyridone (35). 2-pyridone **1fd** (19.6 mg, 0.046 mmol) was dissolved in neat trifluoroacetic acid and added to an oven-dried pressure tube. The reaction vessel was sealed and heated to 110 °C for 12 h. The resulting solution was allowed to cool to 23 °C, concentrated *in vacuo*, and purified with flash chromatography (gradient elution 10:1 EtOAc:MeOH). The isolated solid was dissolved in concentrated aq NaOH solution and extracted 3x with EtOAc. The resulting solution was dried and concentrated *in vacuo* to afford11.1 mg of pyridone **35** (78%). ^{1}H NMR (400 MHz, $CDCl_3$) δ 7.69 (m, 2H), 7.60 (m, 2H), 7.01 (m, 4H), 6.66 (m, 2H), 3.88 (s, 3H), 3.87 (s, 3H). ^{13}C NMR (100 MHz, $CDCl_3$) δ 165.1, 161.1, 160.8, 153.2, 146.1, 130.4, 128.2, 127.9, 126.2, 114.6, 114.4, 103.6, 55.5, 55.4. R_f = 0.51 (10:1 EtOAc:MeOH). IR (NaCl, $CHCl_3$) 3078, 2955, 2904, 1639, 1603, 1234, 1024, 809. HRMS (ESI) $[C_{19}H_{18}NO_3]^+$ calcd 308.12420, found 308.12806.

^{1}H NMR and ^{13}C NMR Spectra of Selected Compounds.

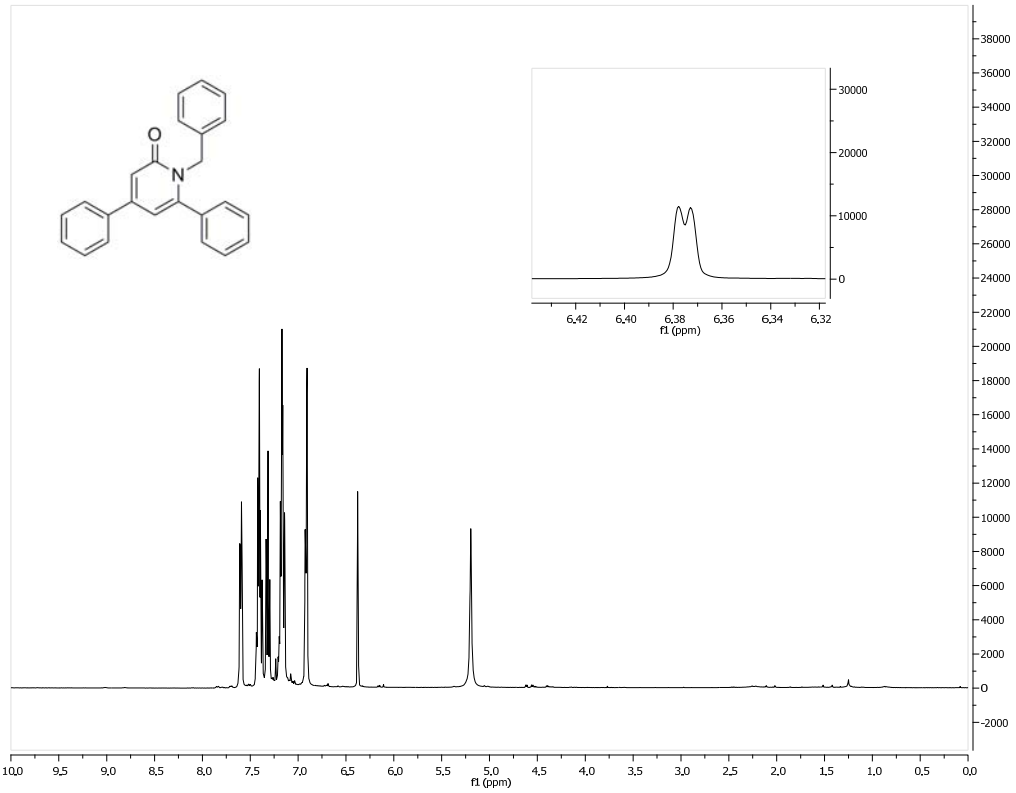

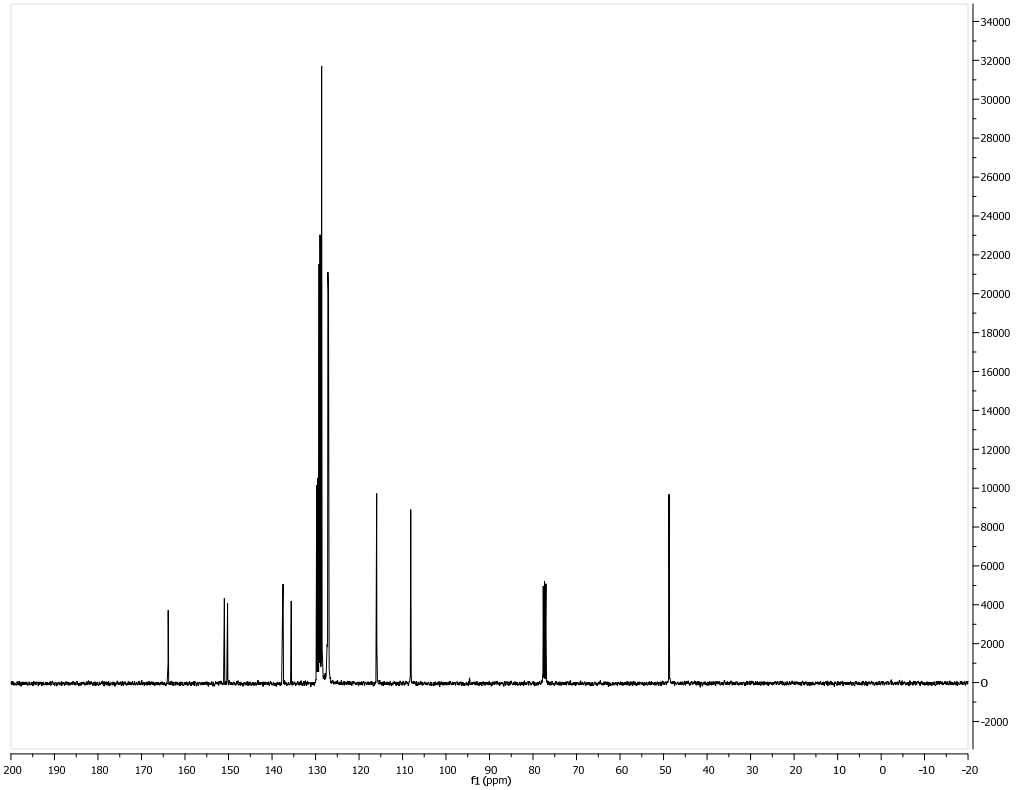

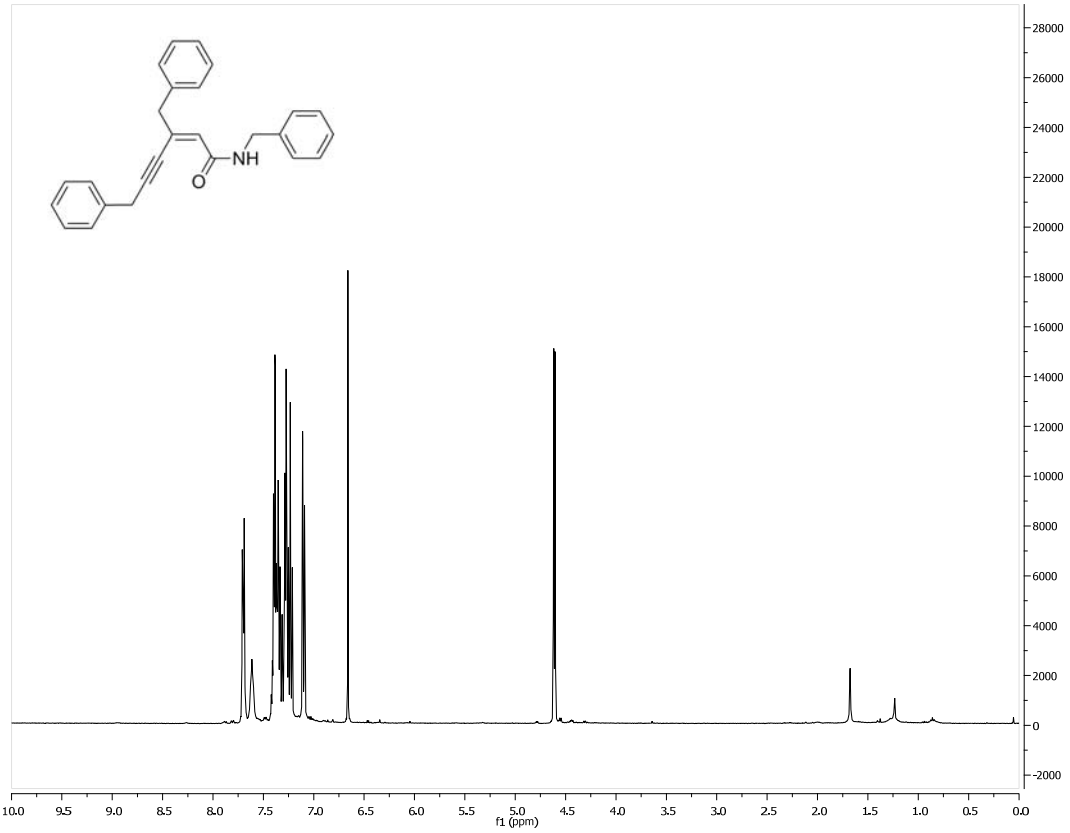
NH
O
28000
26000
24000
22000
20000
18000
16000
14000
12000
10000
8000
6000
4000
2000
0
-2000
10.0 9.5 9.0 8.5 8.0 7.5 7.0 6.5 6.0 5.5 5.0 4.5 4.0 3.5 3.0 2.5 2.0 1.5 1.0 0.5 0.0
f1 (ppm)

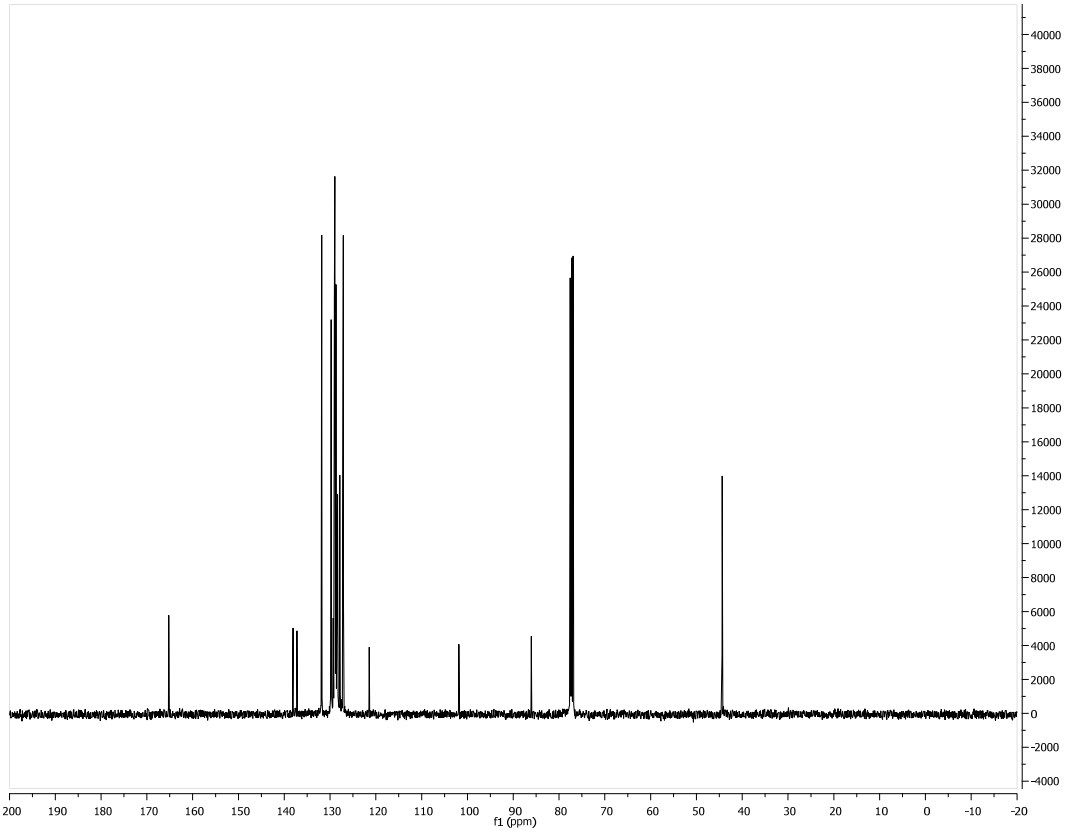
40000
38000
36000
34000
32000
30000
28000
26000
24000
22000
20000
18000
16000
14000
12000
10000
8000
6000
4000
2000
0
-2000
-4000
200 190 180 170 160 150 140 130 120 110 100 90 80 70 60 50 40 30 20 10 0 -10 -20
f1 (ppm)

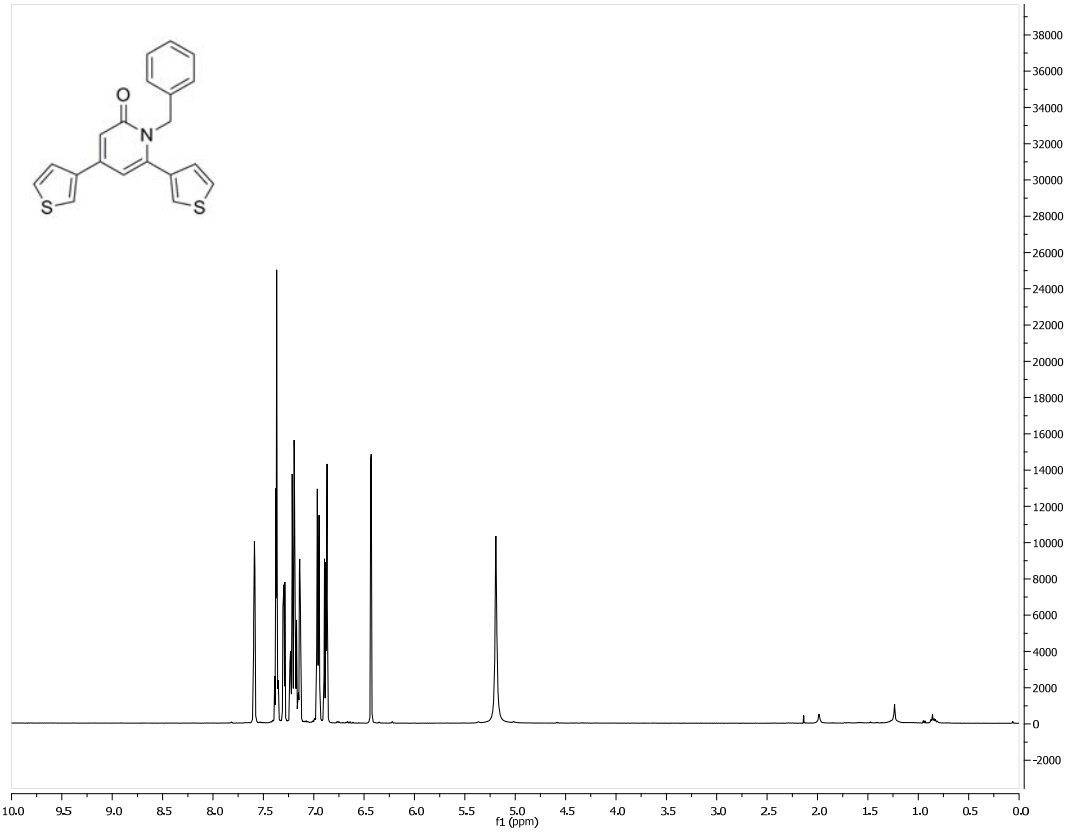
O
N
S
S
38000
36000
34000
32000
30000
28000
26000
24000
22000
20000
18000
16000
14000
12000
10000
8000
6000
4000
2000
0
-2000
10.0 9.5 9.0 8.5 8.0 7.5 7.0 6.5 6.0 5.5 5.0 4.5 4.0 3.5 3.0 2.5 2.0 1.5 1.0 0.5 0.0
f1 (ppm)

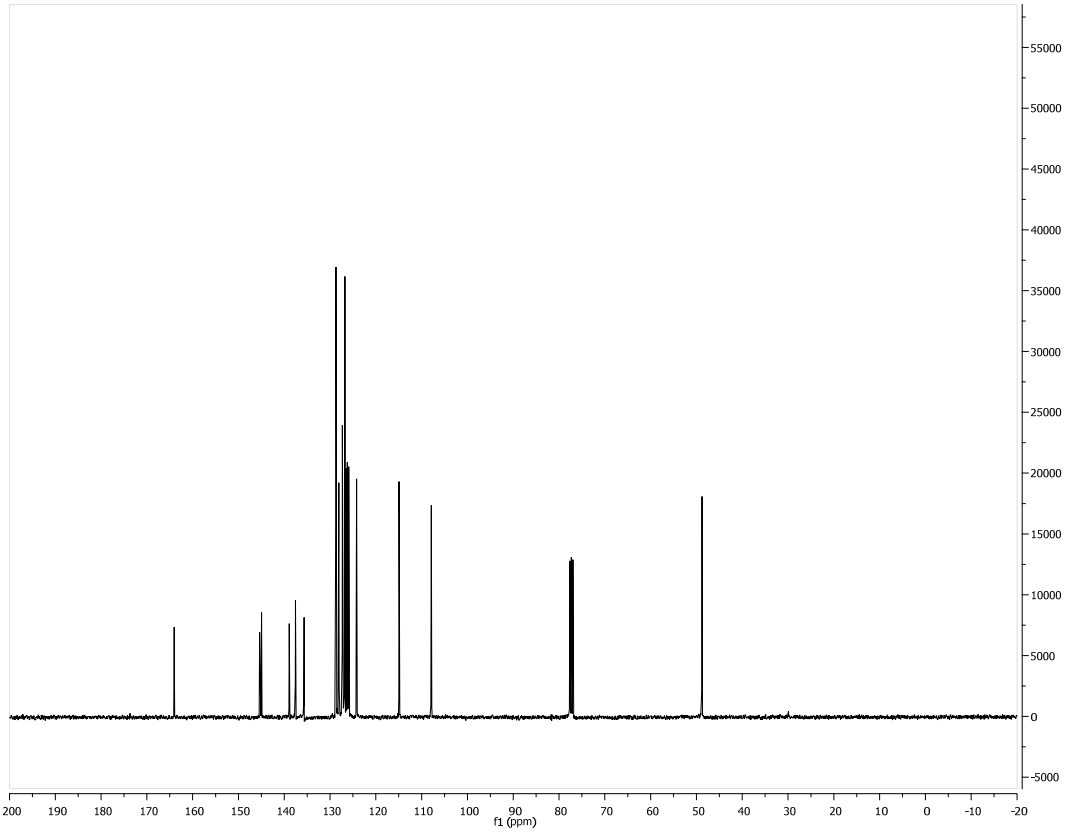
55000
50000
45000
40000
35000
30000
25000
20000
15000
10000
5000
0
-5000
200 190 180 170 160 150 140 130 120 110 100 90 80 70 60 50 40 30 20 10 0 -10 -20
f1 (ppm)

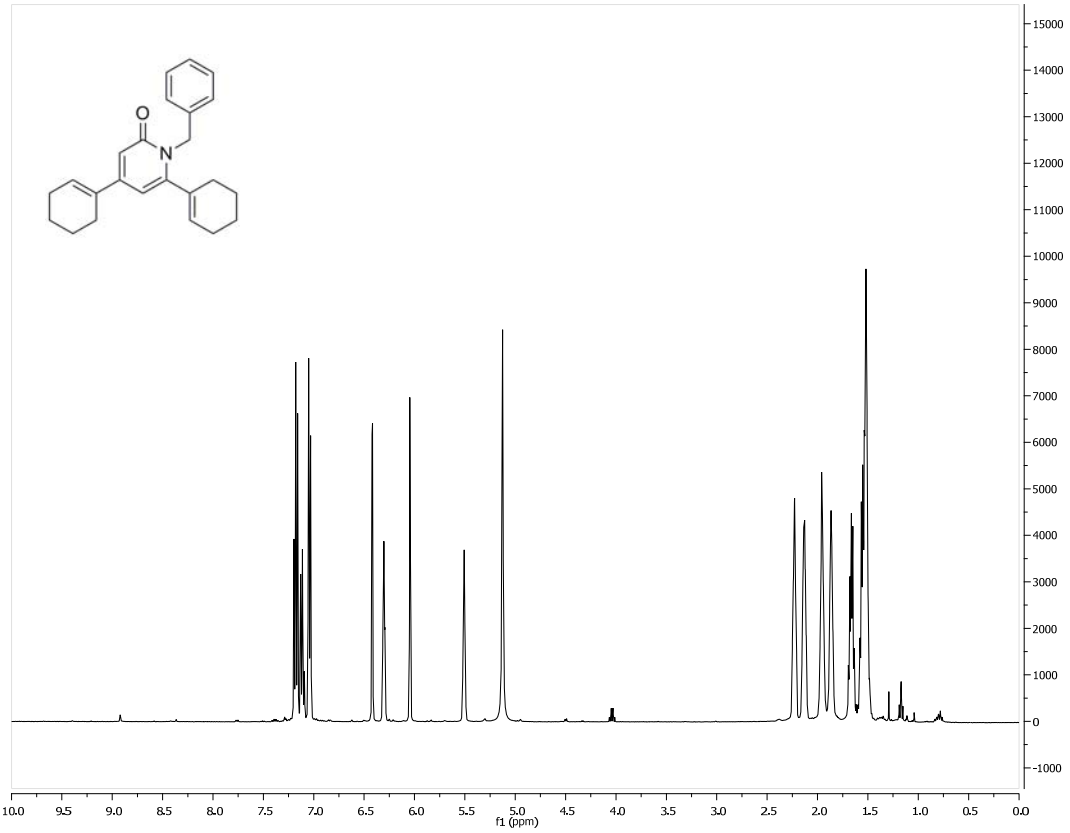
O
N
15000
14000
13000
12000
11000
10000
9000
8000
7000
6000
5000
4000
3000
2000
1000
0
-1000
10.0 9.5 9.0 8.5 8.0 7.5 7.0 6.5 6.0 5.5 5.0 4.5 4.0 3.5 3.0 2.5 2.0 1.5 1.0 0.5 0.0
f1 (ppm)

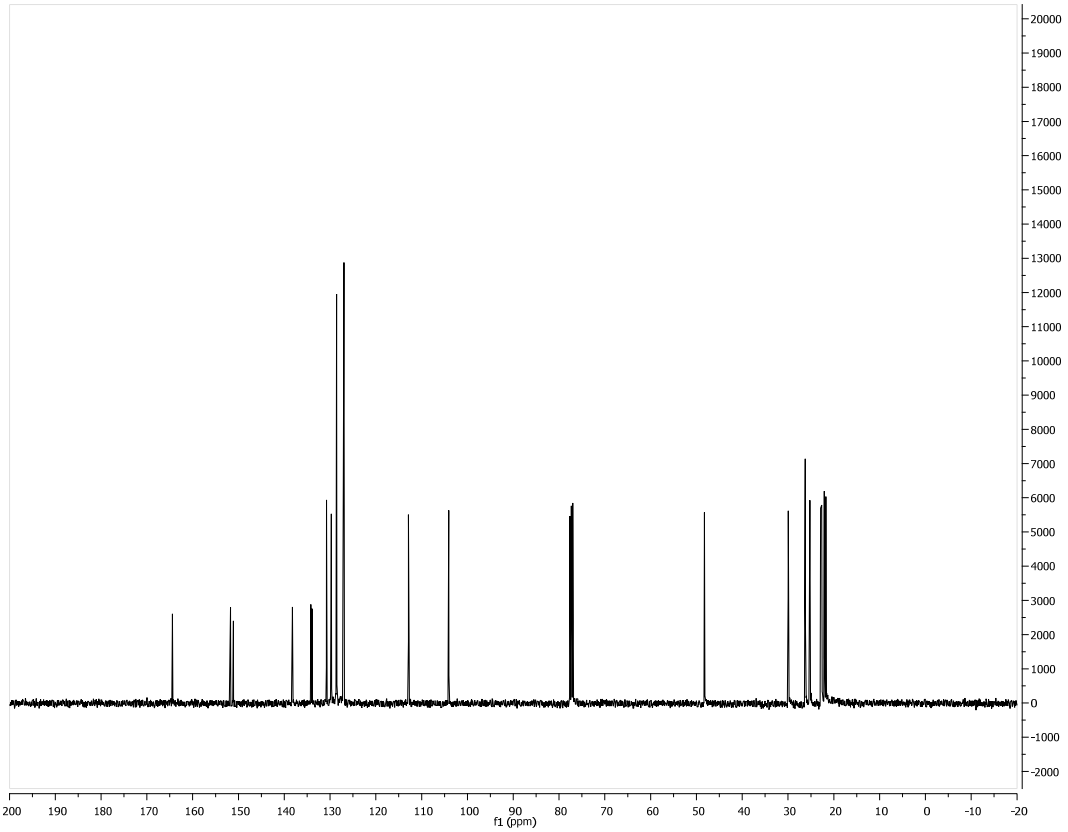
20000
19000
18000
17000
16000
15000
14000
13000
12000
11000
10000
9000
8000
7000
6000
5000
4000
3000
2000
1000
0
-1000
-2000
200 190 180 170 160 150 140 130 120 110 100 90 80 70 60 50 40 30 20 10 0 -10 -20
f1 (ppm)

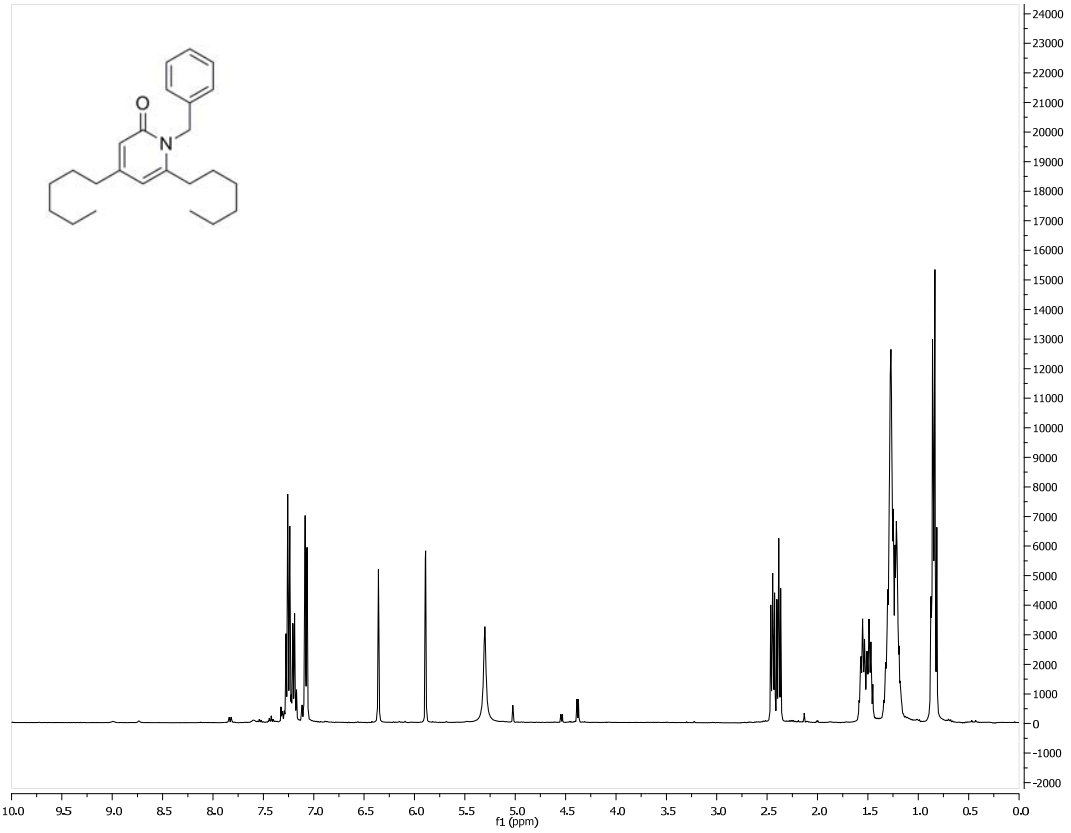
O
N
f1 (ppm)

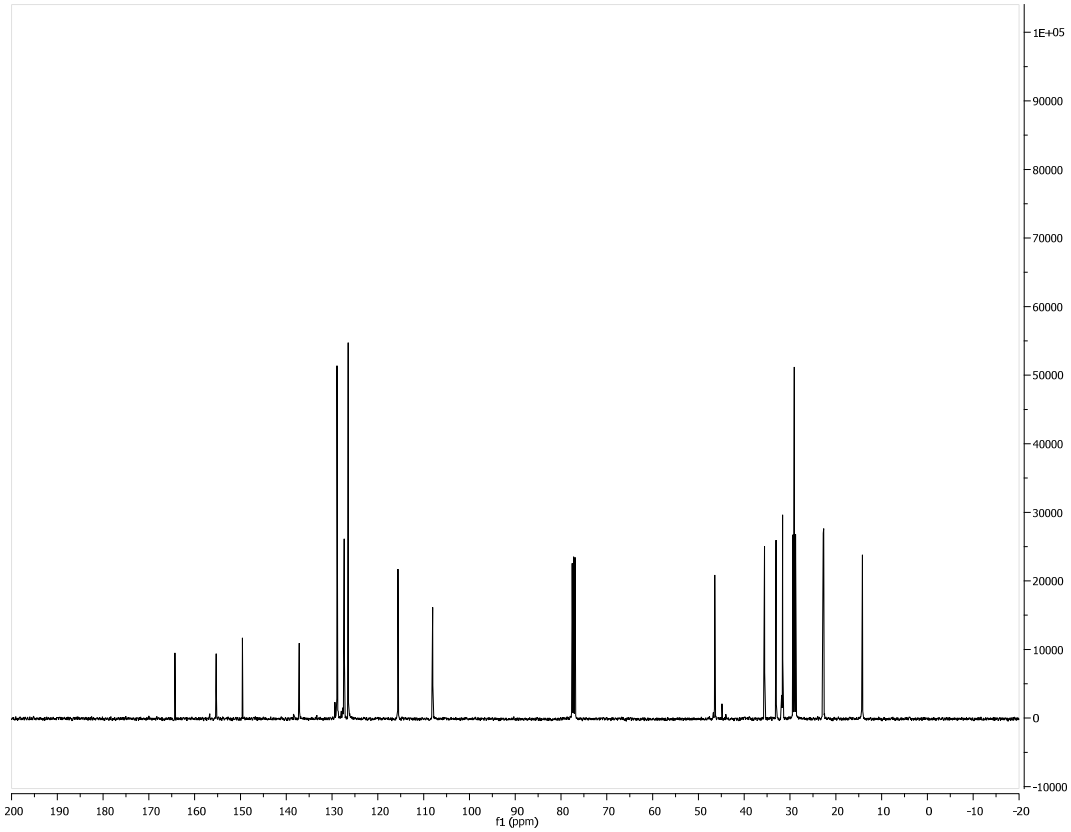
f1 (ppm)

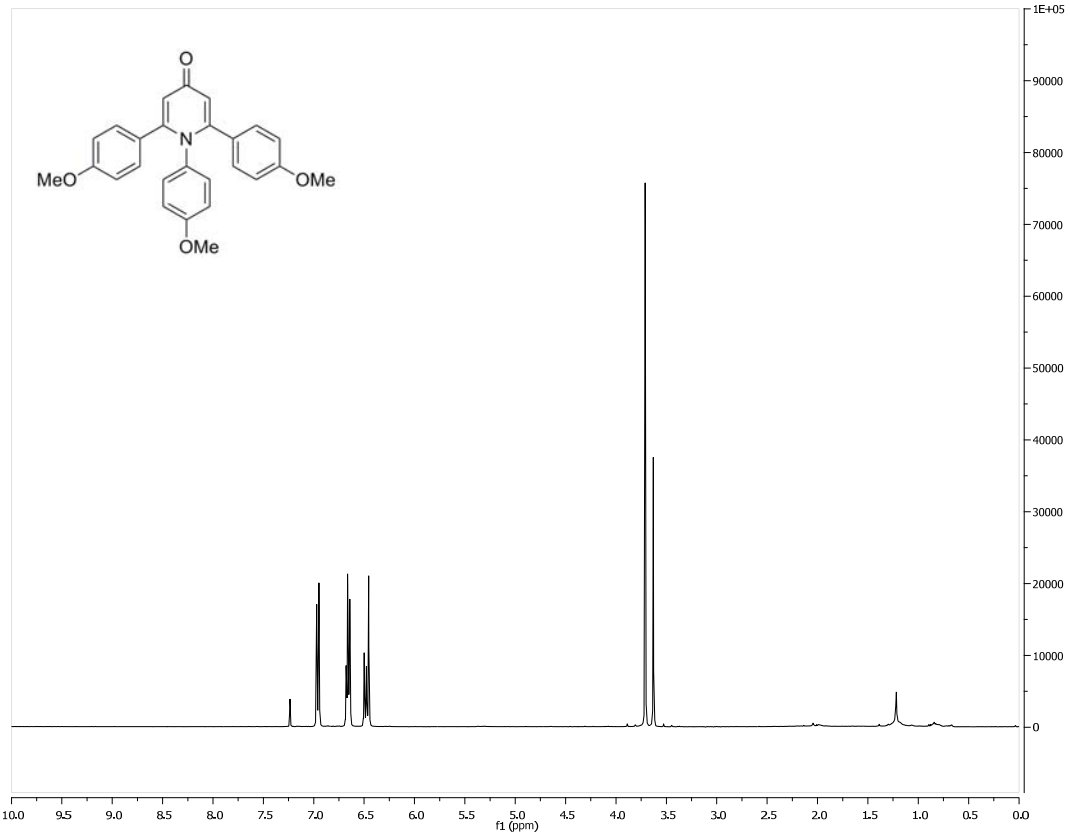
O
N
MeO
OMe
OMe
1E+05
90000
80000
70000
60000
50000
40000
30000
20000
10000
0
10.0 9.5 9.0 8.5 8.0 7.5 7.0 6.5 6.0 5.5 5.0 4.5 4.0 3.5 3.0 2.5 2.0 1.5 1.0 0.5 0.0
f1 (ppm)

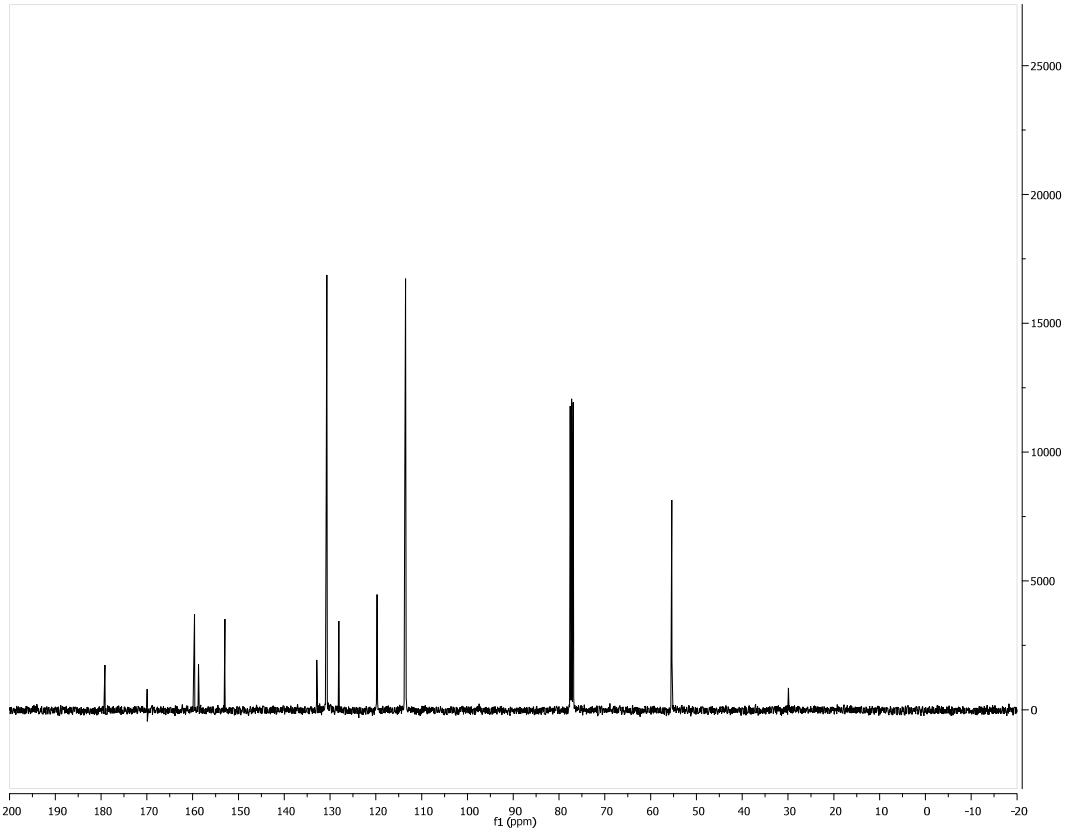
25000
20000
15000
10000
5000
0
200 190 180 170 160 150 140 130 120 110 100 90 80 70 60 50 40 30 20 10 0 -10 -20
f1 (ppm)

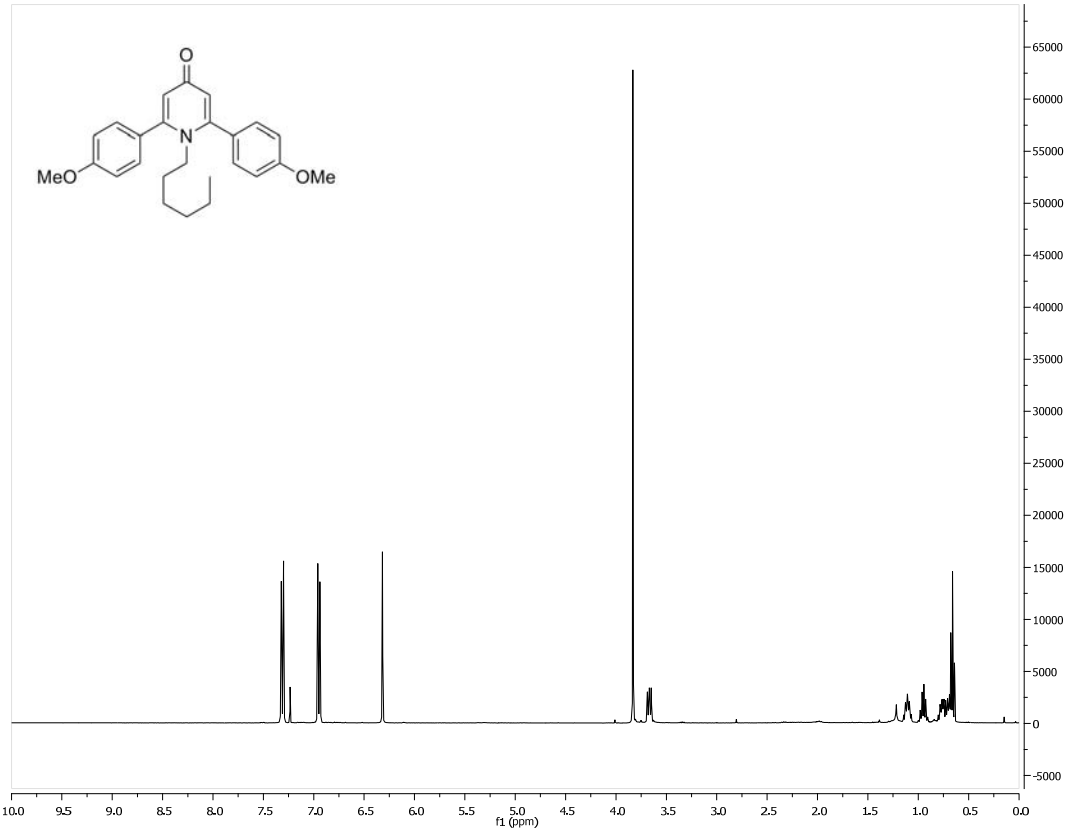
O
N
MeO
OMe
65000
60000
55000
50000
45000
40000
35000
30000
25000
20000
15000
10000
5000
0
-5000
10.0 9.5 9.0 8.5 8.0 7.5 7.0 6.5 6.0 5.5 5.0 4.5 4.0 3.5 3.0 2.5 2.0 1.5 1.0 0.5 0.0
f1 (ppm)

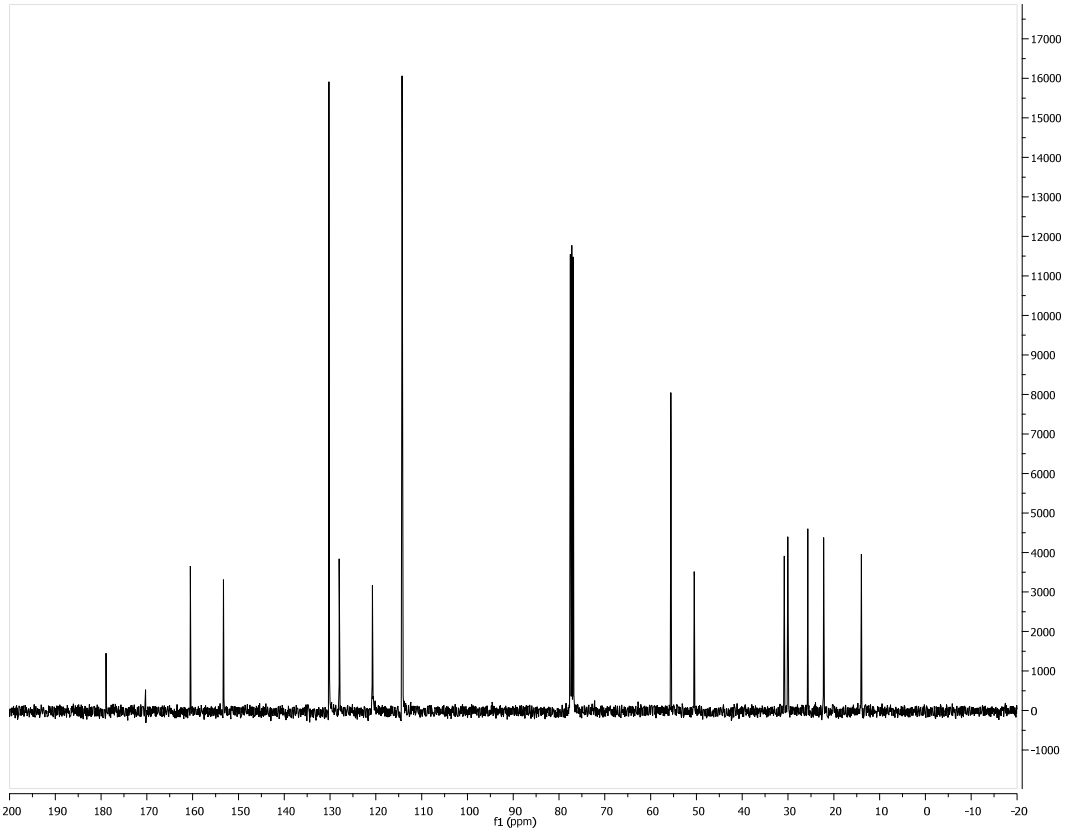
17000
16000
15000
14000
13000
12000
11000
10000
9000
8000
7000
6000
5000
4000
3000
2000
1000
0
-1000
200 190 180 170 160 150 140 130 120 110 100 90 80 70 60 50 40 30 20 10 0 -10 -20
f1 (ppm)

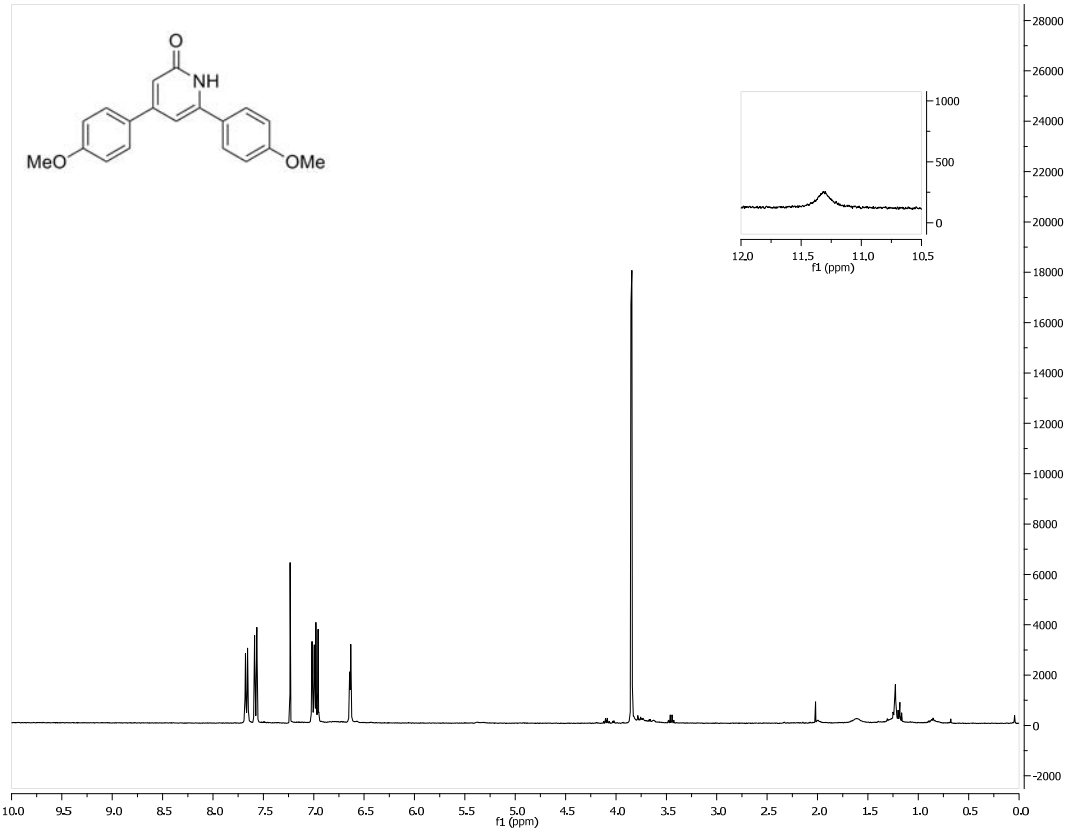
O
NH
MeO
OMe
f1 (ppm)
f1 (ppm)

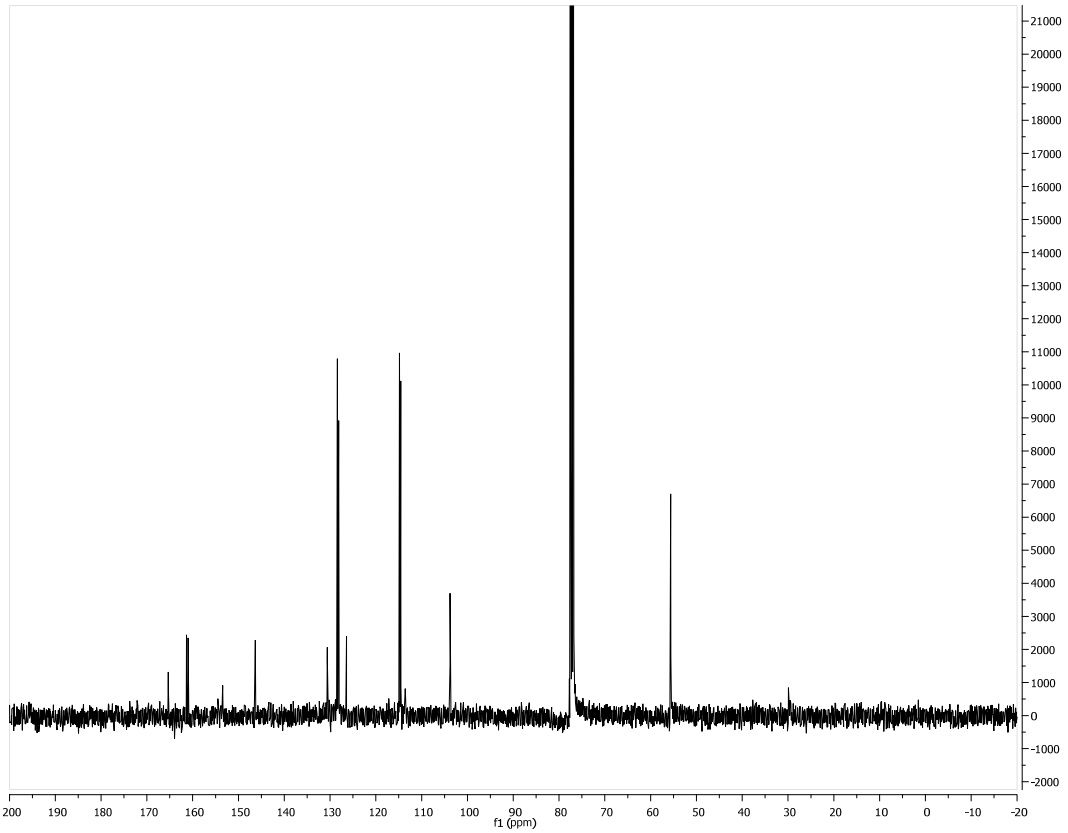
f1 (ppm)

Crystal Structure Tables and Figures.

Table A.1.1. Crystal data and structure refinement for **1db**.

Identification code	rovis122	
Empirical formula	$C_{24}H_{19}NO$	
Formula weight	337.40	
Temperature	120 K	
Wavelength	0.71073 Å	
Crystal system	Monoclinic	
Space group	$P\ 2_1/c$	
Unit cell dimensions	a = 18.0500(9) Å	α= 90°.
	b = 6.2286(3) Å	β= 114.967(3)°.
	c = 17.2636(9) Å	γ = 90°.
Volume	1759.51(15) $Å^3$	
Z	4	
Density (calculated)	1.274 Mg/m^3	
Absorption coefficient	0.077 mm^{-1}	
F(000)	712	
Crystal size	0.19 x 0.19 x 0.09 mm^3	
Theta range for data collection	2.36 to 31.03°.	
Index ranges	-26<=h<=25, -9<=k<=9, -25<=l<=25	
Reflections collected	42377	
Independent reflections	5592 [R(int) = 0.0813]	
Completeness to theta = 31.03°	99.8 %	
Absorption correction	Semi-empirical from equivalents	
Max. and min. transmission	0.9929 and 0.9857	
Refinement method	Full-matrix least-squares on F^2	
Data / restraints / parameters	5592 / 0 / 235	
Goodness-of-fit on F^2	1.041	
Final R indices [I>2sigma(I)]	R1 = 0.0522, wR2 = 0.1342	
R indices (all data)	R1 = 0.1074, wR2 = 0.1814	
Largest diff. peak and hole	0.301 and -0.400 $e.Å^{-3}$	

Table A.1.2. Atomic coordinates (x 10^4) and equivalent isotropic displacement parameters ($Å^2$x 10^3) for **1db**. U(eq) is defined as one third of the trace of the orthogonalized U^{ij} tensor.

	x	y	z	U(eq)
C(1)	1148(1)	7103(3)	747(1)	21(1)
C(2)	2411(1)	7560(2)	2038(1)	19(1)
C(3)	2212(1)	5896(3)	2420(1)	20(1)
C(4)	1459(1)	4766(2)	1990(1)	19(1)
C(5)	960(1)	5356(3)	1175(1)	20(1)
C(6)	2072(1)	10067(3)	819(1)	22(1)
C(7)	2700(1)	9593(3)	477(1)	22(1)
C(8)	2704(1)	7642(3)	95(1)	26(1)
C(9)	3253(1)	7244(3)	-257(1)	32(1)
C(10)	3809(1)	8805(3)	-230(1)	35(1)

C(11)	3811(1)	10756(3)	148(1)	36(1)
C(12)	3260(1)	11146(3)	504(1)	29(1)
C(13)	3214(1)	8662(3)	2481(1)	19(1)
C(14)	3921(1)	7617(3)	2552(1)	25(1)
C(15)	4679(1)	8546(3)	3001(1)	31(1)
C(16)	4743(1)	10521(3)	3387(1)	32(1)
C(17)	4046(1)	11581(3)	3316(1)	31(1)
C(18)	3282(1)	10659(3)	2870(1)	27(1)
C(19)	1252(1)	3007(2)	2442(1)	19(1)
C(20)	1514(1)	3096(3)	3326(1)	22(1)
C(21)	1329(1)	1453(3)	3757(1)	24(1)
C(22)	884(1)	-316(3)	3315(1)	24(1)
C(23)	615(1)	-408(3)	2436(1)	23(1)
C(24)	789(1)	1236(3)	1999(1)	21(1)
N(1)	1883(1)	8209(2)	1227(1)	19(1)
O(1)	719(1)	7671(2)	6(1)	31(1)

Table A.1.3. Bond lengths [Å] and angles [°] for **1db**.

C(1)-O(1)	1.2348(19)	O(1)-C(1)-C(5)	124.73(15)
C(1)-N(1)	1.411(2)	N(1)-C(1)-C(5)	115.85(14)
C(1)-C(5)	1.435(2)	C(3)-C(2)-N(1)	120.42(14)
C(2)-C(3)	1.356(2)	C(3)-C(2)-C(13)	120.17(14)
C(2)-N(1)	1.381(2)	N(1)-C(2)-C(13)	119.39(13)
C(2)-C(13)	1.491(2)	C(2)-C(3)-C(4)	120.85(15)
C(3)-C(4)	1.428(2)	C(5)-C(4)-C(3)	118.26(14)
C(4)-C(5)	1.363(2)	C(5)-C(4)-C(19)	122.61(14)
C(4)-C(19)	1.481(2)	C(3)-C(4)-C(19)	119.13(14)
C(6)-N(1)	1.467(2)	C(4)-C(5)-C(1)	122.62(14)
C(6)-C(7)	1.511(2)	N(1)-C(6)-C(7)	113.42(13)
C(7)-C(8)	1.384(2)	C(8)-C(7)-C(12)	118.50(16)
C(7)-C(12)	1.387(2)	C(8)-C(7)-C(6)	120.94(15)
C(8)-C(9)	1.387(2)	C(12)-C(7)-C(6)	120.50(15)
C(9)-C(10)	1.383(3)	C(7)-C(8)-C(9)	121.01(16)
C(10)-C(11)	1.379(3)	C(10)-C(9)-C(8)	120.09(18)
C(11)-C(12)	1.393(3)	C(11)-C(10)-C(9)	119.53(17)
C(13)-C(14)	1.392(2)	C(10)-C(11)-C(12)	120.20(17)
C(13)-C(18)	1.394(2)	C(7)-C(12)-C(11)	120.67(18)
C(14)-C(15)	1.383(2)	C(14)-C(13)-C(18)	118.92(15)
C(15)-C(16)	1.380(3)	C(14)-C(13)-C(2)	119.15(14)
C(16)-C(17)	1.380(3)	C(18)-C(13)-C(2)	121.82(14)
C(17)-C(18)	1.387(2)	C(15)-C(14)-C(13)	120.47(16)
C(19)-C(20)	1.396(2)	C(16)-C(15)-C(14)	120.31(16)
C(19)-C(24)	1.400(2)	C(17)-C(16)-C(15)	119.78(16)
C(20)-C(21)	1.386(2)	C(16)-C(17)-C(18)	120.40(17)
C(21)-C(22)	1.387(2)	C(17)-C(18)-C(13)	120.12(16)
C(22)-C(23)	1.386(2)	C(20)-C(19)-C(24)	118.49(15)
C(23)-C(24)	1.384(2)	C(20)-C(19)-C(4)	120.15(14)
		C(24)-C(19)-C(4)	121.36(14)
O(1)-C(1)-N(1)	119.42(15)	C(21)-C(20)-C(19)	120.67(15)

C(20)-C(21)-C(22)	120.43(16)	C(2)-N(1)-C(1)	121.84(13)
C(23)-C(22)-C(21)	119.30(15)	C(2)-N(1)-C(6)	121.10(13)
C(24)-C(23)-C(22)	120.69(15)	C(1)-N(1)-C(6)	117.05(13)
C(23)-C(24)-C(19)	120.40(15)		

Symmetry transformations used to generate equivalent atoms:

Table A.1.4. Anisotropic displacement parameters ($Å^2 x\ 10^3$)for **1db**. The anisotropic displacement factor exponent takes the form: $-2\pi^2[\ h^2 a^{*2} U^{11} + ... + 2\ h\ k\ a^*\ b^*\ U^{12}\ ]$

	U^{11}	U^{22}	U^{33}	U^{23}	U^{13}	U^{12}
C(1)	18(1)	26(1)	18(1)	-1(1)	7(1)	-1(1)
C(2)	17(1)	19(1)	20(1)	-1(1)	7(1)	1(1)
C(3)	17(1)	23(1)	19(1)	1(1)	5(1)	0(1)
C(4)	16(1)	19(1)	20(1)	-2(1)	8(1)	-1(1)
C(5)	17(1)	23(1)	20(1)	-2(1)	7(1)	-3(1)
C(6)	23(1)	22(1)	20(1)	2(1)	8(1)	0(1)
C(7)	20(1)	26(1)	16(1)	4(1)	6(1)	1(1)
C(8)	29(1)	26(1)	25(1)	0(1)	13(1)	-3(1)
C(9)	38(1)	34(1)	27(1)	2(1)	16(1)	6(1)
C(10)	29(1)	53(1)	26(1)	9(1)	15(1)	7(1)
C(11)	29(1)	48(1)	33(1)	3(1)	15(1)	-10(1)
C(12)	29(1)	30(1)	27(1)	-1(1)	11(1)	-7(1)
C(13)	18(1)	21(1)	19(1)	1(1)	7(1)	-2(1)
C(14)	22(1)	27(1)	26(1)	-5(1)	10(1)	0(1)
C(15)	17(1)	43(1)	30(1)	-3(1)	8(1)	1(1)
C(16)	24(1)	43(1)	25(1)	-5(1)	8(1)	-13(1)
C(17)	36(1)	28(1)	31(1)	-9(1)	14(1)	-11(1)
C(18)	24(1)	24(1)	32(1)	-4(1)	12(1)	-1(1)
C(19)	15(1)	20(1)	22(1)	1(1)	8(1)	1(1)
C(20)	21(1)	21(1)	21(1)	-1(1)	6(1)	-3(1)
C(21)	24(1)	26(1)	20(1)	2(1)	7(1)	2(1)
C(22)	21(1)	22(1)	28(1)	5(1)	11(1)	0(1)
C(23)	18(1)	21(1)	29(1)	-5(1)	10(1)	-2(1)
C(24)	17(1)	23(1)	21(1)	-2(1)	7(1)	0(1)
N(1)	19(1)	20(1)	18(1)	1(1)	7(1)	-1(1)
O(1)	28(1)	39(1)	19(1)	5(1)	3(1)	-6(1)

Table A.1.5. Hydrogen coordinates ($x\ 10^4$) and isotropic displacement parameters ($Å^2 x\ 10^3$) for **1db**.

	x	y	z	U(eq)
H(3)	2570	5485	2969	24
H(5)	477	4596	885	24
H(6A)	2273	11224	1232	26
H(6B)	1573	10557	353	26

H(8)	2333	6583	73	32
H(9)	3248	5926	-512	38
H(10)	4179	8540	-464	42
H(11)	4181	11814	166	43
H(12)	3269	12462	762	35
H(14)	3884	6283	2296	30
H(15)	5148	7837	3044	37
H(16)	5254	11134	3694	38
H(17)	4087	12922	3568	38
H(18)	2816	11375	2831	32
H(20)	1816	4269	3630	26
H(21)	1503	1538	4345	29
H(22)	768	-1429	3605	28
H(23)	314	-1587	2136	27
H(24)	598	1164	1408	25

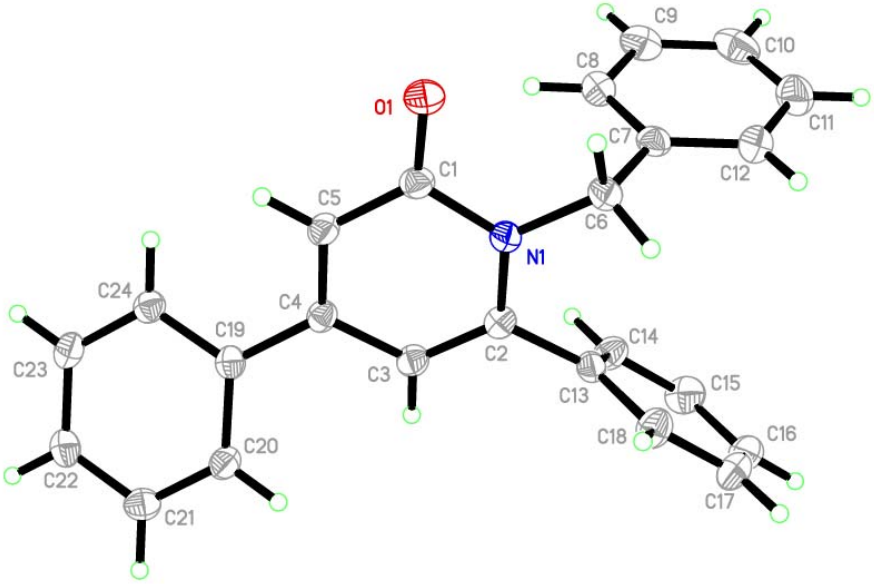

Table A.1.6. Crystal data and structure refinement for **2ff**.

Identification code	rovis121_0m	
Empirical formula	$C_{26}H_{23}NO_4$	
Formula weight	413.45	
Temperature	120 K	
Wavelength	0.71073 Å	
Crystal system	Orthorhombic	
Space group	$P\ 2_12_12_1$	
Unit cell dimensions	a = 10.7001(5) Å	α= 90°.
	b = 18.9198(9) Å	β= 90°.
	c = 20.6478(11) Å	γ = 90°.
Volume	4180.0(4) $Å^3$	
Z	8	
Density (calculated)	1.314 Mg/m^3	
Absorption coefficient	0.089 mm^{-1}	
F(000)	1744	
Crystal size	0.19 x 0.16 x 0.14 mm^3	
Theta range for data collection	1.97 to 30.74°.	
Index ranges	-15<=h<=15, -27<=k<=27, -29<=l<=29	
Reflections collected	94030	
Independent reflections	12898 [R(int) = 0.0919]	
Completeness to theta = 30.74°	99.4 %	
Absorption correction	Semi-empirical from equivalents	
Max. and min. transmission	0.9876 and 0.9837	
Refinement method	Full-matrix least-squares on F^2	
Data / restraints / parameters	12898 / 0 / 565	
Goodness-of-fit on F^2	0.982	
Final R indices [I>2sigma(I)]	R1 = 0.0527, wR2 = 0.1240	
R indices (all data)	R1 = 0.1033, wR2 = 0.1665	
Absolute structure parameter	0.7(9)	
Largest diff. peak and hole	0.333 and -0.534 $e.Å^{-3}$	

Table A.1.7. Atomic coordinates (x 10^4) and equivalent isotropic displacement parameters ($Å^2$x 10^3) for **2ff**. U(eq) is defined as one third of the trace of the orthogonalized U^{ij} tensor.

	x	y	z	U(eq)
C(1)	4574(2)	2811(1)	7635(1)	22(1)
C(2)	4026(2)	2533(1)	8211(1)	23(1)
C(3)	3124(2)	2875(1)	8554(1)	21(1)
C(4)	3258(2)	3854(1)	7822(1)	20(1)
C(5)	4143(2)	3508(1)	7469(1)	23(1)
C(6)	2516(2)	2520(1)	9110(1)	20(1)
C(7)	1207(2)	2445(1)	9149(1)	21(1)
C(8)	682(2)	2051(1)	9642(1)	23(1)
C(9)	1422(2)	1745(1)	10121(1)	24(1)
C(10)	2710(2)	1798(1)	10080(1)	26(1)
C(11)	3242(2)	2176(1)	9571(1)	23(1)

C(12)	1483(3)	1109(2)	11123(1)	33(1)
C(13)	2057(2)	3978(1)	8843(1)	19(1)
C(14)	2732(2)	4242(1)	9359(1)	22(1)
C(15)	2140(2)	4631(1)	9841(1)	23(1)
C(16)	854(2)	4757(1)	9797(1)	21(1)
C(17)	185(2)	4501(1)	9269(1)	22(1)
C(18)	779(2)	4108(1)	8795(1)	22(1)
C(19)	823(3)	5341(1)	10825(1)	30(1)
C(20)	2821(2)	4560(1)	7604(1)	21(1)
C(21)	3672(2)	5109(1)	7523(1)	22(1)
C(22)	3322(2)	5750(1)	7240(1)	24(1)
C(23)	2108(2)	5829(1)	7015(1)	23(1)
C(24)	1233(2)	5286(1)	7107(1)	23(1)
C(25)	1584(2)	4661(1)	7396(1)	22(1)
C(26)	2516(3)	6980(2)	6572(2)	40(1)
C(27)	5497(2)	2353(1)	2601(1)	22(1)
C(28)	6091(2)	2124(1)	3191(1)	22(1)
C(29)	6900(2)	2543(1)	3528(1)	21(1)
C(30)	6662(2)	3466(1)	2742(1)	20(1)
C(31)	5845(2)	3057(1)	2405(1)	22(1)
C(32)	7521(2)	2270(1)	4124(1)	20(1)
C(33)	6796(2)	1991(1)	4618(1)	24(1)
C(34)	7336(2)	1738(1)	5185(1)	24(1)
C(35)	8629(2)	1756(1)	5253(1)	23(1)
C(36)	9364(2)	2000(1)	4745(1)	24(1)
C(37)	8826(2)	2262(1)	4187(1)	23(1)
C(38)	8548(3)	1272(2)	6324(1)	34(1)
C(39)	7899(2)	3684(1)	3732(1)	19(1)
C(40)	9123(2)	3865(1)	3568(1)	22(1)
C(41)	9814(2)	4270(1)	3989(1)	22(1)
C(42)	9306(2)	4480(1)	4579(1)	22(1)
C(43)	8081(2)	4310(1)	4736(1)	24(1)
C(44)	7374(2)	3917(1)	4303(1)	21(1)
C(45)	9615(3)	5093(2)	5574(1)	42(1)
C(46)	7050(2)	4162(1)	2468(1)	21(1)
C(47)	7603(2)	4150(1)	1855(1)	25(1)
C(48)	7916(2)	4762(1)	1533(1)	26(1)
C(49)	7633(2)	5415(1)	1810(1)	22(1)
C(50)	7071(2)	5445(1)	2415(1)	24(1)
C(51)	6807(2)	4818(1)	2744(1)	23(1)
C(52)	7429(3)	6657(1)	1609(2)	33(1)
N(1)	2725(2)	3546(1)	8368(1)	19(1)
N(2)	7177(2)	3221(1)	3318(1)	20(1)
O(1)	5337(2)	2469(1)	7299(1)	29(1)
O(2)	784(2)	1401(1)	10598(1)	32(1)
O(3)	184(2)	5129(1)	10245(1)	26(1)
O(4)	1664(2)	6408(1)	6692(1)	30(1)
O(5)	4769(2)	1966(1)	2279(1)	26(1)
O(6)	9264(2)	1533(1)	5791(1)	31(1)
O(7)	10100(2)	4850(1)	4969(1)	31(1)
O(8)	7919(2)	5983(1)	1431(1)	31(1)

Table A.1.8. Bond lengths [Å] and angles [°] for **2ff**.

C(1)-O(1)	1.252(3)	C(35)-O(6)	1.370(3)
C(1)-C(2)	1.426(4)	C(35)-C(36)	1.389(3)
C(1)-C(5)	1.439(3)	C(36)-C(37)	1.379(3)
C(2)-C(3)	1.360(3)	C(38)-O(6)	1.428(3)
C(3)-N(1)	1.393(3)	C(39)-C(44)	1.379(3)
C(3)-C(6)	1.482(3)	C(39)-C(40)	1.395(3)
C(4)-C(5)	1.363(3)	C(39)-N(2)	1.447(3)
C(4)-N(1)	1.391(3)	C(40)-C(41)	1.375(3)
C(4)-C(20)	1.486(3)	C(41)-C(42)	1.393(3)
C(6)-C(11)	1.389(3)	C(42)-O(7)	1.364(3)
C(6)-C(7)	1.410(3)	C(42)-C(43)	1.388(3)
C(7)-C(8)	1.381(3)	C(43)-C(44)	1.387(3)
C(8)-C(9)	1.392(3)	C(45)-O(7)	1.427(3)
C(9)-O(2)	1.364(3)	C(46)-C(51)	1.391(3)
C(9)-C(10)	1.384(4)	C(46)-C(47)	1.398(3)
C(10)-C(11)	1.394(3)	C(47)-C(48)	1.377(3)
C(12)-O(2)	1.430(3)	C(48)-C(49)	1.394(3)
C(13)-C(14)	1.381(3)	C(49)-O(8)	1.366(3)
C(13)-C(18)	1.393(3)	C(49)-C(50)	1.387(3)
C(13)-N(1)	1.464(3)	C(50)-C(51)	1.395(3)
C(14)-C(15)	1.390(3)	C(52)-O(8)	1.426(3)
C(15)-C(16)	1.400(3)		
C(16)-O(3)	1.366(3)	O(1)-C(1)-C(2)	122.7(2)
C(16)-C(17)	1.391(3)	O(1)-C(1)-C(5)	123.4(2)
C(17)-C(18)	1.384(3)	C(2)-C(1)-C(5)	113.9(2)
C(19)-O(3)	1.435(3)	C(3)-C(2)-C(1)	123.4(2)
C(20)-C(21)	1.390(3)	C(2)-C(3)-N(1)	120.5(2)
C(20)-C(25)	1.404(3)	C(2)-C(3)-C(6)	120.0(2)
C(21)-C(22)	1.397(3)	N(1)-C(3)-C(6)	119.5(2)
C(22)-C(23)	1.388(3)	C(5)-C(4)-N(1)	121.1(2)
C(23)-O(4)	1.367(3)	C(5)-C(4)-C(20)	119.2(2)
C(23)-C(24)	1.402(3)	N(1)-C(4)-C(20)	119.6(2)
C(24)-C(25)	1.377(3)	C(4)-C(5)-C(1)	122.3(2)
C(26)-O(4)	1.436(3)	C(11)-C(6)-C(7)	118.0(2)
C(27)-O(5)	1.259(3)	C(11)-C(6)-C(3)	119.8(2)
C(27)-C(28)	1.440(3)	C(7)-C(6)-C(3)	121.7(2)
C(27)-C(31)	1.441(3)	C(8)-C(7)-C(6)	120.0(2)
C(28)-C(29)	1.365(3)	C(7)-C(8)-C(9)	121.1(2)
C(29)-N(2)	1.387(3)	O(2)-C(9)-C(10)	125.2(2)
C(29)-C(32)	1.491(3)	O(2)-C(9)-C(8)	115.2(2)
C(30)-C(31)	1.361(3)	C(10)-C(9)-C(8)	119.5(2)
C(30)-N(2)	1.389(3)	C(9)-C(10)-C(11)	119.3(2)
C(30)-C(46)	1.494(3)	C(6)-C(11)-C(10)	121.9(2)
C(32)-C(33)	1.387(3)	C(14)-C(13)-C(18)	120.4(2)
C(32)-C(37)	1.402(3)	C(14)-C(13)-N(1)	117.7(2)
C(33)-C(34)	1.390(3)	C(18)-C(13)-N(1)	121.9(2)
C(34)-C(35)	1.391(3)	C(13)-C(14)-C(15)	120.3(2)

C(14)-C(15)-C(16)	119.4(2)	C(37)-C(36)-C(35)	120.8(2)
O(3)-C(16)-C(17)	116.2(2)	C(36)-C(37)-C(32)	119.9(2)
O(3)-C(16)-C(15)	124.0(2)	C(44)-C(39)-C(40)	120.8(2)
C(17)-C(16)-C(15)	119.8(2)	C(44)-C(39)-N(2)	118.8(2)
C(18)-C(17)-C(16)	120.4(2)	C(40)-C(39)-N(2)	120.4(2)
C(17)-C(18)-C(13)	119.6(2)	C(41)-C(40)-C(39)	119.2(2)
C(21)-C(20)-C(25)	118.6(2)	C(40)-C(41)-C(42)	120.2(2)
C(21)-C(20)-C(4)	120.1(2)	O(7)-C(42)-C(43)	124.8(2)
C(25)-C(20)-C(4)	120.8(2)	O(7)-C(42)-C(41)	114.8(2)
C(20)-C(21)-C(22)	121.5(2)	C(43)-C(42)-C(41)	120.4(2)
C(23)-C(22)-C(21)	119.0(2)	C(44)-C(43)-C(42)	119.3(2)
O(4)-C(23)-C(22)	125.1(2)	C(39)-C(44)-C(43)	120.0(2)
O(4)-C(23)-C(24)	114.9(2)	C(51)-C(46)-C(47)	117.8(2)
C(22)-C(23)-C(24)	120.0(2)	C(51)-C(46)-C(30)	125.4(2)
C(25)-C(24)-C(23)	120.3(2)	C(47)-C(46)-C(30)	116.5(2)
C(24)-C(25)-C(20)	120.5(2)	C(48)-C(47)-C(46)	121.7(2)
O(5)-C(27)-C(28)	123.0(2)	C(47)-C(48)-C(49)	119.6(2)
O(5)-C(27)-C(31)	123.3(2)	O(8)-C(49)-C(50)	125.5(2)
C(28)-C(27)-C(31)	113.7(2)	O(8)-C(49)-C(48)	114.4(2)
C(29)-C(28)-C(27)	122.4(2)	C(50)-C(49)-C(48)	120.1(2)
C(28)-C(29)-N(2)	120.9(2)	C(49)-C(50)-C(51)	119.4(2)
C(28)-C(29)-C(32)	120.2(2)	C(46)-C(51)-C(50)	121.4(2)
N(2)-C(29)-C(32)	118.9(2)	C(4)-N(1)-C(3)	118.63(19)
C(31)-C(30)-N(2)	120.3(2)	C(4)-N(1)-C(13)	120.56(18)
C(31)-C(30)-C(46)	119.1(2)	C(3)-N(1)-C(13)	118.33(19)
N(2)-C(30)-C(46)	120.6(2)	C(29)-N(2)-C(30)	119.43(19)
C(30)-C(31)-C(27)	123.2(2)	C(29)-N(2)-C(39)	119.29(19)
C(33)-C(32)-C(37)	119.0(2)	C(30)-N(2)-C(39)	121.01(18)
C(33)-C(32)-C(29)	119.3(2)	C(9)-O(2)-C(12)	118.1(2)
C(37)-C(32)-C(29)	121.7(2)	C(16)-O(3)-C(19)	117.39(19)
C(32)-C(33)-C(34)	121.2(2)	C(23)-O(4)-C(26)	117.9(2)
C(33)-C(34)-C(35)	119.3(2)	C(35)-O(6)-C(38)	117.8(2)
O(6)-C(35)-C(36)	115.7(2)	C(42)-O(7)-C(45)	117.0(2)
O(6)-C(35)-C(34)	124.6(2)	C(49)-O(8)-C(52)	118.3(2)
C(36)-C(35)-C(34)	119.7(2)		

Symmetry transformations used to generate equivalent atoms:

Table A.1.9. Anisotropic displacement parameters ($Å^2 x\ 10^3$)for **2ff**. The anisotropic displacement factor exponent takes the form: $-2\pi^2[\ h^2 a^{*2} U^{11} + ... + 2\ h\ k\ a^*\ b^*\ U^{12}\ ]$

	U^{11}	U^{22}	U^{33}	U^{23}	U^{13}	U^{12}
C(1)	18(1)	23(1)	26(1)	-2(1)	-1(1)	0(1)
C(2)	22(1)	20(1)	25(1)	1(1)	-1(1)	1(1)
C(3)	20(1)	20(1)	22(1)	0(1)	-2(1)	-2(1)
C(4)	21(1)	22(1)	17(1)	0(1)	-1(1)	-4(1)
C(5)	23(1)	28(1)	18(1)	1(1)	3(1)	-2(1)
C(6)	23(1)	17(1)	20(1)	-1(1)	1(1)	1(1)
C(7)	22(1)	19(1)	21(1)	-3(1)	0(1)	0(1)

C(8)	18(1)	24(1)	28(1)	-3(1)	3(1)	-1(1)
C(9)	27(1)	21(1)	23(1)	0(1)	4(1)	-2(1)
C(10)	26(1)	26(1)	26(1)	2(1)	-3(1)	-2(1)
C(11)	21(1)	25(1)	22(1)	-1(1)	0(1)	-3(1)
C(12)	37(2)	35(2)	27(1)	7(1)	3(1)	-2(1)
C(13)	22(1)	16(1)	18(1)	-1(1)	2(1)	-1(1)
C(14)	21(1)	22(1)	23(1)	-3(1)	-2(1)	-1(1)
C(15)	24(1)	25(1)	20(1)	-5(1)	-3(1)	-2(1)
C(16)	25(1)	17(1)	19(1)	-1(1)	3(1)	0(1)
C(17)	18(1)	24(1)	23(1)	1(1)	0(1)	0(1)
C(18)	24(1)	21(1)	19(1)	-1(1)	-2(1)	-1(1)
C(19)	39(1)	30(1)	20(1)	-6(1)	2(1)	2(1)
C(20)	26(1)	22(1)	15(1)	-2(1)	1(1)	-1(1)
C(21)	23(1)	25(1)	19(1)	-1(1)	-2(1)	0(1)
C(22)	27(1)	23(1)	22(1)	2(1)	1(1)	-4(1)
C(23)	29(1)	21(1)	19(1)	1(1)	2(1)	2(1)
C(24)	23(1)	24(1)	21(1)	0(1)	1(1)	1(1)
C(25)	23(1)	22(1)	19(1)	-1(1)	0(1)	-1(1)
C(26)	41(2)	29(1)	51(2)	16(1)	-3(1)	-8(1)
C(27)	20(1)	23(1)	23(1)	-5(1)	2(1)	-1(1)
C(28)	21(1)	21(1)	24(1)	0(1)	0(1)	-1(1)
C(29)	20(1)	21(1)	22(1)	1(1)	1(1)	1(1)
C(30)	21(1)	21(1)	18(1)	-2(1)	-1(1)	2(1)
C(31)	25(1)	23(1)	20(1)	-1(1)	-2(1)	2(1)
C(32)	23(1)	17(1)	21(1)	1(1)	-2(1)	-1(1)
C(33)	22(1)	24(1)	24(1)	1(1)	1(1)	1(1)
C(34)	23(1)	27(1)	22(1)	3(1)	2(1)	-2(1)
C(35)	27(1)	23(1)	19(1)	2(1)	-4(1)	-1(1)
C(36)	20(1)	24(1)	27(1)	0(1)	-3(1)	-2(1)
C(37)	23(1)	22(1)	24(1)	0(1)	2(1)	-2(1)
C(38)	43(2)	37(2)	22(1)	8(1)	-1(1)	-1(1)
C(39)	21(1)	18(1)	19(1)	2(1)	-4(1)	-2(1)
C(40)	22(1)	23(1)	21(1)	2(1)	0(1)	1(1)
C(41)	20(1)	25(1)	22(1)	4(1)	-1(1)	-2(1)
C(42)	23(1)	23(1)	21(1)	0(1)	-5(1)	-6(1)
C(43)	26(1)	24(1)	21(1)	-1(1)	2(1)	-3(1)
C(44)	20(1)	23(1)	21(1)	1(1)	1(1)	-1(1)
C(45)	48(2)	53(2)	24(1)	-11(1)	2(1)	-21(2)
C(46)	21(1)	23(1)	20(1)	1(1)	-3(1)	0(1)
C(47)	29(1)	21(1)	24(1)	-1(1)	0(1)	5(1)
C(48)	30(1)	27(1)	22(1)	1(1)	4(1)	4(1)
C(49)	23(1)	21(1)	23(1)	2(1)	-2(1)	0(1)
C(50)	27(1)	18(1)	26(1)	-4(1)	-2(1)	1(1)
C(51)	27(1)	22(1)	20(1)	-4(1)	0(1)	0(1)
C(52)	34(1)	20(1)	45(2)	2(1)	5(1)	2(1)
N(1)	18(1)	18(1)	21(1)	-3(1)	1(1)	-1(1)
N(2)	19(1)	20(1)	19(1)	-1(1)	-1(1)	-3(1)
O(1)	27(1)	30(1)	30(1)	-3(1)	6(1)	5(1)
O(2)	30(1)	38(1)	28(1)	9(1)	6(1)	-3(1)
O(3)	27(1)	30(1)	21(1)	-6(1)	3(1)	4(1)
O(4)	30(1)	23(1)	37(1)	8(1)	0(1)	1(1)

O(5)	26(1)	28(1)	25(1)	-6(1)	-1(1)	-4(1)
O(6)	28(1)	40(1)	24(1)	7(1)	-6(1)	-3(1)
O(7)	31(1)	42(1)	22(1)	-6(1)	-1(1)	-13(1)
O(8)	35(1)	22(1)	37(1)	5(1)	8(1)	4(1)

Table A.1.10. Hydrogen coordinates (x 10^4) and isotropic displacement parameters (Å^{2}x 10^3) for **2ff**.

	x	y	z	U(eq)
H(2)	4299	2096	8360	27
H(5)	4479	3730	7107	27
H(7)	697	2662	8843	25
H(8)	-180	1989	9654	28
H(10)	3215	1584	10389	31
H(11)	4108	2199	9538	27
H(12A)	2042	753	10962	49
H(12B)	921	900	11431	49
H(12C)	1956	1476	11330	49
H(14)	3588	4160	9384	26
H(15)	2595	4806	10190	28
H(17)	-666	4594	9234	26
H(18)	327	3931	8446	26
H(19A)	1135	4931	11044	44
H(19B)	253	5589	11103	44
H(19C)	1507	5647	10714	44
H(21)	4492	5048	7662	27
H(22)	3894	6117	7204	29
H(24)	411	5349	6971	27
H(25)	999	4304	7454	26
H(26A)	2912	7115	6971	60
H(26B)	2065	7376	6399	60
H(26C)	3139	6831	6267	60
H(28)	5918	1673	3347	26
H(31)	5493	3240	2029	27
H(33)	5932	1972	4569	28
H(34)	6837	1559	5515	29
H(36)	10230	1986	4781	28
H(37)	9327	2432	3854	27
H(38A)	8004	1638	6480	51
H(38B)	9102	1127	6666	51
H(38C)	8059	874	6186	51
H(40)	9467	3712	3178	26
H(41)	10622	4405	3879	26
H(43)	7737	4459	5126	29
H(44)	6546	3810	4398	25
H(45A)	8887	5377	5498	62
H(45B)	10238	5371	5791	62

H(45C)	9395	4695	5838	62
H(47)	7763	3716	1659	30
H(48)	8315	4741	1133	32
H(50)	6871	5879	2599	28
H(51)	6461	4840	3157	28
H(52A)	6542	6620	1671	50
H(52B)	7599	6992	1271	50
H(52C)	7815	6812	2004	50

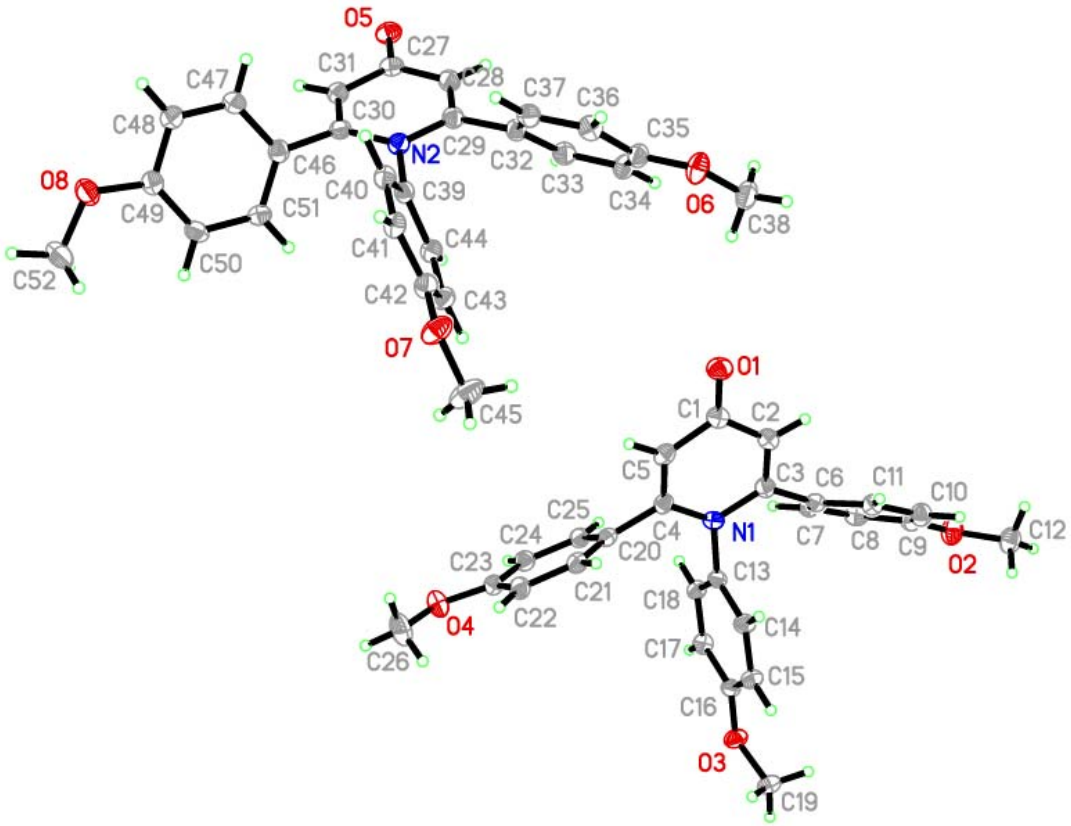

Pyridone Isomers in the Literature

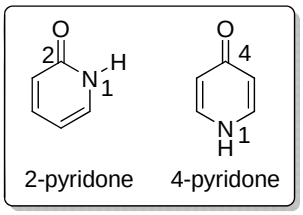

Ref 1

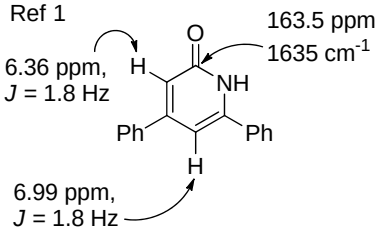

Ref 2

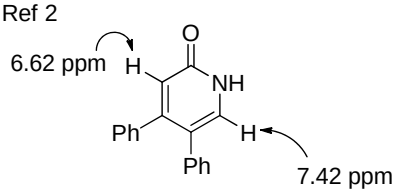

Ref 3

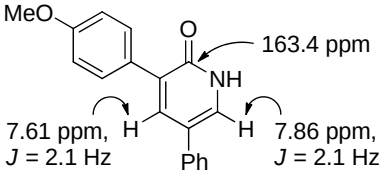

Ref 4

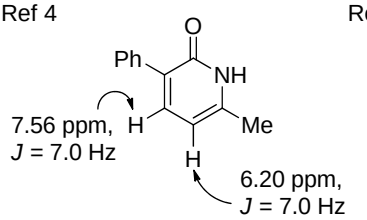

Ref 5

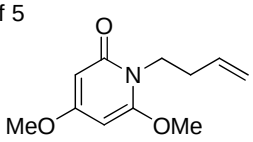

Ref 6

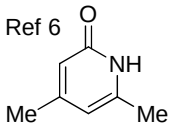

Ref 7

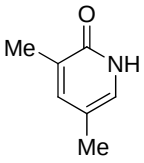

Ref 8

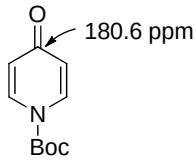

Ref 9

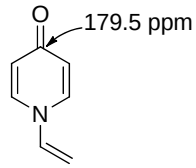

Ref 10

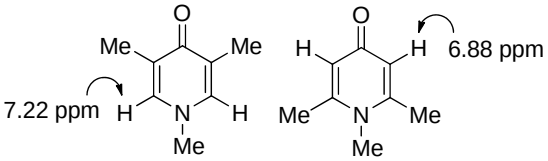

Ref 11

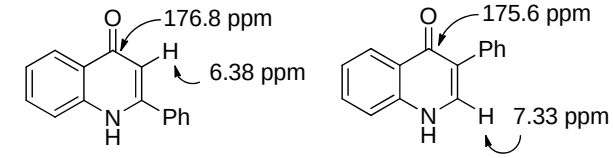

Ref 12

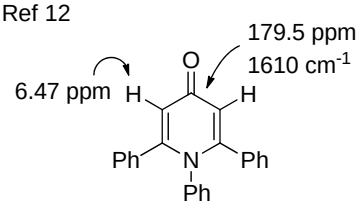

References:
1. Carles, L.; Narkunam, K.; Penlou, S.; Rousset, L.; Bouchu, D.; Ciufolini, M. A. *J. Org. Chem.* **2002**, *67*, 4304-4308.
2. Yamamoto, K.; Yamazaki, S.; Murata, I. *J. Org. Chem.* **1987**, *52*, 5239-5243.
3. Sutherland, A.; Gallagher, T. *J. Org. Chem.* **2003**, *68*, 3352-3355.
4. Overman, L. E.; Tsuboi, S.; Roos, J. P.; Taylor, G. F. *J. Am. Chem. Soc.* **1980**, *102*, 747-754.
5. Kaneko, C.; Uchiyama, K.; Sato, M.; Katagiri, N. *Chem. Pharm. Bull.* **1986**, *34*, 3658-3671.
6. Brun, E.; Gil, S.; Mestres, R.; Parra, M. *Synthesis*. **2000**, *2*, 273-280.
7. Rozen, S.; Hebel, D. *Heterocycles* **1989**, 28, 249-258.
8. Lim, S.; Curtis, M.; Beak, P. *Org. Lett.* **2001**, *3*, 711-714.
9. Blouin, M.; Frenette, R. *J. Org. Chem.* **2001**, *66*, 9043-9045.
10. Beak, P.; Bonham, J. *J. Am. Chem. Soc.* **1965**, *87*, 3365-3371.
11. Patonay, T.; Levai, A.; Riman, E.; Varma, R. S. *ARKIVOK* **2004**, *7*, 183-195.
12. Barluenga, J.; Lopez Ortiz, F.; Palacios, F.; Gotor, V. *Synthetic Commun.* **1983**, *13*, 411.

APPENDIX 2: CHAPTER 2 EXPERIMENTAL

General Methods. All reactions were carried out under an atmosphere of argon in oven-dried glassware with magnetic stirring. Toluene was degassed with argon and passed through one column of neutral alumina and one column of Q5 reactant. Column chromatography was performed on Silicycle Inc. silica gel 60 (230-400 mesh). Thin layer chromatography was performed on Silicycle Inc. 0.25 mm silica gel 60-F plates. Visualization was accomplished with UV light (254 nm), potassium permanganate, and/or cerric ammonium nitrate.

^{1}H NMR and ^{13}C NMR spectra were obtained in $CDCl_3$ at ambient temperature and chemical shifts are expressed in parts per million (δ, ppm). Proton chemical shifts are referenced to 7.26 ppm ($CHCl_3$) and carbon chemical shifts are referenced to 77.0 ppm ($CDCl_3$). Data reporting uses the following abbreviations: s, singlet; bs, broad singlet; d, doublet; dd, doublet of doublets; t, triplet; m, multiplet; and *J*, coupling constant in Hz.

Ligands **T1**-**T9**,[1] **B3**,[2] and **A1**[3] were synthesized as previously described in the literature. The synthesis of ligands **B4** and **B5** are described below. Alkynes and ligands **B1** and **B2** were purchased from Aldrich Chemicals Co. and used without further purification. Alkenyl isocyanate **2** was synthesized as previously described.[4] $[Rh(C_2H_4)_2Cl]_2$ was purchased from Strem Chemical, Inc. and used without further purification.

General Procedure for Synthesis of Phosphoramidite Ligands. The diol (0.27 mmol) was dissolved in THF in an oven-dried round bottom flask with a magnetic stir bar. Et_3N (3.5 eq, 0.95 mmol) was added and the reaction mixture was cooled to 0 °C before dropwise addition of phosphorous trichloride (1.1 eq, 0.30 mmol). The reaction mixture was stirred for 1 h and the amine (10 eq, 2.70 mmol) was added slowly at 0 °C. The reaction was stirred overnight at 23 °C, diluted with ether, and filtered. The filtrate was concentrated in *vacuo* and the resulting crude material was purified by flash column chromatography (98:2 Hex:EtOAc) to afford the desired phosphoramidite.

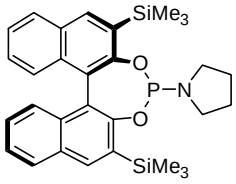

***O,O*-(*R*)-3,3'-bis(trimethylsilyl)-1,1'-binapthyl-2,2'-diyl-pyrrolidinephosphoramidite (B4).** General procedure yielded a white solid (85%). $[\alpha]^{20}_D$ = -550.4°, c = 0.01 g/ml $CHCl_3$. ^{1}H NMR (400 MHz, $CDCl_3$) δ 8.07 (m, 2H), 7.90 (m, 2H), 7.32 (m, 2H), 7.18 (m, 4H), 3.18 (m, 2H), 2.84 (bs, 2H), 1.65 (m, 4H), 0.45 (s, 9H), 0.44 (s, 9H). ^{13}C NMR (75 MHz, $CDCl_3$) δ 137.8, 136.6, 134.0, 133.7, 132.5, 132.2, 130.7, 130.1, 128.5, 128.3, 128.1, 127.5, 126.8, 126.7, 126.1, 124.2, 123.9, 123.6, 45.9, 45.7, 25.9, 25.8, 0.1, 0.0, -0.1, -0.9. ^{31}P NMR (75 MHz, $CDCl_3$) δ 149.82. R_f = 0.62 (98:2 Hex:EtOAc). IR (NaCl, Thin Film) 3534, 3053, 3032, 2960, 2899, 2858, 1578, 1388, 1255, 1086, 968, 835, 753 cm^{-1}. HRMS (ESI) *m/z* $[C_{30}H_{37}NO_2PSi_2]^+$ calcd 530.2095, found 530.2104.

---

[1] (a) Yu, R. T.; Rovis, T. *J. Am. Chem. Soc.* **2006**, *128*, 12370-12371. (b) Lee, E. E.; Rovis, T. *Org. Lett.* **2008**, *10*, 1231-1234. (c) Yu, R. T.; Rovis, T. *J. Am. Chem. Soc.* **2008**, *130*, 3262-3263.

[2] Yu, R. T.; Lee, E. E.; Malik, G.; Rovis, T. *Angew. Chem. Int. Ed.* **2009**, *48*, 2379-2382.

[3] Giacomina, F.; Meetsma, A.; Panella, L.; Lefort, L.; de Vries, A. H. M.; de Vries, J.G. *Angew. Chem. Int. Ed.* **2007**, *46*, 1497-1500.

[4] Lee, E. E.; Rovis, T. *Org. Lett.* **2008**, *10*, 1231-1234.

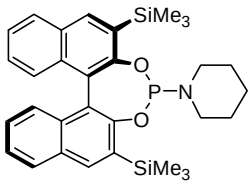

***O,O*-(*R*)-3,3'-bis(trimethylsilyl)-1,1'-binapthyl-2,2'-diyl-piperidinephosphoramidite (B5).** General procedure yielded a white solid (89%). $[\alpha]_D$ = -505.4°, c = 0.01 g/ml $CHCl_3$. ^1H NMR (400 MHz, $CDCl_3$) δ 8.07 (m, 2H), 7.91 (m, 2H), 7.39 (m, 3H), 7.17 (m, 3H), 2.92 (m, 2H), 1.53 (m, 4H), 1.32 (m, 2H), 0.51 (s, 9H), 0.45 (s, 9H). ^{13}C NMR (75 MHz, $CDCl_3$) δ 153.6, 136.7, 133.9, 133.7, 132.6, 132.1, 130.7, 130.0, 128.3, 128.2, 126.8, 126.7, 126.1, 126.0, 124.3, 124.1, 30.3, 27.2, 24.8. ^{31}P NMR (75 MHz, $CDCl_3$) δ 146.25. R_f = 0.40 (98:2 Hex:EtOAc). IR (NaCl, Thin Film) 3052, 2935, 2853, 1368, 1240, 1091, 1055, 979, 943, 840, 748 cm^{-1}. HRMS (ESI) m/z $[C_{31}H_{39}NO_2PSi_2]^+$ calcd 544.2251, found 544.2263.

Synthesis and Crystallography of Rhodium(cod)Cl·Ligand Complexes.

A 10 ml vial was charged with $[Rh(cod)Cl]_2$ (28 mg, 0.057 mmol) and ligand (0.114 mmol) in an inert atmosphere (N_2) glove box. Upon removal from the glove box, 1 ml of CH_2Cl_2 was added via syringe and the resulting yellow solution was layered with heptanes (~2 ml). The cap was loosely sealed and the solvent was allowed to evaporated slowly over 1 or 2 weeks yielding X-ray quality crystals.

All single crystals were coated in oil, transferred to a goniometer head, and mounted on a Bruker Kappa Apex CCD diffractometer under a stream of dinitrogen. All data collections were performed with Mo Kα radiation and a graphite monochromator. Data sets were taken with complete coverage and fourfold redundancy at 120K. Data was integrated and corrected for absorption effects with the Apex 2 software package.[5] Structures were solved with the SHELXTL software package.[6] All non-hydrogen atoms were refined with anisotropic thermal parameters and hydrogen atoms placed in idealized positions. Rhodium alkene bond distances determined in XP using cent/x, join, and bang commands.

General Procedure for Rhodium-Catalyzed [2+2+2] Cycloadditions.

An oven-dried 10 mL round bottom flask was charged with $[Rh(C_2H_4)_2Cl]_2$ (2.3 mg, 0.006 mmol) and ligand (0.012 mmol) and fitted with an oven-dried reflux condenser in an inert atmosphere (N_2) glove box. Upon removal from the glove box, 1 ml of toluene was added via syringe and the resulting yellow solution was stirred at ambient temperature for 15 min. To this solution, alkyne **1** (0.48 mmol) and isocyanate **2** (0.24 mmol) in 2 ml of toluene was added via syringe. An additional 4 ml of toluene was used to wash down the residue and added to the reaction mixture. The reaction mixture was heated to 110 °C in an oil bath and kept at reflux for 16 h. The reaction mixture was cooled to 23 °C, concentrated in vacuo, and purified by flash column chromatography (typically 20:1 EtOAc:MeOH). Evaporation of solvent afforded the analytically pure products. Absolute stereochemistry of lactam **3a**, vinylogous amide **4a**, lactam **3d**, and vinylogous amide **4d** were previously assigned and the spectra for these compounds are reported.[7] Enantioselectivity determination of lactam **3a** used previous HPLC conditions (Chiralcel ADH column, 90:10 Hex:iPrOH, 1 mL/min, 254nm, 23.6 min and 29.7 min). Enantioselectivity determination of vinylogous amide **4a** used previous HPLC conditions (Chiralcel ODH column, 85:15 Hex:iPrOH, 0.3 mL/min, 254nm, 55.4 min and 59.1 min) or Chiralcel IC column, 50:50 Hex:EtOAc, 0.8 mL/min, 330nm, 59.3 min and 63.0 min. Enantioselectivity determination of lactam **3d** used previous HPLC conditions (Chiralcel ODH column, 97:3 Hex:iPrOH, 1 mL/min, 230nm, 25.8 min and 27.2 min) or Chiralcel IC column, 60:40 Hex:iPrOH, 0.9 mL/min, 254nm, 24.1 min and 25.4 min. Enantioselectivity determination of vinylogous amide **4d** used previous HPLC conditions (Chiralcel ADH

[5] Bruker AXS Inc., 5465 East Chervl Parkway, Madison, WI 53711-5373 USA

[6] Sheldrick, G. (1997) *SHELXL-97 Program for Crystal Structure Refinement*, Institüt für Anorganische Chemie der Universität, Göttingen, Germany.

[7] (a) Yu, R. T.; Rovis, T. *J. Am. Chem. Soc.* **2006**, *128*, 12370-12371. (b) Yu, R. T.; Lee, E. E.; Malik, G.; Rovis, T. *Angew. Chem. Int. Ed.* **2009**, *48*, 2379-2382.

column, 95:5 Hex(0.5% DEA):iPrOH, 1 mL/min, 330nm, 24.3 min and 27.8 min) or Chiralcel IA column, 88:7:5 Hex(0.5% DEA):EtOAc:iPrOH, 1 mL/min, 330nm, 23.9 min and 28.4 min.

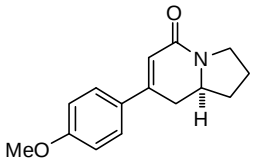

(*S*)-7-(4-methoxyphenyl)-2,3,8,8a-tetrahydroindolizin-5(1H)-one (3g). An oven-dried 50 mL round bottom flask was charged with $[Rh(C_2H_4)_2Cl]_2$ (11.7 mg, 0.03 mmol) and ligand (0.06 mmol) and fitted with an oven-dried reflux condenser in an inert atmosphere (N_2) glove box. Upon removal from the glove box, 20 mL of toluene was added via syringe and the resulting yellow solution was stirred at ambient temperature for 15 min. To this solution, alkyne **1e** (635 mg, 4.8 mmol) and isocyanate **2** (267 mg, 2.4 mmol) in 5 mL of toluene was added via syringe. An additional 10 mL of toluene was used to wash down the residue and added to the reaction mixture. The reaction mixture was heated to 110 °C in an oil bath and kept at reflux for 16 h. The reaction mixture was cooled to 23 °C, concentrated in vacuo, and purified by flash column chromatography (20:1 EtOAc:MeOH). This resulted in 8.4 mg (1 % yield) of (*S*)-7-(4-methoxyphenyl)-2,3,8,8a-tetrahydroindolizin-5(1H)-one **3g** as a brown solid and 459 mg (79 % yield) of (*R*)-5-(4-methoxyphenyl)-2,3,8,8a-tetrahydroindolizin-7(1H)-one **4g** as a light brown solid. Physical characteristics of lactam **3g**: ee not determined. ^{1}H NMR (400 MHz, $CDCl_3$) δ 7.45 (m, 2H), 6.91 (m, 2H), 6.25 (d, *J* = 2.6 Hz, 1H), 3.83 (s, 3H), 3.80 (m, 1H), 3.69 (m, 1H), 3.52 (m, 1H), 2.92 (dd, *J* = 16.4, 4.7 Hz, 1H), 2.47 (ddd, *J* = 16.5, 14.0, 2.6 Hz, 1H), 2.28 (m, 1H), 2.07 (m, 1H), 1.86 (m, 1H), 1.72 (m, 1H). ^{13}C NMR (100 MHz, $CDCl_3$) δ 164.3, 160.6, 148.0, 130.0, 127.2, 118.7, 114.1, 56.5, 55.3, 43.9, 33.5, 33.1, 23.0. R_f = 0.30 (20:1 EtOAc:MeOH). IR (ATR-IR) 2925, 2878, 1648, 1604, 1514, 1444, 1258, 1182, 1031. LRMS (APCI/ESI) *m/z* $[C_{15}H_{18}NO_2]^+$ (M+H) calcd 244.1, found 244.0. Physical characteristics of vinylogous amide **4g** are reported below.

Large Scale Ligand Synthesis and Cycloaddition.

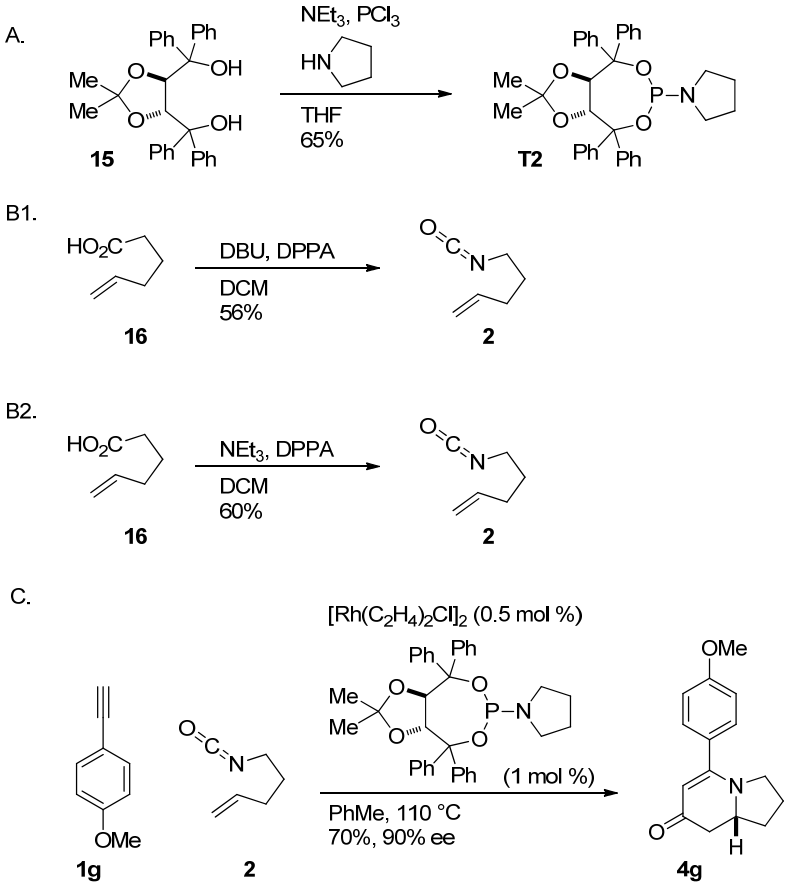

A. *Taddol-pyrrolidine phosphoramidite.* A 250 mL single-necked round bottom flask equipped with a magnetic stir bar is flame dried under vacuum. After cooling to 23 °C, (R,R)-Taddol (2.0 g, 4.29 mmol) (Note 1) is added to the round bottom, a rubber septum is fitted, the reaction flask is put under an atmosphere of Ar, and tetrahydrofuran (75 mL) (Note 2) is added via syringe to the round bottom. To this clear, colorless solution, triethylamine (2.4 mL, 17.2 mmol, 4 equiv) (Note 3) is added via syringe resulting in a clear solution with a slight yellow color. The reaction mixture is cooled to 0 °C with an ice bath and trichlorophosphine (0.39 mL, 4.5 mmol, 1.05 equiv) (Note 4) is added drop wise over 2 min via syringe resulting in a white suspension. The ice bath is removed, the reaction is allowed to warm to 23 °C and stirred for 1 h. The reaction mixture is cooled to 0 °C with an ice bath, and pyrrolidine (1.8 mL, 21.4 mmol, 5 equiv) (Note 5) is added via syringe. The ice bath is removed, the reaction is allowed to warm to 23 °C and stir for 1 h. 50 mL Et_2O is then added, and the reaction mixture is filtered through a medium fritted funnel into a 250 mL round bottom flask. The solid residue in the reaction flask is washed an additional two times with 25 mL Et_2O and filtered into the round bottom flask. The filtrate is transferred to a 500 mL separatory funnel and washed with 50 mL of deionized water (Note 6). The organic layer is dried over $MgSO_4$, filtered through a course fritted funnel into a 250 mL round bottom, and the $MgSO_4$ is rinsed twice with 10 mL Et_2O. The filtrate is concentrated *in vacuo* using a rotovap, and the off-white solid put on a high vac for 30 min. A magnetic stir bar and 5 mL EtOAc are added to the round bottom and a reflux condenser is attached. Using an oil bath, the mixture is heated to reflux with stirring and EtOAc is added dropwise until all the solid dissolves (~20 mL). The stir bar is removed from the clear, slightly yellow solution. The round bottom is allowed to cool slowly in the oil bath to 23 °C,

placed in a -10 °C fridge for 12 h, and then placed in a -24 °C freezer for 12 h. The solid is collected with a Buchner funnel (5 cm) with medium porosity filter paper to yield 1.58 g of Taddol-pyrrolidine phosphoramidite as white crystals (65 % yield) (Note 7).

B1. *Pentenyl isocyanate.* A 500 mL single-necked round bottom flask equipped with a magnetic stir bar is flame dried under vacuum. After cooling to 23 °C, a rubber septum is fitted to the round bottom flask and the flask is put under an atmosphere of Ar. Dichloromethane (50 mL) (Note 8) and 5-hexenoic acid (10.4 mL, 87.6 mmol) (Note 9) are added to the round bottom flask and the flask is cooled to 0 °C with an ice bath. 1,8-diazobicylo[5.4.0]undec-7-ene (14.2 mL, 94.6 mmol, 1.1 equiv) (Note 10) is added to the round bottom via syringe over 5 minutes and the clear solution is stirred for 20 minutes. Diphenyl phosphoryl azide (20.4 mL, 94.6 mmol, 1.1 equiv) (Note 11) is added over 5 min via syringe resulting in a clear, yellow solution. The reaction mixture is stirred for 3 h at 0 °C. The ice bath is removed, the septa is removed, and 200 mL hexanes (Note 12) is added. The reaction is stirred for 5 minutes and transferred to a 500 mL separatory funnel. After the layers separate, the lower (yellow) dichloromethane layer is collected in a 250 mL Erlenmeyer flask and the cloudy hexane layer is transferred to a 1 L round bottom flask. The dichloromethane layer is returned to the separatory flask and the 250 mL Erlenmeyer flask is rinsed with 200 mL hexanes and transferred to the separatory funnel. The dichloromethane layer is extracted with hexanes. The lower dichloromethane layer is collected in the 250 mL Erlenmeyer flask and the cloudy hexane layer is transferred to the 1 L round bottom flask. The 1 L round bottom flask (without a septum) is put into a 23 °C oil bath that is heated to 50 °C for 3 h and then at 55 °C for 3 h (Note 13). After conversion is complete, the solvent is removed via rotovap using a 23 °C bath, resulting in a yellow solution. This oil is transferred to a 25 mL round bottom flask and 1 L flask is rinsed with minimal hexanes and transferred to the 25 mL round bottom flask. The 25 mL flask is concentrated via rotovap using a 23 °C bath. The resultant yellow oil is purified via vacuum distillation and the first clear fraction (Note 14) is collected in a 25 ml round bottom flask cooled to 0 °C. This yields 5.42 g of pentenyl isocyanate as a clear liquid (56 % yield) (Note 15).

B2. *Pentenyl isocyanate.* A 100 mL single-necked round bottom flask equipped with a magnetic stir bar is flame dried under vacuum and is cooled to 23 °C. A rubber septum is fitted to the round bottom, and the round bottom is put under an atmosphere of Ar. Dichloromethane (20 mL) (Note 8), 5-hexenoic acid (9.8 mL, 82.8 mmol) (Note 9), and triethylamine (13 mL, 93.5 mmol, 1.1 equiv) (Note 3) are added to the round bottom and the clear solution is stirred for 20 min. The round bottom flask is cooled to 0 °C with an ice bath and diphenyl phosphoryl azide (20 mL, 92.5 mmol, 1.1 equiv) (Note 11) is added over 1 h via a syringe pump resulting in a clear, yellow solution. The reaction mixture is stirred for 4 h at 0 °C. The reaction mixture is purified directly via flash chromatography (Note 16,17). The last seven fractions containing acyl azide are collected in a 500 mL round bottom flask and concentrated *in vacuo* via rotovap (Note 18). The remaining fractions containing acyl azide are then added to the same round bottom resulting in a volume of ca 400 mL (Note 19). The flask is fitted with a septum containing an Ar inlet and two 18 G needles as outlets, heated to 50 °C for 3 h in an oil bath, and then at 55 °C for 3 h (Note 13). After conversion is complete, the solvent is removed via rotovap resulting in 5.52 g pentenyl isocyanate as a clear liquid (60 % yield) (Note 15).

C. *(R)-5-(4-methoxyphenyl)-2,3,8,8a-tetrahydroindolizin-7(1H)-one.* An oven dried 250mL round bottom flask equipped with a magnetic stir bar and an oven dried reflux condenser with septum attached are loaded into an inert atmosphere (Ar) glove box (Note 20). Chlorobis(ethylene)rhodium(I) dimer (58 mg, 0.15 mmol, 0.005 equiv) (Note 21) and Taddol-pyrrolidine phosphoramidite (170 mg, 0.3 mmol, 0.01 equiv) are added to the round bottom. The reflux condenser is attached, the apparatus is removed from the glove box, and 110 mL PhMe (Note 22) is added via syringe resulting in a clear, gold solution. 5 mL PhMe is added to a vial containing pentenyl isocyanate (3.33 g, 30 mmol) and 4-ethynylanisole (6.0 g, 45 mmol, 1.5 equiv) (Note 23) and this solution is added to the reaction mixture. The vial is rinsed with 5 mL PhMe, added to the reaction vessel, and another 50 mL PhMe is added to the

reaction mixture resulting in a crimson solution. The reaction mixture is heated to 110 °C in an oil bath for 36 h resulting in a dark brown solution. The reaction mixture is concentrated *in vacuo*, and the crude reaction mixture is purified via flash chromatography (Note 24) resulting in 5.11 g (*R*)-5-(4-methoxyphenyl)-2,3,8,8a-tetrahydroindolizin-7(1H)-one as a light brown solid (70% yield, 90% ee) (Note 25,26).

Notes

1. (*R*,*R*)-Taddol was purchased from AK Scientific, Inc. and used as received.
2. Tetrahydrofuran was degassed with Ar and passed through two columns of neutral alumina.
3. Triethylamine was purchased from Sigma-Aldrich and distilled over KOH before use.
4. Trichlorophosphine was purchased from Sigma-Aldrich and distilled before use.
5. Pyrrolidine was purchased from Sigma-Aldrich and distilled over KOH before use.
6. Use of deionized water is necessary. Degradation of ligand is observed by P^{31} NMR if tap or acidic water is used.
7. Physical characteristics of Taddol-pyrrolidine phosphoramidite: $[\alpha]^{20}_{D}$ = -145.5 (conc = 0.0106 g/mL $CHCl_3$). ^{1}H NMR (300 MHz, $CDCl_3$) δ 7.74 (dm, *J* = 6.9 Hz, 2H), 7.60 (dm, *J* = 7.2 Hz, 2H), 7.48 (dm, *J* = 7.2 Hz, 2H), 7.41 (dm, *J* = 7.2 Hz, 2H), 7.34 - 7.15 (m, 12 H), 5.20 (dd, *J* = 8.4, 3.3 Hz, 1H), 4.82 (d, *J* = 8.4 Hz, 1H), 3.44 - 3.34 (m, 2H), 3.26 - 3.17 (m, 2H), 1.87 - 1.73 (m, 4H), 1.26 (s, 3H), 0.28 (s, 3H). ^{13}C NMR (75 MHz, $CDCl_3$) δ 146.9, 146.6, 142.2, 142.0, 129.0, 128.8, 128.7, 128.0, 127.6, 127.4, 127.2, 127.1, 127.1, 127.0, 111.7, 82.6, 82.5, 82.4, 82.2, 81.8, 81.2, 45.1, 44.9, 27.5, 26.0, 25.9, 25.3. ^{31}P NMR (121 MHz, $CDCl_3$) δ 137.7. IR (NaCl, Thin Film) 3060, 2969, 2883, 1492, 1447, 1035, 737. Mp = 215-217 °C. HRMS (ESI) *m/z* $[C_{35}H_{37}NO_4P]^+$ calcd 566.2455, found 566.2454. Anal. calcd for $C_{35}H_{36}NO_4P$: C, 74.32; H, 6.42; N, 2.48; O, 11.31; P, 5.48, found C, 74.29; H, 6.48; N, 2.57; O, 11.58; P, 4.94.
8. Dichloromethane was degassed with Ar and passed through two columns of neutral alumina.
9. 5-Hexenoic acid was purchased from TCI and used as received.
10. 1-8-Diazabicyclo[5.4.0]undec-7-ene was purchased from AK Scientific, Inc. and distilled over KOH before use.
11. Diphenyl phosphoryl azide was purchased from AK Scientific, Inc. and used as received.
12. Hexanes were distilled at ambient pressure over boiling chips.
13. Conversion can be monitored by NMR (2.35 (t, 2H) shifts to 3.32 (t, 2H)) or IR (1720 shifts to 2171) for completion. Physical characteristics for acyl azide: ^{1}H NMR (300 MHz, $CDCl_3$) δ 5.76 (ddt, *J* = 17.1, 10.2, 6.9 Hz, 1H), 5.03 (dm, *J* = 17.1 Hz, 1H), 5.00 (dm, *J* = 10.2 Hz, 1H), 2.35 (t, *J* = 7.5 Hz, 2H), 2.10 (dt, *J* = 7.2, 7.2 Hz, 2H), 1.73 (tt, *J* = 7.5, 7.2 Hz, 2H). ^{13}C NMR (75 MHz, $CDCl_3$) δ 180.5, 137.2, 115.7, 36.0, 32.8, 23.7. R_f = 0.52 (20:1 Hex:EtOAc). IR (NaCl, Thin Film) 2360, 2138, 1720, 1369, 1161.
14. Boiling point: 63 °C at 50 torr.
15. Physical characteristics of pentenyl isocyanate: ^{1}H NMR (300 MHz, $CDCl_3$) δ 5.77 (ddt, J = 17.1, 10.2, 6.9 Hz, 1H), 5.07 (dm, J = 17.1 Hz, 1H), 5.03 (dm, J = 10.2 Hz, 1H), 3.32 (t, J = 6.6 Hz, 2H), 2.16 (dt, J = 6.9, 6.9 Hz, 2H), 1.71 (tt, J = 6.9, 6.9 Hz, 2H). ^{13}C NMR (75 MHz, $CDCl_3$) δ 136.7, 121.9, 115.6, 42.0, 30.4, 30.1. IR (NaCl, Thin Film) 2927, 2171, 1690, 1489, 1183, 966.
16. Column needs to be slurry packed so the column does not heat up during chromatography and should be done behind a hood sash or blast shield. If the column heats up, it will promote the decomposition of the acyl azide releasing large amounts of nitrogen and can result in an explosion (this has not been observed by the authors with this procedure).
17. Column diameter: 6cm, silica: 160 g (Silicycle, Inc. silica 60 (230-400 mesh)), eluant: 1 L (40:1 Hex:EtOAc), 0.5 L (19:1 Hex:EtOAc), fraction size: 50 mL (25 x 150 mm test tubes), product typically in fractions 6-20.
18. Rotovap cold to prevent acyl azide conversion.

19. If all the fractions are collected in a 1 L round bottom flask with ca 700 mL solvent, the solution must be heated overnight at 60 °C for full conversion.

20. The use of a glove box is for simplicity of set up due to the air sensitive nature of chlorobis(ethylene)rhodium(I) dimer. Use of standard Schlenk techniques in place of a glove box should provide similar results if the chlorobis(ethylene)rhodium(I) dimer is of high quality. Chlorobis(cyclooctadiene)rhodium(I) dimer may be used as an air stable alternative, but we observe lower yields (15-25% lower) when this catalyst is used on smaller scale. The phosphoramidite ligand is air stable and can be stored outside the glovebox, but is stored in the glovebox for ease of reaction setup.

21. Chlorobis(ethylene)rhodium(I) dimer was purchased from Strem, Inc., stored cold in an inert atmosphere glove box (Ar), and used as received.

22. Toluene was degassed with Ar and passed through one column of neutral alumina and one column of Q5 reactant.

23. 4-Ethynylanisole was purchased from AK Scientific, Inc. and used as received.

24. Column diameter: 6 cm, silica: 140 g (Silicycle, Inc. silica 60 (230-400 mesh)), eluant: 2.5 L (20:1 EtOAc:MeOH), fraction size: 50 mL (25 x 150 mm test tubes), product typically found in fractions 16-49.

25. Physical characteristics of (*R*)-5-(4-methoxyphenyl)-2,3,8,8a-tetrahydroindolizin-7(1H)-one: 90% ee by HPLC: Chiralcel ODH column, 90:10 Hex:iPrOH, 1 mL/min, 330nm, RT_{major} = 27.72 min, RT_{minor} = 33.82 min. $[\alpha]^{20}_{D}$ = +592.9 (conc = 0.0084 g/mL $CHCl_3$). ^{1}H NMR (300 MHz, $CDCl_3$) δ 7.34 (dm, *J* = 8.7 Hz, 2H), 6.92 (dm, *J* = 8.7 Hz, 2H), 5.08 (s, 1H), 4.05 (dddd, *J* = 13.5, 6.9, 6.9, 6.9 Hz, 1H), 3.84 (s, 3H), 3.55 (ddd, *J* = 11.4, 7.2, 5.7 Hz, 1H), 3.27 (ddd, *J* = 10.8, 7.2, 7.2 Hz, 1H), 2.53 - 2.25 (m, 3H), 2.07 - 1.71 (m, 3H). ^{13}C NMR (75 MHz, $CDCl_3$) δ 191.9, 162.7, 160.8, 129.2, 128.4, 113.8, 99.7, 58.6, 55.3, 49.5, 41.4, 31.6, 24.6. R_f = 0.16 (20:1 EtOAc:MeOH). IR (NaCl, Thin Film) 2967, 2878, 1624, 1507, 1245, 1030. HRMS (ESI) *m/z* $[C_{15}H_{18}NO_2]^+$ calcd 244.1332, found 244.1330. Anal. calcd for $C_{15}H_{17}NO_2$: C, 74.05; H, 7.04; N, 5.76; O, 13.15, found C, 73.99; H, 7.10; N, 5.80; O, 13.28.

26. (*R*)-5-(4-methoxyphenyl)-2,3,8,8a-tetrahydroindolizin-7(1H)-one can be recrystalized from EtOAc to yield light yellow crystals. 86% recovery, 96% ee, mp = 126-129 °C.

^{1}H NMR and ^{13}C NMR Spectra of Selected Compounds.

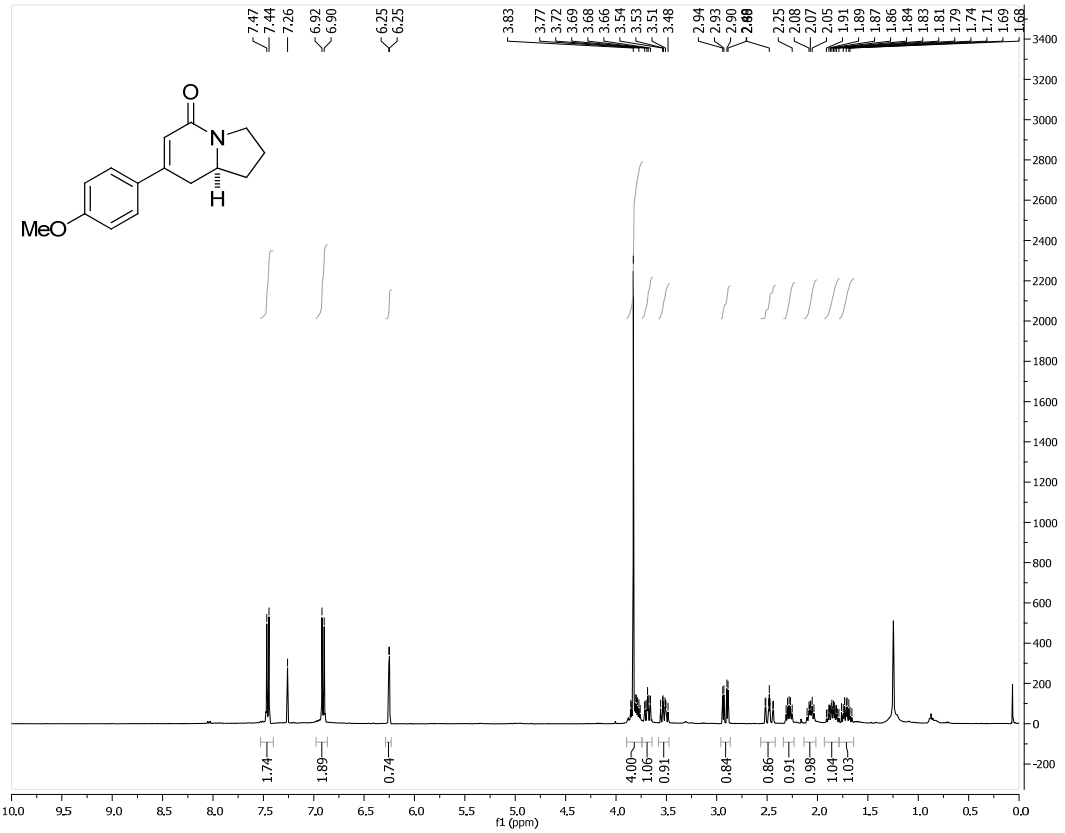

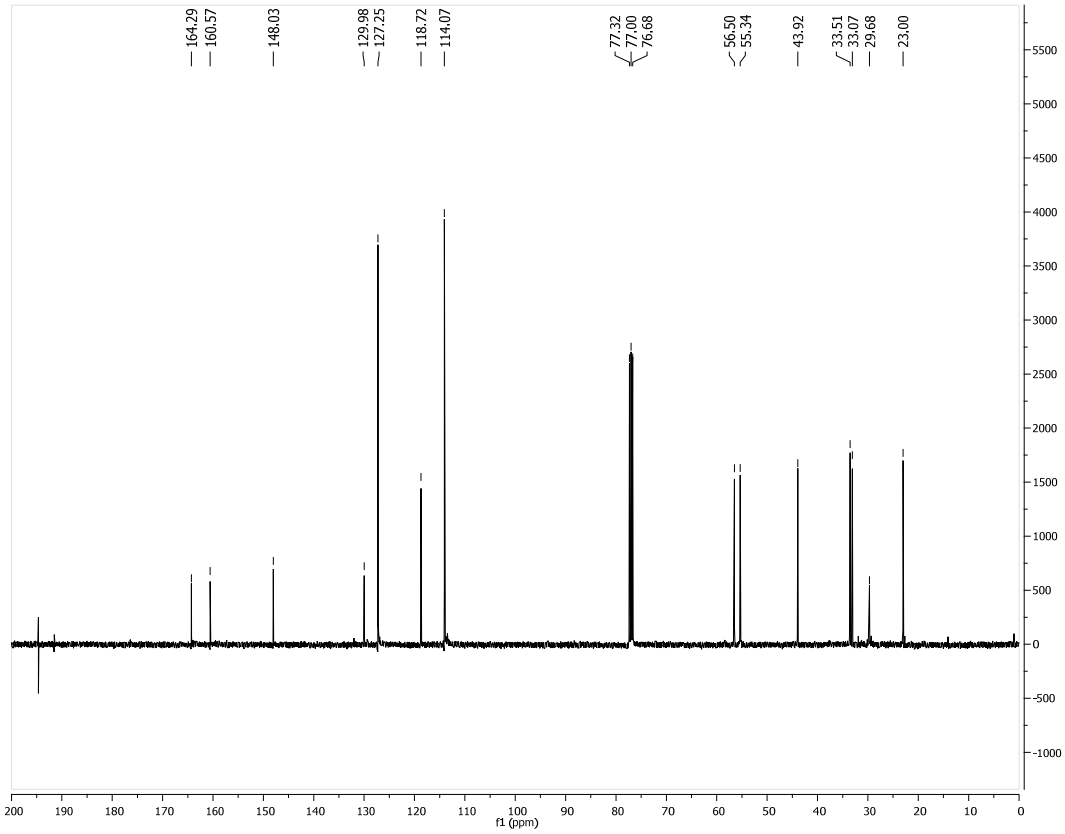

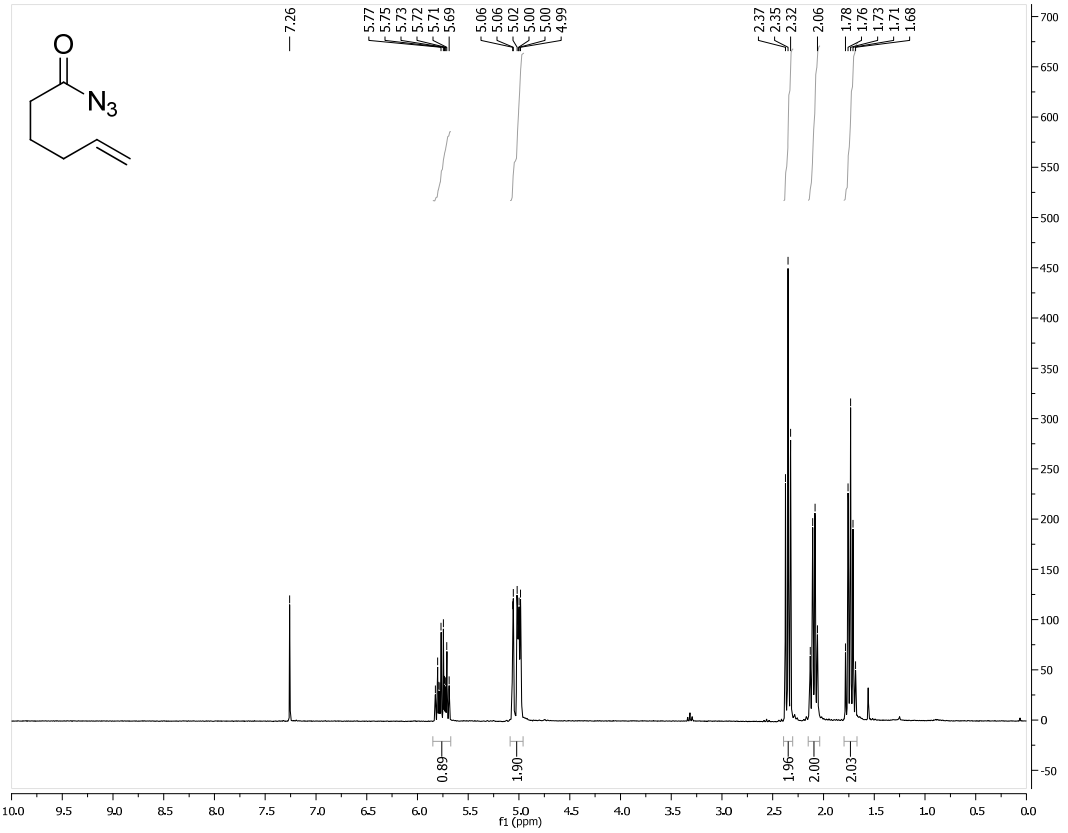
7.26
5.77
5.75
5.73
5.72
5.71
5.69
5.06
5.06
5.02
5.00
5.00
4.99
2.37
2.35
2.32
2.06
1.78
1.76
1.73
1.71
1.68
0.89
1.90
1.96
2.00
2.03
f1 (ppm)

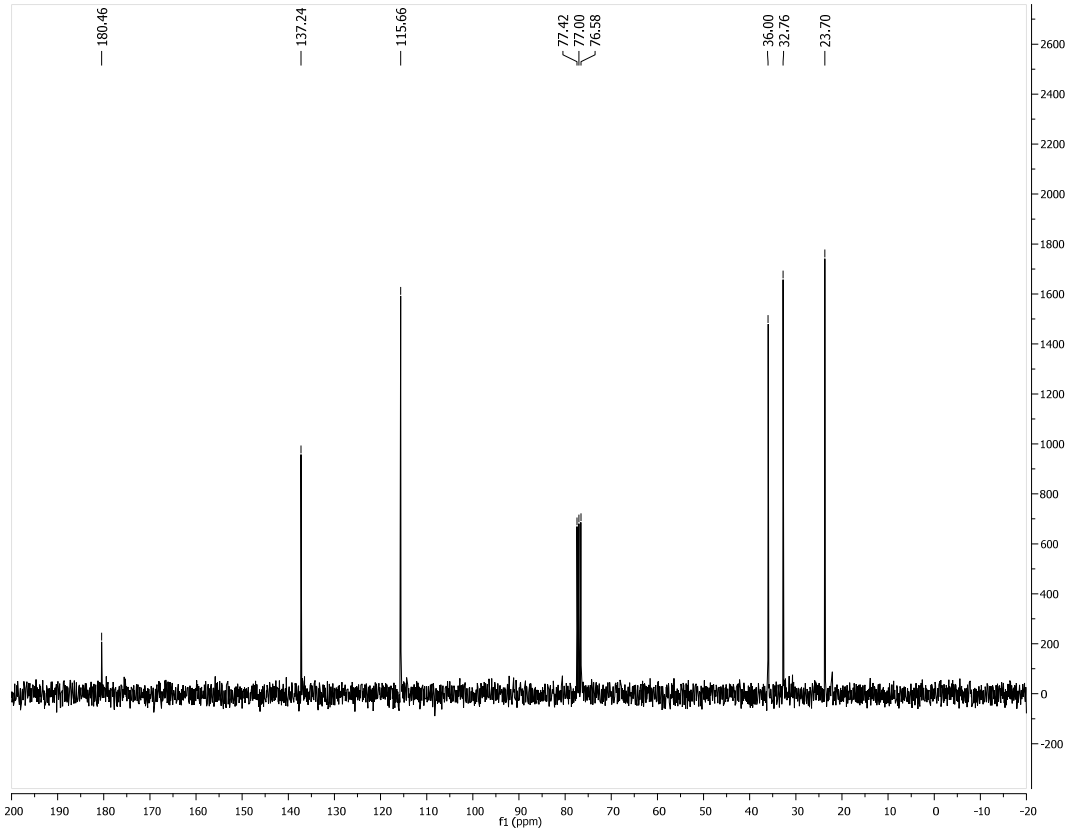
180.46
137.24
115.66
77.42
77.00
76.58
36.00
32.76
23.70
f1 (ppm)

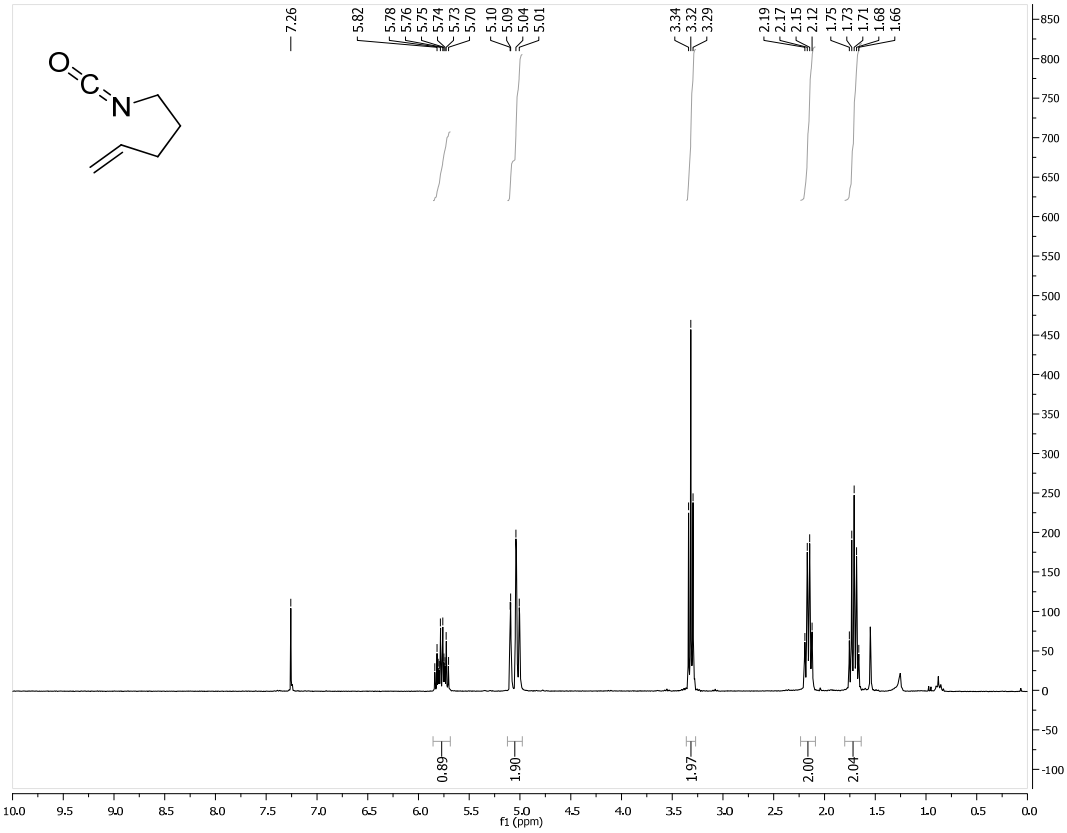
7.26
5.82
5.78
5.76
5.75
5.74
5.73
5.70
5.10
5.09
5.04
5.01
3.34
3.32
3.29
2.19
2.17
2.15
2.12
1.75
1.73
1.71
1.68
1.66
0.89
1.90
1.97
2.00
2.04
f1 (ppm)

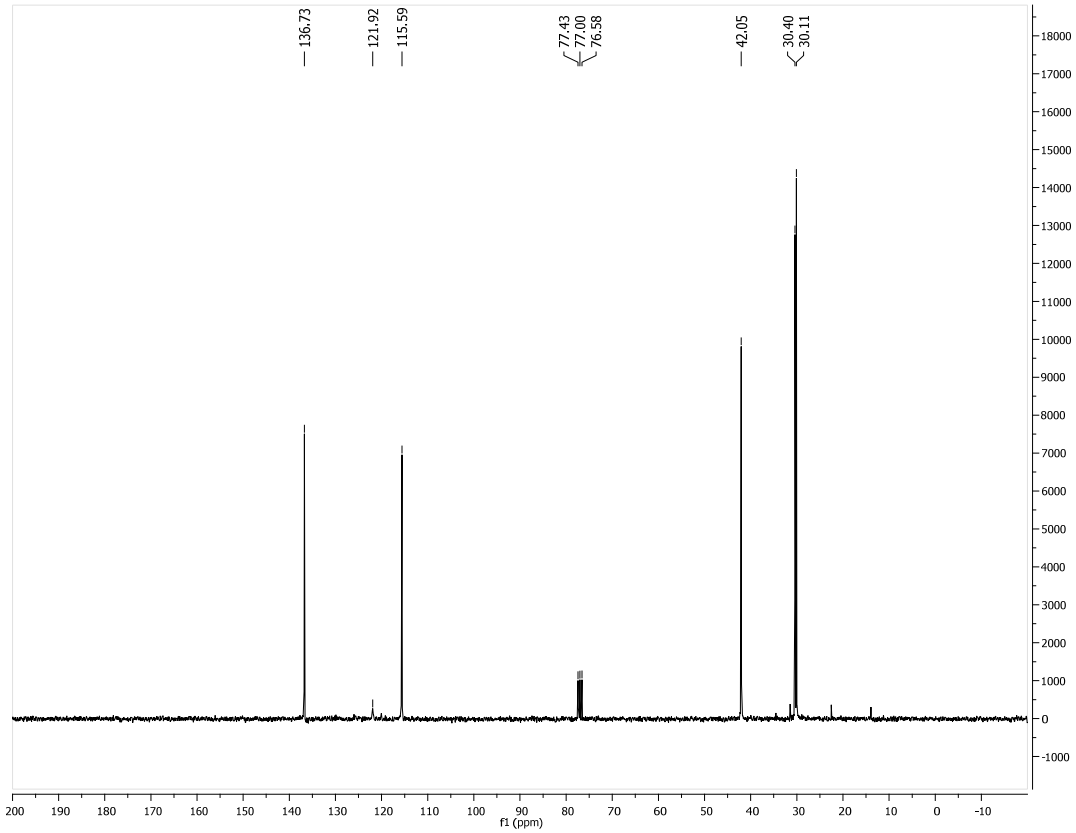
136.73
121.92
115.59
77.43
77.00
76.58
42.05
30.40
30.11
f1 (ppm)

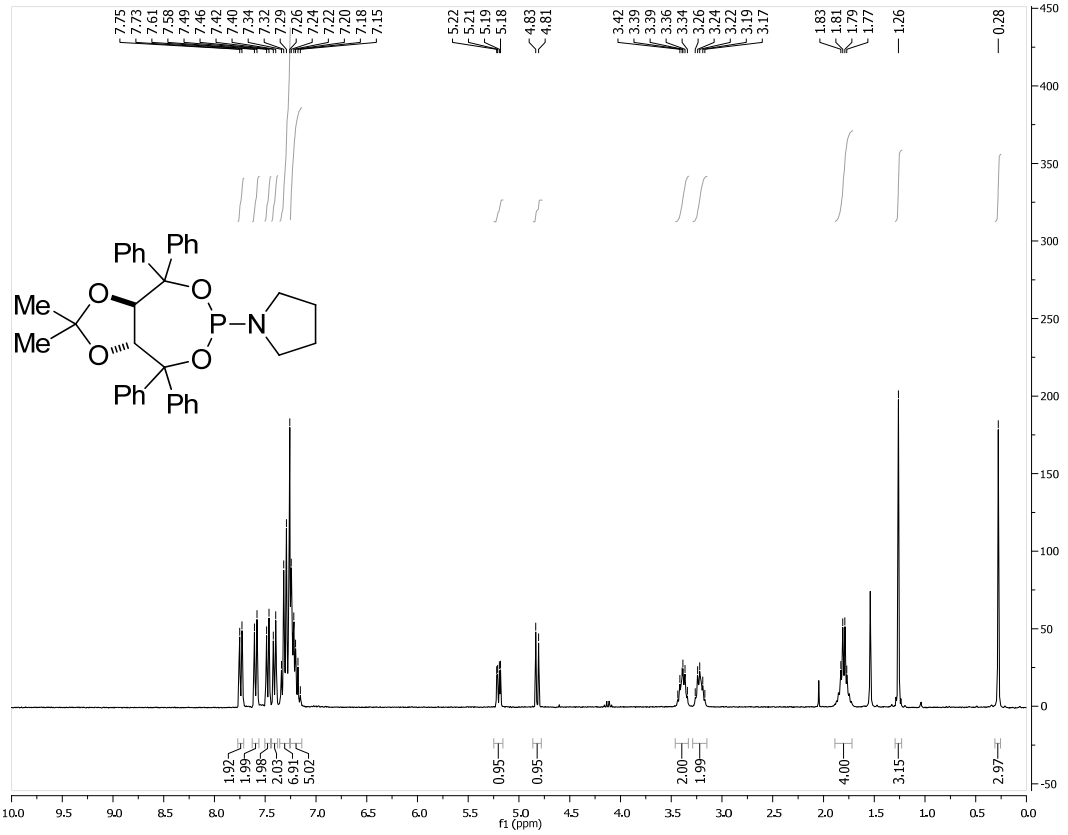
7.75
7.73
7.61
7.58
7.49
7.46
7.42
7.40
7.34
7.32
7.29
7.26
7.24
7.22
7.20
7.18
7.15
5.22
5.21
5.19
5.18
4.83
4.81
3.42
3.39
3.36
3.34
3.26
3.24
3.22
3.19
3.17
1.83
1.81
1.79
1.77
1.26
0.28
Ph
Ph
Me
Me
O
O
P–N
O
O
Ph
Ph
1.92
1.99
1.98
2.03
6.91
5.02
0.95
0.95
2.00
1.99
4.00
3.15
2.97
f1 (ppm)

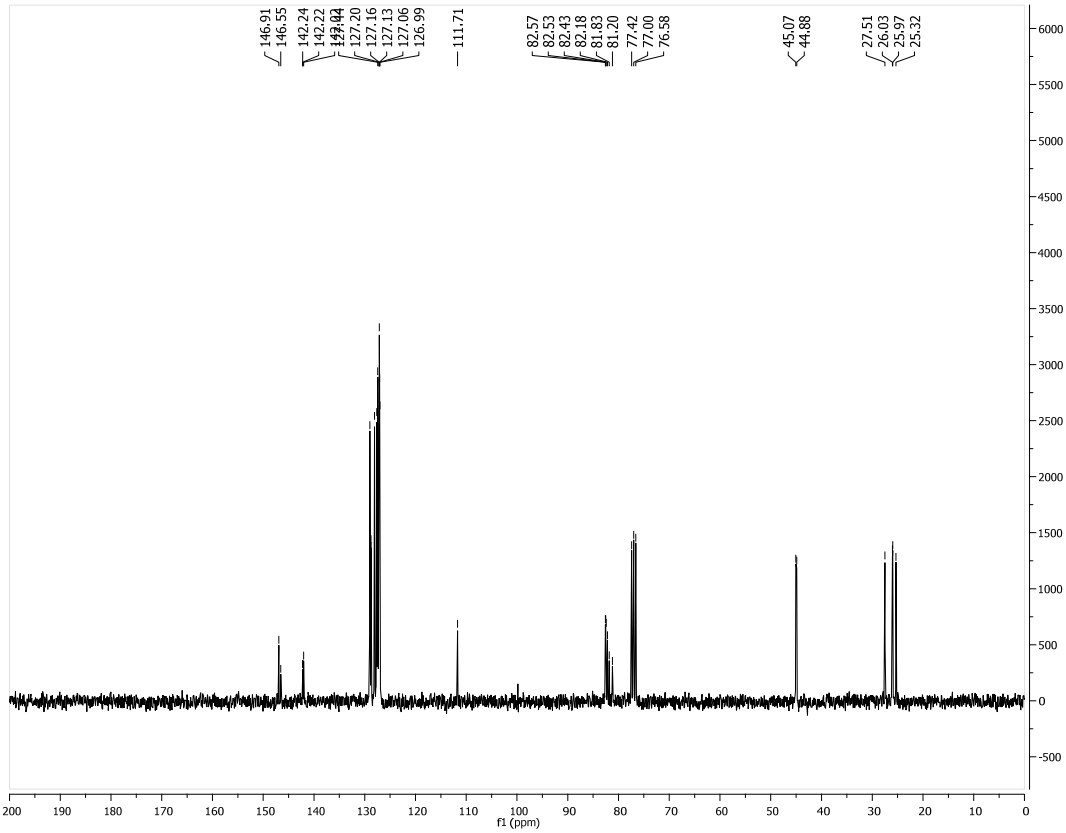
146.91
146.55
142.24
142.22
127.20
127.16
127.13
127.06
126.99
111.71
82.57
82.53
82.43
82.18
81.83
81.20
77.42
77.00
76.58
45.07
44.88
27.51
26.03
25.97
25.32
f1 (ppm)

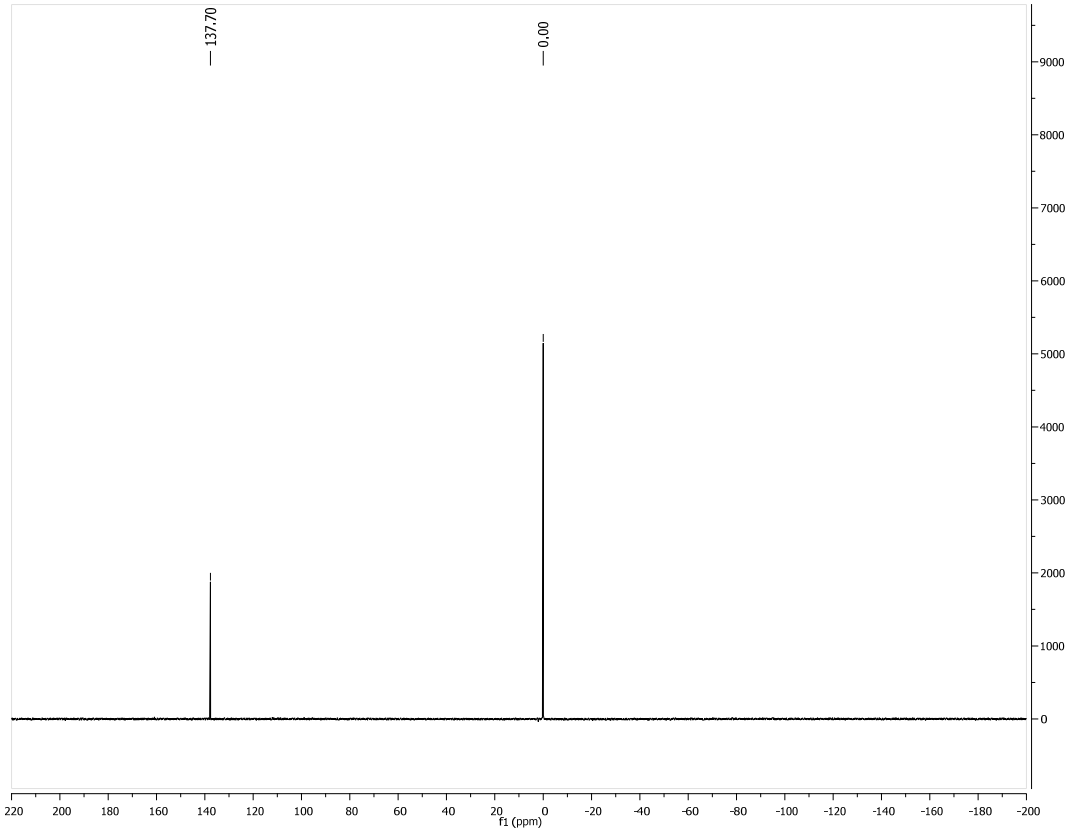
137.70
0.00
f1 (ppm)

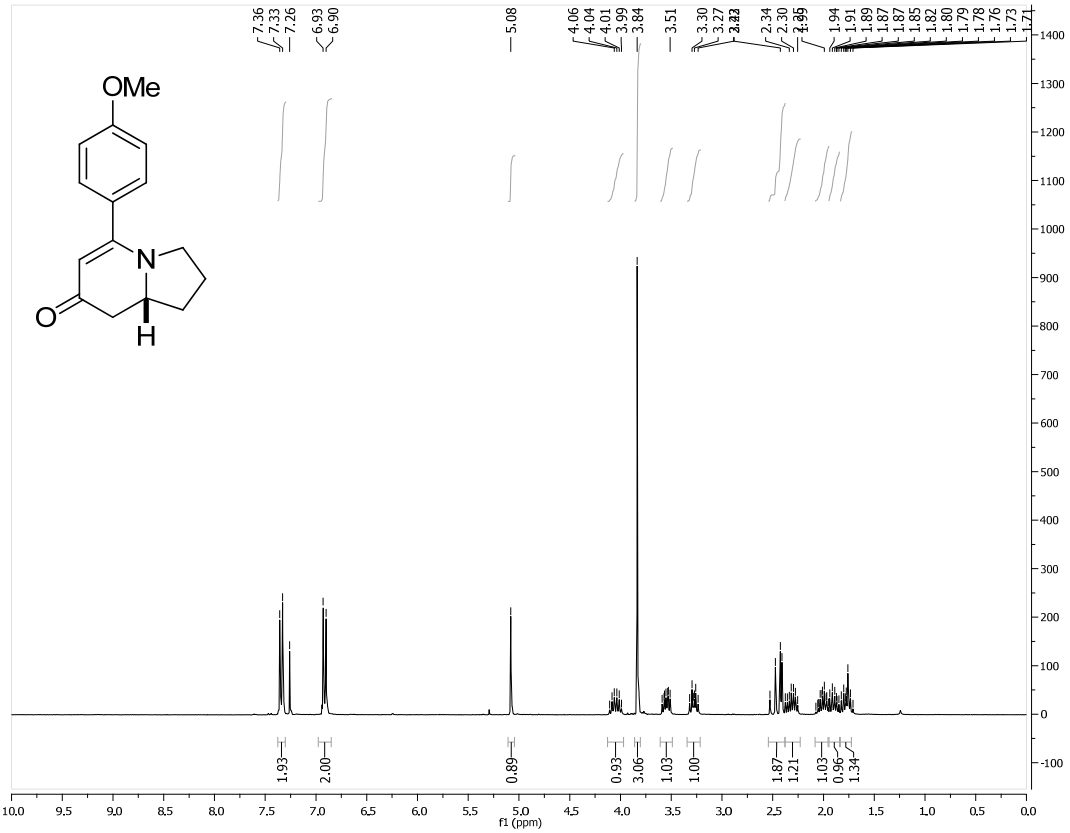
7.36
7.33
7.26
6.93
6.90
5.08
4.06
4.04
4.01
3.99
3.84
3.51
3.30
3.27
2.34
2.30
1.94
1.91
1.89
1.87
1.85
1.82
1.80
1.79
1.78
1.76
1.73
1.71
OMe
N
O
H
1.93
2.00
0.89
0.93
3.06
1.03
1.00
1.87
1.21
1.03
0.96
1.34
f1 (ppm)

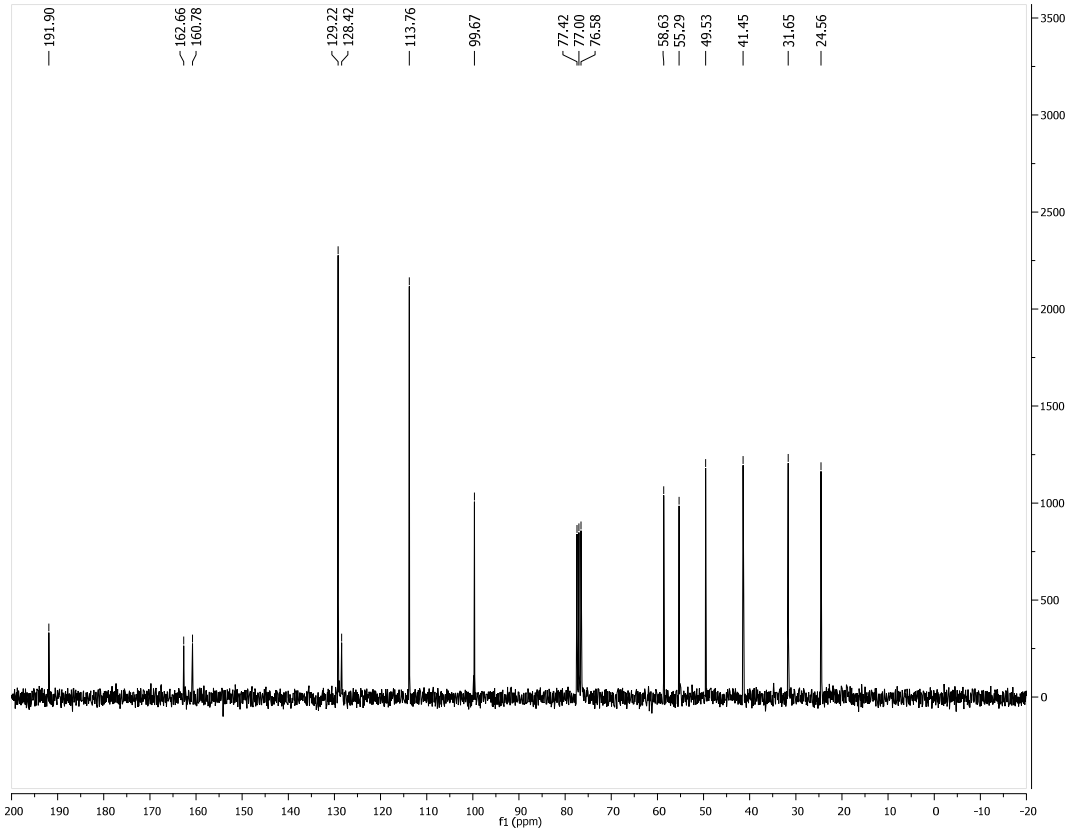

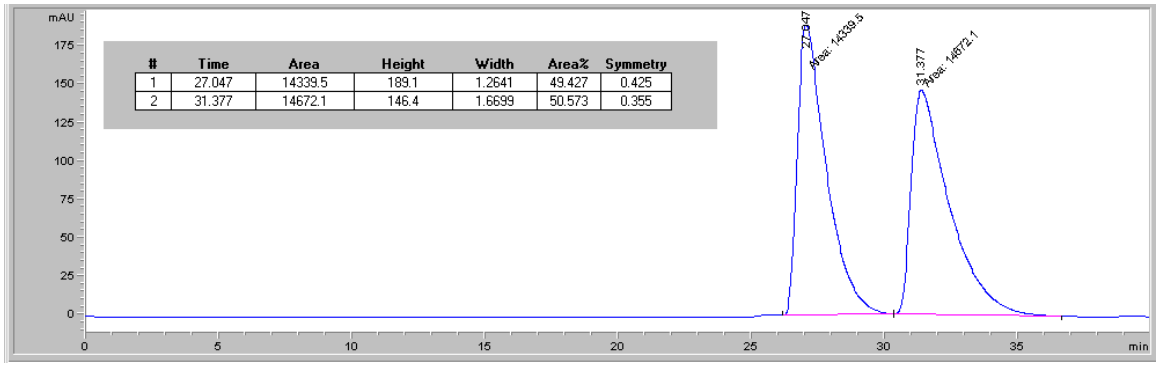

#	Time	Area	Height	Width	Area%	Symmetry
1	27.047	14339.5	189.1	1.2641	49.427	0.425
2	31.377	14672.1	146.4	1.6699	50.573	0.355

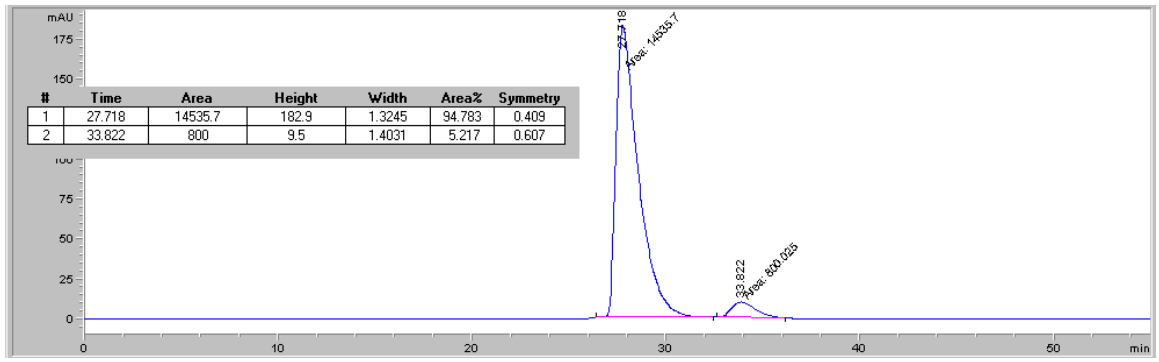

#	Time	Area	Height	Width	Area%	Symmetry
1	27.718	14535.7	182.9	1.3245	94.783	0.409
2	33.822	800	9.5	1.4031	5.217	0.607

Crystal Structure Tables and Figures.

Table A.2.1. Crystal data and structure refinement for Rh(cod)Cl·**T9**.

Identification code	rovis36_0m	
Empirical formula	$C_{52}H_{66}ClNO_4PRh$	
Formula weight	938.39	
Temperature	120(2) K	
Wavelength	0.71073 Å	
Crystal system	Orthorhombic	
Space group	$P\ 2_12_12_1$	
Unit cell dimensions	a = 15.3932(6) Å	α= 90°.
	b = 17.5850(7) Å	β= 90°.
	c = 18.0197(8) Å	γ = 90°.
Volume	4877.7(3) $Å^3$	
Z	4	
Density (calculated)	1.278 Mg/m^3	
Absorption coefficient	0.481 mm^{-1}	
F(000)	1976	
Crystal size	0.63 x 0.45 x 0.30 mm^3	
Theta range for data collection	2.09 to 33.49°.	
Index ranges	-21<=h<=23, -26<=k<=27, -27<=l<=27	
Reflections collected	138707	
Independent reflections	18942 [R(int) = 0.0541]	
Completeness to theta = 33.49°	99.3 %	
Absorption correction	None	
Max. and min. transmission	0.8683 and 0.7527	
Refinement method	Full-matrix least-squares on F^2	
Data / restraints / parameters	18942 / 0 / 568	
Goodness-of-fit on F^2	1.029	
Final R indices [I>2sigma(I)]	R1 = 0.0333, wR2 = 0.0760	
R indices (all data)	R1 = 0.0434, wR2 = 0.0811	
Absolute structure parameter	-0.014(12)	
Largest diff. peak and hole	0.709 and -0.589 e.$Å^{-3}$	

Table A.2.2. Atomic coordinates (x 10^4) and equivalent isotropic displacement parameters ($Å^2$x 10^3) for Rh(cod)Cl·**T9**. U(eq) is defined as one third of the trace of the orthogonalized U^{ij} tensor.

	x	y	z	U(eq)
C(1)	19(1)	5558(1)	5821(1)	16(1)
C(2)	421(1)	4739(1)	5820(1)	18(1)
C(3)	21(1)	4233(1)	5219(1)	19(1)
C(4)	611(1)	4193(1)	4521(1)	18(1)
C(5)	-109(2)	3614(1)	6349(1)	27(1)
C(6)	-1056(2)	3632(1)	6604(1)	35(1)
C(7)	411(2)	3000(1)	6718(1)	41(1)
C(8)	618(1)	6146(1)	6179(1)	17(1)
C(9)	476(1)	6908(1)	6024(1)	18(1)
C(10)	961(1)	7474(1)	6375(1)	21(1)

C(11)	1574(1)	7256(1)	6899(1)	25(1)
C(12)	1715(1)	6499(1)	7071(1)	27(1)
C(13)	1238(1)	5939(1)	6703(1)	23(1)
C(14)	809(1)	8301(1)	6194(1)	28(1)
C(15)	2356(2)	6278(2)	7672(2)	45(1)
C(16)	-862(1)	5565(1)	6212(1)	19(1)
C(17)	-1641(1)	5510(1)	5821(1)	20(1)
C(18)	-2438(1)	5479(1)	6191(1)	24(1)
C(19)	-2443(1)	5508(1)	6967(1)	28(1)
C(20)	-1677(1)	5578(1)	7366(1)	28(1)
C(21)	-886(1)	5604(1)	6988(1)	24(1)
C(22)	-3277(1)	5440(1)	5767(1)	32(1)
C(23)	-1677(2)	5626(2)	8209(1)	42(1)
C(24)	132(1)	3957(1)	3823(1)	18(1)
C(25)	478(1)	4166(1)	3141(1)	21(1)
C(26)	91(1)	3940(1)	2479(1)	24(1)
C(27)	-642(1)	3476(1)	2513(1)	25(1)
C(28)	-998(1)	3249(1)	3187(1)	24(1)
C(29)	-607(1)	3502(1)	3843(1)	21(1)
C(30)	461(2)	4190(2)	1744(1)	40(1)
C(31)	-1774(2)	2728(1)	3200(1)	38(1)
C(32)	1388(1)	3654(1)	4632(1)	21(1)
C(33)	2222(1)	3923(1)	4747(1)	31(1)
C(34)	2926(2)	3425(2)	4811(2)	40(1)
C(35)	2780(2)	2655(1)	4770(1)	39(1)
C(36)	1953(2)	2366(1)	4665(1)	34(1)
C(37)	1257(2)	2867(1)	4593(1)	28(1)
C(38)	3840(2)	3741(2)	4927(3)	74(1)
C(39)	1795(2)	1517(1)	4634(2)	48(1)
C(40)	158(1)	6132(1)	2978(1)	23(1)
C(41)	-484(1)	6708(1)	2635(1)	29(1)
C(42)	-1385(1)	6359(1)	2565(1)	30(1)
C(43)	-1684(1)	6058(1)	3313(1)	27(1)
C(44)	-1028(1)	5493(1)	3623(1)	21(1)
C(45)	2499(1)	5939(1)	3906(1)	22(1)
C(46)	2610(1)	5999(1)	4683(1)	24(1)
C(47)	3361(1)	6420(1)	5043(1)	32(1)
C(48)	3122(1)	7238(1)	5252(1)	32(1)
C(49)	2502(1)	7599(1)	4709(1)	26(1)
C(50)	2551(1)	7548(1)	3949(1)	25(1)
C(51)	3277(1)	7164(1)	3529(1)	31(1)
C(52)	3057(1)	6337(1)	3336(1)	29(1)
Cl(1)	456(1)	7628(1)	4288(1)	21(1)
N(1)	-162(1)	5843(1)	3678(1)	18(1)
O(1)	-162(1)	5763(1)	5051(1)	16(1)
O(2)	981(1)	4949(1)	4424(1)	17(1)
O(3)	275(1)	4342(1)	6495(1)	23(1)
O(4)	-65(1)	3509(1)	5563(1)	24(1)
P(1)	527(1)	5784(1)	4376(1)	14(1)
Rh(1)	1566(1)	6700(1)	4344(1)	16(1)

Table A.2.3. Bond lengths [Å] and angles [°] for Rh(cod)Cl·**T9**.

C(1)-O(1)	1.4606(19)	C(41)-C(42)	1.523(3)
C(1)-C(8)	1.528(2)	C(42)-C(43)	1.519(3)
C(1)-C(16)	1.529(2)	C(43)-C(44)	1.523(3)
C(1)-C(2)	1.567(2)	C(44)-N(1)	1.471(2)
C(2)-O(3)	1.421(2)	C(45)-C(46)	1.413(3)
C(2)-C(3)	1.531(2)	C(45)-C(52)	1.510(3)
C(3)-O(4)	1.421(2)	C(45)-Rh(1)	2.1155(19)
C(3)-C(4)	1.553(2)	C(46)-C(47)	1.519(3)
C(4)-O(2)	1.458(2)	C(46)-Rh(1)	2.1152(19)
C(4)-C(24)	1.516(2)	C(47)-C(48)	1.532(3)
C(4)-C(32)	1.539(2)	C(48)-C(49)	1.506(3)
C(5)-O(4)	1.431(2)	C(49)-C(50)	1.374(3)
C(5)-O(3)	1.433(2)	C(49)-Rh(1)	2.2373(19)
C(5)-C(7)	1.499(3)	C(50)-C(51)	1.510(3)
C(5)-C(6)	1.529(3)	C(50)-Rh(1)	2.2430(19)
C(8)-C(9)	1.387(3)	C(51)-C(52)	1.533(3)
C(8)-C(13)	1.390(2)	Cl(1)-Rh(1)	2.3654(4)
C(9)-C(10)	1.396(2)	N(1)-P(1)	1.6477(15)
C(10)-C(11)	1.389(3)	O(1)-P(1)	1.6149(13)
C(10)-C(14)	1.508(3)	O(2)-P(1)	1.6283(12)
C(11)-C(12)	1.384(3)	P(1)-Rh(1)	2.2703(4)
C(12)-C(13)	1.397(3)		
C(12)-C(15)	1.517(3)	O(1)-C(1)-C(8)	110.47(13)
C(16)-C(17)	1.393(2)	O(1)-C(1)-C(16)	105.39(13)
C(16)-C(21)	1.400(3)	C(8)-C(1)-C(16)	109.64(13)
C(17)-C(18)	1.397(3)	O(1)-C(1)-C(2)	107.50(12)
C(18)-C(19)	1.401(3)	C(8)-C(1)-C(2)	112.59(14)
C(18)-C(22)	1.502(3)	C(16)-C(1)-C(2)	110.99(14)
C(19)-C(20)	1.388(3)	O(3)-C(2)-C(3)	104.78(13)
C(20)-C(21)	1.397(3)	O(3)-C(2)-C(1)	112.89(13)
C(20)-C(23)	1.520(3)	C(3)-C(2)-C(1)	112.15(14)
C(24)-C(25)	1.389(2)	O(4)-C(3)-C(2)	104.52(13)
C(24)-C(29)	1.391(3)	O(4)-C(3)-C(4)	111.47(14)
C(25)-C(26)	1.391(3)	C(2)-C(3)-C(4)	111.30(14)
C(26)-C(27)	1.394(3)	O(2)-C(4)-C(24)	109.83(13)
C(26)-C(30)	1.507(3)	O(2)-C(4)-C(32)	105.88(14)
C(27)-C(28)	1.392(3)	C(24)-C(4)-C(32)	108.47(13)
C(28)-C(29)	1.398(2)	O(2)-C(4)-C(3)	106.56(13)
C(28)-C(31)	1.507(3)	C(24)-C(4)-C(3)	113.60(14)
C(32)-C(33)	1.384(3)	C(32)-C(4)-C(3)	112.20(14)
C(32)-C(37)	1.400(3)	O(4)-C(5)-O(3)	106.10(15)
C(33)-C(34)	1.398(3)	O(4)-C(5)-C(7)	108.68(18)
C(34)-C(35)	1.375(4)	O(3)-C(5)-C(7)	109.99(18)
C(34)-C(38)	1.526(4)	O(4)-C(5)-C(6)	110.15(17)
C(35)-C(36)	1.384(4)	O(3)-C(5)-C(6)	108.71(17)
C(36)-C(37)	1.393(3)	C(7)-C(5)-C(6)	112.99(19)
C(36)-C(39)	1.515(3)	C(9)-C(8)-C(13)	119.84(16)
C(40)-N(1)	1.447(2)	C(9)-C(8)-C(1)	118.26(15)
C(40)-C(41)	1.545(3)	C(13)-C(8)-C(1)	121.60(16)

C(8)-C(9)-C(10)	120.92(16)	C(43)-C(42)-C(41)	110.09(16)
C(11)-C(10)-C(9)	118.33(17)	C(42)-C(43)-C(44)	110.61(16)
C(11)-C(10)-C(14)	121.26(16)	N(1)-C(44)-C(43)	110.65(15)
C(9)-C(10)-C(14)	120.40(17)	C(46)-C(45)-C(52)	124.86(19)
C(12)-C(11)-C(10)	121.59(17)	C(46)-C(45)-Rh(1)	70.48(12)
C(11)-C(12)-C(13)	119.33(18)	C(52)-C(45)-Rh(1)	110.32(13)
C(11)-C(12)-C(15)	120.58(18)	C(45)-C(46)-C(47)	123.42(19)
C(13)-C(12)-C(15)	120.1(2)	C(45)-C(46)-Rh(1)	70.50(12)
C(8)-C(13)-C(12)	119.96(18)	C(47)-C(46)-Rh(1)	114.63(14)
C(17)-C(16)-C(21)	119.04(16)	C(46)-C(47)-C(48)	112.35(17)
C(17)-C(16)-C(1)	122.06(15)	C(49)-C(48)-C(47)	112.80(17)
C(21)-C(16)-C(1)	118.87(16)	C(50)-C(49)-C(48)	125.9(2)
C(16)-C(17)-C(18)	121.17(16)	C(50)-C(49)-Rh(1)	72.37(13)
C(17)-C(18)-C(19)	118.71(18)	C(48)-C(49)-Rh(1)	107.56(14)
C(17)-C(18)-C(22)	120.98(18)	C(49)-C(50)-C(51)	124.6(2)
C(19)-C(18)-C(22)	120.28(18)	C(49)-C(50)-Rh(1)	71.91(12)
C(20)-C(19)-C(18)	121.05(18)	C(51)-C(50)-Rh(1)	111.17(14)
C(19)-C(20)-C(21)	119.41(17)	C(50)-C(51)-C(52)	112.04(17)
C(19)-C(20)-C(23)	121.51(19)	C(45)-C(52)-C(51)	114.17(17)
C(21)-C(20)-C(23)	119.1(2)	C(40)-N(1)-C(44)	113.37(14)
C(20)-C(21)-C(16)	120.60(18)	C(40)-N(1)-P(1)	117.90(12)
C(25)-C(24)-C(29)	119.25(16)	C(44)-N(1)-P(1)	127.45(12)
C(25)-C(24)-C(4)	118.42(16)	C(1)-O(1)-P(1)	126.59(10)
C(29)-C(24)-C(4)	122.22(16)	C(4)-O(2)-P(1)	131.43(10)
C(24)-C(25)-C(26)	121.24(17)	C(2)-O(3)-C(5)	110.34(13)
C(25)-C(26)-C(27)	118.50(17)	C(3)-O(4)-C(5)	108.63(13)
C(25)-C(26)-C(30)	120.56(18)	O(1)-P(1)-O(2)	102.74(6)
C(27)-C(26)-C(30)	120.93(17)	O(1)-P(1)-N(1)	98.83(6)
C(28)-C(27)-C(26)	121.60(17)	O(2)-P(1)-N(1)	111.92(7)
C(27)-C(28)-C(29)	118.50(17)	O(1)-P(1)-Rh(1)	119.87(5)
C(27)-C(28)-C(31)	119.99(17)	O(2)-P(1)-Rh(1)	109.79(4)
C(29)-C(28)-C(31)	121.49(17)	N(1)-P(1)-Rh(1)	112.95(6)
C(24)-C(29)-C(28)	120.88(17)	C(46)-Rh(1)-C(45)	39.03(7)
C(33)-C(32)-C(37)	118.63(18)	C(46)-Rh(1)-C(49)	80.67(8)
C(33)-C(32)-C(4)	122.01(16)	C(45)-Rh(1)-C(49)	96.82(8)
C(37)-C(32)-C(4)	119.33(18)	C(46)-Rh(1)-C(50)	88.06(8)
C(32)-C(33)-C(34)	121.2(2)	C(45)-Rh(1)-C(50)	80.98(7)
C(35)-C(34)-C(33)	119.0(2)	C(49)-Rh(1)-C(50)	35.72(7)
C(35)-C(34)-C(38)	121.1(2)	C(46)-Rh(1)-P(1)	96.58(6)
C(33)-C(34)-C(38)	119.8(2)	C(45)-Rh(1)-P(1)	92.26(6)
C(34)-C(35)-C(36)	121.3(2)	C(49)-Rh(1)-P(1)	161.33(6)
C(35)-C(36)-C(37)	119.2(2)	C(50)-Rh(1)-P(1)	162.90(6)
C(35)-C(36)-C(39)	121.0(2)	C(46)-Rh(1)-Cl(1)	164.48(6)
C(37)-C(36)-C(39)	119.8(2)	C(45)-Rh(1)-Cl(1)	155.62(6)
C(36)-C(37)-C(32)	120.6(2)	C(49)-Rh(1)-Cl(1)	89.47(6)
N(1)-C(40)-C(41)	111.20(15)	C(50)-Rh(1)-Cl(1)	90.90(6)
C(42)-C(41)-C(40)	110.59(17)	P(1)-Rh(1)-Cl(1)	88.919(14)

Symmetry transformations used to generate equivalent atoms:

Table A.2.4. Anisotropic displacement parameters ($Å^2 x\ 10^3$)for Rh(cod)Cl·**T9**. The anisotropic displacement factor exponent takes the form: $-2\pi^2[\ h^2 a^{*2} U^{11} + ... + 2\ h\ k\ a^*\ b^*\ U^{12}\ ]$

	U^{11}	U^{22}	U^{33}	U^{23}	U^{13}	U^{12}
C(1)	18(1)	18(1)	14(1)	-1(1)	0(1)	1(1)
C(2)	22(1)	17(1)	16(1)	-1(1)	0(1)	1(1)
C(3)	22(1)	16(1)	18(1)	0(1)	1(1)	-1(1)
C(4)	20(1)	14(1)	19(1)	-1(1)	-1(1)	1(1)
C(5)	41(1)	20(1)	20(1)	3(1)	-4(1)	-2(1)
C(6)	41(1)	35(1)	29(1)	3(1)	6(1)	-7(1)
C(7)	58(2)	28(1)	38(1)	4(1)	-10(1)	8(1)
C(8)	16(1)	21(1)	15(1)	-4(1)	1(1)	0(1)
C(9)	16(1)	21(1)	19(1)	-4(1)	1(1)	-1(1)
C(10)	19(1)	22(1)	23(1)	-7(1)	2(1)	-3(1)
C(11)	20(1)	30(1)	26(1)	-13(1)	1(1)	-2(1)
C(12)	18(1)	40(1)	23(1)	-13(1)	-3(1)	1(1)
C(13)	22(1)	27(1)	20(1)	-4(1)	-2(1)	4(1)
C(14)	29(1)	23(1)	33(1)	-7(1)	0(1)	-4(1)
C(15)	39(1)	53(2)	43(1)	-16(1)	-23(1)	13(1)
C(16)	20(1)	16(1)	21(1)	-1(1)	4(1)	0(1)
C(17)	22(1)	17(1)	23(1)	-1(1)	2(1)	0(1)
C(18)	21(1)	15(1)	36(1)	1(1)	6(1)	1(1)
C(19)	26(1)	23(1)	35(1)	1(1)	13(1)	0(1)
C(20)	33(1)	25(1)	26(1)	-2(1)	11(1)	-3(1)
C(21)	24(1)	26(1)	22(1)	-2(1)	3(1)	-2(1)
C(22)	20(1)	26(1)	49(1)	0(1)	3(1)	1(1)
C(23)	49(2)	49(1)	28(1)	-4(1)	16(1)	-5(1)
C(24)	20(1)	16(1)	17(1)	-3(1)	0(1)	3(1)
C(25)	21(1)	24(1)	19(1)	-4(1)	2(1)	2(1)
C(26)	24(1)	28(1)	19(1)	-7(1)	2(1)	3(1)
C(27)	27(1)	27(1)	22(1)	-7(1)	-3(1)	0(1)
C(28)	26(1)	22(1)	25(1)	-5(1)	-2(1)	-2(1)
C(29)	25(1)	18(1)	21(1)	-2(1)	1(1)	-2(1)
C(30)	38(1)	61(2)	19(1)	-6(1)	3(1)	-15(1)
C(31)	42(1)	40(1)	33(1)	-6(1)	-2(1)	-16(1)
C(32)	28(1)	19(1)	18(1)	-1(1)	-1(1)	7(1)
C(33)	25(1)	26(1)	41(1)	-1(1)	-5(1)	7(1)
C(34)	29(1)	40(1)	52(1)	1(1)	-8(1)	13(1)
C(35)	46(1)	36(1)	35(1)	0(1)	-6(1)	23(1)
C(36)	50(1)	23(1)	28(1)	0(1)	-3(1)	14(1)
C(37)	37(1)	19(1)	27(1)	-1(1)	-2(1)	7(1)
C(38)	31(1)	57(2)	134(4)	-2(2)	-18(2)	12(1)
C(39)	71(2)	23(1)	49(1)	1(1)	-2(1)	16(1)
C(40)	18(1)	27(1)	25(1)	-3(1)	0(1)	-3(1)
C(41)	35(1)	26(1)	26(1)	3(1)	-10(1)	-1(1)
C(42)	29(1)	28(1)	32(1)	-2(1)	-13(1)	5(1)
C(43)	19(1)	29(1)	34(1)	-9(1)	-6(1)	5(1)
C(44)	16(1)	23(1)	23(1)	-4(1)	-2(1)	-2(1)
C(45)	16(1)	21(1)	29(1)	-2(1)	0(1)	1(1)

C(46)	17(1)	26(1)	30(1)	2(1)	-4(1)	2(1)
C(47)	20(1)	41(1)	36(1)	-3(1)	-10(1)	1(1)
C(48)	21(1)	43(1)	31(1)	-8(1)	-4(1)	-5(1)
C(49)	18(1)	23(1)	36(1)	-6(1)	1(1)	-6(1)
C(50)	21(1)	22(1)	31(1)	1(1)	3(1)	-5(1)
C(51)	24(1)	32(1)	36(1)	-1(1)	8(1)	-5(1)
C(52)	23(1)	32(1)	31(1)	-4(1)	9(1)	-1(1)
Cl(1)	19(1)	19(1)	24(1)	2(1)	0(1)	1(1)
N(1)	15(1)	22(1)	16(1)	0(1)	-3(1)	-2(1)
O(1)	15(1)	17(1)	15(1)	-1(1)	-1(1)	0(1)
O(2)	17(1)	14(1)	19(1)	0(1)	1(1)	1(1)
O(3)	31(1)	21(1)	17(1)	1(1)	-1(1)	-1(1)
O(4)	38(1)	16(1)	19(1)	1(1)	4(1)	-3(1)
P(1)	14(1)	15(1)	14(1)	0(1)	-1(1)	0(1)
Rh(1)	13(1)	18(1)	19(1)	0(1)	-1(1)	-1(1)

Table A.2.5. Hydrogen coordinates (x 10^4) and isotropic displacement parameters ($Å^2$x 10^3) for Rh(cod)Cl·**T9**.

	x	y	z	U(eq)
H(2)	1061	4779	5732	22
H(3)	-566	4431	5079	22
H(6A)	-1370	4028	6331	52
H(6B)	-1080	3741	7136	52
H(6C)	-1326	3137	6507	52
H(7A)	161	2503	6595	62
H(7B)	398	3074	7257	62
H(7C)	1013	3022	6542	62
H(9)	42	7047	5675	22
H(11)	1905	7636	7146	30
H(13)	1336	5417	6810	28
H(14A)	308	8488	6476	42
H(14B)	694	8355	5662	42
H(14C)	1325	8597	6326	42
H(15A)	2935	6469	7542	68
H(15B)	2376	5722	7716	68
H(15C)	2173	6498	8146	68
H(17)	-1629	5494	5294	25
H(19)	-2981	5480	7225	34
H(21)	-359	5649	7259	29
H(22A)	-3582	5927	5809	48
H(22B)	-3641	5034	5971	48
H(22C)	-3155	5334	5243	48
H(23A)	-1384	6095	8365	63
H(23B)	-1369	5186	8414	63
H(23C)	-2277	5629	8390	63
H(25)	988	4470	3126	25

H(27)	-905	3311	2064	30
H(29)	-849	3362	4308	26
H(30A)	88	4585	1529	59
H(30B)	486	3754	1406	59
H(30C)	1047	4393	1818	59
H(31A)	-2214	2915	2851	57
H(31B)	-2020	2715	3702	57
H(31C)	-1595	2214	3055	57
H(33)	2318	4456	4783	37
H(35)	3256	2315	4814	47
H(37)	688	2673	4516	33
H(38A)	4241	3322	5030	111
H(38B)	3837	4095	5347	111
H(38C)	4027	4010	4478	111
H(39A)	1840	1303	5134	71
H(39B)	2230	1279	4311	71
H(39C)	1213	1418	4435	71
H(40A)	246	5704	2629	28
H(40B)	727	6382	3057	28
H(41A)	-514	7168	2951	35
H(41B)	-274	6864	2138	35
H(42A)	-1800	6748	2385	36
H(42B)	-1372	5939	2200	36
H(43A)	-2255	5806	3257	33
H(43B)	-1754	6487	3664	33
H(44A)	-1218	5322	4121	25
H(44B)	-998	5042	3295	25
H(47A)	3860	6428	4697	39
H(47B)	3543	6143	5495	39
H(48A)	2854	7240	5752	38
H(48B)	3658	7548	5277	38
H(51A)	3812	7174	3834	37
H(51B)	3393	7449	3066	37
H(52A)	2751	6328	2853	34
H(52B)	3605	6049	3277	34
H(49)	2103(17)	8006(15)	4886(14)	31(7)
H(50)	2203(17)	7873(15)	3659(14)	30(7)
H(45)	2204(18)	5499(16)	3700(15)	36(7)
H(46)	2348(17)	5594(15)	4956(14)	30(6)

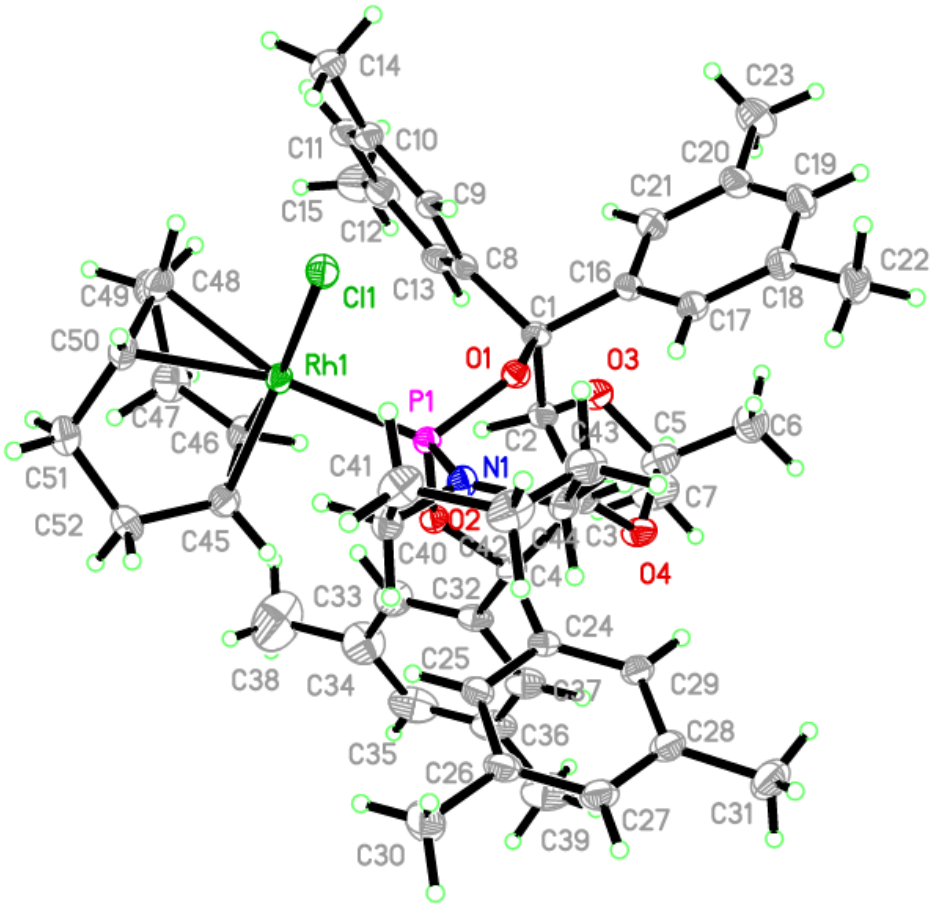
C14
C23
C11
C10
C20
C19
C15
C9
C21
C12
C8
C22
C48
C16
C49
Cl1
C13
C1
C18
C17
C50
Rh1
O1
O3
P1
C47
C2
C43
C5
C6
C46
C41
N1
C7
C51
O2
C52
C45
C40
C42
C44
C3
O4
C4
C33
C32
C24
C25
C38
C34
C37
C29
C36
C28
C35
C26
C27
C31
C39
C30

Table A.2.6. Crystal data and structure refinement for Rh(cod)Cl·**A1**.

Identification code	rovis41_0m	
Empirical formula	$C_{34}H_{50}ClNO_2PRh$	
Formula weight	674.08	
Temperature	296(2) K	
Wavelength	0.71073 Å	
Crystal system	Triclinic	
Space group	*P*-1	
Unit cell dimensions	*a* = 10.4105(5) Å	α= 77.003(3)°.
	b = 10.8685(6) Å	β= 76.360(2)°.
	c = 16.5368(10) Å	γ = 64.354(2)°.
Volume	1622.99(15) $Å^3$	
Z	2	
Density (calculated)	1.379 Mg/m^3	
Absorption coefficient	0.688 mm^{-1}	
F(000)	708	
Crystal size	0.70 x 0.37 x 0.17 mm^3	
Theta range for data collection	2.10 to 33.37°.	
Index ranges	-16<=h<=13, -16<=k<=15, -25<=l<=25	
Reflections collected	19235	
Independent reflections	12140 [R(int) = 0.0176]	
Completeness to theta = 33.37°	96.3 %	
Absorption correction	Semi-empirical from equivalents	
Max. and min. transmission	0.8890 and 0.6455	
Refinement method	Full-matrix least-squares on F^2	
Data / restraints / parameters	12140 / 0 / 389	
Goodness-of-fit on F^2	1.104	
Final R indices [I>2sigma(I)]	R1 = 0.0336, wR2 = 0.0761	
R indices (all data)	R1 = 0.0410, wR2 = 0.0792	
Largest diff. peak and hole	1.056 and -0.844 $e.Å^{-3}$	

Table A.2.7. Atomic coordinates (x 10^4) and equivalent isotropic displacement parameters ($Å^2$x 10^3) for Rh(cod)Cl·**A1**. U(eq) is defined as one third of the trace of the orthogonalized U^{ij} tensor.

	x	y	z	U(eq)
C(1)	1725(2)	5267(2)	3240(1)	13(1)
C(2)	3191(2)	4967(2)	3167(1)	12(1)
C(3)	3711(2)	5600(2)	3586(1)	13(1)
C(4)	2679(2)	6412(2)	4177(1)	18(1)
C(5)	1231(2)	6611(2)	4340(1)	19(1)
C(6)	728(2)	6061(2)	3855(1)	16(1)
C(7)	5251(2)	5552(2)	3354(1)	17(1)
C(8)	5462(2)	6175(2)	2427(1)	24(1)
C(9)	6416(2)	4076(2)	3485(1)	23(1)
C(10)	5482(2)	6415(2)	3879(1)	23(1)
C(11)	212(2)	7467(2)	5014(1)	29(1)
C(12)	-842(2)	6305(2)	4004(1)	22(1)

C(13)	1241(2)	4796(2)	2630(1)	14(1)
C(14)	1684(2)	3384(2)	2628(1)	14(1)
C(15)	1071(2)	2863(2)	2194(1)	18(1)
C(16)	164(2)	3863(2)	1646(1)	22(1)
C(17)	-161(2)	5260(2)	1545(1)	21(1)
C(18)	342(2)	5760(2)	2065(1)	17(1)
C(19)	1264(2)	1357(2)	2277(1)	22(1)
C(20)	1991(2)	396(2)	3020(1)	27(1)
C(21)	2139(2)	773(2)	1460(2)	33(1)
C(22)	-240(2)	1330(2)	2412(2)	36(1)
C(23)	-1070(2)	6240(2)	893(1)	28(1)
C(24)	-45(2)	7279(2)	1987(1)	22(1)
C(25)	4216(2)	1871(2)	4453(1)	25(1)
C(26)	6577(2)	718(2)	3606(1)	22(1)
C(27)	6010(2)	3301(2)	932(1)	16(1)
C(28)	4641(2)	3464(2)	823(1)	16(1)
C(29)	4271(2)	3234(2)	57(1)	21(1)
C(30)	5448(2)	2006(2)	-359(1)	23(1)
C(31)	6145(2)	815(2)	289(1)	19(1)
C(32)	7404(2)	550(2)	552(1)	19(1)
C(33)	8267(2)	1418(2)	274(1)	24(1)
C(34)	7346(2)	2971(2)	255(1)	22(1)
Cl(1)	5896(1)	-687(1)	2247(1)	21(1)
N(1)	5070(2)	1691(2)	3620(1)	16(1)
O(1)	4135(1)	4065(1)	2599(1)	12(1)
O(2)	2774(1)	2508(1)	3105(1)	14(1)
P(1)	4404(1)	2437(1)	2749(1)	12(1)
Rh(1)	5602(1)	1536(1)	1559(1)	12(1)

Table A.2.8. Bond lengths [Å] and angles [°] for Rh(cod)Cl·**A1**.

C(1)-C(2)	1.397(2)	C(15)-C(19)	1.538(3)
C(1)-C(6)	1.407(2)	C(16)-C(17)	1.383(3)
C(1)-C(13)	1.492(2)	C(17)-C(18)	1.407(2)
C(2)-O(1)	1.3982(18)	C(17)-C(23)	1.512(3)
C(2)-C(3)	1.399(2)	C(18)-C(24)	1.503(3)
C(3)-C(4)	1.400(2)	C(19)-C(20)	1.534(3)
C(3)-C(7)	1.538(2)	C(19)-C(21)	1.536(3)
C(4)-C(5)	1.394(2)	C(19)-C(22)	1.541(3)
C(5)-C(6)	1.400(2)	C(25)-N(1)	1.457(2)
C(5)-C(11)	1.513(2)	C(26)-N(1)	1.462(2)
C(6)-C(12)	1.505(2)	C(27)-C(28)	1.409(2)
C(7)-C(10)	1.533(2)	C(27)-C(34)	1.526(2)
C(7)-C(8)	1.536(3)	C(27)-Rh(1)	2.1299(17)
C(7)-C(9)	1.540(3)	C(28)-C(29)	1.508(2)
C(13)-C(14)	1.399(2)	C(28)-Rh(1)	2.1182(17)
C(13)-C(18)	1.403(2)	C(29)-C(30)	1.534(3)
C(14)-C(15)	1.397(2)	C(30)-C(31)	1.510(3)
C(14)-O(2)	1.402(2)	C(31)-C(32)	1.369(3)
C(15)-C(16)	1.403(3)	C(31)-Rh(1)	2.2678(17)

C(32)-C(33)	1.501(3)	C(20)-C(19)-C(15)	115.06(15)
C(32)-Rh(1)	2.2432(16)	C(21)-C(19)-C(15)	109.30(17)
C(33)-C(34)	1.536(3)	C(20)-C(19)-C(22)	106.14(18)
Cl(1)-Rh(1)	2.3485(4)	C(21)-C(19)-C(22)	108.87(17)
N(1)-P(1)	1.6337(15)	C(15)-C(19)-C(22)	108.39(15)
O(1)-P(1)	1.6359(12)	C(28)-C(27)-C(34)	124.82(16)
O(2)-P(1)	1.6333(12)	C(28)-C(27)-Rh(1)	70.19(10)
P(1)-Rh(1)	2.2451(4)	C(34)-C(27)-Rh(1)	113.59(11)
		C(27)-C(28)-C(29)	126.44(15)
C(2)-C(1)-C(6)	119.67(14)	C(27)-C(28)-Rh(1)	71.09(10)
C(2)-C(1)-C(13)	119.01(14)	C(29)-C(28)-Rh(1)	109.09(11)
C(6)-C(1)-C(13)	121.25(14)	C(28)-C(29)-C(30)	113.89(15)
C(1)-C(2)-O(1)	116.60(13)	C(31)-C(30)-C(29)	111.41(15)
C(1)-C(2)-C(3)	122.91(14)	C(32)-C(31)-C(30)	124.64(17)
O(1)-C(2)-C(3)	120.33(13)	C(32)-C(31)-Rh(1)	71.35(10)
C(2)-C(3)-C(4)	114.97(14)	C(30)-C(31)-Rh(1)	110.21(11)
C(2)-C(3)-C(7)	123.15(14)	C(31)-C(32)-C(33)	125.78(17)
C(4)-C(3)-C(7)	121.56(14)	C(31)-C(32)-Rh(1)	73.31(10)
C(5)-C(4)-C(3)	123.69(15)	C(33)-C(32)-Rh(1)	107.07(11)
C(4)-C(5)-C(6)	119.50(15)	C(32)-C(33)-C(34)	113.71(15)
C(4)-C(5)-C(11)	119.57(16)	C(27)-C(34)-C(33)	113.04(15)
C(6)-C(5)-C(11)	120.88(16)	C(25)-N(1)-C(26)	115.22(14)
C(5)-C(6)-C(1)	118.45(14)	C(25)-N(1)-P(1)	123.53(12)
C(5)-C(6)-C(12)	120.17(15)	C(26)-N(1)-P(1)	121.16(12)
C(1)-C(6)-C(12)	121.37(15)	C(2)-O(1)-P(1)	122.20(10)
C(10)-C(7)-C(8)	107.65(15)	C(14)-O(2)-P(1)	117.76(10)
C(10)-C(7)-C(3)	111.50(14)	O(2)-P(1)-N(1)	97.23(7)
C(8)-C(7)-C(3)	107.96(14)	O(2)-P(1)-O(1)	101.98(6)
C(10)-C(7)-C(9)	107.42(15)	N(1)-P(1)-O(1)	109.12(7)
C(8)-C(7)-C(9)	109.48(15)	O(2)-P(1)-Rh(1)	119.26(5)
C(3)-C(7)-C(9)	112.70(14)	N(1)-P(1)-Rh(1)	118.68(5)
C(14)-C(13)-C(18)	120.09(15)	O(1)-P(1)-Rh(1)	108.89(4)
C(14)-C(13)-C(1)	119.49(14)	C(28)-Rh(1)-C(27)	38.73(7)
C(18)-C(13)-C(1)	120.42(15)	C(28)-Rh(1)-C(32)	96.83(7)
C(15)-C(14)-C(13)	122.79(15)	C(27)-Rh(1)-C(32)	81.16(7)
C(15)-C(14)-O(2)	121.46(15)	C(28)-Rh(1)-P(1)	91.19(5)
C(13)-C(14)-O(2)	115.74(14)	C(27)-Rh(1)-P(1)	95.11(5)
C(14)-C(15)-C(16)	114.22(16)	C(32)-Rh(1)-P(1)	161.50(5)
C(14)-C(15)-C(19)	127.09(17)	C(28)-Rh(1)-C(31)	80.89(7)
C(16)-C(15)-C(19)	118.68(16)	C(27)-Rh(1)-C(31)	88.00(7)
C(17)-C(16)-C(15)	124.55(16)	C(32)-Rh(1)-C(31)	35.34(7)
C(16)-C(17)-C(18)	119.32(16)	P(1)-Rh(1)-C(31)	163.15(5)
C(16)-C(17)-C(23)	120.29(17)	C(28)-Rh(1)-Cl(1)	157.29(5)
C(18)-C(17)-C(23)	120.39(18)	C(27)-Rh(1)-Cl(1)	162.92(5)
C(13)-C(18)-C(17)	117.89(16)	C(32)-Rh(1)-Cl(1)	88.04(5)
C(13)-C(18)-C(24)	121.95(16)	P(1)-Rh(1)-Cl(1)	90.953(16)
C(17)-C(18)-C(24)	120.13(16)	C(31)-Rh(1)-Cl(1)	90.81(5)
C(20)-C(19)-C(21)	108.90(17)		

Symmetry transformations used to generate equivalent atoms:

Table A.2.9. Anisotropic displacement parameters ($Å^2 x\ 10^3$)for Rh(cod)Cl·**A1**. The anisotropic displacement factor exponent takes the form: $-2\pi^2[\ h^2 a^{*2} U^{11} + ... + 2\ h\ k\ a^*\ b^*\ U^{12}\ ]$

	U^{11}	U^{22}	U^{33}	U^{23}	U^{13}	U^{12}
C(1)	12(1)	13(1)	14(1)	-3(1)	-2(1)	-5(1)
C(2)	12(1)	11(1)	11(1)	-3(1)	0(1)	-4(1)
C(3)	14(1)	13(1)	14(1)	-2(1)	-3(1)	-5(1)
C(4)	19(1)	18(1)	17(1)	-7(1)	-3(1)	-7(1)
C(5)	17(1)	18(1)	18(1)	-9(1)	2(1)	-5(1)
C(6)	12(1)	16(1)	18(1)	-5(1)	0(1)	-4(1)
C(7)	14(1)	20(1)	18(1)	-6(1)	-1(1)	-9(1)
C(8)	30(1)	29(1)	20(1)	-6(1)	2(1)	-21(1)
C(9)	15(1)	22(1)	33(1)	-7(1)	-6(1)	-5(1)
C(10)	22(1)	31(1)	25(1)	-10(1)	-4(1)	-14(1)
C(11)	23(1)	35(1)	30(1)	-22(1)	5(1)	-8(1)
C(12)	12(1)	25(1)	27(1)	-10(1)	2(1)	-5(1)
C(13)	11(1)	16(1)	14(1)	-4(1)	-1(1)	-5(1)
C(14)	10(1)	17(1)	15(1)	-5(1)	0(1)	-5(1)
C(15)	14(1)	22(1)	20(1)	-11(1)	2(1)	-8(1)
C(16)	18(1)	31(1)	21(1)	-12(1)	-3(1)	-10(1)
C(17)	13(1)	31(1)	17(1)	-5(1)	-3(1)	-6(1)
C(18)	11(1)	20(1)	18(1)	-3(1)	-2(1)	-4(1)
C(19)	16(1)	23(1)	33(1)	-16(1)	4(1)	-9(1)
C(20)	27(1)	20(1)	37(1)	-8(1)	2(1)	-13(1)
C(21)	29(1)	33(1)	37(1)	-23(1)	5(1)	-10(1)
C(22)	20(1)	31(1)	65(2)	-22(1)	1(1)	-14(1)
C(23)	21(1)	40(1)	22(1)	-4(1)	-9(1)	-8(1)
C(24)	19(1)	18(1)	25(1)	1(1)	-7(1)	-4(1)
C(25)	26(1)	28(1)	14(1)	-2(1)	-1(1)	-6(1)
C(26)	16(1)	23(1)	21(1)	0(1)	-4(1)	-4(1)
C(27)	19(1)	12(1)	16(1)	-3(1)	1(1)	-7(1)
C(28)	18(1)	13(1)	15(1)	-2(1)	-2(1)	-3(1)
C(29)	24(1)	19(1)	18(1)	-2(1)	-7(1)	-4(1)
C(30)	32(1)	20(1)	17(1)	-5(1)	-5(1)	-8(1)
C(31)	27(1)	15(1)	15(1)	-7(1)	-1(1)	-7(1)
C(32)	20(1)	14(1)	18(1)	-5(1)	3(1)	-3(1)
C(33)	18(1)	20(1)	26(1)	-4(1)	6(1)	-5(1)
C(34)	20(1)	20(1)	23(1)	-4(1)	5(1)	-9(1)
Cl(1)	22(1)	12(1)	25(1)	-1(1)	2(1)	-6(1)
N(1)	14(1)	16(1)	13(1)	-1(1)	-2(1)	-4(1)
O(1)	12(1)	12(1)	13(1)	-4(1)	1(1)	-4(1)
O(2)	11(1)	14(1)	16(1)	-2(1)	0(1)	-5(1)
P(1)	11(1)	11(1)	12(1)	-3(1)	0(1)	-4(1)
Rh(1)	12(1)	10(1)	13(1)	-3(1)	0(1)	-3(1)

Table A.2.10. Hydrogen coordinates (x 10^4) and isotropic displacement parameters (Å^{2}x 10^3) for Rh(cod)Cl·**A1**.

	x	y	z	U(eq)
H(4)	2976	6842	4478	21
H(8A)	6423	6144	2266	36
H(8B)	4777	7115	2353	36
H(8C)	5319	5656	2083	36
H(9A)	6231	3656	4051	35
H(9B)	7348	4109	3385	35
H(9C)	6396	3545	3100	35
H(10A)	5377	6035	4462	35
H(10B)	4779	7347	3804	35
H(10C)	6433	6403	3700	35
H(11A)	739	7761	5279	44
H(11B)	-220	6923	5427	44
H(11C)	-528	8260	4765	44
H(12A)	-977	5748	3683	33
H(12B)	-1408	7260	3834	33
H(12C)	-1141	6061	4591	33
H(16)	-247	3567	1328	26
H(20A)	1942	-481	3073	41
H(20B)	1504	796	3527	41
H(20C)	2983	272	2926	41
H(21A)	1661	1339	995	49
H(21B)	2216	-150	1498	49
H(21C)	3086	765	1378	49
H(22A)	-726	1885	1947	54
H(22B)	-793	1690	2922	54
H(22C)	-138	398	2450	54
H(23A)	-1369	5738	620	43
H(23B)	-513	6671	483	43
H(23C)	-1905	6933	1161	43
H(24A)	527	7429	2302	34
H(24B)	-1049	7738	2203	34
H(24C)	140	7640	1406	34
H(25A)	3942	1106	4667	38
H(25B)	3365	2711	4419	38
H(25C)	4777	1913	4823	38
H(26A)	7027	984	3940	33
H(26B)	7074	721	3038	33
H(26C)	6619	-191	3831	33
H(29A)	4094	4061	-352	26
H(29B)	3384	3087	216	26
H(30A)	5027	1709	-702	28
H(30B)	6177	2291	-724	28
H(33A)	8802	1246	-283	28
H(33B)	8961	1138	652	28

H(34A)	7932	3417	329	26
H(34B)	7044	3349	-292	26
H(32)	7840(20)	-300(20)	836(13)	14(5)
H(28)	3810(20)	4010(20)	1165(14)	17(5)
H(27)	6040(20)	3770(20)	1363(14)	19(5)
H(31)	5750(30)	180(30)	435(16)	29(6)

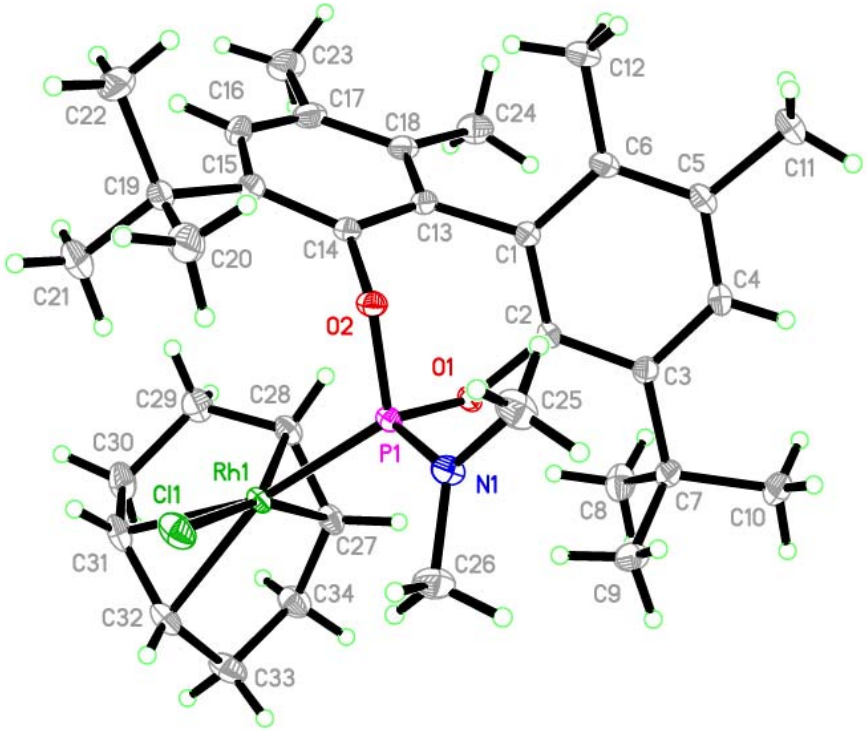

Table A.2.11. Crystal data and structure refinement for Rh(cod)Cl·**T2** (1).

Identification code	rovis81	
Empirical formula	$C_{45}H_{52}Cl_5NO_4PRh$	
Formula weight	982.01	
Temperature	120(2) K	
Wavelength	0.71073 Å	
Crystal system	Monoclinic	
Space group	$P2_1$	
Unit cell dimensions	a = 10.8926(7) Å	α= 90°.
	b = 18.1189(11) Å	β= 91.835(3)°.
	c = 11.2230(7) Å	γ = 90°.
Volume	2213.9(2) $Å^3$	
Z	2	
Density (calculated)	1.473 Mg/m^3	
Absorption coefficient	0.767 mm^{-1}	
F(000)	1012	
Crystal size	0.32 x 0.30 x 0.26 mm^3	
Theta range for data collection	2.14 to 35.63°.	
Index ranges	-17<=h<=17, -29<=k<=29, -18<=l<=17	
Reflections collected	77157	
Independent reflections	20295 [R(int) = 0.0257]	
Completeness to theta = 35.63°	100.0 %	
Absorption correction	Semi-empirical from equivalents	
Max. and min. transmission	0.8249 and 0.7898	
Refinement method	Full-matrix least-squares on F^2	
Data / restraints / parameters	20295 / 1 / 517	
Goodness-of-fit on F^2	1.020	
Final R indices [I>2sigma(I)]	R1 = 0.0232, wR2 = 0.0575	
R indices (all data)	R1 = 0.0246, wR2 = 0.0582	
Absolute structure parameter	-0.017(8)	
Largest diff. peak and hole	1.091 and -0.978 e.$Å^{-3}$	

Table A.2.12. Atomic coordinates (x 10^4) and equivalent isotropic displacement parameters ($Å^2$x 10^3) for Rh(cod)Cl·**T2** (1). U(eq) is defined as one third of the trace of the orthogonalized U^{ij} tensor.

	x	y	z	U(eq)
C(1)	-688(1)	709(1)	7937(1)	13(1)
C(2)	-1052(1)	547(1)	6607(1)	14(1)
C(3)	-697(1)	-229(1)	6211(1)	13(1)
C(4)	541(1)	-228(1)	5541(1)	12(1)
C(5)	-2683(1)	64(1)	5503(1)	17(1)
C(6)	-2777(1)	458(1)	4309(1)	21(1)
C(7)	-3867(1)	-315(1)	5834(1)	27(1)
C(8)	348(1)	44(1)	4262(1)	13(1)
C(9)	-213(1)	-429(1)	3421(1)	17(1)
C(10)	-484(1)	-187(1)	2272(1)	21(1)
C(11)	-179(1)	526(1)	1926(1)	24(1)

C(12)	416(1)	990(1)	2737(1)	22(1)
C(13)	674(1)	752(1)	3905(1)	16(1)
C(14)	1168(1)	-978(1)	5536(1)	13(1)
C(15)	534(1)	-1632(1)	5753(1)	19(1)
C(16)	1139(1)	-2312(1)	5707(1)	24(1)
C(17)	2373(1)	-2343(1)	5436(1)	24(1)
C(18)	3007(1)	-1692(1)	5198(1)	21(1)
C(19)	2408(1)	-1017(1)	5240(1)	16(1)
C(20)	-518(1)	1527(1)	8181(1)	15(1)
C(21)	-1110(1)	2061(1)	7475(1)	19(1)
C(22)	-1039(1)	2806(1)	7778(1)	25(1)
C(23)	-371(1)	3025(1)	8793(1)	28(1)
C(24)	244(1)	2499(1)	9491(1)	26(1)
C(25)	178(1)	1753(1)	9187(1)	19(1)
C(26)	-1638(1)	378(1)	8768(1)	15(1)
C(27)	-1592(1)	-365(1)	9092(1)	19(1)
C(28)	-2481(1)	-667(1)	9816(1)	24(1)
C(29)	-3415(1)	-229(1)	10237(1)	28(1)
C(30)	-3469(1)	512(1)	9928(1)	30(1)
C(31)	-2589(1)	817(1)	9192(1)	23(1)
C(32)	1754(1)	-987(1)	8671(1)	19(1)
C(33)	2784(1)	-1552(1)	8873(1)	25(1)
C(34)	3942(1)	-1072(1)	8945(1)	24(1)
C(35)	3694(1)	-502(1)	7975(1)	18(1)
C(36)	3278(1)	1549(1)	6034(1)	15(1)
C(37)	2212(1)	1947(1)	6320(1)	15(1)
C(38)	2140(1)	2771(1)	6521(1)	20(1)
C(39)	3218(1)	3082(1)	7284(1)	22(1)
C(40)	3669(1)	2544(1)	8237(1)	19(1)
C(41)	4626(1)	2057(1)	8100(1)	19(1)
C(42)	5339(1)	1941(1)	6985(1)	22(1)
C(43)	4523(1)	1910(1)	5841(1)	20(1)
C(44)	6900(1)	4752(1)	7696(1)	26(1)
C(45)	6690(2)	7107(1)	7423(2)	40(1)
Cl(1)	3102(1)	1038(1)	9901(1)	20(1)
Cl(2)	5966(1)	5338(1)	6807(1)	46(1)
Cl(3)	6182(1)	3878(1)	7841(1)	35(1)
Cl(4)	5091(1)	7280(1)	7392(1)	58(1)
Cl(5)	7570(1)	7914(1)	7400(1)	78(1)
N(1)	2348(1)	-391(1)	8009(1)	14(1)
O(1)	445(1)	305(1)	8221(1)	13(1)
O(2)	1332(1)	314(1)	6140(1)	12(1)
O(3)	-1714(1)	-479(1)	5494(1)	16(1)
O(4)	-2352(1)	567(1)	6438(1)	19(1)
P(1)	1729(1)	384(1)	7545(1)	11(1)
Rh(1)	2890(1)	1400(1)	7862(1)	12(1)

Table A.2.13. Bond lengths [Å] and angles [°] for Rh(cod)Cl·**T2** (1).

C(1)-O(1)	1.4606(13)	C(38)-C(39)	1.5384(18)
C(1)-C(20)	1.5187(15)	C(39)-C(40)	1.5171(18)
C(1)-C(26)	1.5373(15)	C(40)-C(41)	1.3780(18)
C(1)-C(2)	1.5595(15)	C(40)-Rh(1)	2.2749(12)
C(2)-O(4)	1.4229(13)	C(41)-C(42)	1.5088(19)
C(2)-C(3)	1.5290(16)	C(41)-Rh(1)	2.2439(11)
C(3)-O(3)	1.4212(13)	C(42)-C(43)	1.5389(19)
C(3)-C(4)	1.5656(14)	C(44)-Cl(2)	1.7589(16)
C(4)-O(2)	1.4570(12)	C(44)-Cl(3)	1.7755(16)
C(4)-C(14)	1.5212(15)	C(45)-Cl(5)	1.749(2)
C(4)-C(8)	1.5260(14)	C(45)-Cl(4)	1.769(2)
C(5)-O(4)	1.4275(15)	Cl(1)-Rh(1)	2.3842(3)
C(5)-O(3)	1.4429(15)	N(1)-P(1)	1.6353(10)
C(5)-C(7)	1.5173(17)	O(1)-P(1)	1.6185(8)
C(5)-C(6)	1.5188(18)	O(2)-P(1)	1.6263(8)
C(8)-C(13)	1.3939(16)	P(1)-Rh(1)	2.2547(3)
C(8)-C(9)	1.4002(15)		
C(9)-C(10)	1.3847(17)	O(1)-C(1)-C(20)	110.62(8)
C(10)-C(11)	1.393(2)	O(1)-C(1)-C(26)	104.67(8)
C(11)-C(12)	1.3846(19)	C(20)-C(1)-C(26)	110.60(9)
C(12)-C(13)	1.3989(16)	O(1)-C(1)-C(2)	107.60(8)
C(14)-C(15)	1.3961(16)	C(20)-C(1)-C(2)	112.42(9)
C(14)-C(19)	1.4031(15)	C(26)-C(1)-C(2)	110.62(9)
C(15)-C(16)	1.4003(18)	O(4)-C(2)-C(3)	104.10(9)
C(16)-C(17)	1.389(2)	O(4)-C(2)-C(1)	110.14(9)
C(17)-C(18)	1.396(2)	C(3)-C(2)-C(1)	113.08(9)
C(18)-C(19)	1.3878(17)	O(3)-C(3)-C(2)	104.92(8)
C(20)-C(21)	1.3948(16)	O(3)-C(3)-C(4)	113.34(9)
C(20)-C(25)	1.4006(16)	C(2)-C(3)-C(4)	111.53(8)
C(21)-C(22)	1.3942(18)	O(2)-C(4)-C(14)	110.20(8)
C(22)-C(23)	1.390(2)	O(2)-C(4)-C(8)	106.17(8)
C(23)-C(24)	1.391(2)	C(14)-C(4)-C(8)	109.46(8)
C(24)-C(25)	1.3954(19)	O(2)-C(4)-C(3)	106.61(8)
C(26)-C(27)	1.3948(17)	C(14)-C(4)-C(3)	113.16(8)
C(26)-C(31)	1.3999(17)	C(8)-C(4)-C(3)	110.97(8)
C(27)-C(28)	1.3960(17)	O(4)-C(5)-O(3)	105.77(9)
C(28)-C(29)	1.385(2)	O(4)-C(5)-C(7)	107.79(10)
C(29)-C(30)	1.386(2)	O(3)-C(5)-C(7)	108.72(10)
C(30)-C(31)	1.3994(19)	O(4)-C(5)-C(6)	110.93(10)
C(32)-N(1)	1.4725(15)	O(3)-C(5)-C(6)	110.08(10)
C(32)-C(33)	1.5303(18)	C(7)-C(5)-C(6)	113.25(10)
C(33)-C(34)	1.532(2)	C(13)-C(8)-C(9)	118.68(10)
C(34)-C(35)	1.5176(18)	C(13)-C(8)-C(4)	122.59(9)
C(35)-N(1)	1.4825(14)	C(9)-C(8)-C(4)	118.71(9)
C(36)-C(37)	1.4130(16)	C(10)-C(9)-C(8)	120.60(11)
C(36)-C(43)	1.5272(16)	C(9)-C(10)-C(11)	120.51(11)
C(36)-Rh(1)	2.1254(11)	C(12)-C(11)-C(10)	119.37(11)
C(37)-C(38)	1.5127(17)	C(11)-C(12)-C(13)	120.35(12)
C(37)-Rh(1)	2.1071(11)	C(8)-C(13)-C(12)	120.43(11)

C(15)-C(14)-C(19)	118.87(10)	C(41)-C(40)-Rh(1)	71.02(7)
C(15)-C(14)-C(4)	122.23(9)	C(39)-C(40)-Rh(1)	110.18(8)
C(19)-C(14)-C(4)	118.81(9)	C(40)-C(41)-C(42)	126.37(12)
C(14)-C(15)-C(16)	120.35(11)	C(40)-C(41)-Rh(1)	73.48(7)
C(17)-C(16)-C(15)	120.21(12)	C(42)-C(41)-Rh(1)	106.32(8)
C(16)-C(17)-C(18)	119.75(12)	C(41)-C(42)-C(43)	113.47(10)
C(19)-C(18)-C(17)	120.10(12)	C(36)-C(43)-C(42)	112.91(10)
C(18)-C(19)-C(14)	120.70(11)	Cl(2)-C(44)-Cl(3)	110.00(8)
C(21)-C(20)-C(25)	118.97(11)	Cl(5)-C(45)-Cl(4)	113.08(11)
C(21)-C(20)-C(1)	121.53(10)	C(32)-N(1)-C(35)	111.37(9)
C(25)-C(20)-C(1)	119.33(10)	C(32)-N(1)-P(1)	127.39(8)
C(22)-C(21)-C(20)	120.79(12)	C(35)-N(1)-P(1)	120.44(8)
C(23)-C(22)-C(21)	119.95(13)	C(1)-O(1)-P(1)	126.14(7)
C(22)-C(23)-C(24)	119.73(12)	C(4)-O(2)-P(1)	129.39(7)
C(23)-C(24)-C(25)	120.40(13)	C(3)-O(3)-C(5)	109.68(9)
C(24)-C(25)-C(20)	120.12(12)	C(2)-O(4)-C(5)	108.01(8)
C(27)-C(26)-C(31)	118.70(11)	O(1)-P(1)-O(2)	103.96(4)
C(27)-C(26)-C(1)	120.95(10)	O(1)-P(1)-N(1)	97.37(4)
C(31)-C(26)-C(1)	120.33(11)	O(2)-P(1)-N(1)	109.63(5)
C(26)-C(27)-C(28)	120.66(12)	O(1)-P(1)-Rh(1)	119.13(3)
C(29)-C(28)-C(27)	120.29(13)	O(2)-P(1)-Rh(1)	110.27(3)
C(28)-C(29)-C(30)	119.69(12)	N(1)-P(1)-Rh(1)	115.29(4)
C(29)-C(30)-C(31)	120.35(13)	C(37)-Rh(1)-C(36)	39.00(4)
C(30)-C(31)-C(26)	120.29(13)	C(37)-Rh(1)-C(41)	96.89(4)
N(1)-C(32)-C(33)	103.48(10)	C(36)-Rh(1)-C(41)	81.65(4)
C(32)-C(33)-C(34)	103.12(10)	C(37)-Rh(1)-P(1)	94.27(3)
C(35)-C(34)-C(33)	102.80(10)	C(36)-Rh(1)-P(1)	94.54(3)
N(1)-C(35)-C(34)	103.12(10)	C(41)-Rh(1)-P(1)	156.70(3)
C(37)-C(36)-C(43)	123.58(10)	C(37)-Rh(1)-C(40)	80.89(4)
C(37)-C(36)-Rh(1)	69.80(6)	C(36)-Rh(1)-C(40)	88.75(4)
C(43)-C(36)-Rh(1)	113.32(8)	C(41)-Rh(1)-C(40)	35.50(5)
C(36)-C(37)-C(38)	125.81(10)	P(1)-Rh(1)-C(40)	167.77(3)
C(36)-C(37)-Rh(1)	71.20(6)	C(37)-Rh(1)-Cl(1)	159.72(3)
C(38)-C(37)-Rh(1)	111.17(8)	C(36)-Rh(1)-Cl(1)	160.95(3)
C(37)-C(38)-C(39)	113.72(10)	C(41)-Rh(1)-Cl(1)	88.66(3)
C(40)-C(39)-C(38)	112.42(10)	P(1)-Rh(1)-Cl(1)	87.891(11)
C(41)-C(40)-C(39)	124.24(12)	C(40)-Rh(1)-Cl(1)	92.84(3)

Symmetry transformations used to generate equivalent atoms:

Table A.2.14. Anisotropic displacement parameters ($Å^2 x\ 10^3$) for Rh(cod)Cl·**T2** (1). The anisotropic displacement factor exponent takes the form: $-2\pi^2[\ h^2\ a^{*2}U^{11} + ...\ + 2\ h\ k\ a^*\ b^*\ U^{12}\ ]$

	U^{11}	U^{22}	U^{33}	U^{23}	U^{13}	U^{12}
C(1)	11(1)	15(1)	12(1)	1(1)	1(1)	1(1)
C(2)	12(1)	16(1)	13(1)	0(1)	0(1)	1(1)
C(3)	11(1)	15(1)	13(1)	0(1)	0(1)	-2(1)
C(4)	11(1)	12(1)	12(1)	0(1)	0(1)	-2(1)
C(5)	11(1)	22(1)	18(1)	0(1)	-1(1)	0(1)

C(6)	18(1)	27(1)	18(1)	0(1)	-3(1)	2(1)
C(7)	12(1)	35(1)	33(1)	5(1)	2(1)	-4(1)
C(8)	12(1)	14(1)	11(1)	0(1)	0(1)	0(1)
C(9)	18(1)	18(1)	14(1)	-1(1)	-2(1)	-2(1)
C(10)	22(1)	26(1)	15(1)	-3(1)	-4(1)	-1(1)
C(11)	27(1)	29(1)	14(1)	3(1)	-4(1)	-1(1)
C(12)	26(1)	22(1)	16(1)	6(1)	-2(1)	-3(1)
C(13)	18(1)	17(1)	13(1)	2(1)	-1(1)	-2(1)
C(14)	14(1)	12(1)	13(1)	0(1)	-1(1)	0(1)
C(15)	20(1)	14(1)	24(1)	0(1)	1(1)	-2(1)
C(16)	30(1)	13(1)	30(1)	0(1)	1(1)	0(1)
C(17)	30(1)	16(1)	27(1)	-2(1)	-3(1)	7(1)
C(18)	19(1)	22(1)	22(1)	-3(1)	0(1)	6(1)
C(19)	15(1)	17(1)	18(1)	-1(1)	2(1)	2(1)
C(20)	14(1)	16(1)	16(1)	0(1)	3(1)	0(1)
C(21)	19(1)	17(1)	21(1)	2(1)	2(1)	4(1)
C(22)	26(1)	16(1)	34(1)	2(1)	9(1)	5(1)
C(23)	33(1)	17(1)	34(1)	-7(1)	12(1)	-1(1)
C(24)	29(1)	24(1)	25(1)	-9(1)	6(1)	-5(1)
C(25)	20(1)	20(1)	17(1)	-3(1)	2(1)	-2(1)
C(26)	12(1)	21(1)	12(1)	2(1)	1(1)	-2(1)
C(27)	20(1)	21(1)	15(1)	1(1)	2(1)	-6(1)
C(28)	23(1)	30(1)	18(1)	5(1)	1(1)	-11(1)
C(29)	14(1)	48(1)	21(1)	10(1)	1(1)	-8(1)
C(30)	15(1)	47(1)	27(1)	12(1)	7(1)	5(1)
C(31)	15(1)	32(1)	21(1)	7(1)	5(1)	5(1)
C(32)	18(1)	17(1)	23(1)	7(1)	2(1)	0(1)
C(33)	23(1)	18(1)	34(1)	9(1)	-1(1)	4(1)
C(34)	20(1)	24(1)	27(1)	4(1)	-6(1)	4(1)
C(35)	12(1)	21(1)	20(1)	1(1)	0(1)	3(1)
C(36)	16(1)	16(1)	14(1)	0(1)	2(1)	-2(1)
C(37)	16(1)	15(1)	14(1)	1(1)	-1(1)	0(1)
C(38)	18(1)	16(1)	24(1)	2(1)	-1(1)	2(1)
C(39)	24(1)	14(1)	27(1)	-1(1)	-1(1)	-1(1)
C(40)	20(1)	15(1)	21(1)	-4(1)	-2(1)	-3(1)
C(41)	15(1)	18(1)	24(1)	0(1)	-4(1)	-4(1)
C(42)	13(1)	24(1)	30(1)	0(1)	2(1)	-2(1)
C(43)	18(1)	21(1)	23(1)	0(1)	6(1)	-3(1)
C(44)	20(1)	32(1)	27(1)	-5(1)	-2(1)	0(1)
C(45)	41(1)	33(1)	47(1)	6(1)	0(1)	5(1)
Cl(1)	22(1)	25(1)	13(1)	1(1)	-2(1)	-1(1)
Cl(2)	44(1)	46(1)	47(1)	-1(1)	-12(1)	16(1)
Cl(3)	35(1)	35(1)	36(1)	-12(1)	11(1)	-8(1)
Cl(4)	40(1)	77(1)	58(1)	-25(1)	-6(1)	24(1)
Cl(5)	83(1)	40(1)	110(1)	18(1)	11(1)	-15(1)
N(1)	11(1)	16(1)	16(1)	4(1)	2(1)	1(1)
O(1)	10(1)	16(1)	13(1)	2(1)	1(1)	0(1)
O(2)	12(1)	13(1)	11(1)	0(1)	0(1)	-2(1)
O(3)	11(1)	18(1)	20(1)	-2(1)	-2(1)	-2(1)
O(4)	12(1)	27(1)	17(1)	-3(1)	-2(1)	4(1)
P(1)	10(1)	12(1)	11(1)	1(1)	0(1)	-1(1)

Rh(1)	12(1)	13(1)	12(1)	0(1)	-1(1)	-2(1)

Table A.2.15. Hydrogen coordinates (x 10^4) and isotropic displacement parameters ($Å^2$x 10^3) for Rh(cod)Cl·**T2** (1).

	x	y	z	U(eq)
H(2)	-667	922	6082	16
H(3)	-607	-553	6930	15
H(6A)	-3482	794	4298	31
H(6B)	-2885	94	3669	31
H(6C)	-2024	741	4189	31
H(7A)	-3747	-563	6605	40
H(7B)	-4096	-680	5221	40
H(7C)	-4522	53	5888	40
H(9)	-409	-920	3641	20
H(10)	-882	-510	1716	25
H(11)	-378	693	1141	28
H(12)	651	1471	2500	26
H(13)	1074	1076	4458	19
H(15)	-311	-1614	5934	23
H(16)	704	-2755	5862	29
H(17)	2784	-2805	5411	29
H(18)	3850	-1712	5007	25
H(19)	2842	-578	5067	20
H(21)	-1568	1914	6780	23
H(22)	-1447	3165	7290	30
H(23)	-335	3531	9011	33
H(24)	712	2649	10177	31
H(25)	605	1397	9664	22
H(27)	-948	-668	8817	22
H(28)	-2446	-1175	10021	29
H(29)	-4015	-434	10735	33
H(30)	-4108	813	10217	35
H(31)	-2636	1323	8978	27
H(32A)	1060	-1203	8198	23
H(32B)	1448	-805	9438	23
H(33A)	2813	-1905	8202	30
H(33B)	2679	-1828	9624	30
H(34A)	4044	-835	9737	29
H(34B)	4685	-1365	8783	29
H(35A)	4142	-37	8150	21
H(35B)	3935	-690	7187	21
H(36)	3114	1103	5527	18
H(37)	1436	1729	5976	18
H(38A)	1362	2886	6916	24
H(38B)	2117	3023	5737	24
H(39A)	3904	3204	6760	26

H(39B)	2955	3545	7670	26
H(40)	3570	2720	9073	23
H(41)	5103	1947	8856	23
H(42A)	5806	1473	7062	27
H(42B)	5940	2347	6912	27
H(43A)	4389	2418	5540	25
H(43B)	4957	1630	5225	25
H(44A)	7041	4975	8494	32
H(44B)	7707	4690	7326	32
H(45A)	6914	6824	8152	49
H(45B)	6889	6799	6727	49

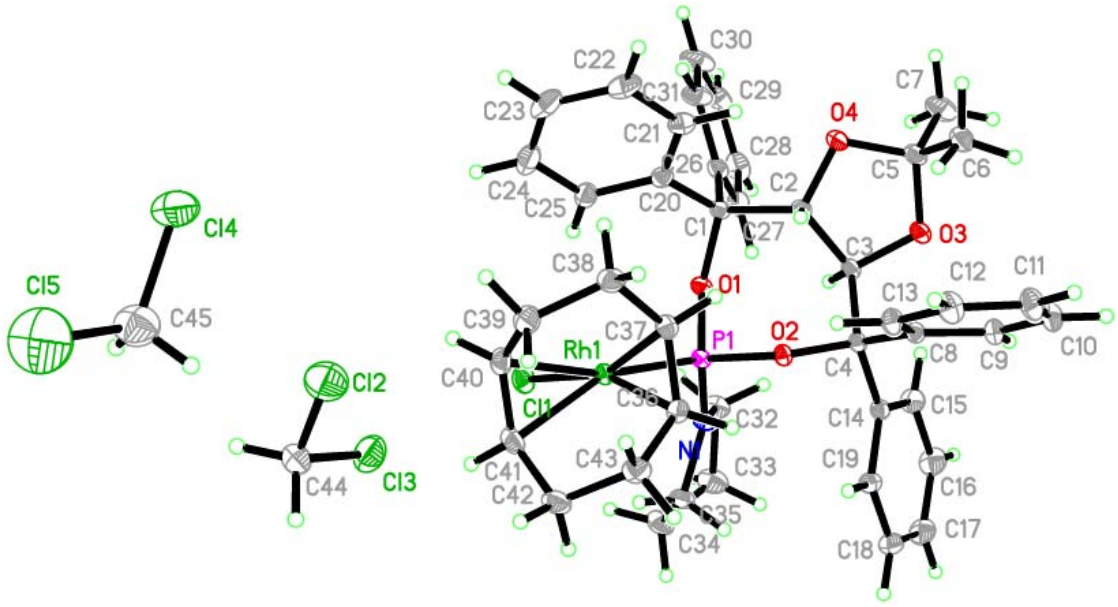

Table A.2.16. Crystal data and structure refinement for Rh(cod)Cl·**T2** (2).

Identification code	rovis49_0m	
Empirical formula	$C_{93}H_{112}Cl_2N_2O_8P_2Rh_2$	
Formula weight	1724.51	
Temperature	296(2) K	
Wavelength	0.71073 Å	
Crystal system	Monoclinic	
Space group	$P\ 2_1$	
Unit cell dimensions	a = 12.9291(3) Å	α= 90°.
	b = 10.9044(3) Å	β= 91.6130(10)°.
	c = 29.3915(7) Å	γ = 90°.
Volume	4142.09(18) $Å^3$	
Z	2	
Density (calculated)	1.383 Mg/m^3	
Absorption coefficient	0.560 mm^{-1}	
F(000)	1804	
Crystal size	0.40 x 0.08 x 0.05 mm^3	
Theta range for data collection	1.99 to 32.58°.	
Index ranges	-19<=h<=19, -13<=k<=16, -44<=l<=44	
Reflections collected	63557	
Independent reflections	25952 [R(int) = 0.0844]	
Completeness to theta = 32.58°	100.0 %	
Absorption correction	Semi-empirical from equivalents	
Max. and min. transmission	0.9731 and 0.8062	
Refinement method	Full-matrix least-squares on F^2	
Data / restraints / parameters	25952 / 1 / 989	
Goodness-of-fit on F^2	0.965	
Final R indices [I>2sigma(I)]	R1 = 0.0573, wR2 = 0.0972	
R indices (all data)	R1 = 0.1048, wR2 = 0.1205	
Absolute structure parameter	-0.04(2)	
Largest diff. peak and hole	0.847 and -0.834 e.$Å^{-3}$	

Table A.2.17. Atomic coordinates (x 10^4) and equivalent isotropic displacement parameters ($Å^2$x 10^3) for Rh(cod)Cl·**T2** (2). U(eq) is defined as one third of the trace of the orthogonalized U^{ij} tensor.

	x	y	z	U(eq)
C(1)	2659(4)	12878(3)	1905(2)	24(1)
C(2)	2859(4)	13037(4)	2413(2)	27(1)
C(3)	3501(4)	11915(4)	2535(2)	30(1)
C(4)	2995(4)	10897(4)	2249(1)	19(1)
C(5)	3329(3)	9888(3)	966(1)	16(1)
C(6)	3043(3)	8637(3)	1181(2)	16(1)
C(7)	1932(3)	8263(3)	1064(2)	17(1)
C(8)	1186(3)	8542(3)	1458(1)	16(1)
C(9)	3026(3)	6646(3)	891(2)	19(1)
C(10)	3136(4)	6424(4)	382(2)	31(1)
C(11)	3301(4)	5542(4)	1173(2)	34(1)

C(12)	3529(4)	9800(3)	460(2)	18(1)
C(13)	4451(4)	9288(4)	321(2)	25(1)
C(14)	4686(4)	9246(4)	-137(2)	28(1)
C(15)	4014(5)	9739(5)	-458(2)	34(1)
C(16)	3093(4)	10236(4)	-326(2)	30(1)
C(17)	2852(4)	10258(4)	131(2)	23(1)
C(18)	4263(3)	10502(3)	1205(1)	18(1)
C(19)	4887(4)	9891(4)	1513(2)	24(1)
C(20)	5758(4)	10449(4)	1708(2)	29(1)
C(21)	6011(4)	11623(4)	1585(2)	28(1)
C(22)	5393(4)	12239(5)	1271(2)	41(1)
C(23)	4521(4)	11688(4)	1085(2)	33(1)
C(24)	65(3)	8679(3)	1284(1)	17(1)
C(25)	-625(4)	9376(4)	1533(2)	22(1)
C(26)	-1644(4)	9464(4)	1387(2)	29(1)
C(27)	-2005(4)	8852(4)	1001(2)	30(1)
C(28)	-1325(4)	8153(4)	757(2)	27(1)
C(29)	-281(4)	8066(4)	895(2)	21(1)
C(30)	1295(3)	7581(3)	1837(1)	16(1)
C(31)	2075(3)	7665(3)	2176(2)	19(1)
C(32)	2180(4)	6794(4)	2513(1)	22(1)
C(33)	1504(4)	5801(4)	2521(2)	24(1)
C(34)	743(4)	5691(4)	2193(2)	26(1)
C(35)	640(4)	6573(3)	1852(2)	21(1)
C(36)	-1179(4)	12926(4)	1068(2)	27(1)
C(37)	-524(4)	13883(4)	1143(2)	27(1)
C(38)	12(5)	14634(4)	786(2)	38(1)
C(39)	532(4)	13873(4)	431(2)	37(1)
C(40)	909(4)	12636(4)	601(2)	24(1)
C(41)	298(4)	11581(4)	579(2)	21(1)
C(42)	-798(4)	11519(4)	400(2)	30(1)
C(43)	-1519(4)	12488(4)	594(2)	36(1)
C(44)	7844(4)	9681(4)	2627(2)	20(1)
C(45)	7546(4)	11022(4)	2665(2)	25(1)
C(46)	7921(4)	11351(4)	3146(2)	26(1)
C(47)	7621(4)	10222(3)	3417(2)	22(1)
C(48)	6810(3)	6908(4)	3998(1)	19(1)
C(49)	7912(3)	6376(4)	4099(1)	17(1)
C(50)	8762(3)	7323(4)	4062(1)	18(1)
C(51)	9299(3)	7223(4)	3599(1)	16(1)
C(52)	8956(4)	6323(4)	4758(2)	26(1)
C(53)	9626(4)	5209(5)	4861(2)	41(2)
C(54)	8712(4)	7083(6)	5174(2)	42(1)
C(55)	6418(4)	7556(4)	4420(2)	21(1)
C(56)	5940(3)	6890(4)	4756(2)	27(1)
C(57)	5646(4)	7466(5)	5158(2)	32(1)
C(58)	5816(4)	8702(5)	5221(2)	34(1)
C(59)	6272(4)	9381(4)	4886(2)	29(1)
C(60)	6579(4)	8797(4)	4485(2)	23(1)
C(61)	6056(3)	5928(4)	3818(1)	18(1)
C(62)	6248(4)	4684(4)	3875(2)	24(1)

C(63)	5544(4)	3817(4)	3714(2)	28(1)
C(64)	4632(4)	4192(5)	3504(2)	35(1)
C(65)	4431(4)	5424(5)	3452(2)	36(1)
C(66)	5139(4)	6293(4)	3605(2)	29(1)
C(67)	9883(3)	8386(3)	3467(1)	14(1)
C(68)	10127(4)	9299(4)	3783(2)	22(1)
C(69)	10644(4)	10349(4)	3646(2)	24(1)
C(70)	10893(4)	10507(4)	3200(2)	24(1)
C(71)	10678(4)	9595(4)	2887(2)	22(1)
C(72)	10178(4)	8539(3)	3022(1)	19(1)
C(73)	10004(4)	6098(4)	3590(1)	16(1)
C(74)	10984(4)	6155(4)	3794(2)	24(1)
C(75)	11618(4)	5113(4)	3822(2)	28(1)
C(76)	11275(4)	4016(4)	3640(2)	28(1)
C(77)	10310(4)	3957(4)	3425(2)	31(1)
C(78)	9676(4)	4991(4)	3399(2)	23(1)
C(79)	7248(4)	5211(4)	2589(2)	27(1)
C(80)	7780(4)	6061(4)	2325(2)	25(1)
C(81)	7754(4)	6140(5)	1815(2)	36(1)
C(82)	6671(4)	5980(4)	1599(2)	33(1)
C(83)	5835(4)	6505(4)	1887(2)	25(1)
C(84)	5290(4)	5842(4)	2187(2)	29(1)
C(85)	5458(4)	4507(4)	2305(2)	33(1)
C(86)	6592(4)	4173(4)	2383(2)	31(1)
C(87)	4486(5)	10502(6)	3672(2)	49(2)
C(88)	3696(5)	9538(5)	3770(2)	43(2)
C(89)	3598(5)	9317(5)	4279(2)	40(1)
C(90)	2819(4)	8337(5)	4411(2)	38(1)
C(91)	2744(4)	8134(4)	4917(2)	37(1)
C(92)	1935(4)	7221(5)	5050(2)	40(1)
C(93)	1877(4)	7071(6)	5567(2)	47(1)
Cl(1)	-5(1)	12266(1)	2045(1)	25(1)
Cl(2)	5210(1)	8484(1)	2682(1)	25(1)
N(1)	2529(3)	11551(3)	1854(1)	20(1)
N(2)	7676(3)	9210(3)	3089(1)	17(1)
O(1)	2420(2)	10672(2)	1006(1)	15(1)
O(2)	1540(2)	9680(2)	1682(1)	15(1)
O(3)	3664(2)	7663(2)	1019(1)	21(1)
O(4)	1979(2)	6986(3)	984(1)	21(1)
O(5)	8471(2)	7003(3)	3260(1)	17(1)
O(6)	6905(2)	7875(2)	3657(1)	18(1)
O(7)	9459(2)	7057(3)	4431(1)	22(1)
O(8)	8003(2)	5914(3)	4548(1)	24(1)
P(1)	1755(1)	10994(1)	1452(1)	15(1)
P(2)	7407(1)	7760(1)	3164(1)	14(1)
Rh(1)	384(1)	12181(1)	1259(1)	18(1)
Rh(2)	6461(1)	6916(1)	2590(1)	16(1)

Table A.2.18. Bond lengths [Å] and angles [°] for Rh(cod)Cl·**T2** (2).

C(1)-N(1)	1.464(5)	C(38)-C(39)	1.507(7)
C(1)-C(2)	1.517(6)	C(39)-C(40)	1.514(6)
C(2)-C(3)	1.517(6)	C(40)-C(41)	1.396(6)
C(3)-C(4)	1.529(6)	C(40)-Rh(1)	2.128(5)
C(4)-N(1)	1.476(5)	C(41)-C(42)	1.498(7)
C(5)-O(1)	1.461(5)	C(41)-Rh(1)	2.105(4)
C(5)-C(12)	1.518(6)	C(42)-C(43)	1.530(6)
C(5)-C(18)	1.534(6)	C(44)-N(2)	1.472(5)
C(5)-C(6)	1.553(5)	C(44)-C(45)	1.517(5)
C(6)-O(3)	1.422(5)	C(45)-C(46)	1.525(6)
C(6)-C(7)	1.523(6)	C(46)-C(47)	1.523(6)
C(7)-O(4)	1.414(5)	C(47)-N(2)	1.469(5)
C(7)-C(8)	1.559(6)	C(48)-O(6)	1.463(5)
C(8)-O(2)	1.471(4)	C(48)-C(55)	1.527(6)
C(8)-C(24)	1.532(6)	C(48)-C(61)	1.530(6)
C(8)-C(30)	1.533(5)	C(48)-C(49)	1.559(6)
C(9)-O(3)	1.426(5)	C(49)-O(8)	1.416(5)
C(9)-O(4)	1.437(5)	C(49)-C(50)	1.514(6)
C(9)-C(11)	1.499(6)	C(50)-O(7)	1.421(5)
C(9)-C(10)	1.524(6)	C(50)-C(51)	1.547(5)
C(12)-C(17)	1.379(6)	C(51)-O(5)	1.461(5)
C(12)-C(13)	1.389(6)	C(51)-C(73)	1.529(6)
C(13)-C(14)	1.387(6)	C(51)-C(67)	1.532(6)
C(14)-C(15)	1.373(7)	C(52)-O(7)	1.421(5)
C(15)-C(16)	1.374(7)	C(52)-O(8)	1.433(6)
C(16)-C(17)	1.389(6)	C(52)-C(54)	1.519(7)
C(18)-C(19)	1.368(6)	C(52)-C(53)	1.518(7)
C(18)-C(23)	1.385(6)	C(55)-C(60)	1.382(6)
C(19)-C(20)	1.389(6)	C(55)-C(56)	1.385(6)
C(20)-C(21)	1.373(6)	C(56)-C(57)	1.399(6)
C(21)-C(22)	1.378(7)	C(57)-C(58)	1.378(7)
C(22)-C(23)	1.377(7)	C(58)-C(59)	1.378(7)
C(24)-C(29)	1.387(6)	C(59)-C(60)	1.407(6)
C(24)-C(25)	1.394(6)	C(61)-C(66)	1.384(6)
C(25)-C(26)	1.378(6)	C(61)-C(62)	1.389(6)
C(26)-C(27)	1.384(7)	C(62)-C(63)	1.387(6)
C(27)-C(28)	1.381(7)	C(63)-C(64)	1.377(7)
C(28)-C(29)	1.401(6)	C(64)-C(65)	1.376(7)
C(30)-C(35)	1.389(5)	C(65)-C(66)	1.384(7)
C(30)-C(31)	1.401(6)	C(67)-C(72)	1.382(6)
C(31)-C(32)	1.375(5)	C(67)-C(68)	1.392(6)
C(32)-C(33)	1.391(6)	C(68)-C(69)	1.392(6)
C(33)-C(34)	1.365(6)	C(69)-C(70)	1.368(6)
C(34)-C(35)	1.391(6)	C(70)-C(71)	1.377(6)
C(36)-C(37)	1.358(7)	C(71)-C(72)	1.384(6)
C(36)-C(43)	1.525(6)	C(73)-C(74)	1.389(6)
C(36)-Rh(1)	2.235(5)	C(73)-C(78)	1.392(6)
C(37)-C(38)	1.514(7)	C(74)-C(75)	1.402(6)
C(37)-Rh(1)	2.217(4)	C(75)-C(76)	1.378(7)

C(76)-C(77)	1.384(7)
C(77)-C(78)	1.395(6)
C(79)-C(80)	1.402(7)
C(79)-C(86)	1.529(6)
C(79)-Rh(2)	2.119(4)
C(80)-C(81)	1.503(7)
C(80)-Rh(2)	2.111(5)
C(81)-C(82)	1.530(7)
C(82)-C(83)	1.505(7)
C(83)-C(84)	1.354(7)
C(83)-Rh(2)	2.244(4)
C(84)-C(85)	1.510(7)
C(84)-Rh(2)	2.228(4)
C(85)-C(86)	1.523(7)
C(87)-C(88)	1.499(8)
C(88)-C(89)	1.524(8)
C(89)-C(90)	1.526(7)
C(90)-C(91)	1.508(8)
C(91)-C(92)	1.504(7)
C(92)-C(93)	1.533(7)
Cl(1)-Rh(1)	2.3777(11)
Cl(2)-Rh(2)	2.3745(11)
N(1)-P(1)	1.643(4)
N(2)-P(2)	1.636(3)
O(1)-P(1)	1.626(3)
O(2)-P(1)	1.612(3)
O(5)-P(2)	1.623(3)
O(6)-P(2)	1.608(3)
P(1)-Rh(1)	2.2545(11)
P(2)-Rh(2)	2.2524(11)

N(1)-C(1)-C(2)	103.3(4)
C(3)-C(2)-C(1)	102.6(4)
C(2)-C(3)-C(4)	103.4(4)
N(1)-C(4)-C(3)	104.0(3)
O(1)-C(5)-C(12)	106.0(3)
O(1)-C(5)-C(18)	109.5(3)
C(12)-C(5)-C(18)	108.9(3)
O(1)-C(5)-C(6)	106.2(3)
C(12)-C(5)-C(6)	113.0(3)
C(18)-C(5)-C(6)	112.9(3)
O(3)-C(6)-C(7)	105.2(3)
O(3)-C(6)-C(5)	112.1(3)
C(7)-C(6)-C(5)	112.2(3)
O(4)-C(7)-C(6)	104.9(3)
O(4)-C(7)-C(8)	110.3(3)
C(6)-C(7)-C(8)	112.2(3)
O(2)-C(8)-C(24)	110.3(3)
O(2)-C(8)-C(30)	103.4(3)
C(24)-C(8)-C(30)	112.2(3)
O(2)-C(8)-C(7)	107.8(3)
C(24)-C(8)-C(7)	111.7(3)
C(30)-C(8)-C(7)	111.1(3)
O(3)-C(9)-O(4)	106.9(3)
O(3)-C(9)-C(11)	110.6(4)
O(4)-C(9)-C(11)	108.2(4)
O(3)-C(9)-C(10)	108.2(4)
O(4)-C(9)-C(10)	110.0(4)
C(11)-C(9)-C(10)	112.8(4)
C(17)-C(12)-C(13)	118.1(4)
C(17)-C(12)-C(5)	122.7(4)
C(13)-C(12)-C(5)	119.1(4)
C(14)-C(13)-C(12)	120.9(4)
C(15)-C(14)-C(13)	120.1(5)
C(14)-C(15)-C(16)	119.9(5)
C(15)-C(16)-C(17)	119.9(5)
C(12)-C(17)-C(16)	121.2(5)
C(19)-C(18)-C(23)	118.8(4)
C(19)-C(18)-C(5)	122.3(4)
C(23)-C(18)-C(5)	118.8(4)
C(18)-C(19)-C(20)	121.0(4)
C(21)-C(20)-C(19)	119.8(5)
C(20)-C(21)-C(22)	119.5(5)
C(23)-C(22)-C(21)	120.4(5)
C(22)-C(23)-C(18)	120.4(5)
C(29)-C(24)-C(25)	119.9(4)
C(29)-C(24)-C(8)	120.6(4)
C(25)-C(24)-C(8)	119.3(4)
C(26)-C(25)-C(24)	119.6(4)
C(25)-C(26)-C(27)	121.3(5)
C(26)-C(27)-C(28)	119.1(5)
C(27)-C(28)-C(29)	120.5(5)
C(24)-C(29)-C(28)	119.5(4)
C(35)-C(30)-C(31)	117.1(4)
C(35)-C(30)-C(8)	121.4(4)
C(31)-C(30)-C(8)	121.5(4)
C(32)-C(31)-C(30)	121.4(4)
C(31)-C(32)-C(33)	120.0(4)
C(34)-C(33)-C(32)	119.8(4)
C(33)-C(34)-C(35)	120.0(4)
C(30)-C(35)-C(34)	121.6(4)
C(37)-C(36)-C(43)	123.5(5)
C(37)-C(36)-Rh(1)	71.5(3)
C(43)-C(36)-Rh(1)	110.6(3)
C(36)-C(37)-C(38)	126.7(5)
C(36)-C(37)-Rh(1)	73.0(3)
C(38)-C(37)-Rh(1)	108.0(3)
C(39)-C(38)-C(37)	113.8(4)
C(40)-C(39)-C(38)	114.0(4)
C(41)-C(40)-C(39)	122.8(4)
C(41)-C(40)-Rh(1)	69.9(3)
C(39)-C(40)-Rh(1)	113.6(3)

C(40)-C(41)-C(42)	125.6(4)	C(68)-C(67)-C(51)	121.8(4)
C(40)-C(41)-Rh(1)	71.6(3)	C(69)-C(68)-C(67)	119.7(4)
C(42)-C(41)-Rh(1)	111.8(3)	C(70)-C(69)-C(68)	120.7(4)
C(41)-C(42)-C(43)	114.7(4)	C(71)-C(70)-C(69)	119.9(4)
C(36)-C(43)-C(42)	113.2(4)	C(70)-C(71)-C(72)	119.8(4)
N(2)-C(44)-C(45)	102.9(3)	C(71)-C(72)-C(67)	121.0(4)
C(44)-C(45)-C(46)	102.7(3)	C(74)-C(73)-C(78)	118.5(4)
C(45)-C(46)-C(47)	102.5(3)	C(74)-C(73)-C(51)	119.6(4)
N(2)-C(47)-C(46)	104.2(3)	C(78)-C(73)-C(51)	121.9(4)
O(6)-C(48)-C(55)	105.1(3)	C(73)-C(74)-C(75)	120.9(4)
O(6)-C(48)-C(61)	109.3(3)	C(76)-C(75)-C(74)	120.0(4)
C(55)-C(48)-C(61)	112.4(3)	C(75)-C(76)-C(77)	119.5(4)
O(6)-C(48)-C(49)	107.8(3)	C(76)-C(77)-C(78)	120.6(4)
C(55)-C(48)-C(49)	109.9(3)	C(73)-C(78)-C(77)	120.5(5)
C(61)-C(48)-C(49)	112.1(3)	C(80)-C(79)-C(86)	123.1(5)
O(8)-C(49)-C(50)	105.6(3)	C(80)-C(79)-Rh(2)	70.3(2)
O(8)-C(49)-C(48)	111.2(3)	C(86)-C(79)-Rh(2)	112.9(3)
C(50)-C(49)-C(48)	113.2(3)	C(79)-C(80)-C(81)	126.3(4)
O(7)-C(50)-C(49)	104.6(3)	C(79)-C(80)-Rh(2)	70.9(3)
O(7)-C(50)-C(51)	111.5(3)	C(81)-C(80)-Rh(2)	110.3(3)
C(49)-C(50)-C(51)	111.1(3)	C(80)-C(81)-C(82)	113.7(4)
O(5)-C(51)-C(73)	106.3(3)	C(83)-C(82)-C(81)	112.8(4)
O(5)-C(51)-C(67)	108.7(3)	C(84)-C(83)-C(82)	124.0(4)
C(73)-C(51)-C(67)	111.2(3)	C(84)-C(83)-Rh(2)	71.7(3)
O(5)-C(51)-C(50)	105.8(3)	C(82)-C(83)-Rh(2)	110.3(3)
C(73)-C(51)-C(50)	110.8(3)	C(83)-C(84)-C(85)	126.2(5)
C(67)-C(51)-C(50)	113.6(3)	C(83)-C(84)-Rh(2)	73.0(3)
O(7)-C(52)-O(8)	106.8(3)	C(85)-C(84)-Rh(2)	107.1(3)
O(7)-C(52)-C(54)	110.2(4)	C(86)-C(85)-C(84)	113.4(4)
O(8)-C(52)-C(54)	108.6(4)	C(85)-C(86)-C(79)	113.8(4)
O(7)-C(52)-C(53)	108.5(4)	C(87)-C(88)-C(89)	112.0(5)
O(8)-C(52)-C(53)	108.4(4)	C(88)-C(89)-C(90)	115.8(5)
C(54)-C(52)-C(53)	114.0(4)	C(91)-C(90)-C(89)	114.5(4)
C(60)-C(55)-C(56)	118.9(4)	C(92)-C(91)-C(90)	114.6(5)
C(60)-C(55)-C(48)	120.8(4)	C(91)-C(92)-C(93)	112.4(5)
C(56)-C(55)-C(48)	120.2(4)	C(1)-N(1)-C(4)	110.7(3)
C(55)-C(56)-C(57)	120.3(4)	C(1)-N(1)-P(1)	120.3(3)
C(58)-C(57)-C(56)	120.5(5)	C(4)-N(1)-P(1)	127.9(3)
C(57)-C(58)-C(59)	119.9(5)	C(44)-N(2)-C(47)	110.8(3)
C(58)-C(59)-C(60)	119.5(4)	C(44)-N(2)-P(2)	120.0(3)
C(55)-C(60)-C(59)	120.9(4)	C(47)-N(2)-P(2)	128.5(3)
C(66)-C(61)-C(62)	118.9(4)	C(5)-O(1)-P(1)	129.5(2)
C(66)-C(61)-C(48)	119.0(4)	C(8)-O(2)-P(1)	128.2(3)
C(62)-C(61)-C(48)	122.0(4)	C(6)-O(3)-C(9)	109.9(3)
C(63)-C(62)-C(61)	120.7(5)	C(7)-O(4)-C(9)	109.3(3)
C(64)-C(63)-C(62)	119.7(5)	C(51)-O(5)-P(2)	129.5(2)
C(63)-C(64)-C(65)	119.8(5)	C(48)-O(6)-P(2)	127.2(2)
C(64)-C(65)-C(66)	120.7(5)	C(50)-O(7)-C(52)	109.8(3)
C(65)-C(66)-C(61)	120.1(5)	C(49)-O(8)-C(52)	109.7(3)
C(72)-C(67)-C(68)	118.8(4)	O(2)-P(1)-O(1)	104.30(14)
C(72)-C(67)-C(51)	119.4(4)	O(2)-P(1)-N(1)	97.78(16)

O(1)-P(1)-N(1)	109.60(19)	C(41)-Rh(1)-Cl(1)	158.09(12)
O(2)-P(1)-Rh(1)	118.14(12)	C(40)-Rh(1)-Cl(1)	162.84(12)
O(1)-P(1)-Rh(1)	110.58(11)	C(37)-Rh(1)-Cl(1)	89.52(13)
N(1)-P(1)-Rh(1)	115.28(13)	C(36)-Rh(1)-Cl(1)	90.93(13)
O(6)-P(2)-O(5)	104.18(15)	P(1)-Rh(1)-Cl(1)	88.01(4)
O(6)-P(2)-N(2)	98.05(16)	C(80)-Rh(2)-C(79)	38.71(18)
O(5)-P(2)-N(2)	109.47(17)	C(80)-Rh(2)-C(84)	96.67(18)
O(6)-P(2)-Rh(2)	118.79(12)	C(79)-Rh(2)-C(84)	81.81(18)
O(5)-P(2)-Rh(2)	111.22(11)	C(80)-Rh(2)-P(2)	91.69(13)
N(2)-P(2)-Rh(2)	113.98(13)	C(79)-Rh(2)-P(2)	96.27(14)
C(41)-Rh(1)-C(40)	38.52(16)	C(84)-Rh(2)-P(2)	163.62(14)
C(41)-Rh(1)-C(37)	95.75(18)	C(80)-Rh(2)-C(83)	81.18(18)
C(40)-Rh(1)-C(37)	81.12(18)	C(79)-Rh(2)-C(83)	89.12(18)
C(41)-Rh(1)-C(36)	81.39(17)	C(84)-Rh(2)-C(83)	35.24(17)
C(40)-Rh(1)-C(36)	89.73(19)	P(2)-Rh(2)-C(83)	161.05(13)
C(37)-Rh(1)-C(36)	35.52(17)	C(80)-Rh(2)-Cl(2)	156.86(13)
C(41)-Rh(1)-P(1)	94.57(13)	C(79)-Rh(2)-Cl(2)	163.85(14)
C(40)-Rh(1)-P(1)	95.33(13)	C(84)-Rh(2)-Cl(2)	89.09(13)
C(37)-Rh(1)-P(1)	158.17(13)	P(2)-Rh(2)-Cl(2)	88.70(4)
C(36)-Rh(1)-P(1)	166.16(13)	C(83)-Rh(2)-Cl(2)	91.10(12)

Symmetry transformations used to generate equivalent atoms:

Table A.2.19. Anisotropic displacement parameters ($Å^2$x 10^3)for Rh(cod)Cl·**T2** (2). The anisotropic displacement factor exponent takes the form: $-2\pi^2[h^2a^{*2}U^{11} + ... + 2 h k a^* b^* U^{12}]$

	U^{11}	U^{22}	U^{33}	U^{23}	U^{13}	U^{12}
C(1)	26(3)	11(2)	34(3)	-1(2)	-4(2)	-2(2)
C(2)	36(3)	19(2)	25(3)	-6(2)	-5(2)	-2(2)
C(3)	37(3)	25(2)	28(2)	-2(2)	-10(2)	1(2)
C(4)	21(3)	21(2)	16(2)	-2(2)	-1(2)	-4(2)
C(5)	13(2)	14(2)	20(2)	5(2)	5(2)	2(2)
C(6)	14(2)	16(2)	17(2)	1(2)	6(2)	3(2)
C(7)	18(2)	14(2)	19(2)	-1(2)	0(2)	-2(2)
C(8)	19(2)	12(2)	16(2)	-2(2)	0(2)	-1(2)
C(9)	19(2)	18(2)	19(2)	0(2)	0(2)	0(2)
C(10)	26(3)	42(3)	24(3)	-10(2)	4(2)	0(2)
C(11)	35(3)	26(2)	39(3)	11(2)	-9(3)	-1(2)
C(12)	21(2)	15(2)	18(2)	0(2)	4(2)	-1(2)
C(13)	28(3)	26(2)	21(2)	3(2)	1(2)	3(2)
C(14)	28(3)	36(3)	22(3)	-1(2)	8(2)	2(2)
C(15)	48(4)	37(3)	17(3)	0(2)	11(2)	-5(2)
C(16)	35(3)	39(3)	17(3)	5(2)	0(2)	2(2)
C(17)	24(3)	25(2)	21(2)	-1(2)	3(2)	0(2)
C(18)	19(2)	16(2)	19(2)	-1(2)	2(2)	-2(2)
C(19)	18(3)	19(2)	35(3)	1(2)	-3(2)	0(2)
C(20)	22(3)	33(2)	32(3)	4(2)	-5(2)	2(2)
C(21)	25(3)	26(2)	33(3)	-7(2)	-1(2)	-10(2)

C(22)	49(3)	25(2)	47(3)	8(2)	-13(3)	-19(2)
C(23)	41(3)	25(2)	32(3)	10(2)	-10(2)	-8(2)
C(24)	18(2)	16(2)	16(2)	2(2)	0(2)	0(2)
C(25)	20(3)	25(2)	20(2)	1(2)	2(2)	-3(2)
C(26)	18(3)	28(2)	42(3)	-1(2)	5(2)	-1(2)
C(27)	13(2)	37(3)	39(3)	10(2)	-6(2)	-5(2)
C(28)	26(3)	25(2)	30(3)	4(2)	-9(2)	-4(2)
C(29)	22(3)	17(2)	24(2)	0(2)	-1(2)	-2(2)
C(30)	20(2)	16(2)	13(2)	1(1)	2(2)	4(2)
C(31)	18(2)	16(2)	22(2)	1(2)	3(2)	0(2)
C(32)	27(3)	24(2)	16(2)	2(2)	-2(2)	5(2)
C(33)	37(3)	16(2)	20(2)	6(2)	10(2)	5(2)
C(34)	35(3)	15(2)	28(3)	2(2)	10(2)	-3(2)
C(35)	24(3)	17(2)	22(2)	-1(2)	2(2)	-4(2)
C(36)	24(3)	29(2)	28(3)	-7(2)	-5(2)	14(2)
C(37)	31(3)	22(2)	29(3)	-1(2)	2(2)	9(2)
C(38)	53(4)	19(2)	42(3)	5(2)	-4(3)	5(2)
C(39)	43(4)	23(2)	44(3)	15(2)	0(3)	6(2)
C(40)	24(3)	23(2)	24(3)	7(2)	3(2)	6(2)
C(41)	27(3)	19(2)	17(2)	-1(2)	2(2)	1(2)
C(42)	24(3)	37(3)	27(3)	-6(2)	-4(2)	-2(2)
C(43)	27(3)	37(3)	43(3)	-15(2)	-15(2)	10(2)
C(44)	23(3)	18(2)	18(2)	4(2)	1(2)	5(2)
C(45)	34(3)	16(2)	26(3)	6(2)	5(2)	0(2)
C(46)	37(3)	15(2)	25(3)	0(2)	-2(2)	-4(2)
C(47)	31(3)	16(2)	18(2)	-6(2)	-1(2)	5(2)
C(48)	15(2)	21(2)	19(2)	6(2)	-4(2)	-1(2)
C(49)	16(2)	21(2)	15(2)	5(2)	5(2)	0(2)
C(50)	21(2)	21(2)	11(2)	2(2)	-2(2)	-1(2)
C(51)	17(2)	16(2)	15(2)	-1(2)	0(2)	0(2)
C(52)	27(3)	32(2)	21(2)	10(2)	-1(2)	-4(2)
C(53)	27(3)	39(3)	57(4)	28(3)	-14(3)	-7(2)
C(54)	45(3)	61(4)	20(2)	-1(3)	1(2)	-12(3)
C(55)	21(3)	26(2)	15(2)	0(2)	1(2)	3(2)
C(56)	25(2)	31(2)	26(2)	5(2)	1(2)	1(2)
C(57)	25(3)	47(3)	26(3)	7(2)	8(2)	5(2)
C(58)	41(4)	43(3)	19(3)	-5(2)	3(2)	11(2)
C(59)	30(3)	34(2)	24(3)	-5(2)	7(2)	2(2)
C(60)	21(3)	28(2)	21(2)	4(2)	7(2)	-2(2)
C(61)	17(2)	26(2)	12(2)	1(2)	-1(2)	-2(2)
C(62)	23(3)	26(2)	23(3)	3(2)	4(2)	-3(2)
C(63)	28(3)	34(2)	22(3)	0(2)	5(2)	-4(2)
C(64)	32(3)	49(3)	25(3)	5(2)	-2(2)	-20(2)
C(65)	25(3)	53(3)	28(3)	15(2)	-5(2)	-8(2)
C(66)	18(3)	33(2)	35(3)	10(2)	-1(2)	-2(2)
C(67)	12(2)	19(2)	13(2)	1(2)	-1(2)	1(2)
C(68)	25(3)	22(2)	18(2)	-2(2)	3(2)	-4(2)
C(69)	27(3)	20(2)	26(3)	-5(2)	-3(2)	-5(2)
C(70)	21(3)	20(2)	32(3)	2(2)	8(2)	-3(2)
C(71)	23(3)	25(2)	17(2)	5(2)	5(2)	-2(2)
C(72)	25(3)	15(2)	16(2)	-6(2)	0(2)	-2(2)

C(73)	19(2)	21(2)	9(2)	2(2)	3(2)	0(2)
C(74)	25(3)	23(2)	23(3)	-2(2)	-3(2)	-3(2)
C(75)	17(3)	34(2)	32(3)	2(2)	-6(2)	3(2)
C(76)	24(3)	22(2)	38(3)	11(2)	0(2)	5(2)
C(77)	33(3)	16(2)	44(3)	1(2)	3(3)	3(2)
C(78)	19(3)	19(2)	31(3)	-1(2)	1(2)	0(2)
C(79)	29(3)	17(2)	36(3)	-5(2)	-10(2)	7(2)
C(80)	23(3)	27(2)	24(3)	-12(2)	1(2)	4(2)
C(81)	37(3)	41(3)	32(3)	-17(2)	11(3)	-2(2)
C(82)	47(4)	32(2)	20(3)	-5(2)	5(2)	-9(2)
C(83)	29(3)	25(2)	21(2)	-1(2)	-10(2)	3(2)
C(84)	22(3)	34(2)	30(3)	-12(2)	-8(2)	-2(2)
C(85)	37(3)	29(2)	32(3)	-6(2)	-2(3)	-13(2)
C(86)	41(3)	17(2)	35(3)	-4(2)	-13(2)	0(2)
C(87)	50(4)	64(4)	33(3)	12(3)	2(3)	-3(3)
C(88)	47(4)	39(3)	42(4)	-3(3)	2(3)	10(3)
C(89)	34(4)	51(3)	36(3)	-1(3)	-4(3)	-3(3)
C(90)	33(3)	36(3)	43(4)	-5(2)	-12(3)	2(2)
C(91)	29(3)	30(2)	51(4)	-2(2)	-12(3)	4(2)
C(92)	30(3)	40(3)	50(3)	6(3)	-6(2)	0(3)
C(93)	49(4)	48(3)	44(3)	15(3)	-13(3)	-11(3)
Cl(1)	30(1)	24(1)	22(1)	-2(1)	6(1)	2(1)
Cl(2)	25(1)	24(1)	26(1)	0(1)	0(1)	8(1)
N(1)	26(2)	14(2)	18(2)	3(1)	-6(2)	-3(1)
N(2)	22(2)	17(2)	11(2)	2(1)	-1(2)	1(1)
O(1)	16(2)	14(1)	15(2)	2(1)	2(1)	3(1)
O(2)	19(2)	11(1)	16(2)	1(1)	2(1)	-1(1)
O(3)	19(2)	19(1)	25(2)	-3(1)	5(1)	2(1)
O(4)	18(2)	15(1)	31(2)	-5(1)	7(1)	-2(1)
O(5)	18(2)	18(1)	14(1)	-1(1)	-3(1)	2(1)
O(6)	22(2)	17(1)	13(2)	3(1)	1(1)	2(1)
O(7)	21(2)	29(2)	16(1)	6(1)	-1(1)	-4(1)
O(8)	18(2)	33(2)	22(2)	14(1)	-2(1)	-4(1)
P(1)	18(1)	12(1)	15(1)	1(1)	0(1)	1(1)
P(2)	17(1)	13(1)	13(1)	1(1)	0(1)	0(1)
Rh(1)	20(1)	15(1)	18(1)	-1(1)	-1(1)	2(1)
Rh(2)	17(1)	16(1)	15(1)	-1(1)	-2(1)	0(1)

Table A.2.20. Hydrogen coordinates (x 10^4) and isotropic displacement parameters (Å^{2}x 10^3) for Rh(cod)Cl·**T2** (2).

	x	y	z	U(eq)
H(1A)	2038	13312	1805	28
H(1B)	3239	13171	1734	28
H(2A)	3239	13787	2478	32
H(2B)	2217	13048	2576	32
H(3A)	3470	11733	2858	36

H(3B)	4218	12030	2457	36
H(4A)	3506	10307	2153	23
H(4B)	2471	10473	2418	23
H(6)	3133	8693	1512	19
H(7)	1690	8685	786	20
H(10A)	2920	7143	217	46
H(10B)	2711	5741	290	46
H(10C)	3846	6248	321	46
H(11A)	4014	5334	1131	50
H(11B)	2870	4865	1080	50
H(11C)	3196	5720	1488	50
H(13)	4917	8969	537	30
H(14)	5299	8883	-226	34
H(15)	4183	9736	-763	41
H(16)	2631	10557	-543	36
H(17)	2224	10588	217	28
H(19)	4726	9090	1593	29
H(20)	6168	10028	1921	35
H(21)	6596	12001	1712	34
H(22)	5565	13031	1184	49
H(23)	4102	12116	877	40
H(25)	-398	9778	1796	26
H(26)	-2098	9944	1550	35
H(27)	-2697	8911	909	36
H(28)	-1561	7736	498	33
H(29)	175	7600	728	25
H(31)	2531	8324	2174	22
H(32)	2702	6868	2735	27
H(33)	1571	5215	2750	29
H(34)	293	5026	2196	31
H(35)	120	6485	1629	25
H(36)	-1700	12820	1300	33
H(37)	-659	14339	1422	33
H(38A)	-494	15165	636	46
H(38B)	527	15153	936	46
H(39A)	48	13745	177	44
H(39B)	1117	14328	318	44
H(40)	1648	12488	560	28
H(41)	693	10830	525	25
H(42A)	-1074	10714	467	35
H(42B)	-799	11608	71	35
H(43A)	-1548	13186	389	43
H(43B)	-2211	12149	607	43
H(44A)	7407	9261	2403	24
H(44B)	8562	9593	2545	24
H(45A)	6804	11130	2629	30
H(45B)	7890	11515	2440	30
H(46A)	7577	12079	3255	31
H(46B)	8664	11481	3160	31
H(47A)	8100	10091	3673	26
H(47B)	6927	10304	3531	26

H(49)	8040	5708	3885	21
H(50)	8475	8148	4097	21
H(53A)	9717	4748	4586	61
H(53B)	9296	4702	5081	61
H(53C)	10288	5470	4980	61
H(54A)	9344	7306	5332	63
H(54B)	8289	6613	5373	63
H(54C)	8348	7812	5080	63
H(56)	5814	6058	4715	33
H(57)	5334	7011	5384	39
H(58)	5623	9078	5490	41
H(59)	6377	10219	4925	35
H(60)	6895	9253	4260	28
H(62)	6856	4429	4023	28
H(63)	5686	2985	3748	33
H(64)	4153	3615	3399	42
H(65)	3813	5675	3311	43
H(66)	4998	7122	3564	35
H(68)	9947	9207	4086	26
H(69)	10821	10950	3858	29
H(70)	11207	11230	3108	29
H(71)	10869	9688	2587	26
H(72)	10038	7923	2810	23
H(74)	11224	6895	3914	28
H(75)	12270	5162	3963	33
H(76)	11689	3320	3662	34
H(77)	10083	3223	3296	37
H(78)	9028	4940	3254	28
H(79)	7599	5004	2879	33
H(80)	8434	6341	2467	30
H(81A)	8204	5512	1696	44
H(81B)	8025	6930	1725	44
H(82A)	6646	6380	1304	40
H(82B)	6539	5114	1551	40
H(83)	5447	7181	1744	30
H(84)	4577	6124	2222	34
H(85A)	5084	4316	2578	39
H(85B)	5171	4005	2060	39
H(86A)	6879	3935	2095	37
H(86B)	6637	3468	2584	37
H(87A)	4251	11281	3781	74
H(87B)	4582	10548	3350	74
H(87C)	5130	10294	3823	74
H(88A)	3889	8778	3624	52
H(88B)	3030	9791	3642	52
H(89A)	3405	10083	4421	48
H(89B)	4272	9086	4404	48
H(90A)	2141	8568	4290	45
H(90B)	3008	7568	4270	45
H(91A)	3412	7857	5036	45
H(91B)	2595	8913	5061	45

H(92A)	2090	6432	4915	48
H(92B)	1266	7486	4929	48
H(93A)	2548	6857	5691	71
H(93B)	1393	6435	5635	71
H(93C)	1655	7829	5699	71

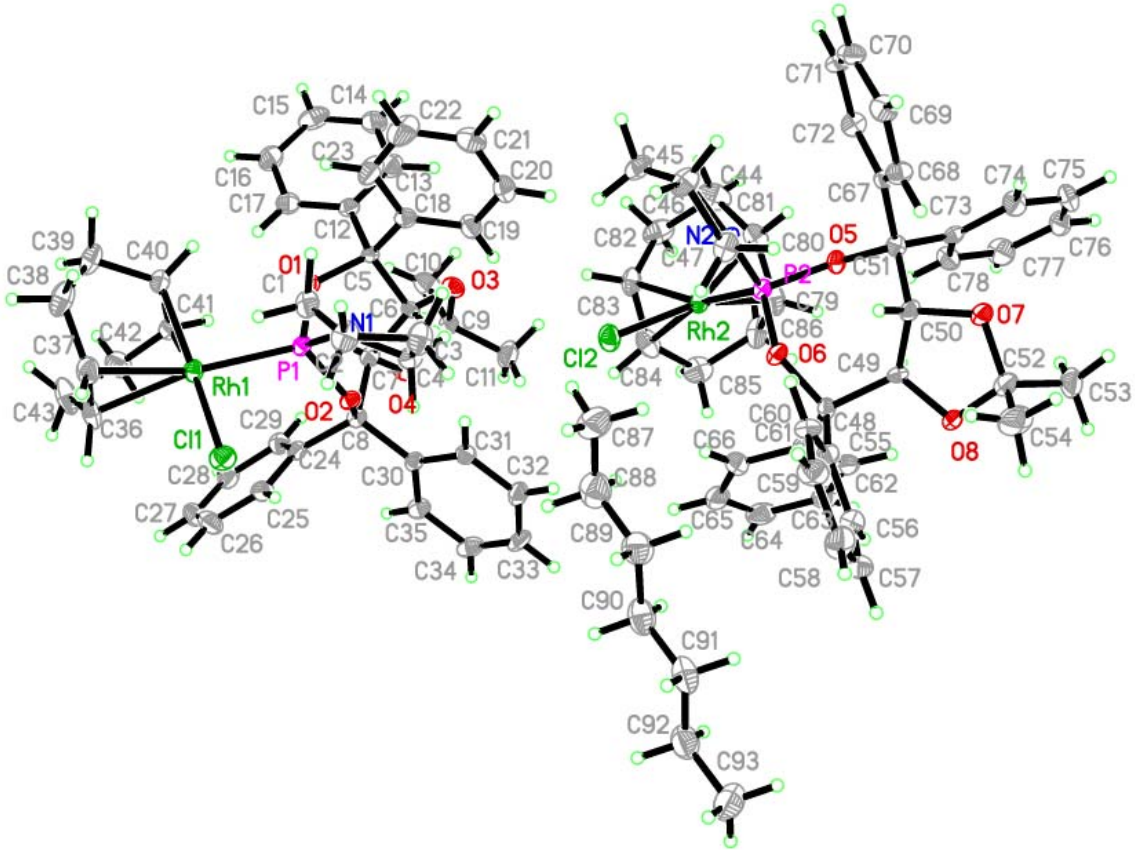

Table A.2.21. Crystal data and structure refinement for Rh(cod)Cl·**B4**.

Identification code	rovis45_0m	
Empirical formula	$C_{36}H_{46}ClNO_2PRhSi_2$	
Formula weight	750.25	
Temperature	296(2) K	
Wavelength	0.71073 Å	
Crystal system	Orthorhombic	
Space group	$P\ 2_12_12_1$	
Unit cell dimensions	a = 11.2417(5) Å	α= 90°.
	b = 14.6792(6) Å	β= 90°.
	c = 21.3614(9) Å	γ = 90°.
Volume	3525.0(3) $Å^3$	
Z	4	
Density (calculated)	1.414 Mg/m^3	
Absorption coefficient	0.706 mm^{-1}	
F(000)	1560	
Crystal size	0.23 x 0.09 x 0.07 mm^3	
Theta range for data collection	1.68 to 33.27°.	
Index ranges	-17<=h<=9, -22<=k<=13, -32<=l<=32	
Reflections collected	31400	
Independent reflections	12869 [R(int) = 0.0581]	
Completeness to theta = 33.27°	99.8 %	
Absorption correction	Semi-empirical from equivalents	
Max. and min. transmission	0.9535 and 0.8516	
Refinement method	Full-matrix least-squares on F^2	
Data / restraints / parameters	12869 / 0 / 422	
Goodness-of-fit on F^2	0.995	
Final R indices [I>2sigma(I)]	R1 = 0.0453, wR2 = 0.0864	
R indices (all data)	R1 = NaN, wR2 = 0.1036	
Absolute structure parameter	-0.02(2)	
Largest diff. peak and hole	0.585 and -0.513 e.$Å^{-3}$	

Table A.2.22. Atomic coordinates (x 10^4) and equivalent isotropic displacement parameters ($Å^2$x 10^3) for Rh(cod)Cl·**B4**. U(eq) is defined as one third of the trace of the orthogonalized U^{ij} tensor.

	x	y	z	U(eq)
C(1)	7261(3)	9780(2)	1414(1)	13(1)
C(2)	7332(3)	9520(2)	2037(1)	13(1)
C(3)	8265(3)	9766(2)	2446(1)	14(1)
C(4)	9178(3)	10266(2)	2185(1)	16(1)
C(5)	9221(3)	10498(2)	1541(1)	15(1)
C(6)	10202(3)	10975(2)	1288(2)	19(1)
C(7)	10256(3)	11172(2)	663(2)	25(1)
C(8)	9340(3)	10898(2)	265(2)	22(1)
C(9)	8356(3)	10454(2)	499(1)	18(1)
C(10)	8261(3)	10247(2)	1149(1)	13(1)
C(11)	6898(3)	9395(3)	3709(2)	28(1)

C(12)	9112(4)	8363(2)	3425(2)	31(1)
C(13)	9281(3)	10386(2)	3681(2)	29(1)
C(14)	6192(3)	9550(2)	1030(1)	14(1)
C(15)	5816(3)	8655(2)	976(1)	14(1)
C(16)	4936(3)	8364(2)	545(1)	18(1)
C(17)	4324(3)	9047(2)	235(1)	20(1)
C(18)	4542(3)	9979(2)	333(1)	18(1)
C(19)	3839(3)	10659(2)	41(2)	25(1)
C(20)	4062(4)	11560(2)	138(2)	28(1)
C(21)	4994(3)	11826(2)	536(2)	25(1)
C(22)	5709(3)	11185(2)	820(1)	21(1)
C(23)	5509(3)	10242(2)	726(1)	16(1)
C(24)	4629(4)	7106(3)	-556(2)	35(1)
C(25)	5711(3)	6298(2)	618(2)	29(1)
C(26)	3052(3)	6855(3)	579(2)	30(1)
C(27)	8050(3)	7068(3)	2062(2)	31(1)
C(28)	6643(3)	6739(2)	2912(2)	28(1)
C(29)	3824(3)	9175(2)	2739(2)	23(1)
C(30)	3607(3)	9198(2)	2095(2)	22(1)
C(31)	2417(3)	9197(2)	1773(2)	27(1)
C(32)	1487(3)	8598(3)	2104(2)	26(1)
C(33)	2014(3)	7731(2)	2352(2)	22(1)
C(34)	2421(3)	7587(2)	2946(2)	22(1)
C(35)	2493(3)	8280(3)	3469(2)	30(1)
C(36)	2885(3)	9224(3)	3253(2)	28(1)
Cl(1)	4189(1)	6265(1)	2189(1)	27(1)
N(1)	6937(2)	7296(2)	2369(1)	19(1)
O(1)	6370(2)	9053(1)	2292(1)	15(1)
O(2)	6349(2)	7999(1)	1361(1)	15(1)
P(1)	5957(1)	8027(1)	2098(1)	14(1)
Rh(1)	4039(1)	7841(1)	2349(1)	15(1)
Si(1)	8353(1)	9484(1)	3307(1)	18(1)
Si(2)	4600(1)	7133(1)	319(1)	20(1)

Table A.2.23. Bond lengths [Å] and angles [°] for Rh(cod)Cl·**B4**.

C(1)-C(2)	1.387(4)	C(11)-Si(1)	1.852(4)
C(1)-C(10)	1.433(4)	C(12)-Si(1)	1.871(4)
C(1)-C(14)	1.494(4)	C(13)-Si(1)	1.866(4)
C(2)-O(1)	1.392(3)	C(14)-C(15)	1.385(4)
C(2)-C(3)	1.411(4)	C(14)-C(23)	1.430(4)
C(3)-C(4)	1.380(4)	C(15)-O(2)	1.402(3)
C(3)-Si(1)	1.888(3)	C(15)-C(16)	1.417(4)
C(4)-C(5)	1.418(4)	C(16)-C(17)	1.385(4)
C(5)-C(6)	1.414(4)	C(16)-Si(2)	1.907(3)
C(5)-C(10)	1.415(4)	C(17)-C(18)	1.406(4)
C(6)-C(7)	1.367(5)	C(18)-C(19)	1.417(4)
C(7)-C(8)	1.394(5)	C(18)-C(23)	1.426(4)
C(8)-C(9)	1.377(4)	C(19)-C(20)	1.363(5)
C(9)-C(10)	1.424(4)	C(20)-C(21)	1.404(5)

C(21)-C(22)	1.378(5)
C(22)-C(23)	1.417(4)
C(24)-Si(2)	1.870(3)
C(25)-Si(2)	1.863(4)
C(26)-Si(2)	1.872(4)
C(27)-N(1)	1.452(4)
C(28)-N(1)	1.457(4)
C(29)-C(30)	1.396(5)
C(29)-C(36)	1.525(5)
C(29)-Rh(1)	2.141(3)
C(30)-C(31)	1.503(5)
C(30)-Rh(1)	2.120(3)
C(31)-C(32)	1.539(5)
C(32)-C(33)	1.500(5)
C(33)-C(34)	1.365(5)
C(33)-Rh(1)	2.282(3)
C(34)-C(35)	1.513(5)
C(34)-Rh(1)	2.252(3)
C(35)-C(36)	1.525(5)
Cl(1)-Rh(1)	2.3455(8)
N(1)-P(1)	1.643(3)
O(1)-P(1)	1.630(2)
O(2)-P(1)	1.634(2)
P(1)-Rh(1)	2.2388(9)

C(2)-C(1)-C(10)	117.8(3)
C(2)-C(1)-C(14)	120.7(3)
C(10)-C(1)-C(14)	121.5(2)
C(1)-C(2)-O(1)	117.8(3)
C(1)-C(2)-C(3)	124.5(3)
O(1)-C(2)-C(3)	117.5(2)
C(4)-C(3)-C(2)	116.0(3)
C(4)-C(3)-Si(1)	118.1(2)
C(2)-C(3)-Si(1)	125.8(2)
C(3)-C(4)-C(5)	123.0(3)
C(6)-C(5)-C(10)	119.8(3)
C(6)-C(5)-C(4)	121.1(3)
C(10)-C(5)-C(4)	119.1(3)
C(7)-C(6)-C(5)	120.8(3)
C(6)-C(7)-C(8)	120.1(3)
C(9)-C(8)-C(7)	120.6(3)
C(8)-C(9)-C(10)	120.9(3)
C(5)-C(10)-C(9)	117.7(3)
C(5)-C(10)-C(1)	119.2(2)
C(9)-C(10)-C(1)	123.1(3)
C(15)-C(14)-C(23)	118.2(3)
C(15)-C(14)-C(1)	120.4(3)
C(23)-C(14)-C(1)	121.4(3)
C(14)-C(15)-O(2)	118.1(3)
C(14)-C(15)-C(16)	123.6(3)
O(2)-C(15)-C(16)	118.2(3)
C(17)-C(16)-C(15)	116.0(3)
C(17)-C(16)-Si(2)	117.8(2)
C(15)-C(16)-Si(2)	126.0(2)
C(16)-C(17)-C(18)	123.2(3)
C(17)-C(18)-C(19)	121.5(3)
C(17)-C(18)-C(23)	119.0(3)
C(19)-C(18)-C(23)	119.5(3)
C(20)-C(19)-C(18)	121.0(3)
C(19)-C(20)-C(21)	119.9(3)
C(22)-C(21)-C(20)	120.8(3)
C(21)-C(22)-C(23)	120.7(3)
C(22)-C(23)-C(18)	118.0(3)
C(22)-C(23)-C(14)	123.0(3)
C(18)-C(23)-C(14)	118.9(3)
C(30)-C(29)-C(36)	125.9(3)
C(30)-C(29)-Rh(1)	70.0(2)
C(36)-C(29)-Rh(1)	113.6(2)
C(29)-C(30)-C(31)	127.3(3)
C(29)-C(30)-Rh(1)	71.7(2)
C(31)-C(30)-Rh(1)	108.7(2)
C(30)-C(31)-C(32)	113.2(3)
C(33)-C(32)-C(31)	112.3(3)
C(34)-C(33)-C(32)	126.2(3)
C(34)-C(33)-Rh(1)	71.30(19)
C(32)-C(33)-Rh(1)	109.4(2)
C(33)-C(34)-C(35)	126.9(3)
C(33)-C(34)-Rh(1)	73.67(19)
C(35)-C(34)-Rh(1)	105.3(2)
C(34)-C(35)-C(36)	113.7(3)
C(35)-C(36)-C(29)	112.0(3)
C(27)-N(1)-C(28)	115.2(3)
C(27)-N(1)-P(1)	124.7(2)
C(28)-N(1)-P(1)	119.7(2)
C(2)-O(1)-P(1)	125.26(19)
C(15)-O(2)-P(1)	115.68(17)
O(1)-P(1)-O(2)	101.02(11)
O(1)-P(1)-N(1)	108.82(13)
O(2)-P(1)-N(1)	98.22(12)
O(1)-P(1)-Rh(1)	108.99(8)
O(2)-P(1)-Rh(1)	119.14(8)
N(1)-P(1)-Rh(1)	118.82(10)
C(30)-Rh(1)-C(29)	38.25(13)
C(30)-Rh(1)-P(1)	92.62(10)
C(29)-Rh(1)-P(1)	95.22(10)
C(30)-Rh(1)-C(34)	96.60(13)
C(29)-Rh(1)-C(34)	80.79(13)
P(1)-Rh(1)-C(34)	159.00(9)
C(30)-Rh(1)-C(33)	80.71(13)
C(29)-Rh(1)-C(33)	87.19(13)
P(1)-Rh(1)-C(33)	165.96(9)
C(34)-Rh(1)-C(33)	35.02(12)

C(30)-Rh(1)-Cl(1)	154.96(10)	C(13)-Si(1)-C(3)	106.95(15)
C(29)-Rh(1)-Cl(1)	165.24(10)	C(12)-Si(1)-C(3)	110.39(15)
P(1)-Rh(1)-Cl(1)	90.89(3)	C(25)-Si(2)-C(24)	108.46(18)
C(34)-Rh(1)-Cl(1)	88.71(9)	C(25)-Si(2)-C(26)	112.20(17)
C(33)-Rh(1)-Cl(1)	90.14(9)	C(24)-Si(2)-C(26)	107.93(17)
C(11)-Si(1)-C(13)	110.21(17)	C(25)-Si(2)-C(16)	113.88(15)
C(11)-Si(1)-C(12)	106.13(18)	C(24)-Si(2)-C(16)	105.61(16)
C(13)-Si(1)-C(12)	108.08(18)	C(26)-Si(2)-C(16)	108.39(16)
C(11)-Si(1)-C(3)	114.94(14)		

Symmetry transformations used to generate equivalent atoms:

Table A.2.24. Anisotropic displacement parameters ($Å^2$x 10^3)for Rh(cod)Cl·**B4**. The anisotropic displacement factor exponent takes the form: $-2\pi^2[h^2a^{*2}U^{11} + ... + 2 h k a^* b^* U^{12}]$

	U^{11}	U^{22}	U^{33}	U^{23}	U^{13}	U^{12}
C(1)	14(1)	12(1)	14(1)	0(1)	-1(1)	1(1)
C(2)	14(1)	11(1)	14(1)	1(1)	3(1)	-1(1)
C(3)	14(1)	14(1)	14(1)	-1(1)	-1(1)	2(1)
C(4)	15(2)	16(1)	17(1)	0(1)	-4(1)	2(1)
C(5)	14(2)	14(1)	17(1)	0(1)	0(1)	-1(1)
C(6)	18(2)	18(2)	21(1)	3(1)	0(1)	-6(1)
C(7)	24(2)	25(2)	26(2)	4(1)	0(1)	-11(2)
C(8)	24(2)	26(2)	17(1)	3(1)	3(1)	-5(1)
C(9)	24(2)	15(1)	14(1)	0(1)	-1(1)	-2(1)
C(10)	15(1)	11(1)	14(1)	-1(1)	2(1)	-1(1)
C(11)	24(2)	43(2)	18(1)	0(2)	0(1)	-1(2)
C(12)	32(2)	29(2)	32(2)	8(2)	-3(2)	3(2)
C(13)	33(2)	34(2)	21(2)	1(1)	-7(2)	-5(2)
C(14)	14(2)	16(1)	12(1)	-2(1)	-1(1)	-2(1)
C(15)	15(2)	15(1)	12(1)	1(1)	2(1)	0(1)
C(16)	18(2)	23(2)	14(1)	2(1)	-1(1)	-5(1)
C(17)	20(2)	24(2)	18(1)	3(1)	-5(1)	-3(1)
C(18)	19(2)	20(2)	14(1)	2(1)	-3(1)	1(1)
C(19)	25(2)	27(2)	22(1)	2(1)	-8(1)	2(1)
C(20)	32(2)	25(2)	26(2)	4(1)	-10(2)	10(2)
C(21)	31(2)	18(2)	27(2)	2(1)	-6(1)	1(1)
C(22)	26(2)	17(1)	20(1)	1(1)	-2(1)	0(1)
C(23)	18(2)	18(1)	13(1)	3(1)	0(1)	-3(1)
C(24)	55(2)	33(2)	19(1)	-3(2)	-5(2)	-13(2)
C(25)	30(2)	22(2)	34(2)	-6(2)	-3(2)	-2(2)
C(26)	24(2)	30(2)	35(2)	3(2)	-4(2)	-9(2)
C(27)	26(2)	41(2)	26(2)	4(2)	4(1)	16(2)
C(28)	28(2)	28(2)	29(2)	16(2)	-5(2)	0(2)
C(29)	20(2)	17(1)	31(2)	-5(1)	-2(1)	-2(1)
C(30)	19(2)	15(2)	32(2)	3(1)	2(1)	4(1)
C(31)	25(2)	28(2)	29(2)	6(2)	1(2)	6(2)
C(32)	19(2)	35(2)	24(2)	2(2)	-2(1)	3(2)
C(33)	19(1)	23(2)	25(1)	-2(2)	0(1)	-1(1)

C(34)	15(2)	25(2)	24(2)	6(1)	4(1)	-3(1)
C(35)	22(2)	47(2)	20(2)	-1(2)	4(1)	2(2)
C(36)	22(2)	35(2)	29(2)	-10(2)	3(2)	-1(2)
Cl(1)	26(1)	15(1)	38(1)	2(1)	2(1)	-2(1)
N(1)	17(1)	21(1)	20(1)	7(1)	3(1)	4(1)
O(1)	14(1)	17(1)	13(1)	0(1)	2(1)	-5(1)
O(2)	18(1)	15(1)	13(1)	2(1)	0(1)	-1(1)
P(1)	14(1)	15(1)	14(1)	2(1)	1(1)	0(1)
Rh(1)	14(1)	14(1)	19(1)	2(1)	1(1)	-1(1)
Si(1)	18(1)	23(1)	14(1)	3(1)	-2(1)	0(1)
Si(2)	23(1)	19(1)	18(1)	-1(1)	-2(1)	-6(1)

Table A.2.25. Hydrogen coordinates (x 10^4) and isotropic displacement parameters (Å^{2}x 10^3) for Rh(cod)Cl·**B4**.

	x	y	z	U(eq)
H(4)	9794	10460	2443	19
H(6)	10818	11158	1550	23
H(7)	10904	11489	503	30
H(8)	9393	11016	-162	27
H(9)	7746	10286	229	21
H(11A)	7024	9304	4149	43
H(11B)	6461	8888	3541	43
H(11C)	6454	9946	3645	43
H(12A)	9258	8272	3864	46
H(12B)	9854	8360	3203	46
H(12C)	8614	7882	3270	46
H(13A)	8994	10975	3558	44
H(13B)	10093	10318	3550	44
H(13C)	9235	10328	4128	44
H(17)	3740	8881	-52	25
H(19)	3217	10487	-220	30
H(20)	3597	11999	-59	33
H(21)	5130	12442	609	30
H(22)	6331	11374	1076	25
H(24A)	5400	7290	-701	53
H(24B)	4038	7516	-717	53
H(24C)	4463	6499	-698	53
H(25A)	5583	5718	421	43
H(25B)	5623	6235	1063	43
H(25C)	6498	6509	524	43
H(26A)	2829	6268	421	44
H(26B)	2512	7308	422	44
H(26C)	3020	6848	1029	44
H(27A)	8666	7005	2370	47
H(27B)	8259	7542	1773	47
H(27C)	7961	6504	1839	47

H(28A)	6626	6109	2792	43
H(28B)	5876	6913	3069	43
H(28C)	7231	6827	3232	43
H(31A)	2519	8982	1347	33
H(31B)	2122	9818	1753	33
H(32A)	1140	8938	2448	32
H(32B)	856	8452	1812	32
H(35A)	3049	8062	3782	36
H(35B)	1719	8329	3666	36
H(36A)	3205	9557	3607	34
H(36B)	2198	9555	3098	34
H(29)	4470(30)	9340(30)	2866(17)	20(10)
H(30)	4210(40)	9430(30)	1837(18)	31(11)
H(33)	1920(30)	7230(20)	2119(15)	16(8)
H(34)	2560(30)	7020(20)	3059(14)	8(8)

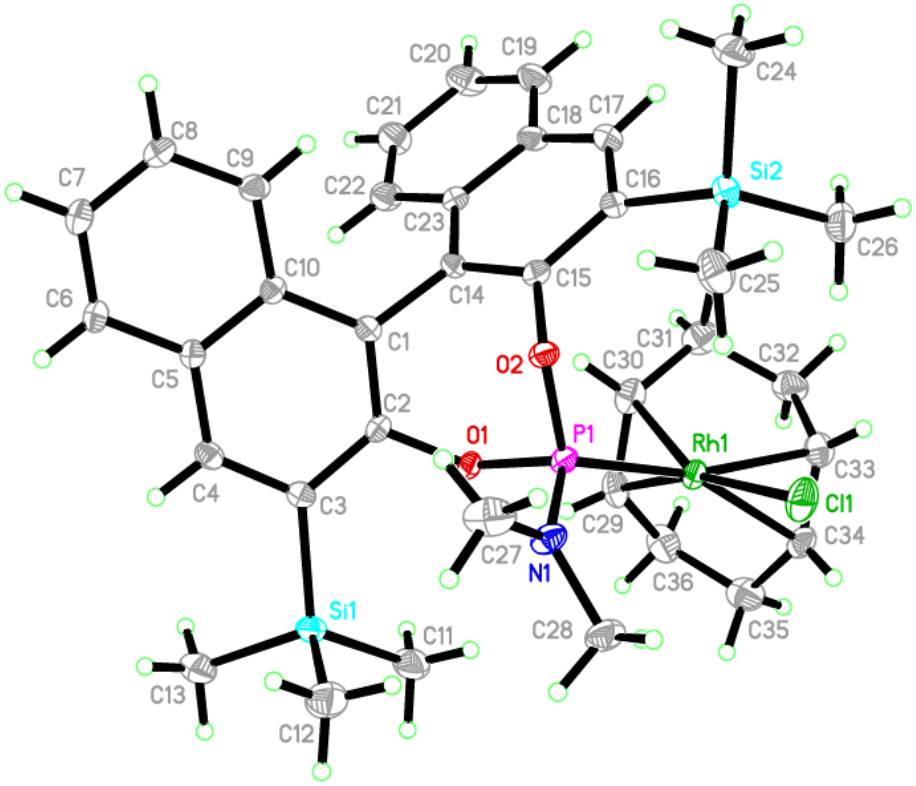

Table A.2.26. Crystal data and structure refinement for Rh(cod)Cl·**T1**.

Identification code	rovis53_0m	
Empirical formula	$C_{43}H_{50}Cl_5NO_4PRh$	
Formula weight	955.97	
Temperature	296(2) K	
Wavelength	0.71073 Å	
Crystal system	Monoclinic	
Space group	$P2_1$	
Unit cell dimensions	a = 10.8877(3) Å	α= 90°.
	b = 18.0279(5) Å	β= 91.9240(10)°.
	c = 11.1484(3) Å	γ = 90°.
Volume	2187.00(10) $Å^3$	
Z	2	
Density (calculated)	1.452 Mg/m^3	
Absorption coefficient	0.774 mm^{-1}	
F(000)	984	
Crystal size	0.39 x 0.13 x 0.11 mm^3	
Theta range for data collection	1.83 to 34.97°.	
Index ranges	-17<=h<=17, -26<=k<=29, -17<=l<=17	
Reflections collected	46802	
Independent reflections	17252 [R(int) = 0.0404]	
Completeness to theta = 34.97°	99.7 %	
Absorption correction	Semi-empirical from equivalents	
Max. and min. transmission	0.9197 and 0.7512	
Refinement method	Full-matrix least-squares on F^2	
Data / restraints / parameters	17252 / 1 / 517	
Goodness-of-fit on F^2	1.032	
Final R indices [I>2sigma(I)]	R1 = 0.0430, wR2 = 0.0935	
R indices (all data)	R1 = 0.0552, wR2 = 0.1010	
Absolute structure parameter	-0.015(17)	
Largest diff. peak and hole	1.210 and -0.966 e.$Å^{-3}$	

Table A.2.27. Atomic coordinates (x 10^4) and equivalent isotropic displacement parameters ($Å^2$x 10^3) for Rh(cod)Cl·**T1**. U(eq) is defined as one third of the trace of the orthogonalized U^{ij} tensor.

	x	y	z	U(eq)
C(1)	589(2)	483(1)	5512(2)	12(1)
C(2)	-646(2)	474(1)	6178(2)	13(1)
C(3)	-1007(2)	1250(1)	6583(2)	14(1)
C(4)	-655(2)	1408(1)	7923(2)	13(1)
C(5)	-2642(2)	765(2)	5463(2)	17(1)
C(6)	-2745(2)	1161(2)	4260(2)	22(1)
C(7)	-3813(2)	381(2)	5799(3)	27(1)
C(8)	1227(2)	-268(1)	5507(2)	14(1)
C(9)	2485(2)	-301(2)	5292(2)	18(1)
C(10)	3092(2)	-976(2)	5259(3)	23(1)
C(11)	2441(3)	-1632(2)	5424(3)	26(1)

C(12)	1197(3)	-1608(2)	5619(3)	24(1)
C(13)	586(2)	-929(2)	5654(2)	19(1)
C(14)	404(2)	764(1)	4225(2)	14(1)
C(15)	-162(2)	292(2)	3374(2)	18(1)
C(16)	-445(3)	539(2)	2218(2)	22(1)
C(17)	-133(3)	1256(2)	1888(2)	28(1)
C(18)	463(3)	1723(2)	2703(2)	26(1)
C(19)	727(2)	1475(2)	3876(2)	19(1)
C(20)	-1614(2)	1070(2)	8743(2)	16(1)
C(21)	-1567(3)	322(2)	9054(2)	21(1)
C(22)	-2487(3)	6(2)	9744(3)	28(1)
C(23)	-3436(3)	436(2)	10134(3)	34(1)
C(24)	-3472(3)	1182(2)	9863(3)	38(1)
C(25)	-2564(3)	1498(2)	9161(3)	29(1)
C(26)	-498(2)	2233(2)	8177(2)	16(1)
C(27)	-1119(2)	2762(2)	7478(3)	20(1)
C(28)	-1075(3)	3513(2)	7792(3)	26(1)
C(29)	-412(3)	3732(2)	8816(3)	30(1)
C(30)	239(3)	3213(2)	9504(3)	27(1)
C(31)	193(2)	2465(2)	9185(2)	20(1)
C(32)	1872(3)	-340(2)	8435(3)	23(1)
C(33)	3801(2)	305(2)	8107(3)	22(1)
C(34)	2225(2)	2687(1)	6316(2)	15(1)
C(35)	3284(2)	2281(1)	6007(2)	17(1)
C(36)	4526(2)	2650(2)	5803(3)	23(1)
C(37)	5355(2)	2684(2)	6934(3)	23(1)
C(38)	4660(2)	2789(2)	8074(3)	20(1)
C(39)	3711(2)	3280(2)	8234(2)	19(1)
C(40)	3247(3)	3825(2)	7280(3)	22(1)
C(41)	2154(2)	3513(2)	6523(2)	21(1)
C(42)	6599(4)	7882(3)	7469(5)	57(1)
C(43)	6926(3)	5445(2)	7837(3)	30(1)
Cl(1)	3137(1)	1804(1)	9920(1)	21(1)
Cl(2)	5112(2)	8186(2)	7633(2)	120(1)
Cl(3)	7633(2)	8570(1)	7149(2)	84(1)
Cl(4)	5882(1)	5954(1)	6915(1)	47(1)
Cl(5)	6251(1)	4595(1)	8296(1)	38(1)
N(1)	2454(2)	344(1)	8050(2)	16(1)
O(1)	1376(2)	1025(1)	6136(2)	12(1)
O(2)	492(2)	1009(1)	8220(2)	14(1)
O(3)	-1663(2)	226(1)	5450(2)	17(1)
O(4)	-2308(2)	1273(1)	6403(2)	19(1)
P(1)	1778(1)	1100(1)	7553(1)	12(1)
Rh(1)	2923(1)	2136(1)	7860(1)	13(1)

Table A.2.28. Bond lengths [Å] and angles [°] for Rh(cod)Cl·**T1**.

C(1)-O(1)	1.461(3)	C(1)-C(2)	1.558(3)
C(1)-C(8)	1.522(3)	C(2)-O(3)	1.423(3)
C(1)-C(14)	1.529(3)	C(2)-C(3)	1.526(4)

C(3)-O(4)	1.425(3)	Cl(1)-Rh(1)	2.3775(6)
C(3)-C(4)	1.555(3)	N(1)-P(1)	1.636(2)
C(4)-O(2)	1.470(3)	O(1)-P(1)	1.6301(17)
C(4)-C(26)	1.523(4)	O(2)-P(1)	1.6158(17)
C(4)-C(20)	1.537(3)	P(1)-Rh(1)	2.2649(6)
C(5)-O(4)	1.429(3)		
C(5)-O(3)	1.443(3)	O(1)-C(1)-C(8)	109.71(18)
C(5)-C(7)	1.508(4)	O(1)-C(1)-C(14)	106.33(18)
C(5)-C(6)	1.521(4)	C(8)-C(1)-C(14)	109.77(19)
C(8)-C(13)	1.393(4)	O(1)-C(1)-C(2)	106.35(18)
C(8)-C(9)	1.399(3)	C(8)-C(1)-C(2)	113.18(19)
C(9)-C(10)	1.387(4)	C(14)-C(1)-C(2)	111.21(18)
C(10)-C(11)	1.393(4)	O(3)-C(2)-C(3)	104.71(18)
C(11)-C(12)	1.380(4)	O(3)-C(2)-C(1)	113.52(19)
C(12)-C(13)	1.395(4)	C(3)-C(2)-C(1)	111.47(19)
C(14)-C(19)	1.387(4)	O(4)-C(3)-C(2)	104.44(19)
C(14)-C(15)	1.403(4)	O(4)-C(3)-C(4)	109.97(19)
C(15)-C(16)	1.389(4)	C(2)-C(3)-C(4)	113.27(19)
C(16)-C(17)	1.388(5)	O(2)-C(4)-C(26)	110.28(18)
C(17)-C(18)	1.384(4)	O(2)-C(4)-C(20)	105.10(19)
C(18)-C(19)	1.403(4)	C(26)-C(4)-C(20)	110.6(2)
C(20)-C(25)	1.384(4)	O(2)-C(4)-C(3)	107.83(18)
C(20)-C(21)	1.393(4)	C(26)-C(4)-C(3)	112.4(2)
C(21)-C(22)	1.404(4)	C(20)-C(4)-C(3)	110.4(2)
C(22)-C(23)	1.374(5)	O(4)-C(5)-O(3)	105.62(18)
C(23)-C(24)	1.379(5)	O(4)-C(5)-C(7)	108.0(2)
C(24)-C(25)	1.402(4)	O(3)-C(5)-C(7)	108.9(2)
C(26)-C(27)	1.392(4)	O(4)-C(5)-C(6)	110.8(2)
C(26)-C(31)	1.395(4)	O(3)-C(5)-C(6)	109.9(2)
C(27)-C(28)	1.399(4)	C(7)-C(5)-C(6)	113.4(2)
C(28)-C(29)	1.388(5)	C(13)-C(8)-C(9)	118.8(2)
C(29)-C(30)	1.389(5)	C(13)-C(8)-C(1)	121.9(2)
C(30)-C(31)	1.394(4)	C(9)-C(8)-C(1)	119.2(2)
C(32)-N(1)	1.458(3)	C(10)-C(9)-C(8)	120.8(3)
C(33)-N(1)	1.468(3)	C(9)-C(10)-C(11)	119.8(3)
C(34)-C(35)	1.418(3)	C(12)-C(11)-C(10)	120.0(3)
C(34)-C(41)	1.509(4)	C(11)-C(12)-C(13)	120.3(3)
C(34)-Rh(1)	2.107(2)	C(8)-C(13)-C(12)	120.3(2)
C(35)-C(36)	1.531(4)	C(19)-C(14)-C(15)	118.7(2)
C(35)-Rh(1)	2.131(2)	C(19)-C(14)-C(1)	122.9(2)
C(36)-C(37)	1.528(4)	C(15)-C(14)-C(1)	118.3(2)
C(37)-C(38)	1.513(4)	C(16)-C(15)-C(14)	120.8(3)
C(38)-C(39)	1.376(4)	C(17)-C(16)-C(15)	119.7(3)
C(38)-Rh(1)	2.233(3)	C(18)-C(17)-C(16)	120.4(3)
C(39)-C(40)	1.522(4)	C(17)-C(18)-C(19)	119.6(3)
C(39)-Rh(1)	2.267(3)	C(14)-C(19)-C(18)	120.7(2)
C(40)-C(41)	1.541(4)	C(25)-C(20)-C(21)	118.6(2)
C(42)-Cl(3)	1.722(5)	C(25)-C(20)-C(4)	120.6(2)
C(42)-Cl(2)	1.724(5)	C(21)-C(20)-C(4)	120.8(2)
C(43)-Cl(4)	1.764(3)	C(20)-C(21)-C(22)	120.5(3)
C(43)-Cl(5)	1.783(4)	C(23)-C(22)-C(21)	120.2(3)

C(22)-C(23)-C(24)	119.8(3)	C(32)-N(1)-C(33)	113.0(2)
C(23)-C(24)-C(25)	120.3(3)	C(32)-N(1)-P(1)	127.55(18)
C(20)-C(25)-C(24)	120.6(3)	C(33)-N(1)-P(1)	119.47(18)
C(27)-C(26)-C(31)	118.9(3)	C(1)-O(1)-P(1)	130.60(15)
C(27)-C(26)-C(4)	121.0(2)	C(4)-O(2)-P(1)	126.14(15)
C(31)-C(26)-C(4)	119.8(2)	C(2)-O(3)-C(5)	110.09(19)
C(26)-C(27)-C(28)	120.7(3)	C(3)-O(4)-C(5)	108.18(18)
C(29)-C(28)-C(27)	119.5(3)	O(2)-P(1)-O(1)	103.21(9)
C(28)-C(29)-C(30)	120.3(3)	O(2)-P(1)-N(1)	98.40(10)
C(29)-C(30)-C(31)	119.8(3)	O(1)-P(1)-N(1)	111.29(11)
C(30)-C(31)-C(26)	120.6(3)	O(2)-P(1)-Rh(1)	119.69(7)
C(35)-C(34)-C(41)	126.4(2)	O(1)-P(1)-Rh(1)	110.07(7)
C(35)-C(34)-Rh(1)	71.38(14)	N(1)-P(1)-Rh(1)	113.34(8)
C(41)-C(34)-Rh(1)	111.09(17)	C(34)-Rh(1)-C(35)	39.08(9)
C(34)-C(35)-C(36)	122.8(2)	C(34)-Rh(1)-C(38)	96.86(10)
C(34)-C(35)-Rh(1)	69.53(14)	C(35)-Rh(1)-C(38)	81.74(10)
C(36)-C(35)-Rh(1)	112.97(17)	C(34)-Rh(1)-P(1)	94.82(7)
C(37)-C(36)-C(35)	113.3(2)	C(35)-Rh(1)-P(1)	94.20(7)
C(38)-C(37)-C(36)	113.6(2)	C(38)-Rh(1)-P(1)	155.60(8)
C(39)-C(38)-C(37)	126.0(3)	C(34)-Rh(1)-C(39)	81.07(10)
C(39)-C(38)-Rh(1)	73.56(15)	C(35)-Rh(1)-C(39)	89.18(10)
C(37)-C(38)-Rh(1)	106.85(18)	C(38)-Rh(1)-C(39)	35.59(10)
C(38)-C(39)-C(40)	124.0(3)	P(1)-Rh(1)-C(39)	168.76(7)
C(38)-C(39)-Rh(1)	70.85(16)	C(34)-Rh(1)-Cl(1)	158.23(7)
C(40)-C(39)-Rh(1)	110.12(17)	C(35)-Rh(1)-Cl(1)	162.17(7)
C(39)-C(40)-C(41)	112.3(2)	C(38)-Rh(1)-Cl(1)	88.52(7)
C(34)-C(41)-C(40)	113.7(2)	P(1)-Rh(1)-Cl(1)	88.51(2)
Cl(3)-C(42)-Cl(2)	114.6(3)	C(39)-Rh(1)-Cl(1)	91.56(7)
Cl(4)-C(43)-Cl(5)	110.48(17)		

Symmetry transformations used to generate equivalent atoms:

Table A.2.29. Anisotropic displacement parameters ($Å^2 x\ 10^3$)for Rh(cod)Cl·**T1**. The anisotropic displacement factor exponent takes the form: $-2\pi^2[\ h^2 a^{*2} U^{11} + ... + 2\ h\ k\ a^*\ b^*\ U^{12}\ ]$

	U^{11}	U^{22}	U^{33}	U^{23}	U^{13}	U^{12}
C(1)	10(1)	11(1)	14(1)	0(1)	1(1)	-1(1)
C(2)	12(1)	14(1)	13(1)	0(1)	0(1)	-1(1)
C(3)	13(1)	15(1)	14(1)	1(1)	-1(1)	2(1)
C(4)	11(1)	16(1)	13(1)	0(1)	1(1)	1(1)
C(5)	14(1)	20(1)	18(1)	-3(1)	-1(1)	1(1)
C(6)	18(1)	27(2)	19(1)	1(1)	-4(1)	2(1)
C(7)	16(1)	35(2)	31(2)	2(1)	2(1)	-2(1)
C(8)	15(1)	12(1)	14(1)	-1(1)	1(1)	0(1)
C(9)	17(1)	19(1)	20(1)	-1(1)	5(1)	-1(1)
C(10)	17(1)	20(1)	32(1)	-4(1)	3(1)	7(1)
C(11)	31(1)	17(1)	30(2)	-2(1)	-2(1)	6(1)
C(12)	31(1)	13(1)	27(1)	-1(1)	3(1)	0(1)
C(13)	20(1)	15(1)	22(1)	0(1)	0(1)	-1(1)

C(14)	15(1)	15(1)	12(1)	0(1)	1(1)	3(1)
C(15)	19(1)	17(1)	18(1)	1(1)	0(1)	-2(1)
C(16)	25(1)	27(1)	14(1)	-2(1)	-3(1)	-2(1)
C(17)	35(2)	37(2)	13(1)	4(1)	-1(1)	-5(1)
C(18)	34(2)	26(2)	18(1)	7(1)	-1(1)	-6(1)
C(19)	23(1)	16(1)	16(1)	1(1)	1(1)	-3(1)
C(20)	13(1)	23(1)	14(1)	5(1)	1(1)	-3(1)
C(21)	24(1)	23(1)	18(1)	0(1)	5(1)	-6(1)
C(22)	31(2)	29(2)	22(1)	7(1)	1(1)	-14(1)
C(23)	15(1)	59(2)	28(2)	22(2)	2(1)	-8(1)
C(24)	20(1)	53(2)	42(2)	16(2)	17(1)	8(1)
C(25)	17(1)	39(2)	32(2)	16(1)	9(1)	7(1)
C(26)	15(1)	19(2)	16(1)	-2(1)	6(1)	-1(1)
C(27)	19(1)	20(1)	21(1)	1(1)	6(1)	3(1)
C(28)	27(1)	18(1)	34(2)	4(1)	12(1)	5(1)
C(29)	36(2)	17(1)	39(2)	-10(1)	18(1)	-3(1)
C(30)	30(1)	23(1)	29(1)	-9(1)	8(1)	-6(1)
C(31)	20(1)	22(1)	18(1)	-2(1)	4(1)	-4(1)
C(32)	22(1)	18(1)	28(1)	10(1)	-4(1)	-3(1)
C(33)	15(1)	23(1)	29(1)	2(1)	1(1)	3(1)
C(34)	16(1)	16(1)	14(1)	0(1)	1(1)	-1(1)
C(35)	18(1)	18(2)	14(1)	1(1)	3(1)	-4(1)
C(36)	19(1)	23(1)	28(1)	-2(1)	9(1)	-4(1)
C(37)	14(1)	23(1)	33(1)	-1(1)	3(1)	-3(1)
C(38)	15(1)	19(1)	27(1)	3(1)	-2(1)	-4(1)
C(39)	21(1)	14(1)	21(1)	-3(1)	1(1)	-4(1)
C(40)	26(1)	13(1)	27(1)	0(1)	1(1)	-2(1)
C(41)	22(1)	17(1)	23(1)	2(1)	0(1)	1(1)
C(42)	53(3)	54(3)	63(3)	22(2)	0(2)	2(2)
C(43)	25(1)	34(2)	30(2)	-8(1)	-1(1)	1(1)
Cl(1)	23(1)	25(1)	14(1)	0(1)	-1(1)	-3(1)
Cl(2)	67(1)	161(2)	132(2)	47(2)	11(1)	49(1)
Cl(3)	118(1)	45(1)	91(1)	13(1)	39(1)	-11(1)
Cl(4)	43(1)	52(1)	45(1)	-6(1)	-12(1)	17(1)
Cl(5)	29(1)	36(1)	51(1)	-10(1)	12(1)	-1(1)
N(1)	12(1)	14(1)	20(1)	4(1)	-1(1)	0(1)
O(1)	13(1)	13(1)	12(1)	0(1)	-1(1)	-3(1)
O(2)	12(1)	15(1)	14(1)	3(1)	2(1)	0(1)
O(3)	12(1)	19(1)	19(1)	-1(1)	-3(1)	-1(1)
O(4)	13(1)	24(1)	18(1)	-5(1)	-2(1)	3(1)
P(1)	11(1)	13(1)	11(1)	1(1)	0(1)	-1(1)
Rh(1)	12(1)	13(1)	13(1)	-1(1)	1(1)	-2(1)

Table A.2.30. Hydrogen coordinates (x 10^4) and isotropic displacement parameters ($Å^2$x 10^3) for Rh(cod)Cl·**T1**.

	x	y	z	U(eq)
H(2)	-557	151	6884	15
H(3)	-625	1621	6073	17
H(6A)	-3393	1522	4276	33
H(6B)	-2925	806	3636	33
H(6C)	-1982	1405	4107	33
H(7A)	-3697	151	6571	41
H(7B)	-4023	10	5209	41
H(7C)	-4465	739	5830	41
H(9)	2918	136	5169	22
H(10)	3930	-992	5127	28
H(11)	2846	-2086	5402	31
H(12)	765	-2046	5728	28
H(13)	-255	-917	5777	23
H(15)	-349	-193	3586	22
H(16)	-842	226	1667	26
H(17)	-325	1422	1115	34
H(18)	688	2199	2474	31
H(19)	1123	1789	4425	22
H(21)	-921	29	8803	26
H(22)	-2454	-496	9937	33
H(23)	-4053	224	10579	40
H(24)	-4101	1476	10146	46
H(25)	-2600	2001	8976	35
H(27)	-1568	2614	6795	24
H(28)	-1487	3864	7317	31
H(29)	-403	4229	9043	36
H(30)	703	3363	10176	33
H(31)	627	2118	9649	24
H(32A)	2173	-749	7977	34
H(32B)	997	-301	8308	34
H(32C)	2061	-421	9272	34
H(33A)	4078	188	8912	33
H(33B)	4135	775	7877	33
H(33C)	4071	-73	7570	33
H(36A)	4945	2376	5188	28
H(36B)	4385	3149	5507	28
H(37A)	5828	2229	6998	28
H(37B)	5931	3091	6857	28
H(40A)	3911	3945	6754	26
H(40B)	2996	4280	7666	26
H(41A)	1399	3624	6924	25
H(41B)	2119	3762	5752	25
H(42A)	6873	7636	8205	68
H(42B)	6601	7516	6831	68

H(43A)	7160	5737	8538	36
H(43B)	7662	5342	7399	36
H(39)	3460(30)	3371(18)	9050(30)	12(7)
H(38)	5010(30)	2555(19)	8900(30)	17(8)
H(34)	1460(30)	2490(18)	6010(30)	13(7)
H(35)	3170(30)	1810(20)	5610(30)	20(8)

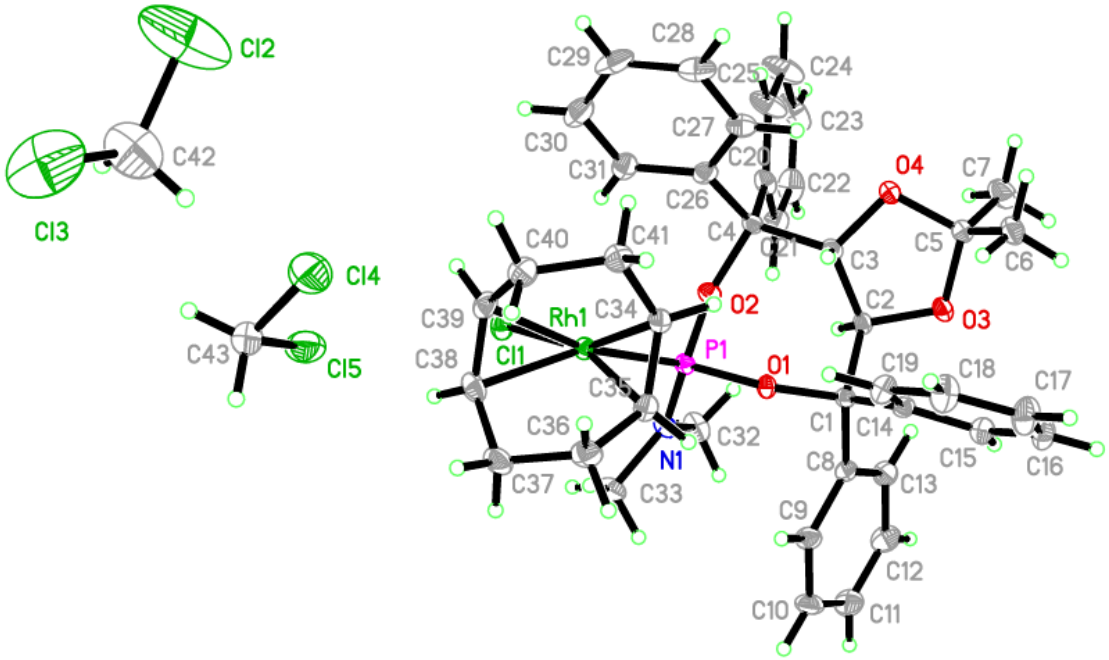

Table A.2.31. Crystal data and structure refinement for Rh(cod)Cl·**T8**.

Identification code	rovis73_0m	
Empirical formula	$C_{51}H_{64}ClNO_4PRh$	
Formula weight	924.36	
Temperature	120 K	
Wavelength	0.71073 Å	
Crystal system	Orthorhombic	
Space group	$P2_12_12_1$	
Unit cell dimensions	a = 15.3754(4) Å	α= 90°.
	b = 17.3853(4) Å	β= 90°.
	c = 18.1214(4) Å	γ = 90°.
Volume	4844.0(2) $Å^3$	
Z	4	
Density (calculated)	1.268 Mg/m^3	
Absorption coefficient	0.483 mm^{-1}	
F(000)	1944	
Crystal size	0.31 x 0.26 x 0.19 mm^3	
Theta range for data collection	2.10 to 36.43°.	
Index ranges	-25<=h<=25, -28<=k<=25, -30<=l<=28	
Reflections collected	52621	
Independent reflections	23450 [R(int) = 0.0546]	
Completeness to theta = 36.43°	99.5 %	
Absorption correction	Semi-empirical from equivalents	
Max. and min. transmission	0.9159 and 0.8658	
Refinement method	Full-matrix least-squares on F^2	
Data / restraints / parameters	23450 / 0 / 542	
Goodness-of-fit on F^2	1.006	
Final R indices [I>2sigma(I)]	R1 = 0.0532, wR2 = 0.1024	
R indices (all data)	R1 = 0.0916, wR2 = 0.1182	
Absolute structure parameter	-0.029(17)	
Largest diff. peak and hole	1.789 and -0.960 e.$Å^{-3}$	

Table A.2.32. Atomic coordinates (x 10^4) and equivalent isotropic displacement parameters ($Å^2$x 10^3) for Rh(cod)Cl·**T8**. U(eq) is defined as one third of the trace of the orthogonalized U^{ij} tensor.

	x	y	z	U(eq)
C(1)	697(1)	10732(1)	4473(1)	16(1)
C(2)	120(2)	10735(1)	5177(1)	18(1)
C(3)	526(2)	10250(1)	5800(1)	18(1)
C(4)	115(2)	9427(1)	5839(1)	17(1)
C(5)	1486(2)	11269(1)	4544(1)	18(1)
C(6)	1388(2)	12061(1)	4420(2)	26(1)
C(7)	2094(2)	12556(2)	4497(2)	34(1)
C(8)	2903(2)	12264(2)	4690(2)	34(1)
C(9)	3007(2)	11484(2)	4823(2)	33(1)
C(10)	2296(2)	10995(2)	4749(2)	26(1)
C(11)	180(2)	10935(1)	3778(1)	17(1)

C(12)	452(2)	10655(1)	3102(1)	19(1)
C(13)	33(2)	10870(2)	2447(2)	23(1)
C(14)	-654(2)	11389(2)	2492(2)	25(1)
C(15)	-943(2)	11677(2)	3164(2)	24(1)
C(16)	-527(2)	11441(1)	3806(2)	21(1)
C(17)	-768(2)	9458(1)	6231(2)	23(1)
C(18)	-806(2)	9415(2)	6996(2)	30(1)
C(19)	-1596(3)	9474(2)	7368(2)	39(1)
C(20)	-2349(2)	9563(2)	6957(2)	45(1)
C(21)	-2339(2)	9599(2)	6187(2)	35(1)
C(22)	-1532(2)	9550(1)	5837(2)	26(1)
C(23)	721(2)	8852(1)	6216(1)	19(1)
C(24)	1323(2)	9082(2)	6741(2)	24(1)
C(25)	1814(2)	8547(2)	7126(2)	29(1)
C(26)	1704(2)	7762(2)	6971(2)	26(1)
C(27)	1104(2)	7519(2)	6444(2)	23(1)
C(28)	614(2)	8068(1)	6076(1)	20(1)
C(29)	244(2)	11465(2)	6258(2)	36(1)
C(30)	2693(2)	8895(2)	4784(2)	29(1)
C(31)	2612(2)	8972(2)	4020(2)	29(1)
C(32)	3169(2)	8601(2)	3429(2)	42(1)
C(33)	3379(2)	7764(2)	3595(2)	37(1)
C(34)	2644(2)	7352(2)	3981(2)	25(1)
C(35)	2602(2)	7271(2)	4736(2)	26(1)
C(36)	3226(2)	7606(2)	5280(2)	32(1)
C(37)	3434(2)	8456(2)	5151(2)	45(1)
C(38)	2452(2)	8795(2)	7718(2)	45(1)
C(39)	992(2)	6675(2)	6273(2)	33(1)
C(40)	-3166(2)	9658(2)	5747(2)	47(1)
C(41)	-1687(2)	12241(2)	3190(2)	37(1)
C(42)	327(2)	10538(2)	1724(2)	33(1)
C(43)	1982(3)	13405(2)	4358(3)	60(1)
C(44)	-1015(2)	9237(2)	3724(2)	23(1)
C(45)	162(2)	8627(2)	3047(2)	26(1)
C(46)	-700(2)	8292(2)	2793(2)	39(1)
C(47)	-1329(2)	8931(2)	2986(2)	39(1)
C(48)	1122(3)	11886(2)	6364(2)	65(1)
C(49)	-1622(3)	9431(2)	8203(2)	60(1)
C(50)	-492(4)	11773(3)	6691(2)	115(3)
C(51)	3897(2)	11161(2)	5042(3)	61(1)
Cl(1)	554(1)	7244(1)	4347(1)	21(1)
N(1)	-78(1)	9020(1)	3742(1)	18(1)
O(1)	-70(1)	9177(1)	5090(1)	16(1)
O(2)	1061(1)	9964(1)	4404(1)	15(1)
O(3)	363(1)	10675(1)	6449(1)	23(1)
O(4)	37(1)	11483(1)	5489(1)	23(1)
P(1)	618(1)	9115(1)	4417(1)	14(1)
Rh(1)	1663(1)	8194(1)	4412(1)	17(1)

Table A.2.33. Bond lengths [Å] and angles [°] for Rh(cod)Cl·**T8**.

C(1)-O(2)	1.454(3)	C(30)-Rh(1)	2.108(3)
C(1)-C(11)	1.531(3)	C(31)-C(32)	1.515(4)
C(1)-C(5)	1.536(3)	C(31)-Rh(1)	2.113(3)
C(1)-C(2)	1.553(3)	C(32)-C(33)	1.521(4)
C(2)-O(4)	1.425(3)	C(33)-C(34)	1.510(4)
C(2)-C(3)	1.541(3)	C(34)-C(35)	1.376(4)
C(3)-O(3)	1.412(3)	C(34)-Rh(1)	2.242(3)
C(3)-C(4)	1.565(3)	C(35)-C(36)	1.495(4)
C(4)-O(1)	1.453(3)	C(35)-Rh(1)	2.236(3)
C(4)-C(23)	1.528(3)	C(36)-C(37)	1.530(4)
C(4)-C(17)	1.533(3)	C(44)-N(1)	1.490(3)
C(5)-C(10)	1.384(4)	C(44)-C(47)	1.518(4)
C(5)-C(6)	1.402(3)	C(45)-N(1)	1.479(3)
C(6)-C(7)	1.392(4)	C(45)-C(46)	1.520(4)
C(7)-C(8)	1.388(5)	C(46)-C(47)	1.513(5)
C(7)-C(43)	1.508(4)	Cl(1)-Rh(1)	2.3764(6)
C(8)-C(9)	1.388(4)	N(1)-P(1)	1.633(2)
C(9)-C(10)	1.392(4)	O(1)-P(1)	1.6188(18)
C(9)-C(51)	1.531(5)	O(2)-P(1)	1.6261(15)
C(11)-C(12)	1.382(3)	P(1)-Rh(1)	2.2688(6)
C(11)-C(16)	1.399(3)		
C(12)-C(13)	1.401(4)	O(2)-C(1)-C(11)	109.86(19)
C(13)-C(14)	1.392(4)	O(2)-C(1)-C(5)	105.16(17)
C(13)-C(42)	1.501(4)	C(11)-C(1)-C(5)	109.80(19)
C(14)-C(15)	1.391(4)	O(2)-C(1)-C(2)	107.07(18)
C(15)-C(16)	1.390(4)	C(11)-C(1)-C(2)	112.30(19)
C(15)-C(41)	1.508(4)	C(5)-C(1)-C(2)	112.36(19)
C(17)-C(22)	1.384(4)	O(4)-C(2)-C(3)	104.19(19)
C(17)-C(18)	1.389(4)	O(4)-C(2)-C(1)	112.35(19)
C(18)-C(19)	1.394(4)	C(3)-C(2)-C(1)	111.6(2)
C(19)-C(20)	1.385(5)	O(3)-C(3)-C(2)	104.58(19)
C(19)-C(49)	1.515(5)	O(3)-C(3)-C(4)	111.60(19)
C(20)-C(21)	1.398(5)	C(2)-C(3)-C(4)	111.7(2)
C(21)-C(22)	1.396(4)	O(1)-C(4)-C(23)	109.97(19)
C(21)-C(40)	1.504(5)	O(1)-C(4)-C(17)	105.61(19)
C(23)-C(24)	1.387(4)	C(23)-C(4)-C(17)	110.8(2)
C(23)-C(28)	1.396(3)	O(1)-C(4)-C(3)	108.04(17)
C(24)-C(25)	1.387(4)	C(23)-C(4)-C(3)	111.9(2)
C(25)-C(26)	1.404(4)	C(17)-C(4)-C(3)	110.31(19)
C(25)-C(38)	1.516(4)	C(10)-C(5)-C(6)	118.6(2)
C(26)-C(27)	1.393(4)	C(10)-C(5)-C(1)	121.5(2)
C(27)-C(28)	1.387(4)	C(6)-C(5)-C(1)	119.9(2)
C(27)-C(39)	1.510(4)	C(7)-C(6)-C(5)	120.4(3)
C(29)-O(3)	1.428(3)	C(8)-C(7)-C(6)	119.9(3)
C(29)-O(4)	1.428(3)	C(8)-C(7)-C(43)	120.1(3)
C(29)-C(50)	1.478(5)	C(6)-C(7)-C(43)	120.0(3)
C(29)-C(48)	1.548(5)	C(9)-C(8)-C(7)	120.3(3)
C(30)-C(31)	1.396(4)	C(8)-C(9)-C(10)	119.3(3)
C(30)-C(37)	1.524(4)	C(8)-C(9)-C(51)	120.4(3)

C(10)-C(9)-C(51)	120.3(3)	C(37)-C(30)-Rh(1)	114.34(19)
C(5)-C(10)-C(9)	121.5(3)	C(30)-C(31)-C(32)	127.5(3)
C(12)-C(11)-C(16)	119.2(2)	C(30)-C(31)-Rh(1)	70.52(17)
C(12)-C(11)-C(1)	119.5(2)	C(32)-C(31)-Rh(1)	110.8(2)
C(16)-C(11)-C(1)	121.2(2)	C(31)-C(32)-C(33)	112.8(3)
C(11)-C(12)-C(13)	121.2(2)	C(34)-C(33)-C(32)	112.7(3)
C(14)-C(13)-C(12)	118.2(2)	C(35)-C(34)-C(33)	123.0(3)
C(14)-C(13)-C(42)	121.9(2)	C(35)-C(34)-Rh(1)	71.89(17)
C(12)-C(13)-C(42)	119.9(3)	C(33)-C(34)-Rh(1)	110.85(18)
C(15)-C(14)-C(13)	121.8(2)	C(34)-C(35)-C(36)	125.8(3)
C(16)-C(15)-C(14)	118.6(2)	C(34)-C(35)-Rh(1)	72.31(17)
C(16)-C(15)-C(41)	121.1(2)	C(36)-C(35)-Rh(1)	107.93(18)
C(14)-C(15)-C(41)	120.3(2)	C(35)-C(36)-C(37)	114.2(2)
C(15)-C(16)-C(11)	120.9(2)	C(30)-C(37)-C(36)	113.2(3)
C(22)-C(17)-C(18)	119.0(2)	N(1)-C(44)-C(47)	103.7(2)
C(22)-C(17)-C(4)	121.1(2)	N(1)-C(45)-C(46)	102.6(2)
C(18)-C(17)-C(4)	119.8(2)	C(47)-C(46)-C(45)	101.8(2)
C(17)-C(18)-C(19)	121.0(3)	C(46)-C(47)-C(44)	105.0(2)
C(20)-C(19)-C(18)	118.5(3)	C(45)-N(1)-C(44)	109.9(2)
C(20)-C(19)-C(49)	121.4(3)	C(45)-N(1)-P(1)	121.38(18)
C(18)-C(19)-C(49)	120.1(4)	C(44)-N(1)-P(1)	128.60(18)
C(19)-C(20)-C(21)	122.2(3)	C(4)-O(1)-P(1)	126.57(15)
C(22)-C(21)-C(20)	117.4(3)	C(1)-O(2)-P(1)	132.17(13)
C(22)-C(21)-C(40)	121.0(3)	C(3)-O(3)-C(29)	108.87(19)
C(20)-C(21)-C(40)	121.5(3)	C(2)-O(4)-C(29)	110.28(19)
C(17)-C(22)-C(21)	121.9(3)	O(1)-P(1)-O(2)	102.94(9)
C(24)-C(23)-C(28)	119.0(2)	O(1)-P(1)-N(1)	98.26(9)
C(24)-C(23)-C(4)	121.7(2)	O(2)-P(1)-N(1)	110.80(10)
C(28)-C(23)-C(4)	119.1(2)	O(1)-P(1)-Rh(1)	120.87(7)
C(25)-C(24)-C(23)	121.0(3)	O(2)-P(1)-Rh(1)	110.09(6)
C(24)-C(25)-C(26)	119.1(3)	N(1)-P(1)-Rh(1)	112.95(8)
C(24)-C(25)-C(38)	121.1(3)	C(30)-Rh(1)-C(31)	38.63(11)
C(26)-C(25)-C(38)	119.8(3)	C(30)-Rh(1)-C(35)	81.15(11)
C(27)-C(26)-C(25)	120.8(3)	C(31)-Rh(1)-C(35)	95.85(12)
C(28)-C(27)-C(26)	118.7(2)	C(30)-Rh(1)-C(34)	89.04(12)
C(28)-C(27)-C(39)	120.6(3)	C(31)-Rh(1)-C(34)	80.58(10)
C(26)-C(27)-C(39)	120.7(2)	C(35)-Rh(1)-C(34)	35.80(10)
C(27)-C(28)-C(23)	121.4(2)	C(30)-Rh(1)-P(1)	97.05(8)
O(3)-C(29)-O(4)	106.7(2)	C(31)-Rh(1)-P(1)	92.20(8)
O(3)-C(29)-C(50)	108.5(3)	C(35)-Rh(1)-P(1)	164.27(8)
O(4)-C(29)-C(50)	109.8(3)	C(34)-Rh(1)-P(1)	159.81(8)
O(3)-C(29)-C(48)	108.2(3)	C(30)-Rh(1)-Cl(1)	162.98(9)
O(4)-C(29)-C(48)	107.7(3)	C(31)-Rh(1)-Cl(1)	157.48(10)
C(50)-C(29)-C(48)	115.4(4)	C(35)-Rh(1)-Cl(1)	88.74(8)
C(31)-C(30)-C(37)	123.2(3)	C(34)-Rh(1)-Cl(1)	90.71(8)
C(31)-C(30)-Rh(1)	70.86(17)	P(1)-Rh(1)-Cl(1)	88.969(19)

Symmetry transformations used to generate equivalent atoms:

Table A.2.34. Anisotropic displacement parameters ($Å^2$x 10^3)for Rh(cod)Cl·**T8**. The anisotropic displacement factor exponent takes the form: $-2\pi^2[h^2a^{*2}U^{11} + ... + 2 h k a^* b^* U^{12}]$

	U^{11}	U^{22}	U^{33}	U^{23}	U^{13}	U^{12}
C(1)	19(1)	12(1)	16(1)	1(1)	0(1)	2(1)
C(2)	21(1)	15(1)	18(1)	0(1)	2(1)	2(1)
C(3)	20(1)	18(1)	15(1)	1(1)	1(1)	0(1)
C(4)	19(1)	16(1)	16(1)	2(1)	2(1)	-2(1)
C(5)	22(1)	18(1)	15(1)	-1(1)	2(1)	-1(1)
C(6)	30(1)	17(1)	29(1)	2(1)	-2(1)	-2(1)
C(7)	41(2)	20(1)	42(2)	1(1)	-8(2)	-8(1)
C(8)	39(2)	26(1)	38(2)	-4(1)	-2(1)	-14(1)
C(9)	22(1)	31(2)	45(2)	1(1)	-5(1)	-8(1)
C(10)	26(1)	19(1)	34(2)	1(1)	-2(1)	-3(1)
C(11)	17(1)	15(1)	20(1)	4(1)	-1(1)	-1(1)
C(12)	19(1)	19(1)	18(1)	3(1)	0(1)	1(1)
C(13)	25(1)	26(1)	18(1)	4(1)	-1(1)	-1(1)
C(14)	25(1)	25(1)	24(1)	11(1)	-3(1)	0(1)
C(15)	22(1)	24(1)	27(1)	5(1)	-1(1)	3(1)
C(16)	24(1)	18(1)	21(1)	2(1)	2(1)	3(1)
C(17)	25(1)	15(1)	28(1)	0(1)	10(1)	-2(1)
C(18)	36(2)	24(1)	30(2)	-3(1)	14(1)	-2(1)
C(19)	53(2)	25(1)	39(2)	-7(1)	25(2)	-8(2)
C(20)	41(2)	22(1)	73(3)	-13(2)	38(2)	-9(1)
C(21)	25(1)	12(1)	66(2)	-5(1)	16(1)	-3(1)
C(22)	20(1)	18(1)	39(2)	0(1)	8(1)	1(1)
C(23)	21(1)	21(1)	15(1)	4(1)	1(1)	-2(1)
C(24)	27(1)	25(1)	19(1)	5(1)	-2(1)	-6(1)
C(25)	30(2)	35(2)	21(1)	6(1)	-8(1)	-5(1)
C(26)	27(1)	26(1)	26(1)	12(1)	-1(1)	0(1)
C(27)	26(1)	24(1)	20(1)	4(1)	3(1)	0(1)
C(28)	22(1)	21(1)	15(1)	3(1)	0(1)	-2(1)
C(29)	62(2)	27(2)	20(1)	-5(1)	-5(1)	14(1)
C(30)	21(1)	18(1)	46(2)	-2(1)	-10(1)	-1(1)
C(31)	20(1)	18(1)	49(2)	4(1)	11(1)	1(1)
C(32)	35(2)	33(2)	58(2)	6(2)	18(2)	7(1)
C(33)	36(2)	30(1)	46(2)	4(1)	17(2)	11(1)
C(34)	24(1)	20(1)	31(2)	-2(1)	2(1)	6(1)
C(35)	22(1)	16(1)	40(2)	3(1)	-6(1)	7(1)
C(36)	29(2)	30(1)	37(2)	3(1)	-9(1)	6(1)
C(37)	30(2)	32(2)	73(2)	-5(2)	-29(2)	2(1)
C(38)	47(2)	48(2)	39(2)	11(2)	-25(2)	-15(2)
C(39)	44(2)	23(2)	33(2)	7(1)	1(1)	6(1)
C(40)	22(1)	20(1)	99(3)	1(2)	20(2)	4(1)
C(41)	34(2)	40(2)	37(2)	9(1)	-3(2)	14(2)
C(42)	38(2)	42(2)	18(1)	3(1)	0(1)	9(1)
C(43)	62(2)	21(1)	97(3)	7(2)	-15(3)	-12(2)
C(44)	17(1)	20(1)	33(1)	3(1)	-4(1)	0(1)
C(45)	28(1)	28(1)	20(1)	-2(1)	-3(1)	3(1)

C(46)	42(2)	42(2)	34(2)	-6(2)	-12(1)	-4(2)
C(47)	31(2)	45(2)	39(2)	-7(2)	-19(1)	6(1)
C(48)	111(4)	35(2)	48(2)	8(2)	-32(2)	-30(2)
C(49)	83(3)	55(2)	41(2)	-9(2)	39(2)	-13(2)
C(50)	175(6)	132(5)	37(2)	35(3)	46(3)	125(5)
C(51)	28(2)	45(2)	109(4)	1(2)	-22(2)	-6(2)
Cl(1)	21(1)	17(1)	25(1)	-2(1)	-1(1)	-2(1)
N(1)	18(1)	20(1)	17(1)	-2(1)	-4(1)	1(1)
O(1)	16(1)	17(1)	15(1)	0(1)	0(1)	-1(1)
O(2)	16(1)	12(1)	18(1)	2(1)	-1(1)	1(1)
O(3)	37(1)	17(1)	16(1)	-2(1)	4(1)	-4(1)
O(4)	34(1)	16(1)	20(1)	-1(1)	5(1)	4(1)
P(1)	14(1)	13(1)	15(1)	1(1)	-1(1)	0(1)
Rh(1)	15(1)	14(1)	21(1)	0(1)	-1(1)	1(1)

Table A.2.35. Hydrogen coordinates (x 10^4) and isotropic displacement parameters (Å^{2}x 10^3) for Rh(cod)Cl·**T8**.

	x	y	z	U(eq)
H(2)	-457	10533	5057	21
H(3)	1155	10207	5722	21
H(6)	848	12256	4286	31
H(8)	3377	12593	4731	41
H(10)	2366	10472	4840	32
H(12)	922	10319	3082	22
H(14)	-927	11547	2060	30
H(16)	-721	11621	4260	25
H(18)	-296	9345	7264	36
H(20)	-2879	9600	7202	55
H(22)	-1507	9579	5325	31
H(24)	1398	9603	6837	29
H(26)	2035	7399	7223	32
H(28)	206	7911	5729	24
H(30)	2501	9348	5061	34
H(31)	2368	9469	3870	34
H(32A)	3708	8887	3383	50
H(32B)	2868	8631	2960	50
H(33A)	3508	7501	3136	45
H(33B)	3895	7741	3902	45
H(34)	2395	6922	3702	30
H(35)	2326	6792	4900	31
H(36A)	3764	7315	5261	38
H(36B)	2986	7548	5772	38
H(37A)	3566	8696	5621	54
H(37B)	3949	8495	4843	54
H(38A)	2450	9346	7757	68
H(38B)	3026	8622	7589	68

H(38C)	2285	8574	8182	68
H(39A)	535	6466	6574	50
H(39B)	1526	6408	6376	50
H(39C)	846	6613	5762	50
H(40A)	-3467	9175	5762	71
H(40B)	-3030	9785	5245	71
H(40C)	-3529	10053	5954	71
H(41A)	-1467	12755	3136	55
H(41B)	-1984	12196	3654	55
H(41C)	-2086	12133	2795	55
H(42A)	63	10043	1654	49
H(42B)	948	10483	1727	49
H(42C)	159	10875	1330	49
H(43A)	2428	13685	4615	90
H(43B)	1422	13567	4533	90
H(43C)	2026	13505	3839	90
H(44A)	-1086	9790	3752	28
H(44B)	-1329	8999	4129	28
H(45A)	588	8226	3134	31
H(45B)	392	8988	2688	31
H(46A)	-698	8189	2267	47
H(46B)	-838	7821	3056	47
H(47A)	-1917	8734	3026	46
H(47B)	-1317	9332	2614	46
H(48A)	1274	11886	6878	97
H(48B)	1069	12407	6193	97
H(48C)	1566	11627	6087	97
H(49A)	-1447	8927	8360	90
H(49B)	-2202	9532	8372	90
H(49C)	-1232	9807	8406	90
H(50A)	-987	11441	6636	172
H(50B)	-636	12279	6516	172
H(50C)	-332	11800	7202	172
H(51A)	4342	11406	4753	91
H(51B)	3909	10617	4953	91
H(51C)	4000	11259	5556	91

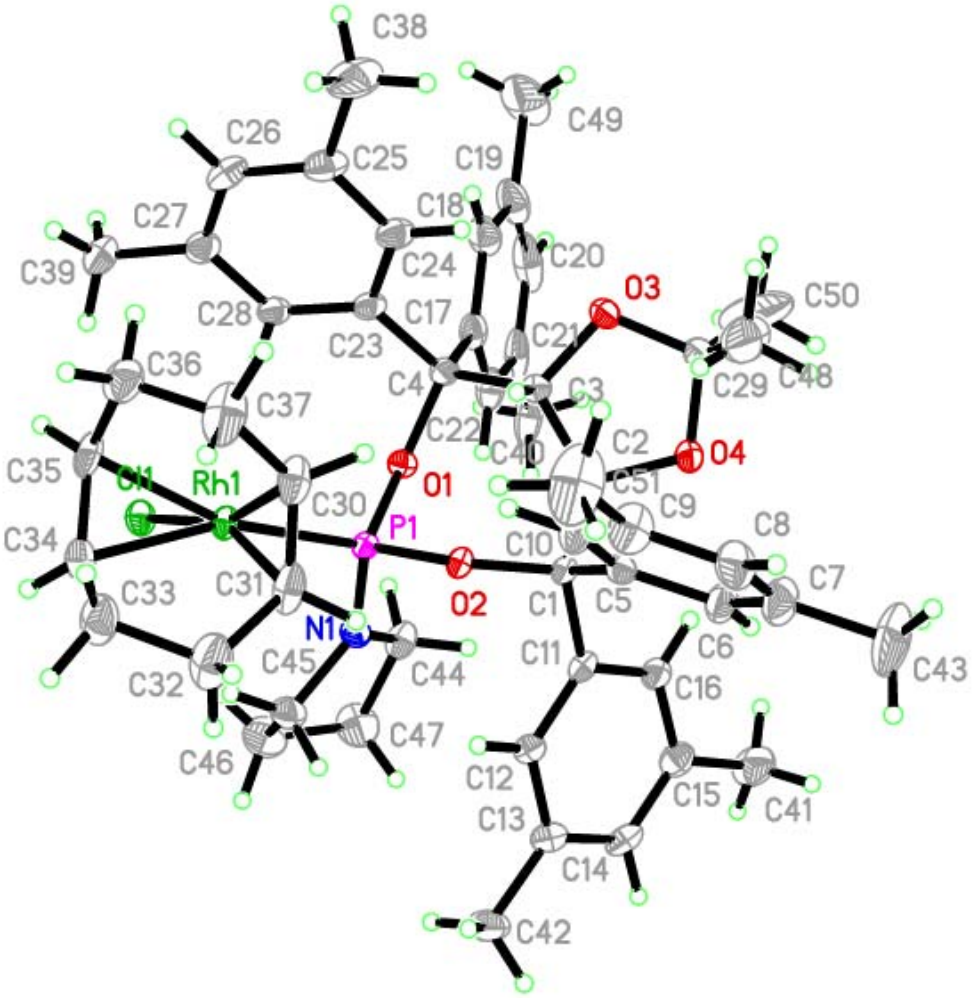
C38
C49
C26
C25
C19
C27
C18
C39
C24
C20
O3
C50
C28
C17
C23
C21
C29
C48
C36
C4
C3
C37
C22
C2
O4
C35
Cl1
Rh1
C30
O1
C40
C51
C9
C34
P1
C10
C8
C31
O2
C1
C5
C7
C33
N1
C45
C44
C11
C6
C43
C32
C16
C47
C46
C12
C15
C41
C13
C14
C42

APPENDIX 3: CHAPTER 3 EXPERIMENTAL

General Methods. All reactions were carried out under an atmosphere of argon in oven-dried glassware with magnetic stirring. Toluene was degassed with argon and passed through one column of neutral alumina and one column of Q5 reactant. Column chromatography was performed on Silicycle Inc. silica gel 60 (230-400 mesh). Thin layer chromatography was performed on Silicycle Inc. 0.25 mm silica gel 60-F plates. Visualization was accomplished with UV light (254 nm), anisaldehyde, and $KMnO_4$.

^1H NMR and ^{13}C NMR spectra were obtained in $CDCl_3$, C_6D_6, or D_3COD at ambient temperature and chemical shifts are expressed in parts per million (δ, ppm). Proton chemical shifts are referenced to 7.26 ppm ($CHCl_3$), 7.16 ppm (C_6D_6), and 3.31 ppm (D_3COD) and carbon chemical shifts are referenced to 77.0 ppm ($CDCl_3$) and 49.00 (D_3COD). Data reporting uses the following abbreviations: s, singlet; bs, broad singlet; d, doublet; t, triplet; m, multiplet; and *J*, coupling constant in Hz.

Unless otherwise indicated, commercially available starting materials were purchased from Aldrich Chemicals. $[Rh(C_2H_4)_2Cl]_2$ was purchased from Strem Chemicals. Amines were distilled over KOH under reduced pressure before use. Ligands **L2** - **L4** were synthesized as previously reported.[1]

Synthesis and Characterization Data of α,β-Unsaturated Imines.

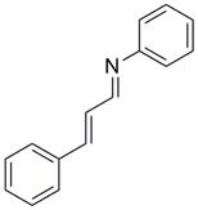

1,4-diphenyl-1-azabuta-1,3-diene (3a). Trans-cinnamaldehyde (6.3 ml, 50 mmol) and aniline (4.6 ml, 50 mmol) were dissolved in toluene and $MgSO_4$ was added. The reaction was stirred at 23 °C for 6 h, filtered, and concentrated *in vacuo*. Recrystallization from Et_2O resulted in yellow-orange needles (6.5 g, 62%, mp: 107 - 109 °C). Spectral data matches literature values.[2] ^1H NMR (300 MHz, $CDCl_3$) δ 8.29 (m, 1H), 7.55 (m, 2H), 7.44 - 7.37 (m, 5H), 7.24 - 7.16 (m, 5H).

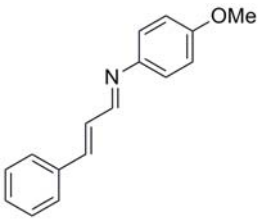

1-(4-methoxyphenyl)-4-phenyl-1-azabuta-1,3-diene (3b). Trans-cinnamaldehyde (2.1 ml, 16.5 mmol) and *p*-anisidine (2.02 g, 16.5 mmol) were dissolved in toluene and $MgSO_4$ was added. The reaction mixture was stirred at 23 °C for 12 h, filtered, and concentrated *in vacuo*. Recrystallization from Et_2O resulted in yellow flakes (2.53 g, 65%, mp: 119 - 121 °C). Spectral data matches literature values.[2] ^1H NMR (300 MHz, $CDCl_3$) δ 8.29 (m, 1H), 7.53 (m, 2H), 7.42 - 7.34 (m, 3H), 7.22 (m, 2H), 7.12 (m, 2H), 6.92 (m, 2H), 3.82 (s, 3H).

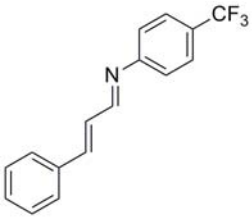

1-(4-trifluoromethylphenyl)-4-phenyl-1-azabuta-1,3-diene (3c). Trans-cinnamaldehyde (1.3 ml, 10 mmol) and 4-(trifluoromethyl)aniline (1.2 ml, 10 mmol) were dissolved in toluene and Na_2SO_4 was added. The reaction mixture was stirred at 23 °C for 2 h, filtered, and concentrated *in vacuo*. Recrystallization from Et_2O resulted in a yellow powder (0.77 g, 28%, mp: 106 - 108 °C). Spectral data matches literature values.[2] ^1H NMR (300 MHz, $CDCl_3$) δ 8.24 (m, 1H), 7.64 (m, 2H), 7.56 (m, 2H), 7.46 - 7.38 (m, 3H), 7.23 (m, 3H), 7.15 (m, 1H).

[1] **L2**, **L4**: Yu, R. T.; Rovis, T. *J. Am. Chem. Soc.* **2006**, *128*, 12370-12371. **L3**: Appendix 2.
[2] Knölker, H.-J.; Baum, G.; Foitzik, N.; Goesmann, H.; Gonser, P.; Jones, P. G.; Röttele, H. *Eur. J. Inorg. Chem.* **1998**, 993-1007.

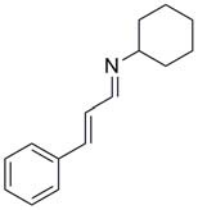

1-cyclohexyl-4-phenyl-1-azabuta-1,3-diene (3d). In a round bottom flask, 3 Å molecular sieves were activated by flame drying under vacuum and toluene was added under Ar. Trans-cinnamaldehyde (2.5 ml, 20 mmol) and cyclohexyl amine (2.3 ml, 20 mmol) were added and the reaction mixture was stirred at 23 °C for 24 h. The resulting mixture was filtered through $MgSO_4$ and Celite and concentrated *in vacuo* resulting in a brown oil (2.99 g, 70%). ^{1}H NMR (300 MHz, $CDCl_3$) δ 8.02 (m, 1H), 7.44 (m, 2H), 7.31 (m, 3H), 6.89 (m, 2H), 3.04 (m, 1H), 1.82 - 1.15 (m, 10H). ^{13}C NMR (75 MHz, $CDCl_3$) δ 160.2, 140.9, 135.7, 128.8, 128.6, 128.4, 127.0, 69.5, 34.3, 25.4, 24.6. IR (NaCl, Thin Film) 3027, 2928, 2852, 1636, 1449, 1166, 981, 749 cm^{-1}. HRMS (ESI) *m/z* $[C_{15}H_{20}N]^+$ calcd 214.1590, found 214.1594.

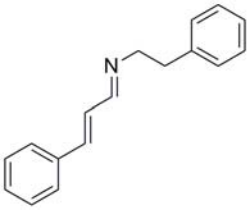

1-phenethyl-4-phenyl-1-azabuta-1,3-diene (3e). In a round bottom flask, 3 Å molecular sieves were activated by flame drying under vacuum and toluene was added under Ar. Trans-cinnamaldehyde (1.9 ml, 15 mmol) and phenethylamine (1.9 ml, 15 mmol) were added and the reaction mixture was stirred at 23 °C for 24 h. The resulting mixture was filtered through $MgSO_4$ and Celite and concentrated *in vacuo*. Recrystallization from Et_2O resulted in clear cubic crystals with a slight yellow hue (1.00 g, 28%, mp: 52 -53 °C). ^{1}H NMR (300 MHz, $CDCl_3$) δ 7.94 (m, 1H), 7.51 - 7.22 (m, 10H), 6.92 (m, 2H), 3.81 (t, *J* = 7.5 Hz, 2H), 3.03 (t, *J* = 7.5 Hz, 2H). ^{13}C NMR (75 MHz, $CDCl_3$) δ 162.9, 141.4, 139.7, 135.6, 128.9, 128.8, 128.6, 128.2, 127.9, 127.0, 126.0, 62.9, 37.3. IR (NaCl, Thin Film) 3028, 2943, 2826, 1634, 1453, 978, 743 cm^{-1}. HRMS (ESI) *m/z* $[C_{17}H_{18}N]^+$ calcd 236.1434, found 236.1436.

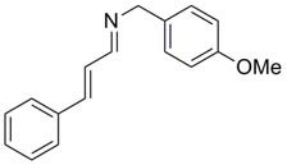

1-(4-methoxybenzyl)-4-phenyl-1-azabuta-1,3-diene (3f). In a round bottom flask, 3 Å molecular sieves were activated by flame drying under vacuum and toluene was added under Ar. Trans-cinnamaldehyde (2.5 ml, 20 mmol) and 4-methoxybenzyl amine (2.2 ml, 20 mmol) were added and the reaction mixture was stirred at 23 °C for 36 h. The resulting mixture was filtered through $MgSO_4$ and Celite and concentrated *in vacuo* resulted in an amorphous pale brown powder (0.98 g, 26%). Spectral data matches literature.[3] ^{1}H NMR (300 MHz, $CDCl_3$) δ 8.12 (m, 1H), 7.48 (m, 2H), 7.36 (m, 3H), 7.25 (m, 2H), 6.98 (m, 2H), 6.89 (m, 2H), 4.66 (s, 2H), 3.80 (s, 3H).

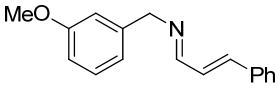

1-(3-methoxyphenyl)-4-phenyl-1-azabuta-1,3-diene (3g). ^{1}H NMR (300 MHz, $CDCl_3$) δ 8.14 (m, 1H), 7.48 (m, 2H), 7.32 (m, 3H), 6.99 (m, 2H), 6.89 (m, 2H), 6.82 (m, 1H), 4.69 (s, 3H), 3.81 (s, 3H).

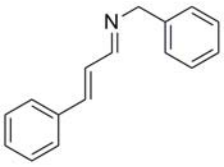

1-benzyl-4-phenyl-1-azabuta-1,3-diene (3h). In a round bottom flask, 3 Å molecular sieves were activated by flame drying under vacuum and toluene was added under Ar. Trans-cinnamaldehyde (2.5 ml, 20 mmol) and benzylamine (2.2 ml, 20 mmol) were added and the reaction mixture was stirred at 23 °C for 36 h. The resulting mixture was filtered through Celite and concentrated *in vacuo* resulting in a brown oil (3.77 g, 85%). Spectral data matches literature.[4] ^{1}H NMR (300 MHz, $CDCl_3$) δ 8.15 (m, 1H), 7.49 (m, 2H), 7.40 - 7.25 (m, 8H), 7.00 (m, 2H), 4.73 (s, 2H).

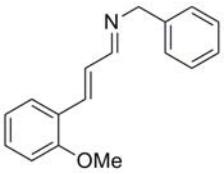

1-benzyl-4-(2-methoxyphenyl)-1-azabuta-1,3-diene (3i). In a round bottom flask, 3 Å molecular sieves were activated by flame drying under vacuum and toluene was added under Ar. *O*-methoxy-trans-cinnamaldehyde (3.2 g, 20 mmol) and benzylamine (2.2 ml, 20 mmol) were added and the reaction mixture was stirred at 23 °C for 24 h. The resulting mixture was filtered through $MgSO_4$ and Celite and concentrated *in vacuo* resulting in a brown oil (3.78 g, 75%). ^{1}H NMR (300 MHz, $CDCl_3$) δ 8.18 (m, 1H), 7.55 (m, 1H), 7.42 - 7.26 (m, 7H), 7.12 - 6.90 (m, 3H), 4.74 (s, 2H), 3.88 (s, 3H). ^{13}C NMR (75 MHz, $CDCl_3$) δ 164.2, 157.2, 139.2, 137.0, 130.2, 128.5, 128.4, 127.9, 127.4, 126.8, 124.4, 120.6, 110.8, 65.1, 55.2. IR (NaCl, Thin Film) 3028, 2837, 1633, 1488, 1246, 1027, 751 cm^{-1}. HRMS (ESI) *m/z* $[C_{17}H_{18}NO]^+$ calcd 252.1383, found 252.1387.

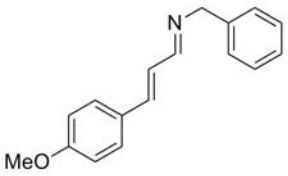

1-benzyl-4-(4-methoxyphenyl)-1-azabuta-1,3-diene (3j). In a round bottom flask, 3 Å molecular sieves were activated by flame drying under vacuum and toluene was added under Ar. *P*-methoxy-trans-cinnamaldehyde (3.2 g, 20 mmol) and benzylamine (2.2 ml, 20 mmol) were added and the reaction mixture was stirred at 23 °C for 24 h. The resulting mixture was filtered through $MgSO_4$ and Celite and concentrated *in vacuo.* Recrystallization from Et_2O resulted in off-white prisms (3.78 g, 75%, mp: 73 - 75 °C). ^{1}H NMR (300 MHz, $CDCl_3$) δ 8.12 (m, 1H), 7.44 (m, 2H), 7.40 - 7.26 (m, 5H), 6.91 (m, 4H), 4.72 (s, 2H), 3.82 (s, 3H). ^{13}C NMR (75 MHz, $CDCl_3$) δ 163.5, 160.3, 141.6, 139.2, 128.6, 128.4, 128.3, 127.9, 126.8, 125.9, 114.1, 65.0, 55.1. IR (NaCl, Thin Film) 3018, 2929, 2837, 1573, 1425, 1207, 1033, 738 cm^{-1}. HRMS (ESI) *m/z* $[C_{17}H_{18}NO]^+$ calcd 252.1383, found 252.1385.

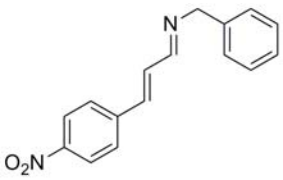

1-benzyl-4-(4-nitrophenyl)-1-azabuta-1,3-diene (3k). In a round bottom flask, 3 Å molecular sieves were activated by flame drying under vacuum and toluene was added under Ar. 4-nitrocinnamaldehyde (1.8 g, 10 mmol) and benzyl amine (1.1 ml, 10 mmol) were added and the reaction mixture was stirred at 23 °C for 24 h. The resulting mixture was filtered through $MgSO_4$ and Celite and concentrated *in vacuo.* Recrystallization from Et_2O resulted in pale yellow flakes (1.74 g, 65%, 104 - 105 °C). ^{1}H NMR (300 MHz, $CDCl_3$) δ 8.18 (m, 3H), 7.58 (m, 2H), 7.38-7.27 (m, 5H), 7.04 (m, 2H), 4.75 (s, 2H). ^{13}C NMR (75 MHz, $CDCl_3$) δ 162.2, 147.5, 141.8, 138.6, 132.1, 128.5, 127.9, 127.6, 127.0, 124.0, 65.2. IR (NaCl, Thin Film) 3058, 3027, 2922, 2814, 1617, 1513, 1345, 741 cm^{-1}. HRMS (ESI) *m/z* $[C_{16}H_{15}N_2O_2]^+$ calcd 267.1128, found 267.1132.

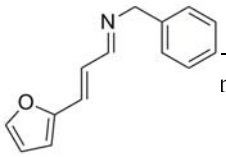

1-benzyl-4-(2-furyl)-1-azabuta-1,3-diene (3l). In a round bottom flask, 3 Å molecular sieves were activated by flame drying under vacuum and toluene was added under Ar. Trans-3-(2furyl)-acrolein (1.8 g, 15 mmol) and benzyl amine (1.6 ml, 15 mmol) were added and the reaction mixture was stirred at 23 °C for 24 h. The resulting mixture was filtered through $MgSO_4$ and Celite and concentrated *in vacuo* resulting in a brown oil (2.76 g, 87%). ^{1}H NMR (300 MHz, $CDCl_3$) δ 8.07 (m, 1H), 7.44 - 7.32 (m, 6H), 6.94 - 6.74 (m, 2H), 6.46 (m, 2H), 4.72 (s, 2H). ^{13}C NMR (75 MHz, $CDCl_3$) δ 162.8, 151.7, 143.6, 139.1, 128.5, 128.4, 127.9, 126.8, 126.1, 111.8, 111.6, 65.1. IR (NaCl, Thin Film) 3062, 3028, 2842, 1633, 1453, 1155, 963, 698 cm^{-1}. HRMS (ESI) *m/z* $[C_{14}H_{14}NO]^+$ calcd 212.1070, found 212.1072.

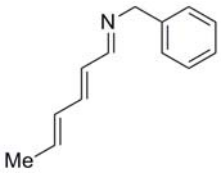

1-benzyl-6-methyl-1-azabuta-1,3,5-triene (3m). In a round bottom flask, 3 Å molecular sieves were activated by flame drying under vacuum and toluene was added under Ar. 2,4-hexadienal (2.2 ml, 20 mmol) and benzyl amine (2.2 ml, 20 mmol) were added and the reaction mixture was stirred at 23 °C for 24 h. The resulting mixture was filtered through $MgSO_4$ and Celite and concentrated *in vacuo* resulting in a brown oil (3.22 g, 87%) as a 1:10 mixture of isomers. ^{1}H NMR (300 MHz, $CDCl_3$) δ 7.98 (m, 1H), 7.28 (m, 5H), 6.60 (m, 1H), 6.27 (m, 2H), 5.98 (m, 1H), 4.65 (s, 2H), 1.83 (d, J = 6.7 Hz, 3H). ^{13}C NMR (75 MHz, $CDCl_3$) δ 163.4, 142.2, 139.2, 136.6, 135.0, 130.7, 129.1, 128.3, 127.8, 126.8, 65.0, 18.4. IR (NaCl, Thin Film) 3386, 3028, 2925, 1631, 1452, 1171, 1001, 698, 665 cm^{-1}. HRMS (ESI) *m/z* $[C_{14}H_{16}N]^+$ calcd 186.1277, found 186.1278.

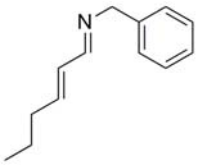

1-benzyl-4-(n-propyl)-1-azabuta-1,3-diene (3n). In a round bottom flask, 3 Å molecular sieves were activated by flame drying under vacuum and toluene was added under Ar. trans-2-hexenal (2.3 ml, 20 mmol) and benzyl amine (2.2 ml, 20 mmol) were added and the reaction mixture was stirred at 23 °C for 24 h. The resulting mixture was filtered through $MgSO_4$ and Celite and concentrated *in vacuo* resulting in a brown oil (3.07 g, 82%). ^{1}H NMR (300 MHz, $CDCl_3$) δ 8.00 (m, 1H), 7.35 - 7.22 (m, 6H), 6.31 (m, 1H), 4.66 (s, 2H), 2.23 (dd, *J* = 13.2, 7.2 Hz, 2H), 1.53 (dt, *J* = 7.5, 7.5 Hz, 2H), 0.98 (t, *J* = 7.5 Hz, 3H). ^{13}C NMR (75 MHz, $CDCl_3$) δ 163.6, 145.8, 139.3, 130.6, 128.4, 128.2, 128.1, 127.9, 126.8, 64.9, 34.6, 21.6, 13.6. IR (NaCl, Thin Film) 3028, 2958, 2930, 2871, 1655, 1454, 969, 698 cm^{-1}. HRMS (ESI) *m/z* $[C_{13}H_{18}N]^+$ calcd 188.1434, found 188.1431.

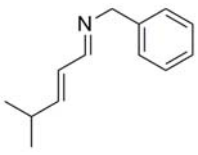

1-benzyl-4-(i-propyl)-1-azabuta-1,3-diene (3o). In a round bottom flask, 3 Å molecular sieves were activated by flame drying under vacuum and toluene was added under Ar. 4-methyl-2-pentenal (1.7 ml, 15 mmol) and benzyl amine (1.6 ml, 15 mmol) were added and the reaction mixture was stirred at 23 °C for 24 h. The resulting mixture was filtered through $MgSO_4$ and Celite and concentrated *in vacuo* resulting in a brown oil (2.49 g, 89%). ^{1}H NMR (300 MHz, $CDCl_3$) δ 7.98 (m, 1H), 7.35 - 7.25 (m, 6H), 6.26 (m, 1H), 4.65 (s, 2H), 2.50 (m, 1H), 1.09 (d, *J* = 6.9 Hz, 6H). ^{13}C NMR (75 MHz, $CDCl_3$) δ 163.8, 152.5, 139.2, 128.4, 127.9, 127.7, 126.8, 64.9, 31.0, 21.5. IR (NaCl, Thin Film) 3029, 2961, 2869, 1652, 1454, 973, 698cm^{-1}. HRMS (ESI) *m/z* $[C_{13}H_{18}N]^+$ calcd 188.1434, found 188.1439.

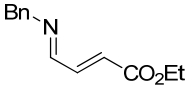

(*E*)-ethyl 4-(benzylimino)but-2-enoate (3p). In a round bottom flask, 3 Å molecular sieves were activated by flame drying under vacuum and toluene was added under Ar.

Ethyl *trans*-4-oxo-2-butenoate (1.2 ml, 10 mmol) and benzyl amine (1.09 ml, 10 mmol) were added and the reaction mixture was stirred at 23 °C for 3 h. The resulting mixture was filtered through $MgSO_4$ and Celite and concentrated *in vacuo* resulting in a red oil (1.82 g, 84%). ^{1}H NMR (400 MHz, $CDCl_3$) δ 8.11 (m, 1H), 7.38-7.32 (m, 3H), 7.29-7.25 (m, 2H),6.29 (d, *J* = 15.9 Hz, 1H), 4.76 (s, 2H), 4.25 (q, *J* = 7.2 Hz, 2H), 1.31 (t, J = 7.2 Hz, 3 H). ^{13}C NMR (100 MHz, $CDCl_3$) δ 165.7, 161.0, 142.4, 138.2, 130.5, 128.6, 128.0, 127.3, 65.6, 60.9, 14.1. IR (NaCl, Thin Film) 3030, 2983, 2875, 1718, 1619, 1257, 1096, 699 cm^{-1}. LRMS (ESI/APCI) *m/z* $[C_{13}H_{16}NO_2]^+$ calcd 218.1, found 218.1.

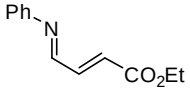

(*E*)-ethyl 4-(phenylimino)but-2-enoate (3q). ^{1}H NMR (300 MHz, $CDCl_3$) δ 8.25 (m, 1H), 7.53-7.37 (m, 3H), 7.27 (m, 1H), 7.19 (m, 2H), 6.43 (d, J = 15.8 Hz, 1H), 4.28 (q, J = 7.2, 2H), 1.34 (t, J = 7.2 Hz, 3H).

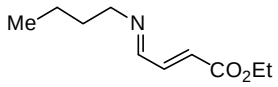

(*E*)-ethyl 4-(butylimino)but-2-enoate (3r). In a round bottom flask, 3 Å molecular sieves were activated by flame drying under vacuum and toluene was added under Ar. Ethyl *trans*-4-oxo-2-butenoate (1.2 ml, 10 mmol) and n-butyl amine (0.99 ml, 10 mmol) were added and the reaction mixture was stirred at 23 °C for 3 h. The resulting mixture was filtered through $MgSO_4$ and Celite and concentrated *in vacuo* resulting in a red oil (1.57 g, 86%). ^{1}H NMR (400 MHz, $CDCl_3$) δ 7.98 (m, 1H), 7.28 (dd, *J* = 15.9, 9.1 Hz, 1H), 6.23 (d, *J* = 15.9 Hz, 1H), 4.24 (q, *J* = 7.2 Hz, 2H), 3.55 (dt, *J* = 7.0, 1.1 Hz, 2H), 1.63 (m, 2H), 1.34 (m, 2H), 1.30 (t, *J* = 7.2 Hz, 3H), 0.92 (t, *J* = 7.4 Hz, 3H). ^{13}C NMR (100 MHz, $CDCl_3$) δ 165.9, 160.1, 142.6, 129.8, 61.8, 60.9, 32.6, 20.4, 14.1, 13.8. IR (NaCl, Thin Film) 2960, 2934, 2874, 1721, 1303, 1256, 1186, 1154 cm^{-1}. LRMS (ESI/APCI) *m/z* $[C_{10}H_{17}NO_2]^+$ calcd 184.1, found 184.1.

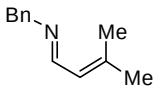

1-benzyl-4,4'-dimethyl-1-azabuta-1,3-diene (3s). In a round bottom flask, 3 Å molecular sieves were activated by flame drying under vacuum and toluene was added under Ar. 3-methyl-2-butenal (1.9 ml, 20 mmol) and benzyl amine (2.2 ml, 20 mmol) were added and the reaction mixture was stirred at 23 °C for 3 h. The resulting mixture was filtered through $MgSO_4$ and Celite and concentrated *in vacuo* resulting in a brown oil (2.91 g, 83%). Spectral data matches literature values.[5] ^{1}H NMR (300 MHz, $CDCl_3$) δ 8.31 (m, 1H), 7.36-7.22 (m, 5), 6.08 (m, 1H), 4.65 (s, 2H), 1.95 (s, 3H), 1.89 (s, 3H).

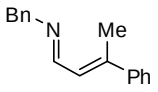

1-benzyl-4-methyl-4'-phenyl-1-azabuta-1,(*E*)-3-diene (3t). Aldehyde was prepared according to literature procedure.[6] Tetrabutylammonium chloride (13.9 g, 50 mmol), sodium acetate (4.29 g, 60 mmol), and palladium acetate (0.10 g, 0.5 mmol) was added to 100 ml round bottom flask. The reaction vessel was evacuated and filled with Ar. To this iodobenzene (5.6 ml, 50 mmol), N-methylpyrolidinone (50 ml), and crotonaldehyde (10.4 ml, 125 mmol) was added. The reaction was heated to 90 °C for 2 h, cooled to 23 °C, and poured into 200 ml sat. $NaHCO_3$. The mixture was extracted with DCM 3x, dried, and concentrated *in vacuo*. The N-methylpyrolidinone was distilled off and the resulting liquid was purified using flash column chromatography 2x. (*Z*)-3-phenylbut-2-enal was isolated as a clear oil (0.10 g, 2%). ^{1}H NMR (300 MHz, $CDCl_3$) δ 9.47 (d, J = 8.2 Hz, 1H),

[5] Joly, G. D.; Jacobsen, E. N. *J. Am. Chem. Soc.* **2004**, *126*, 4102-4103.
[6] Stadler, M.; List, B. *Synlett* **2008**, *4*, 597-599.

7.41 (m, 3H), 7.30 (m, 2H), 6.14 (dd, J = 8.2, 1.2 Hz, 1H), 2.32 (d, J = 1.3 Hz, 3H). (*E*)-3-phenylbut-2-enal was isolated as a clear oil (1.34 g, 18%). ^{1}H NMR (300 MHz, $CDCl_3$) δ 10.18 (d, J = 7.9 Hz, 1H), 7.55 (m, 2H), 7.42 (m, 3H), 6.40 (dd, J = 7.8, 1.1 Hz, 1H), 2.58 (d, J = 1.0 Hz, 3H). In a round bottom flask, 3 Å molecular sieves were activated by flame drying under vacuum and toluene was added under Ar. (*E*)-3-phenylbut-2-enal (0.29 g, 1.97 mmol) and benzyl amine (0.21 ml, 1.97 mmol) were added and the reaction mixture was stirred at 23 °C for 3 h. The resulting mixture was filtered through $MgSO_4$ and Celite and concentrated *in vacuo* resulting in a brown oil. ^{1}H NMR (300 MHz, $CDCl_3$) δ 8.51 (m, 1H), 7.52 (m, 2H), 7.43-7.16 (m, 8H), 6.68 (d, J = 9.3 Hz, 1H), 4.74 (s, 2H), 2.36 (s, 3H).

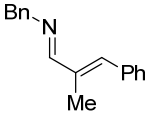

1-benzyl-(*E*)-2-methyl-3-phenyl-1-azabuta-1,3-diene (3u). In a round bottom flask, 3 Å molecular sieves were activated by flame drying under vacuum and toluene was added under Ar. α-methyl-*trans*-cinnamaldehyde (2.1 ml, 15 mmol) and benzyl amine (1.6 ml, 15 mmol) were added and the reaction mixture was stirred at 23 °C for 3 h. The resulting mixture was filtered through $MgSO_4$ and Celite and concentrated *in vacuo* resulting in a gold oil (3.0 g, 86%). ^{1}H NMR (300 MHz, $CDCl_3$) δ 8.10 (s, 1H), 7.42-7.24 (m, 10H), 6.85 (s, 1H), 4.78 (s, 2H), 2.21 (s, 3H).

General Procedure for Rhodium-Catalyzed [4+2] Cycloaddition. $[Rh(C_2H_4)_2Cl]_2$ (5.8 mg, 0.015 mmol) and ligand (**L3** unless otherwise mentioned) (0.03 mmol) were added to an oven-dried 10 ml round bottom flask and the flask was fitted with an oven-dried reflux condenser in an inert atmosphere (Ar) glove box. Upon removal from the glove box, the reaction vessel was put under Ar and 4 ml of toluene was added via syringe and the resulting gold solution was stirred at 23 °C for 15 min. To this solution, imine (0.3 mmol) and isocyanate (0.375 mmol) in 2 ml of toluene was added via syringe. The reaction mixture was heated to 110 °C in an oil bath and kept at reflux for 12 h. The reaction mixture was cooled to 23 °C, concentrated *in vacuo*, and purified by flash column chromatography (typically 2:1 Hex:CH_2Cl_2, followed by CH_2Cl_2). Evaporation of solvent afforded the analytically pure products.

Characterization Data for Pyrimidinones and Pyrrolones.

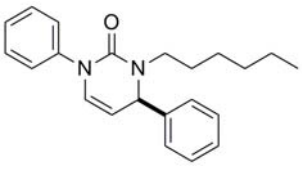

(*R*)-3-hexyl-1,4-diphenyl-3,4-dihydropyrimidine-2-one (4ac). General procedure yielded brown oil (56%). 90% ee by HPLC: Chiralcel IA column, 90:10 Hex:iPrOH, 1ml/min, RT_{major} = 7.68 min, RT_{minor} = 11.08 min, 210 nm. $[\alpha]^{20}_D$ = +110.0, c = 0.0118 g/ml $CHCl_3$. ^{1}H NMR (300 MHz, $CDCl_3$) δ 7.43-7.23 (m, 10H), 6.30 (d, *J* = 7.8 Hz, 1H), 5.10 (d, *J* = 4.5 Hz, 1H), 4.97 (dd, *J* = 7.8, 4.5 Hz, 1H), 3.74 (ddd, *J* = 15.6, 9.6, 6.0 Hz, 1H), 2.76 (ddd, *J* = 14.4, 9.3, 5.4 Hz, 1H), 1.61 (m, 1H), 1.50 (m, 1H), 1.26 (m, 6H), 0.87 (m, 3H). ^{13}C NMR (75 MHz, $CDCl_3$) δ 152.3, 142.6, 141.3, 128.9, 128.7, 128.0, 127.9, 126.5, 126.2, 103.0, 61.6, 46.2, 31.4, 26.8, 26.5, 22.5, 14.0. R_f = 0.42 (98:2 CH_2Cl_2:EtOAc). IR (NaCl, Thin Film) 2957, 2928, 2857, 1665, 1450, 1289, 697 cm^{-1}. HRMS (ESI) *m/z* $[C_{22}H_{27}N_2O]^+$ calcd 335.2118, found 335.2127.

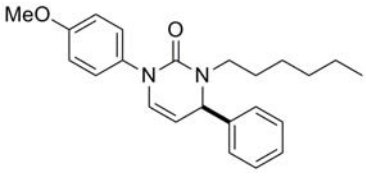

(*R*)-3-hexyl-1-(4-methoxyphenyl)-4-phenyl-3,4-dihydropyrimidin-2-one (4bc). General procedure yielded a brown syrup (49%). 89% ee by HPLC: Chiralcel ODH column, 90:10 Hex:iPrOH, 1ml/min, RT_{major} = 8.76 min, RT_{minor} = 20.42 min, 230 nm. $[\alpha]^{20}_D$ = +151.3, c = 0.0099 g/ml $CHCl_3$. ^1H NMR (300 MHz, $CDCl_3$) δ 7.42 - 7.32 (m, 5H), 7.26 (m, 2H), 6.91 (m, 2H), 6.22 (d, *J* = 7.8 Hz, 1H), 5.08 (d, *J* = 4.5 Hz, 1H), 4.92 (dd, *J* = 7.8, 4.5 Hz, 1H), 3.80 (s, 3H), 3.72 (ddd, *J* = 15.6, 9.6, 6.0 Hz, 1H), 2.73 (ddd, *J* = 14.4, 9.3, 5.4 Hz, 1H), 1.59 (m, 1H), 1.48 (m, 1H), 1.24 (m, 6H), 0.85 (m, 3H). ^{13}C NMR (75 MHz, $CDCl_3$) δ 157.9, 152.6, 142.7, 134.3, 128.8, 128.3, 127.9, 127.6, 126.5, 114.0, 102.5, 61.6, 55.4, 46.2, 31.4, 26.8, 26.5, 22.5, 14.0. R_f = 0.16 (98:2 CH_2Cl_2:EtOAc). IR (NaCl, Thin Film) 3029, 2930, 2857, 1655, 1512, 1246, 1031, 829, 700 cm^{-1}. HRMS (ESI) *m/z* $[C_{23}H_{29}N_2O_2]^+$ calcd 365.2224, found 365.2229.

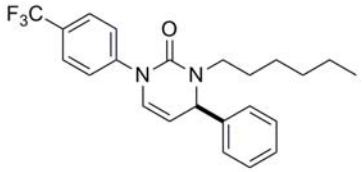

(*R*)-3-hexyl-4-phenyl-1-(4-(trifluoromethyl)phenyl)-3,4-dihydropyrimidin-2-one (4cc). General procedure yielded a brown syrup (65%). 91% ee by HPLC: Chiralcel ODH column, 90:10 Hex:iPrOH, 1ml/min, RT_{major} = 6.40 min, RT_{minor} = 7.11 min, 254 nm. $[\alpha]^{20}_D$ = +159.3°, c = 0.0145 g/ml $CHCl_3$. ^1H NMR (300 MHz, $CDCl_3$) δ 7.64 (m, 2H), 7.50 (m, 2H), 7.39 - 7.33 (m, 5H), 6.32 (d, *J* = 7.8 Hz, 1H), 5.09 (d, *J* = 4.5 Hz, 1H), 5.04 (dd, *J* = 7.8, 4.5 Hz, 1H), 3.71 (ddd, *J* = 15.6, 9.6, 6.0 Hz, 1H), 2.76 (ddd, *J* = 14.4, 9.3, 5.1 Hz, 1H), 1.60 (m, 1H), 1.49 (m, 1H), 1.24 (m, 6H), 0.85 (m, 3H). ^{13}C NMR (75 MHz, $CDCl_3$) δ 151.8, 144.2, 142.1, 129.0, 128.2, 127.0, 126.5, 126.0, 125.9, 125.8, 104.4, 61.6, 46.4, 31.4, 26.8, 26.5, 22.5, 14.0. R_f = 0.32 (98:2 CH_2Cl_2:EtOAc). IR (NaCl, Thin Film) 2958, 2931, 2859, 1667, 1326, 1124, 699 cm^{-1}. HRMS (ESI) *m/z* $[C_{23}H_{26}F_3N_2O]^+$ calcd 403.1992, found 403.1991.

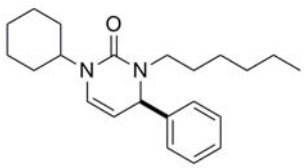

(*R*)-1-cyclohexyl-3-hexyl-4-phenyl-3,4-dihydropyrimidin-2-one (4dc). General procedure yielded a brown syrup (80%). 80% ee by HPLC: Chiralcel ODH column, 90:10 Hex:iPrOH, 1ml/min, RT_{major} = 4.24 min, RT_{minor} = 4.64 min, 210 nm. $[\alpha]^{20}_D$ = +221.0°, c = 0.0090 g/ml $CHCl_3$. ^1H NMR (300 MHz, $CDCl_3$) δ 7.35 - 7.22 (m, 5H), 6.09 (d, *J* = 8.1 Hz, 1H), 4.92 (d, *J* = 4.8 Hz, 1H), 4.83 (dd, *J* = 8.1, 4.8 Hz, 1H), 4.33 (m, 1H), 3.67 (ddd, *J* = 15.3, 9.6, 6.0 Hz, 1H), 2.68 (ddd, *J* = 14.4, 9.3, 5.1 Hz, 1H), 1.82 - 1.64 (m, 5H), 1.39 - 1.08 (m, 16H), 0.84 (m, 3H). ^{13}C NMR (75 MHz, $CDCl_3$) δ 153.1, 143.2, 128.7, 127.7, 126.4, 123.1, 101.9, 60.8, 52.6, 46.2, 32.0, 31.5, 31.3, 27.0, 26.5, 25.9, 25.7, 25.5, 22.5, 14.0. R_f = 0.44 (98:2 CH_2Cl_2:EtOAc). IR (NaCl, Thin Film) 2929, 2856, 1649, 1460, 1226, 699 cm^{-1}. HRMS (ESI) *m/z* $[C_{22}H_{33}N_2O]^+$ calcd 341.2587, found 341.2582.

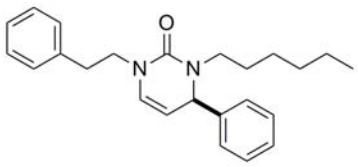

(*R*)-3-hexyl-1-phenethyl-4-phenyl-3,4-dihydropyrimidin-2-one (4ec). General procedure yielded a brown syrup (69%). 94% ee by HPLC: Chiralcel ODH column, 90:10 Hex:iPrOH, 1ml/min, RT_{major} = 7.31 min, RT_{minor} = 8.52 min, 254 nm. $[\alpha]^{20}_D$ = +149.6°, c = 0.0147 g/ml $CHCl_3$. ^1H NMR (300 MHz, $CDCl_3$) δ 7.36 - 7.19 (m, 10H), 5.82 (d, *J* = 7.8 Hz, 1H), 4.97 (d, *J* = 4.5 Hz, 1H), 4.70 (dd, *J* = 7.8, 4.5 Hz, 1H), 3.86 (dt, *J* = 13.8, 7.5 Hz, 1H), 3.72 (ddd, *J* = 15.3, 9.3, 6.3 Hz, 1H), 3.58 (dt, *J* = 13.8, 7.5 Hz, 1H), 2.95 (t, *J* = 7.5 Hz, 2H), 2.66 (ddd, *J* = 14.4, 9.0, 5.4 Hz, 1H), 1.54 (m, 1H), 1.45 (m, 1H), 1.26 (m, 6H), 0.87 (m, 3H). ^{13}C NMR (75 MHz, $CDCl_3$) δ 153.0, 142.9, 138.8, 129.0, 128.7, 128.4, 127.7, 127.6, 126.4, 126.2, 101.6, 61.3, 49.3, 45.7, 35.5, 31.5, 26.9, 26.5, 22.5, 14.0. R_f = 0.50 (98:2 CH_2Cl_2:EtOAc). IR (NaCl, Thin Film) 3028, 2929, 2858, 1653, 1455, 1255, 699 cm^{-1}. HRMS (ESI) *m/z* $[C_{24}H_{31}N_2O]^+$ calcd 363.2431, found 363.2431.

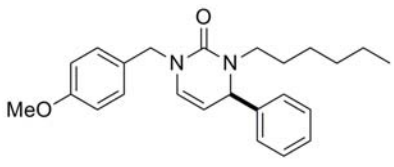

(*R*)-3-hexyl-1-(4-methoxybenzyl)-4-phenyl-3,4-dihydropyrimidin-2-one (4fc). General procedure yielded a brown oil (75%). 94% ee by

HPLC: Chiralcel ODH column, 90:10 Hex:iPrOH, 1ml/min, RT_{major} = 10.37 min, RT_{minor} = 9.20 min, 230 nm. $[\alpha]^{20}_D$ = +171.3, c = 0.0150 g/ml $CHCl_3$. ^1H NMR (300 MHz, $CDCl_3$) δ 7.35 - 7.21 (m, 7H), 6.74 (m, 2H), 5.98 (d, *J* = 7.8 Hz, 1H), 4.98 (d, *J* = 4.5 Hz, 1H), 4.80 (dd, *J* = 7.8, 4.5 Hz, 1H), 4.69 (d, *J* = 15.0 Hz, 1H), 4.59 (d, *J* = 15.0 Hz, 1H), 3.80 (s, 3H), 3.74 (ddd, *J* = 15.3, 9.3, 6.3 Hz, 1H), 2.68 (ddd, *J* = 14.3, 9.0, 5.3 Hz, 1H), 1.55 (m, 1H), 1.47 (m, 1H), 1.24 (m, 6H), 0.86 (m, 3H). ^{13}C NMR (75 MHz, $CDCl_3$) δ 158.8, 153.4, 142.8, 130.3, 128.9, 128.7, 127.8, 126.9, 126.4, 113.9, 102.4, 61.3, 55.2, 49.8, 45.9, 31.5, 26.9, 26.5, 22.5, 14.0. R_f = 0.48 (98:2 CH_2Cl_2:EtOAc). IR (NaCl, Thin Film) 2955, 2929, 2858, 1652, 1248, 1035, 700 cm^{-1}. HRMS (ESI) *m/z* $[C_{24}H_{31}N_2O_2]^+$ calcd 379.2380, found 379.2360.

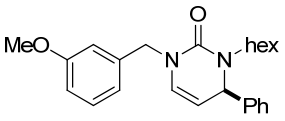

(*R*)-3-hexyl-1-(3-methoxybenzyl)-4-phenyl-3,4-dihydropyrimidin-2-one (4gc). General procedure yielded a brown oil (77%). 93% ee by HPLC: Chiralcel IC column, 80:20 Hex:iPrOH, 1ml/min, RT_{major} = 13.63 min, RT_{minor} = 14.57 min, 230 nm. $[\alpha]^{20}_D$ = +180.2, c = 0.0101 g/ml $CHCl_3$. ^1H NMR (300 MHz, $CDCl_3$) δ 7.37-7.23 (m, 6H), 6.91-6.80 (m, 3H), 5.97 (d, *J* = 7.9 Hz, 1H), 5.02 (d, *J* = 4.6 Hz, 1H), 4.82 (dd, *J* = 7.9, 4.6 Hz, 1H), 4.77 (d, *J* = 15.4 Hz, 1H), 4.63 (d, *J* = 15.4 Hz, 1H), 3.79 (m, 1H), 3.78 (s, 3H), 2.70 (ddd, *J* = 14.1, 9.1, 5.4 Hz, 1H), 1.57 (m, 1H), 1.49 (m, 1H), 1.26 (m, 6H), 0.87 (m, 3H). ^{13}C NMR (75 MHz, $CDCl_3$) δ 159.7, 153.3, 142.7, 139.8, 129.5, 128.7, 127.8, 127.0, 126.3, 119.6, 112.9, 112.6, 102.4, 61.2, 55.0, 50.1, 45.8, 31.4, 26.9, 26.4, 22.4, 13.9. R_f = 0.32 (98:2 CH_2Cl_2:EtOAc). IR (NaCl, Thin Film) 3028, 2929, 2857, 1653, 1463, 1261, 1051, 757, 699 cm^{-1}. HRMS (ESI) *m/z* $[C_{24}H_{31}N_2O_2]^+$ calcd 379.2380, found 379.2370.

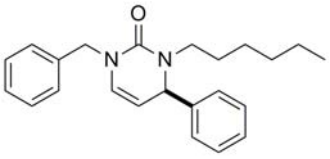

(*R*)-1-benzyl-3-hexyl-4-phenyl-3,4-dihydropyrimidin-2-one (4hc). General procedure yielded a brown oil (67%). 93% ee by HPLC: Chiralcel ODH column, 90:10 Hex:iPrOH, 1ml/min, RT_{major} = 8.12 min, RT_{minor} = 7.56 min, 210 nm. $[\alpha]^{20}_D$ = +38.4, c = 0.0076 g/ml $CHCl_3$. ^1H NMR (300 MHz, $CDCl_3$) δ 7.38 - 7.24 (m, 10H), 5.99 (d, *J* = 7.8 Hz, 1H), 5.02 (d, *J* = 4.5 Hz, 1H), 4.82 (dd, *J* = 7.8, 4.5 Hz, 1H), 4.82 (d, *J* = 15.3 Hz, 1H), 4.66 (d, *J* = 15.3 Hz, 1H), 3.77 (ddd, *J* = 15.6, 9.3, 6.3 Hz, 1H), 2.69 (ddd, *J* = 14.1, 9.0, 5.1 Hz, 1H), 1.56 (m, 1H), 1.48 (m, 1H), 1.26 (m, 6 H), 0.87 (m, 3H). ^{13}C NMR (75 MHz, $CDCl_3$) δ 153.4, 142.7, 138.2, 128.7, 128.5, 127.8, 127.5, 127.2, 127.0, 126.4, 102.4, 61.3, 50.3, 45.9, 31.5, 26.9, 26.5, 22.5, 14.0. R_f = 0.33 (98:2 CH_2Cl_2:EtOAc). IR (NaCl, Thin Film) 3030, 2929, 2858, 1655, 1453, 1253, 701 cm^{-1}. HRMS (ESI) *m/z* $[C_{23}H_{29}N_2O]^+$ calcd 349.2274, found 349.2277.

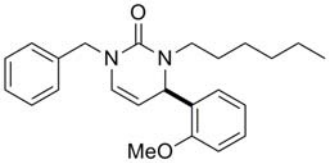

(*R*)-1-benzyl-3-hexyl-4-(2-methoxyphenyl)-3,4-dihydropyrimidin-2-one (4ic). General procedure yielded a brown oil (67%). 94% ee by HPLC: Chiralcel ODH column, 90:10 Hex:iPrOH, 1ml/min, RT_{major} = 9.75 min, RT_{minor} = 7.15 min, 230 nm. $[\alpha]^{20}_D$ = +219.7, c = 0.0081 g/ml $CHCl_3$. ^1H NMR (300 MHz, $CDCl_3$) δ 7.35 - 7.20 (m, 7H), 6.97 - 6.86 (m, 2 H), 5.95 (d, *J* = 7.8 Hz, 1H), 5.46 (d, *J* = 4.8 Hz, 1H), 4.96 (dd, *J* = 7.8, 4.8 Hz, 1H), 4.78 (d, *J* = 15.3 Hz, 1H), 4.63 (d, *J* = 15.3 Hz, 1H), 3.89 (ddd, *J* = 15.3, 8.7, 6.9 Hz, 1H), 3.82 (s, 3H), 2.62 (ddd, *J* = 14.1, 8.4, 5.7 Hz, 1H), 1.66 - 1.49 (m, 2H), 1.28 (m, 6H), 0.88 (m, 3H). ^{13}C NMR (75 MHz, $CDCl_3$) δ 155.8, 154.2, 138.4, 130.3, 128.5, 128.4, 127.4, 127.3, 127.1, 126.8, 120.9, 110.3, 101.8, 55.2, 54.7, 50.2, 46.0, 31.5, 27.3, 26.4, 22.5, 14.0. R_f = 0.32 (98:2 CH_2Cl_2:EtOAc). IR (NaCl, Thin Film) 2954, 2929, 2857, 1654, 1464, 1239, 1029, 704 cm^{-1}. HRMS (ESI) *m/z* $[C_{24}H_{31}N_2O_2]^+$ calcd 379.2380, found 379.2386.

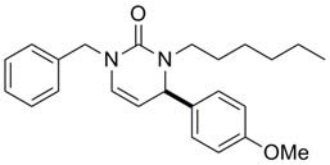

(*R*)-1-benzyl-3-hexyl-4-(4-methoxyphenyl)-3,4-dihydropyrimidin-2-one (4jc). General procedure yielded a gold oil (69%). 92% ee by HPLC: Chiralcel IA column, 90:10 Hex:iPrOH, 1ml/min, RT_{major} = 10.55 min, RT_{minor} = 9.7 min, 210 nm. $[\alpha]^{20}_D$ = +177.8, c = 0.0086 g/ml $CHCl_3$. ^1H NMR (300 MHz, $CDCl_3$) δ 7.35 - 7.20 (m, 5H), 7.16 (m, 2H), 6.85 (m, 2H), 5.98 (d, *J* = 7.8 Hz, 1H), 4.95 (d, *J* = 4.5 Hz, 1H), 4.78 (dd, *J* = 7.8, 4.5 Hz, 1H), 4.75 (d, *J* = 15.3 Hz, 1H), 4.65 (d, *J* = 15.3 Hz, 1H), 3.80 (s, 3H), 3.71 (ddd, *J* = 15.3, 9.3, 6.3 Hz, 1H), 2.69 (ddd, *J* = 14.1, 9.0, 5.1 Hz, 1H), 1.55 (m, 1H), 1.46 (m, 1H), 1.24 (m, 6H), 0.86 (m, 3H). ^{13}C NMR (75 MHz, $CDCl_3$) δ 159.2, 153.3, 138.3, 134.9, 128.6, 127.7, 127.5, 127.3, 126.8, 114.0, 102.7, 60.7, 55.2, 50.3, 45.7, 31.5, 26.9, 26.5, 22.6, 14.0. R_f = 0.35 (98:2 CH_2Cl_2:EtOAc). IR (NaCl, Thin Film) 2929, 2857, 1653, 1510, 1249, 1034, 832, 703 cm^{-1}. HRMS (ESI) *m/z* $[C_{24}H_{31}N_2O_2]^+$ calcd 379.2380, found 379.2376.

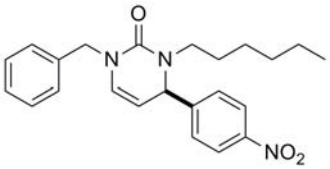

(*R*)-1-benzyl-3-hexyl-4-(4-nitrophenyl)-3,4-dihydropyrimidin-2-one (4kc). General procedure yielded a brown syrup (36%). 95% ee by HPLC: Chiralcel IA column, 90:10 Hex:iPrOH, 1ml/min, RT_{major} = 16.76 min, RT_{minor} = 19.91 min, 210 nm. $[\alpha]^{20}_D$ = +227.3, c = 0.0077 g/ml $CHCl_3$. ^1H NMR (300 MHz, $CDCl_3$) 8.18 (m, 2H), 7.39 - 7.28 (m, 7H), 6.04 (d, *J* = 7.8 Hz, 1H), 5.12 (d, *J* = 4.8 Hz, 1H), 4.80 (dd, *J* = 7.8, 4.8 Hz, 1H), 4.78 (d, *J* = 15.0 Hz, 1H), 4.63 (d, *J* = 15.0 Hz, 1H), 3.80 (ddd, *J* = 15.3, 9.3, 6.3 Hz, 1H), 2.62 (ddd, *J* = 14.4, 9.0, 5.4 Hz, 1H), 1.52 (m, 2H), 1.25 (m, 6H), 0.86 (m, 3H). ^{13}C NMR (75 MHz, $CDCl_3$) δ 153.2, 149.9, 147.5, 137.9, 128.7, 128.3, 127.6, 127.1, 124.2, 101.0, 60.8, 50.5, 46.4, 31.5, 27.0, 26.4, 22.5, 14.0. R_f = 0.44 (98:2 CH_2Cl_2:EtOAc). IR (NaCl, Thin Film) 2930, 2858, 1654, 1522, 1348, 700 cm^{-1}. HRMS (ESI) *m/z* $[C_{23}H_{28}N_3O_3]^+$ calcd 394.2125, found 394.2130.

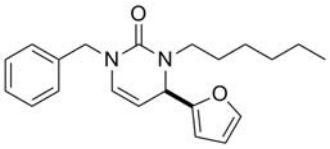

(*R*)-1-benzyl-4-(furan-2-yl)-3-hexyl-3,4-dihydropyrimidin-2-one (4lc). General procedure yielded a brown syrup (82%). 94% ee by HPLC: Chiralcel ODH column, 90:10 Hex:iPrOH, 1ml/min, RT_{major} = 8.86 min, RT_{minor} = 8.00 min, 210 nm. $[\alpha]^{20}_D$ = +138.7, c = 0.0140 g/ml $CHCl_3$. ^1H NMR (300 MHz, $CDCl_3$) 7.36 - 7.22 (m, 6H), 6.32 (dd, J = 3.0, 1.8 Hz, 1H), 6.18 (d, 3.0 Hz, 1H), 6.08 (d, 7.8 Hz, 1H), 5.05 (d, J = 4.8 Hz, 1H), 4.83 (dd, J = 7.8, 4.8 Hz, 1H), 4.79 (d, J = 15.3 Hz, 1H), 4.63 (d, J = 15.3 Hz, 1H), 3.72 (ddd, J = 15.0, 9.3, 6.0 Hz, 1H), 2.98 (ddd, J = 14.1, 9.0, 5.1 Hz, 1H), 1.59 (m, 1H), 1.40 (m, 1H), 1.28 (m, 6H), 0.88 (m, 3H). ^{13}C NMR (75 MHz, $CDCl_3$) δ 154.1, 153.2, 142.2, 138.1, 129.1, 128.4, 127.3, 127.1, 110.2, 106.8, 98.9, 54.1, 50.1, 46.1, 31.5, 27.1, 26.4, 22.5, 14.0. R_f = 0.46 (98:2 CH_2Cl_2:EtOAc). IR (NaCl, Thin Film) 2957, 2929, 2858, 1654, 1497, 1254, 737 cm^{-1}. HRMS (ESI) *m/z* $[C_{21}H_{27}N_2O_2]^+$ calcd 339.2067, found 339.2075.

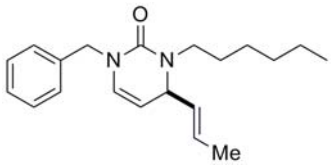

(*S,E*)-1-benzyl-3-hexyl-4-(prop-1-en-1-yl)-3,4-dihydropyrimidin-2-one (4mc). General procedure yielded yellow oil (60%) as a 1:10 mixture of cis:trans isomers. 89% ee by HPLC: Chiralcel IA column, 90:10 Hex:iPrOH, 1ml/min, RT_{major} = 6.79 min, RT_{minor} = 6.53 min, 230 nm. $[\alpha]^{20}_D$ = +121.6, c = 0.0124 g/ml $CHCl_3$. ^1H NMR (300 MHz, $CDCl_3$) δ 7.34 - 7.23 (m, 5H), 5.92 (d, *J* = 7.8 Hz, 1H), 5.59 - 5.33 (m, 2H), 4.70 (d, *J* = 15.3 Hz, 1H), 4.65 (m, 1H), 4.57 (d, *J* = 15.3 Hz, 1H), 4.30 (dd, *J* = 7.8, 4.8 Hz, 1H), 3.72 (ddd, *J* =

15.0, 7.8, 7.2 Hz, 1H), 2.90 (ddd, *J* = 14.1, 8.1, 6.0 Hz, 1H), 1.69 (d, *J* = 6.0 Hz, 3H), 1.56 (m, 2H), 1.29 (m, 6H), 0.88 (m, 3H). ^{13}C NMR (75 MHz, $CDCl_3$) δ 153.5, 138.4, 130.8, 128.4, 127.8, 127.3, 127.1, 126.4, 101.2, 59.1, 50.0, 45.3, 31.5, 27.3, 26.5, 22.6, 17.4, 14.0. R_f = 0.31 (98:2 CH_2Cl_2:EtOAc). IR (NaCl, Thin Film) 3029, 2929, 2857, 1653, 1456, 1253, 964, 703 cm^{-1}. HRMS (ESI) *m/z* $[C_{20}H_{29}N_2O]^+$ calcd 313.2274, found 313.2277.

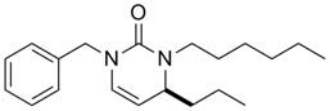

(*S*)-1-benzyl-3-hexyl-4-propyl-3,4-dihydropyrimidin-2-one (4nc). General procedure yielded gold syrup (38%). 77% ee by HPLC: Chiralcel ODH column, 90:10 Hex:iPrOH, 1ml/min, RT_{major} = 5.75 min, RT_{minor} = 5.16 min, 230 nm. $[\alpha]^{20}_D$ = +27.0, c = 0.0117 g/ml $CHCl_3$. ^{1}H NMR (300 MHz, $CDCl_3$) δ 7.33 - 7.23 (m, 5H), 5.95 (d, *J* = 7.8 Hz, 1H), 4.74 (m, 1H), 4.71 (d, *J* = 15.3 Hz, 1H), 4.53 (d, *J* = 15.3 Hz, 1H), 3.93 (m, 1H), 3.78 (ddd, *J* = 14.4, 8.7, 6.6 Hz, 1H), 2.88 (ddd, *J* = 14.4, 8.7, 5.7 Hz, 1H), 1.58 (m, 2H), 1.30 (m, 10H), 0.89 (m, 6H). ^{13}C NMR (75 MHz, $CDCl_3$) δ 154.1, 138.4, 128.4, 127.4, 127.1, 101.7, 56.2, 50.0, 45.8, 37.1, 31.6, 27.8, 26.5, 22.6, 17.0, 14.0. R_f = 0.42 (98:2 CH_2Cl_2:EtOAc). IR (NaCl, Thin Film) 3065, 3032, 2930, 2859, 1653, 1454, 1372, 1259, 700 cm^{-1}. HRMS (ESI) *m/z* $[C_{20}H_{31}N_2O]^+$ calcd 315.2431, found 315.2431.

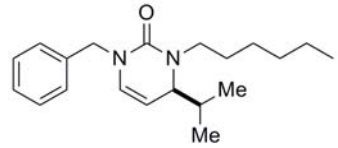

(*S*)-1-benzyl-3-hexyl-4-isopropyl-3,4-dihydropyrimidin-2-one (4oc). General procedure yielded gold syrup (53%). 83% ee by HPLC: Chiralcel ODH column, 90:10 Hex:iPrOH, 1ml/min, RT_{major} = 6.19 min, RT_{minor} = 5.43 min, 210 nm. $[\alpha]^{20}_D$ = +59.0, c = 0.0116 g/ml $CHCl_3$. ^{1}H NMR (300 MHz, $CDCl_3$) δ 7.33 - 7.23 (m, 5H), 6.02 (d, J = 8.1 Hz, 1H), 4.74 (d, J = 15.3 Hz, 1H), 4.64 (dd, J = 8.1, 4.5 Hz, 1H), 4.48 (d, J = 15.3 Hz, 1H), 3.85 (dd, J = 4.5, 4.2 Hz, 1H), 3.77 (ddd, J = 15.3, 9.3, 6.3 Hz, 1H), 2.91 (ddd, J = 14.4, 9.0, 5.4 Hz, 1H), 1.97 (dd, J = 6.6, 4.2 Hz, 1H), 1.59 (m, 2H), 1.30 (m, 6H), 0.89 (m, 3H), 0.83 (m, 6H). ^{13}C NMR (75 MHz, $CDCl_3$) δ 154.2, 138.2, 129.5, 128.4, 127.6, 127.1, 97.5, 62.0, 50.0, 46.3, 31.6, 31.4, 27.7, 26.6, 22.6, 17.8, 15.2, 14.0. R_f = 0.43 (98:2 CH_2Cl_2:EtOAc). IR (NaCl, Thin Film) 2959, 2929, 2871, 1652, 1455, 1257, 702 cm^{-1}. HRMS (ESI) *m/z* $[C_{20}H_{31}N_2O]^+$ calcd 315.2431, found 315.2421.

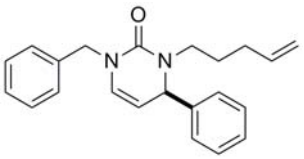

(*R*)-1-benzyl-3-(pent-4-en-1-yl)-4-phenyl-3,4-dihydropyrimidin-2-one (4hb). General procedure yielded gold syrup (53%). 91% ee by HPLC: Chiralcel IC column, 95:5 Hex:iPrOH, 1ml/min, RT_{major} = 20.89 min, RT_{minor} = 18.37 min, 210 nm. $[\alpha]^{20}_D$ = +120.4, c = 0.0098 g/ml $CHCl_3$. ^{1}H NMR (300 MHz, $CDCl_3$) δ 7.38 - 7.23 (m, 10H), 5.99 (d, *J* = 7.8 Hz, 1H), 5.78 (ddt, *J* = 16.8, 10.2, 6.6, 1H), 5.02 - 4.92 (m, 3H), 4.82 (dd, *J* = 7.8, 4.5 Hz, 1H), 4.78 (d, *J* = 15.3 Hz, 1H), 4.65 (d, *J* = 15.3 Hz, 1H), 3.74 (ddd, *J* = 15.3, 9.3, 6.3 Hz, 1H), 2.74 (ddd, *J* = 14.4, 9.0, 5.4 Hz, 1H), 2.03 (dt, *J* = 7.2, 6.6 Hz, 2H), 1.72 - 1.56 (m, 2H). ^{13}C NMR (75 MHz, $CDCl_3$) δ 153.4, 142.7, 138.2, 138.0, 128.8, 128.6, 127.9, 127.5, 127.3, 127.1, 126.4, 114.8, 102.5, 61.6, 50.3, 45.6, 31.0, 26.2. R_f = 0.24 (4:1 Hex:EtOAc). IR (NaCl, Thin Film) 3064, 3030, 2930, 1653, 1452, 1246, 913, 700 cm^{-1}. HRMS (ESI) *m/z* $[C_{22}H_{25}N_2O]^+$ calcd 333.1961, found 333.1965.

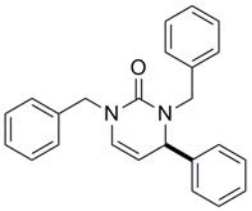

(*R*)-1,3-dibenzyl-4-phenyl-3,4-dihydropyrimidin-2-one (4hd). General procedure yielded gold syrup (65%). 94% ee by HPLC: Chiralcel ODH column, 90:10 Hex:iPrOH, 1ml/min, RT_{major} = 10.53 min, RT_{minor} = 7.97 min, 230 nm. $[\alpha]^{20}_D$ = +202.5, c = 0.0100 g/ml $CHCl_3$. ^{1}H NMR (300 MHz, $CDCl_3$) δ 7.43 -

7.23 (m, 15H), 6.03 (d, *J* = 7.8 Hz, 1H), 5.48 (d, *J* = 15.3 Hz, 1H), 4.89 (d, *J* = 15.3 Hz, 1H), 4.88 (d, *J* = 4.5 Hz, 1H), 4.79 (dd, *J* = 7.8, 4.5 Hz, 1H), 4.71 (d, *J* = 15.3 Hz, 1H), 3.56 (d, *J* = 15.3 Hz, 1H). ^{13}C NMR (75 MHz, $CDCl_3$) δ 153.7, 141.8, 138.1, 137.1, 128.8, 128.6, 128.5, 128.0, 127.5, 127.4, 127.3, 126.9, 126.7, 60.0, 50.6, 47.8. R_f = 0.42 (98:2 CH_2Cl_2:EtOAc). IR (NaCl, Thin Film) 3063, 3029, 2926, 1652, 1449, 1246, 698 cm^{-1}. HRMS (ESI) *m/z* $[C_{24}H_{23}N_2O]^+$ calcd 355.1805, found 355.1808. $[Rh(C_2H_4)_2Cl]_2$ (17.5 mg, 0.045 mmol) and **L3** (50.9 mg, 0.09 mmol) were added to an oven-dried 50 ml round bottom flask and the flask was fitted with an oven-dried reflux condenser in an inert atmosphere (Ar) glove box. Upon removal from the glove box, the reaction vessel was put under Ar and 20 ml of toluene was added via syringe and the resulting gold solution was stirred at 23 °C for 15 min. To this solution, imine **1d** (1.0 g, 4.5 mmol) and isocyanate **2c** (0.75 g, 5.6 mmol) in 15 ml of toluene was added via syringe. The reaction mixture was heated to 110 °C in an oil bath and kept at reflux for 12 h. The reaction mixture was cooled to 23 °C, concentrated *in vacuo*, and purified by flash column chromatography (2:1 Hex:CH_2Cl_2, followed by CH_2Cl_2). Evaporation of solvent afforded 1.13g (71%, 94% ee) of **3gc**.

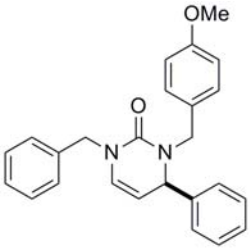

(*R*)-1-benzyl-3-(4-methoxybenzyl)-4-phenyl-3,4-dihydropyrimidin-2-one (4he). General procedure yielded gold syrup (75%). 93% ee by HPLC: Chiralcel ODH column, 90:10 Hex:iPrOH, 1 ml/min, RT_{major} = 14.91 min, RT_{minor} = 11.61 min, 210 nm. $[\alpha]^{20}_D$ = +182.6, c = 0.0113 g/ml $CHCl_3$. ^{1}H NMR (300 MHz, $CDCl_3$) δ 7.42 - 6.88 (m, 12H), 6.89 (m, 2H), 6.00 (d, *J* = 7.8 Hz, 1H), 5.41 (d, *J* = 15.0 Hz, 1H), 4.88 (d, *J* = 15.3 Hz, 1H), 4.88 (d, *J* = 4.5 Hz, 1H), 4.77 (dd, *J* = 7.8, 4.5 Hz, 1H), 4.70 (d, *J* = 15.3 Hz, 1H), 3.82 (s, 3H), 3.49 (d, *J* = 15.0 Hz). ^{13}C NMR (75 MHz, $CDCl_3$) δ 158.8, 153.6, 141.9, 138.1, 129.4, 129.0, 128.8, 128.6, 127.9, 127.5, 127.3, 126.8, 126.6, 113.8, 102.7, 59.7, 55.2, 50.6, 47.1. R_f = 0.42 (98:2 CH_2Cl_2:EtOAc). IR (NaCl, Thin Film) 3028, 2933, 1650, 1511, 1370, 1246, 700 cm^{-1}. HRMS (ESI) *m/z* $[C_{25}H_{25}N_2O_2]^+$ calcd 385.1911, found 385.1892.

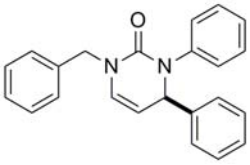

(*R*)-1-benzyl-3,4-diphenyl-3,4-dihydropyrimidin-2-one (4ha). General procedure yielded brown syrup (42%). 84% ee by HPLC: Chiralcel IA column, 90:10 Hex:iPrOH, 1 ml/min, RT_{major} = 13.74 min, RT_{minor} = 15.11 min, 230 nm. $[\alpha]^{20}_D$ = +246.5, c = 0.0123 g/ml $CHCl_3$. ^{1}H NMR (300 MHz, $CDCl_3$) δ 7.39 - 7.07 (m, 15H), 6.17 (d, *J* = 7.8 Hz, 1H), 5.29 (d, *J* = 4.8 Hz, 1H), 5.06 (dd, *J* = 7.8, 4.8 Hz, 1H), 4.84 (d, *J* = 15.0 Hz, 1H), 4.74 (d, *J* = 15.0 Hz, 1H). ^{13}C NMR (75 MHz, $CDCl_3$) δ 153.0, 142.1, 142.0, 137.8, 128.8, 128.6, 127.9, 127.8, 127.6, 127.5, 127.3, 126.7, 126.5, 64.8, 50.4. R_f = 0.50 (98:2 CH_2Cl_2:EtOAc). IR (NaCl, Thin Film) 3062, 3030, 1656, 1416, 1248, 697 cm^{-1}. HRMS (ESI) *m/z* $[C_{23}H_{21}N_2O]^+$ calcd 341.1648, found 341.1656.

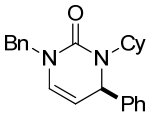

(*R*)-1-benzyl-3-cyclohexyl-4-phenyl-3,4-dihydropyrimidin-2-one (4hf). General procedure yielded brown syrup (4%). 81% ee by HPLC: Chiralcel ODH column, 90:10 Hex:iPrOH, 1 ml/min, RT_{major} = 11.37 min, RT_{minor} = 7.69 min, 210 nm. General procedure using **L8** as ligand yielded brown syrup (58%). 18% ee by HPLC: Chiralcel ODH column, 90:10 Hex:iPrOH, 1 ml/min, RT_{major} = 10.24 min, RT_{minor} = 7.028 min, 210 nm. $[\alpha]^{20}_D$ = +28.5, c = 0.0093 g/ml $CHCl_3$. ^{1}H NMR (300 MHz, $CDCl_3$) δ 7.36-7.21 (m, 10H), 5.95 (d, *J* = 7.3 Hz,

1H), 4.97 (d, *J* = 5.5 Hz, 1H), 4.92 (dd, *J* = 7.3, 5.5 Hz, 1H), 4.79 (d, *J* = 15.2 Hz, 1H), 4.64 (d, *J* = 15.2 Hz, 1H), 4.08 (m, 1H), 1.78-1.52 (m, 6H), 1.36-1.13 (m, 2H), 1.06-0.89 (m, 2H). ^{13}C NMR (75 MHz, $CDCl_3$) δ 153.8, 145.1, 138.3, 128.6, 128.5, 127.6, 127.4, 127.2, 126.8, 125.7, 103.7, 57.5, 56.8, 50.5, 31.8, 30.4, 26.2, 26.0, 25.5. R_f = 0.42 (98:2 CH_2Cl_2:EtOAc). IR (NaCl, Thin Film) 3029, 2931, 2855, 1645, 1450, 1270, 1120, 698 cm^{-1}. LRMS (ESI) *m/z* $[C_{23}H_{26}N_2O]^+$ calcd 346.2, found 347.3.

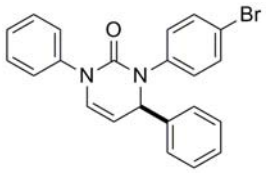

(*R*)-3-(4-bromophenyl)-1,4-diphenyl-3,4-dihydropyrimidin-2-one (4ag). General procedure yielded brown solid (37%). 81% ee by HPLC: Chiralcel IA column, 90:10 Hex:iPrOH, 1ml/min, RT_{major} = 11.44 min, RT_{minor} = 20.74 min, 210 nm. $[\alpha]^{20}_D$ = +161.8, c = 0.0126 g/ml $CHCl_3$. ^{1}H NMR (300 MHz, $CDCl_3$) δ 7.42 - 6.97 (m, 12H), 6.98 (m, 2H), 6.46 (d, *J* = 7.8 Hz, 1H), 5.34 (d, *J* = 4.8 Hz, 1H), 5.20 (dd, *J* = 7.8, 4.8 Hz, 1H). ^{13}C NMR (75 MHz, $CDCl_3$) δ 151.7, 141.4, 140.8, 140.6, 131.9, 129.5, 129.4, 128.9, 128.7, 128.5, 128.4, 128.3, 126.8, 126.7, 126.2, 120.3, 104.1, 65.0. R_f = 0.40 (98:2 CH_2Cl_2:EtOAc). IR (NaCl, Thin Film) 3061, 3029, 2924, 1672, 1489, 1264, 697 cm^{-1}. HRMS (ESI) *m/z* $[C_{22}H_{18}BrN_2O]^+$ calcd 405.0597, found 405.0594. Slow crystallization from CH_2Cl_2 layered with heptanes yielded clear X-ray quality crystals (<99% ee by HPLC: Chiralcel IA column, 90:10 Hex:iPrOH, 1ml/min, RT_{major} = 11.70 min).

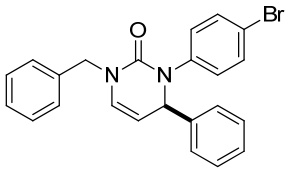

(*R*)-1-benzyl-3-(4-bromophenyl)-4-phenyl-3,4-dihydropyrimidin-2-one (4hg). General procedure yielded brown syrup (58%). ee not determined. $[\alpha]^{20}_D$ = +174.3, c = 0.0103 g/ml $CHCl_3$. ^{1}H NMR (300 MHz, $CDCl_3$) δ 7.39-7.32 (m, 6H), 7.32-7.26 (m, 4H), 7.17-7.14 (m, 2), 6.96 (m, 2H), 6.17 (d, *J* = 7.8 Hz, 1H), 5.25 (d, *J* = 4.8 Hz, 1H), 5.05 (dd, *J* = 7.8, 4.8 Hz, 1H), 4.81 (d, *J* = 15.0 Hz, 1H), 4.73 (d, *J* = 15.0 Hz, 1H). ^{13}C NMR (75 MHz, $CDCl_3$) δ 152.7, 141.6, 141.0 137.6, 131.9, 129.3 128.8, 128.6, 128.1, 127.9, 127.6, 127.2, 126.7, 120.0, 103.6, 64.8, 50.5. R_f = 0.43 (98:2 CH_2Cl_2:EtOAc). IR (NaCl, Thin Film) 3063, 3030, 2929, 1654, 1491, 1249, 1100, 1029, 823, 699 cm^{-1}. HRMS (ESI) *m/z* $[C_{23}H_{20}BrN_2O]^+$ calcd 419.0750, found 419.0750 and 421.0738.

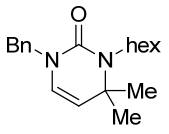

1-benzyl-3-hexyl-4,4-dimethyl-3,4-dihydropyrimidin-2-one (4sc). General procedure using **L8** as ligand yielded brown syrup (25%). ^{1}H NMR (400 MHz, $CDCl_3$) δ 7.34-7.30 (m, 3H), 7.27-7.21 (m, 2H), 5.87 (d, *J* = 7.9 Hz, 1H), 4.65 (s, 2H), 4.57 (d, *J* = 7.9 Hz, 1H), 3.27 (m, 2H), 1.60 (m, 2H), 1.32 (s, 6H), 1.31 (m, 6H), 0.89 (m, 3H). ^{13}C NMR (100 MHz, $CDCl_3$) δ 153.9, 138.5, 128.5, 127.4, 127.1, 125.7, 108.7, 57.3, 50.3, 43.1, 31.6, 30.7, 29.1, 27.0, 22.7, 14.0. R_f = 0.43 (98:2 CH_2Cl_2:EtOAc). IR (NaCl, Thin Film) 2958, 2929, 2857, 1685, 1649, 1398, 1362, 723 cm^{-1}. HRMS (ESI) *m/z* $[C_{19}H_{29}N_2O]^+$ calcd 301.2274, found 301.2271.

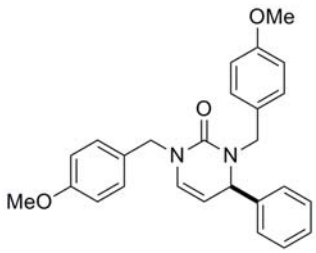

(*R*)-1,3-bis(4-methoxybenzyl)-4-phenyl-3,4-dihydropyrimidin-2-one (4fe). General procedure yielded gold syrup (78%). 92% ee by HPLC: Chiralcel IC column, 80:20 Hex:iPrOH, 1 ml/min, RT_{major} = 32.25 min, RT_{minor} = 22.60 min, 230 nm. $[\alpha]^{20}_D$ = +139.5, c = 0.0124 g/ml $CHCl_3$. ^{1}H NMR (300 MHz, $CDCl_3$) δ 7.37 - 7.17 (m, 9H), 6.92 - 6.86 (m, 4H), 5.99 (d, *J* = 7.8 Hz, 1H), 5.38 (d, *J* = 15.0 Hz, 1H), 4.83 (d, J = 4.5 Hz, 1H), 4.79 (d,

J = 14.7 Hz, 1H), 4.74 (dd, *J* = 7.8, 4.5 Hz, 1H), 4.62 (d, *J* = 15.0 Hz, 1H), 3.82 (s, 3H), 3.81 (s, 3H), 3.46 (d, *J* = 15.0 Hz, 1H). ^{13}C NMR (75 MHz, $CDCl_3$) δ 158.9, 158.8, 153.7, 142.0, 130.2, 129.4, 129.1, 129.0, 128.8, 127.9, 126.8, 126.7, 114.0, 113.8, 102.7, 59.7, 55.2, 50.1, 47.1. R_f = 0.27 (98:2 CH_2Cl_2:EtOAc). IR (NaCl, Thin Film) 3029, 3002, 2933, 2836, 1651, 1512, 1247, 1034, 828, 665 cm^{-1}. HRMS (ESI) *m/z* $[C_{26}H_{27}N_2O_3]^+$ calcd 415.2016, found 415.2018.

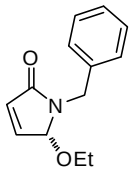

(*R*)-1-benzyl-5-ethoxy-pyrrol-2-one (19p).[7] $[Rh(C_2H_4)_2Cl]_2$ (5.8 mg, 0.015 mmol) and ligand **L3** (17.0 mg, 0.03 mmol) were added to an oven-dried 10 ml round bottom flask and the flask was fitted with an oven-dried reflux condenser in an inert atmosphere (Ar) glove box. Upon removal from the glove box, the reaction vessel was put under Ar and 4 ml of toluene was added via syringe and the resulting gold solution was stirred at 23 °C for 15 min. To this solution, (*E*)-ethyl 4-(benzylimino)but-2-enoate **3p** (69.3 mg, 0.32 mmol) in 2 ml of toluene was added via syringe. The reaction mixture was heated to 110 °C in an oil bath and kept at reflux for 12 h. The reaction mixture was cooled to 23 °C, concentrated *in vacuo*, absorbed onto Celite, and purified by flash column chromatography (2:1 Hex:EtOAc). Evaporation of solvent afforded the 56.9 mg (82%) of (*R*)-1-benzyl-5-ethoxy-pyrrol-2-one **19p** as a brown oil. 20% ee by HPLC: Chiralcel IC column, 80:20 Hex:iPrOH, 1 ml/min, RT_{major} = 14.23 min, RT_{minor} = 15.86 min, 210 nm. $[\alpha]^{20}_D$ = -38.9, c = 0.0099 g/ml $CHCl_3$. ^{1}H NMR (300 MHz, $CDCl_3$) δ 7.36-7.24 (m, 5H), 6.88 (dd, *J* = 6.0, 1.6 Hz, 1H), 6.26 (dd, *J* = 6.1, 0.8 Hz, 1H), 5.27 (bs, 1H), 4.92 (d, *J* = 14.8 Hz, 1H), 4.16 (d, *J* = 14.8 Hz, 1H), 3.28 (q, *J* = 7.0 Hz, 2H), 1.12 (t, *J* = 7.0 Hz, 3H). ^{13}C NMR (75 MHz, $CDCl_3$) δ 169.2, 144.1, 137.1, 129.8, 128.6, 128.4, 127.5, 87.2, 59.2, 43.1, 15.2. R_f = 0.21 (2:1 Hex:EtOAc). IR (NaCl, Thin Film) 2977, 2928, 1704, 1411, 1234, 1094, 703 cm^{-1}. LRMS (ESI/APCI) *m/z* $[C_{13}H_{16}NO_2]^+$ calcd 218.1, found 218.1.

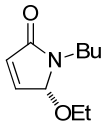

(*R*)-1-butyl-5-ethoxy-pyrrol-2-one (19r). $[Rh(C_2H_4)_2Cl]_2$ (5.8 mg, 0.015 mmol) and ligand **L3** (17.0 mg, 0.03 mmol) were added to an oven-dried 10 ml round bottom flask and the flask was fitted with an oven-dried reflux condenser in an inert atmosphere (Ar) glove box. Upon removal from the glove box, the reaction vessel was put under Ar and 4 ml of toluene was added via syringe and the resulting gold solution was stirred at 23 °C for 15 min. To this solution, (*E*)-ethyl 4-(butylimino)but-2-enoate **3r** (55.5 mg, 0.30 mmol) in 2 ml of toluene was added via syringe. The reaction mixture was heated to 110 °C in an oil bath and kept at reflux for 12 h. The reaction mixture was cooled to 23 °C, concentrated *in vacuo*, absorbed onto Celite, and purified by flash column chromatography (2:1 Hex:EtOAc). Evaporation of solvent afforded the 33.1 mg (60%) of (*R*)-1-butyl-5-ethoxy-pyrrol-2-one **19r** as a brown oil. 9% ee by HPLC: Chiralcel IC column, 90:10 Hex:iPrOH, 1 ml/min, RT_{major} = 19.59 min, RT_{minor} = 23.14 min, 210 nm. ^{1}H NMR (300 MHz, $CDCl_3$) δ 6.88 (dd, *J* = 6.0, 1.6 Hz, 1H), 6.21 (d, *J* = 8.0 Hz, 1H), 5.42 (bs, 1H), 3.57 (ddd, *J* = 14.8, 7.7, 7.7 Hz, 1H), 3.29 (m, 2H), 3.10 (ddd, *J* = 14.1, 7.7, 6.7 Hz, 1H), 1.54 (m, 2H), 1.32 (m, 2H), 1.17 (t, *J* = 7.0 Hz, 3H), 0.92 (t, *J* = 7.3 Hz, 3H). ^{13}C NMR (75 MHz, $CDCl_3$) δ 169.5, 143.6, 130.1, 87.7, 58.7, 39.2, 30.5, 20.1, 15.2, 13.7. R_f = 0.26 (2:1 Hex:EtOAc). IR (NaCl, Thin Film) 2961, 2932, 2875, 1701, 1414, 1102, 704 cm^{-1}. LRMS (ESI/APCI) *m/z* $[C_{10}H_{17}NO_2]^+$ calcd 184.1, found 184.1.

Derivitization of Pyrimidinones.

[7] Stereochemistry was arbitrarily assigned based on optical rotation of a *similar* compound: Cuiper, A. D.; Kellogg, R. M.; Feringa, B. L. *Chem. Commun.* **1998**, 655-656.

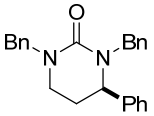

(R)-1,3-dibenzyl-4-phenyltetrahydropyrimidin-2-one (20hb). In a 10 ml round bottom flask, dihydropyrimidinone **4hb** (471.3 mg, 1.33 mmol) was dissolved in MeOH and 10% Pd/C (25 mg) was added. The reaction flask was evacuated and refilled with H_2. After stirring at 23 °C for 12 h, the reaction was filtered through Celite, concentrated *in vacuo*, and purified by flash column chromatography to yield 405.6 mg of **20hb** (86%) as a clear amorphous solid. $[\alpha]^{20}_D$ = +2.6, c = 0.0110 g/ml $CHCl_3$. ^{1}H NMR (400 MHz, $CDCl_3$) δ 7.35-7.24 (m, 13 H), 7.16-7.13 (m, 2H), 5.59 (d, *J* = 15.3 Hz, 1H), 4.71 (d, *J* = 14.9 Hz, 1H), 4.97 (d, *J* = 14.9 Hz, 1H), 4.47 (m, 1H), 3.61 (d, *J* = 15.3 Hz, 1H), 3.03 (m, 1H), 2.20 (m, 1H), 1.82 (m, 1H). ^{13}C NMR (75 MHz, $CDCl_3$) δ 156.4, 140.9, 138.5, 138.2, 128.6, 128.4, 127.8, 127.7, 127.4, 127.1, 127.0, 126.2, 57.3, 51.6, 49.2, 41.0, 29.5. R_f = 0.17 (4:1 Hex:EtOAc). IR (NaCl, Thin Film) 3062, 3029, 2928, 1635, 1498, 1449, 1218, 805, 702 cm^{-1}. HRMS (ESI) *m/z* $[C_{24}H_{25}N_2O]^+$ calcd 357.1961, found 357.1968.

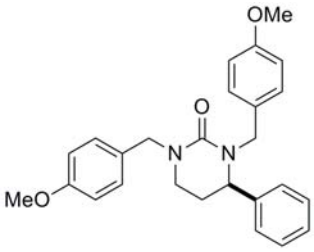

(*R*)-1,3-bis(4-methoxybenzyl)-4-phenyltetrahydropyrimidin-2-one (20fe). In a 10 ml round bottom flask, dihydropyrimidinone **4fe** (127 mg, 0.31 mmol) was dissolved in MeOH and 10% Pd/C (4 mg) was added. The reaction flask was evacuated and refilled with H_2. After stirring at 23 °C for 12 h, the reaction was filtered through Celite, concentrated *in vacuo*, and purified by flash column chromatography to yield 104.5 mg of **20fe** (82%) as a clear amorphous solid. 92% ee by HPLC: Chiralcel IA column, 85:15 Hex:iPrOH, 1 ml/min, RT_{major} = 18.96 min, RT_{minor} = 16.46 min, 254 nm. $[\alpha]^{20}_D$ = +11.5, c = 0.0132 g/ml $CHCl_3$. ^{1}H NMR (300 MHz, $CDCl_3$) δ 7.35 - 7.24 (m, 5H), 7.18 - 7.11 (m, 4H), 6.88 - 6.83 (m, 4H), 5.50 (d, *J* = 15.0 Hz, 1H), 4.63 (d, *J* = 14.8 Hz, 1H), 4.58 (d, *J* = 14.8 Hz, 1H), 4.43 (dd, *J* = 4.8, 3.3 Hz, 1H), 3.80 (s, 6H), 3.51 (d, *J* = 15.0 Hz, 1H), 3.02 - 2.97 (m, 2H), 2.14 (dddd, *J* = 16.8, 12.9, 5.4, 5.4 Hz, 1H), 1.80 (dddd, *J* = 13.2, 3.3, 3.3, 3.3 Hz, 1H). ^{13}C NMR (75 MHz, $CDCl_3$) δ 158.6, 156.3, 141.0, 130.5, 130.3, 129.1, 129.0, 128.5, 127.3, 126.2, 113.6, 56.9, 55.0, 50.9, 48.4, 40.7, 29.5. R_f = 0.19 (2:1 Hex:EtOAc). IR (NaCl, Thin Film) 2931, 2835, 1630, 1510, 1245, 1034 cm^{-1}. HRMS (ESI) *m/z* $[C_{26}H_{29}N_2O_3]^+$ calcd 417.2173, found 417.2162.

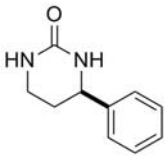

(*R*)-4-phenyltetrahydropyrimidin-2-one (21).[8] In a 10 ml round bottom flask, dihydropyrimidinone **20fe** (91.4 mg, 0.22 mmol) was dissolved in 6 ml TFA and heated to 80 °C for 3 h. The reaction was cooled to 23 °C, concentrated *in vacuo*, and purified by flash column chromatography (eluent 10:1 EtOAc:MeOH). The resulting white powder was tritrated with EtOAc to yield 25.4 mg of **21** (66%) as a white powder. 94% ee by HPLC: Chiralcel IA column, 70:30 Hex:iPrOH, 1 ml/min, RT_{major} = 6.80 min, RT_{minor} = 6.33 min, 254 nm. $[\alpha]^{20}_D$ = +41.7, c = 0.0081 g/ml MeOH. ^{1}H NMR (400 MHz, $CDCl_3$) δ 7.35 - 7.24 (m, 5H), 4.57 (dd, *J* = 6.0, 5.2 Hz, 1H), 3.27 (s, 1H), 3.26 (s, 1H), 3.23 (ddd, *J* = 12.0, 7.2, 4.8 Hz, 1H), 3.10 (ddd, *J* = 12.0, 7.2, 4.8 Hz, 1H), 2.09 (m, 1H), 1.84 (m, 1H). ^{13}C NMR (100 MHz, $CDCl_3$) δ 163.7, 129.7, 128.6, 127.2, 55.5, 38.4, 30.9. R_f = 0.18 (10:1 EtOAc:MeOH). IR (NaCl, Thin Film) 3222, 3074, 2968, 2917, 1684, 1515, 13362, 757 cm^{-1}. HRMS (ESI) *m/z* $[C_{10}H_{13}N_2O]^+$ calcd 177.1022, found 177.1021.

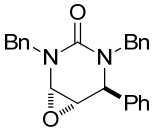

(*1S,5S,6S*)-2,4-dibenzyl-5-phenyl-7-oxa-2,4-diazabicyclo[4.1.0]heptan-3-one (22). In a 10 ml round bottom flask, dihydropyrimidinone **4hb** (62.1 mg, 0.18 mmol) was dissolved in 6 ml DCM. mCPBA (76.8 mg, 0.34 mmol) was added and the reaction was stirred for

[8] He, Z.-Q., Zhou, Q.; Wu, L.; Chen, Y.-C. *Adv. Synth. Catal.* **2010**, *352*, 1904-1908.

24 h at 23 °C. The reaction was diluted with DCM and washed with 5% NaOH. The organic layer was dried and concentrated *in vacuo*. The resulting residue was purified by flash column chromatography (eluent 4:1 Hex:EtOAc) to yield 22.4 mg (34%) of **22** as a clear residue. ^{1}H NMR (300 MHz, $CDCl_3$) δ 7.43 (m, 2H), 7.33 (m, 6H), 7.22 (m, 3H), 7.06 (m, 2H), 6.97 (m, 2H), 5.28 (d, *J* = 15.2 Hz, 1H), 5.12 (d, *J* = 14.0 Hz, 1H), 5.06 (d, *J* = 14.0 Hz, 1H), 4.38 (dd, *J* = 8.1, 2.1 Hz, 1H), 4.30 (d, *J* = 8.1 Hz, 1H), 3.76 (d, *J* = 15.2 Hz, 1H), 3.37 (d, *J* = 2.4 Hz, 1H). R_f = 0.42 (2:1 Hex:EtOAc). LRMS (ESI) *m/z* $[C_{24}H_{23}N_2O_2]^+$ calcd 371.2, found 371.2.

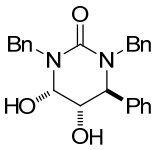

(4S,5S,6S)-1,3-dibenzyl-4,5-dihydroxy-6-phenyltetrahydropyrimidin-2-one (23). In a 10 ml round bottom flask, dihydropyrimidinone 4hb (88.8 mg, 0.25 mmol) was dissolved in 5 ml acetone:H_2O (1:1). To the reaction mixture, $K_2OsO_2(OH)_2$ (4.6 mg, 0.0125 mmol) and NMO (36.6 mg, 0.31 mmol). The reaction was stirred at 23 °C for 12h. The reaction was diluted with EtOAc and H_2O. The layers were seperated and the aqueous was extracted with EtOAc 2x. The organic layer was dried with MgSO4, filtered, and concentrated. The resulting residue was purified by flash column chromatography (eluent 2:1 Hex:EtOAc) to yield 38.3 mg (40%) of 23 as a yellow oil. ^{1}H NMR (300 MHz, $CDCl_3$) δ 7.40-7.20 (m, 11 H), 7.14 (m, 2H), 7.06 (m, 2H), 5.38 (d, *J* = 15.3 Hz, 1H), 5.08 (d, *J* = 14.8 Hz, 1H), 4.62 (d, *J* = 3.2 Hz, 1H), 4.46 (d, *J* = 14.9, 1H), 4.31 (d, *J* = 6.6 Hz, 1H), 3.84 (dd, *J* = 6.8, 3.2 Hz, 1H), 3.56 (d, *J* = 15.3 Hz, 1H), 3.17 (bs, 1H), 2.32 (bs, 1H). R_f = 0.14 (2:1 Hex:EtOAc). LRMS (ESI) *m/z* $[C_{24}H_{25}N_2O_3]^+$ calcd 389.2, found 371.2 (M-H_2O), 389.2 (M+H), 403.2 (M-OH+MeOH).

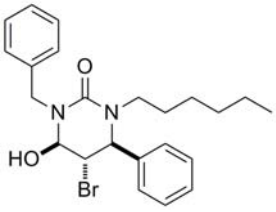

(*4S,5S,6R*)-1-benzyl-5-bromo-3-hexyl-6-hydroxy-4-phenyltetrahydropyrimidin-2-one (24hc). In a 10 ml round bottom, dihydropyrimidinone **4hc** (101.2 mg, 0.29 mmol) was dissolved in 6 ml of wet DMF, NBS (52.7 mg, 0.29 mmol) was added, and the reaction was stirred for 3 h at 23 °C. The reaction was diluted with 50 ml Et_2O and the organic layer was washed with H_2O (3 X 50 ml), concentrated *in vacuo*, dried with $MgSO_4$, and purified by flash column chromatography (eluent 4:1 Hex:EtOAc) to yield 96.7 mg of **6** (75%) as a clear amorphous solid. 94% ee by HPLC: Chiralcel IC column, 80:20 Hex:iPrOH, 1 ml/min, RT_{major} = 7.14 min, RT_{minor} = 5.23 min, 230 nm. $[\alpha]^{20}_D$ = -20.6, c = 0.0060 g/ml $CHCl_3$. ^{1}H NMR (300 MHz, $CDCl_3$) δ 7.44 - 7.24 (m, 10H), 5.13 (d, *J* = 15.3 Hz, 1H), 4.83 (bs, 1H), 4.77 (bd, *J* = 10.2 Hz, 1H), 4.59 (dd, *J* = 2.1, 2.1 Hz, 1H), 4.27 (d, *J* = 15.3 Hz, 1H), 4.08 (ddd, *J* = 15.6, 9.3, 6.6 Hz, 1H), 2.70 (ddd, *J* = 14.4, 9.3, 5.1 Hz, 1H), 1.62 (m, 3H), 1.28 (m, 6H), 0.87 (m, 3H). ^{13}C NMR (75 MHz, $CDCl_3$) δ 153.4, 137.9, 137.5, 129.7, 128.7, 128.3, 128.2, 127.2, 126.0, 83.1, 63.4, 48.4, 48.3, 47.7, 31.6, 27.8, 26.6, 22.6, 14.0. R_f = 0.26 (2:1 Hex:EtOAc). IR (NaCl, Thin Film) 3330, 2955, 2928, 2857, 1616, 1502, 1227, 1045, 696 cm^{-1}. HRMS (ESI) *m/z* $[C_{23}H_{30}BrN_2O_2]^+$ calcd 445.1485, found 445.1494.

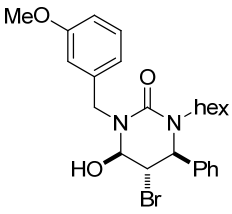

(*4R,5S,6S*)-5-bromo-1-hexyl-4-hydroxy-3-(3-methoxybenzyl)-6-phenyltetrahydropyrimidin-2-one (24gc). In a 10 ml round bottom, dihydropyrimidinone **4gc** (72.0 mg, 0.19 mmol) was dissolved in 6 ml of wet DMF, NBS (36.8 mg, 0.20 mmol) was added, and the reaction was stirred for 3 h at 0 °C. The reaction was diluted with 50 ml Et_2O and the organic layer was washed with H_2O (3 X 50 ml), concentrated *in vacuo*, dried with $MgSO_4$, and purified by flash column chromatography (eluent 4:1 Hex:EtOAc) to yield 58.0 mg of **24gc** (64%) as a clear amorphous solid. $[\alpha]^{20}_D$ = -29.6, c = 0.0094 g/ml $CHCl_3$. ^{1}H NMR (300 MHz, $CDCl_3$) δ 7.45-7.18

(m, 6H), 6.93-6.77 (m, 3H), 5.14 (d, J = 15.3 Hz, 1H), 4.84 (bs, 1H), 4.77 (dt, J = 13.7Hz, 1H), 4.61 (t, J = 1.9 Hz, 1H), 4.25 (d, J = 15.3 Hz, 1H), 4.10 (ddd, J = 13.9, 9.0, 6.7 Hz, 1H), 3.79 (s, 3H), 2.70 (ddd, J = 14.1, 9.3, 5.0 Hz, 1H), 1.63 (m, 2H), 1.48 (d, J = 10.7 Hz, 1H), 1.30 (m, 6H), 0.87 (m, 3H). R_f = 0.30 (2:1 Hex:EtOAc). IR (NaCl, Thin Film) 3320, 2930, 2858, 1616, 1504, 1262, 1045, 727 cm^{-1}. HRMS (ESI) *m/z* $[C_{24}H_{32}BrN_2O_3]^+$ calcd 475.1591, found 475.1595 and 477.1576.

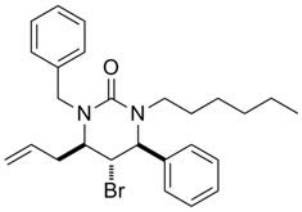

(*4S,5S,6R*)-6-allyl-1-benzyl-5-bromo-3-hexyl-4-phenyltetrahydropyrimidin-2-one (25). In a 10 ml round bottom, bromohydrin **24hc** (54.1 mg, 0.12 mmol) and allyltrimethylsilane (41.4 mg, 0.36 mmol) was dissolved in DCM and cooled to -78 °C. After cooling, 50 µl of boron trifluoride diethyl etherate was added and the reaction vessel was removed from the cooling bath and allowed to warm to 23 °C. The reaction was concentrated *in vacuo*, and purified by flash column chromatography (eluent 10:1 Hex:EtOAc) to yield 43.1 mg of **7** (72%) as a clear syrup. 94% ee by HPLC: Chiralcel ODH column, 90:10 Hex:iPrOH, 1 ml/min, RT_{major} = 5.40 min, RT_{minor} = 4.62 min, 254 nm. $[\alpha]^{20}_D$ = +15.4, c = 0.0105 g/ml $CHCl_3$. ^{1}H NMR (300 MHz, $CDCl_3$) δ 7.42 - 7.22 (m, 10H), 5.29 (d, *J* = 15.3 Hz, 1H), 5.25 (m, 1H), 4.86 (bs, 1H), 4.84 (bd, *J* = 10.8 Hz, 1H), 4.72 (bs, 1H), 4.21 (bd, *J* = 16.5 Hz, 1H), 4.16 (m, 1H), 4.13 (d, *J* = 15.3 Hz, 1H), 3.49 (dd, *J* = 11.4, 4.2 Hz, 1H), 2.62 (ddd, *J* 14.3, 9.9, 4.5 Hz, 1H), 2.14 (dt, *J* = 13.8, 5.1 Hz, 1H), 1.72 (m, 1H), 1.57 (m, 1H), 1.41 (m, 2H), 1.29 (m, 5H), 0.87 (m, 3H). ^{13}C NMR (75 MHz, $CDCl_3$) δ 154.5, 138.8, 137.7, 132.6, 129.0, 128.3, 128.2, 128.1, 127.2, 126.7, 119.2, 65.3, 62.3, 49.1, 47.5, 47.2, 37.3, 31.7, 27.7, 26.6, 22.6, 14.0. R_f = 0.38 (4:1 Hex:EtOAc). IR (NaCl, Thin Film) 3063, 3028, 2955, 2928, 2857, 1636, 1482, 1230, 923, 818, 702 cm^{-1}. HRMS (ESI) *m/z* $[C_{26}H_{34}BrN_2O]^+$ calcd 469.1849, found 469.1841.

High Throughput Experimentation.[9]

The experimental design was accomplished using ChemDraw and Excel. The reaction set up was done in an MBraun duel glovebox. Solvents were purchased from Aldrich (anhydrous, sure-seal) and used with no further purification). The reactions were carried out in 1 mL vials (30 mm height x 8 mm diameter) (Freeslate, Inc.) in a 24-well plate aluminum reactor block (Analytical Sales & Service, Inc.). Chemicals were dosed using an Eppendorf pipettor (20-200 uL). Dosing solvent was removed using a custom blow down box with nitrogen inlet and vacuum outlet. The reactions were heated and stirred using a tumble stirrer (V&P Scientific, Inc.) using parylene coated tumble stir dowels (1.98 mm diameter, 4.80 mm length) (V&P Scientific, Inc.).

The metals (1 umol and 0.5 umol for dimers) were dosed into the reaction vials as solutions (or slurries) (50 uL of an 0.02 M solution in THF). The ligands (1 umol) were dosed into the reaction as solutions (50 uL of an 0.02 M solution in THF). The dosing solvent was removed using the blow down tool. A stir-bar was added to each reaction vial. The starting materials 1-benzyl-4,4'-dimethyl-1-azabuta-1,3-diene **3s** (10 umol), hexyl isocyanate **2c** (15 umol) and trimethoxybenene (internal standard) (1 umol) was added to each vial in the desired reaction solvent (0.1 M solutions). The reactions were sealed and heated to 110 °C for 14 h. After cooling to 23 °C, the reactions were diluted with 400 uL of MeCN. In a seperate 96-1mL-well LC plate, 750 uL of MeCN was added. Aliquots (100 uL) of the diluted reactions

[9] This procedure is based on the HTE platform developed by Merck and Co. Inc. (a) Dreher, S. D.; Dormer, P. G.; Sandrock, D. L.; Molander, G. A. *J. Am. Chem. Soc.* **2008**, *130*, 9257-9259. (b) Spencer D. Dreher, Merck and Co. Inc., Rahway, New Jersey, USA. Personal Communication, 2011.

were added to the LC plate. The LC plate was sealed and inverted to mix the solution. The reactions were analyzed using an Agilent HPLC with a 96-well auto-sampler. HPLC method: Aldrich Ascentis Express C-18 column (4.6 diameter, 100 mm length) with mobile phase A (0.1% H_3PO_4/H_2O) and mobile phase B (MeCN). Gradient of 10-95% B in 6 minutes, hold 95% B for 2 minutes. Flow rate 1.8 mL/min. Temperature 40 °C.

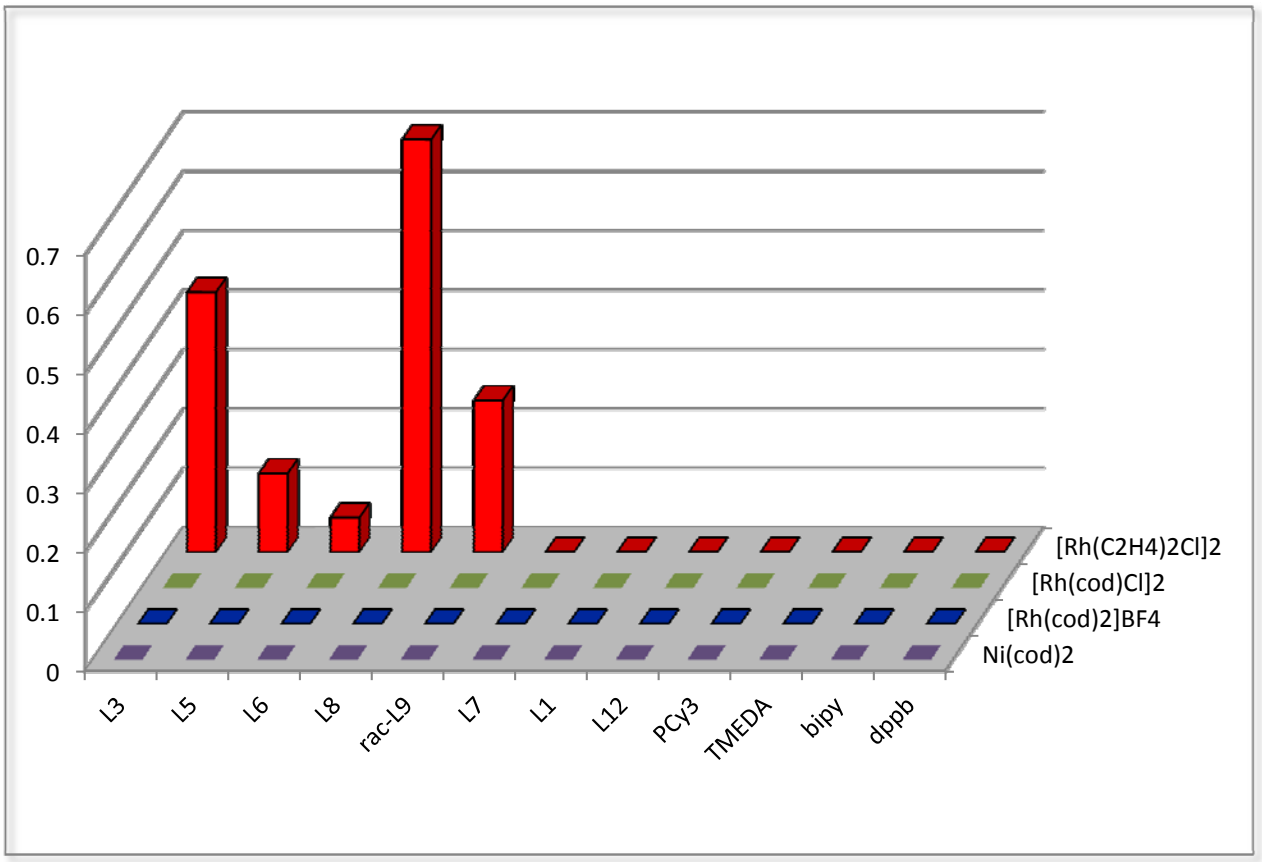

Vial	Metal	Ligand		IS	prod	prod/IS
A1	[Rh(C2H4)2Cl]2	L3		979	428	0.437181
A2	[Rh(C2H4)2Cl]2	L5		914	121	0.132385
A3	[Rh(C2H4)2Cl]2	L6		603	35	0.058043
A4	[Rh(C2H4)2Cl]2	L8		807	560	0.693928
A5	[Rh(C2H4)2Cl]2	L9		819	209	0.255189
A6	[Rh(C2H4)2Cl]2	L7		1027	0	0
B1	[Rh(C2H4)2Cl]2	tBuPhox		929	0	0
B2	[Rh(C2H4)2Cl]2	BINAP		1	0	0
B3	[Rh(C2H4)2Cl]2	PCy3		1	0	0
B4	[Rh(C2H4)2Cl]2	TMEDA		1	0	0
B5	[Rh(C2H4)2Cl]2	bipy		27	0	0
B6	[Rh(C2H4)2Cl]2	dppb		1094	0	0
C1	[Rh(cod)2]BF4	L3		1064	0	0
C2	[Rh(cod)2]BF4	L5		820	0	0
C3	[Rh(cod)2]BF4	L6		994	0	0
C4	[Rh(cod)2]BF4	L8		1	0	0
C5	[Rh(cod)2]BF4	L9		1	0	0
C6	[Rh(cod)2]BF4	L7		1021	0	0
D1	[Rh(cod)2]BF4	tBuPhox		1022	0	0
D2	[Rh(cod)2]BF4	BINAP		1127	0	0
D3	[Rh(cod)2]BF4	PCy3		1106	0	0
D4	[Rh(cod)2]BF4	TMEDA		774	0	0
D5	[Rh(cod)2]BF4	bipy		1076	0	0
D6	[Rh(cod)2]BF4	dppb		1103	0	0

Vial	Metal	Ligand		IS	prod	prod/IS
A1	[Rh(cod)Cl]2	Taddol(Ph,pyr)		979	428	0
A2	[Rh(cod)Cl]2	Taddol(xyl,pip)		914	121	0
A3	[Rh(cod)Cl]2	CKPhos		603	35	0
A4	[Rh(cod)Cl]2	GuiPhos		807	560	0
A5	[Rh(cod)Cl]2	tBuPhos		819	209	0
A6	[Rh(cod)Cl]2	MonoPhos		1027	0	0
B1	[Rh(cod)Cl]2	tBuPhox		929	0	0
B2	[Rh(cod)Cl]2	BINAP		1	0	0
B3	[Rh(cod)Cl]2	PCy3		1	0	0
B4	[Rh(cod)Cl]2	P(fur)3		1	0	0
B5	[Rh(cod)Cl]2	Ad2PBu		27	0	0
B6	[Rh(cod)Cl]2	dppb		1094	0	0
C1	Ni(cod)2	L3		1064	0	0
C2	Ni(cod)2	L5		820	0	0
C3	Ni(cod)2	L6		994	0	0
C4	Ni(cod)2	L8		1	0	0
C5	Ni(cod)2	L9		1	0	0
C6	Ni(cod)2	L7		1021	0	0
D1	Ni(cod)2	tBuPhox		1022	0	0
D2	Ni(cod)2	BINAP		1127	0	0
D3	Ni(cod)2	PCy3		1106	0	0
D4	Ni(cod)2	P(fur)3		774	0	0
D5	Ni(cod)2	Ad2PBu		1076	0	0
D6	Ni(cod)2	dppb		1103	0	0

^{1}H NMR and ^{13}C NMR Spectra of Selected Compounds.

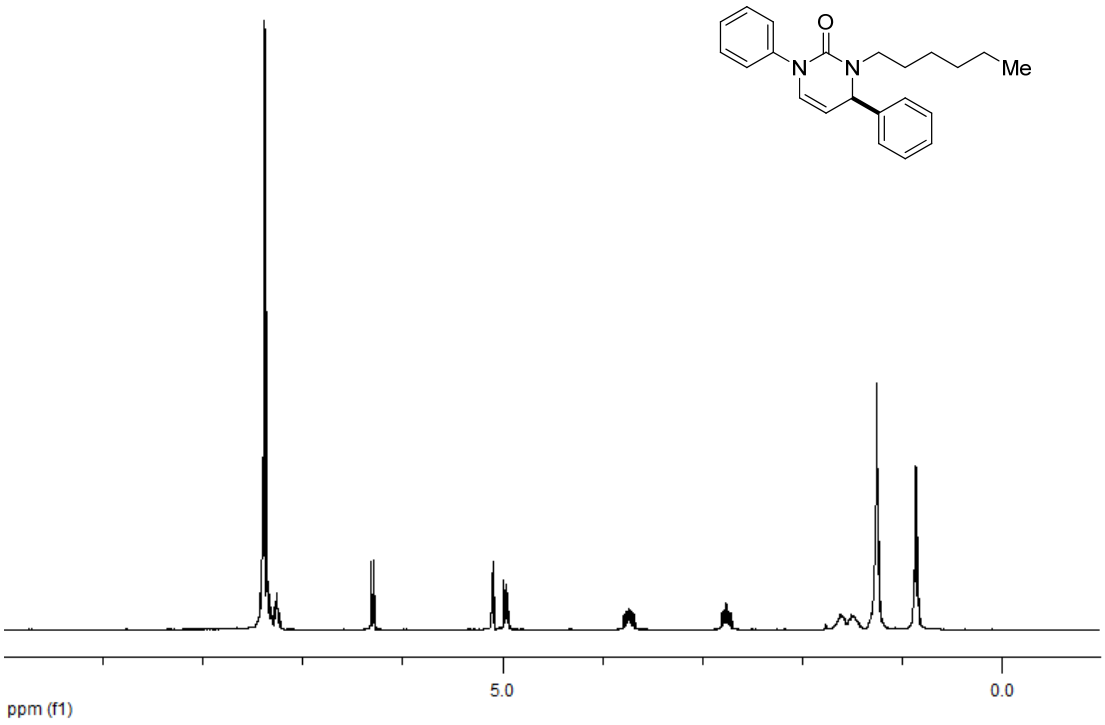

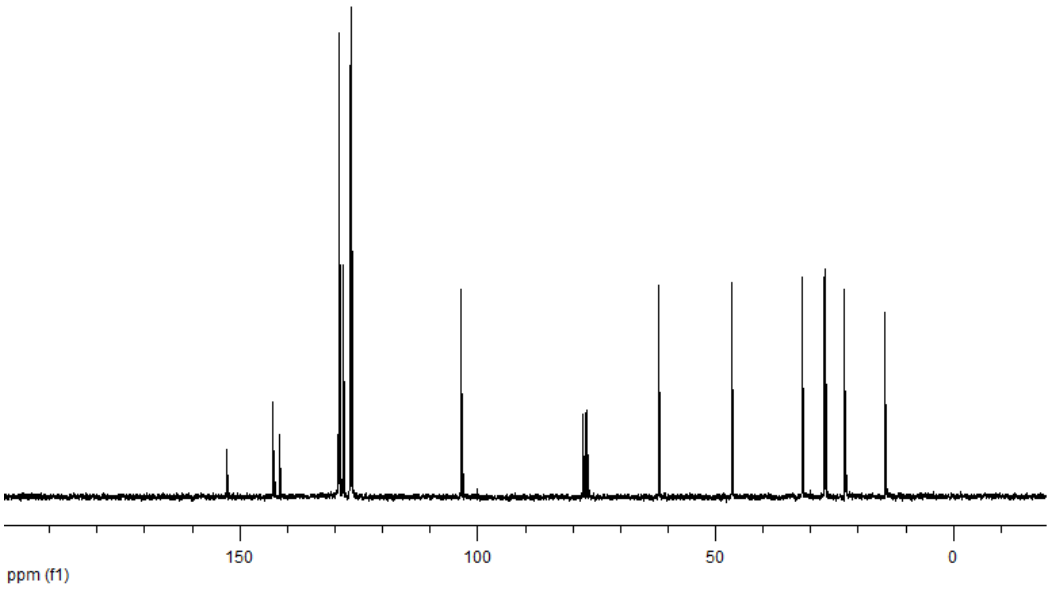

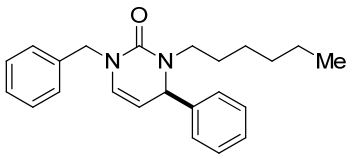
O
N
N
Me

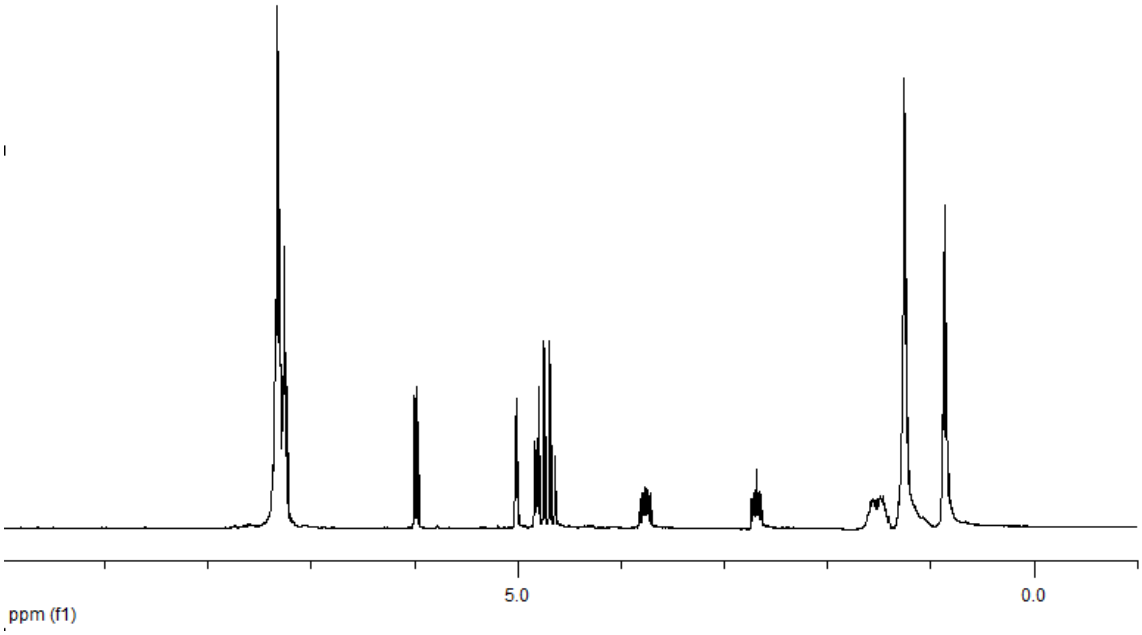
5.0
0.0
ppm (f1)

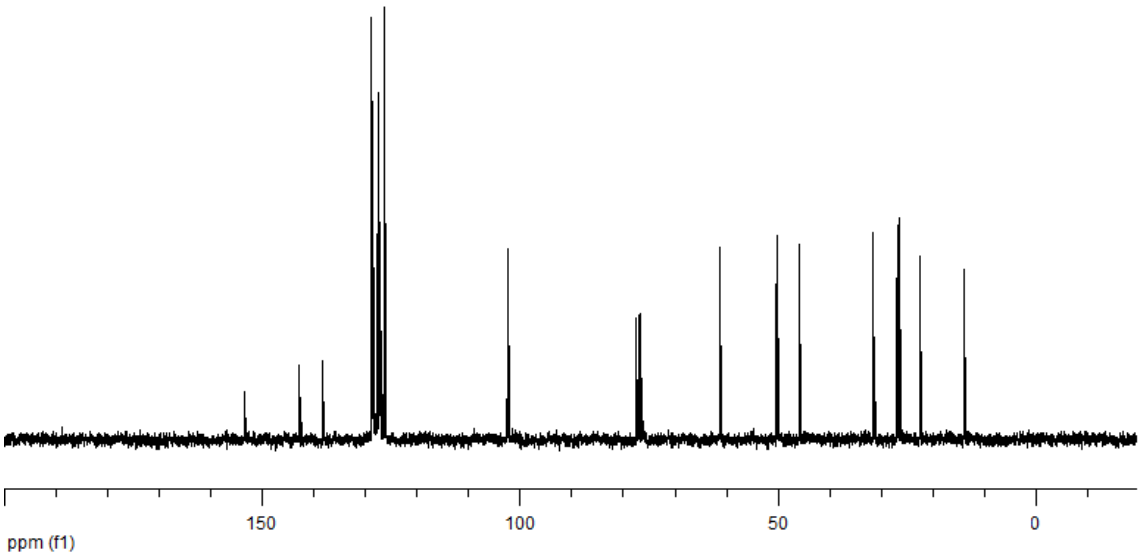
150
100
50
0
ppm (f1)

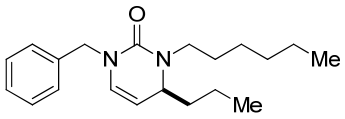
O
N
N
Me
Me

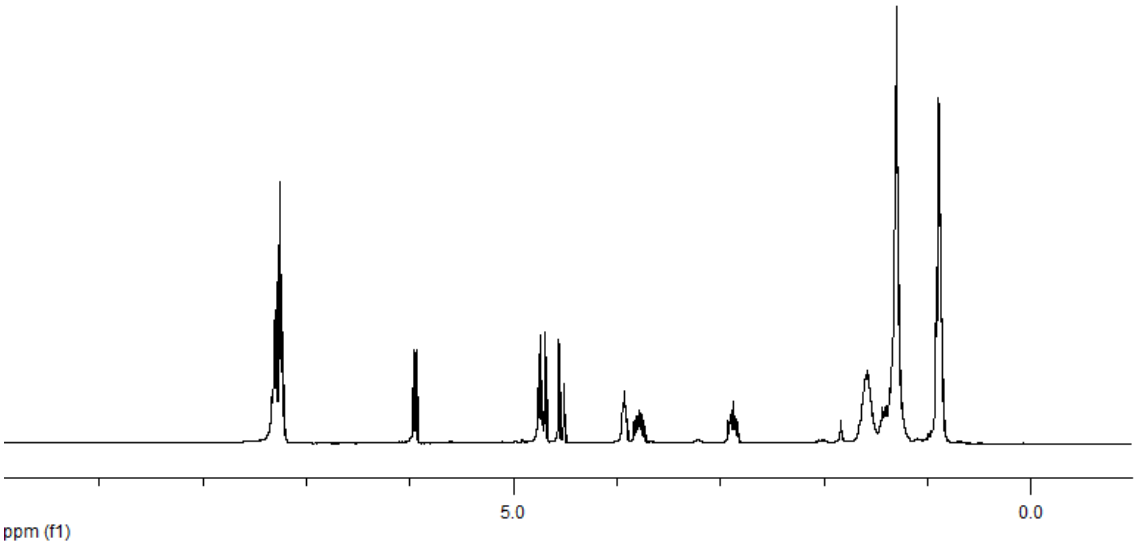
5.0
0.0
ppm (f1)

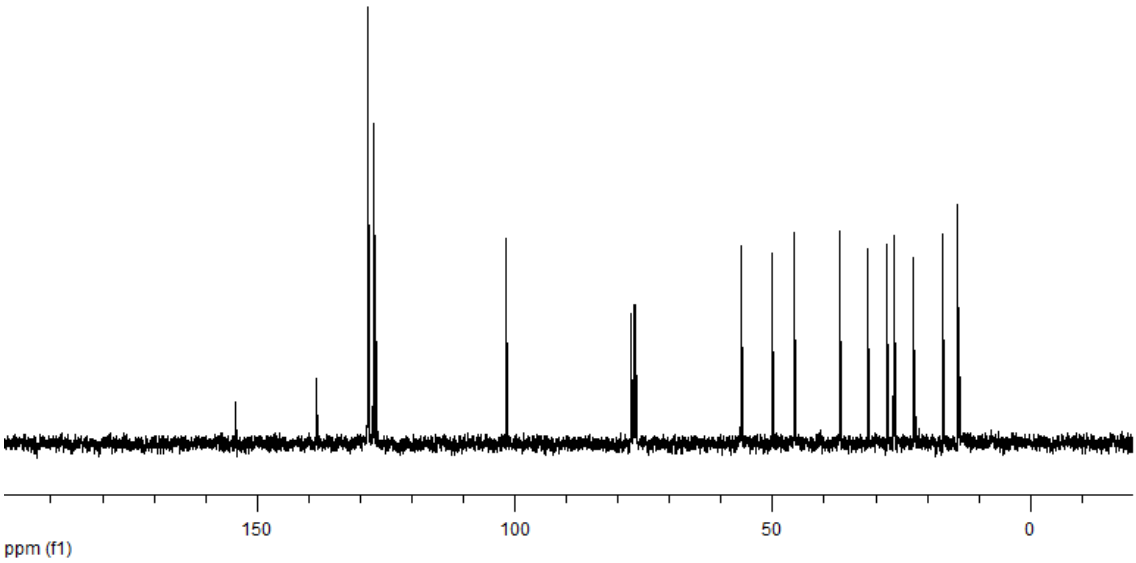
150
100
50
0
ppm (f1)

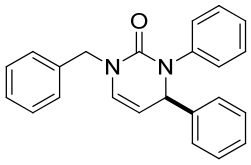
O
N
N

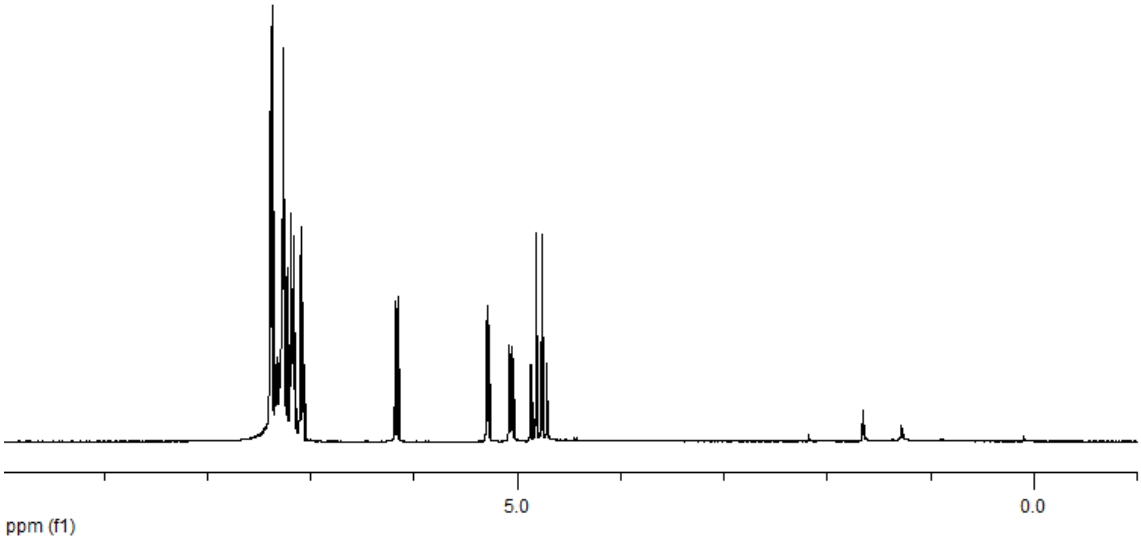
5.0
0.0
ppm (f1)

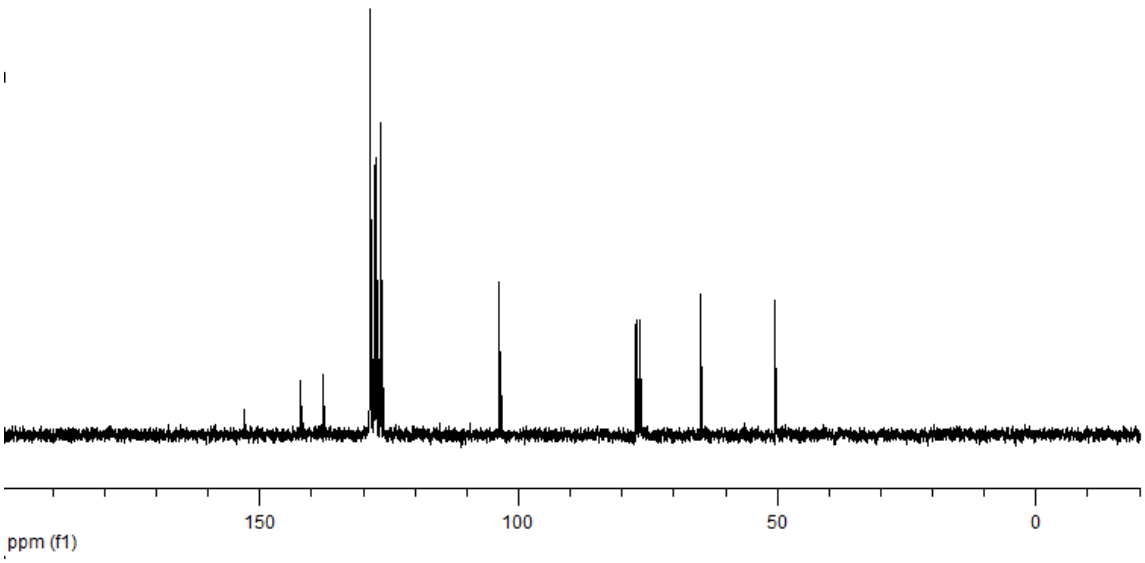
150
100
50
0
ppm (f1)

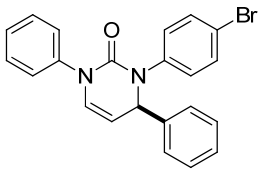
Br
O
N
N

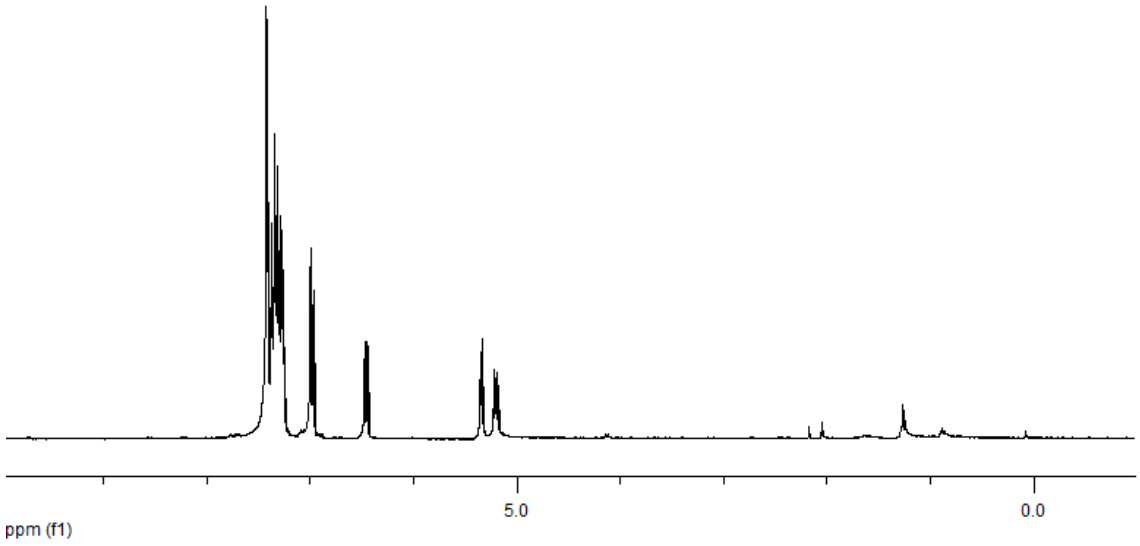
5.0
0.0
ppm (f1)

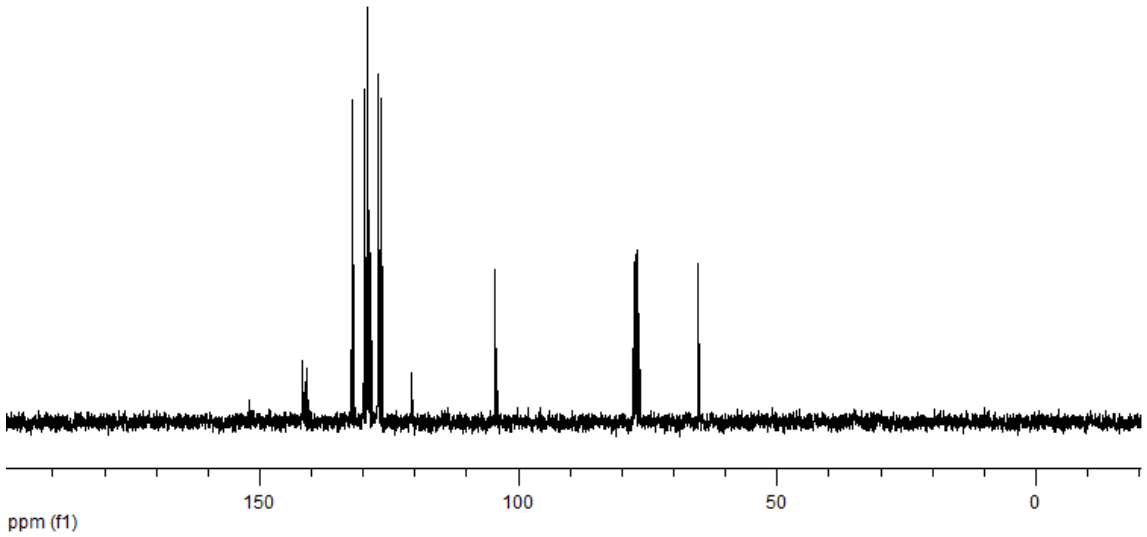
150
100
50
0
ppm (f1)

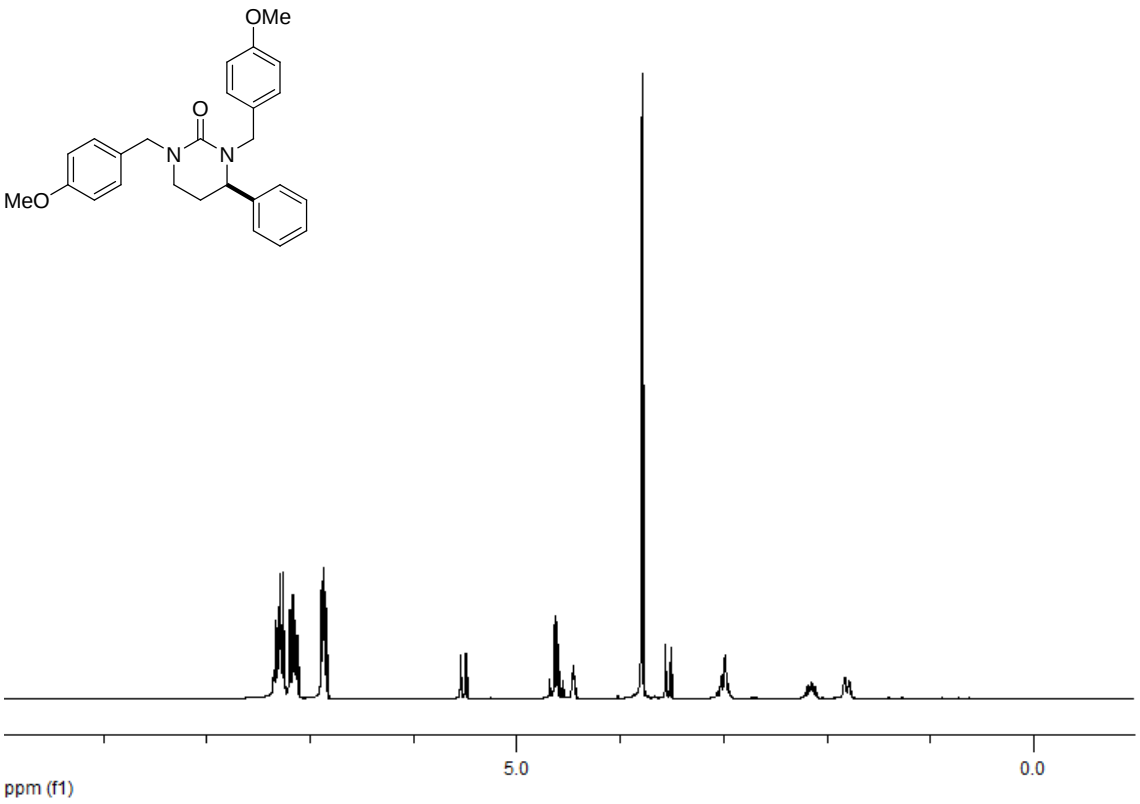
OMe
O
N
N
MeO
5.0
0.0
ppm (f1)

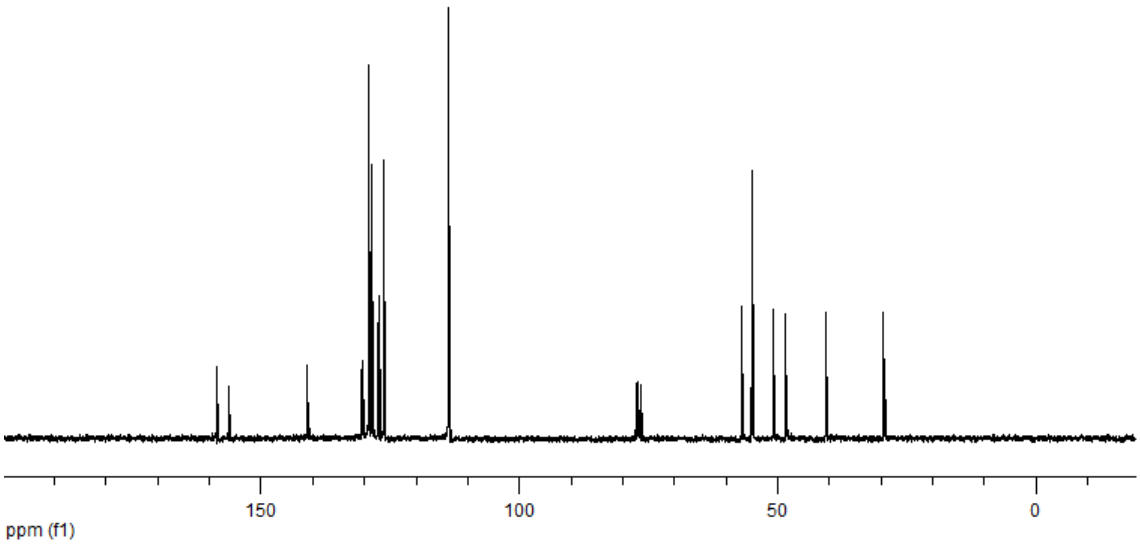
150
100
50
0
ppm (f1)

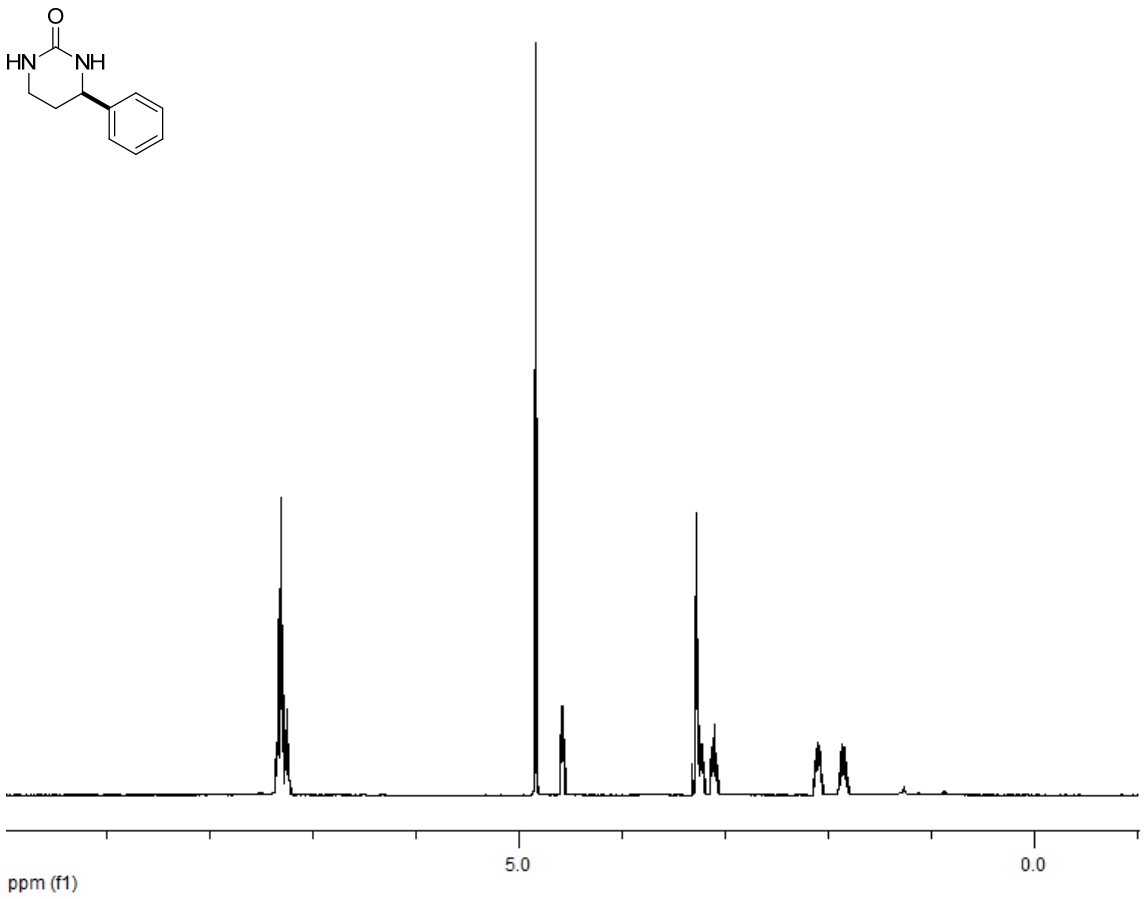
O
HN
NH
5.0
0.0
ppm (f1)

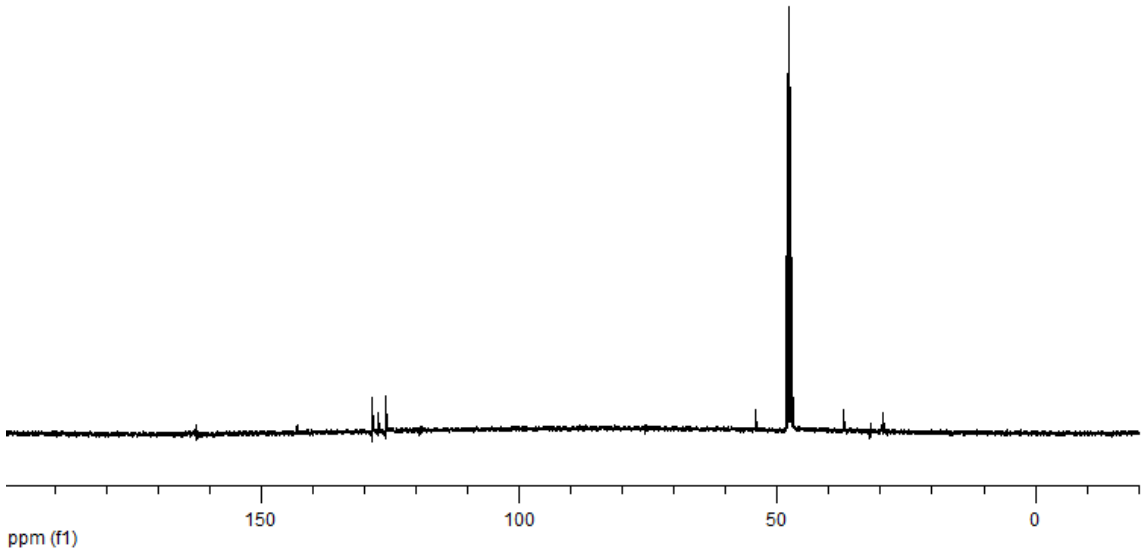
150
100
50
0
ppm (f1)

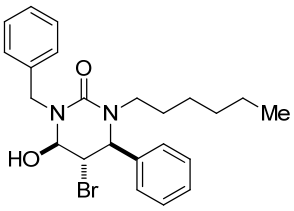
O
N
N
Me
HO
Br

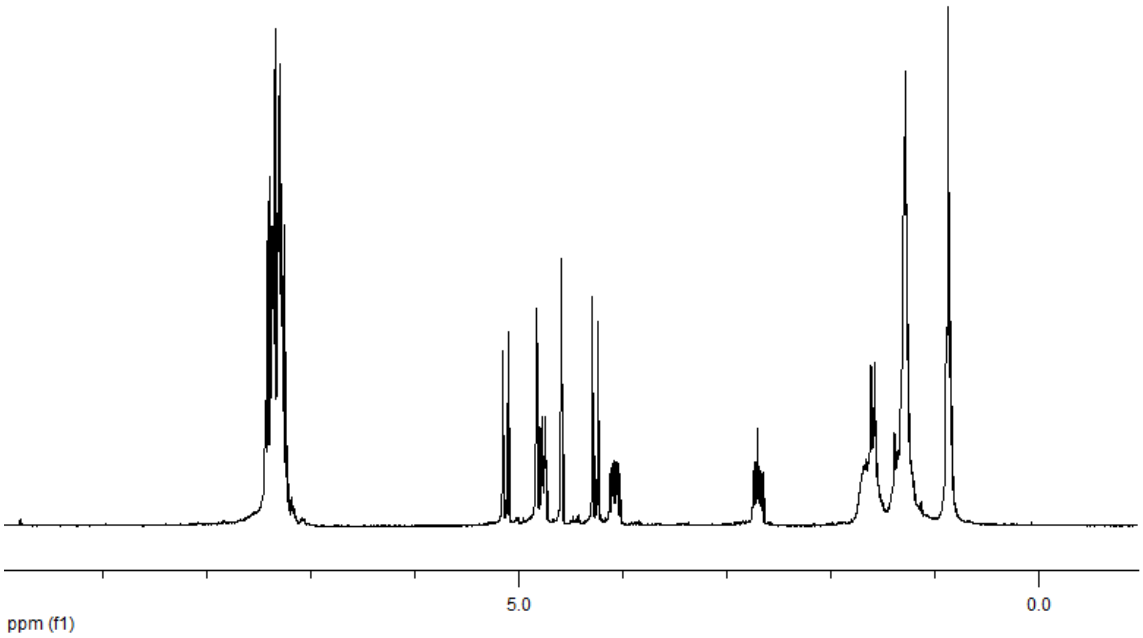
5.0
0.0
ppm (f1)

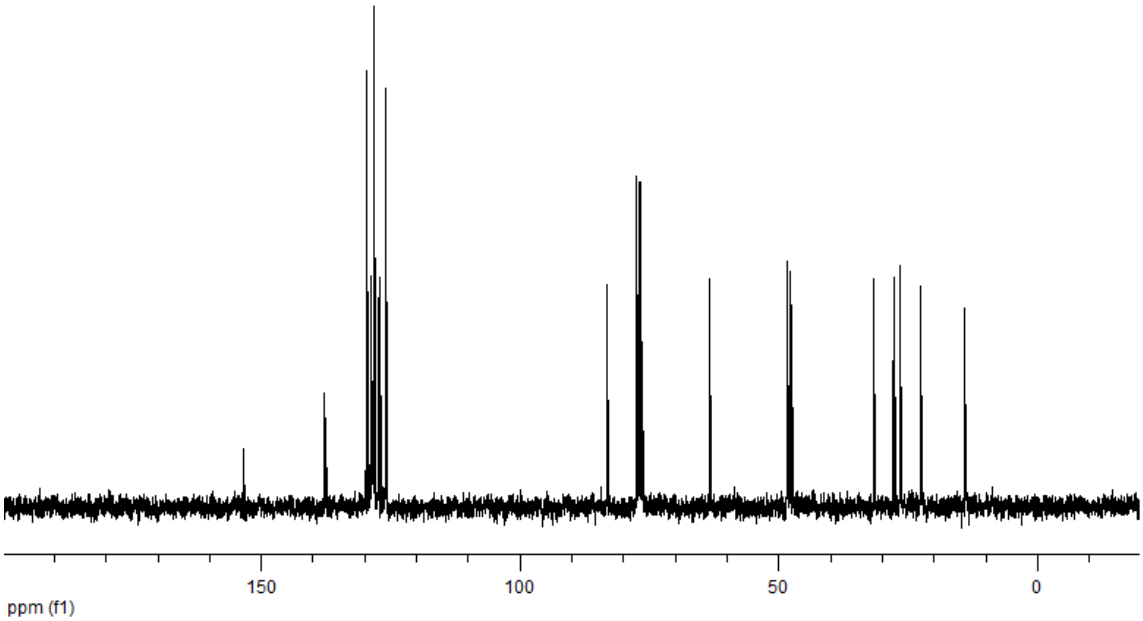
150
100
50
0
ppm (f1)

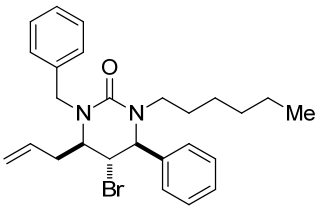
O
N
N
Me
Br

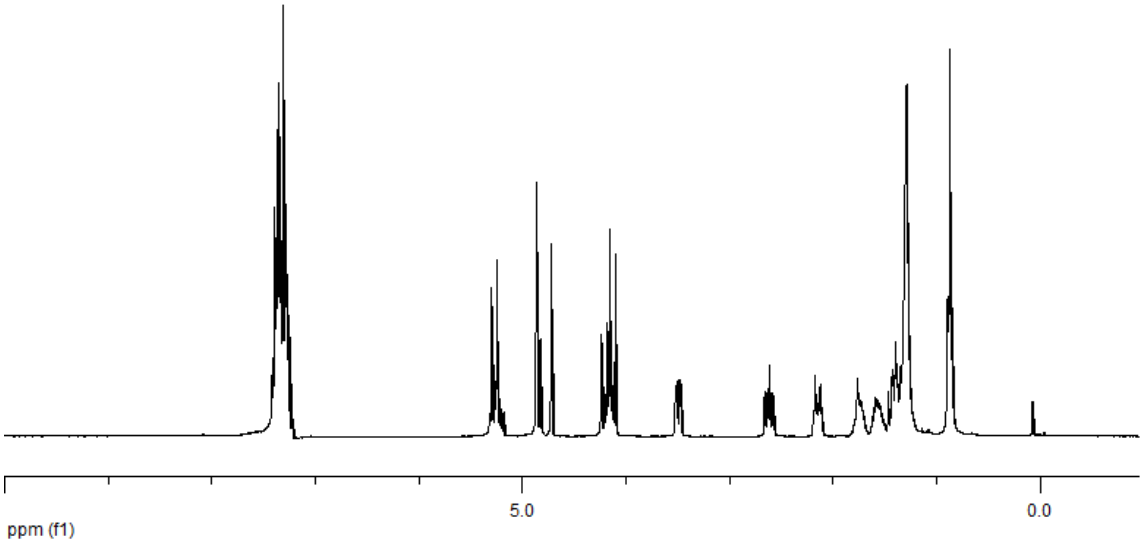
5.0
0.0
ppm (f1)

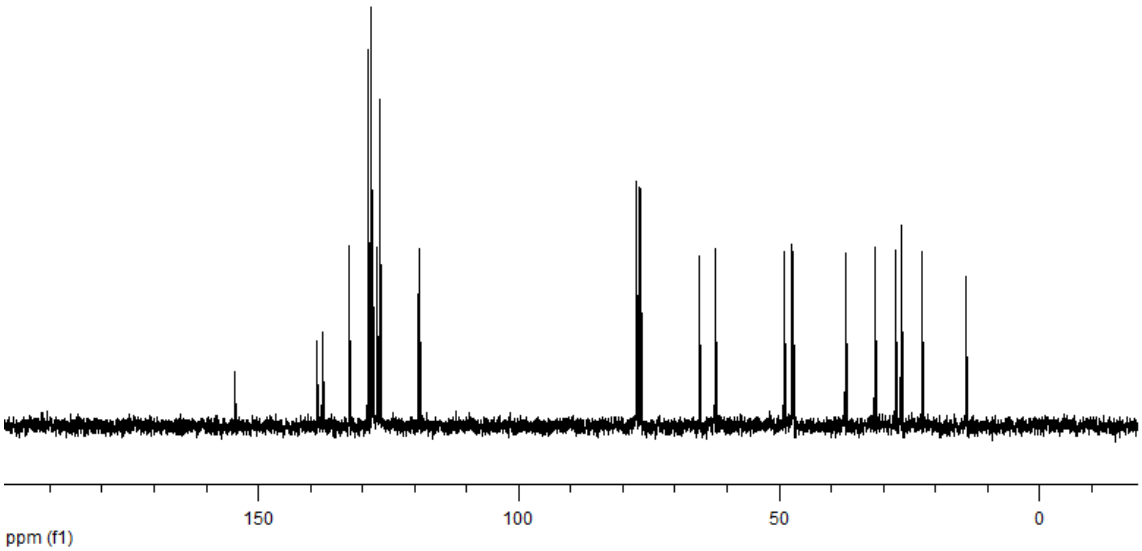
150
100
50
0
ppm (f1)

NOE of 25 in C_6D_6.

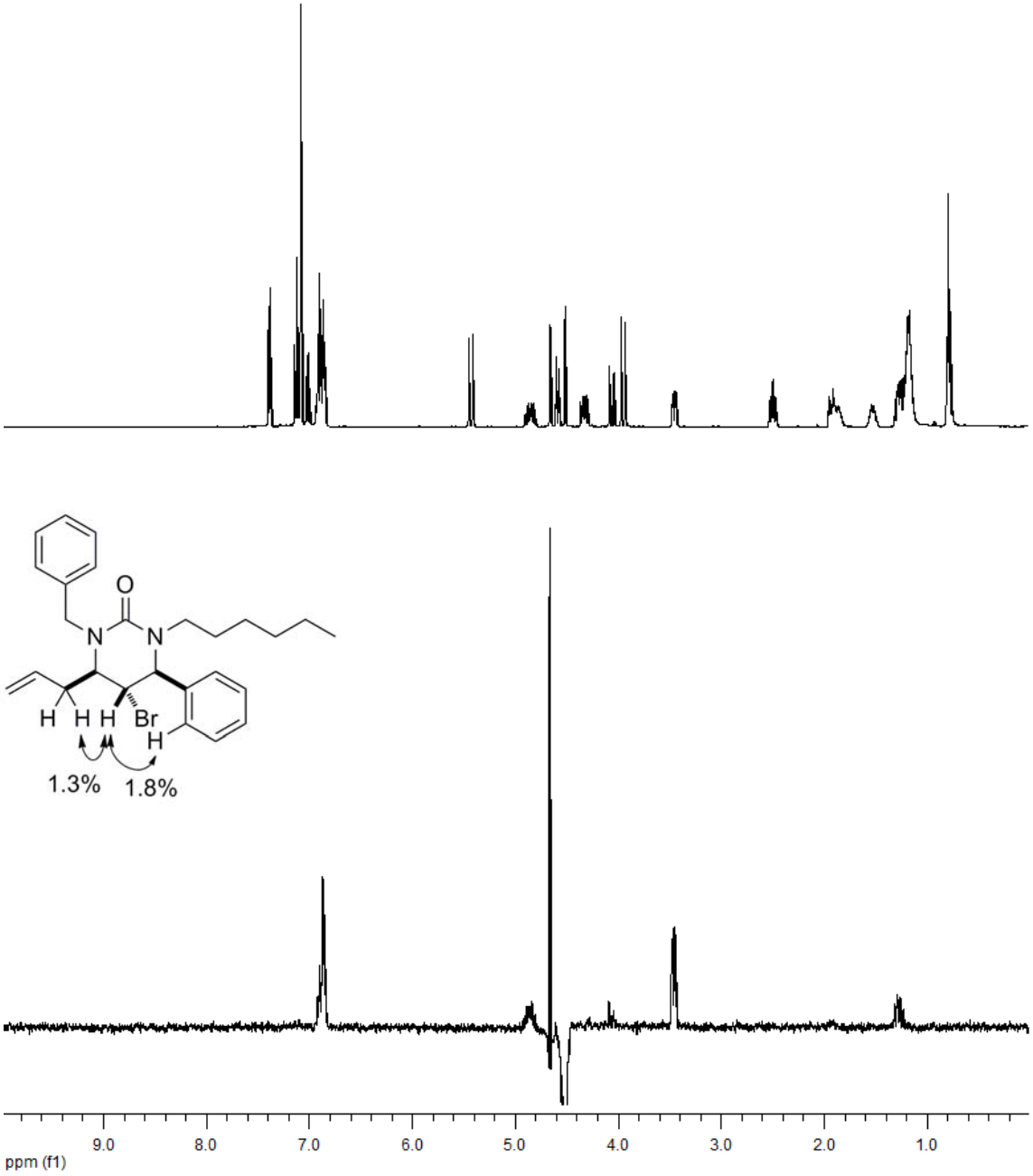

Crystal Structure Tables and Figure for 4ag.

Table A.3.1. Crystal data and structure refinement for **4ag**.

Identification code	rovis102	
Empirical formula	$C_{22}H_{17}BrN_2O$	
Formula weight	405.29	
Temperature	120 K	
Wavelength	0.71073 Å	
Crystal system	Orthorhombic	
Space group	$P\ 2_12_12_1$	
Unit cell dimensions	a = 5.8881(2) Å	α = 90°
	b = 12.0278(3) Å	β = 90°
	c = 24.8051(7) Å	γ = 90°
Volume	1756.72(9) $Å^3$	
Z	4	
Density (calculated)	1.532 Mg/m^3	
Absorption coefficient	2.353 mm^{-1}	
F(000)	824	
Crystal size	0.24 x 0.18 x 0.14 mm^3	
Theta range for data collection	1.64 to 30.52°.	
Index ranges	-8<=h<=8, -17<=k<=17, -35<=l<=35	
Reflections collected	42873	
Independent reflections	5374 [R(int) = 0.0753]	
Completeness to theta = 30.52°	99.9 %	
Absorption correction	Semi-empirical from equivalents	
Max. and min. transmission	0.7387 and 0.5997	
Refinement method	Full-matrix least-squares on F^2	
Data / restraints / parameters	5374 / 0 / 236	
Goodness-of-fit on F^2	1.143	
Final R indices [I>2sigma(I)]	R1 = 0.0497, wR2 = 0.1249	
R indices (all data)	R1 = 0.0869, wR2 = 0.1933	
Absolute structure parameter	-0.013(15)	
Largest diff. peak and hole	0.932 and -1.240 $e.Å^{-3}$	

Table A.3.2. Atomic coordinates (x 10^4) and equivalent isotropic displacement parameters ($Å^2$x 10^3) for **4ag**. U(eq) is defined as one third of the trace of the orthogonalized U^{ij} tensor.

	x	y	z	U(eq)
Br(1)	13764(1)	-2018(1)	447(1)	29(1)
C(1)	7278(8)	1149(4)	2161(2)	17(1)
C(2)	6856(9)	3101(4)	2386(2)	23(1)
C(3)	8429(10)	3419(4)	2029(2)	27(1)
C(4)	9688(9)	2609(4)	1677(2)	20(1)
C(5)	4767(9)	1725(4)	2903(2)	19(1)
C(6)	2777(10)	2333(5)	2945(2)	27(1)
C(7)	1268(10)	2130(5)	3355(2)	32(1)

C(8)	1788(11)	1320(5)	3740(2)	36(2)
C(9)	3831(12)	722(4)	3715(2)	32(1)
C(10)	5316(10)	929(4)	3296(2)	24(1)
C(11)	9860(8)	616(4)	1460(2)	17(1)
C(12)	8836(10)	167(4)	1004(2)	20(1)
C(13)	9999(9)	-645(4)	708(2)	21(1)
C(14)	12136(9)	-972(4)	877(2)	20(1)
C(15)	13142(8)	-538(4)	1332(2)	20(1)
C(16)	12003(8)	258(4)	1619(2)	20(1)
C(17)	9548(8)	3018(4)	1101(2)	19(1)
C(18)	7535(9)	2892(4)	801(2)	23(1)
C(19)	7386(10)	3370(4)	293(2)	26(1)
C(20)	9191(10)	3991(4)	92(2)	30(1)
C(21)	11140(11)	4138(4)	392(2)	29(1)
C(22)	11365(10)	3638(4)	897(2)	23(1)
N(1)	6325(7)	1983(3)	2475(1)	19(1)
N(2)	8716(8)	1489(3)	1749(1)	19(1)
O(1)	6856(6)	158(3)	2231(1)	20(1)

Table A.3.3. Bond lengths [Å] and angles [°] for **4ag**.

Br(1)-C(14)	1.908(5)	C(19)-C(20)	1.392(8)
C(1)-O(1)	1.231(6)	C(20)-C(21)	1.379(9)
C(1)-N(2)	1.388(6)	C(21)-C(22)	1.396(6)
C(1)-N(1)	1.388(6)		
C(2)-C(3)	1.336(7)	O(1)-C(1)-N(2)	120.8(4)
C(2)-N(1)	1.398(6)	O(1)-C(1)-N(1)	122.6(4)
C(3)-C(4)	1.504(7)	N(2)-C(1)-N(1)	116.6(4)
C(4)-N(2)	1.475(6)	C(3)-C(2)-N(1)	122.3(4)
C(4)-C(17)	1.514(6)	C(2)-C(3)-C(4)	122.7(4)
C(5)-C(6)	1.385(8)	N(2)-C(4)-C(3)	109.3(4)
C(5)-C(10)	1.402(7)	N(2)-C(4)-C(17)	112.9(4)
C(5)-N(1)	1.438(6)	C(3)-C(4)-C(17)	108.1(4)
C(6)-C(7)	1.371(8)	C(6)-C(5)-C(10)	120.2(5)
C(7)-C(8)	1.399(9)	C(6)-C(5)-N(1)	118.8(4)
C(8)-C(9)	1.403(9)	C(10)-C(5)-N(1)	120.8(4)
C(9)-C(10)	1.381(7)	C(7)-C(6)-C(5)	120.7(5)
C(11)-C(12)	1.390(6)	C(6)-C(7)-C(8)	119.2(5)
C(11)-C(16)	1.390(7)	C(7)-C(8)-C(9)	121.0(5)
C(11)-N(2)	1.439(6)	C(10)-C(9)-C(8)	118.9(5)
C(12)-C(13)	1.400(7)	C(9)-C(10)-C(5)	120.0(5)
C(13)-C(14)	1.383(7)	C(12)-C(11)-C(16)	120.3(4)
C(14)-C(15)	1.378(7)	C(12)-C(11)-N(2)	119.1(4)
C(15)-C(16)	1.369(7)	C(16)-C(11)-N(2)	120.6(4)
C(17)-C(22)	1.398(7)	C(11)-C(12)-C(13)	119.0(5)
C(17)-C(18)	1.408(7)	C(14)-C(13)-C(12)	119.0(4)
C(18)-C(19)	1.386(7)	C(15)-C(14)-C(13)	122.1(4)

C(15)-C(14)-Br(1)	119.5(4)	C(21)-C(20)-C(19)	120.6(5)
C(13)-C(14)-Br(1)	118.4(4)	C(20)-C(21)-C(22)	120.6(5)
C(16)-C(15)-C(14)	118.7(5)	C(21)-C(22)-C(17)	118.8(5)
C(15)-C(16)-C(11)	121.0(4)	C(1)-N(1)-C(2)	121.0(4)
C(22)-C(17)-C(18)	120.7(4)	C(1)-N(1)-C(5)	121.1(4)
C(22)-C(17)-C(4)	118.2(4)	C(2)-N(1)-C(5)	117.8(4)
C(18)-C(17)-C(4)	120.7(4)	C(1)-N(2)-C(11)	116.0(4)
C(19)-C(18)-C(17)	119.3(5)	C(1)-N(2)-C(4)	126.4(3)
C(18)-C(19)-C(20)	120.0(5)	C(11)-N(2)-C(4)	115.1(4)

Symmetry transformations used to generate equivalent atoms:

Table A.3.4. Anisotropic displacement parameters ($Å^2 x\ 10^3$)for **4ag**. The anisotropic displacement factor exponent takes the form: $-2\pi^2[h^2 a^{*2} U^{11} + ... + 2 h k a^* b^* U^{12}]$

	U^{11}	U^{22}	U^{33}	U^{23}	U^{13}	U^{12}
Br(1)	30(1)	26(1)	30(1)	-7(1)	2(1)	9(1)
C(1)	18(2)	17(2)	15(2)	-3(2)	-2(2)	2(2)
C(2)	31(3)	16(2)	22(2)	1(2)	3(2)	3(2)
C(3)	44(3)	14(2)	23(2)	-3(2)	5(2)	0(2)
C(4)	27(2)	18(2)	15(2)	-1(2)	3(2)	-4(2)
C(5)	21(2)	21(2)	15(2)	-4(2)	3(2)	-4(2)
C(6)	28(3)	29(3)	23(2)	-5(2)	-3(2)	6(2)
C(7)	24(2)	42(3)	28(2)	-18(2)	2(2)	6(3)
C(8)	48(4)	34(3)	27(3)	-13(2)	17(3)	-15(3)
C(9)	43(3)	25(2)	27(2)	0(2)	14(3)	-6(3)
C(10)	27(3)	20(2)	26(2)	1(2)	7(2)	-3(2)
C(11)	22(2)	17(2)	13(2)	0(2)	1(2)	-2(2)
C(12)	21(2)	21(2)	18(2)	-1(2)	-1(2)	2(2)
C(13)	22(3)	20(2)	21(2)	-1(2)	-1(2)	0(2)
C(14)	22(2)	17(2)	22(2)	-2(2)	6(2)	1(2)
C(15)	17(2)	25(2)	18(2)	2(2)	0(2)	1(2)
C(16)	22(2)	24(2)	13(2)	1(2)	-3(2)	1(2)
C(17)	26(2)	15(2)	15(2)	-2(2)	1(2)	3(2)
C(18)	25(3)	20(2)	25(2)	-3(2)	-2(2)	3(2)
C(19)	28(3)	26(2)	24(2)	2(2)	-3(2)	9(2)
C(20)	45(4)	23(2)	23(2)	7(2)	7(2)	8(2)
C(21)	34(3)	29(2)	26(2)	7(2)	9(3)	0(2)
C(22)	28(3)	20(2)	22(2)	1(2)	4(2)	-2(2)
N(1)	22(2)	17(2)	19(2)	1(1)	3(2)	1(2)
N(2)	26(2)	16(2)	14(2)	-1(1)	5(2)	1(2)
O(1)	20(2)	16(1)	24(2)	-1(1)	3(1)	-3(1)

Table A.3.5. Hydrogen coordinates (x 10^4) and isotropic displacement parameters (Å^{2}x 10^3) for **4ag**.

	x	y	z	U(eq)
H(2)	6087	3643	2582	28
H(3)	8758	4173	1998	32
H(4)	11286	2595	1788	24
H(6)	2463	2885	2694	32
H(7)	-85	2527	3376	38
H(8)	765	1175	4017	44
H(9)	4179	194	3976	38
H(10)	6680	542	3273	29
H(12)	7400	402	898	24
H(13)	9345	-959	403	25
H(15)	14567	-782	1443	24
H(16)	12672	565	1924	24
H(18)	6320	2492	941	28
H(19)	6080	3276	88	31
H(20)	9082	4310	-249	36
H(21)	12314	4574	257	35
H(22)	12699	3715	1094	28

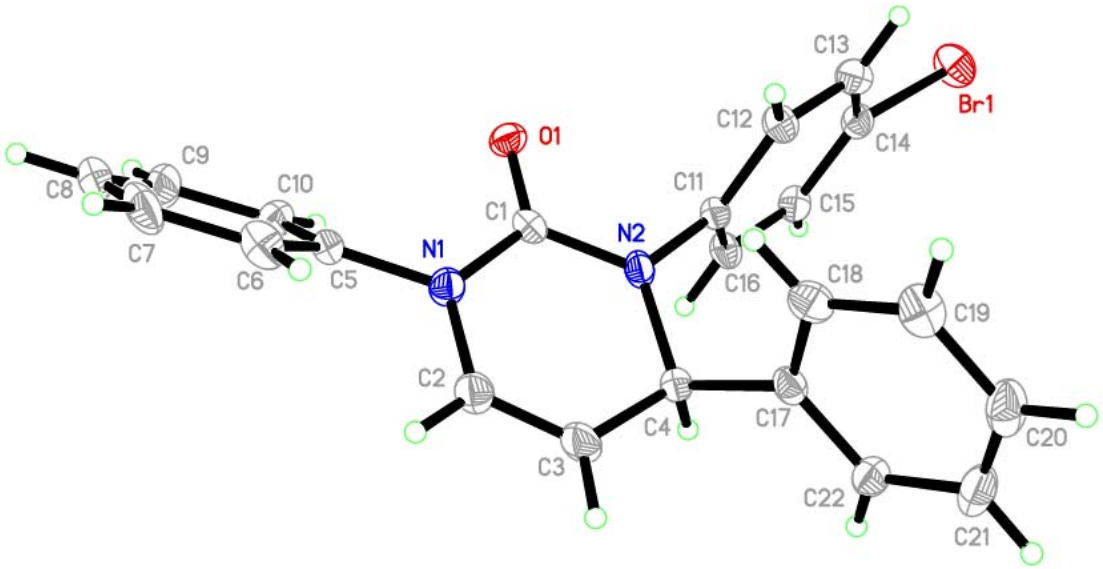

APPENDIX 4: CHAPTER 4 EXPERIMENTAL

General Methods. Toluene was degassed with argon and passed through one column of neutral alumina and one column of Q5 reactant. Ethyl ether, tetrahydrofuran, and dichloromethane were degassed and passed through two columns of neutral alumina. Column chromatography was performed on Silicycle, Inc. silica gel 60 (230-400 mesh). Preparative thin layer chromatography was performed on Silicycle, Inc. 2.00 mm silica 60-F plates and thin layer chromatography was performed on Silicycle, Inc. 0.25 mm silica gel 60-F plates. Chemicals were purchased from Aldrich Chemicals, Inc. unless otherwise stated.

^{1}H NMR and ^{13}C NMR spectra were obtained in $CDCl_3$ at ambient temperature and chemical shifts are expressed in parts per million (δ, ppm). Proton chemical shifts are referenced to 7.26 ppm ($CHCl_3$) and 7.16 ppm (C_6D_6) and carbon chemical shifts are referenced to 77.0 ppm ($CDCl_3$) and 128 (C_6D_6). Data reporting uses the following abbreviations: s, singlet; bs, broad singlet; d, doublet; dd, doublet of doublets; ddd, doublet of doublets of doublets; t, triplet; m, multiplet; and *J*, coupling constant in Hz.

Concentrations of alkyl lithium reagents were determined using diphenyl acetic acid titrations.[1] Concentrations of Grignard reagents were determined using $LiCl/I_2$ titrations.[2]

Spectral data for compounds cis, cis-3-(benzyloxy)-2,4-dimethyl glutaric anhydride (**3b**), (2S,3S,4R)-3-(benzyloxy)-2,4-dimethyl-5-oxohexanoic acid (**4b**), (E)-5-((2R,3R)-3-(hydroxymethyl)-3-methyloxiran-2-yl)-3-methylpent-2-en-1-yl acetate (**S13**), (E)-5-((2R,3S)-3-(iodomethyl)-3-methyloxiran-2-yl)-3-methylpent-2-en-1-ol (**139**), tert-butyl 3-((2R,3R)-3-((E)-5-hydroxy-3-methylpent-3-en-1-yl)-2-methyloxiran-2-yl)propanoate (**S14**), tert-butyl 3-((2R,3R)-3-(2-((2R,3R)-3-(hydroxymethyl)-2-methyloxiran-2-yl)ethyl)-2-methyloxiran-2-yl)propanoate (**140**), (2S,2'R,5'S)-5'-((S)-2-bromo-1-hydroxyethyl)-2,5'-dimethylhexahydro-[2,2'-bifuran]-5(2H)-one (**S15**), and (4R,6S,8S,12R,14S,Z)-ethyl 9-hydroxy-4,6,8,12,14-pentamethyl-11-oxo-16-((1-phenyl-1H-tetrazol-5-yl)sulfonyl)hexadec-9-enoate (**162**) match Dr. Brian Cochran's post doctoral report[3] and his data for these compounds are included for completeness.

Synthesis of Compounds and Characterization Data.

C1-C9 Fragment

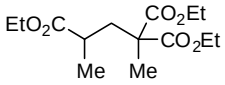

Triethyl pentane-2,2,4-tricarboxylate (S1). Prepared using modified literature procedure.[4] Sodium (17.2 g, 0.75 mol) was slowly added to 500 mL EtOH and dissolved (~3 h). After heating the solution to reflux, diethyl methylmalonate (127.8 mL, 750 mmol) and ethyl α-bromoisobutyrate (110.0 mL, 750 mmol) were added quickly. The solution turned slight yellow. After 1 h, the solution was bright yellow with a yellow precipitate. The reaction was heated for an additional 5 h and cooled to 23 °C. The solution was concentrated *in vacuo* and 200 mL H_2O and 200 mL Et_2O were added. The layers were separated and the aqueous layer was extracted with 200 mL Et_2O 3x. The organic layers were combined, washed with brine, dried over $MgSO_4$, and concentrated to yield 197 g (91%) of triethyl pentane-2,2,4-tricarboxylate as light yellow oil.

[1] Kofron, W. G.; Baclawski, L. M. *J. Org. Chem.* **1976**, *41*, 1879-1880.
[2] Krasovskiy, A.; Knochel, P. *Synthesis* **2006**, *5*, 890-891.
[3] Cochran, B. M. Colorado State University, Fort Collins, CO. Unpublished work, 2012.
[4] Lautens, M.; Colucci, J. T.; Hiebert, S.; Smith, N. D.; Bouchain, G. *Org. Lett.* **2002**, *4*, 1879-1882.

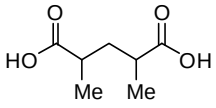

2,4-dimethylpentanedioic acid (S2). Prepared using modified literature procedure.[4] Triethyl pentane-2,2,4-tricarboxylate **S1** (197 g, 683 mmol) was dissolved in 500 mL conc. HCl and refluxed for 36 h. Another 100 mL. conc. HCl was added and the reaction was refluxed for another 24 h. The reaction was cooled to 23 °C and then put in a -20 °C freezer for 12 h. The crystals were filtered off, dissolved in 400 mL Et_2O. The layers were separated and the organic layer was dried with $MgSO_4$ and concentrated to yield 48 g of 2,4-dimethylpentanedioic acid. The aqueous HCl solution was extracted with 200 mL Et_2O 4x. The organic layers were combined, dried with $MgSO_4$, and concentrated to an amorphous solid. The solid was recrystallized from Hex:EtOAc to yield an additional 24 g of 2,4-dimethylpentanedioic acid (72 g total, 66%).

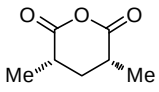

Cis-2,4-dimethyl glutaric anhydride (1). Prepared using modified literature procedures.[4,5] 2,4-dimethylpentanedioic acid **S2** (72 g, 452 mmol) was dissolved in acetic anhydride (100 mL) and heated to 130 °C for 6 h. The reaction was concentrated *in vacuo* by azeotroping with PhMe 3x. The resulting solid was dissolved in minimal refluxing EtOAc and 2 mL DBU was added. The solution was cooled to 23 °C and then 0 °C and the solid was filtered off to yield 33.4 g of dimethyl glutaric anhydride as light brown solid (>20:1 cis:trans). The filtrated was concentrated and the solid was recrystallized from EtOAc 2x (10.69 g, >20:1 cis:trans; 0.68 g, 19:1 cis:trans). All the solids were combined and recrystallized from EtOAc to yield 34.4 g (54%) of cis-2,4-dimethyl glutaric anhydride as clear, cubic crystals. Spectral data matches previous report.[4] ^{1}H NMR (300 MHz, $CDCl_3$) δ 2.73 (m, 2H), 2.06 (dt, *J* = 13.6, 5.3 Hz, 1H), 1.59 (dt, *J* = 13.3, 13.3 Hz, 1H), 1.38 (d, *J* = 6.9 Hz, 6H). X-ray data[6] matches previous report.[7]

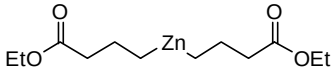

Bis(4-ethoxy-4-oxobutyl)zinc (122). In a 100 ml round bottom flask, ethyl 4-bromobutyrate (6.0 ml, 40.2 mmol: ^{1}H NMR (300 MHz, $CDCl_3$) δ 4.14 (q, *J* = 7.2 Hz, 2H), 3.47 (t, *J* = 6.5 Hz, 2H), 2.49 (t, *J* = 7.2 Hz, 2H), 2.17 (m, 2H), 1.26 (t, *J* = 7.1 Hz, 3H).) was dissolved in 40 ml acetone. Potassium iodide (13.35 g, 80.4 mmol, 2.0 equiv.) was added, a reflux condenser was attached, and the reaction was heated at reflux for 12h. The solution was cooled, filtered through a course fritted funnel, and concentrated *in vacuo.* The resulting yellow oil with fine particulates was taken up in ca 50 ml of 1:1 Hex:Et_2O and filtered through neutral aluminum to remove color. After flushing with an additional 100 ml 1:1 Hex:Et_2O, the solution was concentrated to yield 8.44 g (87%) of ethyl 4-iodobutyrate. ^{1}H NMR (300 MHz, $CDCl_3$) δ 4.14 (q, *J* = 7.2 Hz, 2H), 3.24 (t, *J* = 6.8 Hz, 2H), 2.44 (t, *J* = 7.1 Hz, 2H), 2.13 (m, 2H), 1.26 (t, *J* = 7.2 Hz, 3H). A 50 ml Schlenk flask was flame dried under vacuum, cooled to 23 °C, and charged with ethyl 4-iodobutyrate (8.4 g, 34.7 mmol) and copper(I) iodide (10 mg, 0.05 mmol). After sealing with a greased ground glass stopper, the flask was

[5] Saicic, R. N. *Synthetic Commun.* **2006**, *36*, 2559-2562. For an alternative procedure using Hünig's base, see: Prusov, E.; Röhm, H.; Maier, M. E. *Org. Lett.* **2006**, *8*, 1025-1028.
[6] Oberg, K. M.; Rovis T. (2013) Private communication to the Cambridge Structural Database, deposit number CCDC 946678.
[7] Haltiwanger, R. C.; Walba, D. M.; Wand, M. D. *Acta crystallographica. Sec. C, Cryst. Struct. Comm.* **1980**, *9*, 1195-1200.

evacuated and refilled with Ar. The stopper was replaced with a rubber septum and neat diethyl zinc (14 ml, 137 mmol, 4 equiv) was added via syringe. The reaction was heated at 40 °C for 12 h. The excess diethyl zinc and ethyl iodide were removed under vacuum for 2 h into a trap with methanol cooled to -78 °C with dry ice and acetone. (CAUTION: A trap cooled with liquid nitrogen easily clogs so dry ice/acetone cooling is preferred. Methanol quenches the excess diethyl zinc, but care should be taken when cleaning the trap as some diethyl zinc may remain.) After backfilling with Ar, THF (5 ml) was added to the reaction vessel and heated at 40 °C for 1 h under Ar. The reaction vessel was evacuated for 1 h. This step was repeated another two times. After cooling to 23 °C, the generated bis(4-ethoxy-4-oxobutyl)zinc was diluted with 15 ml of THF and this solution was used directly in the desymmetrization reaction.

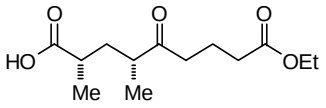

(2S,4R)-9-ethoxy-2,4-dimethyl-5,9-dioxononanoic acid (2a). A flame dried 250 ml round bottom with stirbar was transferred into glove box where $[Rh(nbd)OAc]_2$[8] (142.3 mg, 0.28 mmol, 2 mol %) and (R)-tBuPhox[9] (217.0 mg, 0.56 mmol, 4 mol %) were added. The reaction vessel was removed from the glove box, charged with 15 ml of THF and stirred for 10 min to make a clear, orange solution. The reaction was charged with the bis(4-ethoxy-4-oxobutyl)zinc-THF solution from the above reaction and stirred for 10 min resulting in a deep red solution. Cis-2,4-dimethyl glutaric anhydride **1** (2.0 g, 14.0 mmol) was added as a solid (septa removed, anhydride added in one portion, and reaction flushed after addition of anhydride) and the reaction was stirred at 23 °C for 6 days. The reaction was quenched slowly with 1 M HCl and EtOAc was added. The layers were separated and the aqueous layer was extracted with EtOAc 3x. The organic phase was extracted with sat. $NaHCO_3$ 3x and collected into a beaker. With stirring, the aqueous solution was acidified using conc. HCl. The acidic solution was extracted with DCM 3x and the organic layer was dried with $MgSO_4$, filtered, and concentrated. The resulting oil was absorbed onto Celite and purified via flash column chromatography (89:10:1 Hex:EtOAc:AcOH to 78:20:2 Hex:EtOAc:AcOH) to yield 2.10 g (58%) of (2S,4R)-9-ethoxy-2,4-dimethyl-5,9-dioxononanoic acid as a pale yellow oil. $[\alpha]^{20}_D$ = +3.9, c = 0.0163 g/ml $CHCl_3$. ^{1}H NMR (400 MHz, $CDCl_3$) δ 9.85 (bs, 1H), 4.11 (q, *J* = 7.1 Hz, 2H), 2.64-2.45 (m, 4H), 2.61 (t, *J* = 7.3 Hz, 2H), 2.07 (ddd, *J* = 14.0, 8.8, 6.3, 1H), 1.87 (p, *J* = 7.2 Hz, 2H), 1.36 (ddd, *J* = 13.7, 7.7, 5.8 Hz, 1H), 1.24 (t, *J* = 7.2 Hz, 3H), 1.19 (d, *J* = 7.0 Hz, 3H), 1.09 (d, *J* = 7.0 Hz. 3H). ^{13}C NMR (100 MHz, $CDCl_3$) δ 212.9, 182.0, 173.3, 60.4, 44.0, 39.6, 37.2, 36.0, 33.3, 18.8, 17.6, 16.4, 14.2. R_f = 0.24 (78:20:2 Hex:EtOAc:AcOH; CAM), 0.21 (2:1 Hex:EtOAc). IR (NaCl, Thin Film) 3172, 2977, 2940, 1717, 1462, 1378, 1192, 1031 cm^{-1}. LRMS (ESI) *m/z* $[C_{13}H_{21}O_5]^-$ (M-H) calcd 257.1, found 257.2.

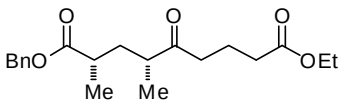

(2S,4R)-1-benzyl 9-ethyl 2,4-dimethyl-5-oxononanedioate (S3). (2S,4R)-9-ethoxy-2,4-dimethyl-5,9-dioxononanoic acid **2a** (212 mg, 0.82 mmol) was dissolved in 15 ml DCM. Benzyl alcohol (0.1 ml, 1 mmol, 1.2 equiv), dicyclohexylcarbodiimide (206 mg, 1 mmol, 1.2 equiv), and dimethylaminopyridine (30.5 mg, 0.25 mmol, 0.3 equiv) were added sequentially. The reaction was stirred at 23 °C for 3 h. The reaction

[8] For synthesis of $[Rh(nbd)OAc]_2$, see: Henderson, D. D.; Cochran, B. M.; Filloux, C. M.; Rovis, T. *Submitted*.
[9] For synthesis of Phox ligands, see: (a) Tani, K.; Behenna, D. C.; McFadden, R. M.; Stoltz, B. M. *Org. Lett.* **2007**, *9*, 2529-2531. (b) Krout, M. R.; Mohr, J. T.; Stoltz, B. M. *Org. Syn.* **2009**, *86*, 181-193.

was concentrated onto Celite and columned to yield 174.9 mg (61%) of (2S,4R)-1-benzyl 9-ethyl 2,4-dimethyl-5-oxononanedioate as a clear oil. ^{1}H NMR (300 MHz, $CDCl_3$) δ 7.38-7.32 (m, 5H), 5.14 (d, *J* = 12.4, 1H), 5.09 (d, *J* = 12.3 Hz, 1H), 4.12 (q, *J* = 7.1 Hz, 2H), 2.28 (t, *J* = 7.3 Hz, 2H), 2.05 (ddd, *J* = 13.9, 9.2, 5.9 Hz, 1H), 1.84 (p, *J* = 7.1 Hz, 2H), 1.35 (ddd, *J* = 13.7, 8.1, 5.5 Hz, 1H), 1.25 (t, *J* = 7.1 Hz, 3H), 1.17 (d, *J* = 7.0 Hz, 3H), 1.05 (d, *J* = 7.0 Hz, 3H). R_f = 0.30 (4:1 Hex:EtOAc; CAM, UV). 89% ee by HPLC: Chiralcel IC column, 95:5 Hex:iPrOH, 1 ml/min, RT_{major} = 35.59 min, RT_{minor} = 37.13 min, 210 nm. *ent*-SX using S-tBuPhox. 92% ee by HPLC: Chiralcel IC column, 95:5 Hex:iPrOH, 1 ml/min, RT_{major} = 36.60 min, RT_{minor} = 35.35 min, 210 nm.

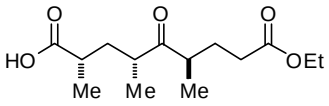

(2S,4R,6R)-9-ethoxy-2,4,6-trimethyl-5,9-dioxononanoic acid (123). Potassium bis(trimethylsilyl)amide (1.328 g, 6.657 mmol, 2.1 equiv.) was added to a flame dried 100 ml round bottom flask in an inert air glove box. After removing from the box, 35 ml of freshly pulled PhMe was added to the reaction flask and stirred until it was a clear, colorless solution. The reaction was cooled to -78 °C and (2S,4R)-9-ethoxy-2,4-dimethyl-5,9-dioxononanoic acid **2a** (0.820 g, 3.17 mmol) was added in 20 ml THF. The solution turned yellow and was stirred for 1 h. Iodomethane (0.79 ml, 12.68 mmol, 4 equiv.) was added neat and the reaction was stirred for 16 h at -78 °C. The reaction was quenched at -78 °C with the addiition of 23 ml 1M HCl and allowed to warm to 23 °C for 1 h. The reaction was extracted with EtOAc 3x and the organic layer was washed with sat. $Na_2S_2O_3$ 2x, dried with $MgSO_4$, filtered, and concentrated. The resulting oil was loaded onto Celite and purified via flash column chromatography to yield 0.631 g (73%, 5:1 dr) of (2S,4R,6R)-9-ethoxy-2,4,6-trimethyl-5,9-dioxononanoic acid as clear liquid. $[\alpha]^{20}_D$ = +2.3, c = 0.0222 g/ml C_6H_6. ^{1}H NMR (400 MHz, $CDCl_3$) δ 8.82 (bs, 1H), 4.11 (q, *J* = 7.1 Hz, 2H), 2.73 (m, 2H), 2.50 (m, 1H), 2.26 (m, 2H), 2.06-1.92 (m, 2H), 1.61 (m, 1H), 1.30 (m, 1H), 1.24 (t, *J* = 7.2 Hz, 3H), 1.20 (d, *J* = 7.0 Hz, 3H), 1.08 (d, *J* = 6.7 Hz, 3H), 1.07 (d, *J* = 6.9 Hz, 3H). ^{13}C NMR (100 MHz, $CDCl_3$) δ 216.5, 181.9, 173.2, 60.4, 43.8, 42.7, 37.0, 36.0, 31.8, 27.6, 17.8, 16.5, 16.1, 14.2. R_f = 0.18 (78:20:2 Hex:EtOAc:AcOH; CAM). IR (ATR) 2974, 2937, 2878, 1732, 1705, 1462, 1377, 1179, 1032 cm^{-1}. HRMS (APCI) *m/z* $[C_{14}H_{25}O_5]^+$ (M+H) calcd 273.1697, found 273.1703.

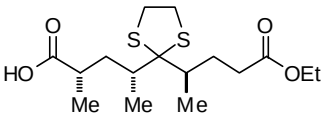

(2S,4R)-4-(2-((R)-5-methoxy-5-oxopentan-2-yl)-1,3-dithiolan-2-yl)-2-methylpentanoic acid (124). In a 20 ml Scintillation vial under Ar, (2S,4R,6R)-9-ethoxy-2,4,6-trimethyl-5,9-dioxononanoic acid **123** (570 mg, 2.09 mmol) was dissolved in 2 ml 1,2-ethanedithiol. Boron trifluoride diethyl etherate (0.33 ml, 2.61 mmol, 1.25 equiv.) was added via syringe. The reaction was stirred for 15 min (long reaction times lead to epimerization) and the entire reaction was immediately subject to flash column chromatography (20:1 Hex:EtOAc to 9:1 Hex:EtOAc to 4:1 Hex:EtOAc) to yield 640.5 mg (91%) of (2S,4R)-4-(2-((R)-5-methoxy-5-oxopentan-2-yl)-1,3-dithiolan-2-yl)-2-methylpentanoic acid as a clear oil. $[\alpha]^{20}_D$ = +17.8, c = 0.0181 g/ml $CHCl_3$. ^{1}H NMR (400 MHz, $CDCl_3$) δ 9.58 (bs, 1H), 4.13 (q, *J* = 7.1 Hz, 2H), 3.24-3.11 (m, 4H), 2.62 (m, 1H), 2.43 (m, 1H), 2.32-2.04 (m, 5H), 1.55 (m, 1H), 1.25 (t, *J* = 7.1 Hz, 3H), 1.22 (d, *J* = 7.1 Hz, 3H), 1.16 (d, *J* = 6.4 Hz, 3H), 1.11 (m, 1H), 1.05 (d, *J* = 6.5 Hz, 3H). ^{13}C NMR (100 MHz, $CDCl_3$) δ 182.43, 173.8, 83.0, 60.3, 41.3, 40.9, 40.2, 39.8, 37.7, 37.5, 32.8, 28.5, 18.8, 16.0, 15.7, 14.2. R_f

= 0.38 (2:1 Hex:EtOAc; CAM). IR (ATR) 2973, 2924, 2877, 1732, 1703, 1375, 1296, 1178, 958 cm^{-1}. HRMS (ESI/APCI) *m/z* $[C_{16}H_{27}O_4S_2]^+$ (M-H) calcd 347.1356, found 347.1337.

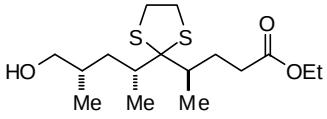

(R)-ethyl 4-(2-((2R,4S)-5-hydroxy-4-methylpentan-2-yl)-1,3-dithiolan-2-yl)pentanoate (125). In a 25 ml round bottom flask, (2S,4R)-4-(2-((R)-5-methoxy-5-oxopentan-2-yl)-1,3-dithiolan-2-yl)-2-methylpentanoic acid **124** (1.52 g, 4.4 mmol) was dissolved in 12 ml THF. Borane·tetrahydrofuran (5.6 ml, 5.63 mmol, 1M in THF, 1.25 equiv.) was added and the reaction was stirred for 1 h. The reaction was quenched with H_2O and after bubbling ceased, 1M HCl was added. The reaction was extracted with EtOAc 3x. The organic layer was washed with 1M HCl 1x and brine 1x, dried with $MgSO_4$, filtered, and concentrated. The crude reaction was loaded onto Celite and purified via flash column chromatography to yield 0.939 g (64%) of (R)-ethyl 4-(2-((2R,4S)-5-hydroxy-4-methylpentan-2-yl)-1,3-dithiolan-2-yl)pentanoate as a clear oil. $[\alpha]^{20}_D$ = +17.3, c = 0.0169 g/ml $CHCl_3$. ^1H NMR (400 MHz, $CDCl_3$) δ 4.12 (q, *J* = 7.1 Hz, 2H), 3.57-3.50 (m, 2H), 3.23-3.16 (m, 4H), 2.43 (m, 1H), 2.27 (m, 1H), 2.17 (m, 1H), 2.06 (m, 1H), 1.78-1.66 (m, 2H), 1.67 (s, 1H), 1.45 (m, 1H), 1.25 (t, *J* = 7.1 Hz, 3H), 1.12 (d, *J* = 6.2 Hz, 3H), 1.10 (d, *J* = 6.2 Hz, 3H), 1.10 (m, 1H), 0.98 (d, *J* = 6.5 Hz, 3H). ^{13}C NMR (100 MHz, $CDCl_3$) δ 173.6, 83.6, 66.5, 60.3, 41.4, 41.0, 40.3, 39.7, 37.4, 33.6, 32.7, 28.2, 18.9, 17.4, 15.8, 14.2. R_f = 0.31 (3x 4:1 Hex:EtOAc; anisaldehyde, CAM). IR (NaCl, Thin Film) 3448, 2967, 2926, 2874, 1733, 1374, 1179, 1039 cm^{-1}. HRMS (ESI/APCI) *m/z* $[C_{16}H_{30}NaO_3S_2]^+$ calcd 357.1529, found 357.1534. Longer reaction times and excess borane lead to diol [(2S,4R)-4-(2-((R)-5-hydroxypentan-2-yl)-1,3-dithiolan-2-yl)-2-methylpentan-1-ol]. ^1H NMR (400 MHz, $CDCl_3$) δ3.72-3.45 (m, 2H), 3.65 (m, 1H), 3.54 (m, 1H), 3.24-3.18 (m, 4H), 2.20 (m, 1H), 2.17-1.71 (m, 8H), 1.50 (m, 1H), 1.24 (m, 1H), 1.13 (d, *J* = 6.9 Hz, 3H), 1.11 (m, 3H), 0.99 (d, *J* = 6.8 Hz, 3H). R_f = 0.30 (1:1 Hex:EtOAc; anisaldehyde, CAM). IR (ATR) 3320, 2952, 2922, 2871, 1462, 1376, 1039 cm^{-1}. LRMS (ESI/APCI) *m/z* $[C_{12}H_{22}O_2]^+$ (M-SCH_2CH_2SH) calcd 199.2, found 199.2.

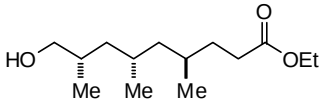

(4R,6S,8S)-methyl 9-hydroxy-4,6,8-trimethylnonanoate (146). (R)-ethyl 4-(2-((2R,4S)-5-hydroxy-4-methylpentan-2-yl)-1,3-dithiolan-2-yl)pentanoate **125** (486 mg, 1.45 mmol) was dissolved in 10 ml EtOH in an acid washed 100 ml round bottom flask. To this, Raney®-nickel (slurry in H_2O: Aldrich 221678) was added via pippette (~8) until starting dithiolane gone by TLC (visualization of progress easiest through use of anisaldehyde stain). Upon completion, the reaction was filtered through Celite and eluted with EtOH (Caution: dry Raney®-nickel is flammable.). The filtrate was concentrated and took up into DCM. The organic layer was washed with 1M HCl 2x, dried with $MgSO_4$, concentrated. The crude oil was loaded onto Celite and purified via flash column chromatography to yield 192.2 mg (54%) of (4R,6S,8S)-methyl 9-hydroxy-4,6,8-trimethylnonanoate as a clear oil. $[\alpha]^{20}_D$ = -3.6, c = 0.0106 g/ml $CHCl_3$. ^1H NMR (400 MHz, $CDCl_3$) δ 4.12 (q, *J* = 7.1 Hz, 2H), 3.52 (dd, *J* = 10.4, 5.0 Hz, 1H), 3.38 (dd, *J* = 10.4, 6.7 Hz, 1H), 2.37-2.21 (m, 2H), 1.75-1.45 (m, 5H), 1.49 (bs, 1H), 1.34-1.13 (m, 4H), 1.25 (t, *J* = 7.2 Hz, 3H), 0.92 (d, *J* = 6.7 Hz, 3H), 0.91 (m, 1H), 0.87 (d, *J* = 6.6 Hz, 3H), 0.86 (d, *J* = 6.6 Hz, 3H). ^{13}C NMR (100 MHz, $CDCl_3$) δ 174.1, 68.1, 60.2, 44.7, 41.2, 33.0, 31.9, 31.3, 29.6, 27.5, 20.8, 20.0, 17.6, 14.2. R_f = 0.20 (4:1 Hex:EtOAc; CAM, anisaldehyde). IR (ATR) 3444, 2955, 2916, 2872, 1735, 1461, 1377, 1178, 1036 cm^{-1}. HRMS (ESI/APCI) *m/z* $[C_{14}H_{28}NaO_3]^+$ (M+Na) calcd 267.1931, found 267.1936.

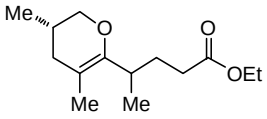

ethyl 4-(3,5-dimethyl-3,4-dihydro-2H-pyran-6-yl)pentanoate (166). From reaction above, this compound was isolated in small amounts. ^{1}H NMR (400 MHz, $CDCl_3$) δ 3.95 (m, 2H), 3.68 (m, 1H), 3.14 (m, 1H), 2.64 (m, 1H), 2.37-2.16 (m, 2H), 2.00 (m, 1H), 1.80-1.56 (m, 2H), 1.50 (m, 3H), 1.39-1.30 (m, 2H), 1.13 (d, J = 6.8 Hz, 1.5H), 1.09 (d, J = 6.8 Hz, 1.5H), 0.94 (t, J = 7.1 Hz, 1.5H), 0.94 (t, J = 7.1 Hz, 1.5H), 0.62 (d, J = 6.6 Hz, 1.5H), 0.61 (d, J = 6.6 Hz, 1.5H). ^{13}C NMR (100 MHz, $CDCl_3$) δ 173.2/173.2, 149.7/149.4, 101.4/101.2, 71.0/71.0, 59.9/59.9, 35.9/35.8, 33.3/33.2, 32.7/32.6, 29.8/29.5, 28.0/28.0, 18.8/18.8, 17.6/17.6, 17.2/17.1, 14.3. R_f = 0.68 (4:1 Hex:EtOAc; CAM). IR (ATR) 2959, 2927, 2871, 1736, 1459, 1374, 1177, 1092 cm^{-1}. HRMS (ESI/APCI) *m/z* $[C_{14}H_{25}O_3]^+$ (M+H) calcd 241.1798, found 241.1803.

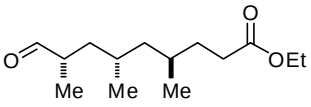

(4R,6S,8S)-ethyl 4,6,8-trimethyl-9-oxononanoate (116). (4R,6S,8S)-methyl 9-hydroxy-4,6,8-trimethylnonanoate **146** (192 mg, 0.786 mmol) was dissolved in 5 ml DCM in a 20 ml Scintillation vial. To this solution, 4Å molecular sieves, 4-methylmorpholine *N*-oxide (128.9 mg, 1.1 mmol, 1.4 equiv), and tetrapropylammonium perruthenate (27.6 mg, 0.08 mmol, 0.10 equiv.) was added. The mixture was stirred for 12 h at 23 °C. The reaction was loaded onto Celite and purified via flash column chromatography to yield 141.6 mg (74%) of (4R,6S,8S)-ethyl 4,6,8-trimethyl-9-oxononanoate as a clear oil. $[\alpha]^{20}_D$ = -2.7, c = 0.0077 g/ml $CHCl_3$. ^{1}H NMR (300 MHz, $CDCl_3$) δ 9.57 (d, *J* = 2.6 Hz, 1H), 4.11 (q, *J* = 7.1 Hz, 2H), 2.48-2.19 (m, 3H), 1.75-1.49 (m, 4H), 1.39-1.25 (m, 1H), 1.24 (t, *J* = 7.1 Hz, 3H), 1.18-0.93 (m, 3H), 1.08 (d, *J* = 7.0 Hz, 3H), 0.88 (d, *J* = 6.5 Hz, 3H), 0.86 (d, *J* = 6.5 Hz, 3H). ^{13}C NMR (100 MHz, $CDCl_3$) δ 205.2, 173.9, 60.2, 44.7, 44.0, 38.2, 31.9, 31.5, 29.6, 27.8, 20.3, 19.8, 14.4, 14.2. R_f = 0.48 (4:1 Hex:EtOAc; CAM). IR (NaCl, Thin Film) 2959, 29926, 2872, 1734, 1459, 1177, 1037 cm^{-1}. HRMS (ESI/APCI) *m/z* $[C_{14}H_{30}NO_3]^+$ (M+NH_4) calcd 260.2220, found 260.2226.

C10-C16 Fragment

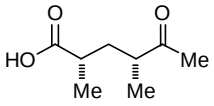

(2S,4R)-2,4-dimethyl-5-oxohexanoic acid (2b). Zinc(II) bromide (14.25 g, 63.3 mmol, 3 equiv.) was added to a flame dried 250 ml round bottom flask in a glove box. The reaction flask was removed from the glove box and the zinc bromide was dissolved in 150 ml THF under Ar. The reaction was cooled to 0 °C and methyl magnesium bromide (24.3 ml, 63.3 mmol, 2.6M in Et_2O, 3.0 equiv.) was added slowly. A white precipitate formed and the reaction was stirred for 10 min. Stirring was discontinued and the precipitate was allowed to settle for 1 h at 0 °C. $[Rh(nbd)Cl]_2$ (48.7 mg, 0.105 mmol, 0.5 mol %) and (R)-tBuPhox (81.8 mg, 0.211 mmol, 1 mol %) were added to a separate 300 ml flame dried round bottom flask in glove box. The reaction flask was removed from the glove box, charged with 16 ml THF, and stirred for 10 min resulting in an yellow solution. The freshly prepared THF solution of methyl zinc bromide was added to the rhodium precatalyst via syringe, leaving behind precipitate. The resulting reddish orange solution was stirred for 10 min and cis-2,4-dimethyl glutaric anhydride **1** (3.0 g, 21.1 mmol) was added as a solid (septa removed, anhydride added in one portion, and reaction flushed after addition of anhydride). The reaction was stirred at 23 °C for 16 h and precipitate formed. The reaction was quenched slowly with 1 M HCl and EtOAc was added.

The layers were separated and the aqueous layer was extracted with EtOAc 3x. The organic phase was extracted with sat. $NaHCO_3$ 3x and collected into a beaker. With stirring, the aqueous solution was acidified using conc. HCl. The acidic solution was extracted with DCM 3x and the organic layer was dried with $MgSO_4$, filtered, and concentrated to yield 3.29 g (99%) of (2S,4R)-2,4-dimethyl-5-oxohexanoic acid as a pale yellow oil. Spectral data matches previous report.[10] $[\alpha]^{20}_D$ = +17.5, c = 0.0227 g/ml $CHCl_3$. ^{1}H NMR (400 MHz, $CDCl_3$) δ 9.54 (s, 1H), 2.62 (m, 1H), 2.52 (m, 1H), 2.17 (s, 3H), 2.10 (m, 1H), 1.38 (m, 1H), 1.21 (d, *J* = 7.0 Hz, 3H), 1.13 (d, *J* = 7.0 Hz). ^{13}C NMR (100 MHz, $CDCl_3$) δ 211.8, 181.7, 44.9, 37.1, 36.0, 28.0, 17.6, 16.3. R_f = 0.22 (78:20:2 Hex:EtOAc:AcOH; CAM). IR (ATR) 2974, 2938, 1734, 1704, 1462, 1357, 1179,1133, 941 cm^{-1}. LRMS (ESI/APCI) *m/z* $[C_8H_{13}O_3]^-$ (M-H) calcd 157.1, found 157.3.

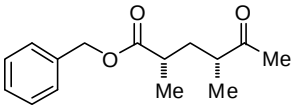

(2S,4R)-benzyl 2,4-dimethyl-5-oxohexanoate (S4). (2S,4R)-2,4-dimethyl-5-oxohexanoic acid **2b** (31.6 mg, 0.20 mmol) was dissolved in 3 ml DCM. Benzyl alcohol (28.1 mg, 0.26 mmol, 1.3 equiv), dicyclohexylcarbodiimide (53.6 mg, 0.20 mmol, 1.3 equiv), and dimethylaminopyridine (7.3 mg, 0.06 mmol, 0.3 equiv.) were added sequentially. The reaction was stirred at 23 °C for 2 h. The reaction was concentrated onto Celite and columned to yield 30.7 mg (62%) of (2S,4R)-benzyl 2,4-dimethyl-5-oxohexanoate as a clear oil. ^{1}H NMR (300 MHz, $CDCl_3$) δ 7.38-7.32 (m, 5H), 5.14 (d, *J* = 13.4 Hz, 1H), 5.10 (d, *J* = 13.4 Hz, 1H), 2.61-2.42 (m, 2H), 2.08 (s, 3H), 2.08 (m, 1H),1.35 (m, 1H), 1.18 (d, *J* = 7.0 Hz, 3H), 1.08 (d, *J* = 7.0 Hz, 3H). R_f = 0.37 (4:1 Hex:EtOAc; UV, CAM). 87% ee by HPLC: Chiralcel IC column, 95:5 Hex:iPrOH, 1 ml/min, RT_{major} = 11.12 min, RT_{minor} = 11.83 min, 210 nm.

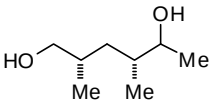

(2S,4R)-2,4-dimethylhexane-1,5-diol (S5). In a flame-dried 50 ml round bottom, lithium aluminum hydride (0.67 g, 17.7 mmol, 2 equiv.) was suspended in 10 ml THF and cooled to 0 °C. To this suspension, (2S,4R)-2,4-dimethyl-5-oxohexanoic acid **2b** (1.4 g, 8.85 mmol) dissolved in THF (5 ml) was added slowly. The solution was allowed to warm to 23 °C and stirred for 12 h. The reaction was quenched by adding $Na_2SO_4 \cdot 10H_2O$ portion wise until bubbling ceased. The mixture was allowed to stir for 45 minutes and filtered. The supernatant was concentrated to yield 1.28 g (99%) of (2S,4R)-2,4-dimethylhexane-1,5-diol as a clear oil of a 1:1.2 mixture of diastereomers (inseparable by flash column chromotography). Spectral data matches previous report.[10] ^{1}H NMR (300 MHz, $CDCl_3$) δ 3.76 (diastereomer a, dq, J = 9.6, 3.0 Hz, 1 H), 3.56 (diastereomer b, dq, J = 6.0, 6.0 Hz, 1.2 H), 3.44 (m, 5.4 H), 2.71 (s, 5.4 H), 1.69 (m, 2.41 H), 1.58 (m, 5.3 H), 1.11 (d, J = 6.3 Hz, 7.7 H), 0.89 (m, 19.3 H). ^{13}C NMR (75 MHz, $CDCl_3$) δ 72.0, 69.8, 67.4, 37.7, 36.9, 36.5, 35.7, 33.3, 32.9, 19.6, 19.5, 18.2, 17.8, 15.7, 15.0. R_f = 0.33 (EtOAc; CAM). IR (NaCl, Thin Film) 3356, 2968, 2927, 2876, 1460, 1379, 1033 cm^{-1}. HRMS (DART) *m/z* $[C_8H_{22}O_2N]^+$ ($M+NH_4$) calcd 146.1307, found 146.1641.

[10] Guo, X.; Liu, T.; Valenzano, C. R.; Deng, Z.; Cane, D. E. *J. Am. Chem. Soc.* **2010**, *132*, 14694-14696.

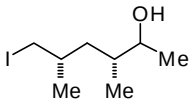

(3R,5S)-6-iodo-3,5-dimethylhexan-2-ol (S6). In a 50 ml round bottom, (2S,4R)-2,4-dimethylhexane-1,5-diol (0.969 g, 6.60 mmol) was dissolved in 30 ml DCM. Imidazole (0.472 g, 6.93 mmol, 1.1 equiv.) and triphenylphosphine (1.82 g, 6.93 mmol, 1.1 equiv.) were added and the reaction mixture was cooled to 0 °C with an ice bath. To this solution, iodine (1.76 g, 6.93 mmol, 1.05 equiv.) was added in 3 portions. The reaction was heated to 45 °C for 1 h in an oil bath and cooled to room temperature. The reaction was absorbed onto Celite and purified via flash column chromatography to yield 1.15 g (68%) of (3R,5S)-6-iodo-3,5-dimethylhexan-2-ol as a clear oil of a mixture of diastereomers. ^{1}H NMR (300 MHz, $CDCl_3$) δ 3.66 (m, 1H), 3.25 (m 1H), 3.12 (m, 1H), 1.61 (bs, 1H), 1.45 (m, 3 H), 1.12 (m, 3H), 1.04 (m, 1H), 0.96 (m, 3H), 0.86 (m, 3H). ^{13}C NMR (75 MHz, $CDCl_3$) δ 71.4, 70.8, 39.4, 39.2, 37.0, 36.8, 31.5, 31.4, 21.8, 21.7, 20.3, 19.2, 18.0, 17.8, 14.8, 14.1. R_f = 0.30 (4:1 Hex:EtOAc). IR (NaCl, Thin Film) 3385, 3967, 2927, 1457, 1378, 1195 cm^{-1}. HRMS (DART) *m/z* $[C_8H_{21}ION]^+$ (M+NH_4) calcd 274.0668, found 274.0660.

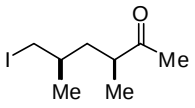

(3S,5R)-6-iodo-3,5-dimethylhexan-2-one (129). In a 50 ml round bottom, (3S,5R)-6-iodo-3,5-dimethylhexan-2-ol ent-**S6** (0.714g, 2.86 mmol) was dissolved in 10 ml DCM. To this solution, 4Å molecular seives, 4-methylmorpholine *N*-oxide (0.369 g, 3.15 mmol, 1.1 equiv), and tetrapropylammonium perruthenate (50 mg, 0.14 mmol, 0.05 equiv) was added. The mixture was stirred for 12 h at 23 °C. The reaction was loaded onto Celite and purified via flash column chromatography to yield 0.665 g (94%) of (3S,5R)-6-iodo-3,5-dimethylhexan-2-one as a clear oil. $[\alpha]^{20}_D$ = +5.8, c = 0.0100 g/ml $CHCl_3$. ^{1}H NMR (300 MHz, $CDCl_3$) δ 3.21 (dd, J = 9.8, 4.4 Hz, 1H), 3.14 (dd, J = 9.8 Hz, 5.4 Hz, 1H), 2.56 (ddq, J = 7.2, 7.0, 7.0 Hz, 1H) 2.15 (s, 3H), 1.76 (ddd, J = 13.9, 7.7, 6.2 Hz, 1H), 1.39 (m, 1H), 1.16 (ddd, J = 13.9, 7.1, 7.1 Hz, 1H), 1.09 (d, J = 7.0 Hz, 3H), 0.96 (d, J = 6.5 Hz, 3H). ^{13}C NMR (75 MHz, $CDCl_3$) δ 212.0, 44.6, 39.5, 31.8, 27.9, 20.7, 17.4, 16.6. R_f = 0.31 (4:1 Hex:EtOAc). IR (NaCl, Thin Film) 2965, 2931, 2875, 1712, 1459, 1237 cm^{-1}. HRMS (DART) *m/z* $[C_8H_{19}ION]^+$ (M+NH_4) calcd 272.0511, found 272.0504.

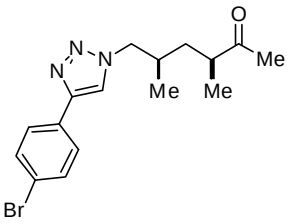

(3S,5R)-6-(4-(4-bromophenyl)-1H-1,2,3-triazol-1-yl)-3,5-dimethylhexan-2-one (170). (3S,5R)-6-iodo-3,5-dimethylhexan-2-one **129** (70.0 mg, 0.28 mmol) was dissolved in 4 mL DMF and sodium azide (36.4 mg, 0.56 mmol, 2.0 equiv) was added. The reaction was heated to 50 °C overnight. After cooling to 23 °C, the reaction was diluted with EtOAc. The organic layer was washed with 10 % LiCl 3x, dried with $MgSO_4$, and concentrated to yield 20.9 mg (45%) of (3S,5R)-6-azido-3,5-dimethylhexan-2-one (**S7**). ^{1}H NMR (300 MHz, $CDCl_3$) δ 3.20 (dd, *J* = 12.1, 5.8 Hz, 1H), 3.13 (dd, *J* = 12.0, 6.3 Hz, 1H), 2.63 (m, 1H), 2.15 (s, 3H), 1.85-1.62 (m, 2H), 1.11 (m, 1H), 1.11 (d, *J* = 7.0 Hz, 3H), 0.96 (d, *J* = 6.7 Hz, 3H). (3S,5R)-6-azido-3,5-dimethylhexan-2-one **S7** (20.9 mg, 0.123 mmol) and 1-bromo-4-ethynyl benzene (22.4 mg, 0.123 mmol, 1.0 equiv) were dissolved in 4 mL 1:1 H_2O:tBuOH. Copper sulfate (4.0 mg, 0.025 mmol, 0.2 equiv.) and (+)-sodium (L)-ascorbate (24.0 mg, 0.123 mmol, 1.0 equiv) were added, resulting in an orange slurry. The reaction was stirred overnight and turned green. The reaction was diluted with H_2O and EtOAc. The layers were separated and the aqueous was extracted with EtOAc 2x, the organic layers were combined and dried with $MgSO_4$. The organic layer was concentrated and purified by flash column chromatography to yield 31.5 mg (73%) of

(3S,5R)-6-(4-(4-bromophenyl)-1H-1,2,3-triazol-1-yl)-3,5-dimethylhexan-2-one as a white powder. $[\alpha]^{20}_D$ = -4.2, c = 0.0315 g/ml $CHCl_3$. ^1H NMR (400 MHz, $CDCl_3$) δ 7.77 (s, 1H), 7.71 (m, 2H), 7.53 (m, 2H), 4.28 (dd, *J* = 13.7, 6.3 Hz, 1H), 4.18 (dd, *J* = 13.7, 7.3 Hz, 1H), 2.67 (m, 1H), 2.11 (s, 3H), 2.08 (m, 1H), 1.78 (ddd, *J* = 14.0, 9.2, 5.0 Hz, 1H), 1.14 (m, 1H), 1.12 (d, *J* = 7.1 Hz, 3H), 0.92 (d, *J* = 6.7 Hz, 3H). ^{13}C NMR (100 MHz, $CDCl_3$) δ 211.9, 146.7, 131.9, 129.6, 127.2, 121.9, 120.0, 56.2, 44.4, 36.9, 32.2, 28.1, 17.6, 17.5. R_f = 0.16 (2:1 Hex:EtOAc). IR (ATR) 3130, 2966, 2933, 1708, 1457, 1356, 1227, 1069, 1010, 972, 826 cm^{-1}. LRMS (APCI/ESI) *m/z* $[C_{16}H_{21}Br_3O]^+$ (M+H) calcd 350.1, found 350.0 and 351.0. Slow evaporation of an Et_2O solution yielded clear, X-ray quality needles.[11]

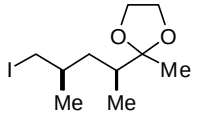

2-((2S,4R)-5-iodo-4-methylpentan-2-yl)-2-methyl-1,3-dioxolane (S8). (3S,5R)-6-iodo-3,5-dimethylhexan-2-one **129** (0.665 g, 2.6 mmol) was dissolved in 7 ml benzene in a 10 ml round bottom flask. To this solution, p-toluenesulfonic acid monohydrate (89 mg, 0.52 mmol, 0.1 equiv) and ethylene glycol (0.7 ml, 13 mmol, 5 equiv) was added. A Dean Stark apparatus and reflux condenser were attached and the reaction was placed into a 100 °C oil bath for 1 h (longer reaction times lead to epimerization). The reaction was cooled to 23 °C and sat. $NaHCO_3$ and EtOAc was added. The layers were separated and the aqueous layer was extracted with EtOAc 3x. The organic layer was washed with sat. NaCl, dried with $MgSO_4$, concentrated, and purified via flash column chromatography to yield 0.658 g (85%) of 2-((2S,4R)-5-iodo-4-methylpentan-2-yl)-2-methyl-1,3-dioxolane as a clear oil. $[\alpha]^{20}_D$ = -19.7, c = 0.0102 g/ml $CHCl_3$. ^1H NMR (300 MHz, $CDCl_3$) δ 3.92 (m, 4H), 3.3 (dd, J = 9.7, 3.2 Hz, 1H), 3.1 (dd, J = 9.7, 5.7 Hz, 1H), 1.69 (m, 1H), 1.53 (m, 2H), 1.24 (s, 3H), 1.05 (m, 1H), 0.99 (d, J = 6.2 Hz, 3H), 0.94 (d, J = 6.8 Hz, 3H). ^{13}C NMR (75 MHz, $CDCl_3$) δ 112.1, 64.6, 64.5, 38.6, 38.5, 31.9, 22.1, 20.3, 17.4, 14.9. R_f = 0.42 (4:1 Hex:EtOAc). IR (NaCl, Thin Film) 2960, 2937, 2879, 1380, 1182, 1093, 1047 cm^{-1}. MS (APCI) m/z $[C_{10}H_{20}IO_2]^+$ calcd 299.1, found 299.1.

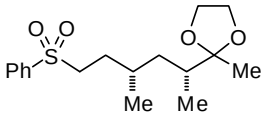

2-methyl-2-((2R,4S)-4-methyl-6-(phenylsulfonyl)hexan-2-yl)-1,3-dioxolane (169d). Methyl phenyl sulfone (25.9 mg, 1.66 mmol, 1.66 equiv.) was added to an oven dried 10 mL round bottom flask. The flask was put under Ar and the methyl phenyl sulfone was dissolved in 2 mL THF. The reaction was cooled to -78 °C and nBuLi (0.1 mL, 1.5M in hexanes, 1.4 equiv.) was added. After stirring for 30 minutes, 2-((2R,4S)-5-iodo-4-methylpentan-2-yl)-2-methyl-1,3-dioxolane **S8** (29.8 mg, 0.1 mmol) was added in 2 mL THF. After 5 minutes, HMPA was added. The reaction was stirred for 2.5 hours at -78 °C and then quenched with sat. NH_4Cl. The reaction was extracted with Et2O 2x, dried with $MgSO_4$, filtered, and purified by preparative thin layer chromatography to yield 19.4 mg (59%) of 2-methyl-2-((2R,4S)-4-methyl-6-(phenylsulfonyl)hexan-2-yl)-1,3-dioxolane as a clear oil. ^1H NMR (400 MHz, C_6D_6) δ 7.83-7.81 (m, 2H), 6.98-6.90 (m, 3H), 3.53-3.45 (m, 4H), 2.95 (ddd, *J* = 13.4, 11.4, 4.2 Hz, 1H), 2.78 (ddd, *J* = 13.8, 11.0, 5.0 Hz, 1H), 1.80 (m, 1H), 1.63 (m, 1H), 1.54-1.27 (m, 3H), 1.14 (s, 3H), 0.92 (d, *J* = 6.8 Hz, 3H), 0.85 (m, 1H), 0.58 (d, *J* = 5.9 Hz, 3H). ^{13}C NMR (100 MHz, C_6D_6) δ 140.7, 133.0, 129.0, 112.3, 64.6, 64.4, 53.6, 39.0, 38.8, 29.6, 28.1, 20.3, 19.9, 15.6. R_f = 0.56 (1:1 Hex:EtOAc). IR (ATR) 2957, 2919, 2875,

[11] Oberg, K. M.; Rovis T. (2014) Private communication to the Cambridge Structural Database, deposit number CCDC 991677.

1447, 1305, 1144, 1071, 742 cm^{-1}. HRMS (APCI) *m/z* $[C_{17}H_{27}O_4S]^+$ (M+H) calcd 327.1552, found 327.1630.

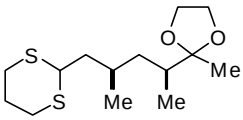

2-((2S,4R)-5-(1,3-dithian-2-yl)-4-methylpentan-2-yl)-2-methyl-1,3-dioxolane (S9). 1,3-Dithiane (0.94 g, 7.8 mmol, 5 equiv) was dissolved in 16 ml THF:HMPA (15:1). The solution was cooled to -30 °C with a dry ice:ethylene glycol:water bath. To this solution, n-BuLi (4.9 ml, 7.8 mmol, 5 equiv, 1.6 M in hexanes) was added and the solution went from clear to yellow. The mixture was stirred for 30 minutes and 2-((2S,4R)-5-iodo-4-methylpentan-2-yl)-2-methyl-1,3-dioxolane **S8** (0.466 g, 1.56 mmol) was added in 1 ml THF. The reaction was allowed to warm to 23 °C and stirred for 1 h. The reaction was quenched with addition of water and then EtOAc was added. The layers were separated and the aqueous layer was extracted with EtOAc 3x. The organic layer was washed with sat. NaCl, dried with $MgSO_4$, concentrated, and purified via flash column chromatography to yield 0.43 g (95%) of 2-((2S,4R)-5-(1,3-dithian-2-yl)-4-methylpentan-2-yl)-2-methyl-1,3-dioxolane as a clear oil. $[\alpha]^{20}_D$ = -31.3, c = 0.0107 g/ml $CHCl_3$. ^{1}H NMR (300 MHz, $CDCl_3$) δ 4.10 (dd, J = 10.2, 4.6 Hz, 1H), 3.91 (m, 4H), 2.86 (m, 4H), 2.12 (m, 1H), 1.86 (m, 1H), 1.75 (m, 1H), 1.47 (m, 1H), 1.38 (m, 1H), 1.22 (s, 3H), 1.02 (m, 1H), 0.95 (d, J = 6.5 Hz, 3H), 0.94 (d, J = 6.8 Hz, 3H). ^{13}C NMR (100 MHz, $CDCl_3$) δ 112.4, 64.6, 64.5, 45.6, 41.4, 39.5, 38.5, 30.7, 30.3, 27.5, 26.1, 20.9, 20.2, 15.0. R_f = 0.26 (9:1 Hex:EtOAc). IR (NaCl, Thin Film) 2932, 2896, 1379, 1145, 1048, 867 cm^{-1}. HRMS (ESI/APCI) m/z $[C_{14}H_{27}O_2S_2]^+$ calcd 291.1447, found 291.1448.

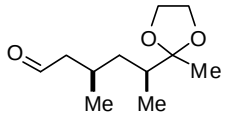

(3R,5S)-3-methyl-5-(2-methyl-1,3-dioxolan-2-yl)hexanal (147). 2-((2S,4R)-5-(1,3-dithian-2-yl)-4-methylpentan-2-yl)-2-methyl-1,3-dioxolane **S9** (0.4 g, 1.38 mmol) was dissolved in 20 ml MeCN:H_2O (1:1). Sodium bicarbonate (1.88 g, 22.4 mmol, 16 equiv) and iodomethane (1.4 ml, 22.4 mmol, 16 equiv) was added and the reaction was stirred for 16 h. The reaction was quenched with addition of water and then EtOAc was added. The layers were separated and the aqueous layer was extracted with EtOAc 3x. The organic layer was washed with sat. NaCl, dried with $MgSO_4$, concentrated, and purified via flash column chromatography to yield 0.20 g (73%) of (3R,5S)-3-methyl-5-(2-methyl-1,3-dioxolan-2-yl)hexanal as a clear oil. $[\alpha]^{20}_D$ = -14.6, c = 0.0105 g/ml $CHCl_3$. ^{1}H NMR (300 MHz, $CDCl_3$) δ 9.77 (dd, J = 2.0, 1.9 Hz, 1H), 3.92 (m, 4H), 2.43 (ddd, J = 19.4, 7.9, 1.9 Hz, 1H), 2.16 (m, 2H), 1.68 (m, 1H), 1.53 (ddd, J = 13.5, 8.8, 3.6 Hz, 1H), 1.23 (s, 3H), 1.09 (m, 1H), 1.00 (d, J = 6.6 Hz, 3H), 0.96 (d, J = 6.8 Hz, 3H). ^{13}C NMR (75 MHz, $CDCl_3$) δ 202.8, 112.1, 64.5, 64.4, 50.0, 39.2, 38.8, 26.1, 21.3, 19.9, 15.2. R_f = 0.27 (4:1 Hex:EtOAc). IR (NaCl, Thin Film) 2961, 2880, 1724, 1381, 1167, 1047 cm^{-1}. HRMS (ESI/APCI) m/z $[C_{11}H_{21}O_3]^+$ calcd 201.1485, found 201.1489.

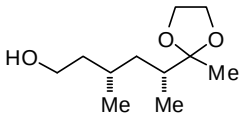

(3S,5R)-3-methyl-5-(2-methyl-1,3-dioxolan-2-yl)hexan-1-ol (167). (3S,5R)-3-methyl-5-(2-methyl-1,3-dioxolan-2-yl)hexanal **147** (0.337 g, 1.68 mmol) was dissolved in 30 ml MeOH in a 100 ml round bottom flask. The reaction was cooled to 0 °C and sodium borohydride (0.127 g, 3.36 mmol, 2 equiv.) was added. The reaction was stirred at 0 °C for 2 h and quenched with sat. NH_4Cl. The reaction was diluted with EtOAc, layers separated, and the

aqueous layer was extracted with EtOAc 2x. The organic layer was dried with $MgSO_4$, filtered, concentrated. The resulting residue was purified by flash column chromotography to yield 0.289 g (85%) of (3S,5R)-3-methyl-5-(2-methyl-1,3-dioxolan-2-yl)hexan-1-ol as a clear oil. $[\alpha]^{20}_D$ = +4.1, c = 0.0043 g/ml $CHCl_3$. ^{1}H NMR (400 MHz, C_6D_6) δ 3.60-3.46 (m, 6H), 1.84 (m, 1H), 1.72-1.58 (m, 3H), 1.48 (m, 1H), 1.24 (m, 4H), 1.05 (m, 1H), 1.05 (d, *J* = 6.8 Hz, 3H), 0.90 (d, *J* = 6.3 Hz, 3H). ^{13}C NMR (100 MHz, C_6D_6) δ 113.0, 65.0, 64.9, 61.0, 40.4, 39.7, 39.5, 28.3, 21.7, 20.6, 16.1. R_f = 0.16 (2:1 Hex:EtOAc). IR (NaCl, Thin Film) 3422, 2934, 2880, 1380, 1166, 1005, 871 cm^{-1}. HRMS (APCI) *m/z* $[C_{11}H_{21}O_3]^-$ calcd 201.16, found 201.1122.

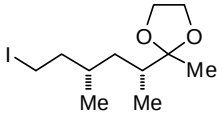

2-((2R,4S)-6-iodo-4-methylhexan-2-yl)-2-methyl-1,3-dioxolane (160). (3S,5R)-3-methyl-5-(2-methyl-1,3-dioxolan-2-yl)hexan-1-ol **167** (162.4 mg, 0.80 mmol) was dissolved in DCM. Triphenyl phosphine (230.8 mg, 0.88 mmol, 1.1 equiv.) and imidizole (60.0 mg, 0.88 mmol, 1.1 equiv.) was added and the reaction mixture was cooled to 0 °C. Iodine (106.6 mg, 0.42 mmol, 0.52 equiv.) was added in 3 portions, the reaction was stirred for 4 h and allowed to warm to 23 °C. The reaction was diluted with DCM and absorbed onto Celite. The reaction was purified by flash column chromatography to yield 114.8 mg (46%) of 2-((2R,4S)-6-iodo-4-methylhexan-2-yl)-2-methyl-1,3-dioxolane as a clear oil. ^{1}H NMR (400 MHz, C_6D_6) δ 3.54-3.46 (m, 4H), 2.93 (ddd, J = 9.5, 8.6, 5.0 Hz, 1H), 2.75 (m, 1H), 1.78 (m, 1H), 1.71 (m, 1H), 1.57-1.50 (m, 2H), 1.28 (m, 1H), 1.19 (s, 3H), 1.01 (d, J = 6.8 Hz, 3H), 0.91 (m, 1H), 0.67 (d, J 6.3 Hz, 3H). ^{13}C NMR (100 MHz, C_6D_6) δ 112.8, 65.0, 64.9, 40.5, 39.7, 39.5, 32.2, 20.6, 20.4, 16.0, 5.2. R_f = 0.23 (20:1 Hex:EtOAc). IR (NaCl, Thin Film) 2959, 2933, 2877, 1380, 1160, 1045, 872 cm^{-1}. LRMS (ESI/APCI) *m/z* $[C_{11}H_{21}IO_2]^+$ calcd 313.0, found 313.1.

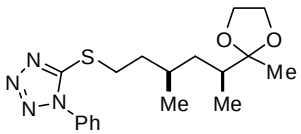

5-(((3R,5S)-3-methyl-5-(2-methyl-1,3-dioxolan-2-yl)hexyl)thio)-1-phenyl-1H-tetrazole (168). 2-((2S,4R)-6-iodo-4-methylhexan-2-yl)-2-methyl-1,3-dioxolane **160** (250 mg, 0.8 mmol), 1-phenyl-tetrazole-5-thiol (214 mg, 1.2 mmol, 1.5 equiv), and potassium carbonate (166 mg, 1.2 mmol, 1.5 equiv) were added to 6 ml DMF. The solution was heated to 50 °C for 2 h. After cooling to 23 °C, EtOAc was added and the organic solution was washed with 10 % LiCl 3x. The organic layer was dried with $MgSO_4$, filtered, concentrated, and purified by flash column chromatography to yield 124.1 mg (92%) of 5-(((3R,5S)-3-methyl-5-(2-methyl-1,3-dioxolan-2-yl)hexyl)thio)-1-phenyl-1H-tetrazole as a clear oil. $[\alpha]^{20}_D$ = -18.2, c = 0.00103 g/ml $CHCl_3$. ^{1}H NMR (300 MHz, $CDCl_3$) δ 7.55 (m, 5H), 3.9 (m, 4H), 3.51 (ddd, J = 12.3, 9.8, 5.1 Hz, 1H), 3..31 (ddd, J = 12.7, 9.5, 6.7 Hz, 1H), 1.87 (m, 1H), 1.71 (m, 2H), 1.55 (m, 2H), 1.22 (s, 3H), 1.05 (m, 1H), 0.98 (d, J = 6.5 Hz, 3H), 0.92 (d, J = 6.8 Hz, 3H). ^{13}C NMR (75 MHz, $CDCl_3$) δ 154.4, 133.7, 130.0, 129.7, 123.8, 112.3, 64.5, 64.4, 39.0, 38.7, 34.7, 31.0, 30.0, 20.5, 20.0, 15.2. R_f = 0.42 (2:1 Hex:EtOAc). IR (NaCl, Thin Film) 2959, 2935, 2879, 1500, 1412, 1075, 762 cm^{-1}. HRMS (ESI/APCI) *m/z* $[C_{18}H_{27}N_4O_2S]^+$ calcd 363.1849, found 363.1837.

(3S,5R)-3-methyl-5-(2-methyl-1,3-dioxolan-2-yl)hexan-1-ol **167** (47.2 mg, 0.23 mmol), triphenyl phosphine (73.3 mg, 0.28 mmol, 1.2 equiv.), 1-phenyl-tetrazole-5-thiol (49.9 mg, 0.28 mmol, 1.2 equiv.) were dissolved in 5 mL THF and the reaction vessel was cooled to 0 °C under Ar. Diisopropyl azodicarboxylate (0.034 mL, 0.24 mmol, 1.02 equiv.) was added and the reaction was stirred for 12 h and

allowed to warm to 23 °C. The reaction was quenched with sat. NH_4Cl and separated. The aqueous layer was extracted with EtOAc 2x. The organic layers were combined, washed with brine, and dried with $MgSO_4$, filtered, and concentrated. The resulting residue was purified by flash column chromatography to yield 63.2 mg (75%) of 5-(((3S,5R)-3-methyl-5-(2-methyl-1,3-dioxolan-2-yl)hexyl)thio)-1-phenyl-1H-tetrazole.

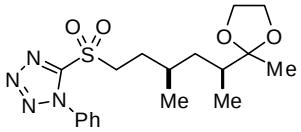

5-(((3R,5S)-3-methyl-5-(2-methyl-1,3-dioxolan-2-yl)hexyl)sulfonyl)-1-phenyl-1H-tetrazole (169a). 5-(((3R,5S)-3-methyl-5-(2-methyl-1,3-dioxolan-2-yl)hexyl)thio)-1-phenyl-1H-tetrazole **168** (107.7 mg, 0.30 mmol) and meta-chloroperoxybenzoic acid (235 mg, 1.05 mmol, 3.5 equiv.) were dissolved in 10 ml DCM and stirred for 12 h. The organic solution was diluted with DCM and washed with sat. $NaHCO_3$ 3x and brine. The organic layer was dried with $MgSO_4$, concentrated, and purified via flash column chromatography to yield 99.1 mg (85%) of 5-(((3R,5S)-3-methyl-5-(2-methyl-1,3-dioxolan-2-yl)hexyl)sulfonyl)-1-phenyl-1H-tetrazole as an amorphous solid. $[\alpha]^{20}_D$ = -11.1, c = 0.00103 g/ml $CHCl_3$. ^{1}H NMR (300 MHz, $CDCl_3$) δ 7.68 (m, 2H), 7.60 (m, 3H), 3.91 (m, 4H), 3.81 (m, 1H), 3.66 (m, 1H), 1.98 (m, 1H), 1.72 (m, 2H), 1.51 (ddd, J = 12.8, 9.0, 3.3 Hz, 1H), 1.21 (s, 3H), 1.06 (m, 1H), 0.98 (d, J = 6.4 Hz, 3H), 0.94 (d, J = 6.8 Hz, 3H). ^{13}C NMR (75 MHz, $CDCl_3$) δ 153.4, 133.0, 131.4, 129.6, 125.0, 112.2, 64.6, 64.5, 53.6, 38.7, 38.4, 29.5, 26.9, 20.3, 19.8, 15.3. R_f = 0.14 (4:1 Hex:EtOAc). IR (NaCl, Thin Film) 2961, 2938, 2880, 1498, 1342, 1152, 1047 cm^{-1}. HRMS (ESI/APCI) *m/z* $[C_{18}H_{26}N_4O_4SNa]^+$ calcd 417.1567, found 417.1570.

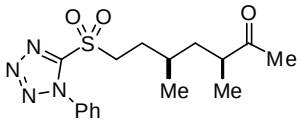

(3S,5R)-3,5-dimethyl-7-((1-phenyl-1H-tetrazol-5-yl)sulfonyl)heptan-2-one (119a). 5-(((3R,5S)-3-methyl-5-(2-methyl-1,3-dioxolan-2-yl)hexyl)sulfonyl)-1-phenyl-1H-tetrazole **169a** (197 mg, 0.5 mmol) was dissolved in MeCN and then sodium iodide (12 mg, 0.08 mmol, 0.15 equiv.) and cerium trichloride heptahydrate (280 mg, 0.75 mmol, 1.5 equiv.) were added.[12] The solution was stirred for 16 h before being diluted with Et_2O and 0.5M HCl. The layers were separated and the aqueous was extracted with Et_2O 3x. The organic layer was washed 3x with sat. $NaHCO_3$ and 1x with brine, dried with $MgSO_4$, concentrated, and columned to yield 154.3 mg of (3S,5R)-3,5-dimethyl-7-((1-phenyl-1H-tetrazol-5-yl)sulfonyl)heptan-2-one (88%) as a clear oil. $[\alpha]^{20}_D$ = -1.6, c = 0.0153 g/ml $CHCl_3$. ^{1}H NMR (300 MHz, $CDCl_3$) δ 7.69 (m, 2H), 7.60 (m, 3H), 3.78 (m, 1H), 3.70 (m, 1H), 2.64 (m, 1H), 2.14 (s, 3H), 1.93 (dddd, J = 13.6, 11.2, 5.7, 5.7 Hz, 1H), 1.76 (m, 2H), 1.60 (m, 1H), 1.13 (m, 1H), 1.10 (d, J = 7.1 Hz, 3H), 0.96 (d, J = 6.6 Hz, 3H). ^{13}C NMR (75 MHz, $CDCl_3$) δ 212.0, 153.4, 133.0, 131.4, 129.7, 125.0, 54.0, 44.5, 39.1, 30.0, 28.6, 28.3, 19.3, 17.4. R_f = 0.27 (2:1 Hex:EtOAc). IR (NaCl, Thin Film) 2966, 2933, 2877, 1710, 1342, 1104 cm^{-1}. HRMS (ESI/APCI) *m/z* $[C_{16}H_{23}N_4O_3S]^+$ calcd 351.1485, found 351.1493.

[12] For use of $CeCl_3 \cdot 7H_2O$/NaI in dioxolane deprotection, see: Marcantoni, E.; Nobili, F.; Bartoli, G.; Bosco, M.; Sambri, L. *J. Org. Chem.* **1997**, *62*, 4183-4184.

C17-C22 Fragment

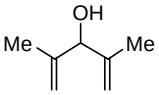

2,4-dimethylpenta-1,4-dien-3-ol (S10). Magnesium (3 g, 123 mmol, 1.4 equiv.) and stir bar were flame dried in a 250 ml round bottom flask. After cooling to 23 °C, a small I_2 crystal and 60 ml THF was added. A reflux condenser was attached and the reaction was flushed with Ar. 1 ml of freshly distilled 2-bromopropene (7.5 ml, 84.4 mmol) was added and the reaction was stirred until initiation. After initiation, the 2-bromopropene was added to keep the reaction at reflux. After addition, the reaction was stirred until it cooled to 23 °C and was then further cooled to 0 °C with an ice bath. Freshly distilled methacrolein (10 ml, 121 mmol, 1.4 equiv.) was slowly added. The ice bath was removed and the reaction was stirred for 3 h. The reaction was decanted away from the excess magnesium into a 500 ml Erlenmeyer and rinsed with 50 mL Et_2O. The organic layer was quenched by addition of 1 M HCl. The reaction was added to a seperatory funnel and the aqueous was extracted 2x with 100 mL Et_2O. The organic was washed with 100 mL sat. brine, dried with $MgSO_4$, and concentrated to yield 8.0-8.5 g (85-90%) of 2,4-dimethylpenta-1,4-dien-3-ol as a viscous oil. The crude product was used directly in the next reaction. Attempts to purify by flash column chromatography or distillation lead to decomposition. ^{1}H NMR (300 MHz, $CDCl_3$) δ 5.06 (m, 2H), 4.94 (m, 2H), 4.48 (bs, 1H), 2.23 (bs, 1H), 1.64 (bs, 6H). bp: 74 °C at 48 torr.

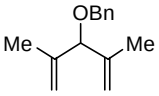

(((2,4-dimethylpenta-1,4-dien-3-yl)oxy)methyl)benzene (132b). Sodium hydride (5.3 g, 133.5 mmol, 1.5 equiv., 60% in mineral oil) was suspended in 100 ml THF under Ar. The reaction vessel was cooled to 0 °C with an ice bath. 2,4-dimethylpenta-1,4-dien-3-ol **S10** (9.98 g, 89.0 mmol) was dissolved in 10 ml THF and added slowly to the reaction vessel. The reaction was stirred for 45 min and benzyl bromide (12.7 ml, 106.8 mmol, 1.2 equiv.) was added. The reaction was stirred at 23 °C for 12 h. The reaction was quenched with H_2O and extracted with Et_2O 3x. The organic layer was dried and concentrated to yield a yellow syrup consisting of a mixture of (((2,4-dimethylpenta-1,4-dien-3-yl)oxy)methyl)benzene, benzyl bromide, and mineral oil. This mixture can be used directly in the hydroboration reaction or purified. Vacuum distillation yields (((2,4-dimethylpenta-1,4-dien-3-yl)oxy)methyl)benzene as a clear oil with minor benzyl bromide impurities, but free of mineral oil. Purification via flash column chromatography yields 9.37 g (52%) of (((2,4-dimethylpenta-1,4-dien-3-yl)oxy)methyl)benzene as a clear oil. ^{1}H NMR (400 MHz, $CDCl_3$) δ 7.38-7.32 (m, 4H), 7.29-7.25 (1H), 5.10 (m, 2H), 5.00 (m, 2H), 4.47 (s, 2H), 4.12 (s, 1H), 1.65 (m, 6H). ^{13}C NMR (100 MHz, $CDCl_3$) δ 143.0, 138.8, 128.2, 127.4, 127.2, 112.9, 85.7, 69.7, 18.0. R_f = 0.14 (95:5 Hex:DCM). bp: 55 °C at 4 torr. IR (ATR) 3068, 2973, 2856, 1453, 1074, 900, 733, 695 cm^{-1}. HRMS (APCI) *m/z* $[C_{14}H_{19}O]^+$ (M+H) calcd 203.1430, found 203.1433.

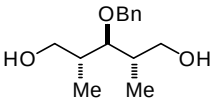

(2R,3s,4S)-3-(benzyloxy)-2,4-dimethylpentane-1,5-diol (133b). A 500 ml pressure equalizing addition funnel and 2000 ml round bottom flask were flame dried under vacuum. (((2,4-dimethylpenta-1,4-dien-3-yl)oxy)methyl)benzene **132b** (7.00 g, 34.6 mmol) was dissolved in 200 ml THF under Ar in the round bottom flask. The reaction flask was cooled to -78 °C and 9-borabicyclo[3.3.1]nonane (276 ml, 138.4 mmol, 0.5 M in THF, 4 equiv.) was added to the

addition funnel. The 9-borabicyclo[3.3.1]nonane solution was added to the reaction over 1 h. The reaction was stirred 36 h and allowed to warm to 23 °C.[13] The reaction was cooled to 0 °C and aqueous sodium hydroxide (140 ml, 42 mmol, 3M, 12.1 equiv.) was added slowly over 1.5 h. While still maintaining 0 °C, hydrogen peroxide (56 ml, 554 mmol, 30% wt. in H_2O, 16 equiv.) was added slowly over 1.5 h. The reaction was stirred for 24 h and allowed to warm to 23 °C. The solution was filtered through Celite to remove the formed solids and extracted with Et_2O 3x. The organic layer was washed with D.I. H_2O 2x (to remove some cyclooctane-1,5-diol) and brine 1x. The organic layer was dried with $MgSO_4$, filtered, and concentrated to a thick syrup. This syrup was dissolved in minimal Et_2O; a seed crystal of cyclooctane-1,5-diol was added and the flask was cooled to -15 °C for 12h. The mother liquor was decanted away from the solid cyclooctane-1,5-diol, concentrated, and purified via flash column chromatography to yield 4.90 g (58%) of (2R,3s,4S)-3-(benzyloxy)-2,4-dimethylpentane-1,5-diol as a clear oil and a 3.5:1 mixture of diastereomers (anti, anti diol: anti, syn diol). ^{1}H NMR (400 MHz, $CDCl_3$) δ 7.36-7.29 (m, 5H), 4.66 (s, 2H), 3.77 (dd, *J* = 11.0, 4.1 Hz, 2H), 3.66 (dd, *J* = 11.0, 5.3 Hz, 2H), 3.45 (t, *J* = 5.8 Hz, 1H), 2.07 (s, 2H), 2.00 (m, 2H), 1.08 (d, *J* = 7.1 Hz, 6H). ^{13}C NMR (100 MHz, $CDCl_3$) δ 137.7, 128.6, 128.1, 128.0, 88.4, 75.8, 65.3, 37.8, 15.4. R_f = 0.22 (1:1 Hex:EtOAc; CAM). IR (ATR) 3345, 2961, 2926, 2876, 1454, 1066, 1028 cm^{-1}. LRMS (ESI/APCI) *m/z* $[C_{14}H_{23}O_3]^+$ (M+H) calcd 239.2, found 239.1.

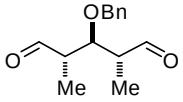

(2R,3r,4S)-3-(benzyloxy)-2,4-dimethylpentanedial (149b). Dimethyl sulfoxide (2.07 ml, 29.28 mmol, 3.05 equiv.) was dissolved in 22 ml DCM under Ar and the reaction was cooled to -78 °C. Oxalyl chloride (2.43 ml, 28.3 mmol, 2.95 equiv.) was added slowly and the reaction was stirred for 20 min. (2R,3s,4S)-3-(benzyloxy)-2,4-dimethylpentane-1,5-diol **133b** (2.29 g, 9.6 mmol) was dissolved in 10 mml DCM and added slowly to the reaction. After stirring for 45 min, triethyl amine (13.4 ml, 96 mmol, 10.0 equiv.) and the reaction was placed in an ice bath for 2 h. At this time, 45 ml PhMe was added and the reaction was filtered through a pad of Celite eluting with 30 ml Et_2O 2x. The filtrate was quickly concentrated to ~1/10 volume via rotovap. The filtrate was diluted with E_2O and filtered through a pad of Celite. The reaction was concentrated to ~1/10 volume and quickly used in the next reaction. If the product is overly concentrated or allowed to sit, the product decomposes (light yellow to orange to brown). ^{1}H NMR (300 MHz, $CDCl_3$) δ 9.7 (d, *J* = 1.9 Hz, 2H), 7.36-7.13 (m, 5H), 4.59 (s, 2H), 4.08 (t, *J* = 5.8 Hz, 1H), 2.78 (m, 2H), 1.13 (d, *J* = 7.2 Hz, 6H).

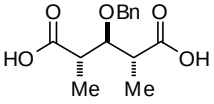

(2R,3r,4S)-3-(benzyloxy)-2,4-dimethylpentanedioic acid (S11). (2R,3r,4S)-3-(benzyloxy)-2,4-dimethylpentanedial **149b** (~9.6 mmol) and 2-methyl-2-butene (10.2 ml, 96 mmol, 10.0 equiv.) were dissolved in 30 ml of a 1:1 THF:tBuOH mixture. The reaction was cooled to 0 °C with an ice bath. Sodium chlorite (5.43 g, 48 mmol, 5.0 equiv., technical grade, 80%) and sodium phosphate monobasic monohydrate (13.24 g, 96 mmol, 10.0 equiv.) was dissolved in 60 ml H2O. This solution was added to the dialdehyde solution via additional funnel over 20 min. The reaction was allowed to stir overnight. The reaction mixture was made acidic (pH = 1) using

[13] If reaction is not stirred at 23 °C for extended time, the second hydroboration does not occur. Early workup of the reaction leads to alkenol: 3-(benzyloxy)-2,4-dimethylpent-4-en-1-ol. ^{1}H NMR (300 MHz, $CDCl_3$) δ 7.38-7.29 (m, 5H), 5.07 (m, 1H), 4.93 (m, 1H), 4.53 (d, J = 11.6 Hz, 1H), 4.25 (d, J = 11.6 Hz, 1H), 3.63-3.59 (m, 2H), 1.98 (m, 1H), 1.72 (m, 3H), 1.53 (m, 1H), 0.72 (d, J = 7.0 Hz, 3H). R_f = 0.54 (1:1 Hex:EtOAc; CAM). After purification via flash column chromatography, this compound can be resubjected to the reaction to get diol **133b**.

conc. HCl and the reaction was extracted with EtOAc 3x. The organic layer was dried and concentrated to yield (2R,3r,4S)-3-(benzyloxy)-2,4-dimethylpentanedioic acid as an impure oil that was used in the next reaction. ^{1}H NMR (400 MHz, $CDCl_3$) δ 9.81 (bs, 2H), 7.31-7.23 (m, 5H), 4.63 (s, 2H), 4.06 (t, *J* = 6.2 Hz, 1H), 2.91 (m, 2H), 1.22 (d, *J* = 7.2 Hz, 6H). ^{13}C NMR (100 MHz, $CDCl_3$) δ 179.4, 137.4, 128.4, 127.8, 127.8, 82.1, 74.0, 42.1, 12.8. IR (ATR) 2981, 2943, 2887, 1705, 1218, 1069 cm^{-1}. LRMS (ESI/APCI) *m/z* $[C_{14}H_{18}O_5]^-$ (M-H) calcd 265.1, found 265.4.

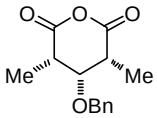

Cis, cis-3-(benzyloxy)-2,4-dimethyl glutaric anhydride (3b). (2R,3r,4S)-3-(benzyloxy)-2,4-dimethylpentanedioic acid **S11** (~9.6 mmol) was dissolved in 20 ml DCM and cooled to °C. Trifluoroacetic anhydride (2.6 ml, 18.6 mmol, 2.0 equiv.) was added slowly and the reaction was stirred for 1 h. The reaction mixture was concentrated *en vacuo* and the resulting light brown paste was tritrated with Et_2O to yield 0.644 g (27% over three steps) of cis, cis-3-(benzyloxy)-2,4-dimethyl glutaric anhydride as a white powder. ^{1}H NMR (400 MHz, $CDCl_3$) δ 7.36-7.25 (m, 5H), 4.68 (s, 2H), 3.81 (t, *J* = 2.4 Hz, 1H), 2.84 (dq, *J* = 6.8, 2.4 Hz, 2H), 1.40 (d, *J* = 6.8 Hz, 6H). ^{13}C NMR (100 MHz, $CDCl_3$) δ 168.6, 136.9, 128.5, 128.2, 127.8, 78.5, 76.0, 43.7, 12.9. IR (NaCl, Thin Film) 2979, 1802, 1773, 1053 cm^{-1}. LRMS (ESI/APCI) *m/z* $[C_{14}H_{16}O_4Na]^+$ (M+Na) calcd 271.1, found 271.1. Slow evaporation of an Et_2O solution yielded clear, X-ray quality needles.[14]

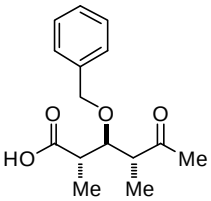

(2S,3S,4R)-3-(benzyloxy)-2,4-dimethyl-5-oxohexanoic acid (4b). Zinc(II) bromide (5.123 g, 22.75 mmol, 3.5 equiv.) was added to a flame dried 300 ml round bottom flask in a glove box. The reaction flask was removed from the glove box and the zinc bromide was dissolved in 115 ml THF under Ar. The reaction was cooled to 0 °C and methyl magnesium bromide (8.75 ml, 22.75 mmol, 2.6M in Et_2O, 3.5 equiv.) was added slowly. A white precipitate formed and the reaction was stirred for 10 min. Stirring was discontinued and the precipitate was allowed to settle for 1 h at 0 °C. $[Rh(nbd)Cl]_2$ (59.9 mg, 0.13 mmol, 2 mol %) and (R)-tBuPhox (100.7 mg, 0.26 mmol, 4 mol %) were added to a separate 250 ml flame dried round bottom flask in glove box. The reaction flask was removed from the glove box, charged with 16 ml THF, and stirred for 10 min resulting in an yellow solution. The freshly prepared THF solution of methyl zinc bromide was added to the rhodium precatalyst via syringe, leaving behind precipitate. The resulting reddish orange solution was stirred for 10 min and cis, cis-3-(benzyloxy)-2,4-dimethyl glutaric anhydride **3b** (1.61 g, 6.5 mmol) was added as a solid (septa removed, anhydride added in one portion, and reaction flushed after addition of anhydride). The reaction was stirred at 23 °C for 16 h and precipitate formed. The reaction was quenched slowly with 1 M HCl and EtOAc was added. The layers were separated and the aqueous layer was extracted with EtOAc 3x. The organic phase was extracted with sat. $NaHCO_3$ 3x and collected into a beaker. With stirring and cooled to 0 °C (excessive heat causes benzyl alcohol elimination), the aqueous solution was acidified using conc. HCl. The acidic solution was extracted with DCM 3x and the organic layer was dried with $MgSO_4$, filtered, and concentrated to yield 1.03 g (60%) of (2S,3S,4R)-3-(benzyloxy)-2,4-dimethyl-5-oxohexanoic acid as a pale yellow oil. $[\alpha]^{20}_D$ = -6.5, c = 0.0110 g/ml CH_2Cl_2. ^{1}H NMR (400 MHz, $CDCl_3$) δ 11.12 (br, 1H),

[14] Oberg, K. M.; Rovis T. (2014) Private communication to the Cambridge Structural Database, deposit number CCDC 991874.

7.24-7.18 (m, 5H), 4.53 (d, *J* = 11.2 Hz, 1H), 4.45 (d, *J* = 11.2 Hz, 1H), 3.96 (dd, *J* = 8.0, 4.0 Hz, 1H), 2.90 (m, 1H), 2.78 (m, 1H), 2.17 (s, 3H), 1.25 (d, *J* = 7.2 Hz, 3H), 1.07 (d, *J* = 7.2 Hz, 3H). ^{13}C NMR (100 MHz, $CDCl_3$) δ 211.2, 179.1, 137.6, 128.4, 127.8, 82.7, 74.2, 49.2, 41.6, 30.3, 12.9, 12.6. R_f = 0.15 (78:20:2 Hex:EtOAc:AcOH; CAM). IR (ATR) 3090, 3032, 2982, 2886, 1738, 1711, 1497, 1087 cm^{-1}. LRMS (ESI/APCI) *m/z* $[C_{15}H_{20}O_4Na]^+$ (M+Na) calcd 287.1, found 287.1.

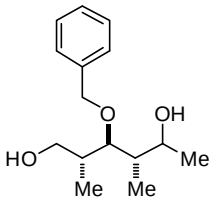

(2R,3R,4S)-3-(benzyloxy)-2,4-dimethylhexane-1,5-diol (S12). Lithium aluminum hydride (167 mg, 4.4 mmol, 2.0 equiv.) was suspended in 20 ml THF and cooled to 0 °C. (2S,3S,4R)-3-(benzyloxy)-2,4-dimethyl-5-oxohexanoic acid **4b** (581.5 mg, 2.2 mmol) was added slowly in 15 ml THF. The reaction was stirred and allowed to warm to 23 °C for 16 h. The reaction was quenched by adding $Na_2SO_4 \cdot 10H_2O$ portion wise until bubbling ceased. The mixture was allowed to stir for 45 minutes and filtered. The supernatant was concentrated to yield 410.8 mg (74%) of (2R,3R,4S)-3-(benzyloxy)-2,4-dimethylhexane-1,5-diol as a clear oil. The crude mixture of diastereomers can be used in the next reaction or purified via flash column chromatography. Less polar diastereomer: ^{1}H NMR (400 MHz, $CDCl_3$) δ 7.37-7.28 (m, 5H), 4.70 (d, J = 14.8 Hz, 1H), 4.67 (d, J = 14.8 Hz, 1H), 4.24 (dq, J = 6.5, 1.6 Hz, 1H), 3.76 (dd, J = 10.8, 4.1 Hz, 1H), 3.68 (dd, J = 10.8, 4.7 Hz, 1H), 3.50 (dd, J = 7.6, 4.2 Hz, 1H), 2.47 (bs, 2H), 2.04 (m, 1H), 1.72 (m, 1H), 1.16 (d, J = 6.5 Hz, 3H), 1.08 (d, J = 7.1 Hz, 3H), 1.01 (d, J = 7.0 Hz, 3H). ^{13}C NMR (100 MHz, $CDCl_3$) δ 137.6, 128.6, 128.1, 127.9, 88.5, 76.2, 66.2, 65.4, 40.0, 37.8, 20.9, 15.2, 11.2. R_f = 0.30 (1:1 Hex:EtOAc; CAM). IR (NaCl, Thin Film) 3386, 2970, 2932, 2879, 1455, 1064 cm^{-1}. HRMS (APCI) *m/z* $[C_{15}H_{23}O_3]^-$ (M-H) calcd 251.1653, found 251.1658. More polar diastereomer: ^{1}H NMR (400 MHz, $CDCl_3$) δ 7.37-7.29 (m, 5H), 4.65 (d, J = 14.8 Hz, 1H), 4.62 (d, J = 14.8 Hz, 1H), 3.88 (dd, J = 7.6, 1.2 Hz, 1H), 3.72 (dd, J = 11.1, 4.2 Hz, 1H), 3.64 (dd, J = 11.1, 5.7 Hz, 1H), 3.44 (m, 1H), 2.02 (m, 1H), 1.90 (m, 1H), 1.18 (d, J = 6.2 Hz, 3H), 1.09 (d, J = 7.1 Hz, 3H), 0.92 (d, J = 7.0 Hz, 3H). ^{13}C NMR (100 MHz, $CDCl_3$) δ 137.5, 128.6, 128.1, 128.0, 88.9, 75.3, 69.8, 65.4, 43.5, 38.2, 20.7, 15.7, 14.4. R_f = 0.20 (1:1 Hex:EtOAc; CAM).

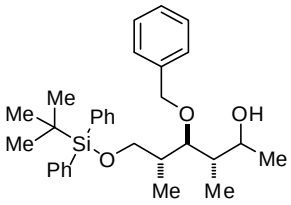

(3S,4R,5R)-4-(benzyloxy)-6-((tert-butyldiphenylsilyl)oxy)-3,5-dimethylhexan-2-ol (S13). Procedure adapted from literature procedure.[15] (3S,4R,5R)-4-(benzyloxy)-6-((tert-butyldiphenylsilyl)oxy)-3,5-dimethylhexan-2-ol **S12** (122.8 mg, 0.49 mmol) dissolved in 6 mL DMF. Imidazole (73.0 mg, 1.07 mmol, 2.2 equiv.) and then tert-butyldiphenylsilyl chloride (0.14 mL, 0.535 mmol, 1.1 equiv.) was added. The reaction was stirred overnight at 23 °C. The reaction was diluted with EtOAc (100 mL) and washed with 10% LiCl 3x. The organic layer was dried with $MgSO_4$, filtered, and concentrated. The resulting residue was loaded onto Celite and purified by flash column chromatography to yield 202.3 mg (85%) of (3S,4R,5R)-4-(benzyloxy)-6-((tert-butyldiphenylsilyl)oxy)-3,5-dimethylhexan-2-ol as a clear oil. Less polar diastereomer: ^{1}H NMR (400 MHz, $CDCl_3$) δ 7.72-7.62 (m, 4H), 7.44-7.31 (m, 6H), 7.24 (m, 3H), 7.09 (m, 2H), 4.54 (d, *J* = 10.7 Hz, 1H), 4.50 (d, *J* = 10.7 Hz, 1H), 4.16 (dd, *J* = 6.4, 1.1 Hz, 1H), 3.81 (dd, *J* = 9.9, 5.2 Hz, 1H), 3.74 (dd, *J* = 9.9, 3.8 Hz, 1H), 1.10 (d, *J* = 6.5 Hz, 3H), 1.08 (s, 9H), 1.07 (m, 3H), 0.97 (d, *J* = 6.9 Hz, 3H). ^{13}C NMR

[15] Hanessian, S.; Lavallee, P. *Can. J. Chem.* **1975**, *53*, 2975-2977.

(100 MHz, $CDCl_3$) δ 138.0, 135.8, 135.7, 135.2, 134.8, 133.7, 133.6, 129.6, 129.6, 129.6, 128.4, 127.7, 127.7, 127.7, 127.6, 86.6, 75.6, 66.2, 65.6, 38.8, 38.6, 27.0, 26.6, 20.6, 19.3, 19.0, 14.7, 11.5. R_f = 0.32 (9:1 Hex:EtOAc). More polar diastereomer: ^{1}H NMR (400 MHz, $CDCl_3$) δ 7.67-7.65 (m, 4H), 7.44-7.21 (m, 11H), 4.58 (d, *J* = 11.0 Hz, 1H), 4.54 (d, *J* = 11.0 Hz, 1H), 3.81 (m, 1H), 3.78 (dd, *J* = 10.1, 5.4 Hz, 1H), 3.67 (dd, *J* = 10.1, 6.6 Hz, 1H), 3.40 (dd, *J* = 6.8 Hz, 4.9 Hz, 1H), 3.24 (bs, 1H), 2.07 (m, 1H), 1.76 (m, 1H), 1.12 (d, *J* = 6.2 Hz, 3H), 1.07 (s, 9H), 1.06 (m, 3H), 0.83 (d, *J* = 7.0 Hz, 3H). ^{13}C NMR (100 MHz, $CDCl_3$) δ 138.0, 135.7, 135.6, 133.8, 133.7, 129.6, 129.5, 128.4, 127.7, 127.7, 127.6, 127.6, 87.0, 74.7, 70.3, 65.4, 42.4, 39.6, 26.9, 20.5, 19.2, 15.2, 14.7. R_f = 0.12 (9:1 Hex:EtOAc). IR (ATR) 3428, 2962, 2930, 2857, 1427, 1390, 1111, 1062, 700 cm^{-1}. HRMS (APCI) *m/z* $[C_{31}H_{42}NaO_3Si]^+$ (M+Na) calcd 513.2795, found 513.2790.

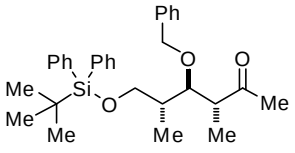

(3R,4R,5R)-4-(benzyloxy)-6-((tert-butyldiphenylsilyl)oxy)-3,5-dimethylhexan-2-one (182). (3S,4R,5R)-4-(benzyloxy)-6-((tert-butyldiphenylsilyl)oxy)-3,5-dimethylhexan-2-ol **S13** (101.7 mg, 0.21 mmol) was dissolved in 8 mL DCM and two scoops of 4 A MS was added. 4-methylmorpholine N-oxide (30.3 mg, 0.26 mmol, 1.25 equiv.) and then tetrapropylammonium perruthenate (7.3 mg, 0.21 mmol, 0.1 equiv.) were added. The reaction was stirred for 12 h at 23 °C. The entire reaction was loaded onto Celite and purified by flash column chromatography to yield 86.0 mg (85%) of (3R,4R,5R)-4-(benzyloxy)-6-((tert-butyldiphenylsilyl)oxy)-3,5-dimethylhexan-2-one as a clear oil [Caution: this compound decomposes at ambient conditions over time through elimination of benzyl alcohol and should be stored frozen in benzene or used soon after making]. $[\alpha]^{20}_D$ = -23.0, c = 0.0078 g/ml $CHCl_3$. ^{1}H NMR (400 MHz, $CDCl_3$) δ 7.72-7.69 (m, 4H), 7.46-7.21 (m, 11H), 4.52 (d, *J* = 11.0 Hz, 1H), 4.48 (d, *J* = 11.0 Hz, 1H), 3.82 (dd, *J* = 10.0, 5.8 Hz, 1H), 3.73 (dd, *J* = 7.8, 4.4 Hz, 1H), 3.70 (dd, *J* = 10.0, 6.2 Hz, 1H), 3.03 (m, 1H), 2.16 (s, 3H), 2.03 (m, 1H), 1.10 (s, 9H), 1.04 (d, *J* = 7.0 Hz, 3H), 1.04 (d, *J* = 7.0 Hz, 3H). ^{13}C NMR (100 MHz, $CDCl_3$) δ 212.3, 138.6, 135.6, 135.6, 134.8, 133.6, 129.6, 128.2, 127.6, 127.6, 127.5, 127.4, 83.8, 74.4, 65.1, 49.2, 38.1, 30.6, 26.9, 19.2, 14.9, 13.4. R_f = 0.32 (9:1 Hex:EtOAc). IR (ATR) 3071, 2961, 2930, 2857, 1714, 1428, 1112, 1067, 740, 701 cm^{-1}. HRMS (APCI) *m/z* $[C_{31}H_{44}NO_3Si]^+$ (M+NH_4) calcd 506.3090, found 506.3085.

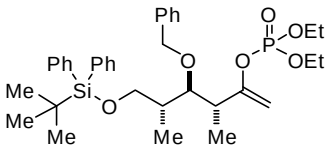

(3R,4R,5R)-4-(benzyloxy)-6-((tert-butyldiphenylsilyl)oxy)-3,5-dimethylhex-1-en-2-yl diethyl phosphate (205). Lithium bis(trimethylsilyl)amide (52.2 mg, 0.312 mmol, 1.05 equiv.) was added to a 25 mL round bottom flask in an inert air glove box. The reaction vessel was sealed and 6 mL of freshly pulled toluene was added. The reaction flask was cooled to -78 °C and (3R,4R,5R)-4-(benzyloxy)-6-((tert-butyldiphenylsilyl)oxy)-3,5-dimethylhexan-2-one **182** (145.0 mg, 0.297 mmol) was added in 6 mL THF. The reaction was stirred for 30 min and diethyl chlorophosphate (0.05 mL, 0.327 mmol, 1.1 equiv) was added. The reaction was stirred for 12 h and allowed to warm to 23 °C. The reaction was quenched with sat. NH_4Cl and extracted with EtOAc 3x. The organic layers were combined, dried with $MgSO_4$, filtered, and dried. The resulting residue was loaded onto Celite and purified via flash column chromatography to yield 119.2 mg of (3R,4R,5R)-4-(benzyloxy)-6-((tert-butyldiphenylsilyl)oxy)-3,5-dimethylhex-1-en-2-yl diethyl phosphate (64%) as an oil. $[\alpha]^{20}_D$ = -1.7, c = 0.0131 g/ml $CHCl_3$. ^{1}H NMR (300 MHz, $CDCl_3$) δ 7.68-7.64 (m, 4H), 7.41-7.23 (m, 11), 4.90 (dd, *J* = 2.1, 1.7 Hz, 1H), 4.63 (d, *J* = 11.0 Hz, 1H), 4.58 (dd, *J* = 2.2, 2.2 Hz, 1H), 4.47 (d, *J* = 11.0 Hz, 1H), 4.13

(m, 4 H), 3.78 (dd, *J* = 9.9, 4.9 Hz, 1H), 3.68 (dd, *J* = 9.9, 6.2 Hz, 1H), 3.49 (t, *J* = 6.0 Hz, 1H), 2.71 (m, 1H), 2.01 (m, 1H), 1.30 (m, 6H), 1.11 (d, *J* = 7.0 Hz, 3H), 1.06 (s, 9H), 1.04 (d, *J* = 7.0 Hz, 3H). ^{13}C NMR (75 MHz, $CDCl_3$) δ 157.2 (d, $^2J_{CP}$ = 9.5 Hz), 138.9, 135.7, 135.6, 133.8, 133.7, 129.5, 129.5, 128.1, 127.6, 127.6, 127.2, 97.1, 97.0, 82.6, 74.4, 65.2, 64.2 (d, $^2J_{CP}$ = 6.0 Hz), 64.2 (d, $^2J_{CP}$ = 5.9 Hz), 41.9 (d, $^3J_{CP}$ = 6.6 Hz), 37.9, 26.9, 19.2, 16.1 (d, $^3J_{CP}$ = 6.8 Hz), 15.4, 15.1. ^{31}P NMR (121 MHz, $CDCl_3$) δ -5.59. R_f = 0.34 (2:1 Hex:EtOAc). IR (ATR) 3070, 2961, 2931, 2857, 1472, 1273, 1062, 1029, 998, 702 cm^{-1}. HRMS (APCI) *m/z* $[C_{35}H_{53}NO_6PSi]^+$ (M+NH_4) calcd 642.3380, found 642.3379.

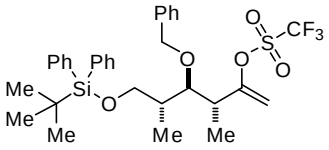

(3R,4R,5R)-4-(benzyloxy)-6-((tert-butyldiphenylsilyl)oxy)-3,5-dimethylhex-1-en-2-yl trifluoromethanesulfonate (238). Potassium bis(trimethylsilyl)amide (10.2 mg, 0.051 mmol, 1.1 equiv) was added to an oven dried 10 ml round bottom flask in an inert air glovebox. The reaction flask was removed and put under Ar. The potassium bis(trimethylsilyl)amide was dissolved in 1.5 mL of PhMe and the flask was cooled to -78 °C. (3R,4R,5R)-4-(benzyloxy)-6-((tert-butyldiphenylsilyl)oxy)-3,5-dimethylhexan-2-one **182** (22.4 mg, 0.046 mmol) was dissolved in 1 mL THF and added to the cooled reaction flask. After stirring for 30 min, N-phenyl-bis(trifluoromethanesulfonimide) (21.4 mg, 0.060 mmol, 1.3 equiv) dissolved in 1 mL of THF was added. After stirring for 30 min at -78 °C, the reaction was warmed to 0 °C and quenched with brine. The aqueous layers were extracted with Et_2O 2x. The organic layer was dried with $MgSO_4$, filtered, and concentrated. The resulting residue was purified via column chromatography that resulted in 12.3 mg of slightly impure (3R,4R,5R)-4-(benzyloxy)-6-((tert-butyldiphenylsilyl)oxy)-3,5-dimethylhex-1-en-2-yl trifluoromethanesulfonate (43%) as a clear oil. $[\alpha]^{20}_D$ = -8.6, c = 0.0120 g/ml $CHCl_3$. ^{1}H NMR (400 MHz, $CDCl_3$) δ 7.66-7.63 (m, 4H), 7.42-7.39 (m, 2H), 7.35-7.32 (m, 4H), 7.29-7.26 (m, 3H), 7.20-7.18 (m, 2H), 5.14 (d, *J* = 3.8 Hz, 1H), 5.03 (d, *J* = 3.8 Hz, 1H), 4.57 (d, *J* = 11.1 Hz, 1H), 4.53 (d, *J* = 11.1 Hz, 1H), 3.74 (d, *J* = 5.1 Hz, 2H), 3.51 (t, *J* = 5.7 Hz, 1H), 2.86 (m, 1H), 1.99 (m, 1H), 1.20 (d, *J* = 7.0 Hz, 3H), 1.07 (s, 9H), 1.02 (d, *J* = 7.0 Hz, 3H). ^{13}C NMR (100 MHz, $CDCl_3$) δ 158.5, 138.4, 135.7, 135.5, 133.6, 133.6, 132.1, 131.0, 130.0, 129.6, 129.6, 128.2, 127.6, 127.6, 127.5, 127.4, 120.0, 116.8, 104.7, 82.4, 74.7, 65.2, 41.5, 38.1, 26.9, 19.2, 15.5, 15.1. R_f = 0.40 (20:1 Hex:EtOAc). IR (ATR) 2961, 2932, 2859, 1418, 1212, 1112, 933, 701 cm^{-1}. HRMS (APCI) *m/z* $[C_{32}H_{43}F_3NO_5SSi]^+$ (M+NH_4) calcd 638.2578, found 638.2574.

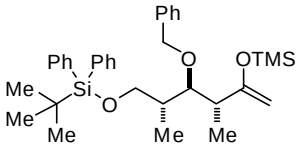

(5R,6R,7R)-6-(benzyloxy)-2,2,5,7,11,11-hexamethyl-4-methylene-10,10-diphenyl-3,9-dioxa-2,10-disiladodecane (183). (3R,4R,5R)-4-(benzyloxy)-6-((tert-butyldiphenylsilyl)oxy)-3,5-dimethylhexan-2-one **182** (145.0 mg, 0.297 mmol) was dissolved in 10 mL DCM. After cooling the solution to 0 °C, triethyl amine (0.41 mL, 2.97 mmol, 10 equiv.) and trimethylsilyl trifluoromethanesulfonate (0.11 mL, 0.594 mmol, 2 equiv.) were added sequentially. The reaction was stirred for 1 h and then transferred to a separatory funnel. The reaction was diluted with 40 mL DCM and then washed with 0.5 M NH_4OH 3x. The organic layer was dried with $MgSO_4$ and concentrated to yield 148.0 mg (89%) of mostly pure (5R,6R,7R)-6-(benzyloxy)-2,2,5,7,11,11-hexamethyl-4-methylene-10,10-diphenyl-3,9-dioxa-2,10-disiladodecane as a clear oil. $[\alpha]^{20}_D$ = -3.0, c = 0.0103 g/ml C_6H_6. ^{1}H NMR (400 MHz, C_6D_6) δ 7.83-7.75 (m, 5H), 7.34 (m, 1H), 7.21-7.18 (m, 8H), 7.09 (m, 1H), 4.74 (d, *J* = 11.3 Hz, 1H), 4.50 (d, *J* = 11.3 Hz, 1H), 4.22 (d, *J* = 1.0 Hz, 1H), 4.10 (d, *J* = 1.1 Hz, 1H), 4.00 (dd, *J* = 9.9, 5.0 Hz, 1H), 3.89 (dd, *J* = 9.8, 6.6 Hz, 1H), 3.62 (dd, *J* = 6.7, 5.2 Hz, 1H), 2.71 (m, 1H), 2.14 (m, 1H), 1.20 (s, 9H), 1.15 (d, *J* = 6.9 Hz,

3H), 1.10 (d, *J* = 7.0 Hz, 3H), 0.18 (s, 9H). ^{13}C NMR (100 MHz, C_6D_6) δ 161.5, 140.0, 136.1, 136.0, 135.4, 134.3, 129.9, 129.8, 129.7, 127.3, 89.9, 83.3, 74.4, 65.9, 43.4, 38.3, 27.2, 27.1, 27.0,19.5, 15.8, 15.4, 22.15, 0.14, 0.13. IR (ATR) 3070, 2959, 2857,1622, 1428, 1110, 1037, 842 cm^{-1}.

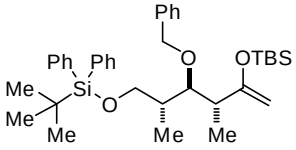

(6R,7R,8R)-7-(benzyloxy)-2,2,3,3,6,8,12,12-octamethyl-5-methylene-11,11-diphenyl-4,10-dioxa-3,11-disilatridecane (S14). (3R,4R,5R)-4-(benzyloxy)-6-((tert-butyldiphenylsilyl)oxy)-3,5-dimethylhexan-2-one **182** (50.0 mg, 0.10 mmol) was dissolved in 5 ml DCM. After cooling the solution to 0 °C, triethyl amine (0.14 ml, 1.0 mmol, 10 equiv.) and tert-butyldimethylsilyl trifluoromethanesulfonate (0.05 mL, 0.20 mmol, 2 equiv.) were added sequentially. The reaction was stirred for 1 h and then transferred to a separatory funnel. The reaction was diluted with 20 ml DCM and then washed with 0.5 M NH_4OH 3x. The organic layer was dried with $MgSO_4$ and concentrated to yield mostly pure (6R,7R,8R)-7-(benzyloxy)-2,2,3,3,6,8,12,12-octamethyl-5-methylene-11,11-diphenyl-4,10-dioxa-3,11-disilatridecane as a clear oil. ^{1}H NMR (300 MHz, $CDCl_3$) δ 7.73-7.63 (m, 6H), 7.42-7.23 (m, 9H), 4.64 (d, J = 11.0 Hz, 1H), 4.41 (d, J = 11.0 Hz, 1H), 4.07 (d, J = 1.0 Hz, 1H), 3.99 (d, J = 1.0 Hz, 1H), 3.79 (dd, J = 9.8, 5.2 Hz, 1H), 3.62 (dd, J = 9.9, 7.1 Hz, 1H), 3.50 (m, 1H), 2.51 (m, 1H), 1.98 (m, 1H), 1.07-1.04 (m, 3H), 1.04 (s, 9H), 0.94 (s, 9H), 0.94-0.91 (m, 3H), 0.19 (s, 3H), 0.18(s, 3H).

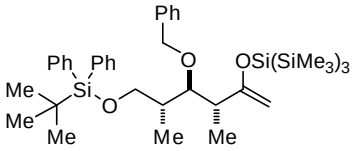

(6R,7R,8R)-7-(benzyloxy)-2,2,6,8,12,12-hexamethyl-5-methylene-11,11-diphenyl-3,3-bis(trimethylsilyl)-4,10-dioxa-2,3,11-trisilatridecane (S15). Tris(trimethylsilyl)silyl trifluoromethanesulfonate was prepared according to a literature procedure.[16] Trifluoromethanesulfonic acid (30.0 mg, 0.20 mmol, 2.0 equiv.) was dissolved in 1 ml DCM in a 10 ml round bottom flask. The reaction flask was put under Ar and tri(trimethylsilyl)silane (49.7 mg, 0.20 mmol, 2.0 equiv.) was added in 1 ml DCM. The reaction was stirred for 30 min and cooled to 0 °C. (3R,4R,5R)-4-(benzyloxy)-6-((tert-butyldiphenylsilyl)oxy)-3,5-dimethylhexan-2-one **182** (48.8 mg, 0.10 mmol) and triethyl amine (0.14 ml, 1.0 mmol, 10 equiv.) were dissolved in 1 ml DCM and added to the reaction. The reaction was stirred for 2 h and then transferred to a separatory funnel. The reaction was diluted with 20 ml DCM and then washed with 0.5 M NH_4OH 3x. The organic layer was dried with $MgSO_4$ and concentrated to yield 77.9 mg (53%) of mostly pure (6R,7R,8R)-7-(benzyloxy)-2,2,6,8,12,12-hexamethyl-5-methylene-11,11-diphenyl-3,3-bis(trimethylsilyl)-4,10-dioxa-2,3,11-trisilatridecane as a clear oil. ^{1}H NMR (300 MHz, $CDCl_3$) δ 7.74-7.63 (m, 6H), 7.42-7.22 (m, 9H), 4.62 (d, J = 11.1 Hz, 1H), 4.65 (d, J = 11.2 Hz, 1H), 4.07 (d, J = 1.4 Hz, 1H), 3.95 (d, J = 1.4 Hz, 1H), 3.80 (dd, J = 9.8, 4.9 Hz, 1H), 3.58 (dd, J = 9.7, 7.4 Hz, 1H), 3.44 (dd, J = 7.6, 4.2 Hz, 1H), 2.50 (m, 1H), 1.98 (m, 1H), 1.07-1.04 (m, 3H), 1.04 (s, 9H), 0.94 (d, J = 6.9 Hz, 3H), 0.20-0.18 (m, 27H).

[16] Boxer, M. B.; Yamamoto, H. *J. Am. Chem. Soc.* **2006**, *128*, 48-49.

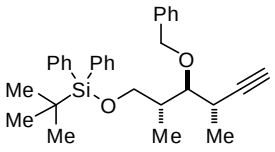

(((2R,3S,4S)-3-(benzyloxy)-2,4-dimethylhex-5-yn-1-yl)oxy)(tert-butyl)diphenylsilane (239). (3R,4R,5R)-4-(benzyloxy)-6-((tert-butyldiphenylsilyl)oxy)-3,5-dimethylhex-1-en-2-yl diethyl phosphate **205** (119.2 mg, 0.19 mmol) was dissolved in THF and cooled to -78 °C. tert-butyl lithium (0.4 ml, 0.57 mmol, 1.4M in pentanes, 3 equiv.) was added and the reaction was stirred for 30 min. The reaction was quenched at -78 °C with sat. NH_4Cl and allowed to warm to 23 °C. The reaction was extracted with EtOAc 3x, dried with $MgSO_4$, filtered, and concentrated. The resulting residue was loaded onto Celite and purified via flash column chromatography to yield 63.4 mg (71%) of (((2R,3S,4S)-3-(benzyloxy)-2,4-dimethylhex-5-yn-1-yl)oxy)(tert-butyl)diphenylsilane as a clear oil. $[\alpha]^{20}_D$ = +5.1, c = 0.0100 g/ml $CHCl_3$. ^{1}H NMR (400 MHz, $CDCl_3$) δ 7.69-7.64 (m, 5H), 7.43-7.21 (m, 10H), 4.64 (d, *J* = 11.2 Hz, 1H), 4.56 (d, *J* = 11.2 Hz, 1H), 3.82 (dd, *J* = 9.9, 5.1 Hz, 1H), 3.72 (dd, *J* = 9.9, 4.0 Hz, 1H), 3.38 (dd, *J* = 7.9, 3.9 Hz, 1H), 2.82 (m, 1H), 2.09 (m, 1H), 2.06 (d, *J* = 2.5 Hz, 1H), 1.26 (d, *J* = 7.1 Hz, 3H), 1.08 (s, 9H), 1.06 (d, *J* = 6.9 Hz, 3H). ^{13}C NMR (100 MHz, $CDCl_3$) δ 138.6, 135.7, 135.7, 133.7, 133.6, 129.6, 129.5, 128.2, 127.7, 127.6, 127.6, 127.4, 86.2, 82.9, 74.3, 69.8, 65.4, 38.9, 29.0, 27.0, 26.8, 19.3, 18.1, 14.6. R_f = 0.25 (20:1 Hex:EtOAc). IR (ATR) 3307, 2960, 2931, 2857, 1472, 1428, 1111, 1068, 823, 739, 701 cm^{-1}. HRMS (APCI) *m/z* $[C_{31}H_{39}O_2Si]^+$ (M+H) calcd 471.2641, found 471.2714.

C23-C32 Fragment

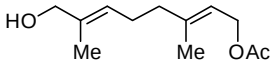

(2E,6E)-8-hydroxy-3,7-dimethylocta-2,6-dien-1-yl acetate (138). Procedure adapted from literature procedures.[17] Selenium dioxide (0.742 g, 6.68 mmol, 14 mol %) was suspended in 75 ml DCM in a 500 ml round bottom flask. tert-Butyl hydroperoxide (25 ml, 186.8 mmol, 2 equiv.; Luperox® 70 wt. % in H_2O) was added and the reaction was stirred for 30 min generating a clear, biphasic solution. Geranial acetate (20 ml, 93.3 mmol; Alfa Aesar) was added via syringe. A reflux condenser was attached and the reaction was stirred for 48 h without heating. The reaction was diluted with 100 ml MeOH and cooled to 0 °C. Sodium borohydride was added slowly until aldehyde not observed by TLC (R_f = 0.52 (2:1 Hex:EtOAc; $KMnO_4$). Solution turned from clear to red to yellow to clear during this process. The reaction was diluted with another 100 ml DCM and 100 ml H_2O and transferred to a separatory funnel rinsing with DCM and H_2O. The layers were separated and the aqueous layer was extracted with DCM 2x. The organic layer was washed with sat. NaCl, dried with $MgSO_4$, filtered, and concentrated. The crude reaction was purified via flash column chromatography to yield 12.78 g (59%) of (2E,6E)-8-hydroxy-3,7-dimethylocta-2,6-dien-1-yl acetate as a pale yellow oil. Spectral data matches literature.[18] ^{1}H NMR (300 MHz, $CDCl_3$) δ 5.39-5.32 (m, 2H), 4.58 (d, J = 7.1 Hz, 2H), 3.99 (s, 2H), 2.21-2.14 (m, 2H), 2.11-2.03 (m, 2H), 2.05 (s, 3H), 1.70 (s, 3H), 1.66 (s, 3H) 1.46 (s, 1H). R_f = 0.32 (2:1 Hex:EtOAc; $KMnO_4$).

[17] (a) Umbreit, M. A.; Sharpless, K. B. *J. Am. Chem. Soc.* **1977**, *99*, 5526-5528. (b) Cole, K. P.; Hsung, R. P. *Org. Lett.* **2003**, *5*, 4843-4846.
[18] Paz, J. L.; Rodrigues, J. A. R. *J. Braz. Chem. Soc.* **2003**, *14*, 975-981.

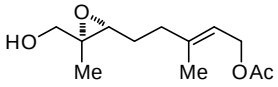

(E)-5-((2R,3R)-3-(hydroxymethyl)-3-methyloxiran-2-yl)-3-methylpent-2-en-1-yl acetate (S16). Procedure adapted from literature procedure.[19] In a flame dried 500 ml round bottom flask, two scoops of 4 Å molecular sieves was suspended in 200 ml DCM under Ar. Titanium(IV) isopropoxide (18.6 ml, 63.2 mmol, 1.05 equiv.) was added and the reaction was cooled to -35 °C. (-)-Diethyl D-tartrate (11.3 ml, 66.2 mmol, 1.1 equiv.; Chem-Impex International or AK Scientific) and anhydrous tert-butyl hydrogen peroxide[20] (40 ml, 120.4 mmol, ~3.0M in DCM, 2.0 equiv.) was added and the reaction was allowed to stir for 45 min. (2E,6E)-8-hydroxy-3,7-dimethylocta-2,6-dien-1-yl acetate **138** (12.78 g, 60.2 mmol) in 18 ml DCM was added slowly. The reaction was stirred at -30 °C for 6 h. At -20 °C, NaOH (48 ml, 240.8 mmol, aq. 5 M, 4 equiv.) was added and the reaction was stirred for 1h. The reaction was transferred to a seperatory funnel and the lower layer was transferred to an 800 ml beaker. $MgSO_4$ was added until the solution stopped bubbling. The solution was filtered through Celite and concentrated to form a milky oil. The crude reaction was purified via flash column chromatography to yield 10.09 g (73%) of (E)-5-((2R,3R)-3-(hydroxymethyl)-3-methyloxiran-2-yl)-3-methylpent-2-en-1-yl acetate as a clear oil (product contaminated with diethyl tartrate can be used in the next reaction without a negative impact on yield). Spectral data matches literature.[21] $[\alpha]^{20}_D$ = +5.4, c = 0.2300 g/ml CH_2Cl_2. ^{1}H NMR (400 MHz, $CDCl_3$) δ 5.38 (dd, J = 7.2, 1.2 Hz, 1H), 4.58 (d, J = 7.2 Hz, 2H), 3.65 (dd, J = 8.0, 4.0 Hz, 1H), 3.56 (dd, J = 12.0, 8.4 Hz, 1H), 3.00 (t, J = 6.4 Hz, 1H), 2.27-2.12 (m, 2H), 2.04 (s, 3H), 1.82 (dd, J = 8.4, 4.8 Hz, 1H), 1.74-1.67 (m, 2H), 1.72 (s, 3H), 1.27 (s, 3H). ^{13}C NMR (100 MHz, $CDCl_3$) δ 171.1, 140.9,119.1, 65.3, 61.2, 60.9, 59.6, 36.1, 26.3, 21.0, 16.4, 14.2. R_f = 0.25 (1:1 Hex:EtOAc; $KMnO_4$). IR (NaCl, Thin Film) 3353, 2932, 1739, 1670, 1446, 1383, 1234,1028, 955 cm^{-1}. LRMS (ESI/APCI) *m/z* $[C_{12}H_{20}O_4Na]^+$ (M+Na) calcd 251.1, found 251.2.

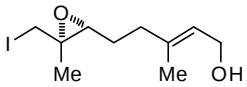

(E)-5-((2R,3S)-3-(iodomethyl)-3-methyloxiran-2-yl)-3-methylpent-2-en-1-ol (139). In a 500 ml flask, (E)-5-((2R,3R)-3-(hydroxymethyl)-3-methyloxiran-2-yl)-3-methylpent-2-en-1-yl acetate **S16** (5.33 g, 23.3 mmol) (if contaminated with DET, an extra equivalent of PPh_3, im, and I_2 was added for every mmol of DET) was dissolved in 120 ml DCM and the flask was put under Ar. After cooling to 0 °C, imidazole (1.67 g, 24.5 mmol, 1.05 equiv.) and triphenyl phosphine (6.43 g, 24.5 mmol, 1.05 equiv.) were added. After dissolution, iodine (6.22 g, 24.5 mmol, 1.05 equiv.) was added in three portions. After stirring for 2 h, 150 ml methanol and potassium carbonate (32.0 g, 233 mmol, 10.0 equiv.) was added sequentially. The reaction flask was covered with aluminum foil and stirred for 12 h. The reaction was quenched with sat. $Na_2S_2O_3$ and extracted with Et_2O 3x. The organic layer was washed with sat. $Na_2S_2O_3$ and brine, dried with $MgSO_4$, and concentrated. The crude reaction was loaded onto Celite and purified via flash column chromatography to yield 5.43 g (78%) of (E)-5-((2R,3S)-3-(iodomethyl)-3-methyloxiran-2-yl)-3-

[19]For procedure, see: Gao, Y.; Hanson, R. M.; Klunder, J. M.; Ko, S. Y.; Masamune, H.; Sharpless, K. B. *J. Am. Chem. Soc.* **1987**, *109*, 5765-5780. In our hands, this particular workup is excellent for small scale work (>400 mg), but becomes cumbersome on larger scale.

[20] 3M anhydrous tert-butyl hydrogen peroxide was obtained by swirling 85 mL of commercial TBHP (70 wt. % in H_2O) with 140 mL DCM in a separatory funnel. The phases were separated and the lower organic layer was stored over 4 Å MS. See: (a) Sharpless, K. B.; Verhoeven, T. R. *Aldrichimica Acta* **1979**, *12*, 4, 63-74. (b) Armarego, W. L. F.; Chai, C. L. L. *Purification of Laboratory Chemicals*, 5th ed. Elsevier Science: Burlington, MA., 2003; pg 148-149.

[21] Li, X.; Borhan, B. *J. Am. Chem. Soc.* **2008**, *130*, 16126-16127.

methylpent-2-en-1-ol as a pale yellow oil. Spectral data matches literature.[22] $[\alpha]^{20}_D$ = -6.3, c = 0.1800 g/ml CH_2Cl_2. ^{1}H NMR (400 MHz, $CDCl_3$) δ 5.46 (m, 1H), 4.15 (d, *J* = 6.8 Hz, 2H), 3.22 (d, *J* = 10.0 Hz, 1H), 3.07 (d, *J* = 9.6 Hz, 1H), 2.86 (t, *J* = 6.4 Hz, 1H), 2.24-2.11 (m, 2H), 1.70-1.65 (m, 2H), 1.68 (s, 3H), 1.44 (s, 3H). ^{13}C NMR (100 MHz, $CDCl_3$) δ 138.0, 124.3, 66.0, 60.1, 59.2, 36.0, 27.2, 16.2,16.0,13.8. R_f = 0.33 (1:1 Hex:EtOAc; $KMnO_4$). IR (NaCl, Thin Film) 3417, 2966, 2927, 1669, 1452, 1385,1175, 1002, 867 cm^{-1}. LRMS (ESI/APCI) *m/z* $[C_{10}H_{17}IO_2Na]^+$ (M+Na) calcd 319.0, found 319.1.

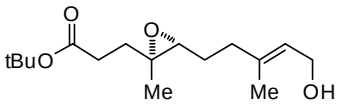

tert-butyl 3-((2R,3R)-3-((E)-5-hydroxy-3-methylpent-3-en-1-yl)-2-methyloxiran-2-yl)propanoate (S17). Procedure adapted from the literature.[23] In a flame dried 500 ml round bottom flask, diisopropylamine (10.4 ml, 73.8 mmol, 3.1 equiv.) was dissolved in 150 ml THF under Ar. The solution was cooled to -78 °C and n-butyllitium (49.2 ml, 71.4 mmol, 1.45 M in hexanes, 3.0 equiv.) was added. The reaction was stirred for 10 min and neat tert-butyl acetate (9.9 ml, 73.8 mmol, 3.1 equiv.; Chem-Impex International) was added via syringe. The reaction was stirred for 1h and (E)-5-((2R,3S)-3-(iodomethyl)-3-methyloxiran-2-yl)-3-methylpent-2-en-1-ol **139** (7.06 g, 23.8 mmol) in 15 ml THF was added. The reaction was stirred for 5 min and freshly distilled hexamethylphosphoramide (24.9 ml, 143 mmol, 6.0 equiv.) was added. After stirring for 2 h at -78 °C, the reaction was quenched with 35 ml sat. NH_4Cl. The cold bath was removed and the reaction was allowed to warm ~0°C. The reaction was transferred to a seperatory funnel and diluted with Et_2O and D.I. H_2O. The layers were separated and the aqueous was extracted with Et_2O 2x. The organic layers were washed with sat. NaCl, dried with $MgSO_4$, filtered, and concentrated. The crude reaction was purified via flash column chromatography to yield 5.28 g (78%) of tert-butyl 3-((2R,3R)-3-((E)-5-hydroxy-3-methylpent-3-en-1-yl)-2-methyloxiran-2-yl)propanoate as a clear oil. $[\alpha]^{20}_D$ = +7.44, c = 0.0166 g/ml CH_2Cl_2. ^{1}H NMR (400 MHz, $CDCl_3$) δ 5.44 (m, 1H), 4.14 (d, *J* = 6.8 Hz, 2H), 2.71 (t, *J* = 6.8 Hz, 1H), 2.28 (t, *J* = 7.2 Hz, 2H), 2.22-2.07 (m, 2H), 1.89-1.73 (m, 2H), 1.69-1.62 (m, 2H), 1.67 (s, 3H), 1.59 (s, 1H), 1.42 (s, 9H), 1.23 (s, 3H). ^{13}C NMR (100 MHz, $CDCl_3$) δ 172.4, 138.3, 124.1, 80.4, 62.8, 60.0, 59.2, 36.2, 33.1, 31.0, 28.0, 26.8, 16.7, 16.2. R_f = 0.23 (2:1 Hex:EtOAc; $KMnO_4$). IR (NaCl, Thin Film) 3435, 2976, 2931, 1730, 1456, 1368, 1255, 1152, 1009, 847 cm^{-1}. HRMS (DART) *m/z* $[C_{16}H_{32}NO_4]^+$ (M+NH_4) calcd 302.2326, found 302.2328.

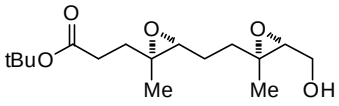

tert-butyl 3-((2R,3R)-3-(2-((2R,3R)-3-(hydroxymethyl)-2-methyloxiran-2-yl)ethyl)-2-methyloxiran-2-yl)propanoate (140). In a flame dried 300 ml round bottom flask, two scoops of 4 Å molecular sieves was suspended in 75 ml DCM under Ar. Titanium(IV) isopropoxide (2.07 ml, 7.01 mmol, 1.05 equiv.) was added and the reaction was cooled to -35 °C. (-)-Diethyl D-tartrate (1.26 ml, 7.35 mmol, 1.1 equiv.; Chem-Impex International or AK Scientific) and anhydrous tert-butyl hydrogen peroxide (4.5 ml, 13.36 mmol, ~3.0M in DCM, 2.0 equiv.) was added and the reaction was allowed to stir for 45 min. tert-butyl 3-((2R,3R)-3-((E)-5-hydroxy-3-methylpent-3-en-1-yl)-2-methyloxiran-2-yl)propanoate **S17** (1.90 g, 6.68 mmol) in 9 ml DCM was added slowly. The reaction was stirred at -30 °C for 6 h. At -20 °C, NaOH (5.3 ml, 26.72 mmol, aq. 5 M, 4 equiv.) was added and the reaction was stirred for 1h. The reaction was

[22] Marshall, J. A.; Chobanian, H. R. *Org. Lett.* **2003**, *5*, 1931-1933.
[23] Tanuwidjaja, J.; Ng, S.-S.; Jamison, T. F. *J. Am. Chem. Soc.* **2009**, *131*, 12084-12085.

transferred to an 800 ml beaker. $MgSO_4$ was added until the solution stopped bubbling. The solution was filtered through Celite and concentrated to form a milky oil. The crude reaction was purified via flash column chromatography to yield 1.298 g (65%) of tert-butyl 3-((2R,3R)-3-(2-((2R,3R)-3-(hydroxymethyl)-2-methyloxiran-2-yl)ethyl)-2-methyloxiran-2-yl)propanoate as a clear oil. $[\alpha]^{20}_D$ = +11.7, c = 0.0093 g/ml CH_2Cl_2. ^{1}H NMR (400 MHz, $CDCl_3$) δ 3.83-3.71 (m, 2H), 2.99 (t, *J* = 5.6 Hz, 1H), 2.76 (m, 1H), 2.28 (dt, *J* = 7.6, 1.6 Hz, 2H), 1.90-1.76 (m, 4H), 1.66-1.58 (m, 3H), 1.44 (s, 9H), 1.33 (s, 3H), 1.25 (s, 3H). ^{13}C NMR (100 MHz, $CDCl_3$) δ 172.4, 80.5, 62.4, 62.3, 61.3, 60.5, 60.2, 35.0, 33.2, 31.0, 28.1, 24.2, 16.9, 16.7. R_f = 0.18 (1:1 Hex:EtOAc; $KMnO_4$). IR (NaCl, Thin Film) 3444, 2975, 2933, 1730, 1458, 1255, 1036, 848 cm^{-1}. HRMS (DART) *m/z* $[C_{12}H_{21}O_5]^+$ (M-C_4H_9(tBu$^+$)) calcd 245.1384, found 245.1375.

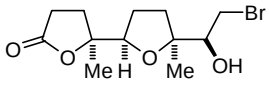

(2S,2'R,5'S)-5'-((S)-2-bromo-1-hydroxyethyl)-2,5'-dimethylhexahydro-[2,2'-bifuran]-5(2H)-one (S18). In an 100 ml round bottom flask, tert-butyl 3-((2R,3R)-3-(2-((2R,3R)-3-(hydroxymethyl)-2-methyloxiran-2-yl)ethyl)-2-methyloxiran-2-yl)propanoate **140** (1.368 g, 4.55 mmol) was dissolved in 20 ml DCM. Triphenyl phosphine (1.254 g, 4.78 mmol, 1.05 equiv.) and tetrabromomethane (1.585 g, 4.78 mmol, 1.05 equiv.) was added and the reaction was heated to reflux for 4h. The reaction mixture was cooled to 23 °C and dry p-toluenesulfonic acid[24] (0.783 g, 4.55 mmol, 1.0 equiv.) was added. The reaction was stirred for 2 h and then quenched with sat. $NaHCO_3$. The reaction was extracted with DCM 3x and the organic layer was dried with $MgSO_4$, filtered, and concentrated. The crude was loaded onto Celite and purified via flash column chromatography to yield 1.11 g (71%) of (2S,2'R,5'S)-5'-((S)-2-bromo-1-hydroxyethyl)-2,5'-dimethylhexahydro-[2,2'-bifuran]-5(2H)-one as a clear oil. $[\alpha]^{20}_D$ = +6.9, c = 0.0076 g/ml $CHCl_3$. ^{1}H NMR (400 MHz, $CDCl_3$) δ 4.04 (m, 1H), 3.74 (m, 1H), 3.67 (dd, *J* = 10.0, 2.0 Hz, 1H), 3.35 (t, *J* = 10.0 Hz, 1H), 2.60 (m, 2H), 2.50 (d, *J* = 3.0 Hz, 1H), 2.28-2.20 (m, 1H), 2.18-2.11 (m, 1H), 2.04-1.96 (m, 1H), 1.93-1.85 (m, 1H), 1.76-1.68 (m, 2H), 1.38 (s, 3H), 1.18 (s, 3H). ^{13}C NMR (100 MHz, $CDCl_3$) δ 176.5, 86.9, 85.3, 82.7, 77.2, 36.5, 34.6, 29.2, 29.1, 26.8, 23.4, 21.0. R_f = 0.27 (1:1 Hex:EtOAc; CAM). IR (NaCl, Thin Film) 3459, 2975, 2878, 1768, 1454, 1381, 1081, 944 cm^{-1}. HRMS (APCI) *m/z* $[C_{12}H_{20}O_4Br]^+$ (M+H) calcd 307.0539, found 307.0542, 309.0521.

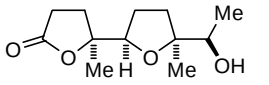

(2S,2'R,5'S)-5'-((R)-1-hydroxyethyl)-2,5'-dimethylhexahydro-[2,2'-bifuran]-5(2H)-one (141). (2S,2'R,5'S)-5'-((S)-2-bromo-1-hydroxyethyl)-2,5'-dimethylhexahydro-[2,2'-bifuran]-5(2H)-one **S18** (1.79g, 5.82 mmol) was dissolved in 20 ml EtOAc. Pd/C (200 mg, 10% by wt.) and 11 ml triethyl amine were added to the reaction. The reaction flask was evacuated and backfilled with Ar 2x. The reaction was then evacuated and refilled with hydrogen 2x using a balloon. The reaction was stirred for 18 h and recharged with hydrogen. After stirring for another 18 h, the reaction was filtered through Celite. The crude reaction was purified via flash column chromatography to yield 0.962 g (72%) of (2S,2'R,5'S)-5'-((R)-1-hydroxyethyl)-2,5'-dimethylhexahydro-[2,2'-bifuran]-5(2H)-one as a clear oil that solidified upon standing. Spectral data

[24] Dry acid was obtained by the azeotropic removal of water from a benzene solution of p-toluenesulfonic acid monohydrate using a Dean-Stark apparatus. The dried acid was recrystallized from benzene. Use of the monohydrate was less reproducible and resulted in a messy reaction.

matches literature.[25] $[\alpha]^{20}_D$ = +1.3, c = 0.0053 g/ml CH_2Cl_2. ^{1}H NMR (300 MHz, $CDCl_3$) δ 4.02 (dd, *J* = 8.4, 6.8 Hz, 1H), 3.75 (dq, *J* = 6.5, 2.6 Hz, 1H), 2.60 (m, 2H), 2.27-2.04 (m, 3H), 2.02-1.86 (m, 2H), 1.75-1.60 (m, 1H), 1.57-1.50 (m, 1H), 1.40 (s, 3H), 1.14 (s, 3H), 1.13 (d, *J* = 6.3 Hz, 3H). R_f = 0.14 (1:1 Hex:EtOAc; CAM). IR (NaCl, Thin Film) 3468, 2976, 2872, 1770, 1453, 1244, 1083, 943 cm^{-1}. HRMS (APCI) *m/z* $[C_{12}H_{21}O_4]^+$ (M+H) calcd 229.1428, found 229.1428.

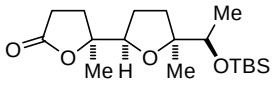

(2S,2'R,5'S)-5'-((R)-1-((tert-butyldimethylsilyl)oxy)ethyl)-2,5'-dimethylhexahydro-[2,2'-bifuran]-5(2H)-one (184). (2S,2'R,5'S)-5'-((R)-1-hydroxyethyl)-2,5'-dimethylhexahydro-[2,2'-bifuran]-5(2H)-one **141** (0.962 g, 4.20 mmol) was dissolved in 30 ml DCM, put under Ar, and cooled to -78 °C.[26] Triethyl amine (2.0 ml, 14.7 mmol, 3.5 equiv.) was added and then tert-butyldimethylsilyl trifluoromethanesulfonate (1.93 ml, 8.4 mmol, 2.0 equiv.; Oakwood Chemical) was added slowly. The reaction was stirred at -78 °C for 4 h. The reaction was quenched with sat. $NaHCO_3$ and warmed to 23 °C. The reaction was extracted with DCM 3x and the organic layer was dried with MgSO4, filtered, and concentrated. The crude reaction was purified via flash column chromatography to yield 1.325 g (92%) of (2S,2'R,5'S)-5'-((R)-1-((tert-butyldimethylsilyl)oxy)ethyl)-2,5'-dimethylhexahydro-[2,2'-bifuran]-5(2H)-one as a clear oil that solidified upon standing. Spectral data matches literature.[24] $[\alpha]^{20}_D$ = -9.5, c = 0.0107 g/ml $CHCl_3$. ^{1}H NMR (300 MHz, $CDCl_3$) δ 4.04-3.98 (m, 1 H) 3.58 (q, *J* = 6.3 Hz, 1H), 2.70-2.48 (m, 2H), 2.25 (ddd, *J* = 12.8, 10.3, 5.9, 1H), 1.98-1.80 (m, 3H), 1.72-1.54 (m, 2H), 1.35 (s, 3H), 1.11 (d, *J* = 6.2 Hz, 3H), 1.10 (s, 3H), 0.87 (s, 9H), 0.06 (s, 3H), 0.04 (s, 3H). R_f = 0.24 (4:1 Hex:EtOAc; CAM).

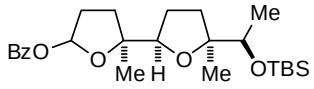

(2S,2'R,5'S)-5'-((R)-1-((tert-butyldimethylsilyl)oxy)ethyl)-2,5'-dimethyloctahydro-[2,2'-bifuran]-5-yl benzoate (185). (2S,2'R,5'S)-5'-((R)-1-((tert-butyldimethylsilyl)oxy)ethyl)-2,5'-dimethylhexahydro-[2,2'-bifuran]-5(2H)-one **184** (97.8 mg, 0.286 mmol) was dissolved in 6 mL DCM and cooled to -78 °C. DIBAL (0.31 mL, 1M Hexanes, 1.1 equiv.) was added and the reaction was stirred for 1.5 h. 10 mL of sat. Rochelle's salt was added and the cold bath was removed. The reaction was stirred for 4 h. The reaction was extracted with DCM 3x, the resulting organic layer was washed with sat. brine 2x, dried with $MgSO_4$, and concentrated to yield 92.8 mg (94%) of (2S,2'R,5'S)-5'-((R)-1-((tert-butyldimethylsilyl)oxy)ethyl)-2,5'-dimethyloctahydro-[2,2'-bifuran]-5-ol (**S19**) as clear oil. ^{1}H NMR (300 MHz, $CDCl_3$) δ 5.36 (diastereomer a, dd, J = 4.4, 0.8 Hz, 0.37H), 5.33 (diastereomer b, dd, J = 4.4, 0.8 Hz, 0.41 H), 4.50 (diastereomer b, s, 0.37 H), 4.46 (diastereomer a, s, 0.35H), 4.01 (diastereomer a, d, J = 5.8 Hz, 0.34H), 3.98 (diastereomer b, d, J = 5.8 Hz, 0.43H), 3.64 (q, J = 6.2 Hz, 1H), 2.18-1.40 (m, 8H), 1.18-1.12 (m, 8H), 0.87 (s, 9H), 0.07-0.03 (m, 6H). Crude (2S,2'R,5'S)-5'-((R)-1-((tert-butyldimethylsilyl)oxy)ethyl)-2,5'-dimethyloctahydro-[2,2'-bifuran]-5-ol **S19** (93 mg, 0.270 mmol) was dissolved in 6 mL DCM. Benzoic anhydride (122 mg, 0.540 mmol, 2 equiv.), triethyl amine (0.11 mL, 0.810 mmol, 3 equiv.), and 4-(dimethylamino)pyridine (23 mg, 0.188 mmol, 0.7 equiv.) was added and the reaction was stirred for 14 h. The entire reaction was loaded onto Celite and purified by flash column

[25] Li, Y.; Cooksey, J. P.; Gao, Z.; Kocieński, P. J.; McAteer, S. M.; Snaddon, T. N. *Synthesis*, **2011**, 104-108.
[26] Smaller scale reactions (0.37 mmol) can be done at 0 °C, but yields suffer at larger scales if the reaction is not done at -78 °C.

chromatography to yield 93.2 mg (75%) of (2S,2'R,5'S)-5'-((R)-1-((tert-butyldimethylsilyl)oxy)ethyl)-2,5'-dimethyloctahydro-[2,2'-bifuran]-5-yl benzoate as a clear oil with slight benzoic anhydride contamination. Less polar diastereomer: ^{1}H NMR (400 MHz, C_6D_6) δ 8.19-8.15 (m, 2H), 7.12-7.03 (m, 3H), 6.72 (d, *J* = 4.1 Hz, 1H), 3.81 (dd, *J* = 7.9, 6.5 Hz, 1H), 3.67 (q, *J* = 6.2 Hz, 1H), 2.01-1.88 (m, 4H), 1.73-1.61 (m, 2H), 1.59-1.48 (m, 2H), 1.37 (s, 3H), 1.23 (d, *J* = 6.2 Hz, 3H), 1.19 (s, 3H), 0.98 (s, 9H), 0.07 (s, 6H). ^{13}C NMR (100 MHz, C_6D_6) δ 165.4, 132.8, 129.9, 128.5, 100.7, 87.8, 85.6, 83.3, 74.0, 36.4, 33.3, 32.0, 27.0, 26.1, 26.0, 24.7, 19.6, 18.7, 18.1, -3.8, -4.8. R_f = 0.33 (20:1 Hex:EtOAc). IR (ATR) 2973, 2955, 2931, 2857, 1723, 1451, 1271, 1082 cm^{-1}. LRMS (APCI+ESI) *m/z* $[C_{18}H_{35}O_3Si]^+$ (M-OBz) calcd 327.2, found 327.2. More polar diastereomer: ^{1}H NMR (400 MHz, C_6D_6) δ 8.20-8.16 (m, 2H), 7.12-7.05 (m, 3H), 6.62 (dd, *J* = 3.6, 1.4 Hz, 1H), 4.04 (t, *J* = 6.6 Hz, 1H), 3.78 (q, *J* = 6.2 Hz, 1H), 2.02-1.91 (m, 3H), 1.81-1.74 (m, 3H), 1.49-1.44 (m, 1H), 1.37 (m, 1H), 1.29 (d, *J* = 6.2 Hz, 3H), 1.20 (s, 3H), 1.17 (s, 3H), 0.94 (s, 9H), 0.06 (s, 3H), 0.02 (s, 3H). ^{13}C NMR (100 MHz, C_6D_6) δ 165.3, 132.9, 129.9, 128.5, 100.0, 87.9, 85.9, 84.5, 73.7, 36.5, 32.6, 32.0, 26.6, 26.0, 22.4, 19.6, 18.7, 18.1, -3.9, -4.8. R_f = 0.27 (20:1 Hex:EtOAc).

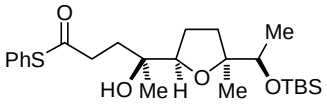

(S)-S-phenyl 4-((2R,5S)-5-((R)-1-((tert-butyldimethylsilyl)oxy)ethyl)-5-methyltetrahydrofuran-2-yl)-4-hydroxypentanethioate (120). Procedure adapted from the literature .[27] Thiophenol (0.12 ml, 1.15 mmol, 2.0 equiv.) was dissolved into 2 ml DCM under Ar and cooled to 0 °C. Trimethyl aluminum (0.57 ml, 1.15 mmol, 2.0 equiv., 2 M in PhMe) was added slowly over 5 min. After stirring the reaction for 10 min at 0 °C, the ice bath was removed and the reaction was stirred for another 10 min. The reaction was cooled back to 0 °C and (2S,2'R,5'S)-5'-((R)-1-((tert-butyldimethylsilyl)oxy)ethyl)-2,5'-dimethylhexahydro-[2,2'-bifuran]-5(2H)-one **184** (196.2 mg, 0.573 mmol) in 3 ml DCM was added slowly. The reaction was stirred and allowed to warm to 23 °C over 12 h. The reaction was cooled to -78 °C and 10 ml Et2O was added. After stirring for 10 min, 3.5 ml 1 M HCl was added and the reaction was allowed to warm to ~0 °C. The reaction was extracted with EtOAc (the emulsion can be removed by addition of more 1 M HCl, ~ 2 ml) and the organic fractions were dried with MgSO4. The crude reaction was loaded onto Celite and purified via flash column chromatography to yield 92.8 mg (36%) of (S)-S-phenyl 4-((2R,5S)-5-((R)-1-((tert-butyldimethylsilyl)oxy)ethyl)-5-methyltetrahydrofuran-2-yl)-4-hydroxypentanethioate as a clear oil and 68.9 mg (35% rsm) of (2S,2'R,5'S)-5'-((R)-1-((tert-butyldimethylsilyl)oxy)ethyl)-2,5'-dimethylhexahydro-[2,2'-bifuran]-5(2H)-one. $[\alpha]^{20}_{D}$ = +11.8, c = 0.0180 g/ml C_6H_6. ^{1}H NMR (400 MHz, C_6D_6) δ 7.40-7.36 (m, 2H), 7.03-6.94 (m, 3H), 3.59 (q, *J* = 6.2 Hz, 1H), 3.51 (dd, *J* = 7.5, 7.1 Hz, 1H), 2.85 (ddd, *J* = 15.7, 10.1, 5.5 Hz, 1H), 2.65 (ddd, *J* = 15.9, 10.2, 5.8 Hz, 1H), 1.97 (s, 1H), 1.96-1.84 (m, 2H), 1.68 (m, 1H), 1.58 (m, 1H), 1.43 (m, 1H), 1.33 (m, 1H), 1.08-1.03 (m, 9H), 0.92 (s, 9H), 0.02 (s, 3H), 0.0 (s, 3H). ^{13}C NMR (100 MHz, C_6D_6) δ 196.5, 134.8, 129.2, 129.2, 128.8, 85.6, 84.6, 73.5, 72.2, 38.6, 34.8, 33.0, 26.0, 25.5, 23.8, 20.6, 19.0, 18.1, -4.0, -4.6. R_f = 0.19 (9:1 Hex:EtOAc; UV, CAM). IR (ATR) 3446, 2955, 2930, 2856, 1710, 1371, 1255, 1096, 970, 832 cm^{-1}. HRMS (APCI) *m/z* $[C_{24}H_{39}O_3SSi]^+$ (M-H_2O) calcd 435.2389, found 435.2384.

[27] Gierasch, T. M.; Shi, Z.; Verdine, G. L. *Org. Lett.* **2003**, *5*, 621-624.

Fragment Couplings and derivatizations

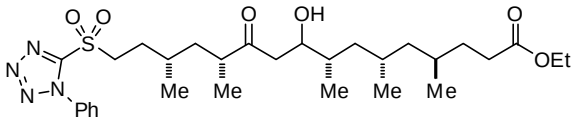

(4R,6S,8S,12R,14S)-ethyl 9-hydroxy-4,6,8,12,14-pentamethyl-11-oxo-16-((1-phenyl-1H-tetrazol-5-yl)sulfonyl)hexadecanoate (161). 9-iodo-9-borabicyclo[3.3.1]nonane (0.28 ml, 0.278 mmol, 1.36 equiv., 1M in Hex) was dissolved in 1 ml DCM. The reaction was cooled to 0 °C and triethyl amine (0.04 ml, 0.278 mmol, 1.36 equiv.) was added. The reaction went from pink to orange. After stirring for 5 min, (3R,5S)-3,5-dimethyl-7-((1-phenyl-1H-tetrazol-5-yl)sulfonyl)heptan-2-one **119a** (71.7 mg, 0.205 mmol) was added in 1 ml DCM. After stirring for 5 min, the reaction was cooled to -78 °C and (4R,6S,8S)-ethyl 4,6,8-trimethyl-9-oxononanoate **116** (59.6 mg, 0.246 mmol, 1.2 equiv.) was added in 1 ml DCM. After stirring for 1 h, the cold bath was removed and the reaction was stirred for 12 h. The reaction was quenched by the addition of 0.5 ml pH = 7.00 buffer, 2.0 ml MeOH, and 0.5 ml 30% H_2O_2. After 15 min, the reaction was extracted with Et_2O 3x. The organic layers were washed with sat. $NaHCO_3$ 2x, dried with $MgSO_4$, and concentrated. The crude reaction was purified via column chromatography to yield 70.2 mg (56%) of (4R,6S,8S,12R,14S)-ethyl 9-hydroxy-4,6,8,12,14-pentamethyl-11-oxo-16-((1-phenyl-1H-tetrazol-5-yl)sulfonyl)hexadecanoate. ^{1}H NMR (400 MHz, $CDCl_3$) δ 7.71-7.69 (m, 2H), 7.64-7.58 (m, 3H), 4.12 (q, J = 7.1 Hz, 2H), 3.96 (m, 0.25H), 3.90 (m, 0.68H), 3.82-3.68 (m, 2H), 2.71-2.24 (m, 6H), 1.98-1.48 (m, 10H), 1.33-1.07 (m, 2H), 1.32 (d, J = 6.3 Hz, 3H), 1.25 (t, J = 7.1 Hz, 3H), 1.11 (d, J = 7.1 Hz, 3H), 0.98 (d, J = 6.6 Hz, 3H), 0.97-0.84 (m, 2H), 0.89 (d, J = 6.9 Hz, 3H), 0.86 (d, J = 6.9 Hz, 3H). R_f = 0.24 (2:1 Hex:EtOAc; UV, CAM). IR (ATR) 2962, 2931, 2874, 1730, 1342, 1153 cm^{-1}. LRMS (ESI/APCI) *m/z* $[C_{30}H_{49}N_4O_6S]^+$ (M+H) calcd 593.3, found 593.1.

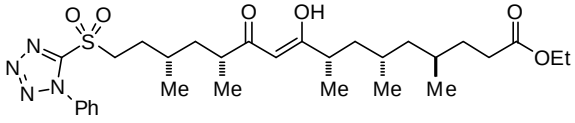

(4R,6S,8S,12R,14S,Z)-ethyl 9-hydroxy-4,6,8,12,14-pentamethyl-11-oxo-16-((1-phenyl-1H-tetrazol-5-yl)sulfonyl)hexadec-9-enoate (162). (4R,6S,8S,12R,14S)-ethyl 9-hydroxy-4,6,8,12,14-pentamethyl-11-oxo-16-((1-phenyl-1H-tetrazol-5-yl)sulfonyl)hexadecanoate **161** (70.0 mg, 0.118 mmol) was dissolved into 10 ml EtOAc. 2-iodoxybenzoic acid (165 mg, 0.591 mmol, 5.0 equiv.) was added and the reaction was heated to 80 °C for 4h. The reaction was cooled to 23 °C, filtered through Celite, and purified via preparative thin layer chromatography to yield 31.0 mg (44%) (4R,6S,8S,12R,14S,Z)-ethyl 9-hydroxy-4,6,8,12,14-pentamethyl-11-oxo-16-((1-phenyl-1H-tetrazol-5-yl)sulfonyl)hexadec-9-enoate and 31.0 mg (44% rsm) of (4R,6S,8S,12R,14S)-ethyl 9-hydroxy-4,6,8,12,14-pentamethyl-11-oxo-16-((1-phenyl-1H-tetrazol-5-yl)sulfonyl)hexadecanoate. $[\alpha]^{20}_D$ = +18.0, c = 0.0105 g/ml $CHCl_3$. ^{1}H NMR (400 MHz, $CDCl_3$) δ 7.70-7.68 (m, 2H), 7.63-7.57 (m, 3H), 5.48 (m, 1H), 4.11 (q, J = 7.1 Hz, 2H), 3.79-3.66 (m, 2H), 2.51-2.17 (m, 5H), 1.91 (m, 1H), 1.83-1.32 (m, 10H), 1.25 (t, J = 7.1 Hz, 3H), 1.14 (d, J = 7.1 Hz, 3H), 1.15-1.07 (m, 1H), 1.12 (d, J = 7.0 Hz, 3H), 0.98 (d, J = 6.5 Hz, 3H), 0.92 (m, 1H), 0.86 (d, J = 6.5 Hz, 3H), 0.82 (d, J = 6.5 Hz, 3H). ^{13}C NMR (100 MHz, $CDCl_3$) δ 198.7, 197.8, 174.0, 153.4, 133.0, 131.4, 129.7, 125.0, 97.4, 60.2, 54.1, 44.9, 41.3, 40.3, 40.1, 40.0, 32.0, 31.8, 29.9, 29.5, 28.7, 27.9, 20.3, 19.6, 19.2, 18.8, 18.8, 14.2. R_f = 0.67 (2:1 Hex:EtOAc; UV, CAM). IR (NaCl, Thin Film) 2965, 2933,

1732, 1596, 1342, 1153 cm^{-1}. HRMS (ESI/APCI) *m/z* $[C_{30}H_{47}N_4O_6S]^+$ (M+H) calcd 591.3211, found 591.3205.

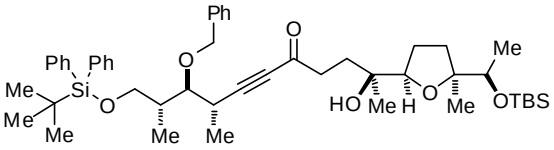

(2S,8S,9S,10R)-9-(benzyloxy)-2-((2R,5S)-5-((R)-1-((tert-butyldimethylsilyl)oxy)ethyl)-5-methyltetrahydrofuran-2-yl)-11-((tert-butyldiphenylsilyl)oxy)-2-hydroxy-8,10-dimethylundec-6-yn-5-one (240). Procedure adapted from the literature.[28] In an oven dried 25 mL round bottom flask, [1,1'-Bis(diphenylphosphino)ferrocene]dichloropalladium (II) (16.7 mg, 0.021 mmol, 10 mol %), tri-(2-furyl)phosphine (11.9 mg, 0.051 mmol, 25 mol %), and copper(I) iodide (94.0 mg, 0.494 mmol, 2.4 equiv.) was added in an inert air glove box. The reaction vessel was sealed, removed from the glove box, and 3.0 mL of DMF was added. In a vial, (((2R,3S,4S)-3-(benzyloxy)-2,4-dimethylhex-5-yn-1-yl)oxy)(tert-butyl)diphenylsilane **239** (106.1 mg, 0.226 mmol, 1.1 equiv.), (S)-S-phenyl 4-((2R,5S)-5-((R)-1-((tert-butyldimethylsilyl)oxy)ethyl)-5-methyltetrahydrofuran-2-yl)-4-hydroxypentanethioate **120** (92.8 mg, 0.205 mmol), and *N*,*N*-diisopropylethylamine (36.9 mg, 0.286 mmol, 1.4 equiv.) was added to a vial and dissolved in 3.0 mL DMF. After adding this solution to the reaction, the reaction was heated to 60 °C and stirred overnight. The reaction was cooled to 23 °C, Celite was added, and stirred for 30 min. Et_2O and H_2O was added and the solution was filtered through a pad of Celite. The filtrate was extracted with Et_2O 3x. The organic layers were combined, washed with 10% LiCl 2x, dried with $MgSO_4$, and concentrated. The residue was purified by flash column chromatography to yield 71.4 mg (43%) of (2S,8S,9S,10R)-9-(benzyloxy)-2-((2R,5S)-5-((R)-1-((tert-butyldimethylsilyl)oxy)ethyl)-5-methyltetrahydrofuran-2-yl)-11-((tert-butyldiphenylsilyl)oxy)-2-hydroxy-8,10-dimethylundec-6-yn-5-one as a clear oil. $[\alpha]^{20}_D$ = +7.6, c = 0.0166 g/ml CH_2Cl_2. ^{1}H NMR (400 MHz, $CDCl_3$) δ 7.64 (m, 4H), 7.44-7.22 (m, 11H), 4.64 (d, *J* = 11.2 Hz, 1H), 4.57 (d, *J* = 11.2 Hz, 1H), 3.80-3.69 (m, 3H), 3.64 (q, *J* = 6.3 Hz, 1H), 3.46 (dd, *J* = 7.3, 4.2 Hz, 1H), 3.01 (dq, *J* = 7.0, 4.3 Hz, 1H), 2.72 (ddd, *J* = 17.2, 9.9, 5.6 Hz, 1H), 2.60 (ddd, *J* = 17.2, 9.9, 5.8 Hz, 1H). 2.16 (bs, 1H), 2.06 (m, 1H), 1.94 (m, 1H), 1.85-1.76 (m, 3H), 1.64-1.53 (m, 2H), 1.30 (d, *J* = 7.0 Hz, 3H), 1.29 (m, 1H), 1.12-1.03 (m, 2H), 1.10 (s, 3H), 1.09 (s, 3H), 1.07 (s, 9H), 1.04 (d, *J* = 6.9 Hz, 3H), 0.87 (m, 9H), 0.05 (m, 6H). ^{13}C NMR (100 MHz, $CDCl_3$) δ 188.2, 138.4, 135.7, 135.6, 133.6, 133.5, 129.6, 129.6, 128.2, 127.6, 127.6, 127.5, 127.4, 95.9, 85.6, 84.4, 82.8, 82.1, 74.3, 73.0, 72.4, 65.3, 40.0, 38.7, 34.4, 30.9, 29.5, 27.0, 25.8, 25.4, 23.8, 20.4, 19.3, 18.8, 17.9, 17.2, 14.6, -4.1, -4.6. R_f = 0.36 (9:1 Hex:EtOAc; UV/CAM). IR (ATR) 3467, 2957, 2932, 2858, 2210, 1673, 1471, 1256, 1111, 832, 702 cm^{-1}. HRMS (APCI) *m/z* $[C_{49}H_{72}NaO_6Si_2]^+$ (M+Na) calcd 835.4765, found 835.4748.

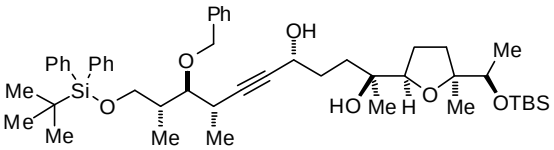

(2S,5R,8S,9S,10R)-9-(benzyloxy)-2-((2R,5S)-5-((R)-1-((tert-butyldimethylsilyl)oxy)ethyl)-5-methyltetrahydrofuran-2-yl)-11-((tert-butyldiphenylsilyl)oxy)-8,10-dimethylundec-6-yne-2,5-diol (246). (2S,8S,9S,10R)-9-(benzyloxy)-2-((2R,5S)-5-((R)-1-((tert-butyldimethylsilyl)oxy)ethyl)-5-methyltetrahydrofuran-2-yl)-11-((tert-butyldiphenylsilyl)oxy)-2-hydroxy-8,10-dimethylundec-6-yn-5-one

[28] Magdziak, D.; Lalic, G.; Lee, H. M.; Fortner, K. C.; Aloise, A. D.; Shair, M. D. *J. Am. Chem. Soc.* **2005**, *127*, 7284-7285.

240 (29.1 mg, 0.036 mmol) was dissolved in 4 ml iPrOH and Ru(*p*-cymene)[(R,R)-Ts-DPEN][29] (2.2 mg, 0.004 mmol, 10 mol %) was added. The reaction was stirred for 1.5 h and the reaction was homogenous and starting material was gone by thin layer chromatography. The reaction was loaded onto silica and purified via flash column chromatography to yield 20.0 mg (68%) of (2S,5R,8S,9S,10R)-9-(benzyloxy)-2-((2R,5S)-5-((R)-1-((tert-butyldimethylsilyl)oxy)ethyl)-5-methyltetrahydrofuran-2-yl)-11-((tert-butyldiphenylsilyl)oxy)-8,10-dimethylundec-6-yne-2,5-diol as a light brown oil. $[\alpha]^{20}_{D}$ = +10.8, c = 0.0051 g/ml $CHCl_3$. ^{1}H NMR (400 MHz, $CDCl_3$) δ 7.68-7.63 (m, 4H), 7.43-7.21 (m, 11H), 4.65 (d, *J* = 11.2 Hz, 1H), 4.54 (d, *J* = 11.2 Hz, 1H), 4.41 (bs, 1H), 3.81-3.69 (m, 3H), 3.66 (q, *J* = 6.2 Hz, 1H), 3.37 (dd, *J* = 7.7, 4.1 Hz, 1H), 3.09 (bs, 1H), 2.85 (m, 1H), 2.57 (bs, 1H), 2.06 (m, 1H), 1.97-1.68 (m, 6H), 1.51-1.35 (m, 2H), 1.26-1.16 (m, 2H), 1.24 (d, *J* = 7.1 Hz, 3H), 1.17 (s, 3H), 1.12-1.04 (m, 7H), 1.07 (s, 9H), 0.88 (s, 9H), 0.07-0.04 (m, 6H). ^{13}C NMR (100 MHz, $CDCl_3$) δ 138.8, 135.7, 135.7, 135.6, 133.8, 133.7, 129.6, 129.5, 128.2, 127.6, 127.6, 127.6, 127.3, 86.1, 85.6, 84.5, 83.3, 82.6, 74.2, 73.0, 72.9, 65.5, 62.4, 38.8, 33.7, 32.6, 31.8, 29.1, 27.0, 25.9, 25.2, 23.9, 21.0, 19.3, 19.0, 18.1, 18.0, 14.8, -4.2, -4.4. R_f = 0.12 (9:1 Hex:EtOAc; UV, CAM). IR (ATR) 3404, 2957, 2930, 2857, 1257, 1111, 833, 701 cm^{-1}. HRMS (APCI) *m/z* $[C_{49}H_{74}NaO_6Si_2]^+$ (M+Na) calcd 837.4922, found 837.4927.

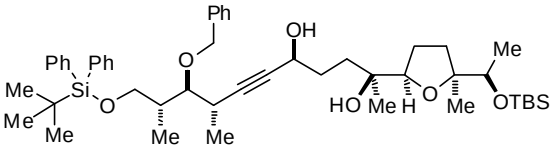

(2S,5S,8S,9S,10R)-9-(benzyloxy)-2-((2R,5S)-5-((R)-1-((tert-butyldimethylsilyl)oxy)ethyl)-5-methyltetrahydrofuran-2-yl)-11-((tert-butyldiphenylsilyl)oxy)-8,10-dimethylundec-6-yne-2,5-diol (247). (2S,8S,9S,10R)-9-(benzyloxy)-2-((2R,5S)-5-((R)-1-((tert-butyldimethylsilyl)oxy)ethyl)-5-methyltetrahydrofuran-2-yl)-11-((tert-butyldiphenylsilyl)oxy)-2-hydroxy-8,10-dimethylundec-6-yn-5-one **240** (44.0 mg, 0.054 mmol) was dissolved in 2 ml iPrOH and Ru(*p*-cymene)[(S,S)-Ts-DPEN] (3.3 mg, 0.005 mmol, 10 mol %) was added. The reaction was stirred for 1.5 h and the reaction was homogenous and starting material was gone by thin layer chromatography. The reaction was loaded onto silica and purified via flash column chromatography to yield 21.7 mg (49%) of (2S,5S,8S,9S,10R)-9-(benzyloxy)-2-((2R,5S)-5-((R)-1-((tert-butyldimethylsilyl)oxy)ethyl)-5-methyltetrahydrofuran-2-yl)-11-((tert-butyldiphenylsilyl)oxy)-8,10-dimethylundec-6-yne-2,5-diol as a light brown oil. ^{1}H NMR (400 MHz, $CDCl_3$) δ 7.70-7.64 (m, 4H), 7.43-7.21 (m, 11H), 4.64 (d, J = 11.3 Hz, 1H), 4.55 (d, J = 11.3 Hz, 1H), 4.35 (m, 1H), 3.81-3.71 (m, 3H), 3.66 (q, J = 6.2 Hz, 1H), 3.38 (dd, J = 7.6, 4.2 Hz, 1H), 2.86 (m, 1H), 2.41 (bs, 2H), 2.05 (m, 1H), 1.96 (m, 1H), 1.88-1.67 (m, 4H), 1.62-1.41 (m, 4H), 1.23 (d, J = 7.0 Hz, 3H), 1.17 (s, 3H), 1.12-1.10 (m, 5H), 1.07 (s, 9H), 1.05 (d, J = 6.9 Hz, 3H), 0.88 (s, 9H), 0.07 (s, 3H), 0.05 (s, 3H). ^{13}C NMR (100 MHz, $CDCl_3$) δ 138.8, 135.7, 135.7, 135.5, 135.5, 133.8, 133.7, 129.6, 129.5, 128.2, 127.6, 127.6, 127.5, 127.3, 87.0, 85.6, 84.2, 83.4, 82.7, 74.2, 73.0, 72.8, 65.4, 63.2, 38.8, 33.9, 33.7, 32.5, 29.1, 27.0, 25.9, 25.2, 24.2, 20.8, 19.3, 19.0, 18.0, 18.0, 14.8, -4.2, -4.5. R_f = 0.10 (9:1 Hex:EtOAc; UV, CAM).

[29] Ru(p-cymene)[(R,R)-Ts-DPEN] was obtained by deprotonation of commercially available RuCl(*p*-cymene)[(R,R)-Ts-DPEN]. RuCl(*p*-cymene)[(R,R)-Ts-DPEN] (248 mg, 0.393 mmol) was dissolved in 10 ml DCM and flushed with Ar. Freshly powdered potassium hydroxide (228 mg, 3.93 mmol, 10 equiv.) was added and the reaction was stirred for 10 min. 10 ml H_2O was added and the layers were separated. The dark purple DCM layer was dried with calcium hydride and filtered through glass wool into a vial. Concentration resulted in 212 mg (91%) of RuCl(*p*-cymene)[(R,R)-Ts-DPEN] as a purple solid. See: (a) Haack, K. J.; Hashiguchi, S.; Fujii, A.; Ikariya, T.; Noyori, R. *Angew. Chem. Int. Ed.* **1997**, *36*, 285-288. (b) Wang, Q.; Kobayashi, Y. *Org. Lett.* **2011**, *13*, 6252-6255.

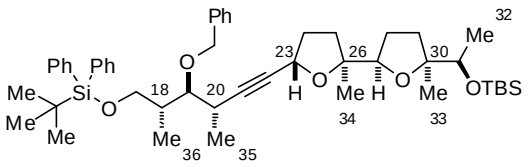

(((2R,3S,4S)-3-(benzyloxy)-6-((2S,2'R,5S,5'S)-5'-((R)-1-((tert-butyldimethylsilyl)oxy)ethyl)-2,5'-dimethyloctahydro-[2,2'-bifuran]-5-yl)-2,4-dimethylhex-5-yn-1-yl)oxy)(tert-butyl)diphenylsilane (248). (2S,5R,8S,9S,10R)-9-(benzyloxy)-2-((2R,5S)-5-((R)-1-((tert-butyldimethylsilyl)oxy)ethyl)-5-methyltetrahydrofuran-2-yl)-11-((tert-butyldiphenylsilyl)oxy)-8,10-dimethylundec-6-yne-2,5-diol **246** (20.3 mg, 0.025 mmol) was dissolved in 2 ml DCM and cooled to 0 °C. An 8 ml solution of methanesulfonic anhydride (43.6 mg, 0.250 mmol, 10.0 equiv.) and pyridine (19.8 mg, 0.250 mmol, 10.0 equiv.) was added and the reaction was stirred for 2 h. At this time starting material had disappeared (R_f = 0.14 (4:1 Hex:EtOAc; CAM)) and a new spot (R_f = 0.23 (4:1 Hex:EtOAc; CAM)) was present by TLC. The reaction was quenched by two drops of MeOH and then with sat. $NaHCO_3$. The reaction was extracted with DCM 3x, dried with $MgSO_4$, and concentrated onto silica. The reaction was purified to yield 11.8 mg (59%) of (((2R,3S,4S)-3-(benzyloxy)-6-((2S,2'R,5S,5'S)-5'-((R)-1-((tert-butyldimethylsilyl)oxy)ethyl)-2,5'-dimethyloctahydro-[2,2'-bifuran]-5-yl)-2,4-dimethylhex-5-yn-1-yl)oxy)(tert-butyl)diphenylsilane as a clear oil. $[\alpha]^{20}_D$ = -19.3 , c = 0.0066 g/ml $CHCl_3$. ^{1}H NMR (400 MHz, $CDCl_3$) δ 7.66-7.63 (m, 4H), 7.42-7.21 (m, 11H), 4.64 (d, *J* = 11.2 Hz, 1H), 4.64 (m, 1H), 4.54 (d, *J* = 11.3 Hz, 1H), 3.88 (dd, *J* = 8.2, 6.4 Hz, 1H), 3.77 (dd, *J* = 9.9, 5.4 Hz, 1H), 3.72 (dd, *J* = 9.8, 4.0 Hz, 1H), 3.56 (q, *J* = 6.2 Hz, 1H), 3.36 (dd, *J* = 7.6, 4.2 Hz, 1H), 2.85 (m, 1H), 2.13-1.82 (m, 5H), 1.71-1.55 (m, 4H), 1.21 (s, 3H), 1.21 (d, *J* = 7.0 Hz, 3H), 1.11 (d, *J* = 6.3 Hz, 3H), 1.10 (s, 3H), 1.07 (s, 9H), 1.05 (d, *J* = 7.0 Hz, 3H), 0.87 (s, 9H), 0.05 (s, 3H), 0.03 (s, 3H). ^{13}C NMR (100 MHz, $CDCl_3$) δ 138.9, 135.7, 135.7, 134.8, 133.9, 133.8, 129.6, 129.5, 129.5, 128.1, 127.7, 127.6, 127.6, 127.5, 127.2, 86.4, 85.5, 85.1, 84.0, 83.4, 82.3, 73.9, 73.2, 68.9, 65.5, 38.7, 35.9, 34.2, 33.0, 29.1, 27.4, 27.0, 26.6, 25.8, 24.1, 19.5, 19.3, 18.3, 17.9, 17.7, 14.8, -3.9, -4.9. ^{1}H NMR (500 MHz, C_6D_6) δ 7.77-7.74 (m, 4H; Ph), 7.31-7.28 (m, 2H; Ph), 7.22-7.11 (m, 9H; Ph), 4.74 (m, 1H; C23-H), 4.62 (d, J = 11.4 Hz, 1H; Bn), 4.49 (d, J = 11.4 Hz, 1H; Bn), 3.87-3.83 (m, 3H; C27-H, C17-H_2), 3.68 (q, J = 6.2 Hz, 1H; C31-H), 3.28 (dd, J = 7.5, 4.3 Hz, 1H; C19-H), 2.86 (m, 1H; C20-H), 2.23 (m, 1H; C18-H), 2.00-1.96 (m, 2H; C24-H_2), 1.94-1.87 (m, 2H; C25-H, C29-H), 1.70-1.64 (m, 2H; C25-H, C28-H), 1.62-1.58 (m, 1H; C28-H), 1.54-1.48 (m, 1H; C29-H), 1.36 (s, 3H; C33-H_3), 1.24 (d, J = 6.2 Hz, 3H; C32-H_3), 1.22 (d, J = 7.0 Hz, 3H; C35-H_3), 1.19 (s, 9H; TBDPS-Me_3), 1.19 (s, 3H; C34-H_3), 1.14 (d, J = 6.9 Hz, 3H; C36-H_3), 0.97 (s, 9H; TBS-Me_3), 0.06 (s, 6H; TBS-Me_2). R_f = 0.68 (4:1 Hex:EtOAc; CAM). IR (ATR) 2957, 2930, 2856, 1471, 1371, 1257, 1112, 833, 702 cm^{-1}. HRMS (ESI/APCI) *m/z* $[C_{49}H_{76}NO_5Si_2]^+$ (M+NH_4) calcd 814.5257, found 814.5254.

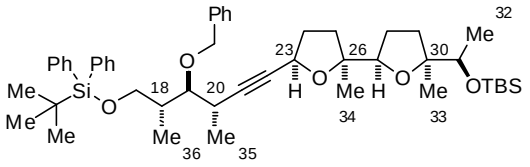

(((2R,3S,4S)-3-(benzyloxy)-6-((2S,2'R,5R,5'S)-5'-((R)-1-((tert-butyldimethylsilyl)oxy)ethyl)-2,5'-dimethyloctahydro-[2,2'-bifuran]-5-yl)-2,4-dimethylhex-5-yn-1-yl)oxy)(tert-butyl)diphenylsilane (245). (2S,8S,9S,10R)-9-(benzyloxy)-2-((2R,5S)-5-((R)-1-((tert-butyldimethylsilyl)oxy)ethyl)-5-methyltetrahydrofuran-2-yl)-11-((tert-butyldiphenylsilyl)oxy)-2-hydroxy-8,10-dimethylundec-6-yn-5-one **240** (47.0 mg, 0.058 mmol) was dissolved into 3 ml trifluoroethanol. Sodium cyanoborohydride (10.9 mg, 0.174 mmol, 3.0 equiv.) was added to the reaction

and then dichloroacetic acid (22.4 mg, 0.174 mmol, 3.0 equiv.) in 3 ml trifluoroethanol was added. The reaction was stirred for 10 min and quenched with sat. $NaHCO_3$. H_2O and DCM were added to the reaction and the mixture was extracted with DCM 3x. The organic layer was dried with MgSO4, concentrated, and purified by preparative thin layer chromatography to yield 31.2 mg (68%) of (((2R,3S,4S)-3-(benzyloxy)-6-((2S,2'R,5R,5'S)-5'-((R)-1-((tert-butyldimethylsilyl)oxy)ethyl)-2,5'-dimethyloctahydro-[2,2'-bifuran]-5-yl)-2,4-dimethylhex-5-yn-1-yl)oxy)(tert-butyl)diphenylsilane as a clear oil. $[\alpha]^{20}_D$ = +11.6, c = 0.0104 g/ml $CHCl_3$. ^{1}H NMR (400 MHz, $CDCl_3$) δ 7.65 (m, 4H), 7.42-7.31 (m, 6H), 7.29-7.22 (m, 5H), 4.64 (d, *J* = 11.3 Hz, 1H), 4.64 (m, 1H), 4.54 (d, *J* = 11.3 Hz, 1H), 3.98 (m, 1H), 3.78 (dd, *J* = 9.9, 5.3 Hz, 1H), 3.72 (dd, *J* = 9.9, 4.0 Hz, 1H), 3.60 (q, *J* = 6.2 Hz, 1H), 3.38 (dd, *J* = 7.6, 4.3 Hz, 1H), 2.84 (m, 1H), 2.14 (m, 1H), 2.08-2.01 (m, 2H), 1.97-1.80 (m, 3H), 1.65-1.55 (m, 3H), 1.22 (d, *J* = 7.0 Hz, 3H), 1.12 (d, *J* = 6.0 Hz, 3H), 1.12 (s, 3H), 1.07 (s, 9H), 1.07 (s, 3H), 1.06 (d, *J* = 6.9 Hz, 3H), 0.87 (s, 9H), 0.05 (s, 3H), 0.04 (s, 3H). ^{13}C NMR (100 MHz, $CDCl_3$) δ 138.8, 135.7, 135.6, 133.8, 133.7, 129.5, 129.5, 128.2, 127.6, 127.6, 127.5, 127.2, 86.4, 85.5, 85.1, 83.6, 83.2, 82.0, 73.9, 73.2, 68.5, 65.5, 38.7, 36.2, 35.2, 33.6, 29.0, 27.0, 26.4, 25.8, 22.0, 19.3, 19.1, 18.4, 17.9, 17.6, 14.7, -3.9, -4.9. ^{1}H NMR (400 MHz, C_6D_6) δ 7.78-7.75 (m, 4H; Ph), 7.30 (m, 2H; Ph), 7.22-7.09 (m, 9H; Ph), 4.64 (m, 1H; C23-H), 4.62 (d, J = 12.0 Hz, 1H; Bn-H), 4.50 (d, J = 11.4 Hz, 1H; Bn-H), 4.09 (m, 1H; C27-H), 3.94-3.87 (m, 2H; C17-H2), 3.78 (q, J = 6.2 Hz, 1H; C31-H), 3.30 (dd, J = 7.6, 4.4 Hz, 1H; C19-H), 2.87 (m, 1H; C20-H), 2.24 (m, 1H; C18-H), 2.07-1.98 (m, 3H; C25-H, C28-H, C29-H), 1.98-1.83 (m, 3H; C24-H_2, C28-H), 1.62-1.57 (m, 1H; C29-H), 1.43-1.38 (m, 1H; C25-H), 1.30 (d, J = 6.2 Hz, 3H; C32-H_3), 1.23 (d, J = 7.0 Hz, 3H; C35-H_3), 1.22 (s, 3H; C34-H_3), 1.20 (s, 9H; TBDPS-Me_3), 1.18 (d, J = 7.1 Hz, 3H; C36-H_3), 1.17 (s, 3H; C33-H_3), 0.98 (s, 9H; TBS-Me_3), 0.09 (s, 3H; TBS-Me), 0.07 (s, 3H; TBS-Me). ^{13}C NMR (100 MHz, C_6D_6) δ 139.4, 136.1, 136.1, 134.2, 134.0, 129.9, 129.9, 128.5, 128.4, 128.1, 127.9, 127.4, 86.4 (C21), 85.6 (C30), 85.0 (C22), 84.2 (C27), 83.8 (C19), 83.2 (C26), 74.3 (Bn), 74.0 (C31), 68.8 (C23), 66.0 (C17), 39.3 (C18), 36.8 (C29), 35.9 (C25), 33.9 (C24), 29.6 (C20), 27.2 (TBDPS-Me_3), 26.7 (C28), 26.1 (TBS-Me_3), 22.2 (C34), 19.6 (TBDPS-CMe_3), 19.4 (C33), 18.8 (C32), 18.1 (TBS-CMe_3), 17.9 (C35), 15.1 (C36), -3.8 (TBS-Me), -4.7 (TBS-Me). R_f = 0.38 (9:1 Hex:EtOAc; UV, CAM). IR (ATR) 2958, 2930, 2857, 1461, 1256, 1105, 833, 739 cm^{-1}. HRMS (APCI) *m/z* $[C_{49}H_{76}NO_5Si_2]^+$ ($M+NH_4$) calcd 814.5257, found 814.5258.

(2S,5S,8S,9S,10R)-9-(benzyloxy)-2-((2R,5S)-5-((R)-1-((tert-butyldimethylsilyl)oxy)ethyl)-5-methyltetrahydrofuran-2-yl)-11-((tert-butyldiphenylsilyl)oxy)-8,10-dimethylundec-6-yne-2,5-diol **247** (16.9 mg, 0.021 mmol) was dissolved in 2 ml DCM and cooled to 0 °C. An 8 ml solution of methanesulfonic anhydride (36.5 mg, 0.210 mmol, 10.0 equiv.) and pyridine (33.2 mg, 0.210 mmol, 20.0 equiv.) was added and the reaction was stirred for 2 h. At this time starting material had disappeared (R_f = 0.14 (4:1 Hex:EtOAc; CAM)) and a new spot (R_f = 0.23 (4:1 Hex:EtOAc; CAM)) was present by TLC. The reaction was quenched with sat. $NaHCO_3$. The reaction was extracted with DCM 3x, dried with $MgSO_4$, and concentrated onto silica. The reaction was purified to yield 6.2 mg (30%) of (((2R,3S,4S)-3-(benzyloxy)-6-((2S,2'R,5S,5'S)-5'-((R)-1-((tert-butyldimethylsilyl)oxy)ethyl)-2,5'-dimethyloctahydro-[2,2'-bifuran]-5-yl)-2,4-dimethylhex-5-yn-1-yl)oxy)(tert-butyl)diphenylsilane as a clear oil.

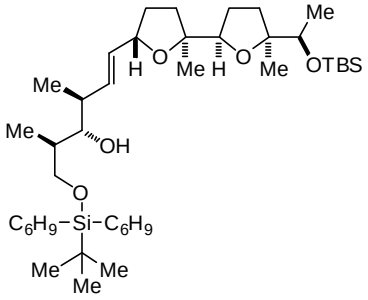

(2R,3S,4S)-1-((tert-butyldicyclohexenylsilyl)oxy)-6-((2S,2'R,5S,5'S)-5'-((R)-1-((tert-butyldimethylsilyl)oxy)ethyl)-2,5'-dimethyloctahydro-[2,2'-bifuran]-5-yl)-2,4-dimethylhex-5-en-3-ol (249). Ammonium was condensed into a 250 ml three neck round bottom flask. Sodium metal was added until a deep blue color was produced. In a 50 ml three neck round bottom flask, (((2R,3S,4S)-3-(benzyloxy)-6-((2S,2'R,5S,5'S)-5'-((R)-1-((tert-butyldimethylsilyl)oxy)ethyl)-2,5'-dimethyloctahydro-[2,2'-bifuran]-5-yl)-2,4-dimethylhex-5-yn-1-yl)oxy)(tert-butyl)diphenylsilane **248** (90.9 mg, 0.114 mmol) was dissolved in 5 ml THF and 1 ml tBuOH. Ammonium was condensed into 50 ml round bottom flask from 250 ml round bottom flask and lithium metal was added until a blue color persisted. Lithium was added over two hours to maintain a blue solution. The reaction was quenched by addition of MeOH until the blue color disappeared. H_2O was added and the reaction was allowed to warm to ~10 °C. The reaction was extracted with Et_2O 3x, dried with $MgSO_4$, and the crude material was purified via flash column chromatography to yield 52.3 mg (64%) of (2R,3S,4S)-1-((tert-butyldicyclohexenylsilyl)oxy)-6-((2S,2'R,5S,5'S)-5'-((R)-1-((tert-butyldimethylsilyl)oxy)ethyl)-2,5'-dimethyloctahydro-[2,2'-bifuran]-5-yl)-2,4-dimethylhex-5-en-3-ol as an oil. ^{1}H NMR (300 MHz, $CDCl_3$) δ 5.81-5.72 (m, 4H), 5.57-5.44 (m, 2H), 3.98-3.57 (m, 4H), 3.35 (m, 1H), 2.73 (m, 2H), 2.34-0.80 (m, 57H), 0.05 (m, 6H). R_f = 0.32 (9:1 Hex:EtOAc; CAM). LRMS (ESI/APCI) *m/z* $[C_{42}H_{80}NO_5Si_2]^+$ (M+NH_4) calcd 734.6, found 734.6.

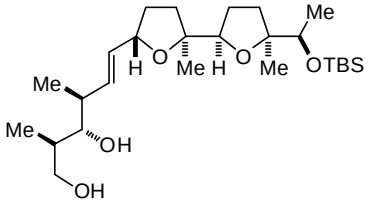

(2R,3S,4S)-6-((2S,2'R,5S,5'S)-5'-((R)-1-((tert-butyldimethylsilyl)oxy)ethyl)-2,5'-dimethyloctahydro-[2,2'-bifuran]-5-yl)-2,4-dimethylhex-5-ene-1,3-diol (250). (2R,3S,4S)-1-((tert-butyldicyclohexenylsilyl)oxy)-6-((2S,2'R,5S,5'S)-5'-((R)-1-((tert-butyldimethylsilyl)oxy)ethyl)-2,5'-dimethyloctahydro-[2,2'-bifuran]-5-yl)-2,4-dimethylhex-5-en-3-ol **249** (52.3 mg, 0.073 mmol) was dissolved in 5 ml THF. Tetrabutylammonium fluoride (0.15 ml, 0.146 mmol, 2.0 equiv., 1 M in THF) was added. After 10 min., 4 drops of AcOH was added. The reaction was loaded onto silica and purified via flash column chromatography to yield 26.0 mg (76%) of (2R,3S,4S)-6-((2S,2'R,5S,5'S)-5'-((R)-1-((tert-butyldimethylsilyl)oxy)ethyl)-2,5'-dimethyloctahydro-[2,2'-bifuran]-5-yl)-2,4-dimethylhex-5-ene-1,3-diol as a 1.5:1 E:Z ratio. ^{1}H NMR (400 MHz, C_6D_6) δ 5.82-5.76 (m, 0.7H), 5.57-5.51 (m, 1.6H), 4.46 (m, 1H), 3.96 (m, 1H), 3.77-3.54 (m, 3H), 3.42 (m, 1H), 3.18 (m, 1H), 2.38-2.11 (m, 3H), 2.05-1.86 (m, 3H), 1.74-1.43 (m, 5H), 1.28 (m, 3H), 1.23 (m, 3H), 1.14 (m, 3H), 1.03 (m, 3H), 0.98-0.91 (m, 9H), 0.77-0.71 (m, 3H), 0.07 (m, 6H). R_f = 0.16 (1:1 Hex:EtOAc; CAM). IR (ATR) 3342, 2958, 2930, 2858, 1462, 1371, 1256, 1098 cm^{-1}. LRMS (APCI) *m/z* $[C_{26}H_{54}NO_5Si]^+$ (M+NH_4) calcd 488.4, found 488.4.

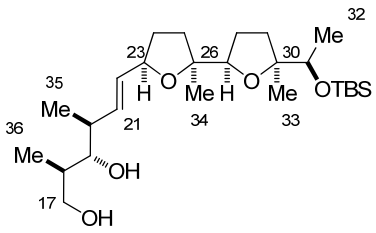

(2R,3S,4S)-6-((2S,2'R,5R,5'S)-5'-((R)-1-((tert-butyldimethylsilyl)oxy)ethyl)-2,5'-dimethyloctahydro-[2,2'-bifuran]-5-yl)-2,4-dimethylhex-5-ene-1,3-diol (S20). Ammonium was condensed into a 250 ml three neck round bottom flask. Sodium metal was added until a deep blue color was produced. In a 50 ml three neck round bottom flask, (((2R,3S,4S)-3-(benzyloxy)-6-((2S,2'R,5R,5'S)-5'-((R)-1-((tert-butyldimethylsilyl)oxy)ethyl)-2,5'-dimethyloctahydro-[2,2'-bifuran]-5-yl)-2,4-dimethylhex-5-yn-1-yl)oxy)(tert-butyl)diphenylsilane **245** (66.0 mg, 0.083 mmol) was dissolved in 5 ml THF and 1 ml tBuOH. Ammonium was condensed into 50 ml round bottom flask from 250 ml round bottom flask and lithium metal was added until a blue color persisted. Lithium was added over two hours to maintain a blue solution. The reaction was quenched by addition of MeOH until the blue color disappeared. H_2O was added and the reaction was allowed to warm to ~10 °C. The reaction was extracted with Et_2O 3x, dried with $MgSO_4$, and the crude material was purified via flash column chromatography to yield 44.6 mg (75%) of (2R,3S,4S)-1-((tert-butyldicyclohexenylsilyl)oxy)-6-((2S,2'R,5R,5'S)-5'-((R)-1-((tert-butyldimethylsilyl)oxy)ethyl)-2,5'-dimethyloctahydro-[2,2'-bifuran]-5-yl)-2,4-dimethylhex-5-en-3-ol **S21**. ^{1}H NMR (400 MHz, $CDCl_3$) δ 5.79-5.44 (m, 6H), 4.38 (m, 1H), 3.95-3.65 (m, 4H), 3.60 (q, J = 6.2 Hz, 1H), 3.36 (m, 1H), 2.73 (m, 2H), 2.34-0.82 (m, 55H), 0.05 (m, 6H). HRMS (APCI) *m/z* $[C_{42}H_{80}NO_5Si]^+$ (M+NH_4) calcd 734.5575, found 734.5555. (2R,3S,4S)-1-((tert-butyldicyclohexenylsilyl)oxy)-6-((2S,2'R,5R,5'S)-5'-((R)-1-((tert-butyldimethylsilyl)oxy)ethyl)-2,5'-dimethyloctahydro-[2,2'-bifuran]-5-yl)-2,4-dimethylhex-5-en-3-ol **S21** (44.6 mg, 0.062 mmol) was dissolved in 5 ml THF. Tetrabutylammonium fluoride (0.16 ml, 0.156 mmol, 2.5 equiv., 1 M in THF) was added. After 10 min., 4 drops of AcOH was added. The reaction was loaded onto silica and purified via flash column chromatography to yield 18.7 mg (64%) of (2R,3S,4S)-6-((2S,2'R,5R,5'S)-5'-((R)-1-((tert-butyldimethylsilyl)oxy)ethyl)-2,5'-dimethyloctahydro-[2,2'-bifuran]-5-yl)-2,4-dimethylhex-5-ene-1,3-diol as a 2:1 E:Z ratio. ^{1}H NMR (400 MHz, C_6D_6) δ 5.78 (dd, J = 15.6, 7.8/8.5 Hz, 1H; C21-H), 5.61 (dd, J = 15.6, 6.7 Hz, 1H; C22-H), 4.33 (ddd, J = 13.6, 6.6, 6.6 Hz, 1H; C23-H), 3.95 (m, 1H; C27-H), 3.75 (q, J = 6.3 Hz, 1H; C31-H), 3.58 (m, 1H; C17-HA), 3.46 (m, 1H; C17-HB), 3.18 (bs, 1H; OH), 3.16 (m, 1H; C19-H), 2.24 (m; C20-H), 1.96 (m, 1H; C29-HA), 1.93 (m, 1H; C25-HA), 1.78 (m, 2H; C28-HA/HB), 1.71 (m, 1H; C24-HA), 1.60 (m, 1H; C29-HB), 1.58 (m, 1H; C18-H), 1.57 (m, 1H; C24-HB), 1.54 (bs, 1H; OH), 1.39 (m, 1H; C25-HB), 1.30 (d, J = 6.2 Hz, 3H; C32-H3), 1.19 (s, 3H; C34-H3), 1.17 (s, 3H; C33-H3), 0.98 (s, 9H; TBS-tBu), 0.94 (m; C35-H3), 0.74 (d, J = 6.7/7.0 Hz, 3H; C36-H3), 0.09 (s, 3H; TBS-Me), 0.08 (s, 3H; TBS-Me). R_f = 0.23 (1:1 Hex:EtOAc; CAM). HRMS (APCI) *m/z* $[C_{26}H_{51}O_5Si]^+$ (M+H) calcd 471.3500, found 471.3509.

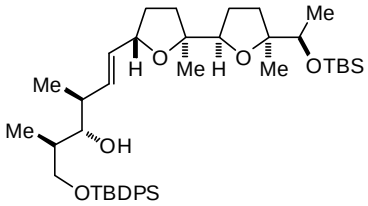

(2R,3S,4S)-6-((2S,2'R,5S,5'S)-5'-((R)-1-((tert-butyldimethylsilyl)oxy)ethyl)-2,5'-dimethyloctahydro-[2,2'-bifuran]-5-yl)-1-((tert-butyldiphenylsilyl)oxy)-2,4-dimethylhex-5-en-3-ol (251). (2R,3S,4S)-6-((2S,2'R,5S,5'S)-5'-((R)-1-((tert-butyldimethylsilyl)oxy)ethyl)-2,5'-dimethyloctahydro-[2,2'-bifuran]-5-yl)-2,4-dimethylhex-5-ene-1,3-diol **250** (18.7 mg, 0.0397 mmol) was dissolved in 0.5 ml DMF. Imidazole (6.0 mg, 0.0873 mmol, 2.0 equiv.) and tertbutyldiphenyl silylchloride (0.01 ml, 0.0405 mmol, 1.02 equiv.) was added. The reaction was stirred for 12 h. EtOAc and H_2O were added and the reaction was extracted with EtOAc 3x. The organic layer was dried with

$MgSO_4$, concentrated, and purified via preparative thin layer chromatography to yield 5.5 mg (20%) of (2R,3S,4S)-6-((2S,2'R,5S,5'S)-5'-((R)-1-((tert-butyldimethylsilyl)oxy)ethyl)-2,5'-dimethyloctahydro-[2,2'-bifuran]-5-yl)-1-((tert-butyldiphenylsilyl)oxy)-2,4-dimethylhex-5-en-3-ol. Spectral data matches literature.[30] ^{1}H NMR (300 MHz, $CDCl_3$) δ 7.73-7.67 (m, 4H), 7.44-7.36 (m, 6H), 5.78 (dd, *J* = 15.5, 7.9 Hz, 0.6 H), 5.54-5.45 (m, 1.4H), 4.41 (m, 0.6 H), 3.99 (m, 0.6 H), 3.84-3.58 (m, 3H), 3.40 (m, 1H), 2.36-1.56 (m, 14H), 1.15-1.12 (m, 9H), 1.07 (s, 9H), 0.87 (s, 9H), 0.78 (d, *J* = 6.8 Hz, 3H), 0.06 (m, 6H). R_f = 0.45 (4:1 Hex:EtOAc; UV, CAM). LRMS (APCI) *m/z* $[C_{42}H_{72}NO_5Si_2]^+$ ($M+NH_4$) calcd 726.5, found 726.5.

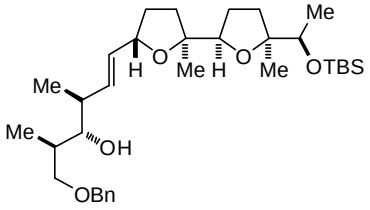

(2R,3S,4S)-1-(benzyloxy)-6-((2S,2'R,5S,5'S)-5'-((R)-1-((tert-butyldimethylsilyl)oxy)ethyl)-2,5'-dimethyloctahydro-[2,2'-bifuran]-5-yl)-2,4-dimethylhex-5-en-3-ol (S22). Sodium hydride (1.2 mg, 0.031 mmol, 2.0 equiv., 60% in mineral oil) was added to 1 ml THF. To this (2R,3S,4S)-6-((2S,2'R,5S,5'S)-5'-((R)-1-((tert-butyldimethylsilyl)oxy)ethyl)-2,5'-dimethyloctahydro-[2,2'-bifuran]-5-yl)-2,4-dimethylhex-5-ene-1,3-diol **250** (7.3 mg, 0.0156 mmol) was added in 1 ml THF. The reaction was cooled to 0 °C and stirred for 20 min. A solution of benzyl bromide in THF (2.7 mg, 0.0156 mmol, 1.0 equiv.) was added and the reaction was stirred for 2 h. Starting material remained by TLC and 5 equiv. of sodium hydride and benzyl bromide were added and the reaction was stirred overnight. The reaction was quenched with sat. NH_4Cl, extracted with EtOAc 3x, dried with $MgSO_4$, and purified via flash column chromatography to yield 3.6 mg (41%) of (2R,3S,4S)-1-(benzyloxy)-6-((2S,2'R,5S,5'S)-5'-((R)-1-((tert-butyldimethylsilyl)oxy)ethyl)-2,5'-dimethyloctahydro-[2,2'-bifuran]-5-yl)-2,4-dimethylhex-5-en-3-ol. ^{1}H NMR (300 MHz, $CDCl_3$) δ 7.34-7.27 (m, 5H), 5.72 (dd, *J* = 15.7, 8.2 Hz, 0.6 H), 5.54-5.42 (m, 1.6H), 4.51 (s, 2H), 4.37 (m, 0.6H), 3.95 (m, 1H), 3.81 (m, 0.5H), 3.69-3.46 (m, 3H), 3.32 (m, 1H), 2.37-1.79 (m, 8H), 1.69-1.52 (m, 5H), 1.19-1.10 (m, 9H), 1.06 (d, *J* = 6.9 Hz, 3H), 0.88-0.86 (m, 9H), 0.05 (m, 6H). R_f = 0.05 (9:1 Hex:EtOAc; CAM). HRMS (APCI) *m/z* $[C_{33}H_{60}NO_5Si]^+$ ($M+NH_4$) calcd 578.4241, found 578.4252.

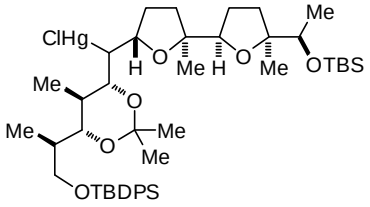

(((2S,2'R,5S,5'S)-5'-((R)-1-((tert-butyldimethylsilyl)oxy)ethyl)-2,5'-dimethyloctahydro-[2,2'-bifuran]-5-yl)((4R,5R,6R)-6-((R)-1-((tert-butyldiphenylsilyl)oxy)propan-2-yl)-2,2,5-trimethyl-1,3-dioxan-4-yl)methyl)mercury(II) chloride (252). Procedure adapted from literature.[31] (2R,3S,4S)-6-((2S,2'R,5S,5'S)-5'-((R)-1-((tert-butyldimethylsilyl)oxy)ethyl)-2,5'-dimethyloctahydro-[2,2'-bifuran]-5-yl)-1-((tert-butyldiphenylsilyl)oxy)-2,4-dimethylhex-5-en-3-ol **251** (5.5 mg, 0.0078 mmol) was dissolved in 1 ml acetone. Chloromercury(II) acetate[32] (6.0 mg, 0.0203 mmol, 2.6 equiv.) and ytterbium(III) trifluoromethane sulfonate (2.0 mg, 0.0032 mmol, 0.4 equiv.) were added at 0 °C. After stirring for 12 h,

[30] Gao, Z.; Li, Y.; Cooksey, J. P.; Snaddon, T. N.; Schunk, S.; Viseux, E. M. E.; McAteer, S. M.; Kocienski, P. J. *Angew. Chem. Int. Ed.* **2009**, *48*, 5022-5025.
[31] Dreher, S. D.; Hornberger, K. R.; Sarraf, S. T.; Leighton, J. L. *Org. Lett.* **2000**, *2*, 3197-3199.
[32] Sarraf, S. T.; Leighton, J. L. *Org. Lett.* **2000**, *2*, 403-405.

the reaction was quenched with sat. $NaHCO_3$ and extracted with DCM. The organic layer was dried with $MgSO_4$ and purified via flash column chromatography to yield 4.2 mg (54%) of (((2S,2'R,5S,5'S)-5'-((R)-1-((tert-butyldimethylsilyl)oxy)ethyl)-2,5'-dimethyloctahydro-[2,2'-bifuran]-5-yl)((4R,5R,6R)-6-((R)-1-((tert-butyldiphenylsilyl)oxy)propan-2-yl)-2,2,5-trimethyl-1,3-dioxan-4-yl)methyl)mercury(II) chloride as a white powder. ^{1}H NMR (400 MHz, $CDCl_3$) δ 7.69-7.64 (m, 4H), 7.44-7.35 (m, 6H), 4.22-4.06 (m, 1H), 3.97 (m, 1H), 3.75-3.38 (m, 3H), 2.03-1.77 (m, 6H), 1.66-1.50 (m, 4H), 1.54 (s, 3H), 1.26 (s, 3H), 1.15 (d, *J* = 7.1 Hz, 3H), 1.12 (m, 9H), 1.05 (s, 9H), 0.98 (d, *J* = 7.0 Hz, 3H), 0.88-0.86 (m, 3H), 0.87 (s, 9H), 0.06 (s, 3H), 0.04 (s, 3H). R_f = 0.30 (9:1 Hex:EtOAc; CAM). HRMS (APCI) *m/z* $[C_{45}H_{74}ClHgO_6Si_2]^+$ (M+H) calcd 1003.44, found 1003.4567.

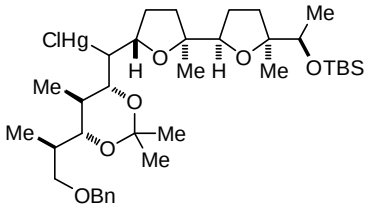

(((4R,5R,6R)-6-((R)-1-(benzyloxy)propan-2-yl)-2,2,5-trimethyl-1,3-dioxan-4-yl)((2S,2'R,5S,5'S)-5'-((R)-1-((tert-butyldimethylsilyl)oxy)ethyl)-2,5'-dimethyloctahydro-[2,2'-bifuran]-5-yl)methyl)mercury(II) chloride (S23). (2R,3S,4S)-1-(benzyloxy)-6-((2S,2'R,5S,5'S)-5'-((R)-1-((tert-butyldimethylsilyl)oxy)ethyl)-2,5'-dimethyloctahydro-[2,2'-bifuran]-5-yl)-2,4-dimethylhex-5-en-3-ol **S22** (3.0 mg, 0.0054 mmol) was dissolved in 1 ml acetone. Chloromercury(II) acetate (2.4 mg, 0.0081 mmol, 1.5 equiv.) and ytterbium(III) trifluoromethane sulfonate (0.3 mg, 0.0005 mmol, 0.1 equiv.) were added at 0 °C. After stirring for 12 h, the reaction was quenched with sat. $NaHCO_3$ and extracted with DCM. The organic layer was dried with $MgSO_4$ and purified via flash column chromatography to yield 0.8 mg (17%) of (((4R,5R,6R)-6-((R)-1-(benzyloxy)propan-2-yl)-2,2,5-trimethyl-1,3-dioxan-4-yl)((2S,2'R,5S,5'S)-5'-((R)-1-((tert-butyldimethylsilyl)oxy)ethyl)-2,5'-dimethyloctahydro-[2,2'-bifuran]-5-yl)methyl)mercury(II) chloride as a white powder. ^{1}H NMR (400 MHz, $CDCl_3$) δ 7.33 (m, 5H), 4.51 (m, 2H), 4.39 (m, 0.6H), 4.12-3.29 (m, 7H), 2.06-0.76 (m, 39H), 0.06 (m, 6H). R_f = 0.30 (4:1 Hex:EtOAc; CAM). LRMS (ESI/APCI) *m/z* $[C_{36}H_{61}HgO_6Si]^+$ (M-Cl) calcd 819.4, found 819.3.

Model Reactions

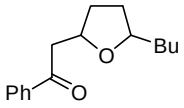

2-(5-butyltetrahydrofuran-2-yl)-1-phenylethanone (197). Trimethyl((1-phenylvinyl)oxy)silane **143** (38.5 mg, 0.20 mmol) and 5-butyltetrahydrofuran-2-yl benzoate **196** (49.7 mg, 0.20 mmol) were dissolved in 2 ml DCM and the reaction was cooled to -78 °C. Trifluoromethanesulfonimide (14.0 mg, 0.05 mmol, 0.25 equiv.) in 2 ml DCM was added and the reaction was stirred for 1 h. The reaction was quenched with sat. $NaHCO_3$ and warmed to 23 °C. The reaction was extracted with DCM 3x and the organic layer was dried with $MgSO_4$, concentrated, and purified via flash column chromatography to yield 40.9 mg (83%, 1.3:1 dr) of 2-(5-butyltetrahydrofuran-2-yl)-1-phenylethanone. Spectral data matches literature.[33] ^{1}H NMR (300 MHz, $CDCl_3$) δ 7.99-7.95 (m, 2H), 7.58-7.40 (m, 3H), 4.52 (m, 0.5H), 4.36 (m, 0.5H), 3.96 (m, 0.44H), 3.82 (m, 0.52H), 3.42 (m, 1H), 3.03 (m, 1H), 2.27-1.94 (m, 2H), 1.63-1.25 (m, 8H), 0.89 (m, 3H). R_f = 0.29 (9:1 Hex:EtOAc; UV, CAM).

[33] Zhang, Y.; Reynolds, N. T; Manju, K.; Rovis, T. *J. Am. Chem. Soc.* **2002**,*124*, 9720-9721.

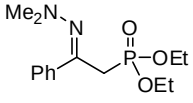

Diethyl (2-(2,2-dimethylhydrazono)-2-phenylethyl)phosphonate (210). 1,1-dimethyl-2-(1-phenylethylidene)hydrazine **209**[34] (108.8 mg, 0.68 mmol) was dissolved in THF. The reaction was cooled to -78 °C and nBuLi (0.42 ml, 0.68 mmol, 1.0 equiv., 1.6 M in Hex) was added. After 10 min, diethyl chlorophosphate (0.1 ml, 0.68 mmol, 1.0 equiv.) was added. The reaction was allowed to stir and warm to 23 °C over 12 h. The reaction was quenched with H_2O and extracted with EtOAc 3x. The organic layer was dried with $MgSO_4$, concentrated, and purified via flash column chromatography to yield 127.2 mg (64%) of diethyl (2-(2,2-dimethylhydrazono)-2-phenylethyl)phosphonate. ^{1}H NMR (300 MHz, $CDCl_3$) δ 7.54-7.51 (m, 2H), 7.32-7.26 (m, 3H), 5.34 (m, 2H), 4.25-4.10 (m, 4H), 2.42 (s, 6H), 1.30 (m, 6H). ^{31}P NMR (75 MHz, $CDCl_3$) δ 4.36. R_f = 0.23 (EtOAc; $KMnO_4$). LRMS (ESI/APCI) *m/z* $[C_{14}H_{24}N_2O_3P]^+$ (M+H) calcd 299.1, found 299.1.

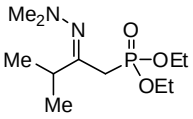

Diethyl (2-(2,2-dimethylhydrazono)-3-methylbutyl)phosphonate (213). 1,1-dimethyl-2-(3-methylbutan-2-ylidene)hydrazine **212** (127.2 mg, 1.0 mmol) was dissolved in THF. The reaction was cooled to -78 °C and nBuLi (0.63 ml, 1.0 mmol, 1.0 equiv., 1.6 M in Hex) was added. After 10 min, diethyl chlorophosphate (0.15 ml, 1.0 mmol, 1.0 equiv.) was added. The reaction was allowed to stir and warm to 23 °C over 12 h. The reaction was quenched with H_2O and extracted with EtOAc 3x. The organic layer was dried with $MgSO_4$, concentrated, and purified via flash column chromatography to yield 138.0 mg (53%) of diethyl (2-(2,2-dimethylhydrazono)-3-methylbutyl)phosphonate. ^{1}H NMR (300 MHz, $CDCl_3$) δ 4.89 (m, 2H), 4.08 (m, 4H), 2.67 (s, 6H), 2.42 (m, 1H), 1.32 (m, 6H), 1.12 (d, J = 6.8 Hz, 6H). ^{31}P NMR (75 MHz, $CDCl_3$) δ 4.91. R_f = 0.16 (1:1 Hex:EtOAc; $KMnO_4$). LRMS (ESI/APCI) *m/z* $[C_{11}H_{26}N_2O_3P]^+$ (M+H) calcd 265.2, found 265.1.

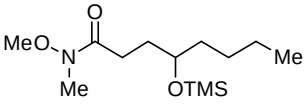

N-methoxy-N-methyl-4-((trimethylsilyl)oxy)octanamide (232). N,O-dimethyl hydroxylamine·HCl (2.61 g, 26.8 mmol, 2 equiv.) was suspended in DCM and cooled to 0 °C. Trimethyl aluminum (13.4 mL, 26.8 mmol, 2M in PhMe, 2 equiv.) was added very slowly. The reaction was stirred for 20 min and resulted in a clear solution. γ-octalactone (2 mL, 13.4 mmol) was added slowly via syringe. After stirring for 1h, the reaction was quenched with 1M HCl and extracted with DCM 3x. The organic layer was dried with $MgSO_4$ and concentrated. The residue was dissolved in DCM. Imidizole (2.28g, 33.5 mmol, 2.5 equiv.) was added and then chlorotrimethylsilane (2 mL, 16.9 mmol, 1.25 equiv.) was added slowly via syringe. After 5 min, a spatula tip of 4-(dimethylamino)pyridine was added and thre reaction was stirred. The reaction was quenched with water and the organic layer was seperated and dried with MgSO4. The residue was purified by flash column chromatography to yield 2.75 g of N-methoxy-N-methyl-4-((trimethylsilyl)oxy)octanamide (74%) as a clear oil. ^{1}H NMR (400 MHz, $CDCl_3$) δ 3.70 (m, 1H), 3.68 (s, 3H), 3.17 (s, 3H), 2.50 (m, 2H), 1.84 (m, 1H), 1.65 (m, 1H), 1.49-1.23 (6H), 0.89 (m, 3H), 0.11 (s, 9H). R_f = 0.47 (2:1 Hex:EtOAc). IR (ATR) 2956, 2861, 1668, 1380, 1249, 1063, 999, 837 cm^{-1}. LRMS (APCI/ESI) *m/z* $[C_{13}H_{30}NO_3Si]^+$ (M+H) calcd 276.2, found 276.2.

[34] Newkome, G. R.; Fishel, D. L. *Org. Syn.* **1970**, *50*, 102-105.

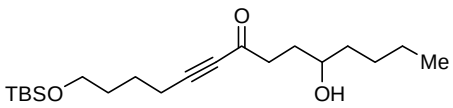

1-((tert-butyldimethylsilyl)oxy)-10-hydroxytetradec-5-yn-7-one (235). Tert-butyl(hex-5-yn-1-yloxy)dimethylsilane (63.7 mg, 0.300 mmol) was dissolved in 2 mL THF and cooled to -78 °C. n-BuLi (1.4 M, 0.22 mL, 0.315 mmol, 1.05 equiv) was added and the reaction was stirred for 30 min. A solution of $BF_3 \cdot OEt_2$ in THF (0.315 mmol, 1.05 equiv) was added and the reaction was stirred for 30 min. γ-octalactone (42.7 mg, 0.300 mmol) was dissolved in 2 mL THF and added to the reaction mixture. After stirring for 4 h, the reaction was quenched with sat NH_4Cl, extracted with Et_2O 2x, dried with $MgSO_4$, and concentrated. The resulting residue was purified via column chromatography that resulted in 44.4 mg of 1-((tert-butyldimethylsilyl)oxy)-10-hydroxytetradec-5-yn-7-one (41%) as a clear oil. ^{1}H NMR (400 MHz, $CDCl_3$) δ 3.63 (t, *J* = 5.8 Hz, 2H), 3.62 (s, 1H), 2.69 (m, 2H), 2.40 (t, *J* = 6.8 Hz, 2H), 1.86 (m, 1H), 1.71 (m, 1H), 1.6 (m, 4H), 1.45 (m, 3H), 1.32 (m, 4H), 0.90 (m, 3H), 0.89 (s, 9H), 0.05 (s, 6H). ^{13}C NMR (100 MHz, $CDCl_3$) δ 188.4, 94.5, 81.0, 71.1, 62.4, 42.0, 37.3, 31.8, 31.2, 27.8, 25.9, 24.3, 22.7, 18.8, 14.0, -5.3. R_f = 0.30 (4:1 Hex:EtOAc). IR (ATR) 3570, 2954, 2929, 2858, 1673, 1471, 1255, 1106, 837, 776 cm^{-1}. LRMS (APCI/ESI) *m/z* $[C_{20}H_{37}O_2Si]^+$ (M-OH) calcd 337.2, found 337.2 and *m/z* $[C_{21}H_{41}O_3Si]^+$ (M-OH+MeOH) calcd 369.3, found 369.3.

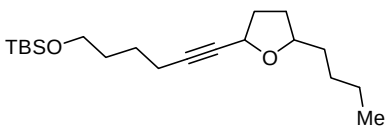

Tert-butyl((6-(5-butyltetrahydrofuran-2-yl)hex-5-yn-1-yl)oxy)dimethylsilane (236). 1-((tert-butyldimethylsilyl)oxy)-10-hydroxytetradec-5-yn-7-one **235** (44.0 mg, 0.124 mmol) was dissolved in 2mL DCM and cooled to -78 °C. Triethylsilane (0.05 mL, 0.590 mmol, 4.7 equiv) was added and the reaction was stirred for 20 min. A solution of $BF_3 \cdot OEt_2$ in THF (0.372 mmol, 0.372 mmol, 3.0 equiv) was added and the reaction was warmed to 0 °C over 30 min. The reaction was quenched with sat NaHCO3 and extracted with DCM 2x. The organic layer was dried with MgSO4, concentrated, and purified via column chromatography to yield 7.1 mg of tert-butyl((6-(5-butyltetrahydrofuran-2-yl)hex-5-yn-1-yl)oxy)dimethylsilane (17 %) as a clear oil. ^{1}H NMR (400 MHz, $CDCl_3$) δ 4.64 (diastereomer a, ddd, *J* = 6.4, 1.8, 1.8 Hz, 0.34 H), 4.47 (diastereomer b, ddd, *J* = 6.3, 1.9, 1.9 Hz, 0.46 H), 4.05 (diastereomer a, m, 0.38 H), 3.79 (diastereomer b, m, 0.55 H), 3.61 (t, J = 6.1 Hz, 2H), 2.22 (ddd, *J* = 6.9, 1.7, 1.7 Hz, 2H), 2.14-1.88 (m, 3H), 1.72-1.25 (m, 11H), 0.89 (s, 9H), 0.89 (m, 3H), 0.04 (s, 6H). ^{13}C NMR (100 MHz, $CDCl_3$) δ 84.9, 84.8, 80.6, 80.4, 80.1, 78.9, 68.2, 68.0, 62.7, 35.7, 35.3, 33.8, 33.6, 32.0, 31.2, 31.1, 28.4, 28.3, 26.0, 25.1, 25.0, 22.8, 22.8, 18.6, 18.6, 18.3, 14.0, -5.3. R_f = 0.21 (20:1 Hex:EtOAc). IR (ATR) 2954, 2929, 2858, 1463, 1255, 1106, 836, 776 cm^{-1}. LRMS (APCI/ESI) *m/z* $[C_{20}H_{39}O_2Si]^+$ (M+H) calcd 339.3, found 339.2.

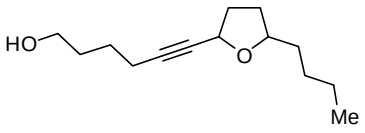

6-(5-butyltetrahydrofuran-2-yl)hex-5-yn-1-ol (237). Isolated from above reaction 5.8 mg (21 %) as a clear oil. ^{1}H NMR (400 MHz, $CDCl_3$) δ 4.63 (diastereomer a, ddd, *J* = 6.4, 1.9, 1.9 Hz, 0.48 H), 4.47 (diastereomer b, ddd, *J* = 6.2, 1.8, 1.8 Hz, 0.48 H), 4.05 (diastereomer a, m, 0.53 H), 3.79 (diastereomer b, m, 0.60 H), 3.66 (t, *J* = 6.2 Hz, 2H), 2.25 (ddd, *J* = 6.9, 1.6, 1.6 Hz, 2H), 2.18-1.88 (m, 3H), 1.71-1.25 (m, 12 H), 0.89 (m, 3H). ^{13}C NMR (100 MHz, $CDCl_3$) δ 84.6, 84.5, 80.8, 80.7, 80.1, 79.0, 68.1, 67.9, 62.4, 62.4, 35.7, 35.3, 33.8, 33.6, 31.8, 31.2, 31.1, 28.4, 28.3, 24.8, 24.8, 22.8, 22.8, 18.6, 18.6, 14.0. R_f = 0.35 (1:1 Hex:EtOAc). IR (ATR) 3408, 2931, 2861, 1457, 1332, 1027, 668 cm^{-1}. LRMS (APCI/ESI) *m/z* $[C_{14}H_{25}O_2]^+$ (M+H) calcd 225.2, found 225.1.

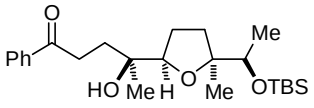

(S)-4-((2R,5S)-5-((R)-1-((tert-butyldimethylsilyl)oxy)ethyl)-5-methyltetrahydrofuran-2-yl)-4-hydroxy-1-phenylpentan-1-one (241). Dried cerium trichloride (12.9 mg, 0.0525 mmol, 1.4 equiv.) was added to an oven dried 10 mL round bottom flask in an inert air glovebox. After sealing and removing, the cerium trichloride was suspended in 1 mL THF and cooled to -78 °C. Phenyl lithium (0.03 mL, 0.0525 mmol, 1.75 M in dibutyl ether, 1.4 equiv.) was added and stirred for 15 min. (2S,2'R,5'S)-5'-((R)-1-((tert-butyldimethylsilyl)oxy)ethyl)-2,5'-dimethylhexahydro-[2,2'-bifuran]-5(2H)-one **184** (13.1 mg, 0.038 mmol) in 0.5 mL THF was added and the reaction was stirred for 30 min. The reaction was quenched at -78 °C with sat. NH_4Cl, allowed to warm, and extracted 3x with Et_2O. The organic layers were combined, dried with $MgSO_4$, filtered, and concentrated. The resultant residue was purified by flash column chromatography to yield 7.0 mg of mostly (S)-4-((2R,5S)-5-((R)-1-((tert-butyldimethylsilyl)oxy)ethyl)-5-methyltetrahydrofuran-2-yl)-4-hydroxy-1-phenylpentan-1-one (43%) as a clear oil. ^{1}H NMR (300 MHz, $CDCl_3$) δ 7.99 (m, 2H), 7.54 (m, 1H), 7.43 (m, 2H), 3.86 (t, *J* = 7.3 Hz, 1H), 3.87 (q, *J* = 6.3 Hz, 1H), 3.24 (ddd, *J* = 17.2, 9.8, 5.3 Hz, 1H), 3.05 (ddd, *J* = 17.2, 9.9, 5.7 Hz, 1H), 2.33-1.00) (m, 5H), 1.21 (s, 3H), 1.13 (m, 6H), 0.90-0.82 (m, 2H), 0.88 (s, 9H), 0.07 (s, 3H), 0.05 (s, 3H). R_f = 0.36 (4:1 Hex:EtOAc). HRMS (APCI/ESI) *m/z* $[C_{24}H_{39}O_3Si]^+$ (M-H_2O) calcd 403.2668, found 403.2668.

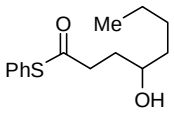

S-phenyl 4-hydroxyoctanethioate (243). Procedure adapted from literature.[35] In an oven dried 100 mL flask, benzene thiol (0.88 mL, 8.6 mmol, 2.5 equiv.) was added to 20 mL of DCM. The reaction flask was cooled to 0 °C and trimethyl aluminum (4.3 mL, 8.6 mmol, 2 M in PhMe, 2.5 equiv.) was added very slowly. The reaction was stirred for 10 minutes at 0 °C, the ice bath was removed and the reaction was stirred for another 10 minutes, and then the reaction was cooled back to 0 °C. γ-octalactone (0.5 mL, 3.45 mmol) was added slowly and the reaction was stirred overnight and allwed to warm to 23 °C. The reaction mixture was cooled to -78 °C and diluted with 20 mL of Et_2O. 12 mL of 1 M HCl was added and the reaction was allowed to warm to 0 °C. The reaction was extracted with Et_2O 3x, and the organic layer was washed with 1 M HCl 1x, sat. $NaHCO_3$ 1x, and sat. brine 1x. The organic layer was dried with $MgSO_4$, filtered, loaded onto Celite and purified via flash column chromatography to yield 261 mg (28%) of S-phenyl 4-hydroxyoctanethioate as a clear oil. [Caution: this compound is acid sensitive and decomposes in $CDCl_3$ over a few hours]. ^{1}H NMR (400 MHz, C_6D_6) δ 7.43-7.40 (m, 2H), 7.08-6.99 (m, 3H), 3.26 (bs, 1H), 2.60 (m, 2H), 1.68 (m, 1H), 1.53 (m, 1H), 1.23-1.05 (m, 7H), 0.85 (m, 3H). ^{13}C NMR (100 MHz, C_6D_6) δ 196.5, 134.8, 129.3, 129.2, 128.7, 70.5, 40.3, 37.5, 33.0, 28.0, 23.0, 14.2. R_f = 0.26 (4:1 Hex:EtOAc). IR (ATR) 3398, 2955, 2928, 2859, 1705, 1441, 1023, 989, 745, 706 cm^{-1}. LRMS (APCI/ESI) *m/z* $[C_{14}H_{19}OS]^+$ (M-H_2O) calcd 235.1, found 234.9.

[35] Gierasch, T. M.; Shi, Z.; Verdine, G. L. *Org. Lett.* **2003**, *5*, 621-624.

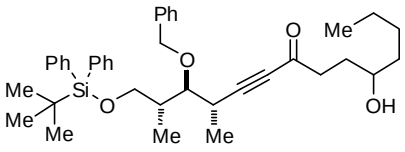

(2R,3S,4S)-3-(benzyloxy)-1-((tert-butyldiphenylsilyl)oxy)-10-hydroxy-2,4-dimethyltetradec-5-yn-7-one (244). Procedure adapted from literature.[36] In a 10 mL round bottom flask, [1,1'-Bis(diphenylphosphino)ferrocene]dichloropalladium (II) (2.4 mg, 0.003 mmol, 10 mol %), tri-(2-furyl)phosphine (1.7 mg, 0.0075 mmol, 25 mol %), and copper(I) iodide (10.3 mg, 0.054 mmol, 2 equiv.) was added in an inert air glove box. The reaction vessel was sealed, removed from the glove box, and 1.5 mL of DMF was added. In a vial, (((2R,3S,4S)-3-(benzyloxy)-2,4-dimethylhex-5-yn-1-yl)oxy)(tert-butyl)diphenylsilane **239** (12.7 mg, 0.027 mmol), S-phenyl 4-hydroxyoctanethioate **243** (8.8 mg, 0.035 mmol, 1.3 equiv.), and *N*,*N*-diisopropylethylamine (6.9 mg, 0.053mmol, 2 equiv.) was added to a vial and dissolved in 0.5 mL DMF. After adding this solution to the reaction, the reaction was heated to 60 °C and stirred overnight. The reaction was cooled to 23 °C, Celite was added, and stirred for 30 min. Et_2O and H_2O was added and the solution was filtered through a pad of Celite. The filtrate was extracted with Et_2O 3x. The organic layers were combined, washed with 10% LiCl 2x, dried with $MgSO_4$, and concentrated. The residue was purified by preparative thin layer chromatography to yield 2.8 mg of (2R,3S,4S)-3-(benzyloxy)-1-((tert-butyldiphenylsilyl)oxy)-10-hydroxy-2,4-dimethyltetradec-5-yn-7-one (17%) as a clear oil. ^{1}H NMR (300 MHz, C_6D_6) δ 7.76-7.72 (m, 4H), 7.28-7.09 (m, 11H), 4.53 (d, *J* = 11.2 Hz, 1H), 4.46 (d, *J* = 11.4 Hz, 1H), 3.80 (m, 2H), 3.24 (m, 2H), 2.81 (m, 1H), 2.53 (t, *J* = 7.4 Hz, 2H), 2.11 (m, 1H), 1.88-1.50 (m, 2H), 1.40-0.75 (m, 7H), 1.18 (s, 9H), 1.12 (d, *J* = 7.0 Hz, 3H), 1.02 (d, *J* = 7.0 Hz, 3H), 0.84 (m, 3H). R_f = 0.08 (9:1 Hex:EtOAc). IR (ATR) 2957, 2929, 2857, 2210, 1775, 1671, 1456, 1185, 1112, 1069, 702 cm^{-1}. HRMS (APCI/ESI) *m/z* $[C_{39}H_{56}NO_4Si]^+$ (M+NH_4) calcd 630.3979, found 630.3983.

[36] Magdziak, D.; Lalic, G.; Lee, H. M.; Fortner, K. C.; Aloise, A. D.; Shair, M. D. *J. Am. Chem. Soc.* **2005**, *127*, 7284-7285.

^{1}H NMR and ^{13}C NMR Spectra of Selected Compounds

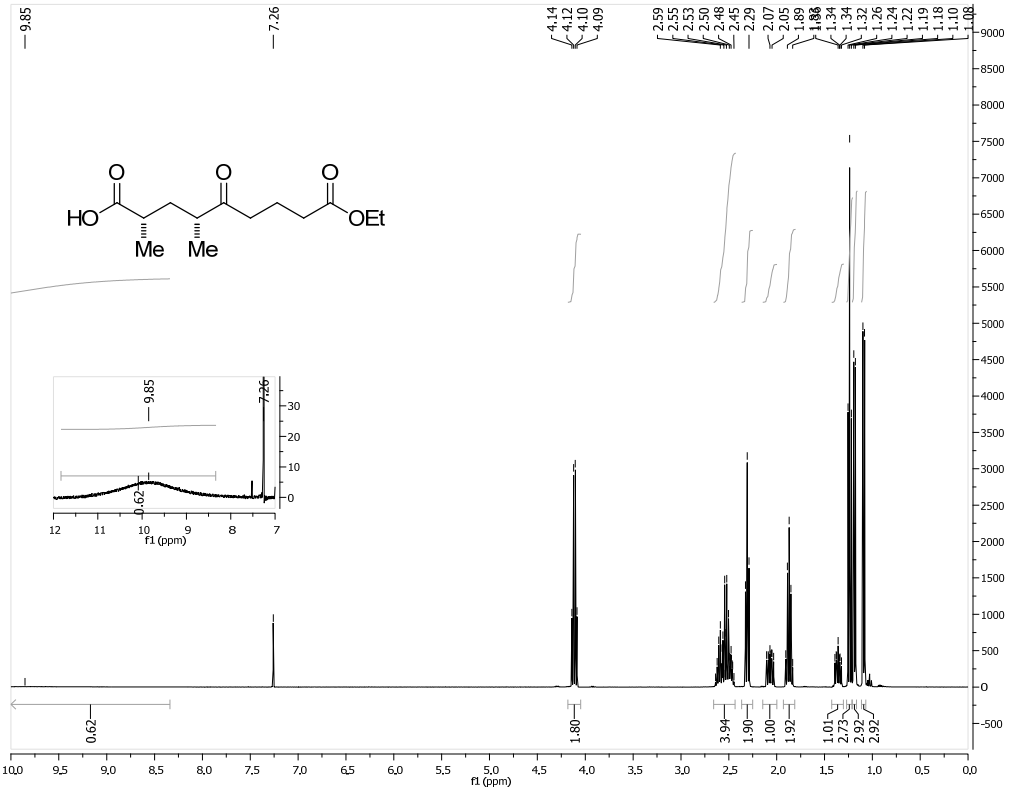

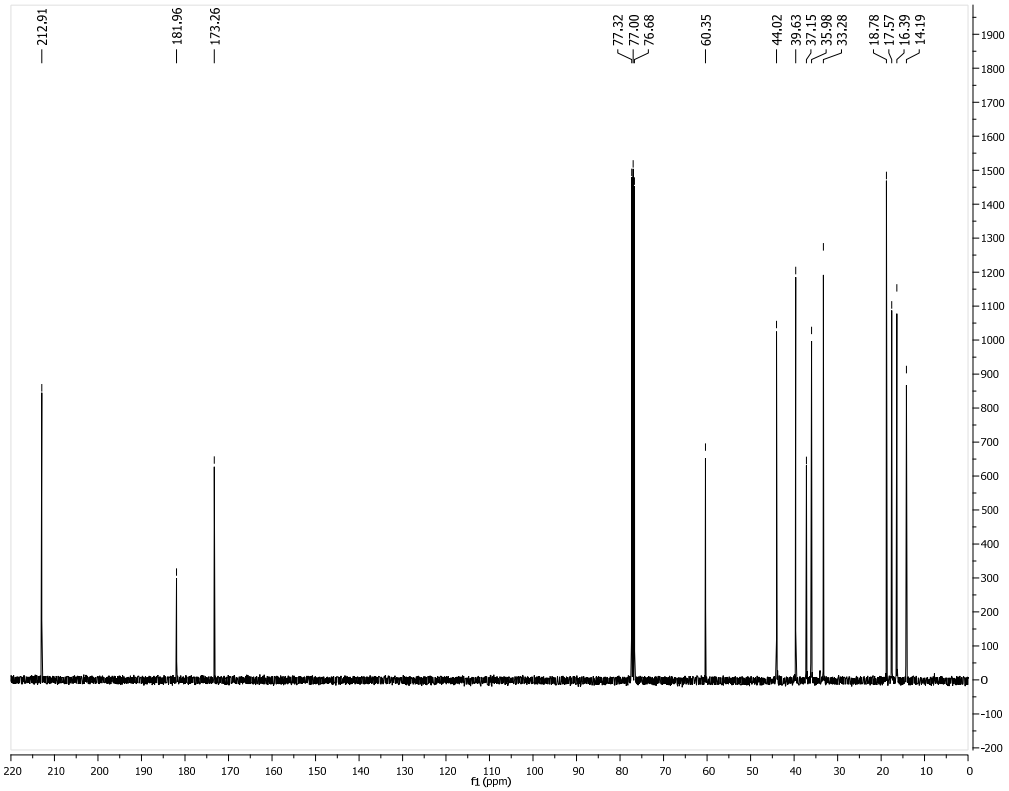

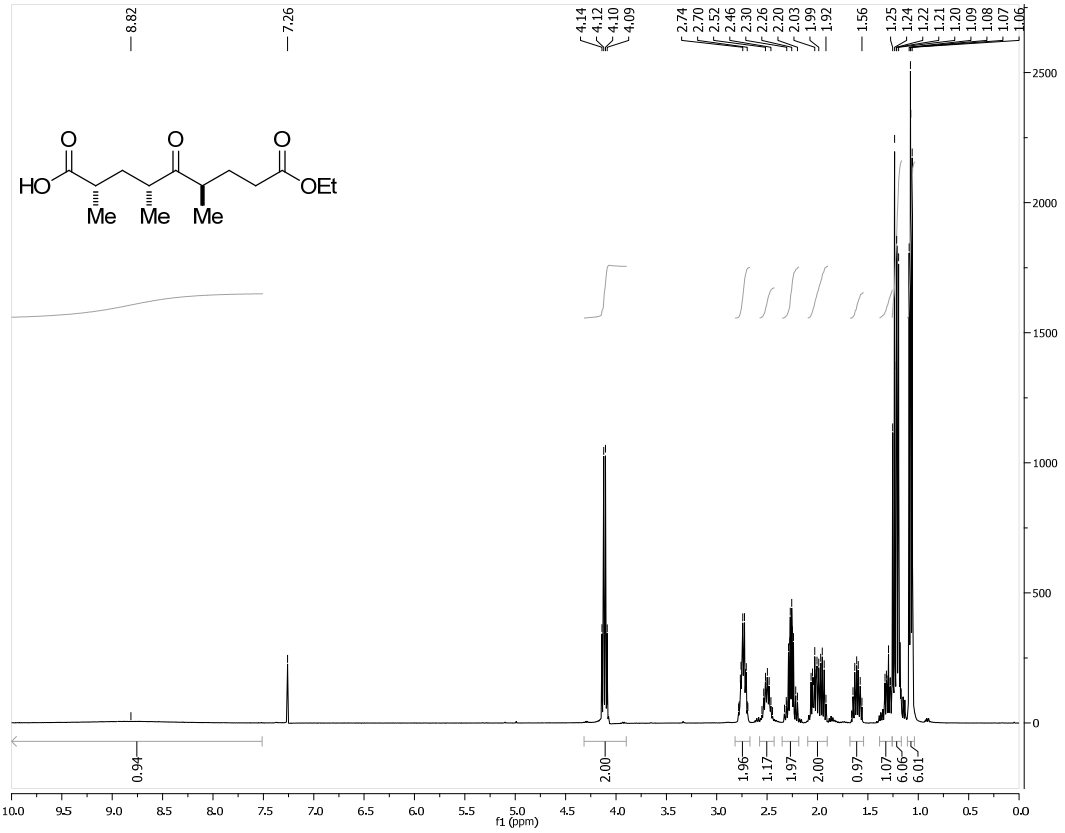
8.82
7.26
4.14
4.12
4.10
4.09
2.74
2.70
2.52
2.46
2.30
2.26
2.20
2.03
1.99
1.92
1.56
1.25
1.24
1.22
1.21
1.20
1.09
1.08
1.07
1.06
HO
O
O
O
OEt
Me
Me
Me
0.94
2.00
1.96
1.17
1.97
2.00
0.97
1.07
6.06
6.01
f1 (ppm)

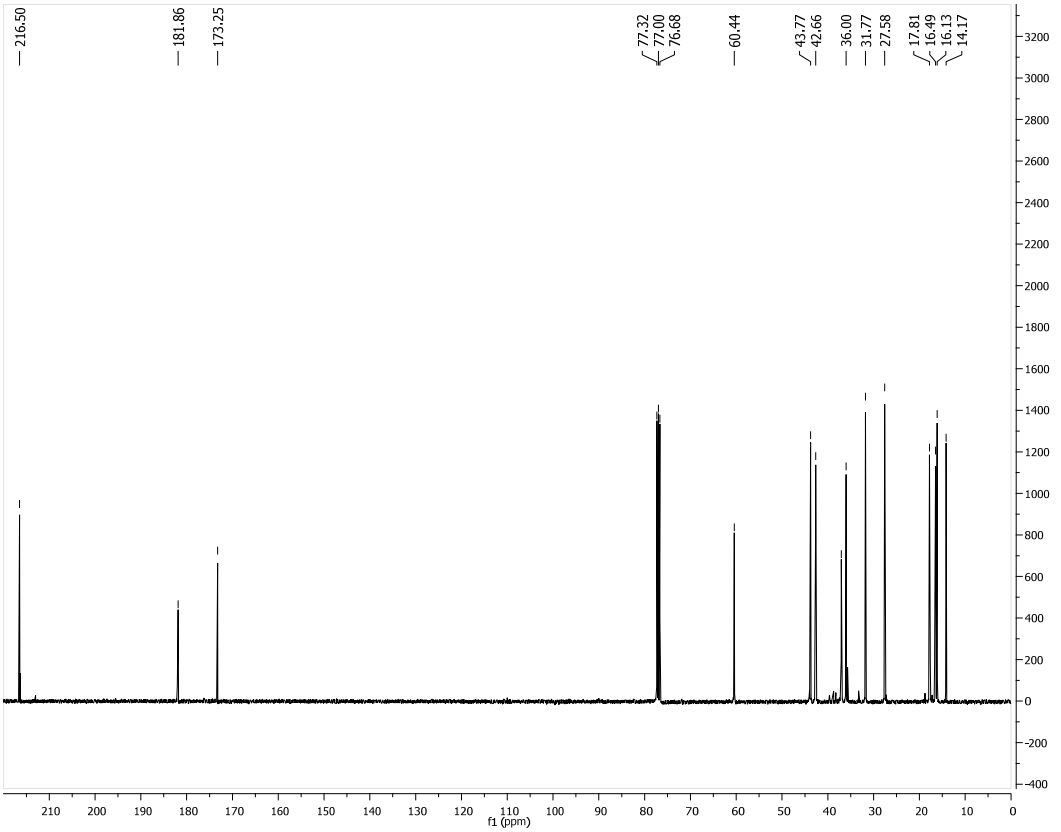
216.50
181.86
173.25
77.32
77.00
76.68
60.44
43.77
42.66
36.00
31.77
27.58
17.81
16.49
16.13
14.17
f1 (ppm)

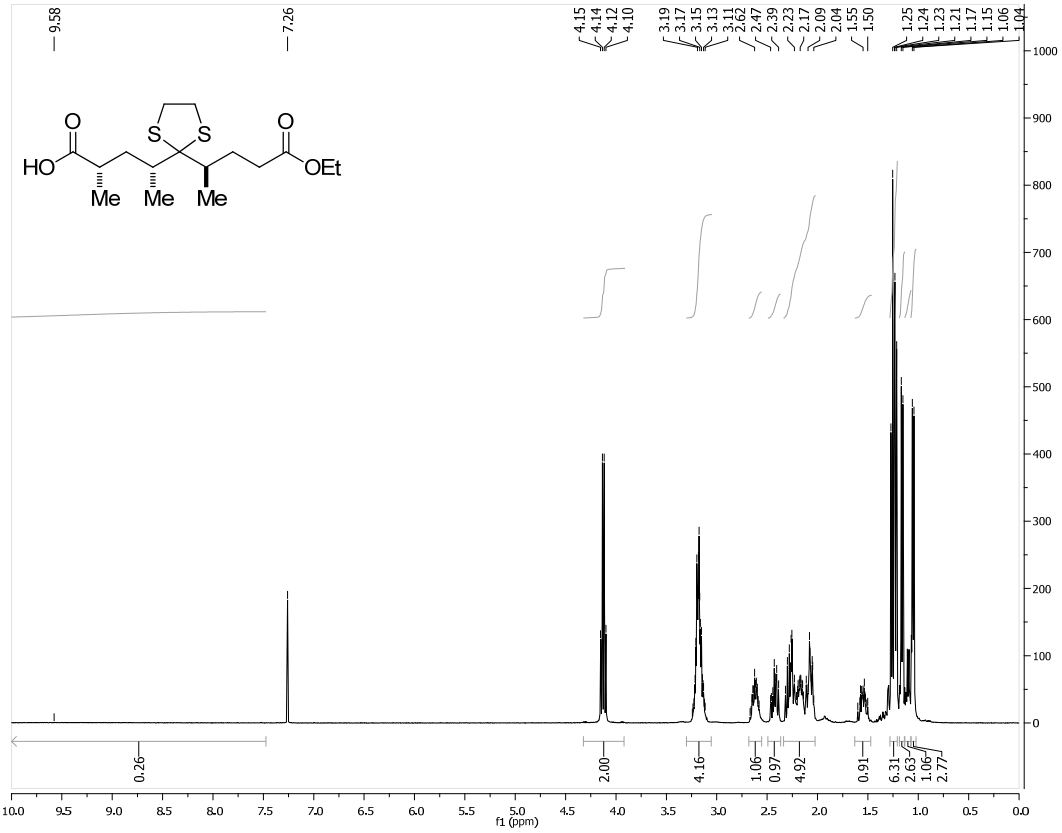
9.58
7.26
4.15
4.14
4.12
4.10
3.19
3.17
3.15
3.13
3.11
2.62
2.47
2.39
2.23
2.17
2.09
2.04
1.55
1.50
1.25
1.24
1.23
1.21
1.17
1.15
1.06
1.04
HO
O
S
S
O
OEt
Me
Me
Me
0.26
2.00
4.16
1.06
0.97
4.92
0.91
6.31
2.63
1.06
2.77
f1 (ppm)

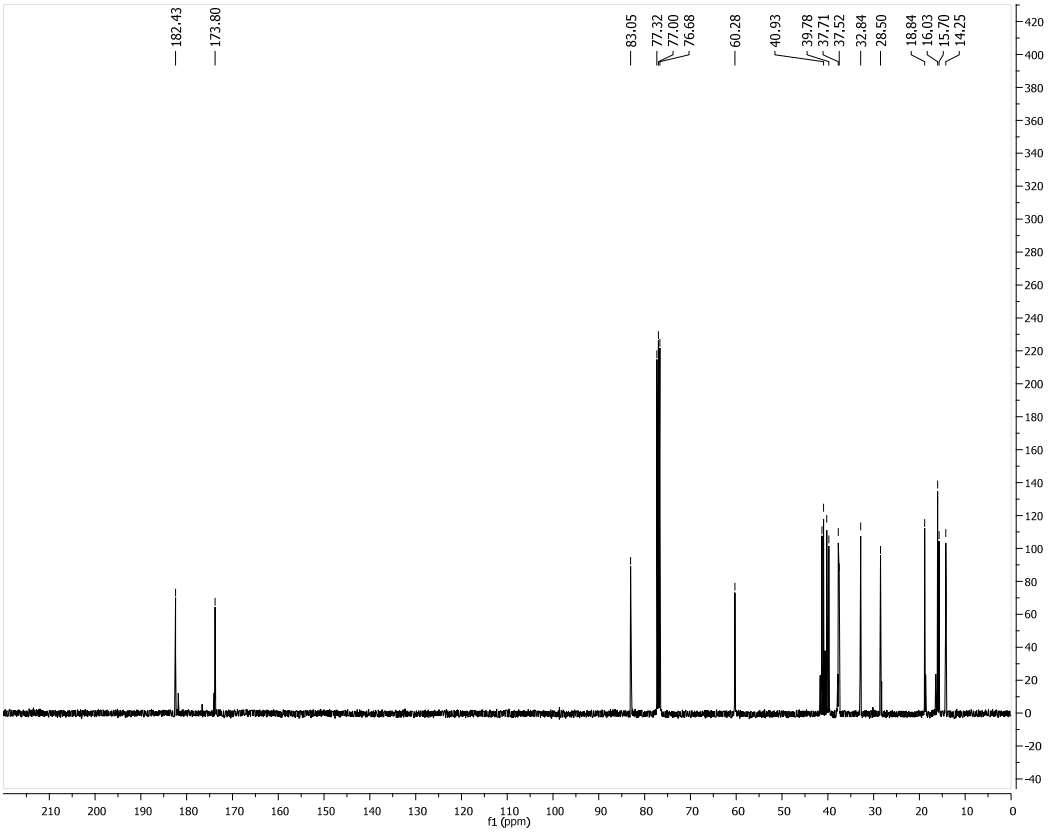
182.43
173.80
83.05
77.32
77.00
76.68
60.28
40.93
39.78
37.71
37.52
32.84
28.50
18.84
16.03
15.70
14.25
f1 (ppm)

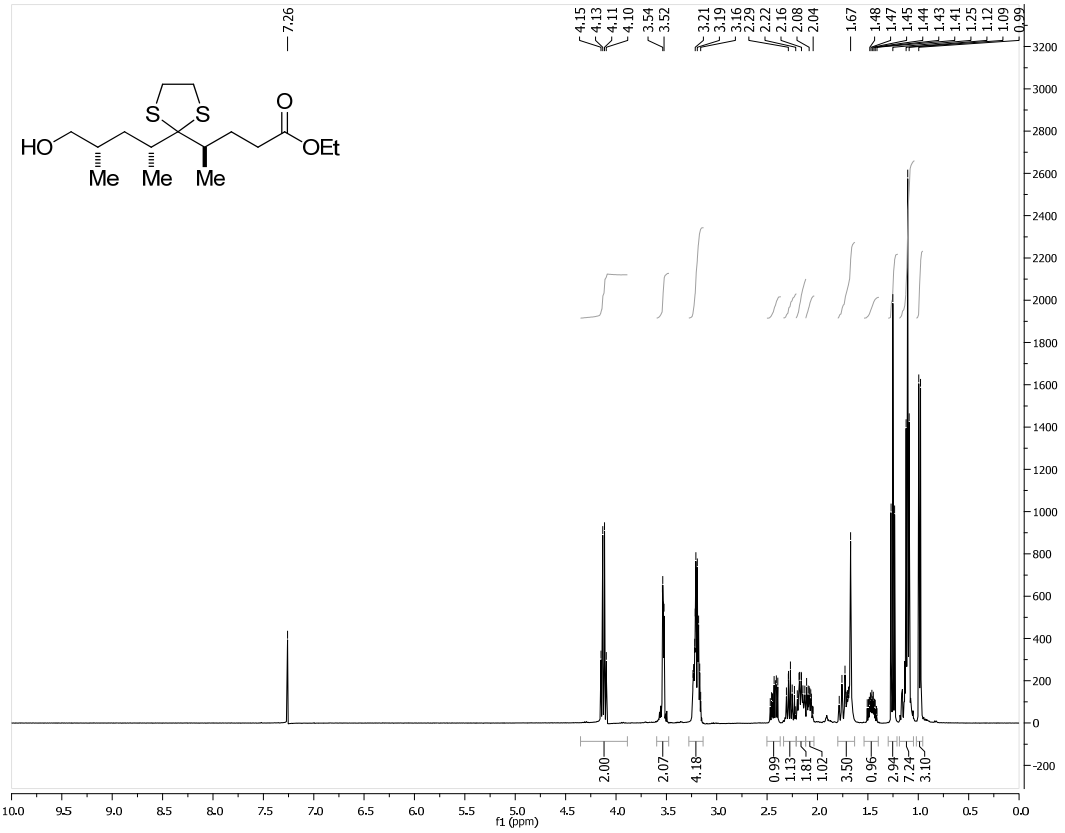
7.26
4.15
4.13
4.11
4.10
3.54
3.52
3.21
3.19
3.16
2.29
2.22
2.16
2.08
2.04
1.67
1.48
1.47
1.45
1.44
1.43
1.41
1.25
1.12
1.09
0.99
HO
Me
Me
Me
S
S
O
OEt
2.00
2.07
4.18
0.99
1.13
1.81
1.02
3.50
0.96
2.94
7.24
3.10
f1 (ppm)

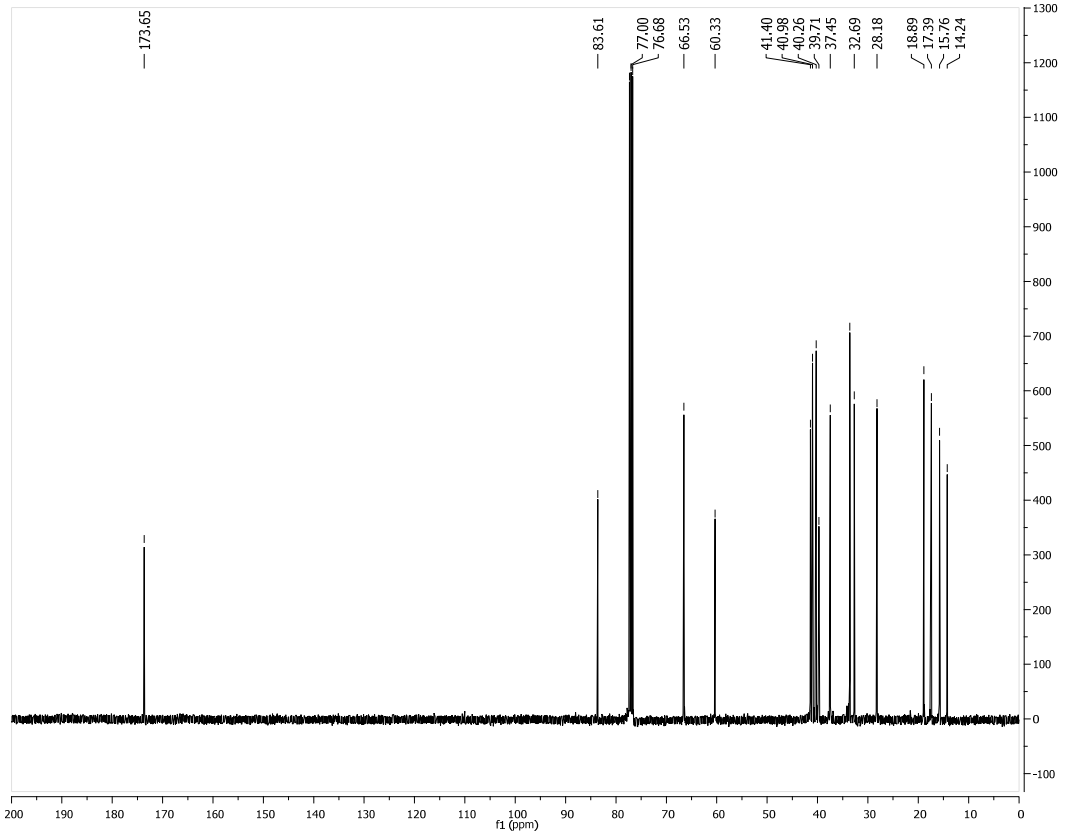
173.65
83.61
77.00
76.68
66.53
60.33
41.40
40.98
40.26
39.71
37.45
32.69
28.18
18.89
17.39
15.76
14.24
f1 (ppm)

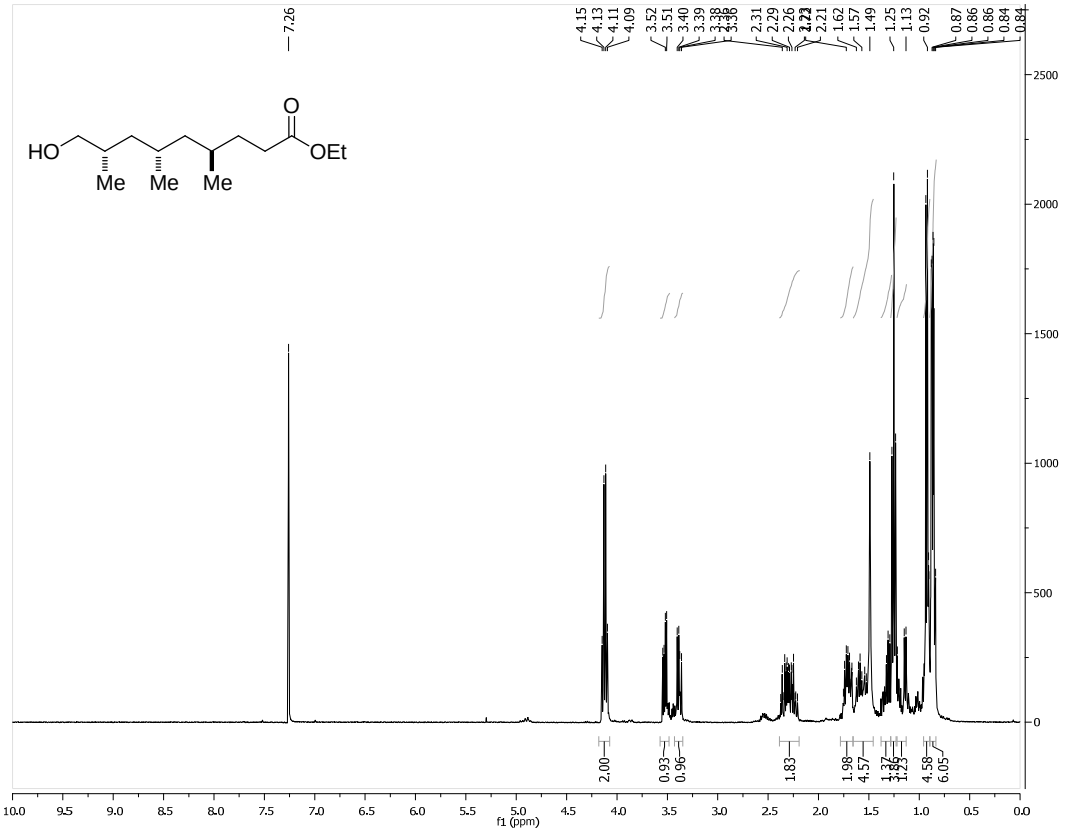
HO
Me
Me
Me
O
OEt
f1 (ppm)

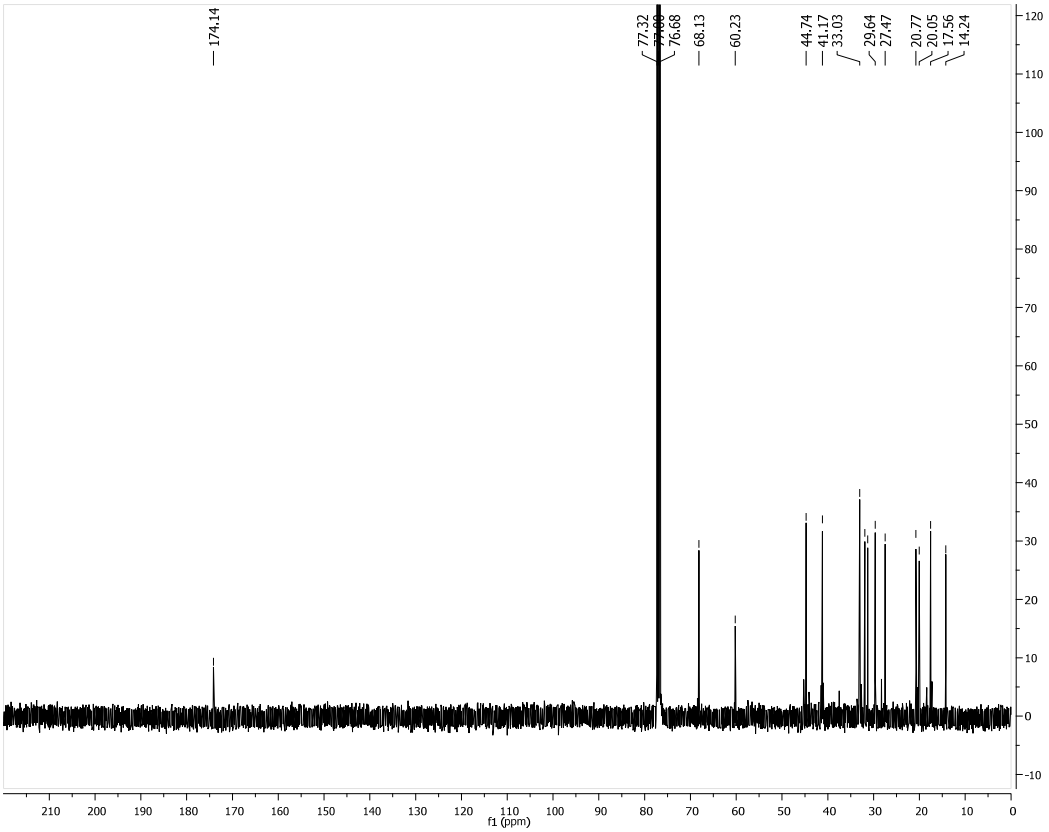
f1 (ppm)

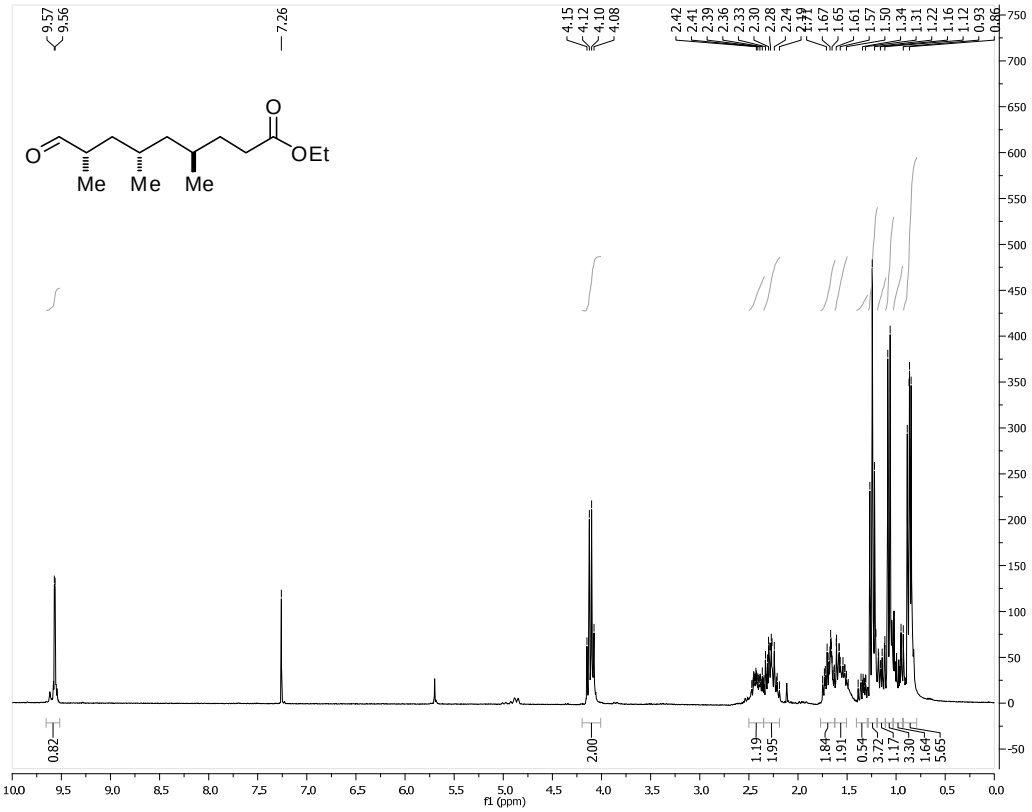
9.57
9.56
7.26
4.15
4.12
4.10
4.08
2.42
2.41
2.39
2.36
2.33
2.30
2.28
2.24
1.67
1.65
1.61
1.57
1.50
1.34
1.31
1.22
1.16
1.12
0.93
0.86
O
O
OEt
Me
Me
Me
0.82
2.00
1.19
1.95
1.84
1.91
0.54
3.72
1.17
3.30
1.64
5.65
f1 (ppm)

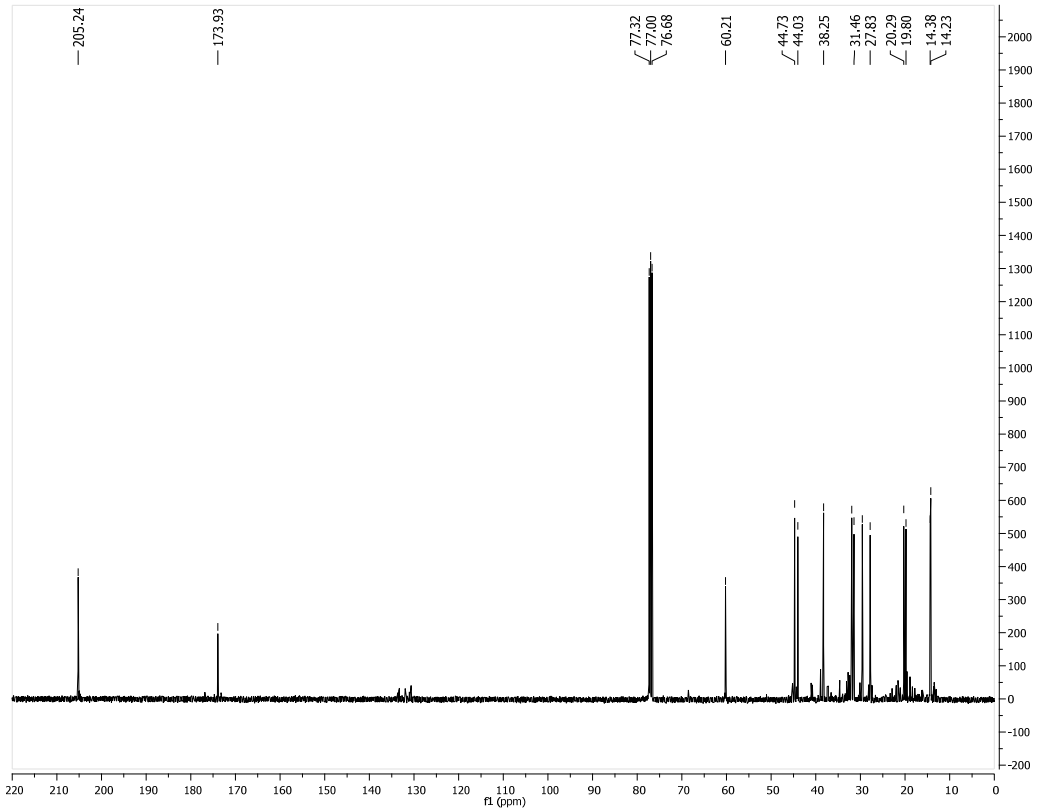
205.24
173.93
77.32
77.00
76.68
60.21
44.73
44.03
38.25
31.46
27.83
20.29
19.80
14.38
14.23
f1 (ppm)

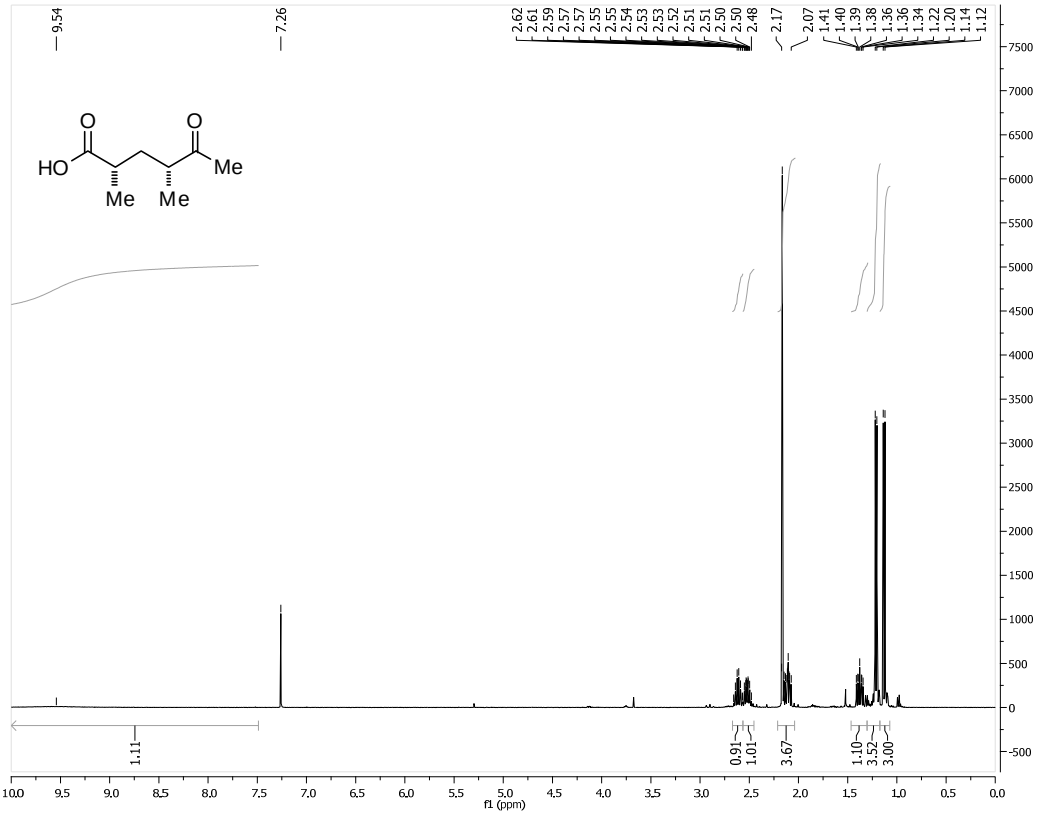
9.54
7.26
2.62
2.61
2.59
2.57
2.57
2.55
2.55
2.54
2.53
2.53
2.52
2.51
2.51
2.50
2.50
2.48
2.17
2.07
1.41
1.40
1.39
1.38
1.36
1.36
1.34
1.22
1.20
1.14
1.12
HO
O
O
Me
Me
Me
1.11
0.91
1.01
3.67
1.10
3.52
3.00
f1 (ppm)

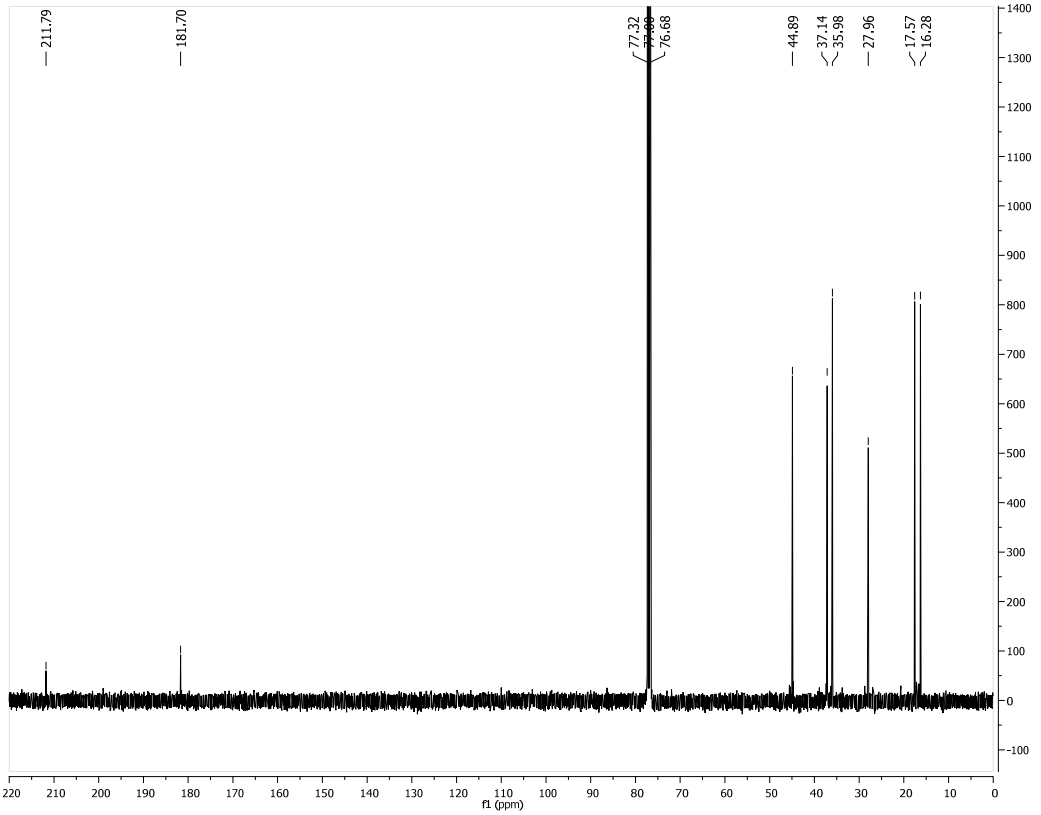
211.79
181.70
77.32
77.00
76.68
44.89
37.14
35.98
27.96
17.57
16.28
f1 (ppm)

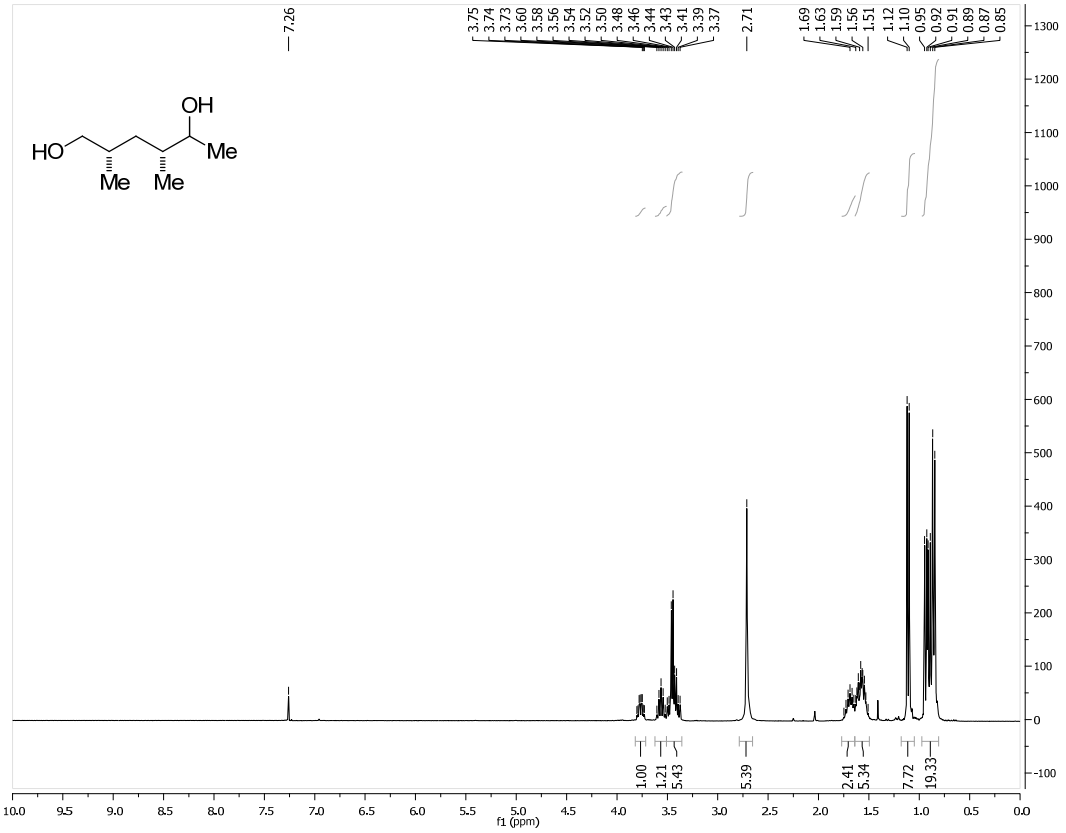
OH
HO
Me
Me
Me
7.26
3.75
3.74
3.73
3.60
3.58
3.56
3.54
3.52
3.50
3.48
3.46
3.44
3.43
3.41
3.39
3.37
2.71
1.69
1.63
1.59
1.56
1.51
1.12
1.10
0.95
0.92
0.91
0.89
0.87
0.85
1.00
1.21
5.43
5.39
2.41
5.34
7.72
19.33
f1 (ppm)

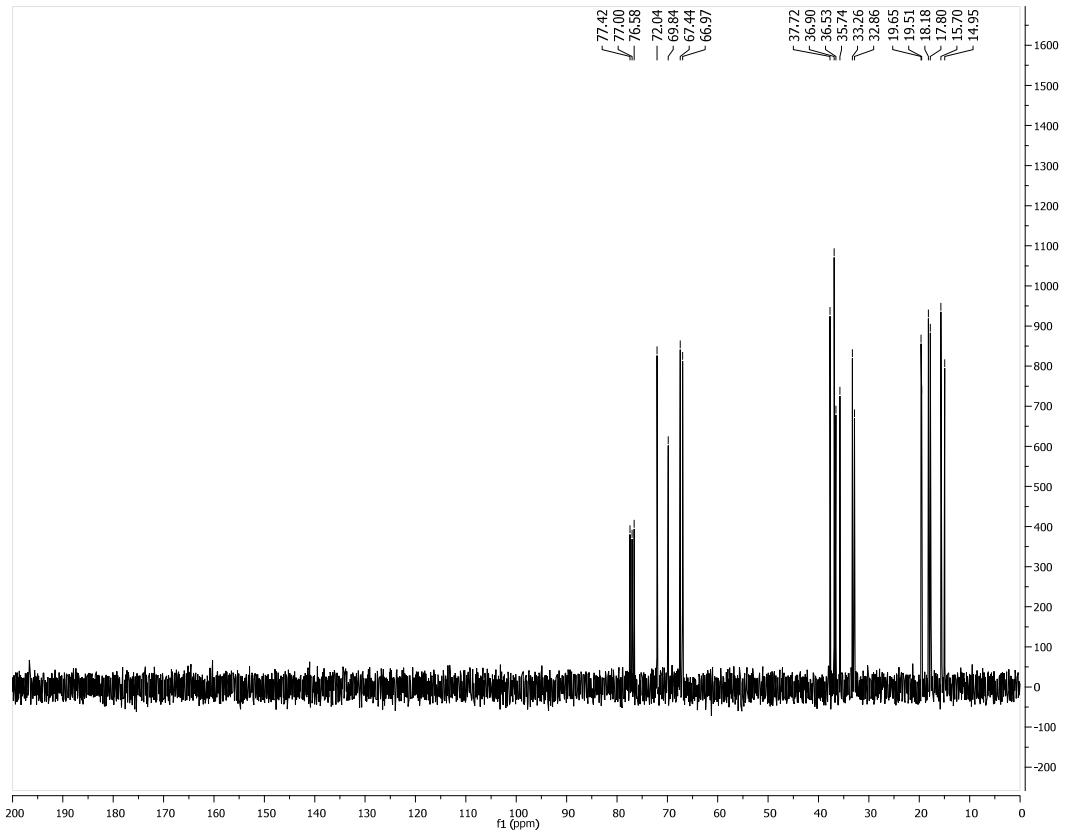
77.42
77.00
76.58
72.04
69.84
67.44
66.97
37.72
36.90
36.53
35.74
33.26
32.86
19.65
19.51
18.18
17.80
15.70
14.95
f1 (ppm)

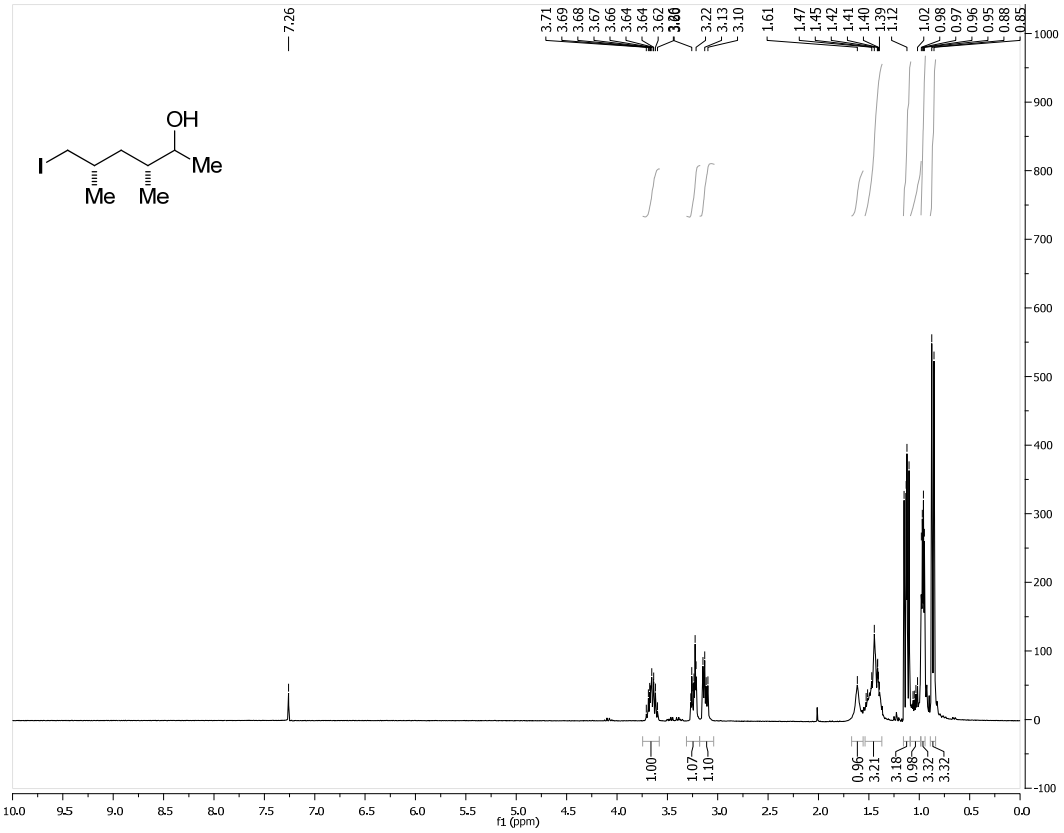
OH
I
Me
Me
Me
7.26
3.71
3.69
3.68
3.67
3.66
3.64
3.64
3.62
3.22
3.13
3.10
1.61
1.47
1.45
1.42
1.41
1.40
1.39
1.12
1.02
0.98
0.97
0.96
0.95
0.88
0.85
1.00
1.07
1.10
0.96
3.21
3.18
0.98
3.32
3.32
f1 (ppm)

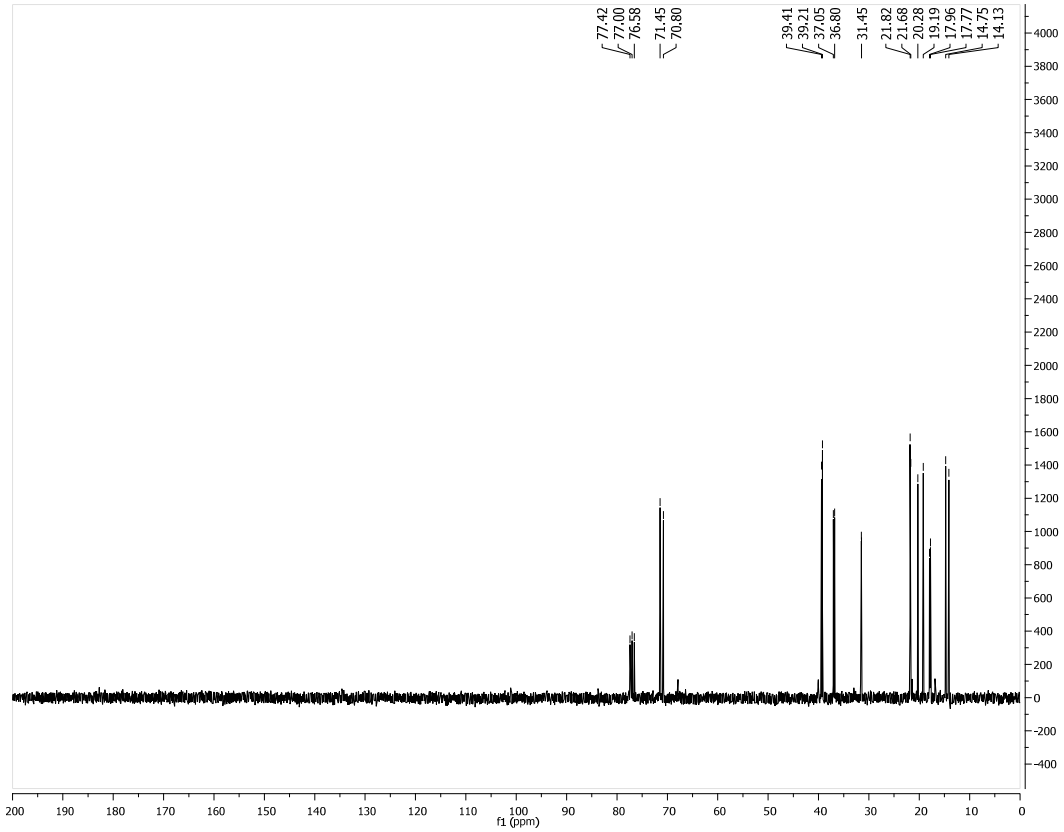
77.42
77.00
76.58
71.45
70.80
39.41
39.21
37.05
36.80
31.45
21.82
21.68
20.28
19.19
17.96
17.77
14.75
14.13
f1 (ppm)

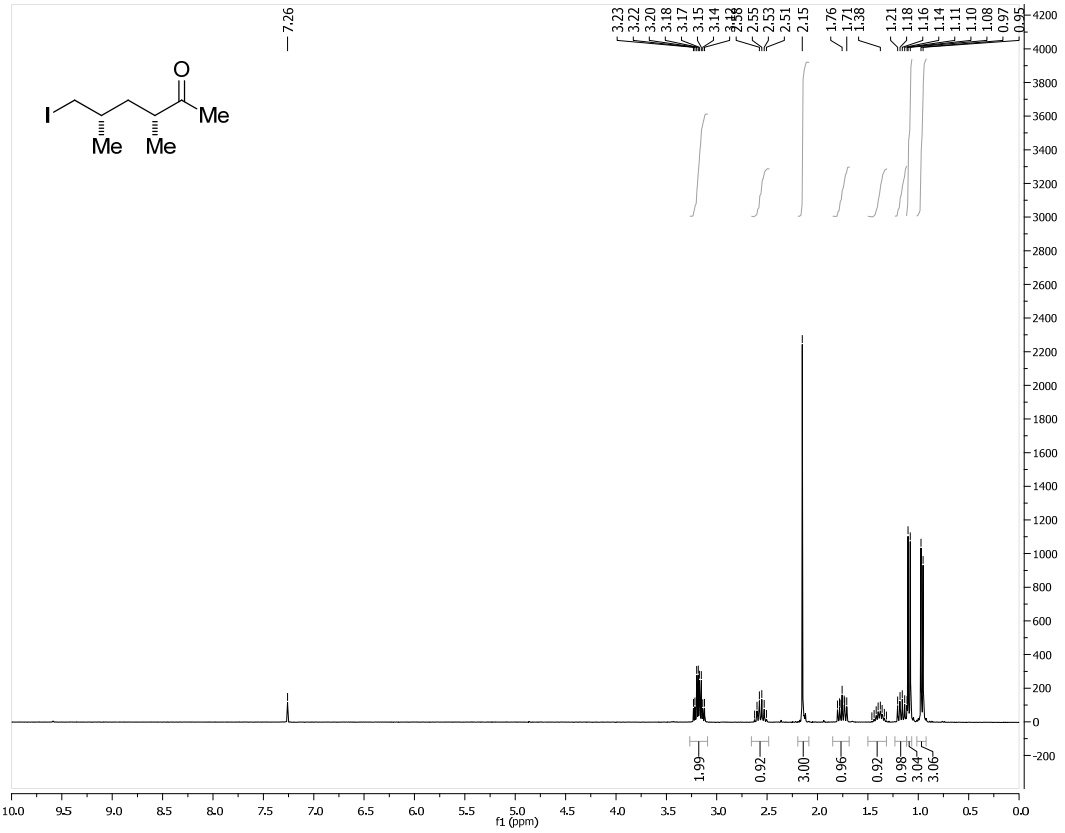
I
O
Me
Me
Me
7.26
3.23
3.22
3.20
3.18
3.17
3.15
3.14
2.55
2.53
2.51
2.15
1.76
1.71
1.38
1.21
1.18
1.16
1.14
1.11
1.10
1.08
0.97
0.95
1.99
0.92
3.00
0.96
0.92
0.98
3.04
3.06
f1 (ppm)

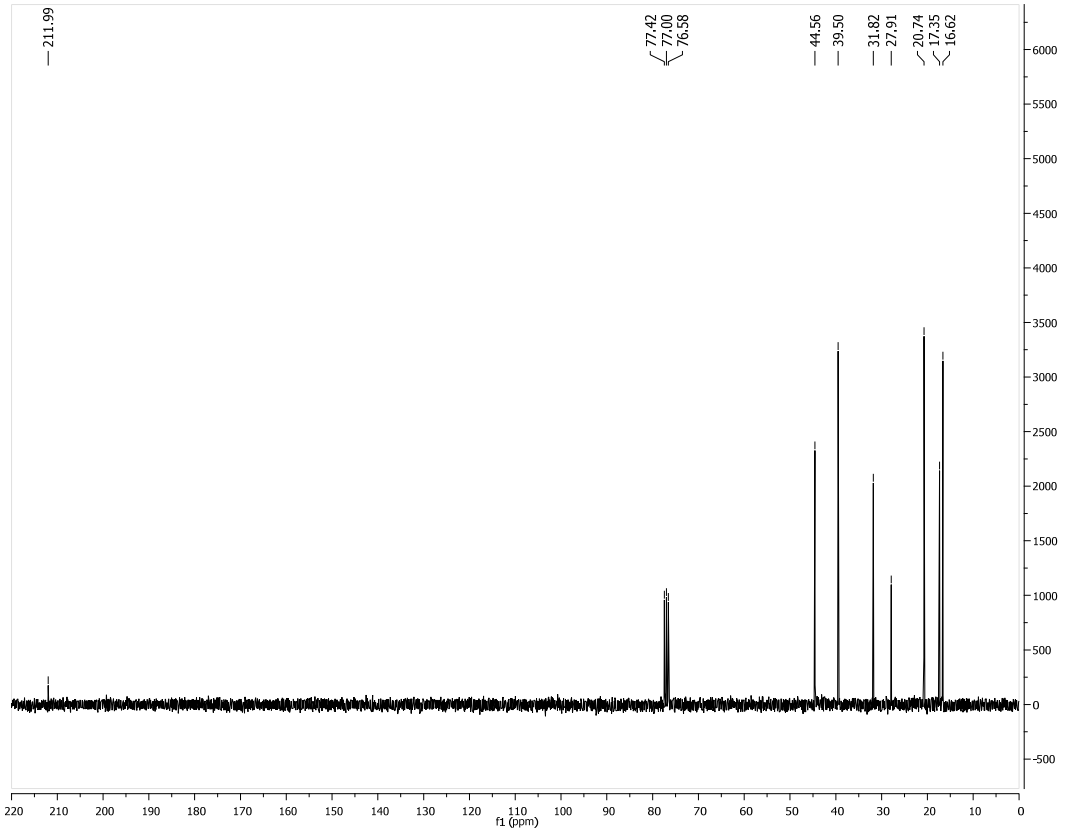
211.99
77.42
77.00
76.58
44.56
39.50
31.82
27.91
20.74
17.35
16.62
f1 (ppm)

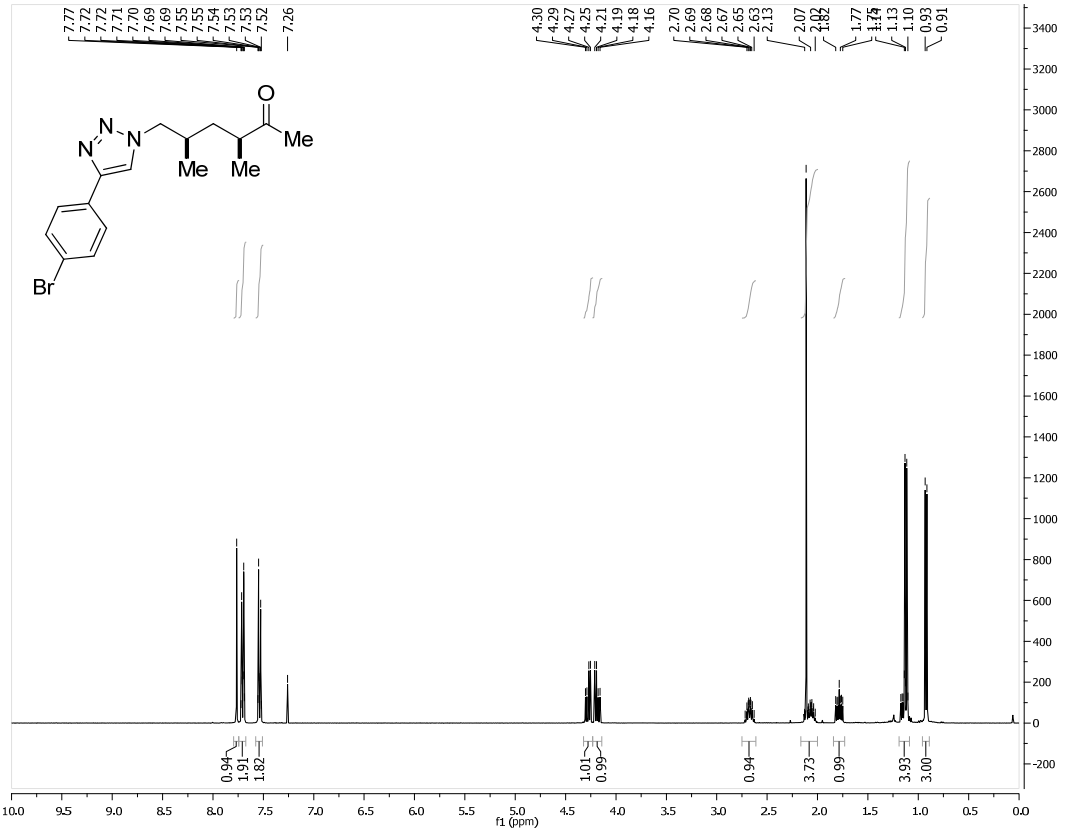
7.77
7.72
7.72
7.71
7.70
7.69
7.69
7.55
7.55
7.54
7.53
7.53
7.52
7.26
4.30
4.29
4.27
4.25
4.21
4.19
4.18
4.16
2.70
2.69
2.68
2.67
2.65
2.63
2.13
2.07
1.82
1.77
1.13
1.10
0.93
0.91
O
Me
N
N
N
Me
Me
Br
0.94
1.91
1.82
1.01
0.99
0.94
3.73
0.99
3.93
3.00
f1 (ppm)

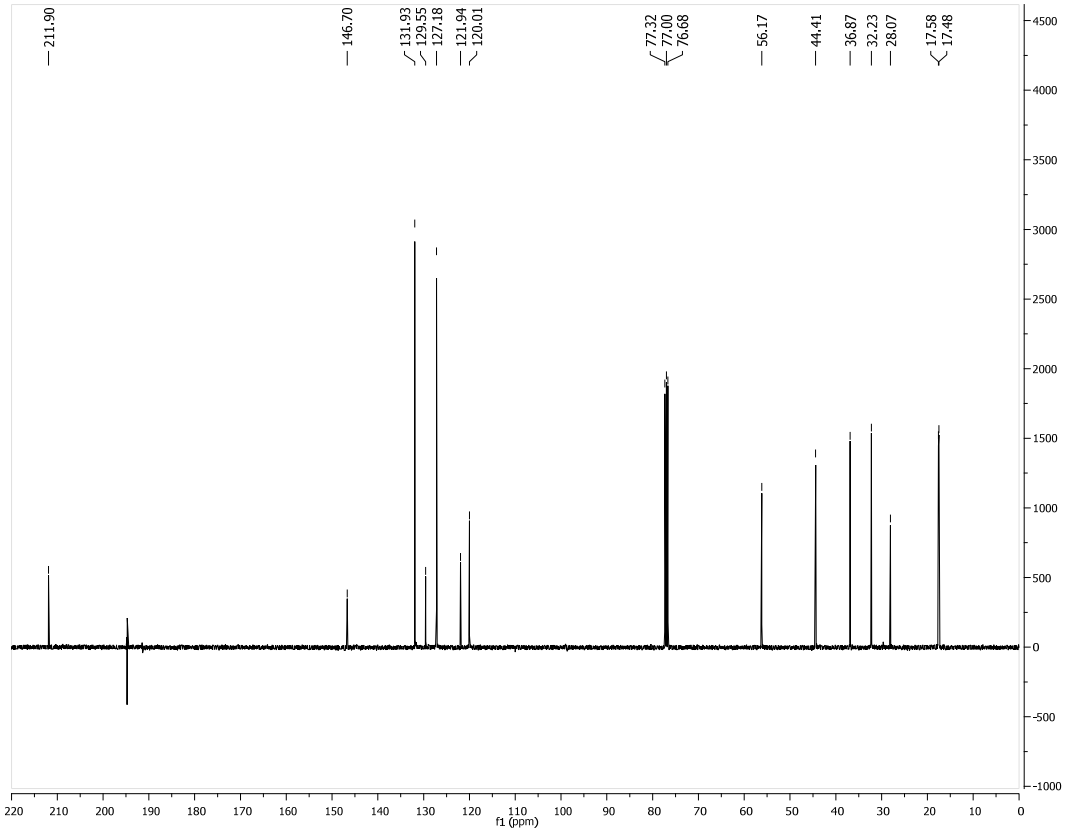
211.90
146.70
131.93
129.55
127.18
121.94
120.01
77.32
77.00
76.68
56.17
44.41
36.87
32.23
28.07
17.58
17.48
f1 (ppm)

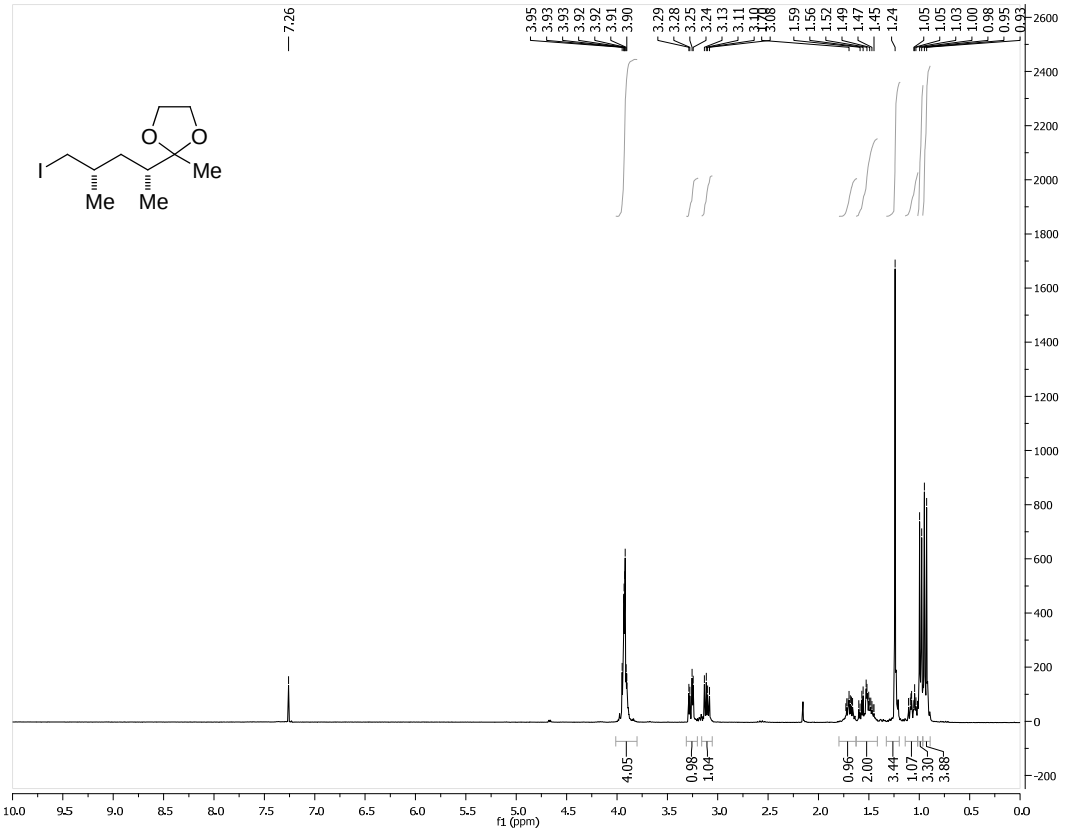
7.26
3.95
3.93
3.92
3.91
3.90
3.29
3.28
3.25
3.24
3.13
3.11
3.10
3.08
1.59
1.56
1.52
1.49
1.47
1.45
1.24
1.05
1.05
1.03
1.00
0.98
0.95
0.93
O
O
I
Me
Me
Me
4.05
0.98
1.04
0.96
2.00
3.44
1.07
3.30
3.88
f1 (ppm)

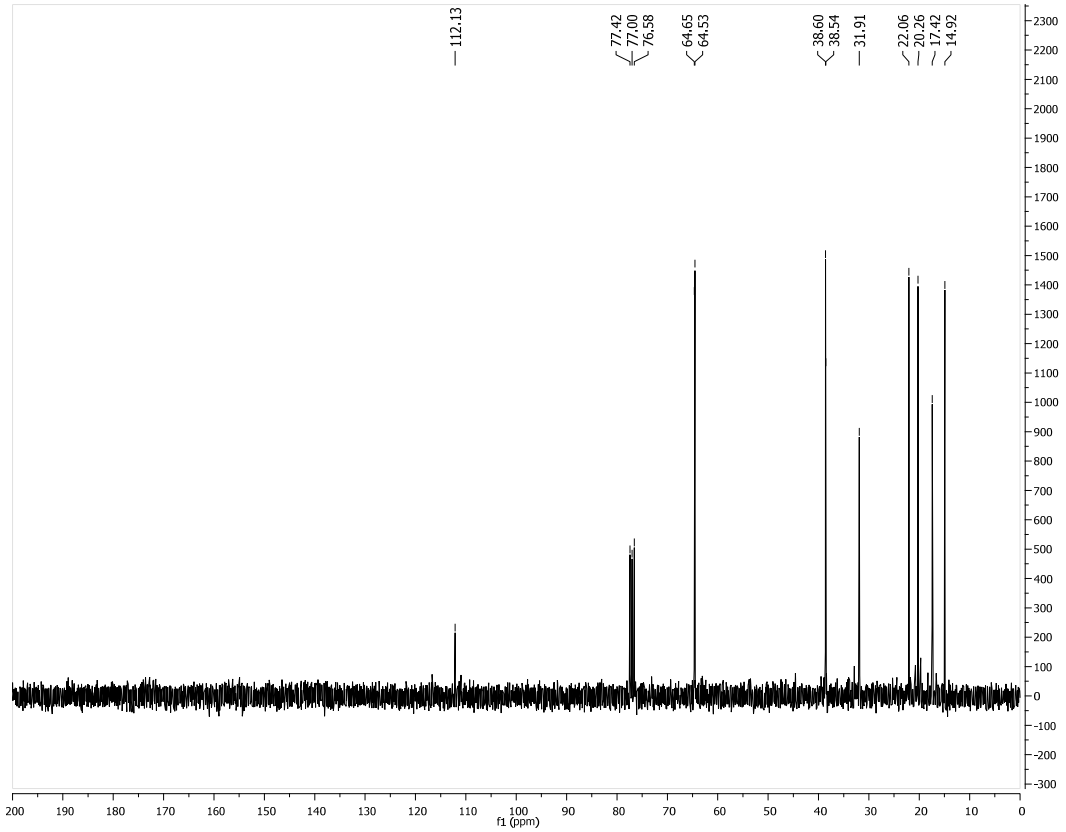
112.13
77.42
77.00
76.58
64.65
64.53
38.60
38.54
31.91
22.06
20.26
17.42
14.92
f1 (ppm)

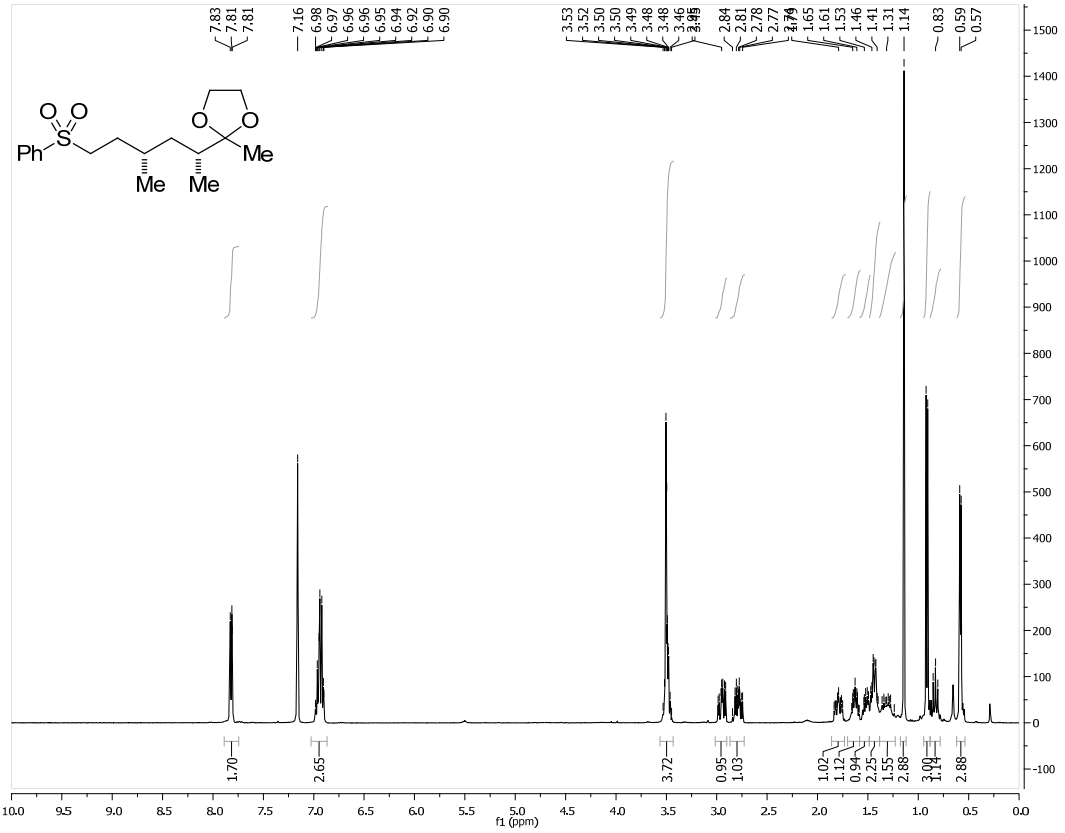
7.83
7.81
7.81
7.16
6.98
6.97
6.96
6.96
6.95
6.94
6.92
6.90
6.90
3.53
3.52
3.50
3.50
3.49
3.48
3.48
3.46
2.84
2.81
2.78
2.77
1.65
1.61
1.53
1.46
1.41
1.31
1.14
0.83
0.59
0.57
1.70
2.65
3.72
0.95
1.03
1.02
1.12
0.94
2.25
1.55
2.88
3.00
3.04
2.88
f1 (ppm)

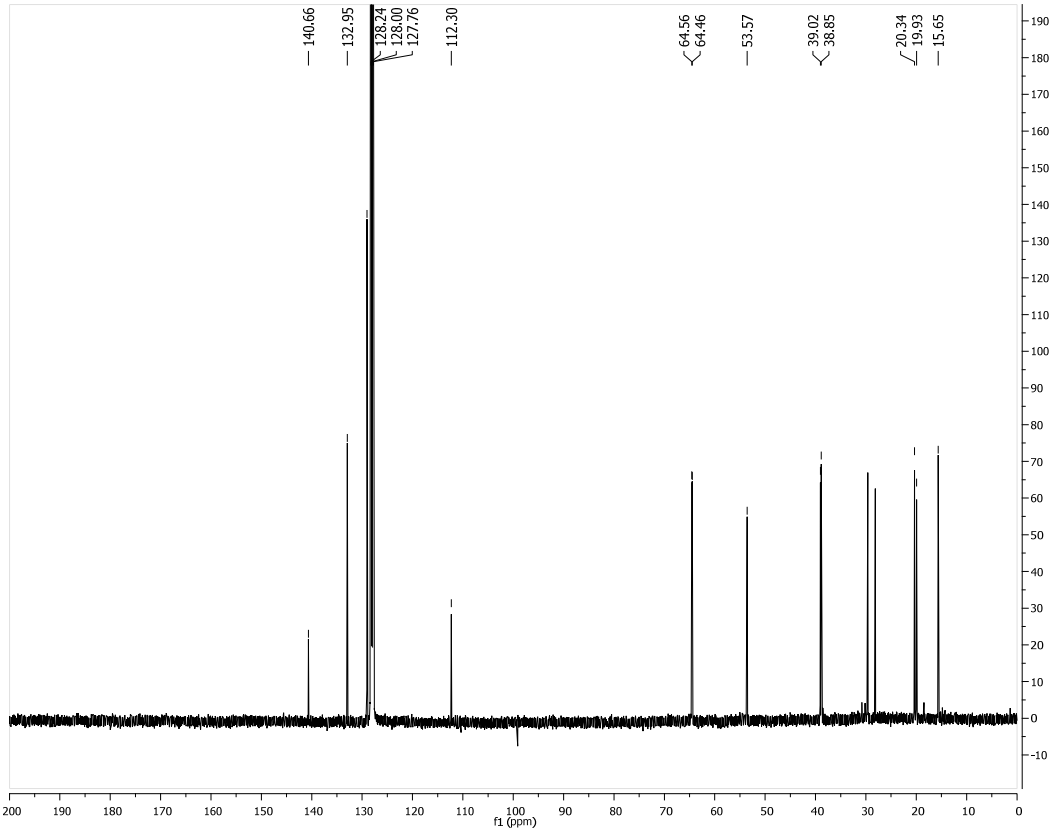
140.66
132.95
128.24
128.00
127.76
112.30
64.56
64.46
53.57
39.02
38.85
20.34
19.93
15.65
f1 (ppm)

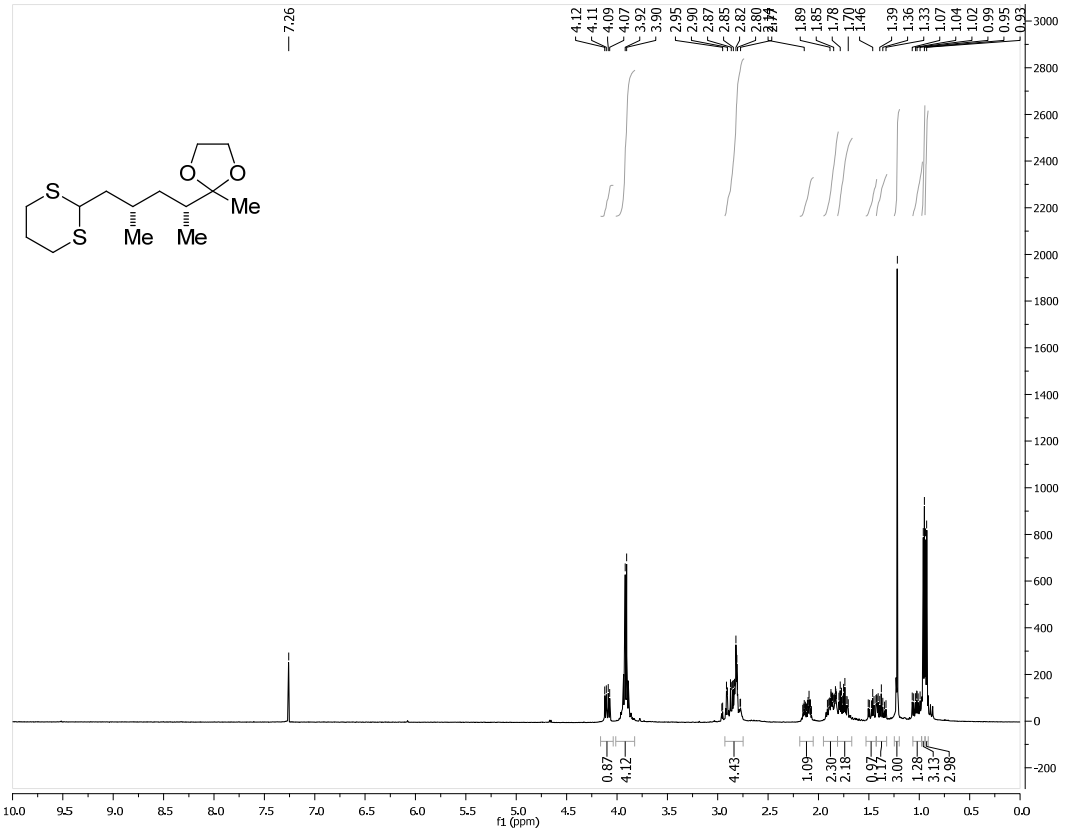
7.26
4.12
4.11
4.09
4.07
3.92
3.90
2.95
2.90
2.87
2.85
2.82
2.80
1.89
1.85
1.78
1.70
1.46
1.39
1.36
1.33
1.07
1.04
1.02
0.99
0.95
0.93
S
S
O
O
Me
Me
Me
0.87
4.12
4.43
1.09
2.30
2.18
0.97
1.17
3.00
1.28
3.13
2.98
f1 (ppm)

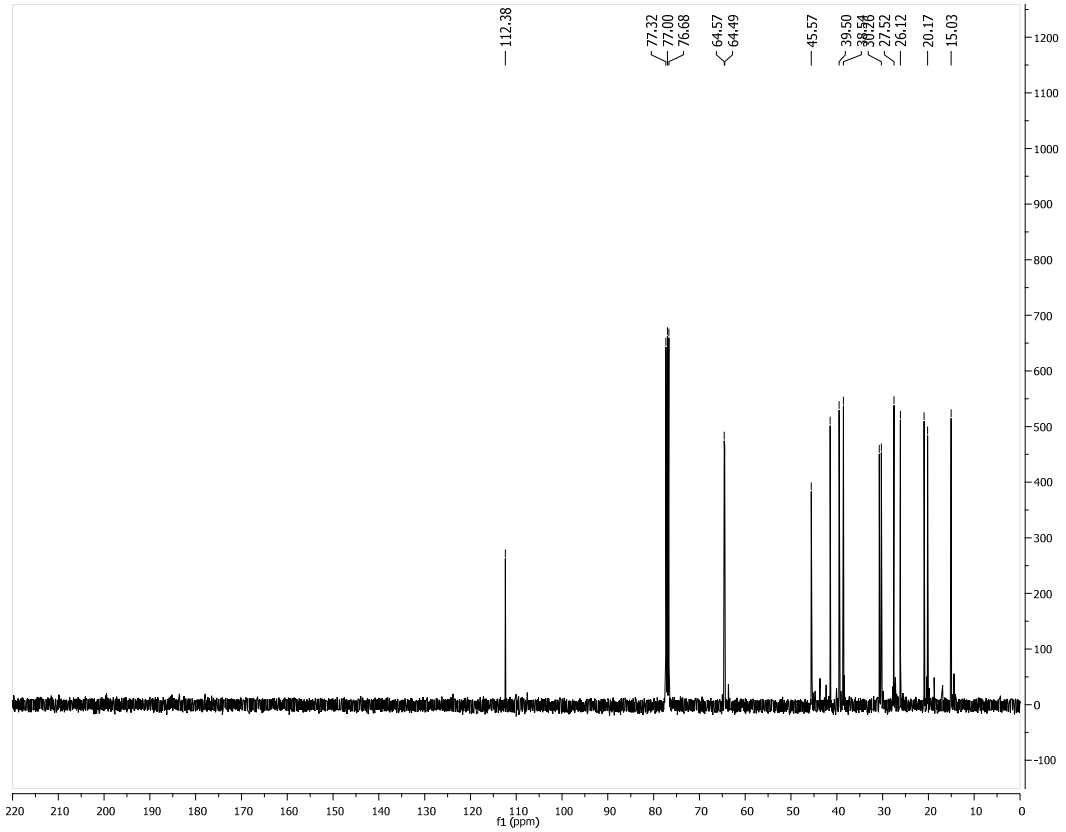
112.38
77.32
77.00
76.68
64.57
64.49
45.57
39.50
38.54
30.26
27.52
26.12
20.17
15.03
f1 (ppm)

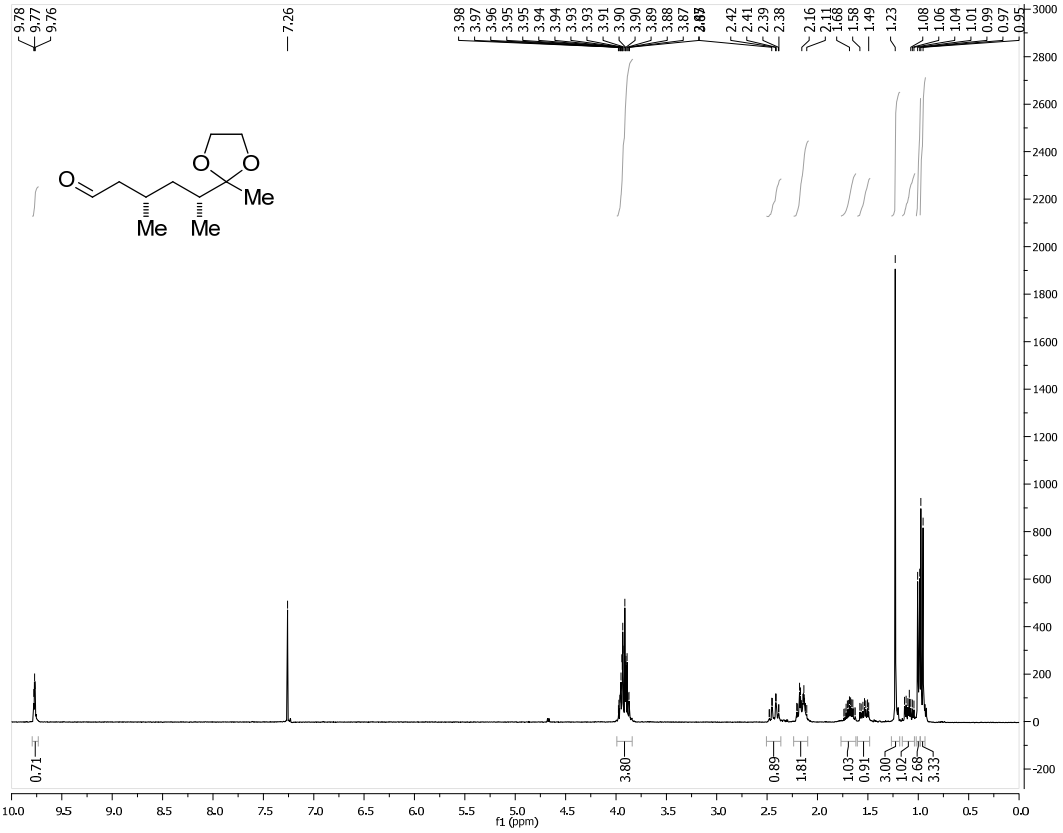
9.78
9.77
9.76
7.26
3.98
3.97
3.96
3.95
3.95
3.94
3.94
3.93
3.93
3.91
3.90
3.90
3.89
3.88
3.87
2.42
2.41
2.39
2.38
2.16
2.11
1.68
1.58
1.49
1.23
1.08
1.06
1.04
1.01
0.99
0.97
0.95
O
O
O
Me
Me
Me
0.71
3.80
0.89
1.81
1.03
0.91
3.00
1.02
2.68
3.33
f1 (ppm)

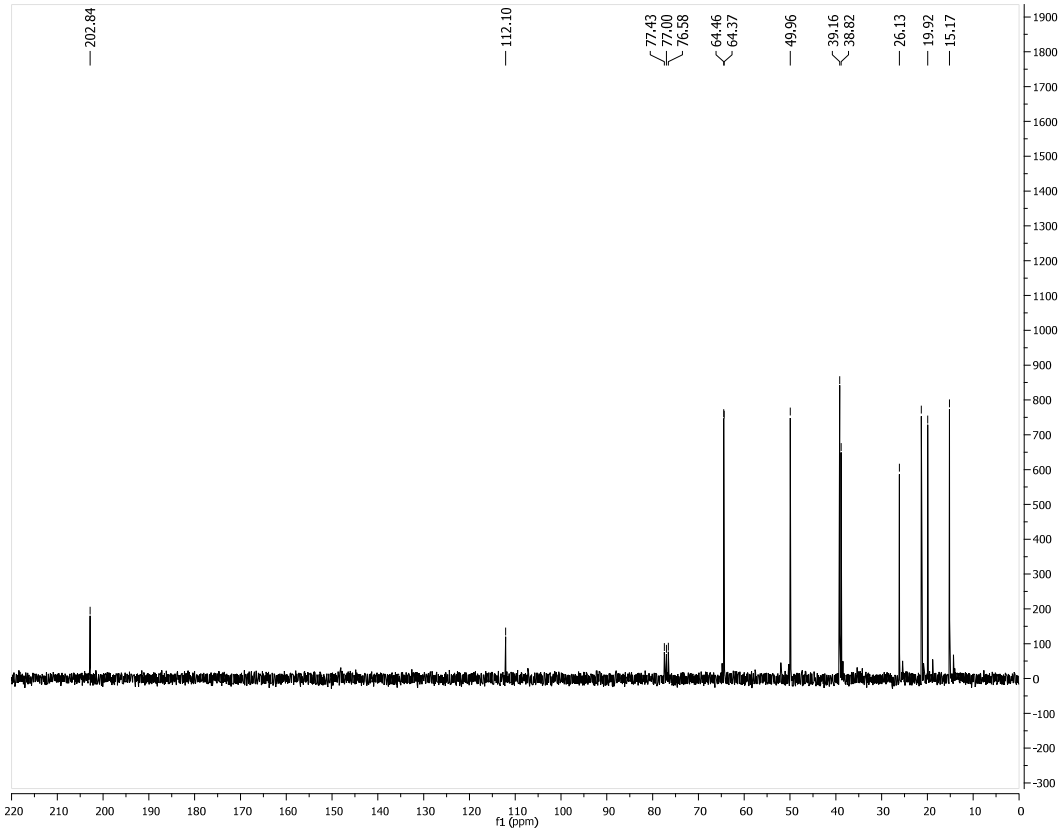
202.84
112.10
77.43
77.00
76.58
64.46
64.37
49.96
39.16
38.82
26.13
19.92
15.17
f1 (ppm)

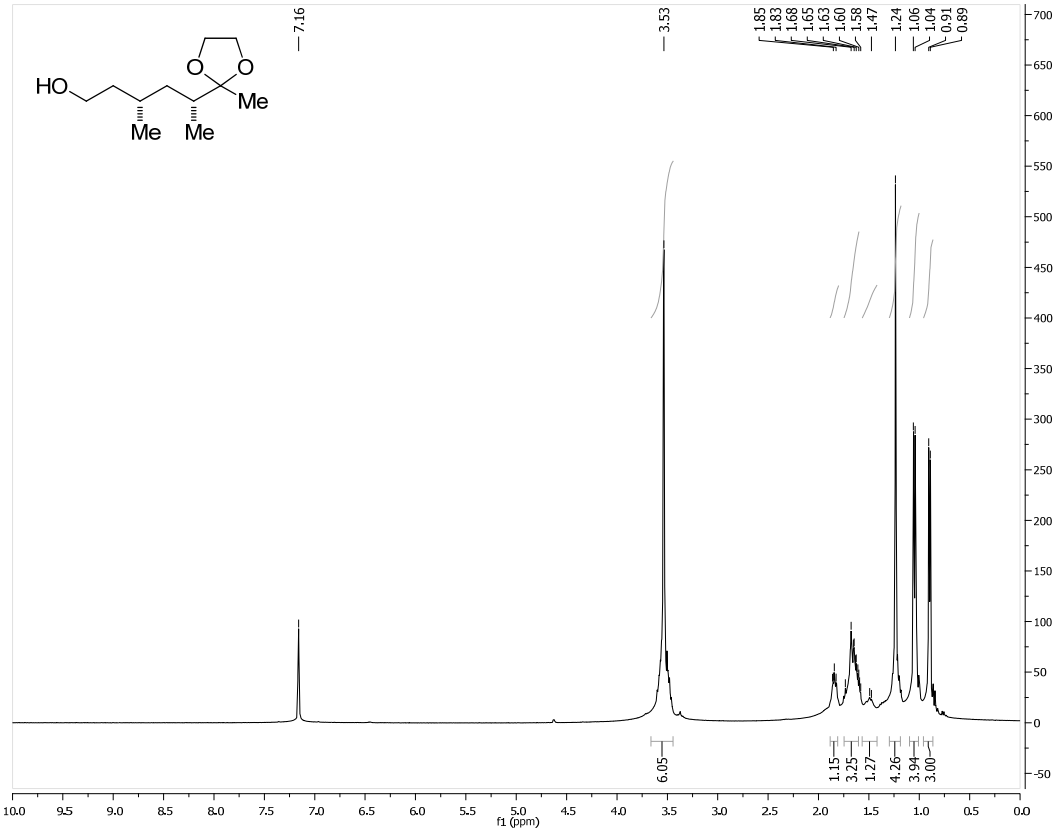
HO
O
O
Me
Me
Me
7.16
3.53
1.85
1.83
1.68
1.65
1.63
1.60
1.58
1.47
1.24
1.06
1.04
0.91
0.89
6.05
1.15
3.25
1.27
4.26
3.94
3.00
f1 (ppm)

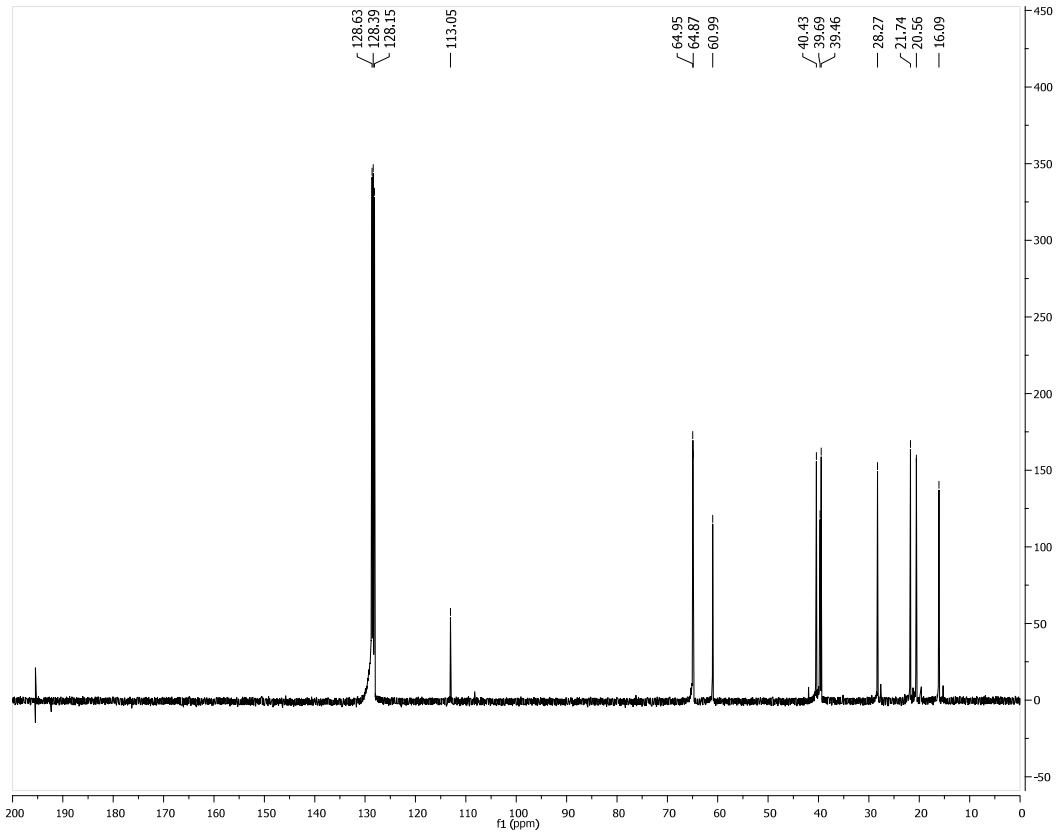
128.63
128.39
128.15
113.05
64.95
64.87
60.99
40.43
39.69
39.46
28.27
21.74
20.56
16.09
f1 (ppm)

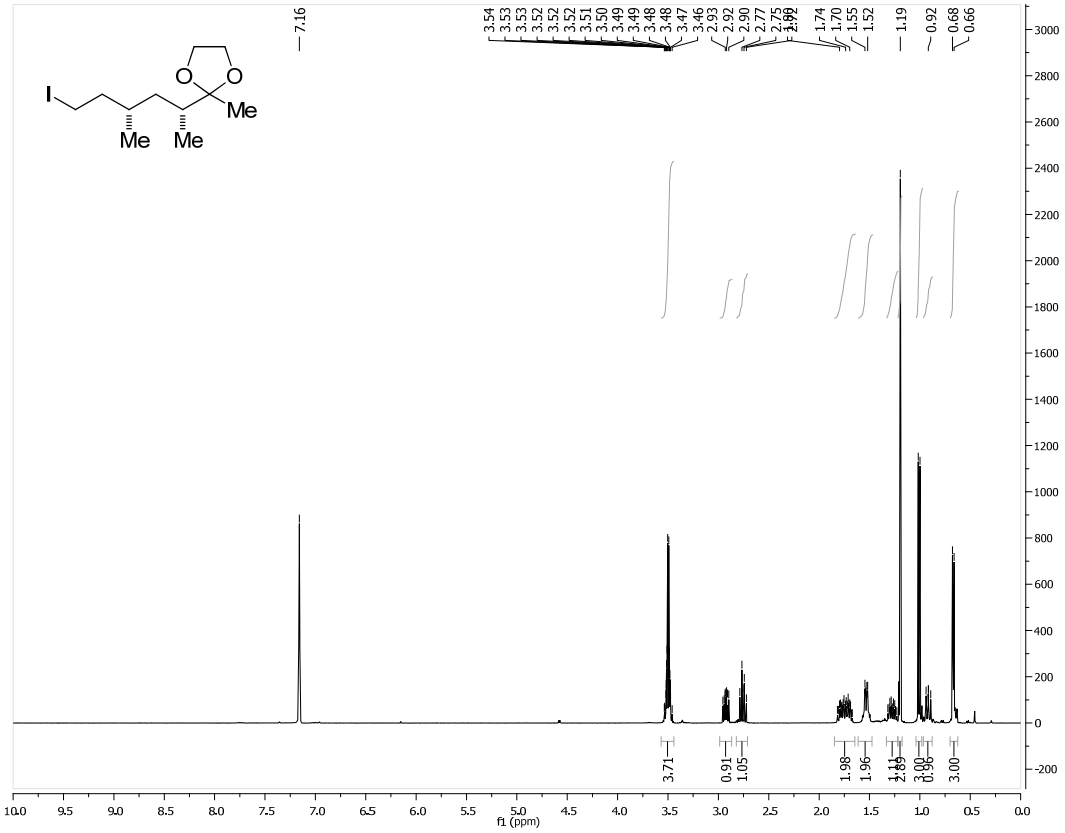
I
O
O
Me
Me
Me
7.16
3.54
3.53
3.53
3.52
3.52
3.52
3.51
3.50
3.49
3.49
3.48
3.48
3.47
3.46
2.93
2.92
2.90
2.77
2.75
1.74
1.70
1.55
1.52
1.19
0.92
0.68
0.66
3.71
0.91
1.05
1.98
1.96
1.11
3.00
0.96
3.00
f1 (ppm)

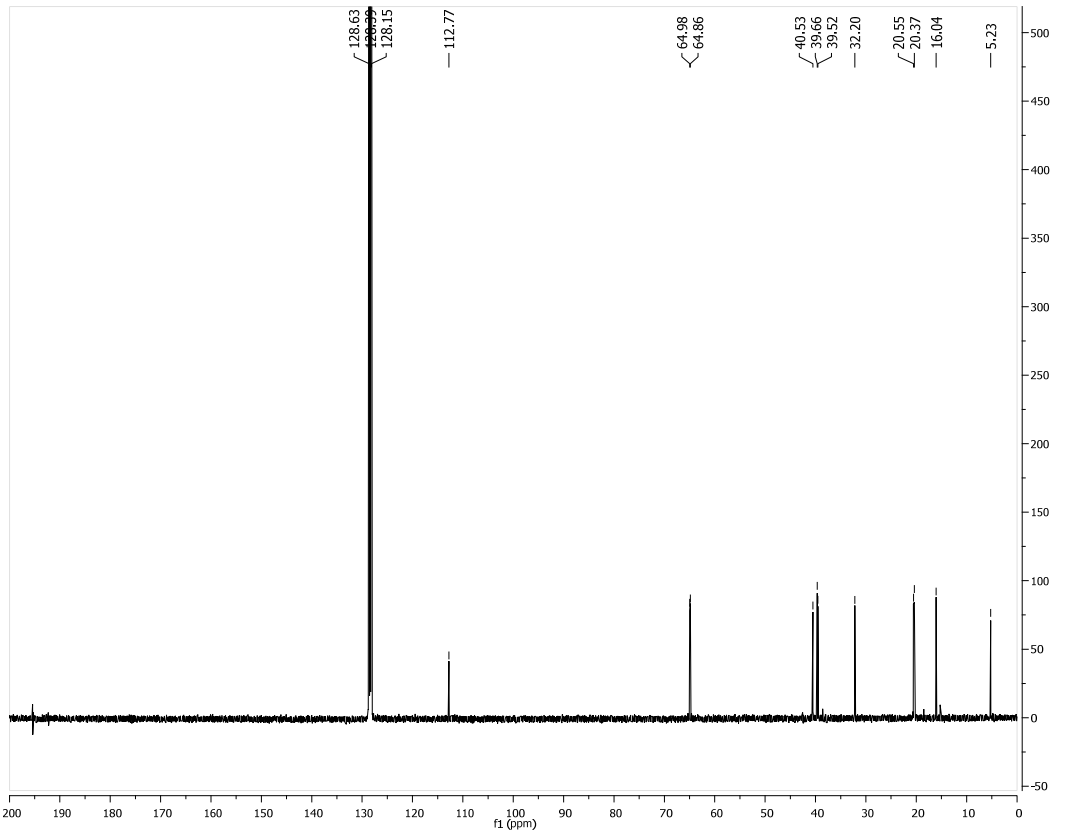
128.63
128.39
128.15
112.77
64.98
64.86
40.53
39.66
39.52
32.20
20.55
20.37
16.04
5.23
f1 (ppm)

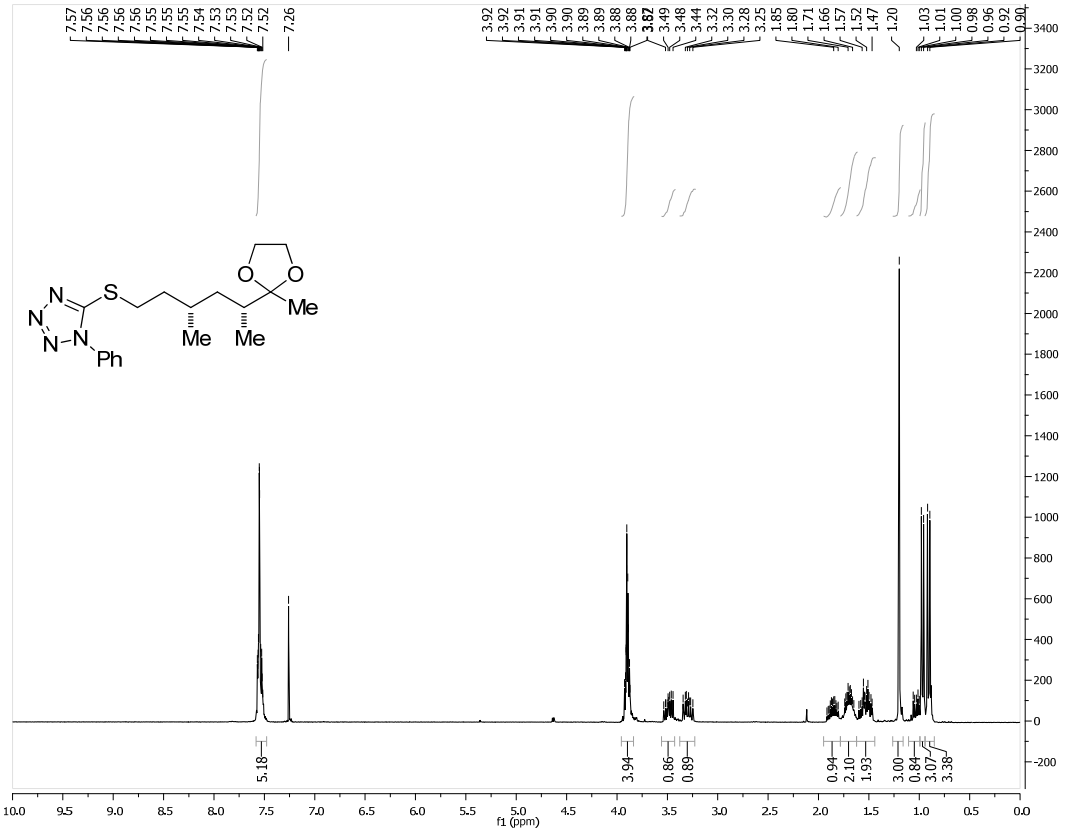
7.57 7.56 7.56 7.56 7.56 7.55 7.55 7.55 7.54 7.53 7.53 7.52 7.52 7.26
3.92 3.92 3.91 3.91 3.90 3.90 3.89 3.89 3.88 3.88 3.82 3.49 3.48 3.44 3.32 3.30 3.28 3.25 1.85 1.80 1.71 1.66 1.57 1.52 1.47 1.20 1.03 1.01 1.00 0.98 0.96 0.92 0.90
N
N
N
N
S
Ph
Me
Me
O
O
Me
5.18
3.94
0.86
0.89
0.94
2.10
1.93
3.00
0.84
3.07
3.38
f1 (ppm)

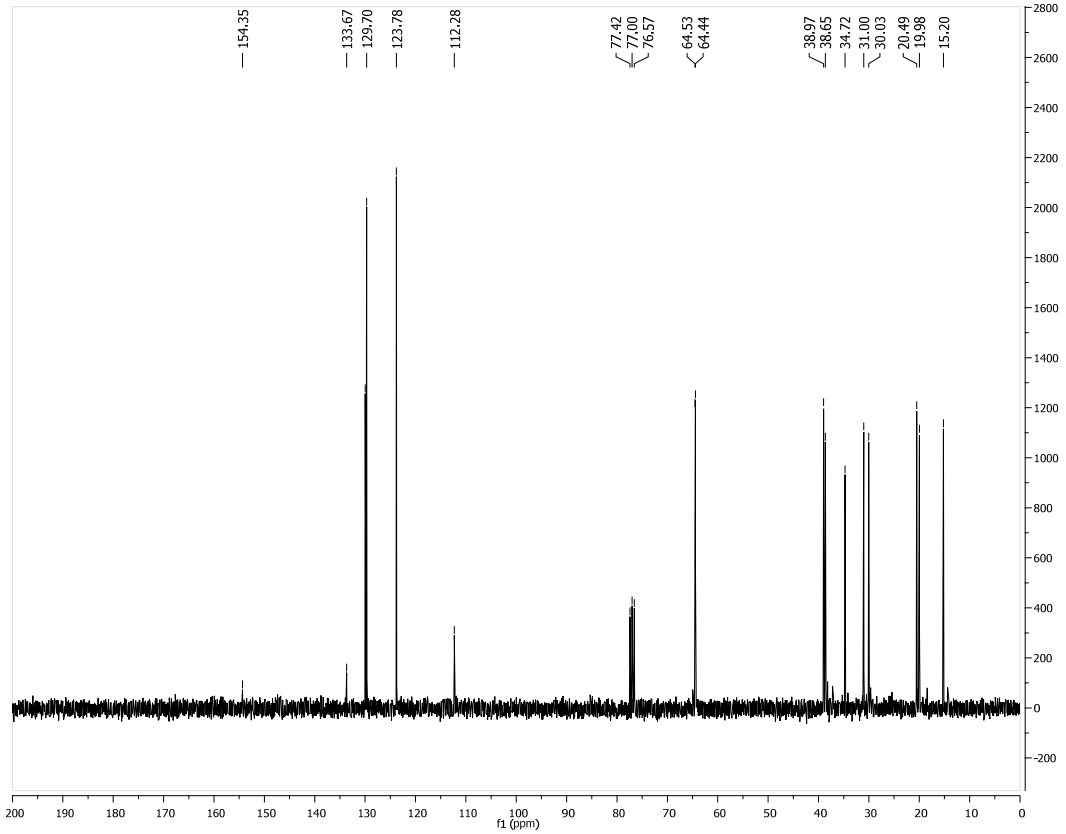
154.35
133.67
129.70
123.78
112.28
77.42
77.00
76.57
64.53
64.44
38.97
38.65
34.72
31.00
30.03
20.49
19.98
15.20
f1 (ppm)

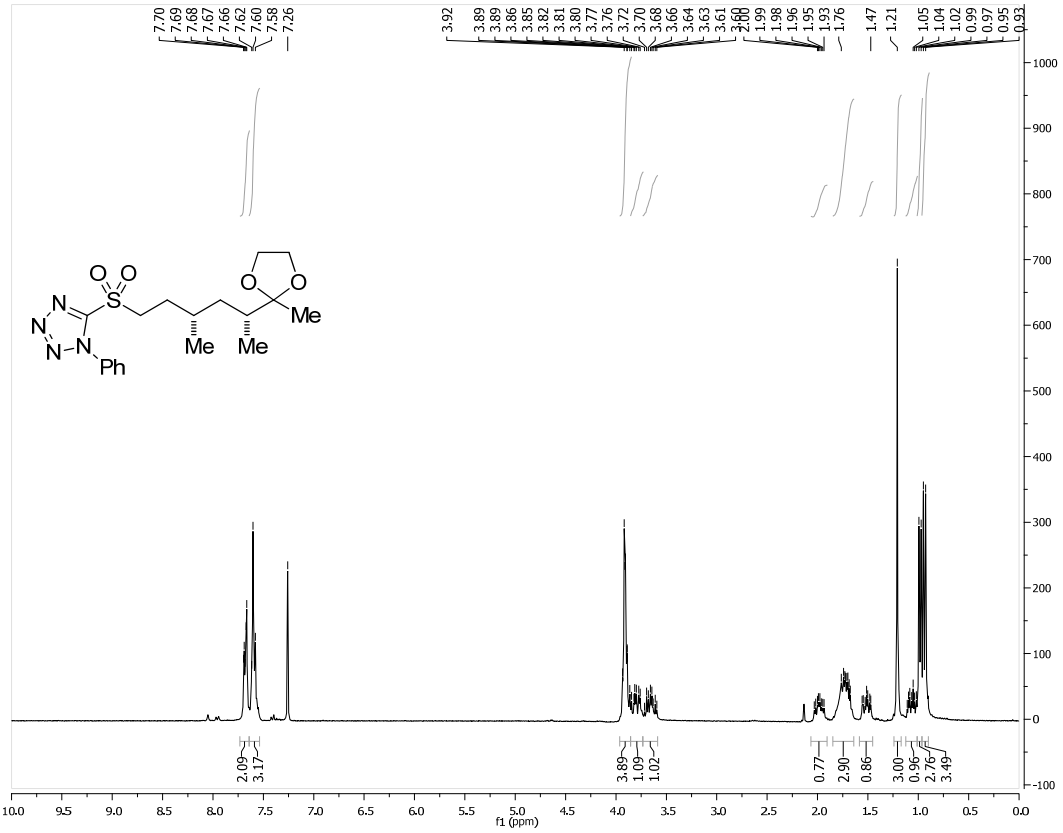
7.70
7.69
7.68
7.67
7.66
7.62
7.60
7.58
7.26
3.92
3.89
3.89
3.86
3.85
3.82
3.81
3.80
3.77
3.76
3.72
3.70
3.68
3.66
3.64
3.63
3.61
3.60
2.00
1.99
1.98
1.96
1.95
1.93
1.76
1.47
1.21
1.05
1.04
1.02
0.99
0.97
0.95
0.93
O
O
S
N
N
N
N
Ph
Me
Me
O
O
Me
2.09
3.17
3.89
1.09
1.02
0.77
2.90
0.86
3.00
0.96
2.76
3.49
f1 (ppm)

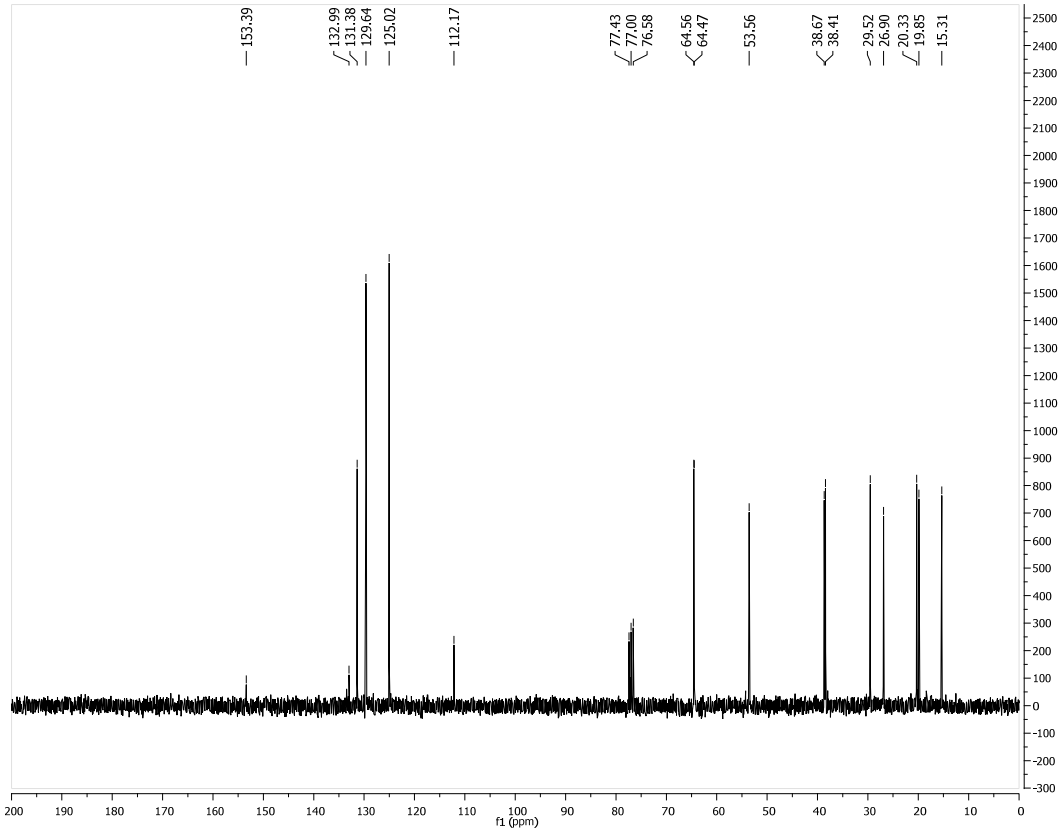
153.39
132.99
131.38
129.64
125.02
112.17
77.43
77.00
76.58
64.56
64.47
53.56
38.67
38.41
29.52
26.90
20.33
19.85
15.31
f1 (ppm)

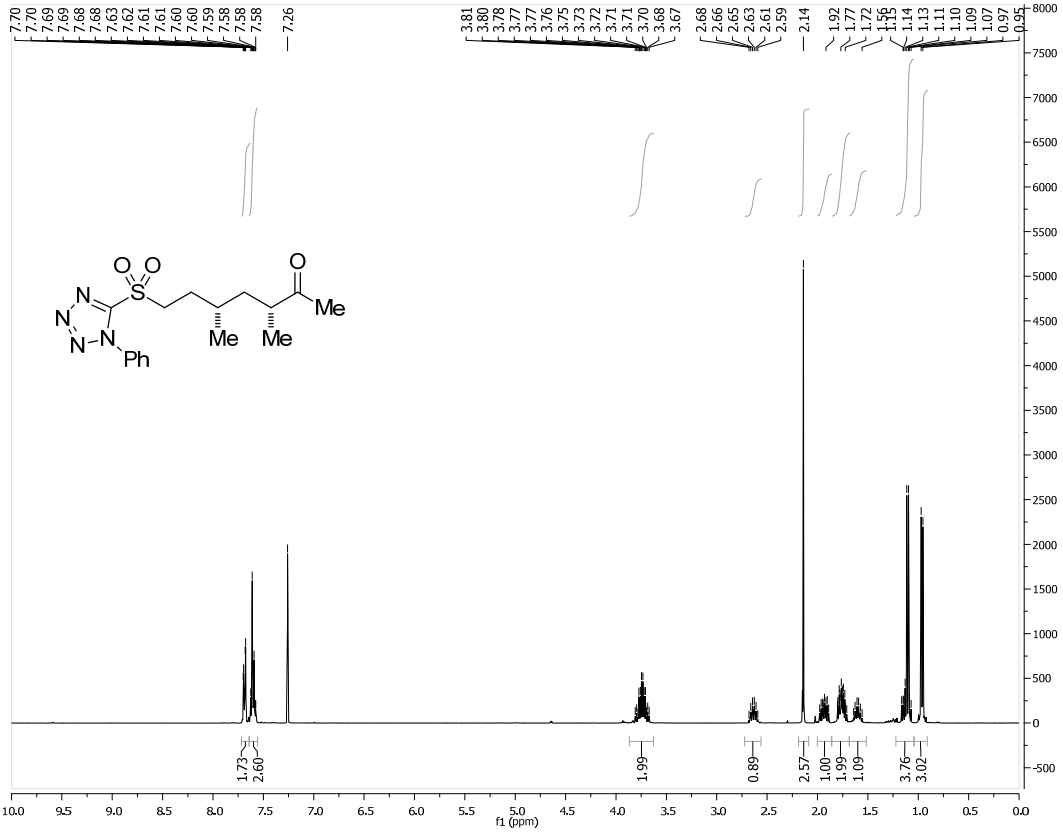
7.70 7.70 7.69 7.69 7.68 7.68 7.63 7.62 7.61 7.61 7.60 7.60 7.59 7.58 7.58 7.58 7.26
3.81 3.80 3.78 3.77 3.77 3.76 3.75 3.73 3.72 3.71 3.71 3.70 3.68 3.67
2.68 2.66 2.65 2.63 2.61 2.59
2.14
1.92 1.77 1.72 1.56 1.15 1.14 1.13 1.11 1.10 1.09 1.07 0.97 0.95
O O S N N N Ph O Me Me Me
1.73 2.60 1.99 0.89 2.57 1.00 1.99 1.09 3.76 3.02
f1 (ppm)

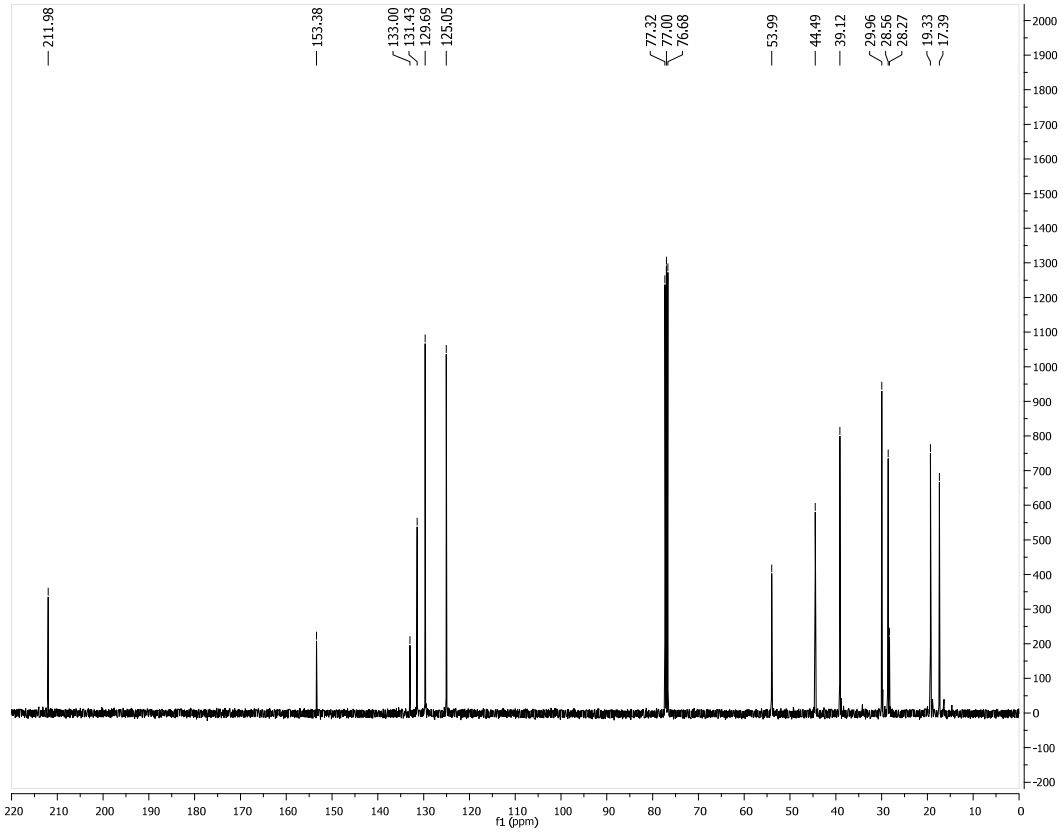
211.98 153.38 133.00 131.43 129.69 125.05 77.32 77.00 76.68 53.99 44.49 39.12 29.96 28.56 28.27 19.33 17.39
f1 (ppm)

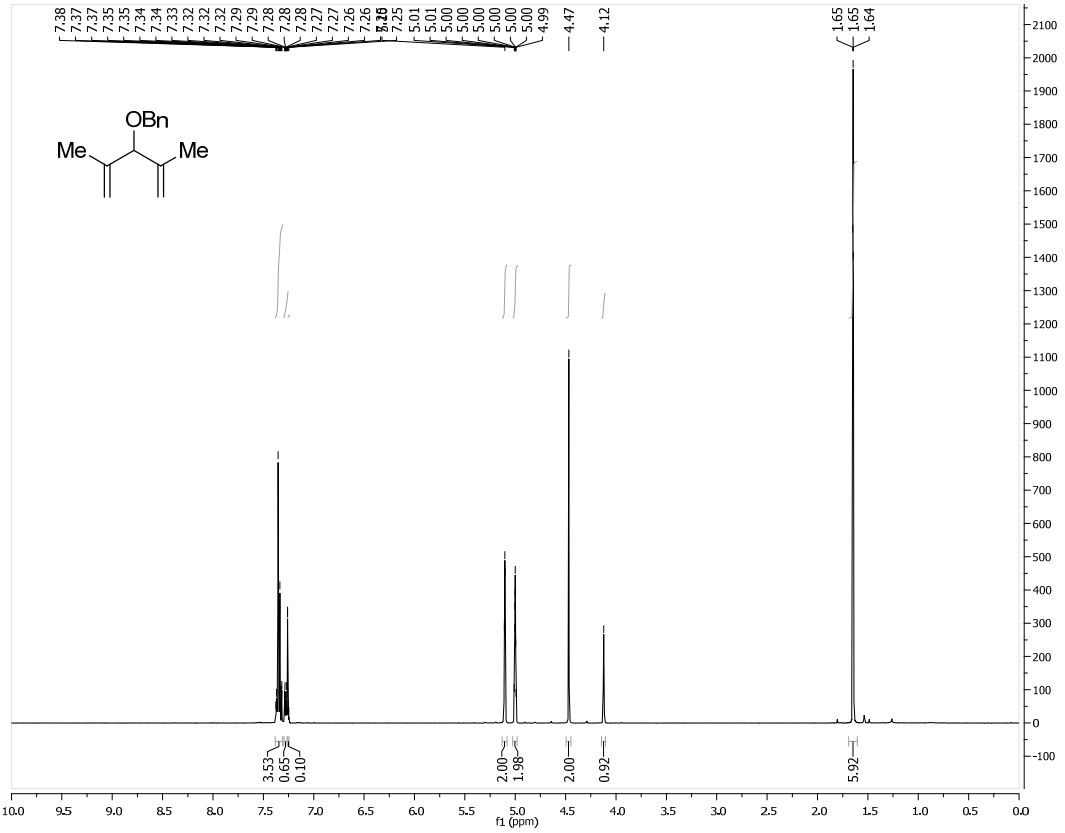
7.38
7.37
7.37
7.35
7.35
7.34
7.34
7.33
7.32
7.32
7.32
7.29
7.29
7.28
7.28
7.28
7.27
7.27
7.26
7.26
7.25
5.01
5.01
5.00
5.00
5.00
5.00
5.00
4.99
4.47
4.12
1.65
1.65
1.64
OBn
Me
Me
3.53
0.65
0.10
2.00
1.98
2.00
0.92
5.92
f1 (ppm)

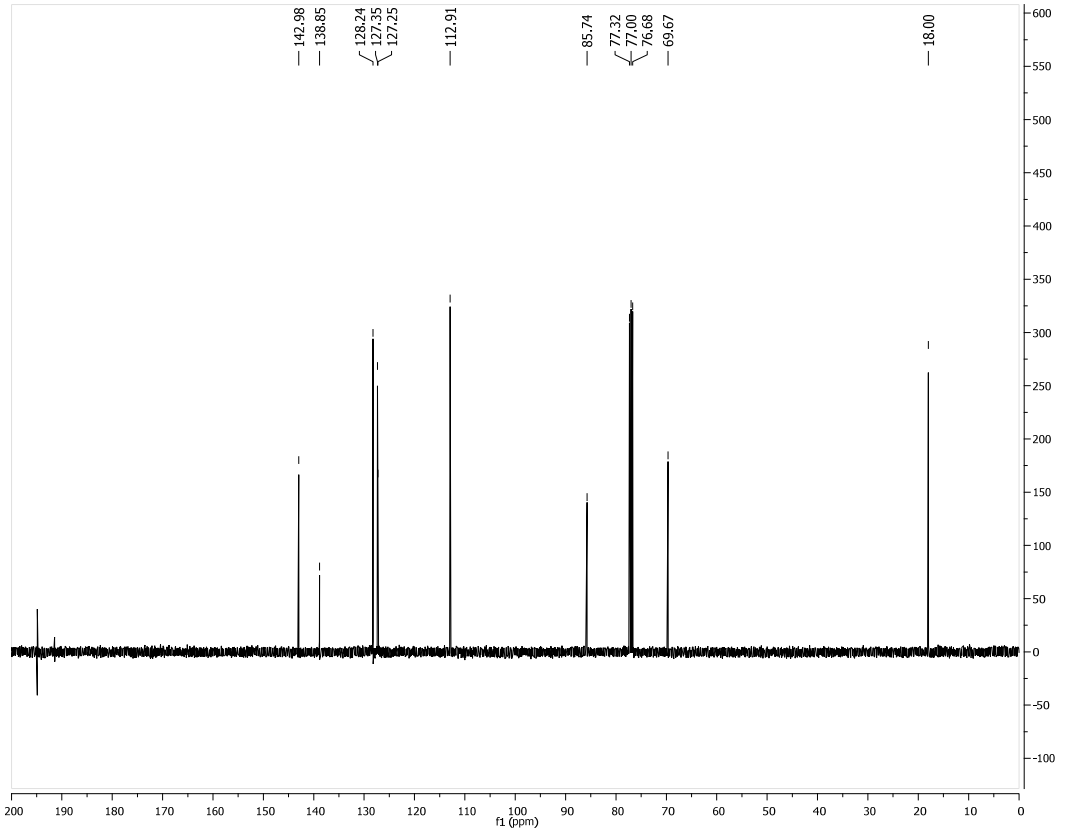
142.98
138.85
128.24
127.35
127.25
112.91
85.74
77.32
77.00
76.68
69.67
18.00
f1 (ppm)

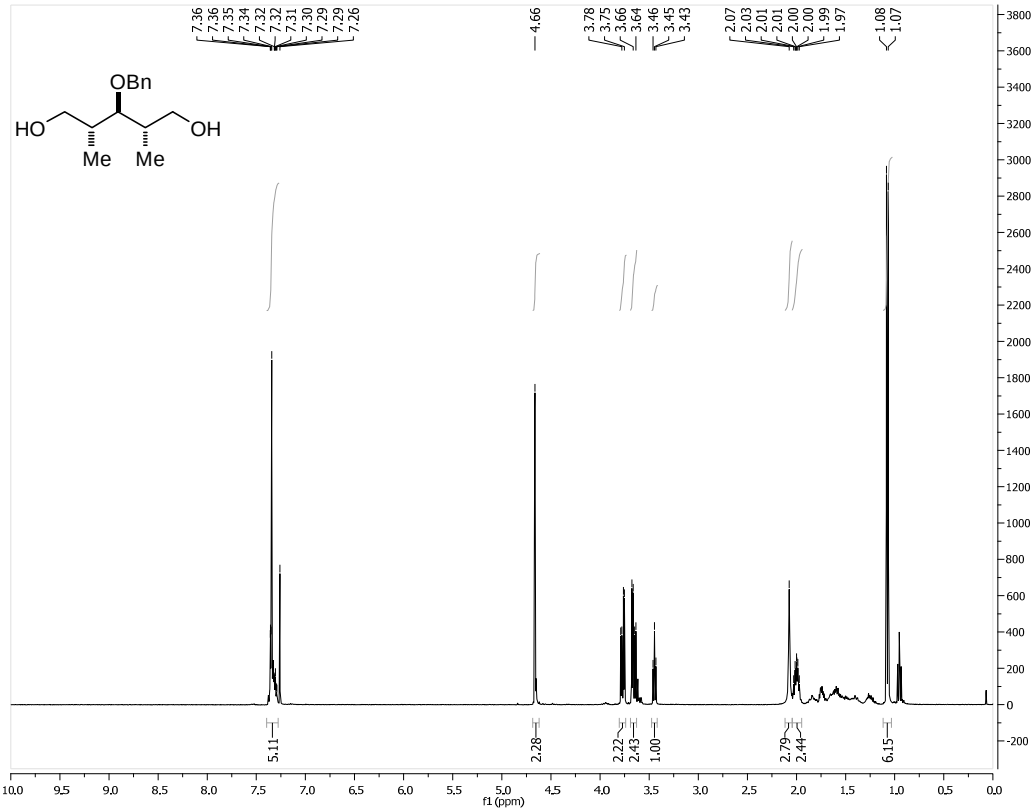
OBn
HO
OH
Me
Me
7.36
7.36
7.35
7.34
7.32
7.32
7.31
7.30
7.29
7.29
7.26
4.66
3.78
3.75
3.66
3.64
3.46
3.45
3.43
2.07
2.03
2.01
2.01
2.00
2.00
1.99
1.97
1.08
1.07
5.11
2.28
2.22
2.43
1.00
2.79
2.44
6.15
f1 (ppm)

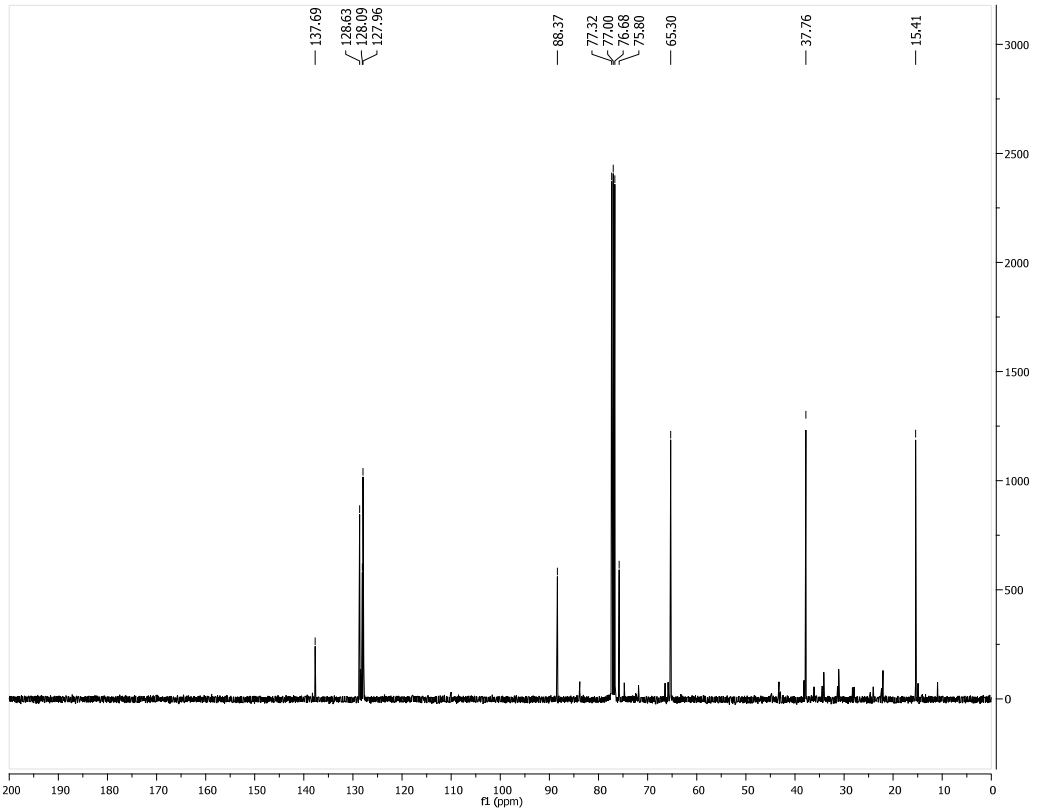
137.69
128.63
128.09
127.96
88.37
77.32
77.00
76.68
75.80
65.30
37.76
15.41
f1 (ppm)

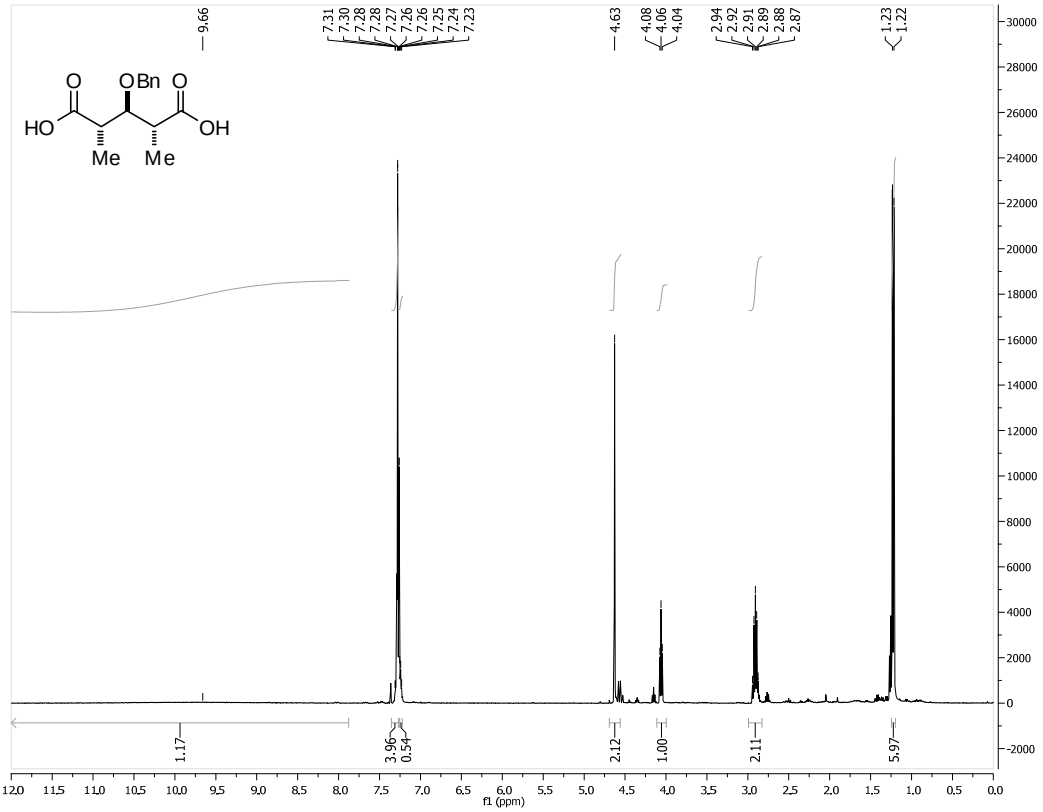
9.66
7.31
7.30
7.28
7.27
7.26
7.26
7.25
7.24
7.23
4.63
4.08
4.06
4.04
2.94
2.92
2.91
2.89
2.88
2.87
1.23
1.22
O
OBn
O
HO
OH
Me
Me
1.17
3.96
0.54
2.12
1.00
2.11
5.97
f1 (ppm)

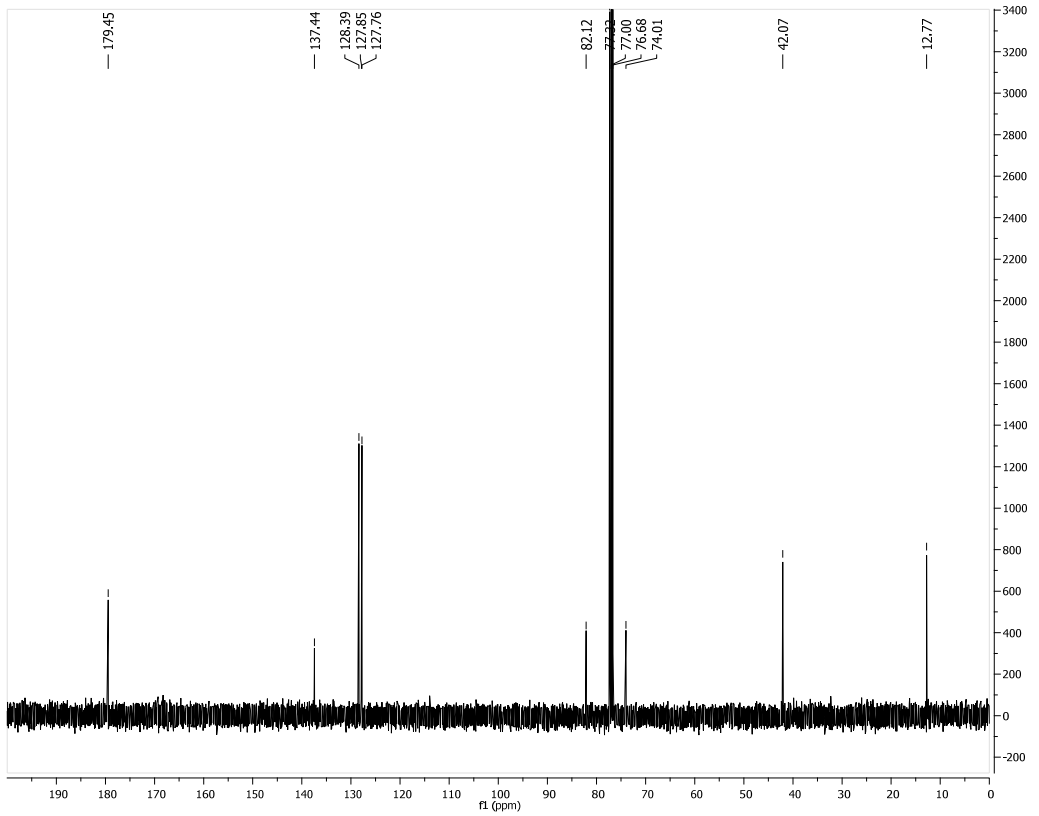
179.45
137.44
128.39
127.85
127.76
82.12
77.33
77.00
76.68
74.01
42.07
12.77
f1 (ppm)

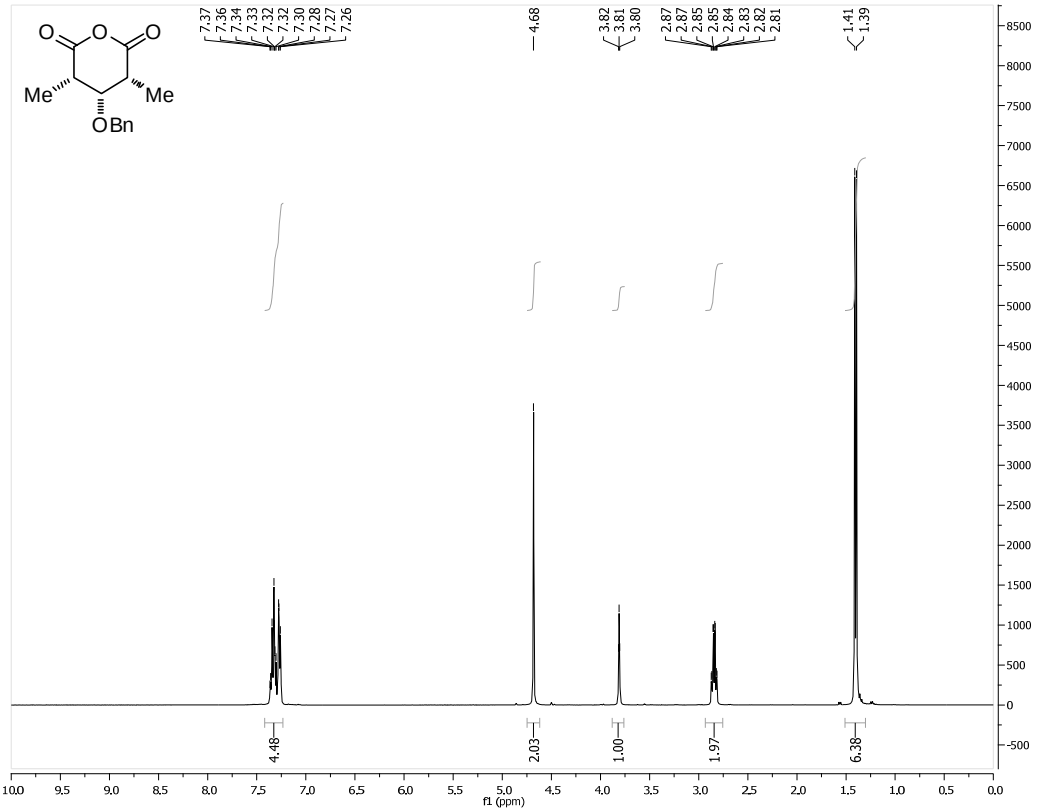
Me
Me
OBn
7.37
7.36
7.34
7.33
7.32
7.32
7.30
7.28
7.27
7.26
4.68
3.82
3.81
3.80
2.87
2.87
2.85
2.85
2.84
2.83
2.82
2.81
1.41
1.39
4.48
2.03
1.00
1.97
6.38
f1 (ppm)

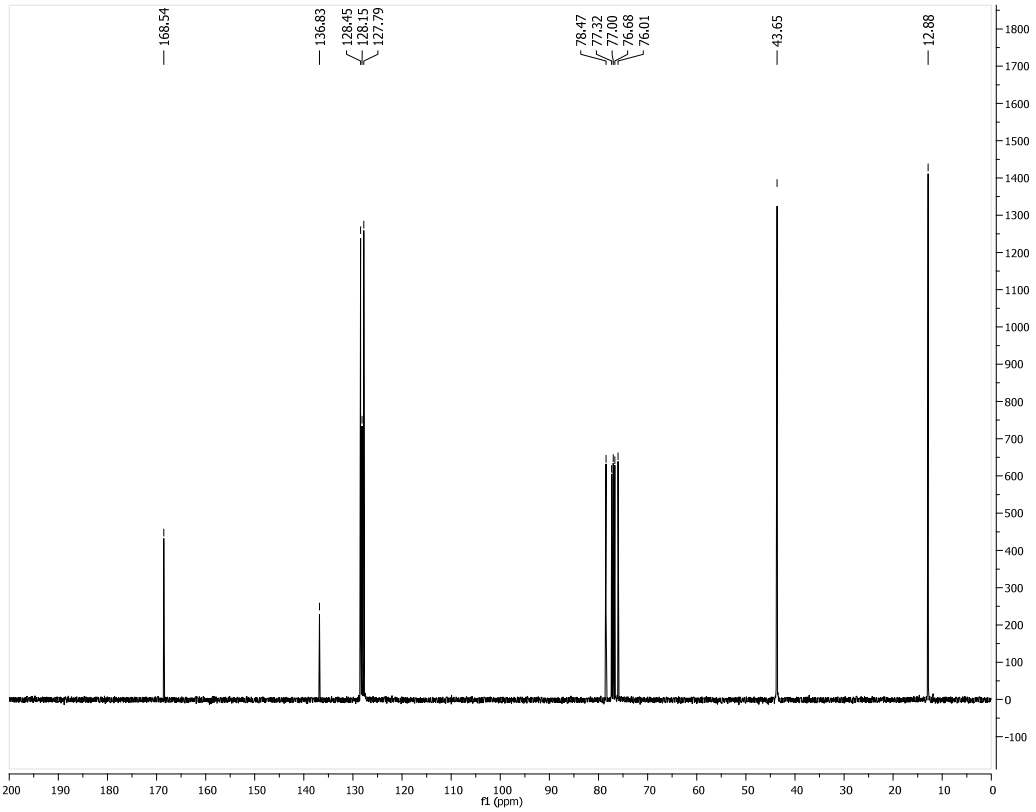
168.54
136.83
128.45
128.15
127.79
78.47
77.32
77.00
76.68
76.01
43.65
12.88
f1 (ppm)

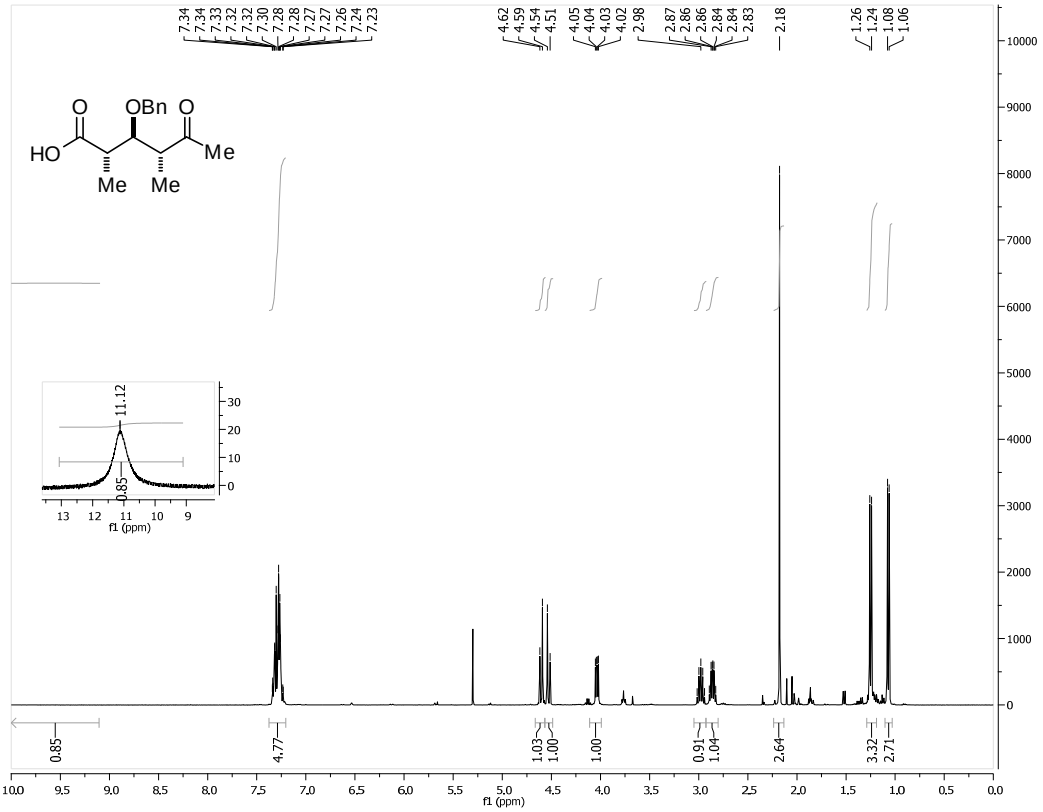
7.34
7.34
7.33
7.32
7.32
7.30
7.28
7.28
7.27
7.27
7.26
7.24
7.23
4.62
4.59
4.54
4.51
4.05
4.04
4.03
4.02
2.98
2.87
2.86
2.86
2.84
2.84
2.83
2.18
1.26
1.24
1.08
1.06
O
OBn
O
HO
Me
Me
Me
11.12
0.85
f1 (ppm)
0.85
4.77
1.03
1.00
1.00
0.91
1.04
2.64
3.32
2.71
f1 (ppm)

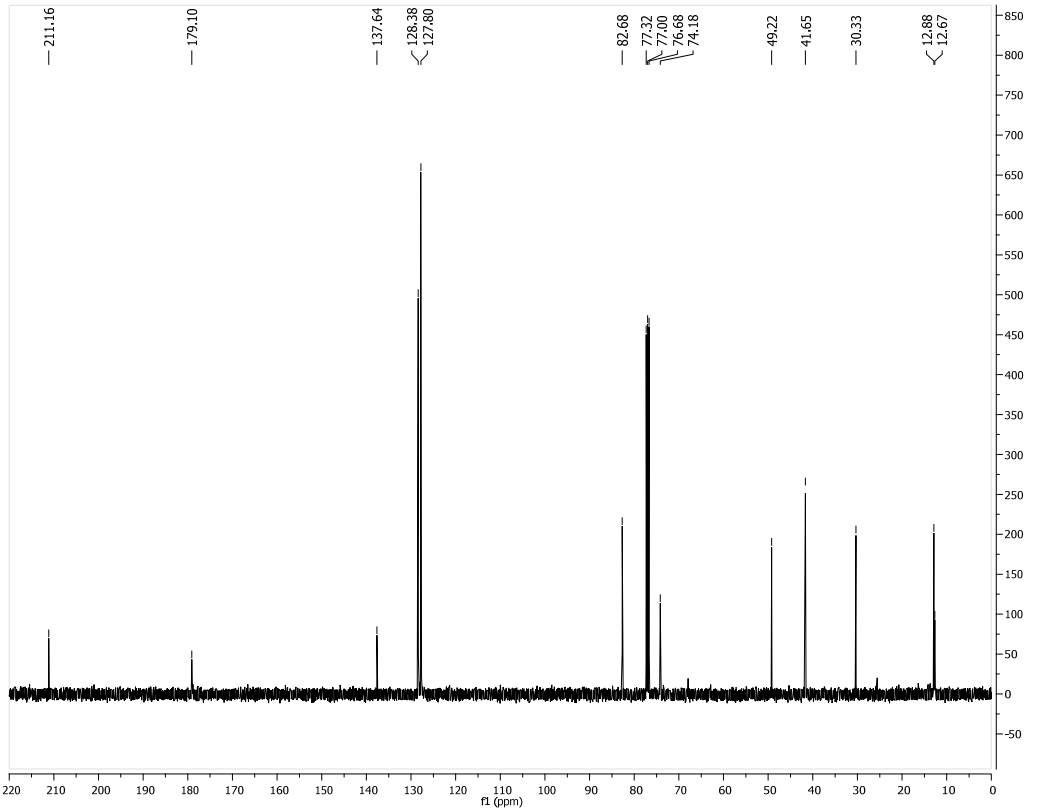
211.16
179.10
137.64
128.38
127.80
82.68
77.32
77.00
76.68
74.18
49.22
41.65
30.33
12.88
12.67
f1 (ppm)

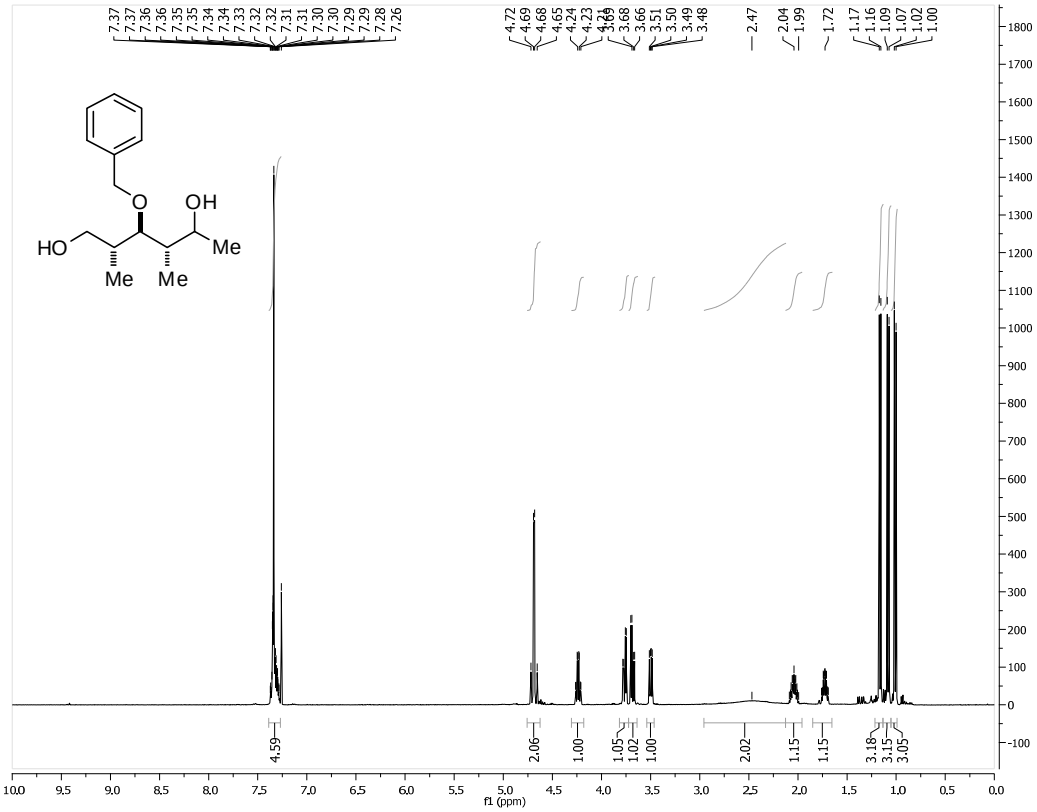
7.37 7.37 7.36 7.36 7.35 7.35 7.34 7.34 7.33 7.32 7.32 7.31 7.31 7.30 7.30 7.29 7.29 7.28 7.26
4.72 4.69 4.68 4.65 4.24 4.23 4.21 3.69 3.68 3.66 3.51 3.50 3.49 3.48
2.47 2.04 1.99 1.72 1.17 1.16 1.09 1.07 1.02 1.00
O OH HO Me Me Me
4.59 2.06 1.00 1.05 1.02 1.00 2.02 1.15 1.15 3.18 3.15 3.05
f1 (ppm)

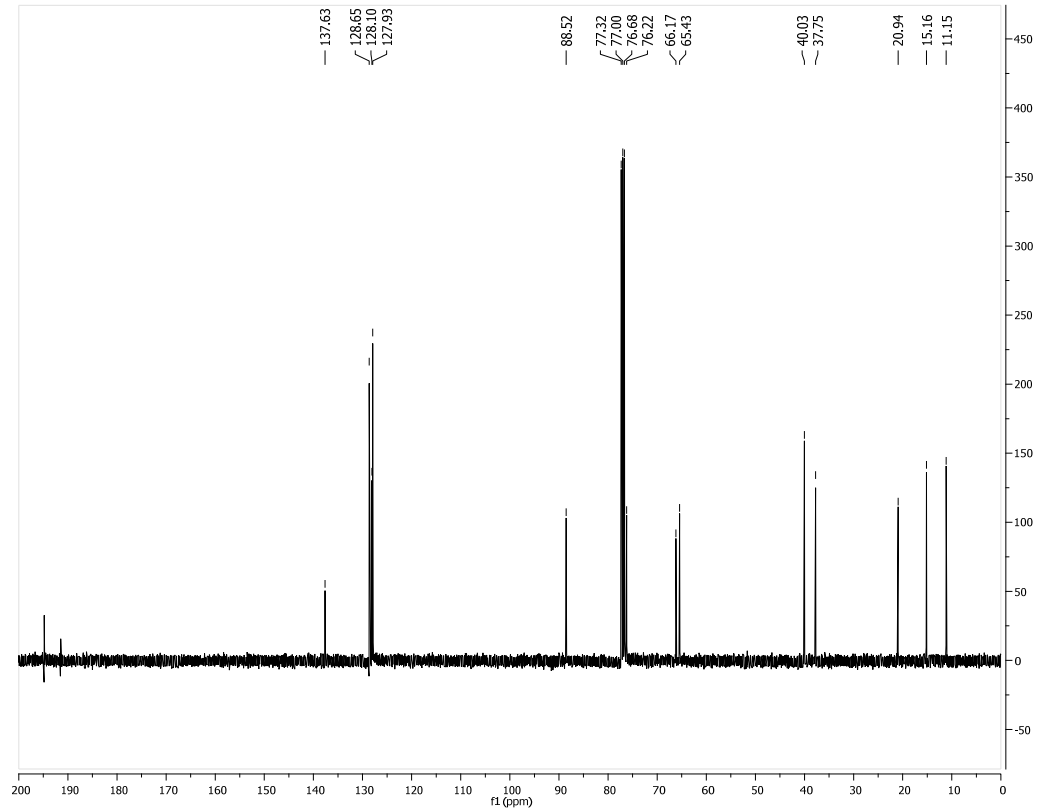
137.63 128.65 128.10 127.93 88.52 77.32 77.00 76.68 76.22 66.17 65.43 40.03 37.75 20.94 15.16 11.15
f1 (ppm)

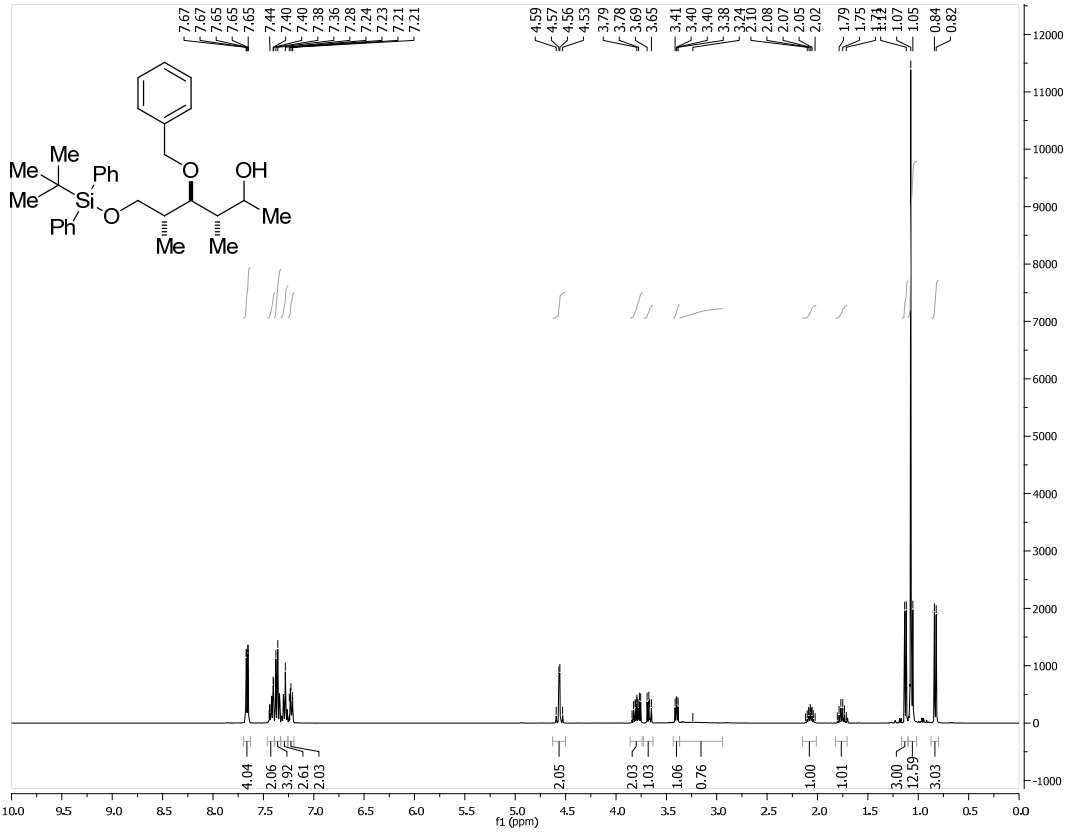
7.67
7.67
7.65
7.65
7.65
7.44
7.40
7.40
7.38
7.36
7.28
7.24
7.23
7.21
7.21
4.59
4.57
4.56
4.53
3.79
3.78
3.69
3.65
3.41
3.40
3.40
3.38
3.24
2.10
2.08
2.07
2.05
2.02
1.79
1.75
1.71
1.07
1.05
0.84
0.82
Me
Me
Ph
Si
Ph
O
O
OH
Me
Me
Me
4.04
2.06
3.92
2.61
2.03
2.05
2.03
1.03
1.06
0.76
1.00
1.01
3.00
12.99
3.03
f1 (ppm)

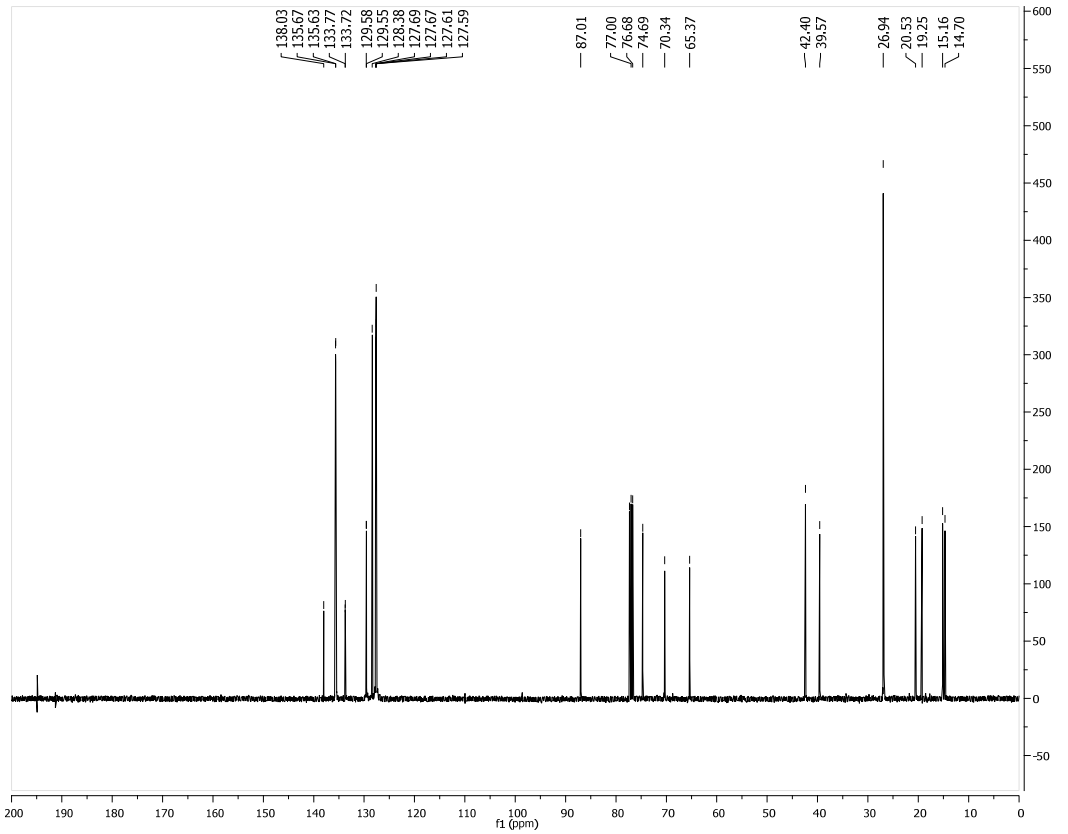
138.03
135.67
135.63
133.77
133.72
129.58
129.55
128.38
127.69
127.67
127.61
127.59
87.01
77.00
76.68
74.69
70.34
65.37
42.40
39.57
26.94
20.53
19.25
15.16
14.70
f1 (ppm)

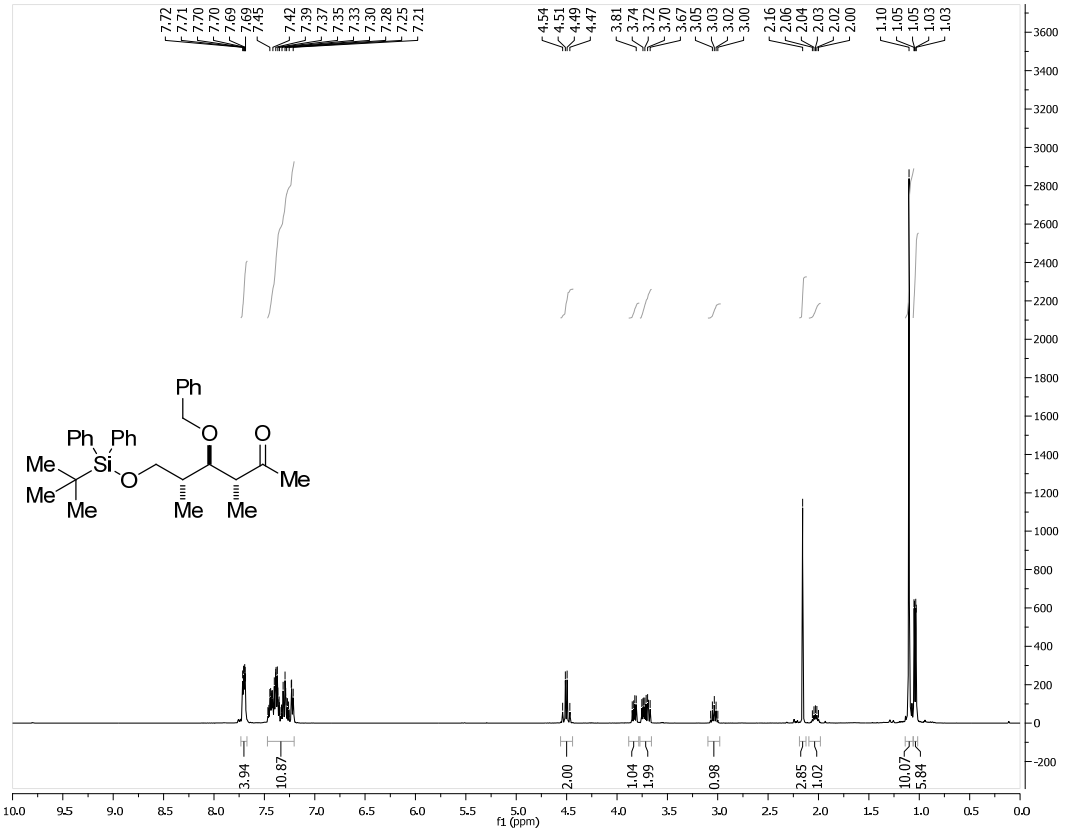
7.72
7.71
7.70
7.70
7.69
7.69
7.45
7.42
7.39
7.37
7.35
7.33
7.30
7.28
7.25
7.21
4.54
4.51
4.49
4.47
3.81
3.74
3.72
3.70
3.67
3.05
3.03
3.02
3.00
2.16
2.06
2.04
2.03
2.02
2.00
1.10
1.05
1.05
1.03
1.03
Ph
Ph
Ph
Si
O
O
O
Me
Me
Me
Me
Me
Me
3.94
10.87
2.00
1.04
1.99
0.98
2.85
1.02
10.07
5.84
f1 (ppm)

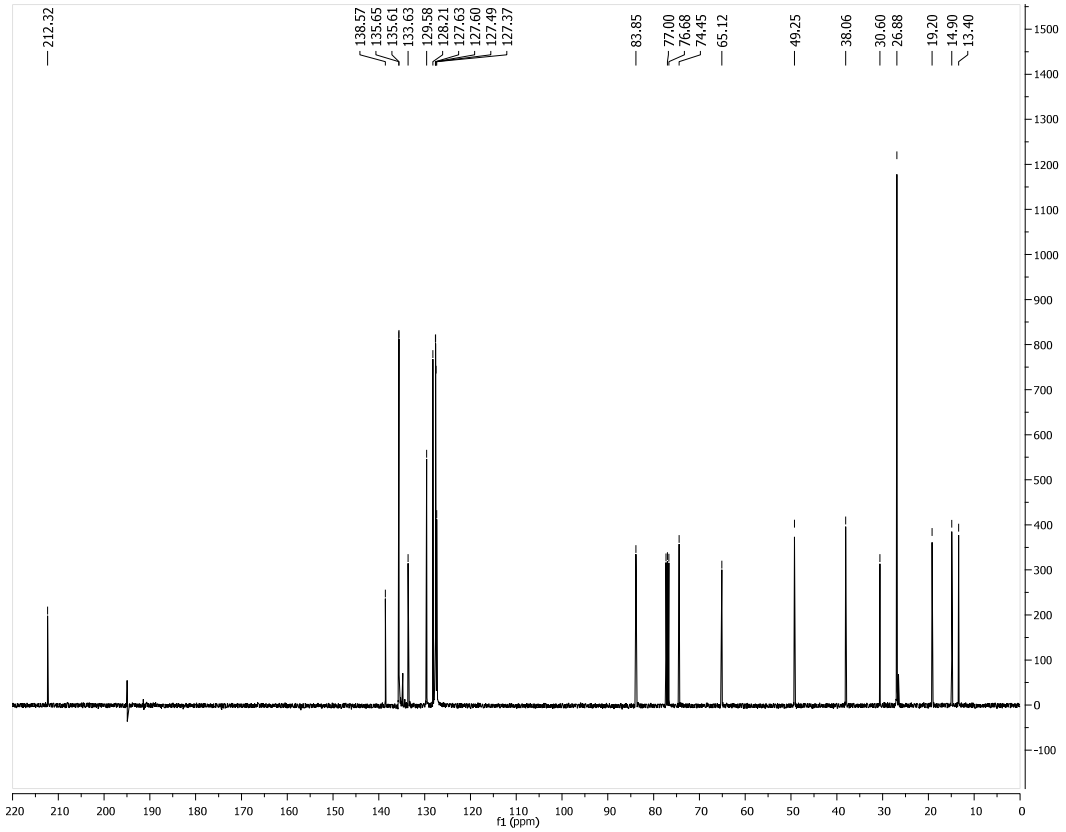
212.32
138.57
135.65
135.61
133.63
129.58
128.21
127.63
127.60
127.49
127.37
83.85
77.00
76.68
74.45
65.12
49.25
38.06
30.60
26.88
19.20
14.90
13.40
f1 (ppm)

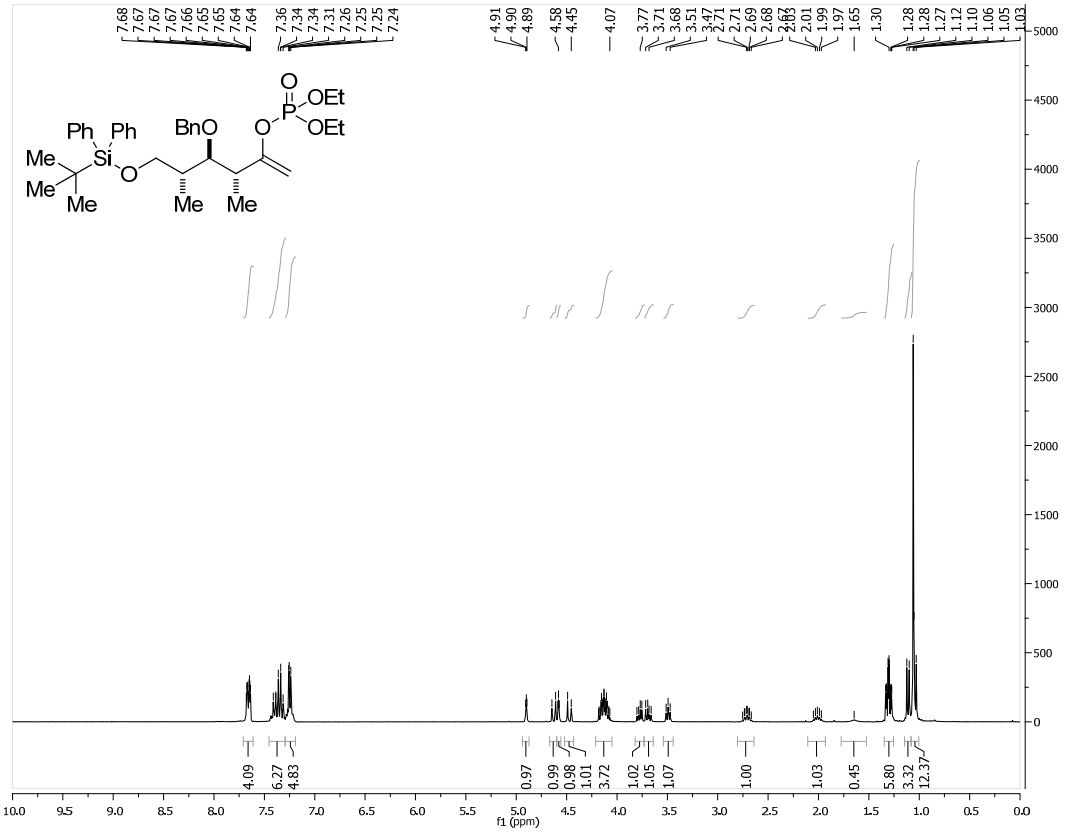
7.68 7.67 7.67 7.66 7.65 7.65 7.64 7.64 7.36 7.34 7.34 7.31 7.26 7.25 7.25 7.24
4.91 4.90 4.89 4.58 4.45 4.07 3.77 3.71 3.68 3.51 3.47 2.71 2.69 2.68 2.67 2.03 2.01 1.99 1.97 1.65 1.30 1.28 1.28 1.27 1.12 1.10 1.06 1.05 1.03
O
OEt
P
OEt
Ph Ph
BnO
O
Me
Me
Me
Si
O
Me Me
4.09 6.27 4.83 0.97 0.99 0.98 1.01 3.72 1.02 1.05 1.07 1.00 1.03 0.45 5.80 3.32 12.37
f1 (ppm)

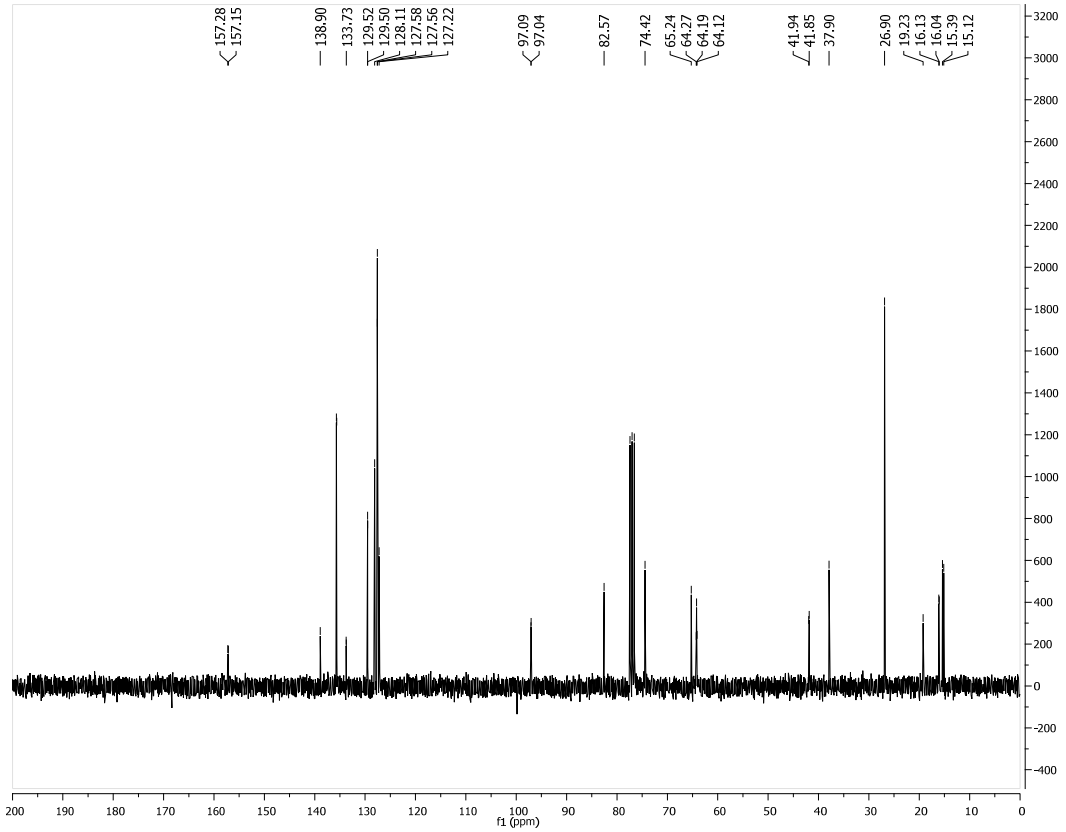
157.28 157.15 138.90 133.73 129.52 129.50 128.11 127.58 127.56 127.22 97.09 97.04 82.57 74.42 65.24 64.27 64.19 64.12 41.94 41.85 37.90 26.90 19.23 16.13 16.04 15.39 15.12
f1 (ppm)

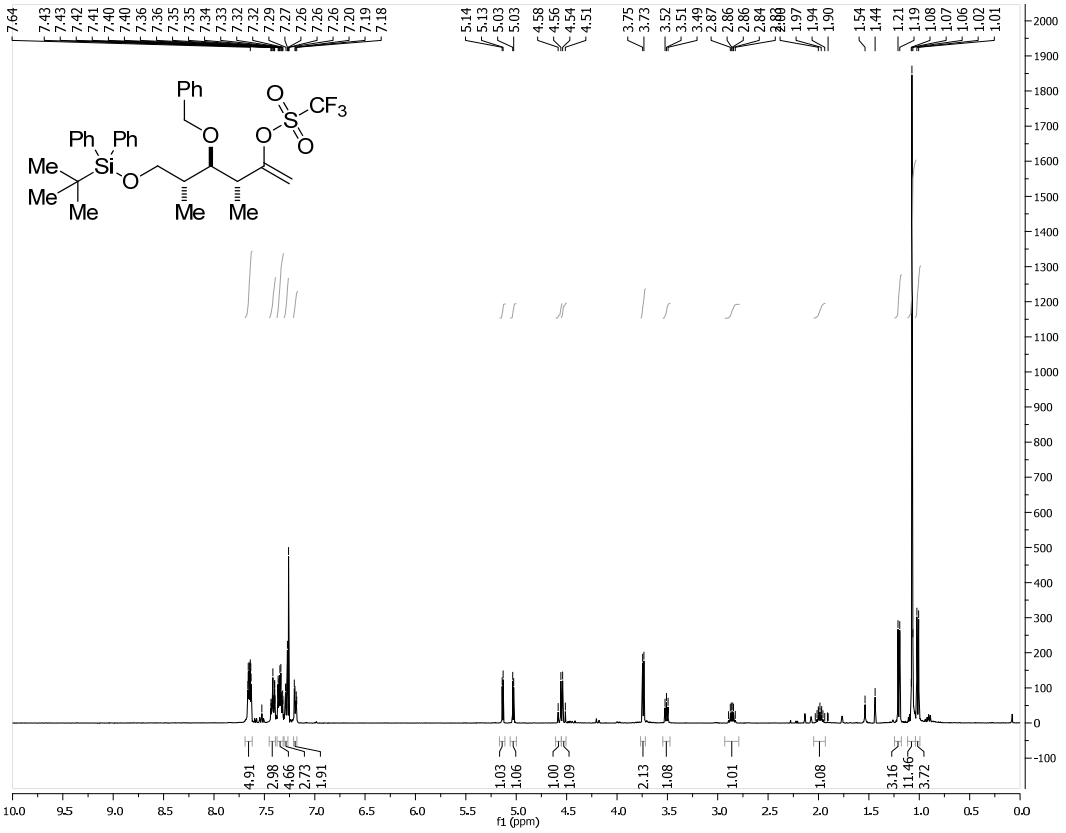
Ph
O
CF3
Ph
Ph
O
O
Me
Si
O
Me
Me
Me
Me
f1 (ppm)

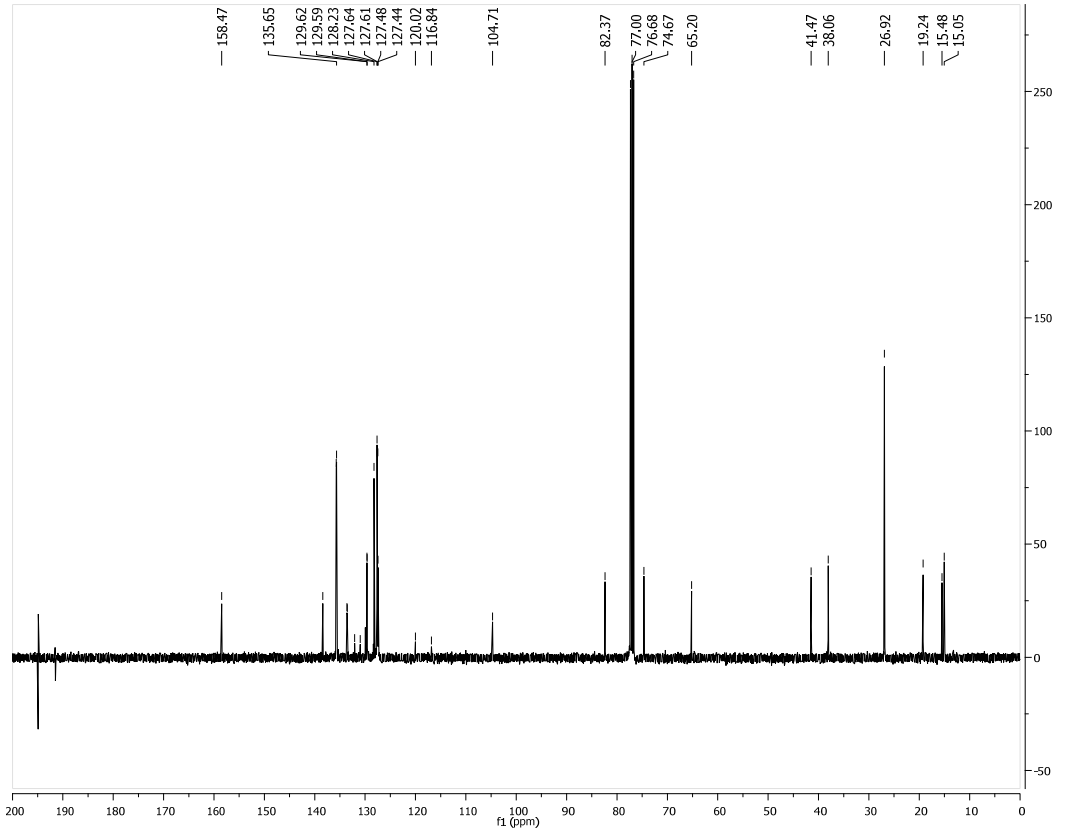
158.47
135.65
129.62
129.59
128.23
127.64
127.61
127.48
127.44
120.02
116.84
104.71
82.37
77.00
76.68
74.67
65.20
41.47
38.06
26.92
19.24
15.48
15.05
f1 (ppm)

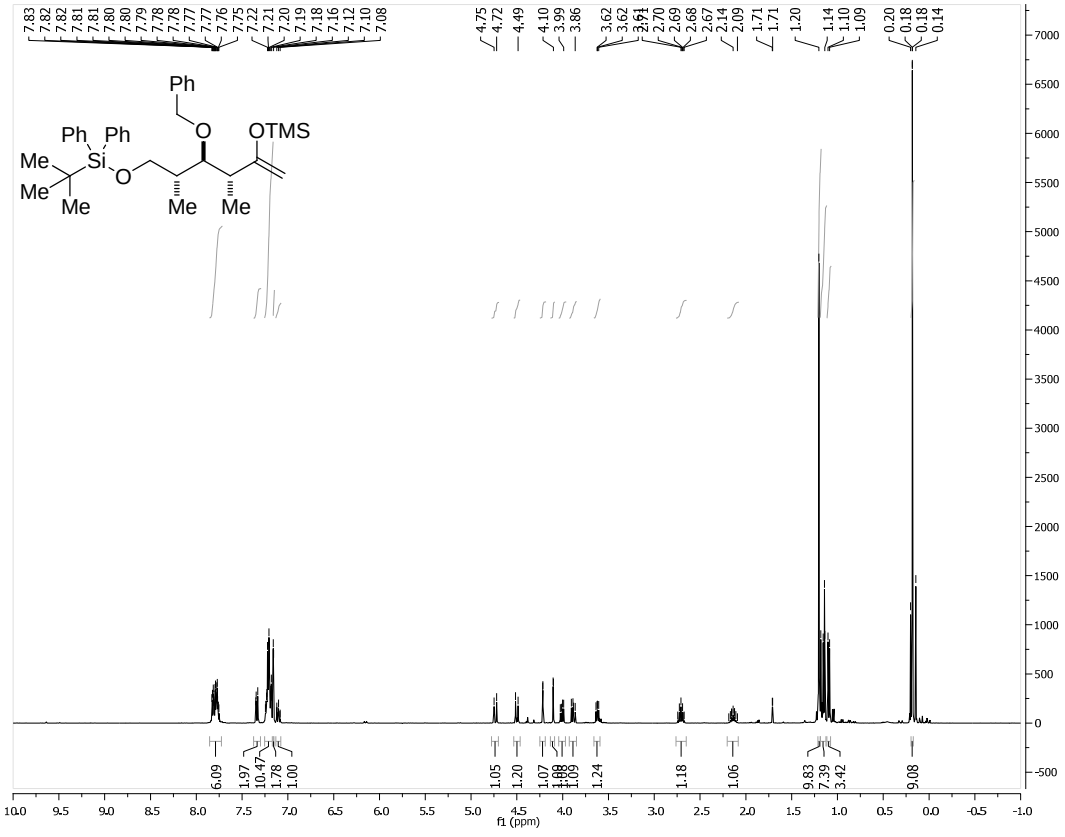
Ph
O
OTMS
Ph Ph
Si
Me
Me
Me
O
Me
Me
f1 (ppm)

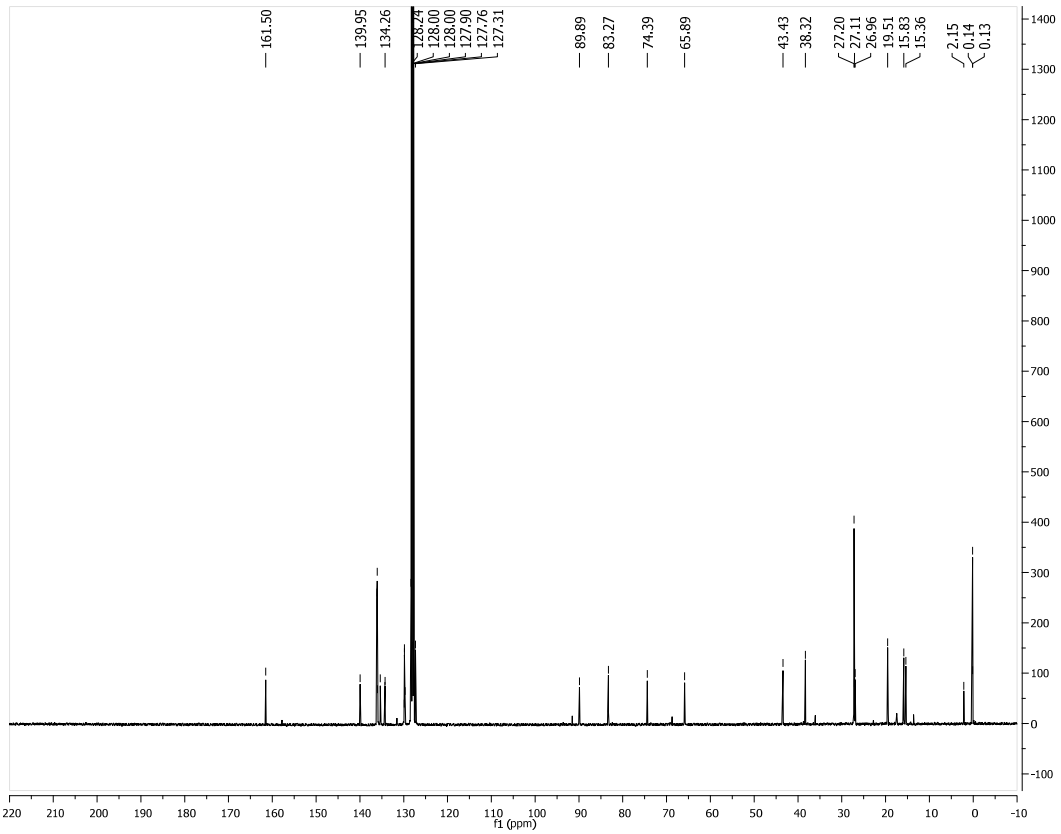
f1 (ppm)

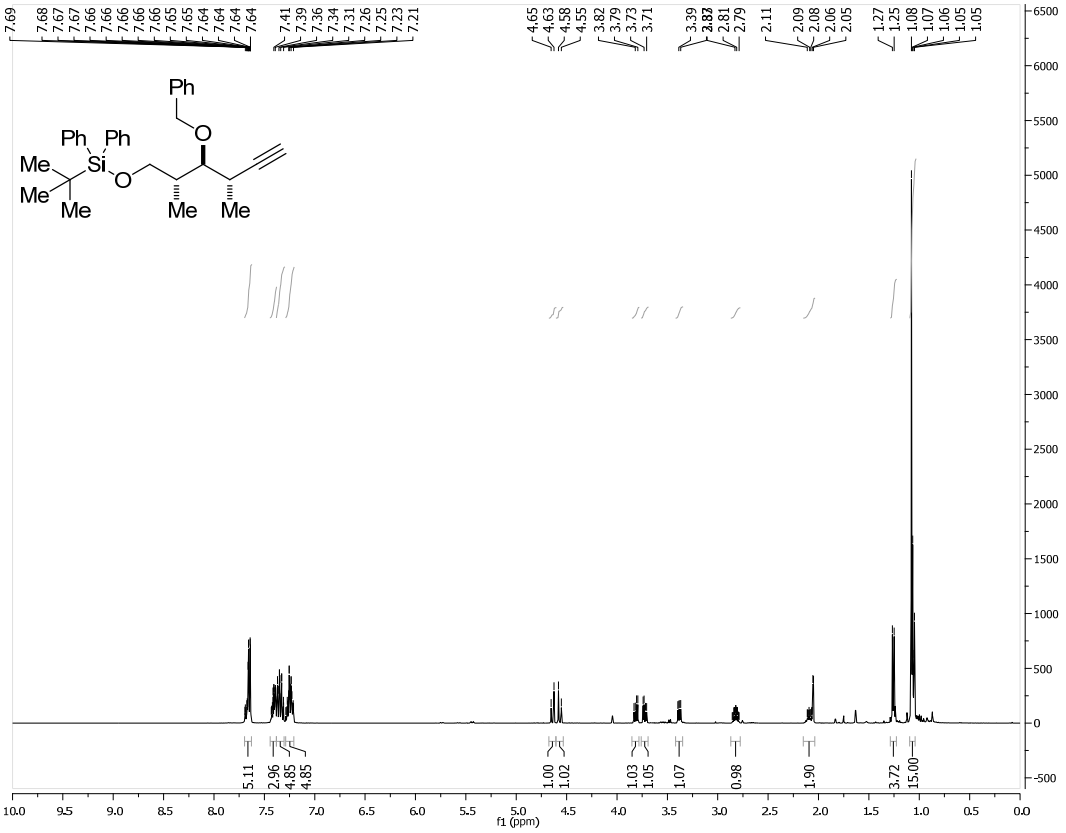
Ph
O
Ph
Ph
Si
Me
Me
Me
O
Me
Me
f1 (ppm)

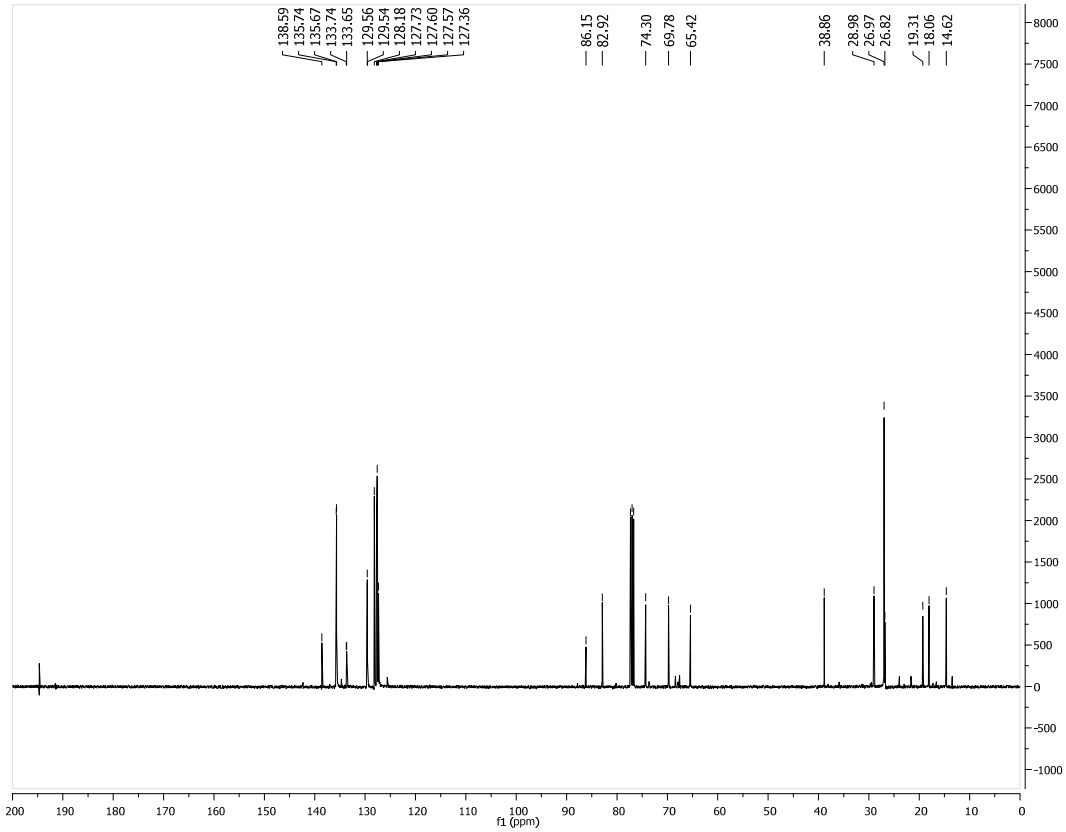
f1 (ppm)

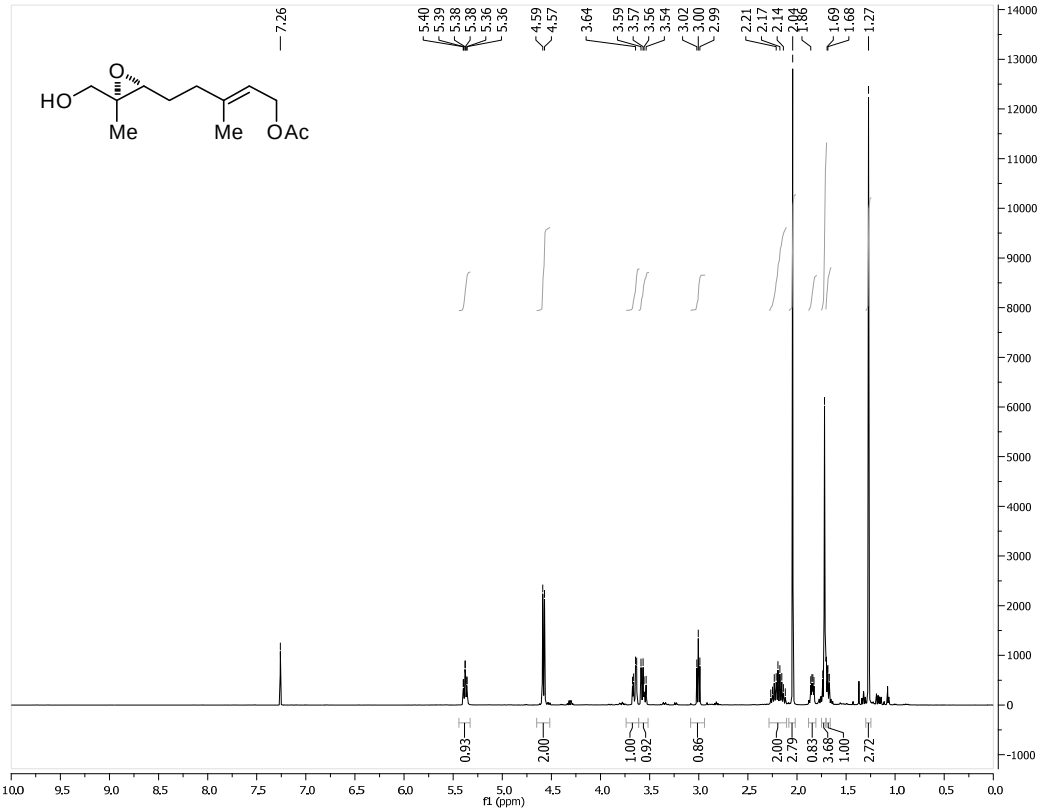
HO
Me
Me
OAc
7.26
5.40
5.39
5.38
5.38
5.36
5.36
4.59
4.57
3.64
3.59
3.57
3.56
3.54
3.02
3.00
2.99
2.21
2.17
2.14
2.04
1.86
1.69
1.68
1.27
0.93
2.00
1.00
0.92
0.86
2.00
2.79
0.83
3.68
1.00
2.72
f1 (ppm)

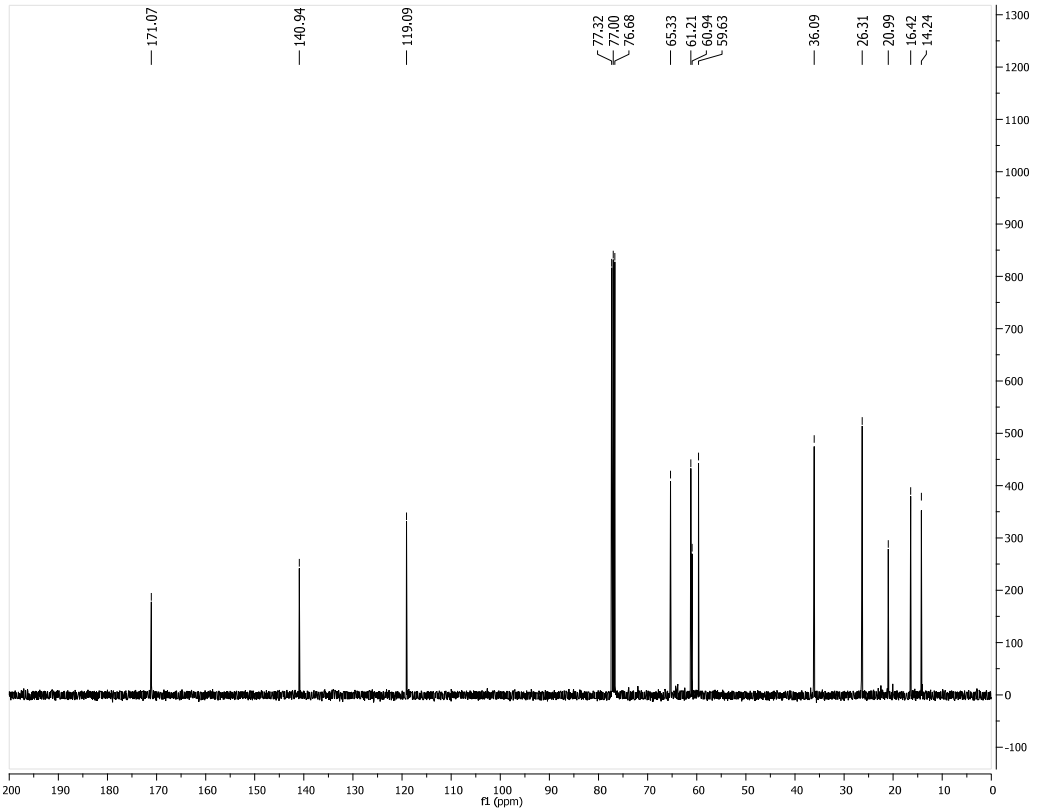
171.07
140.94
119.09
77.32
77.00
76.68
65.33
61.21
60.94
59.63
36.09
26.31
20.99
16.42
14.24
f1 (ppm)

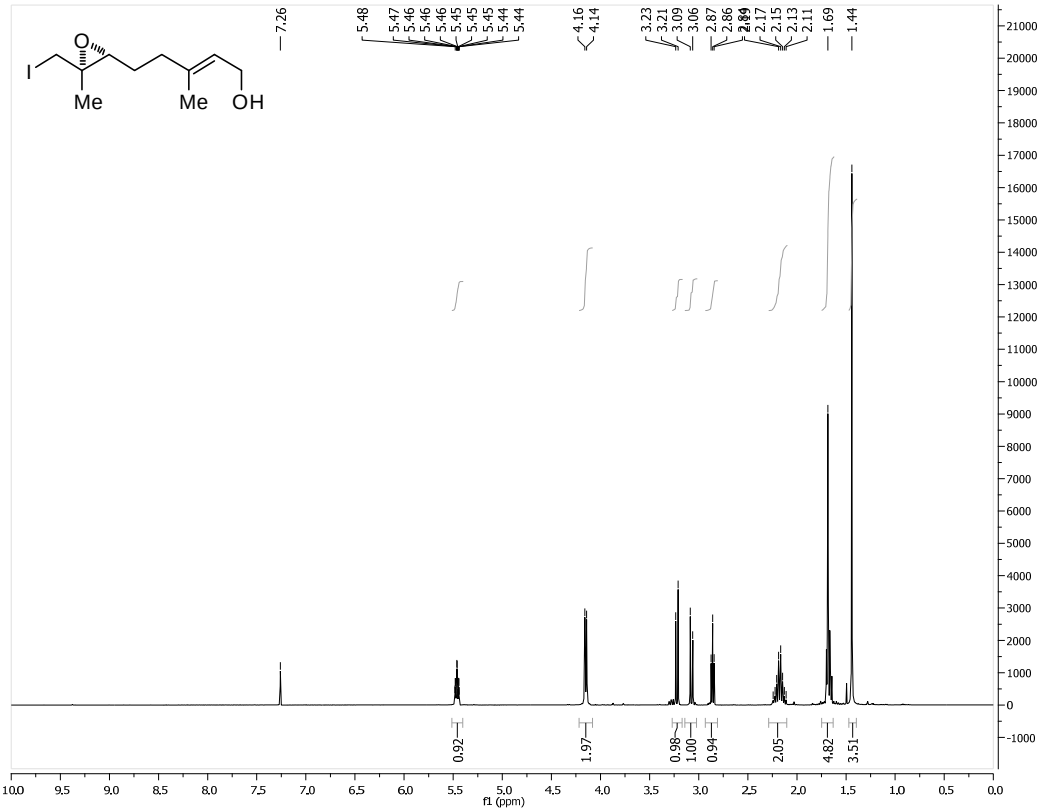
I
O
Me
Me
OH
7.26
5.48
5.47
5.46
5.46
5.46
5.45
5.45
5.45
5.44
5.44
4.16
4.14
3.23
3.21
3.09
3.06
2.87
2.86
2.17
2.15
2.13
2.11
1.69
1.44
0.92
1.97
0.98
1.00
0.94
2.05
4.82
3.51
f1 (ppm)

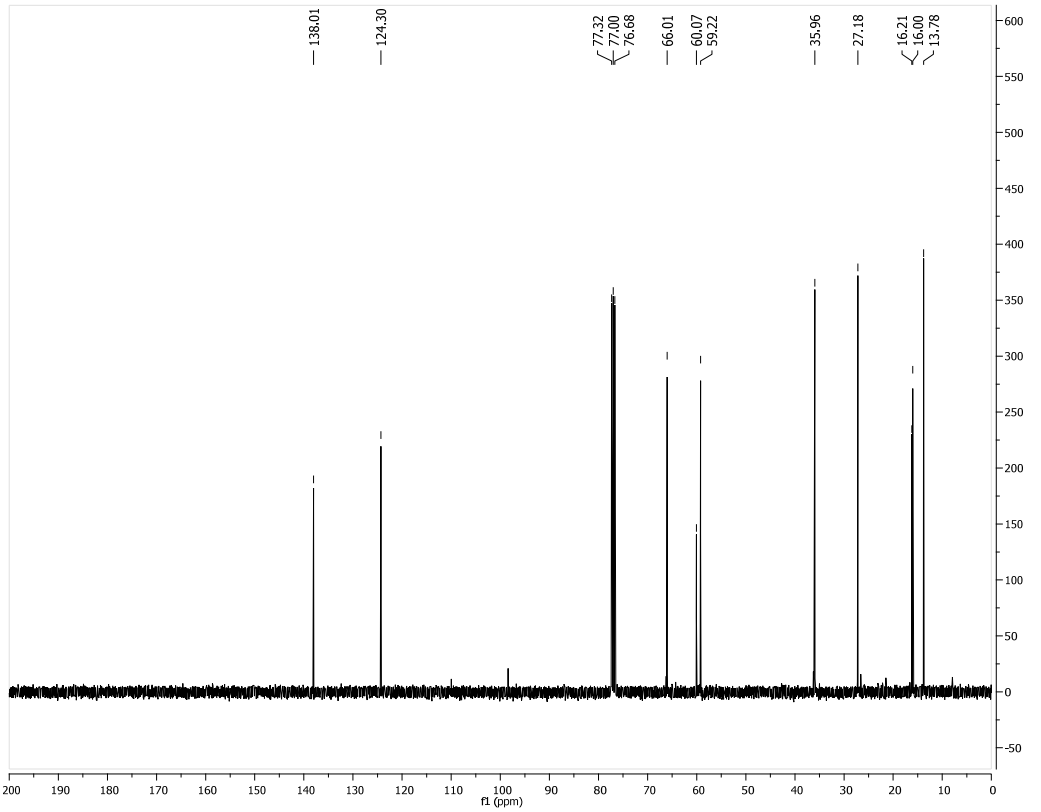
138.01
124.30
77.32
77.00
76.68
66.01
60.07
59.22
35.96
27.18
16.21
16.00
13.78
f1 (ppm)

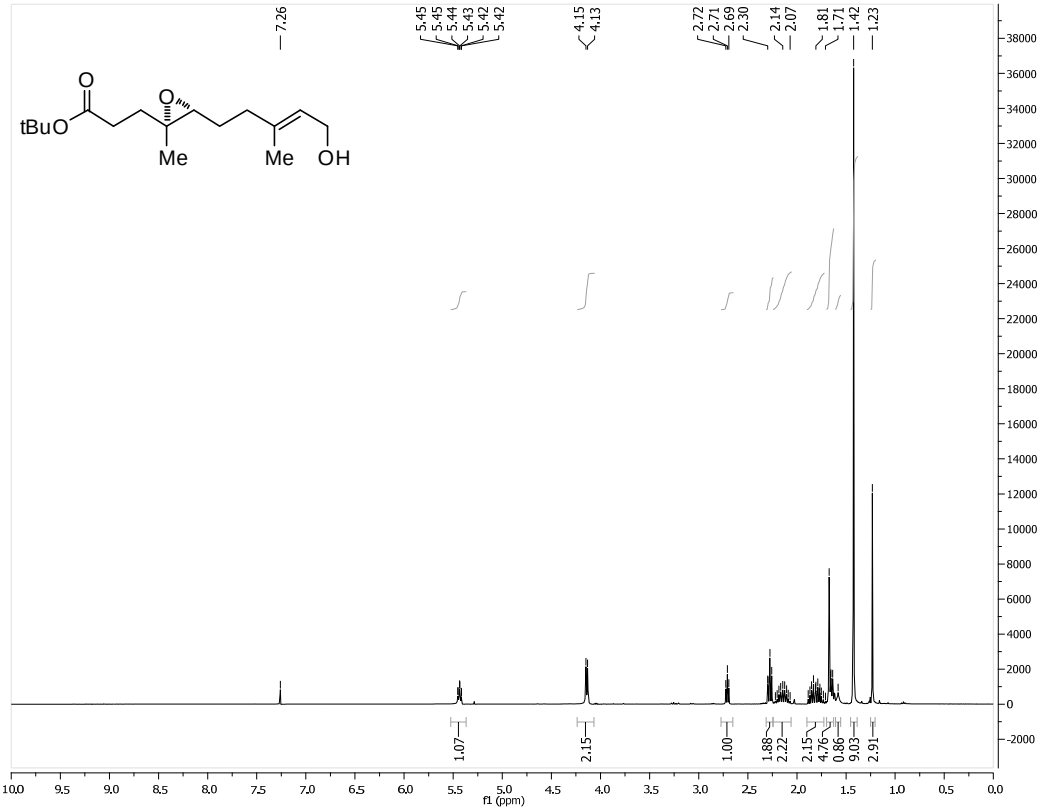
7.26
5.45
5.45
5.44
5.43
5.42
5.42
4.15
4.13
2.72
2.71
2.69
2.30
2.14
2.07
1.81
1.71
1.42
1.23
tBuO
Me
Me
OH
1.07
2.15
1.00
1.88
2.22
2.15
4.76
0.86
9.03
2.91
f1 (ppm)

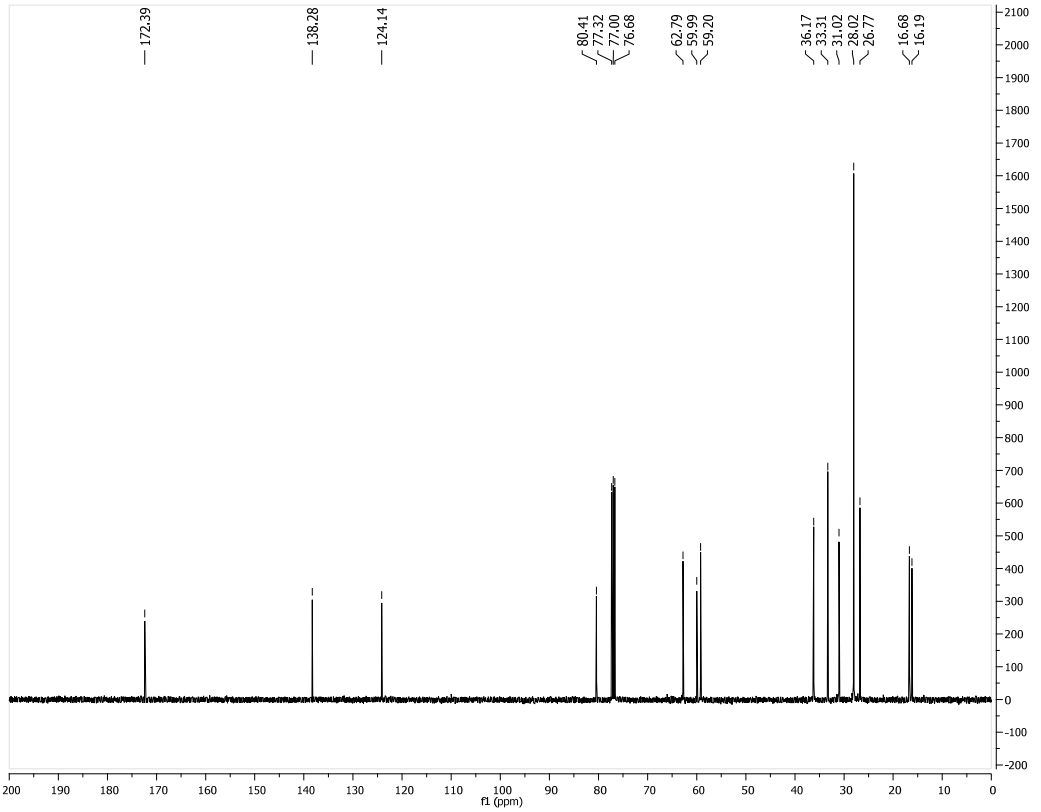
172.39
138.28
124.14
80.41
77.32
77.00
76.68
62.79
59.99
59.20
36.17
33.31
31.02
28.02
26.77
16.68
16.19
f1 (ppm)

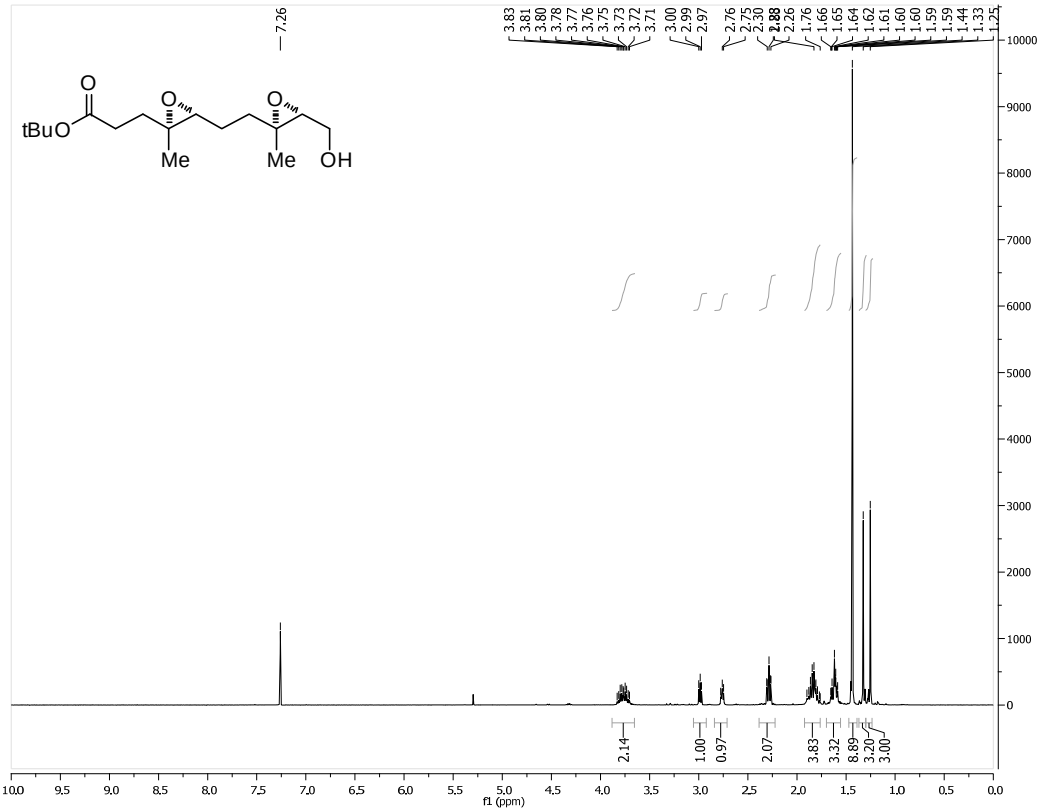
7.26
3.83
3.81
3.80
3.78
3.77
3.76
3.75
3.73
3.72
3.71
3.00
2.99
2.97
2.76
2.75
2.30
2.26
1.76
1.66
1.65
1.64
1.62
1.61
1.60
1.60
1.59
1.59
1.44
1.33
1.25
O
O
O
tBuO
Me
Me
OH
2.14
1.00
0.97
2.07
3.83
3.32
8.89
3.20
3.00
f1 (ppm)

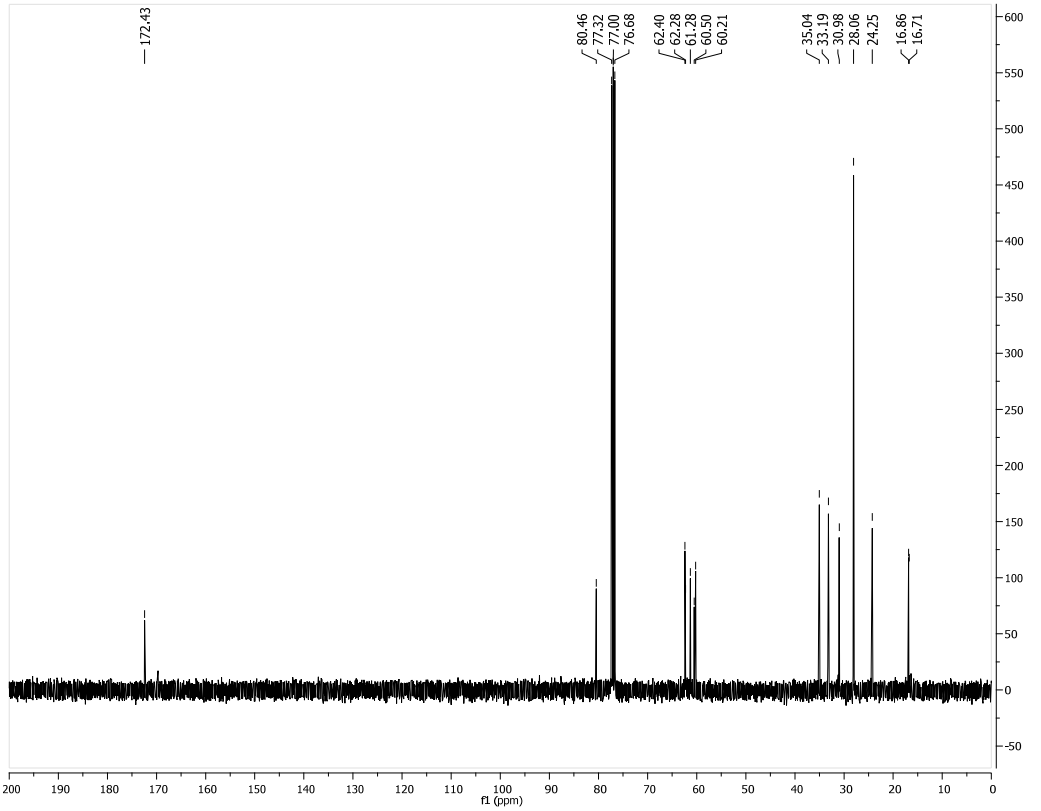
172.43
80.46
77.32
77.00
76.68
62.40
62.28
61.28
60.50
60.21
35.04
33.19
30.98
28.06
24.25
16.86
16.71
f1 (ppm)

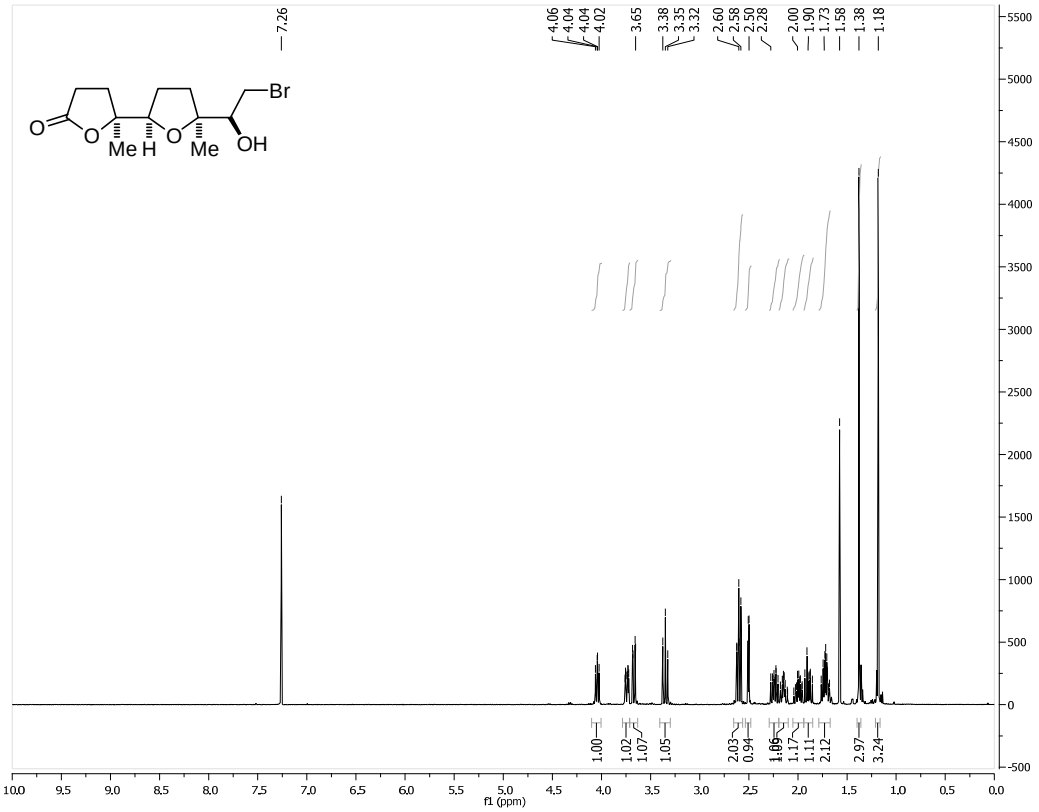
7.26
4.06
4.04
4.04
4.02
3.65
3.38
3.35
3.32
2.60
2.58
2.50
2.28
2.00
1.90
1.73
1.58
1.38
1.18
Br
O
O
Me H
O
Me
OH
1.00
1.02
1.07
1.05
2.03
0.94
1.17
1.11
2.12
2.97
3.24
f1 (ppm)

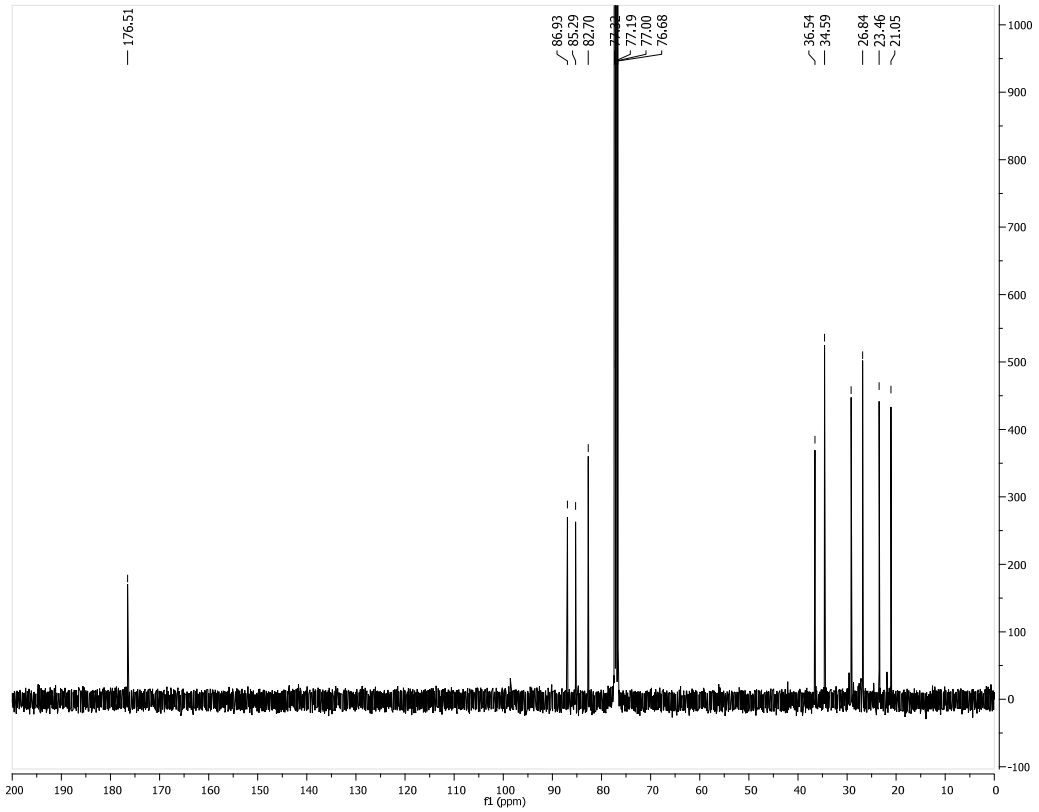
176.51
86.93
85.29
82.70
77.19
77.00
76.68
36.54
34.59
26.84
23.46
21.05
f1 (ppm)

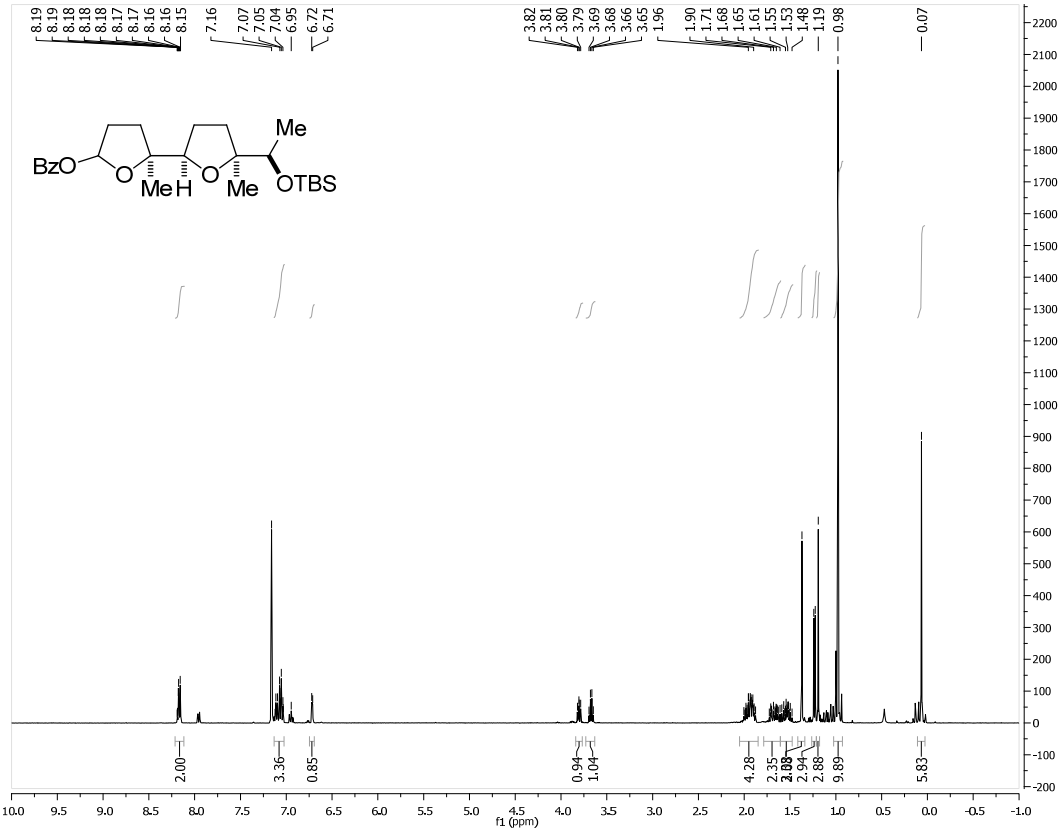
8.19
8.19
8.18
8.18
8.18
8.17
8.17
8.16
8.16
8.15
7.16
7.07
7.05
7.04
6.95
6.72
6.71
3.82
3.81
3.80
3.79
3.69
3.68
3.66
3.65
1.96
1.90
1.71
1.68
1.65
1.61
1.55
1.53
1.48
1.19
0.98
0.07
BzO
O
Me H
O
Me
Me
OTBS
2.00
3.36
0.85
0.94
1.04
4.28
2.35
2.94
2.88
9.89
5.83
f1 (ppm)

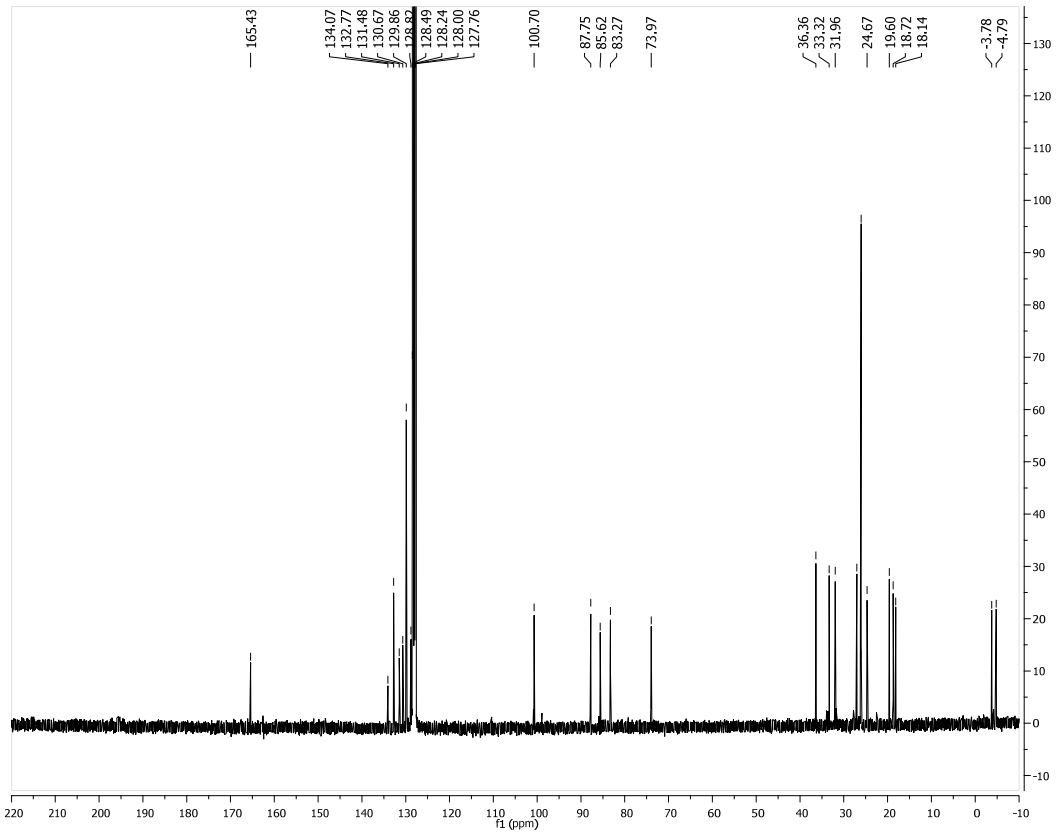
165.43
134.07
132.77
131.48
130.67
129.86
128.82
128.49
128.24
128.00
127.76
100.70
87.75
85.62
83.27
73.97
36.36
33.32
31.96
24.67
19.60
18.72
18.14
-3.78
-4.79
f1 (ppm)

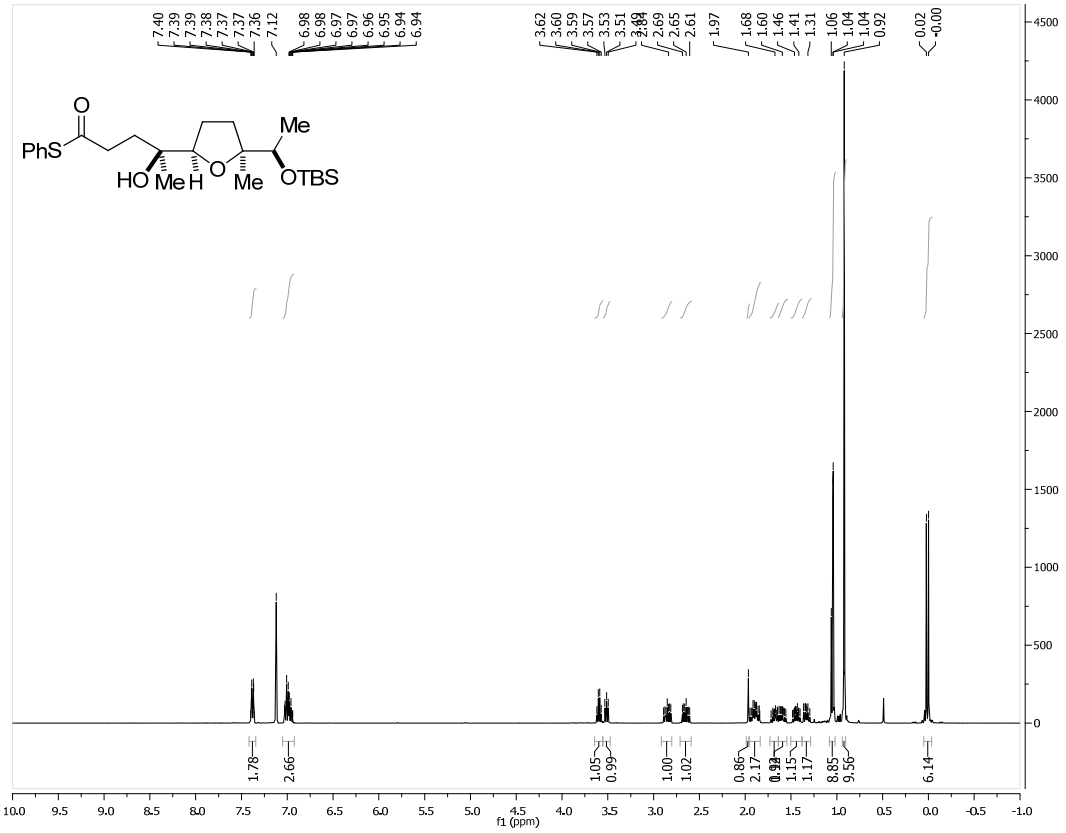
7.40
7.39
7.39
7.38
7.37
7.37
7.36
7.12
6.98
6.98
6.97
6.97
6.96
6.95
6.94
6.94
3.62
3.60
3.59
3.57
3.53
3.51
2.69
2.65
2.61
1.97
1.68
1.60
1.46
1.41
1.31
1.06
1.04
1.04
0.92
0.02
-0.00
O
PhS
Me
HO
Me
H
O
Me
OTBS
1.78
2.66
1.05
0.99
1.00
1.02
0.86
2.17
1.15
1.17
8.85
9.56
6.14
f1 (ppm)

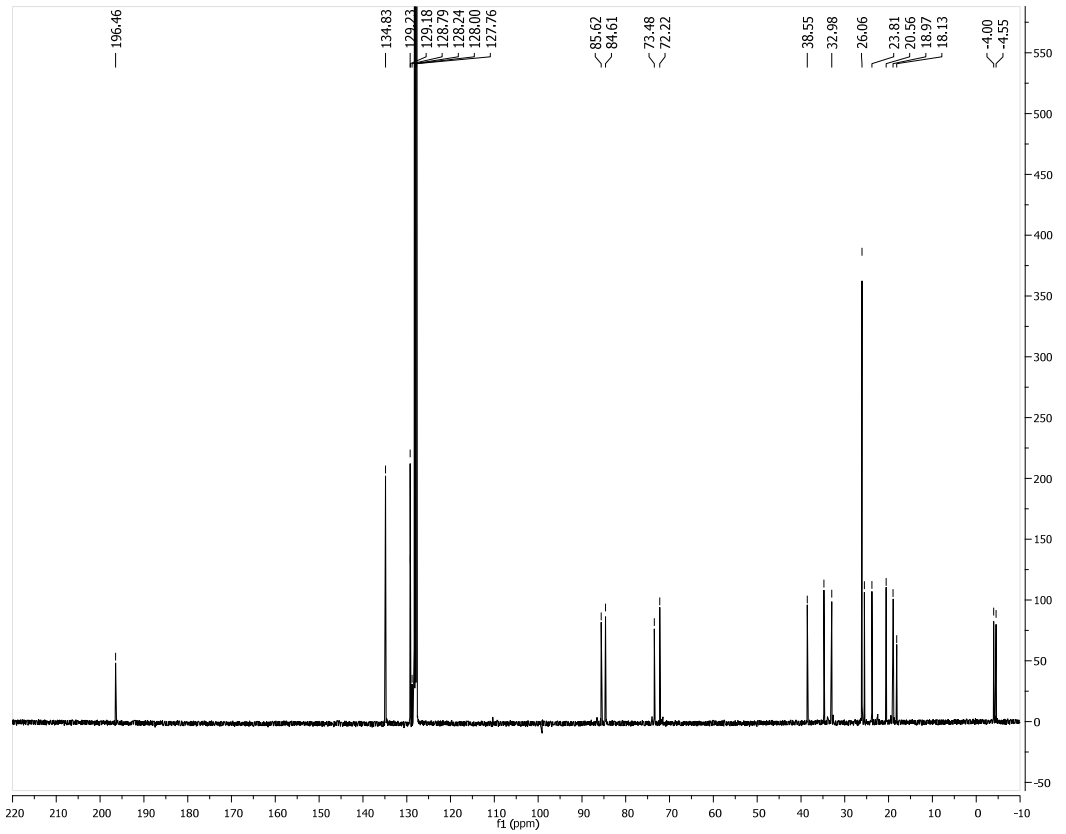
196.46
134.83
129.22
129.18
128.79
128.24
128.00
127.76
85.62
84.61
73.48
72.22
38.55
32.98
26.06
23.81
20.56
18.97
18.13
-4.00
-4.55
f1 (ppm)

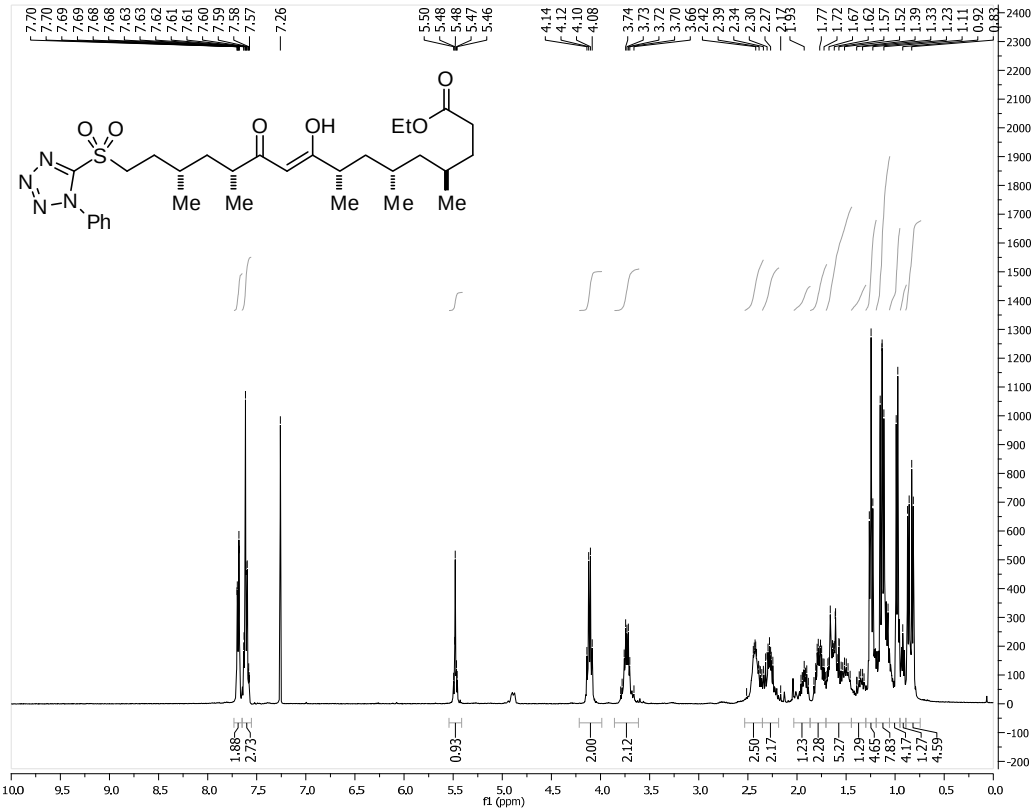
7.70 7.70 7.69 7.69 7.68 7.68 7.63 7.63 7.62 7.61 7.61 7.60 7.59 7.58 7.57
7.26
5.50 5.48 5.48 5.47 5.46
4.14 4.12 4.10 4.08
3.74 3.73 3.72 3.70 3.66 2.42 2.39 2.34 2.30 2.27 2.17 1.93
1.77 1.72 1.67 1.62 1.57 1.52 1.39 1.33 1.23 1.11 0.92 0.83
O
O O
S
O
OH
EtO
N
N
N
N
Ph
Me Me Me Me Me
1.88 2.73 0.93 2.00 2.12 2.50 2.17 1.23 2.28 5.27 1.29 4.65 7.83 4.17 1.27 4.59
f1 (ppm)

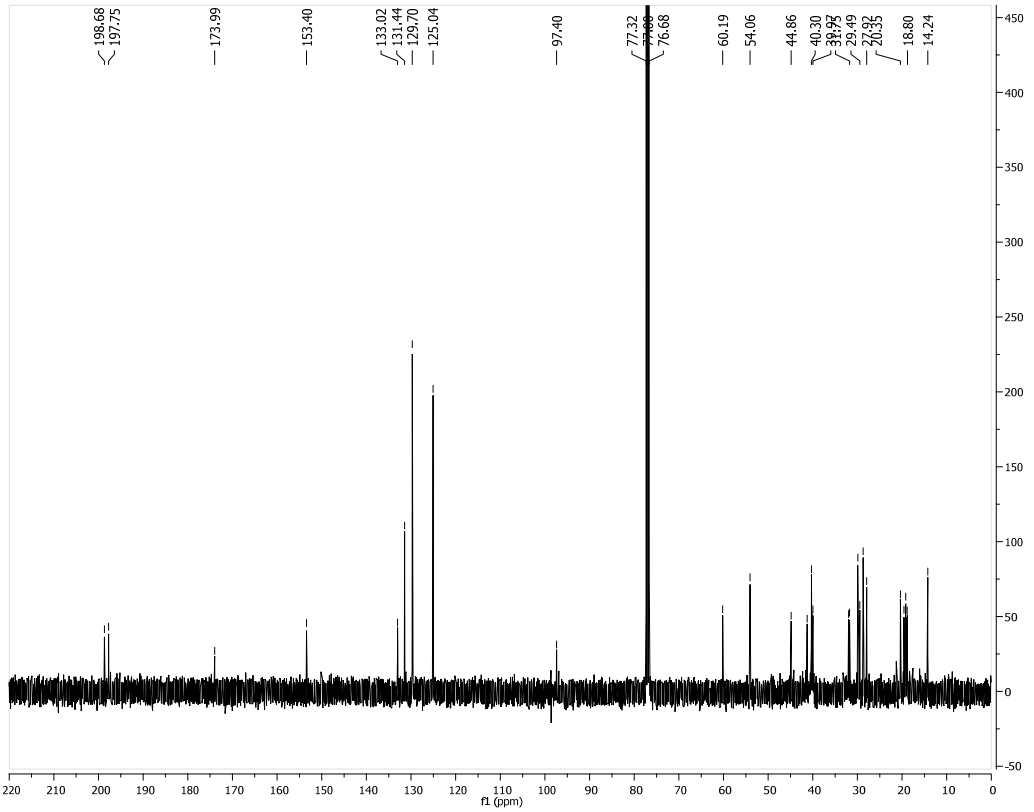
198.68
197.75
173.99
153.40
133.02
131.44
129.70
125.04
97.40
77.32
77.00
76.68
60.19
54.06
44.86
40.30
29.49
27.92
20.35
18.80
14.24
f1 (ppm)

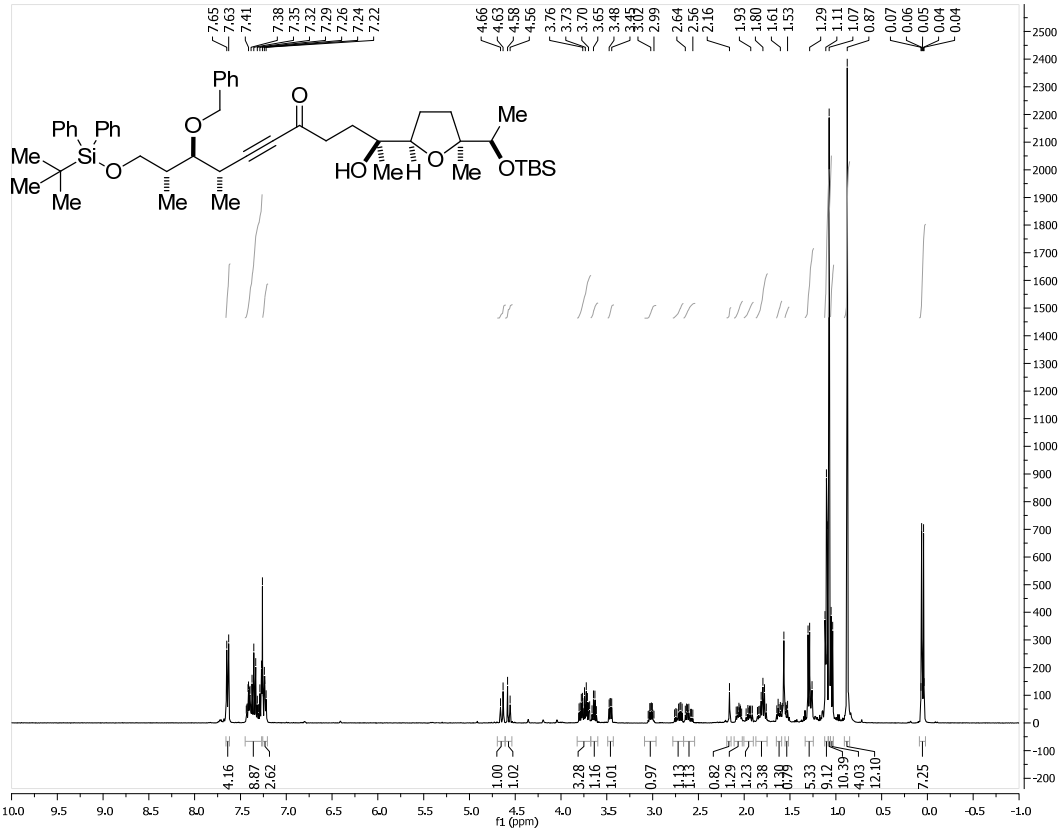
Ph
Ph Ph
Si
O
Me
Me
Me
O
Me Me
O
HO Me H
O
Me
Me
OTBS
f1 (ppm)

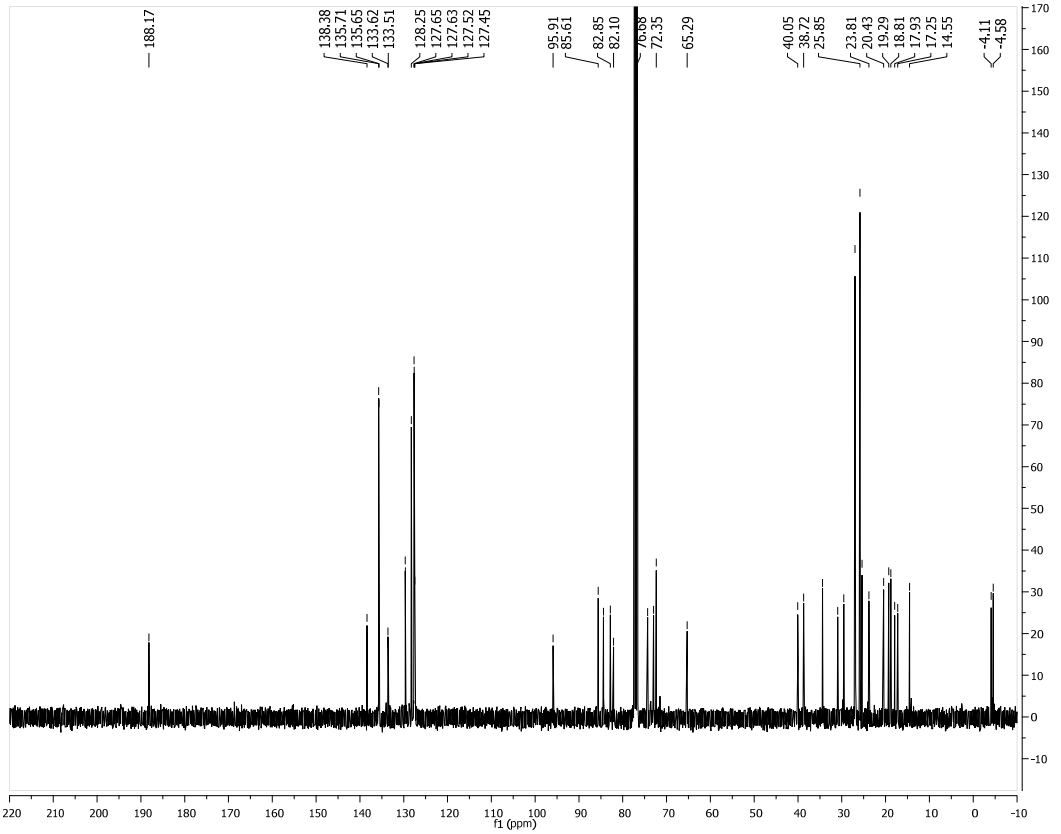
f1 (ppm)

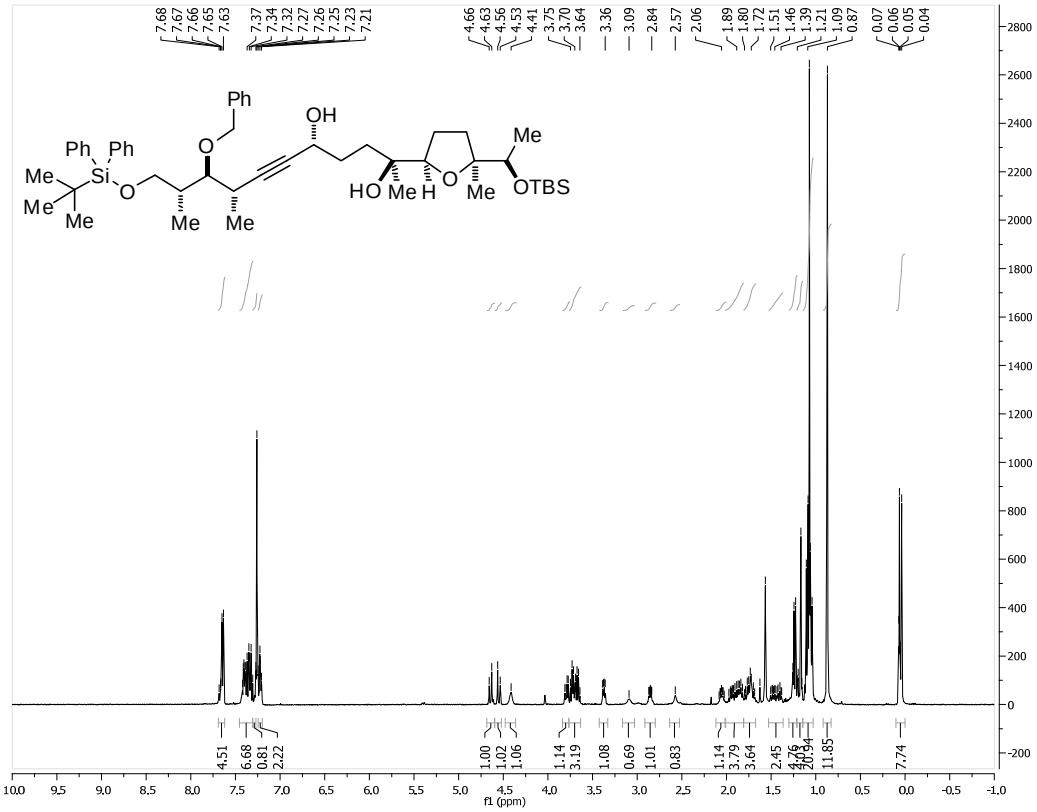
Ph
OH
Ph Ph
O
Me
Si
O
Me
Me
Me
Me
HO Me H
O
Me
OTBS
f1 (ppm)

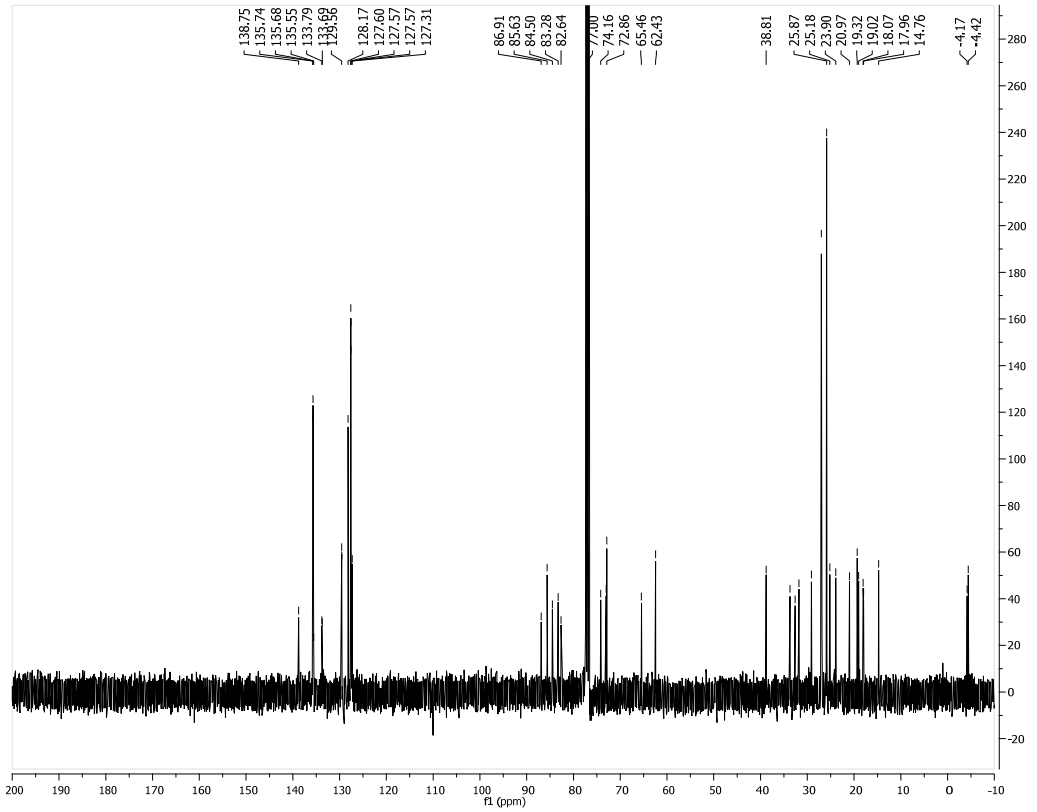
f1 (ppm)

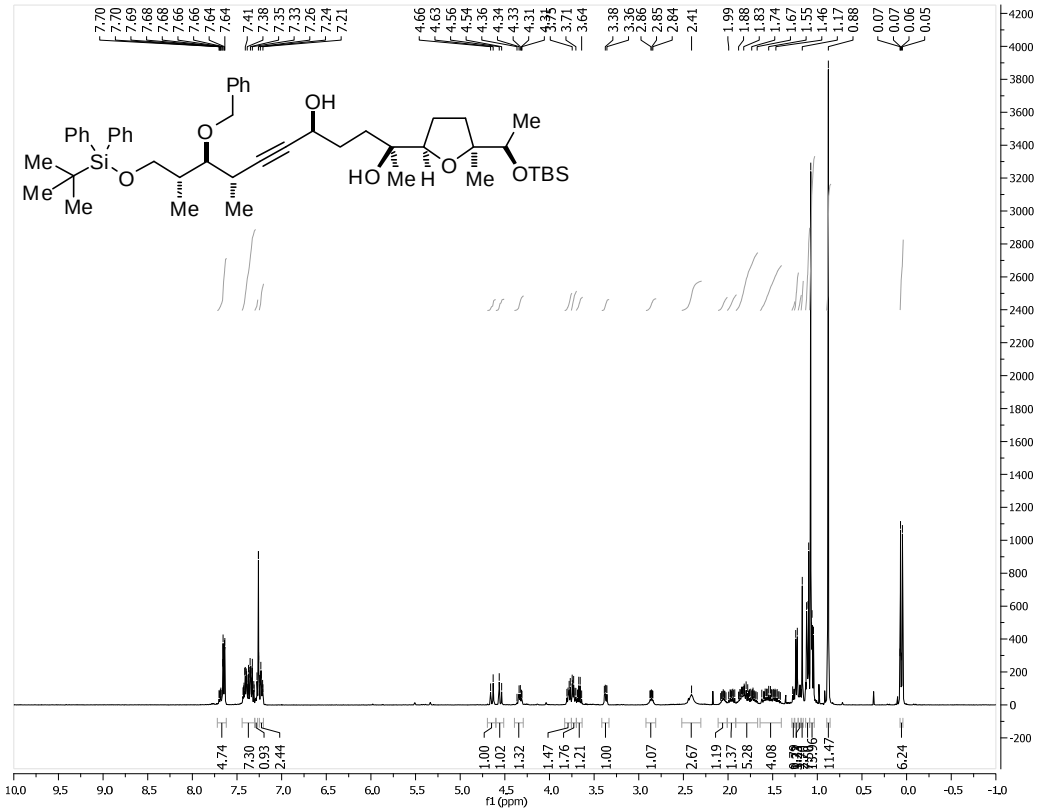
Ph
OH
Ph Ph
O
Me
Si
Me
Me
O
HO Me H
O
Me
OTBS
Me
Me
Me
f1 (ppm)

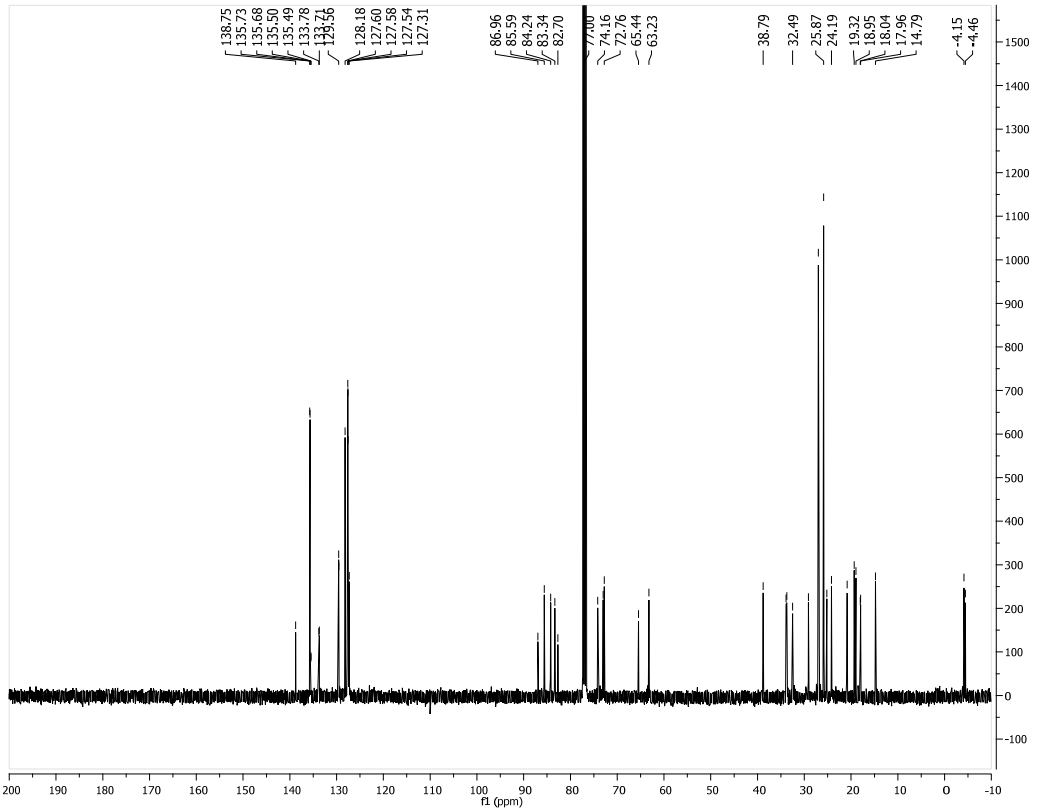
f1 (ppm)

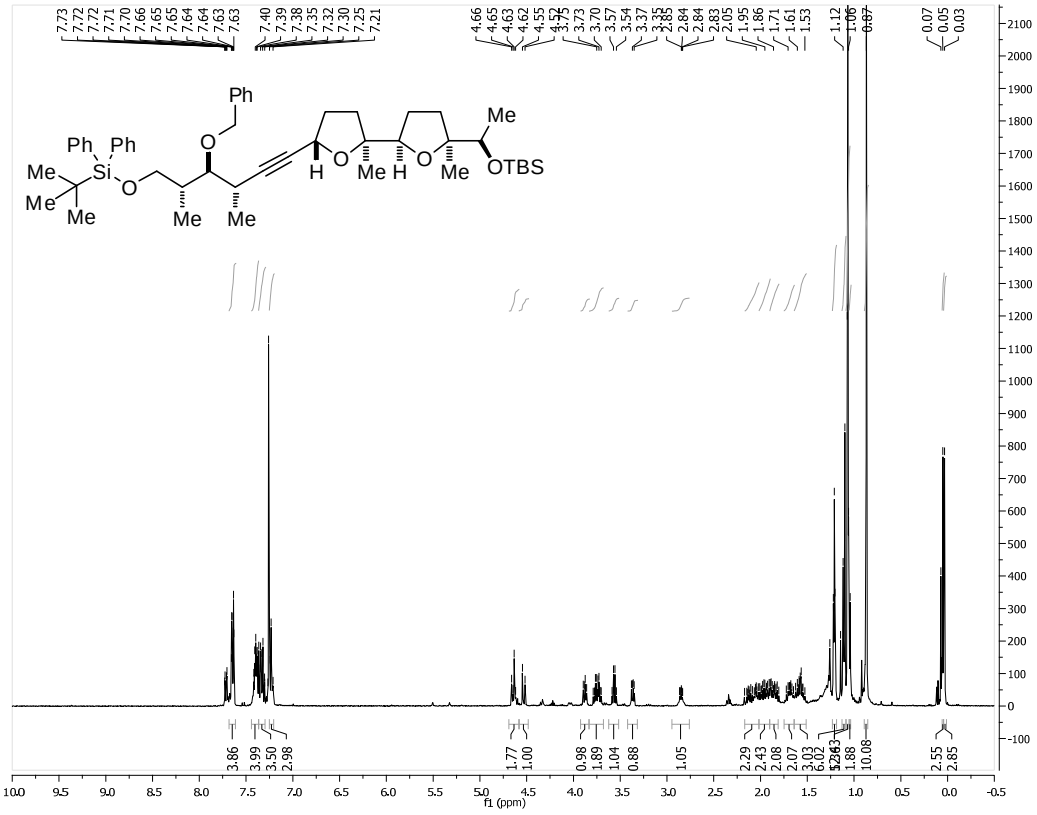
Ph
Ph Ph
O
Me
Si
O
Me
Me
Me
Me
Me
H
O
Me H
O
Me
OTBS
f1 (ppm)

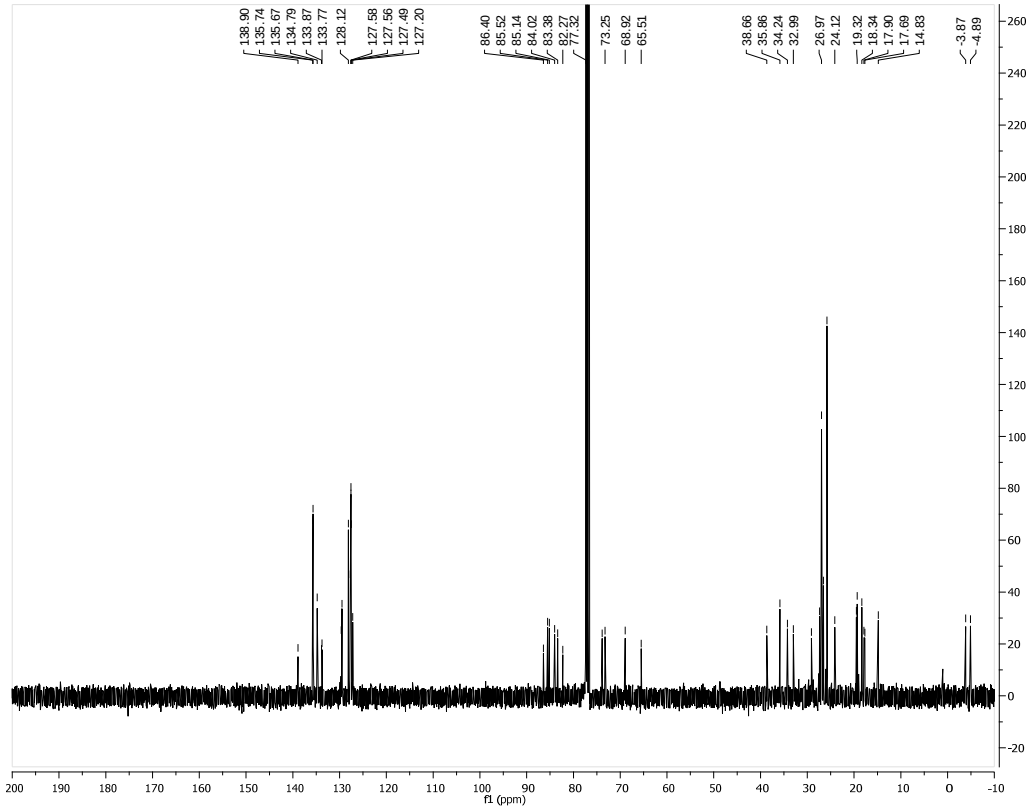
f1 (ppm)

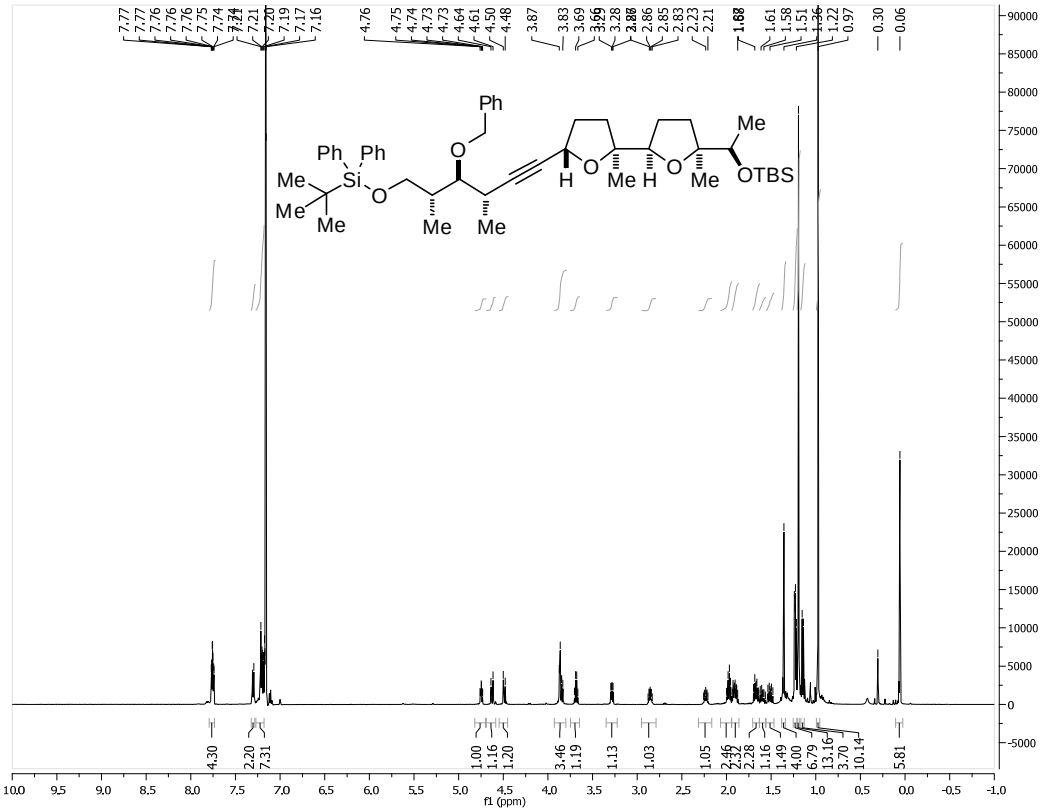
Ph
Ph Ph
Si
O
Me
Me
Me
Me Me
O
Ph
O
H
O
Me H
O
Me
Me
OTBS
f1 (ppm)

COSY-C_6D_6

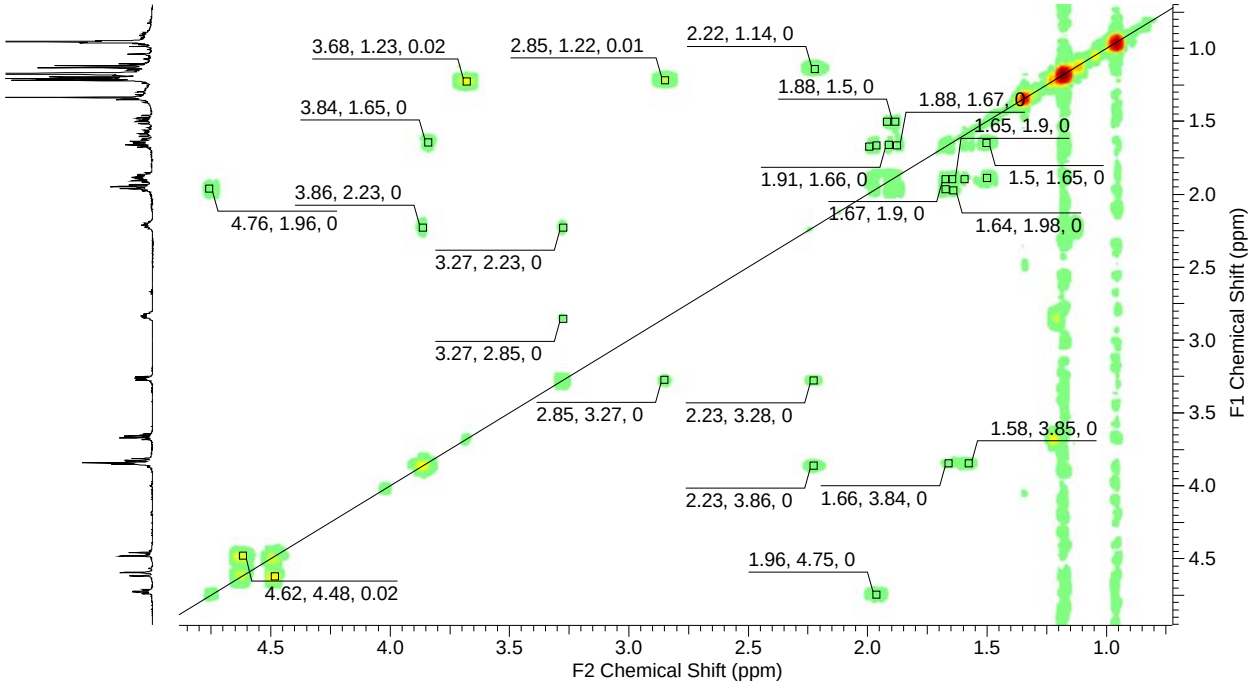
3.68, 1.23, 0.02
2.85, 1.22, 0.01
2.22, 1.14, 0
1.88, 1.5, 0
1.88, 1.67, 0
3.84, 1.65, 0
1.65, 1.9, 0
1.91, 1.66, 0
1.5, 1.65, 0
3.86, 2.23, 0
4.76, 1.96, 0
1.67, 1.9, 0
1.64, 1.98, 0
3.27, 2.23, 0
3.27, 2.85, 0
2.85, 3.27, 0
2.23, 3.28, 0
1.58, 3.85, 0
2.23, 3.86, 0
1.66, 3.84, 0
1.96, 4.75, 0
4.62, 4.48, 0.02
F2 Chemical Shift (ppm)
F1 Chemical Shift (ppm)

HSQC-C_6D_6

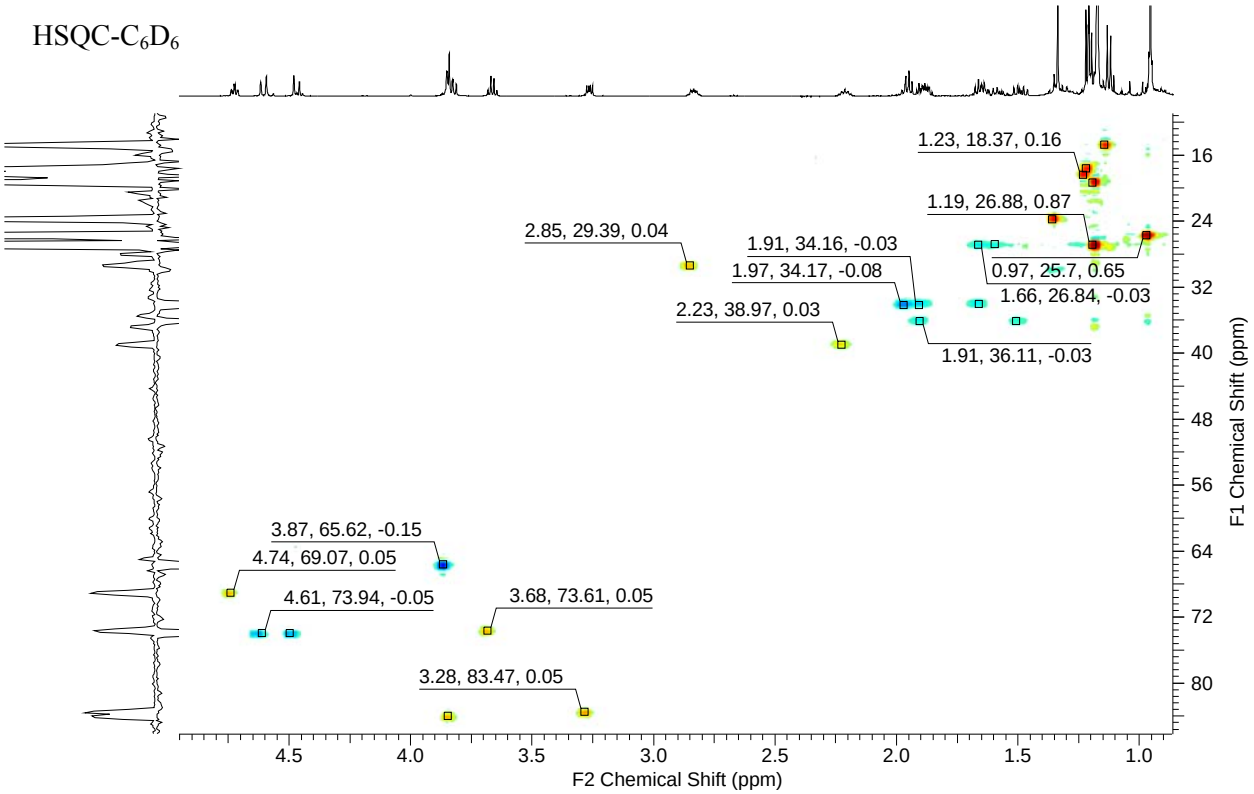

HMBC-C_6D_6

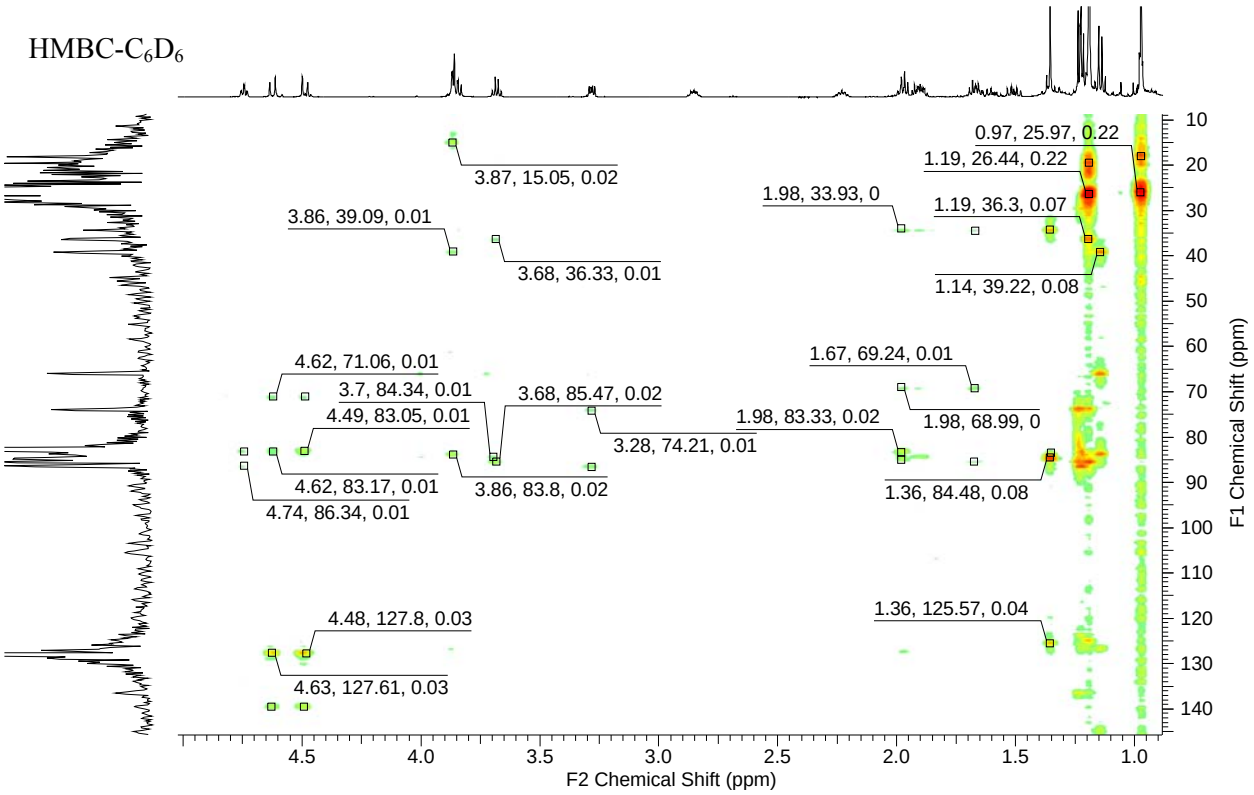

ROESY-C_6D_6

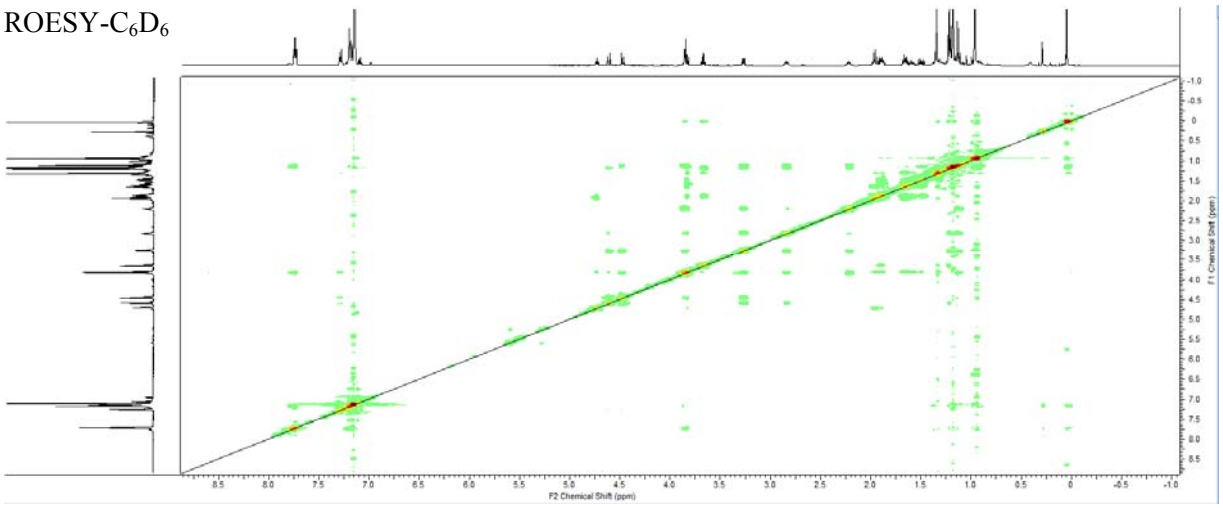

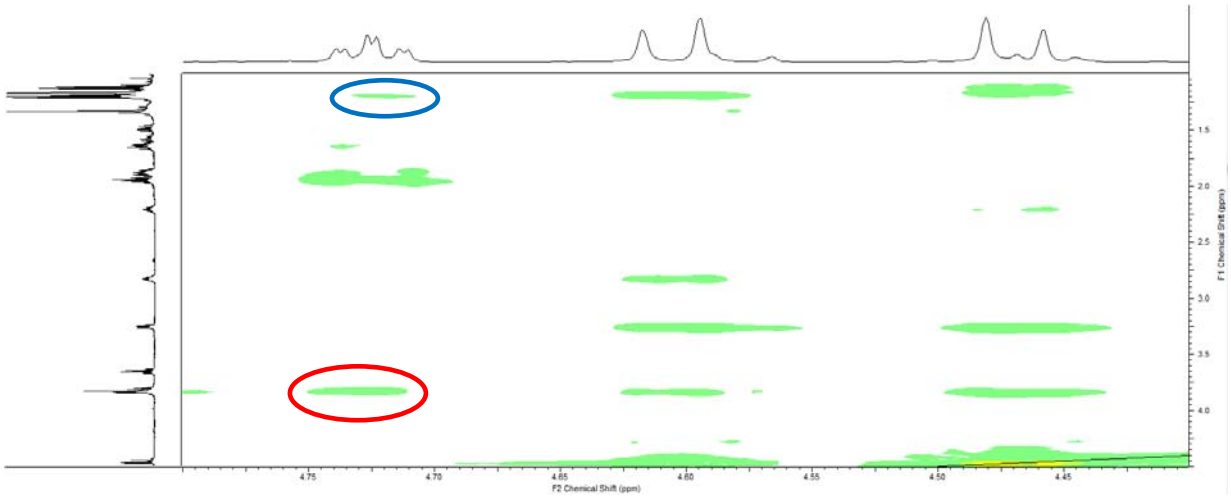

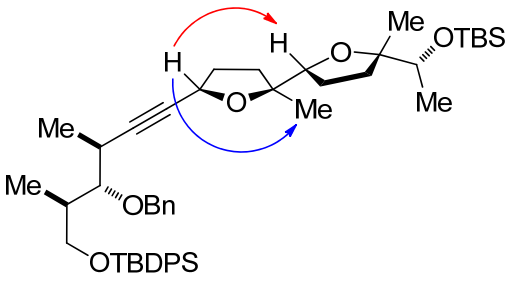

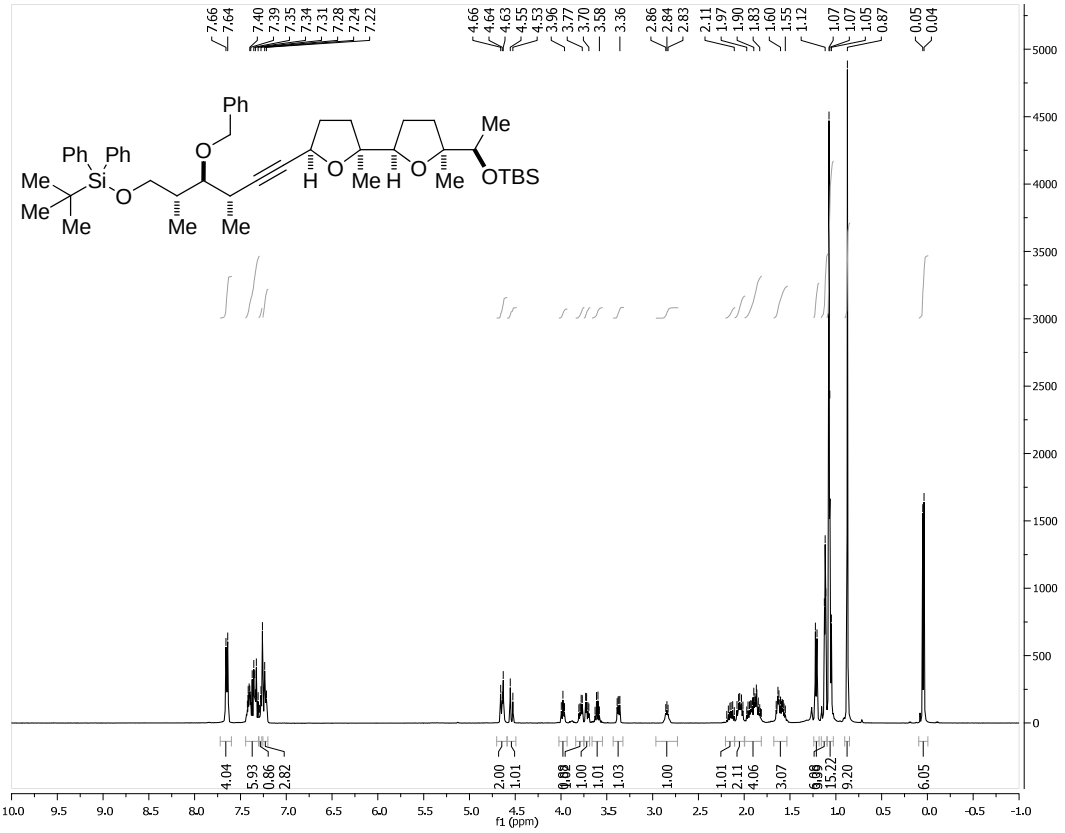
Ph
Ph Ph
O
Me
Si
O
Me
Me
Me Me
H O Me H O Me
Me
OTBS
f1 (ppm)

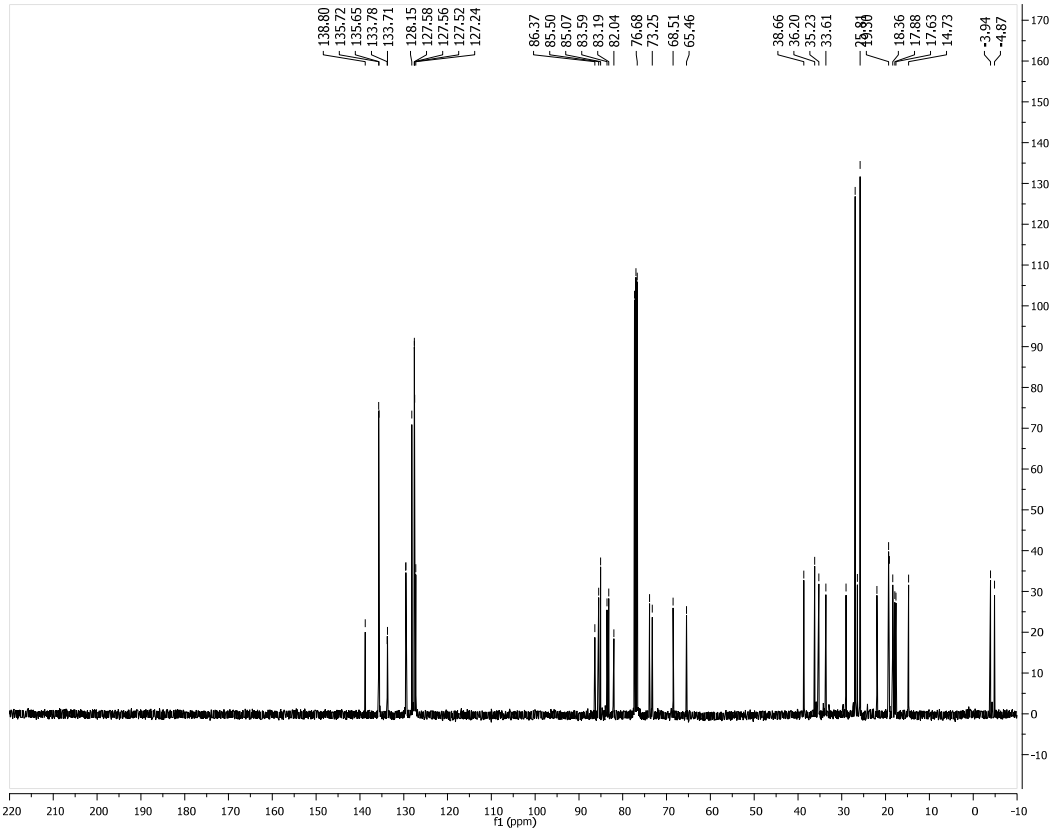
f1 (ppm)

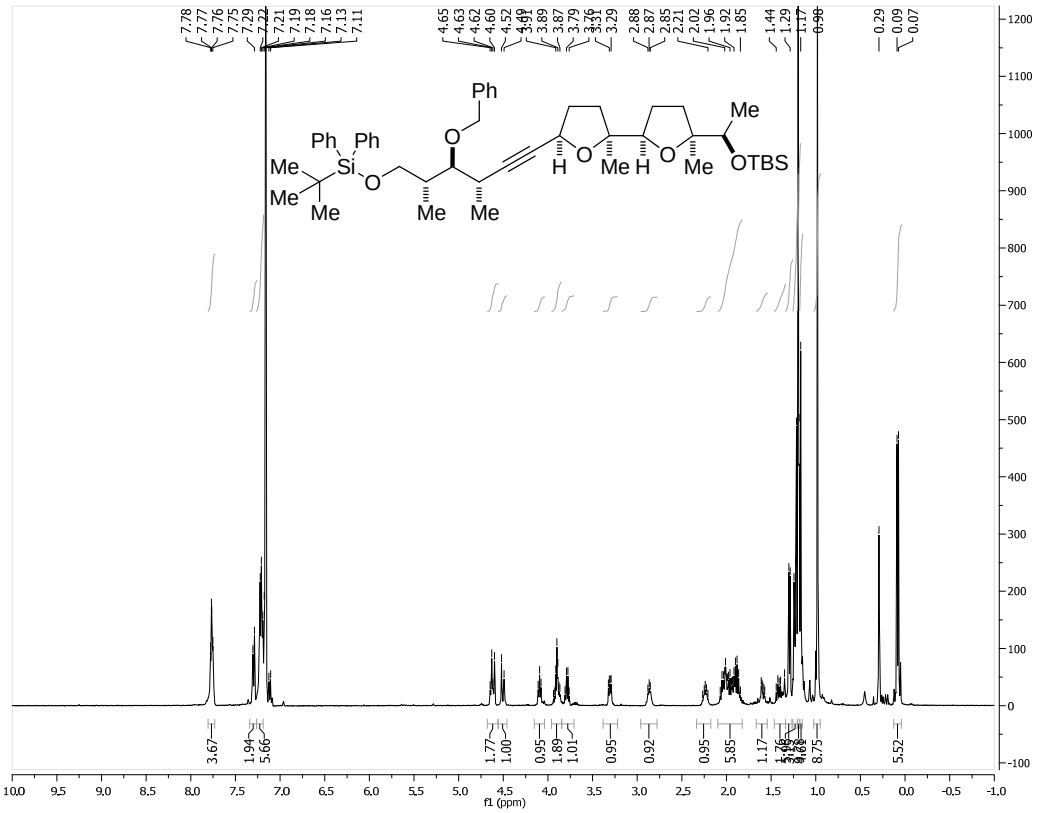
Ph
Ph Ph
Si
O
Me
Me
Me
Me Me
O
H
O
Me H
O
Me
Me
OTBS
f1 (ppm)

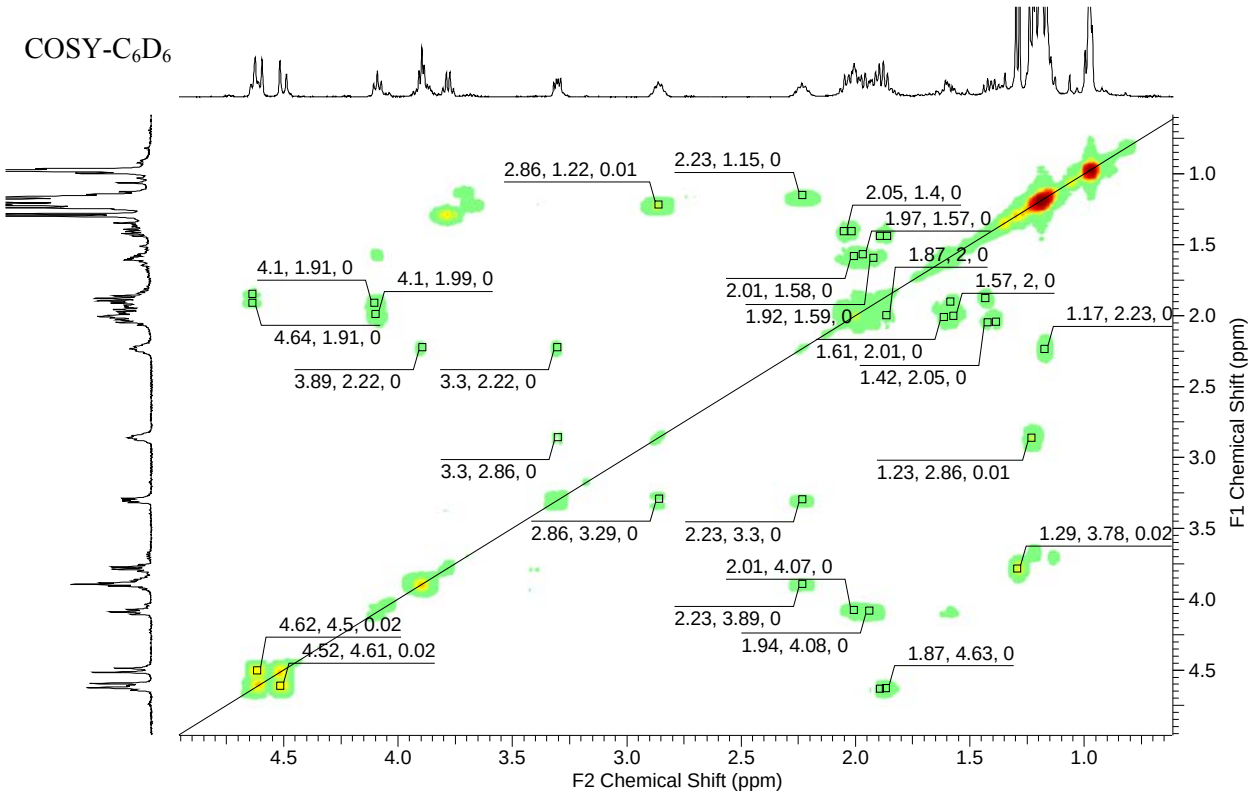
COSY-C6D6
2.86, 1.22, 0.01
2.23, 1.15, 0
2.05, 1.4, 0
1.97, 1.57, 0
1.87, 2, 0
4.1, 1.91, 0
4.1, 1.99, 0
2.01, 1.58, 0
1.92, 1.59, 0
1.57, 2, 0
4.64, 1.91, 0
1.17, 2.23, 0
3.89, 2.22, 0
3.3, 2.22, 0
1.61, 2.01, 0
1.42, 2.05, 0
3.3, 2.86, 0
1.23, 2.86, 0.01
2.86, 3.29, 0
2.23, 3.3, 0
1.29, 3.78, 0.02
2.01, 4.07, 0
2.23, 3.89, 0
1.94, 4.08, 0
4.62, 4.5, 0.02
4.52, 4.61, 0.02
1.87, 4.63, 0
F2 Chemical Shift (ppm)
F1 Chemical Shift (ppm)

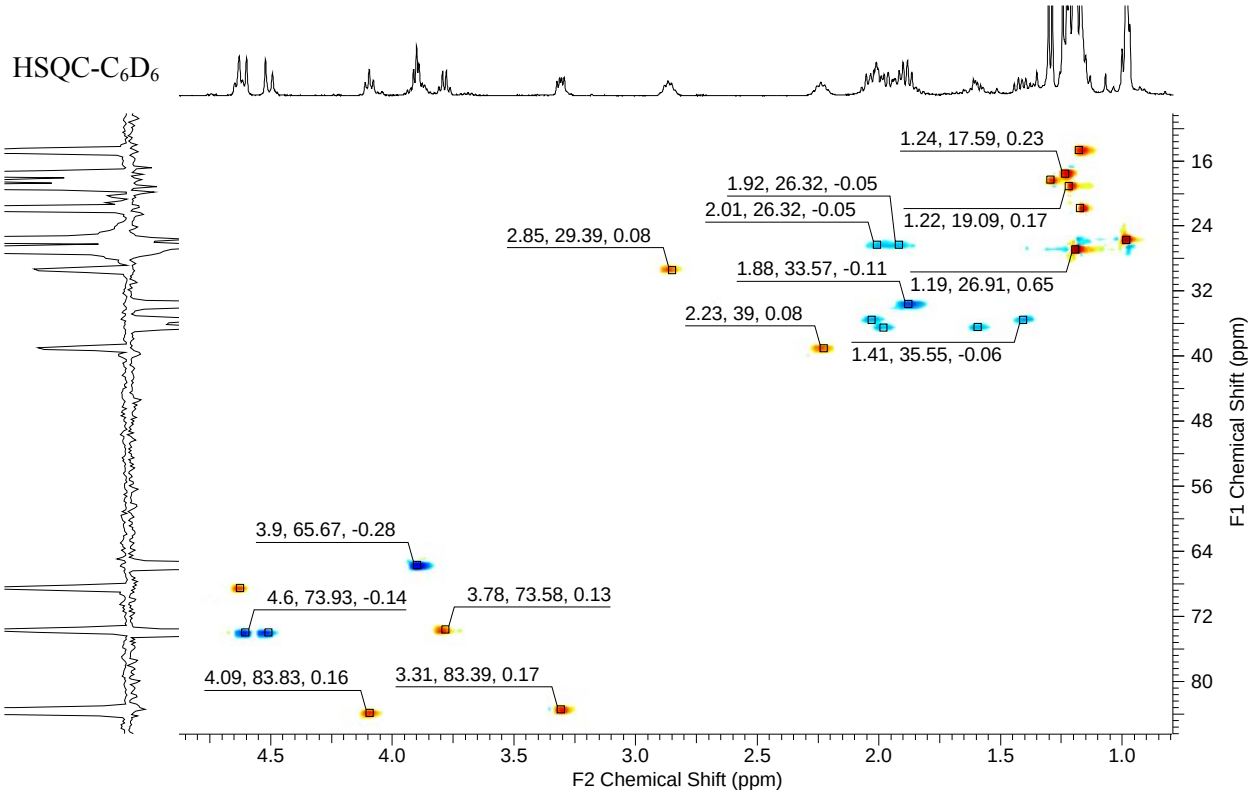
HSQC-C6D6
1.24, 17.59, 0.23
1.92, 26.32, -0.05
2.01, 26.32, -0.05
1.22, 19.09, 0.17
2.85, 29.39, 0.08
1.88, 33.57, -0.11
1.19, 26.91, 0.65
2.23, 39, 0.08
1.41, 35.55, -0.06
3.9, 65.67, -0.28
4.6, 73.93, -0.14
3.78, 73.58, 0.13
4.09, 83.83, 0.16
3.31, 83.39, 0.17
F2 Chemical Shift (ppm)
F1 Chemical Shift (ppm)

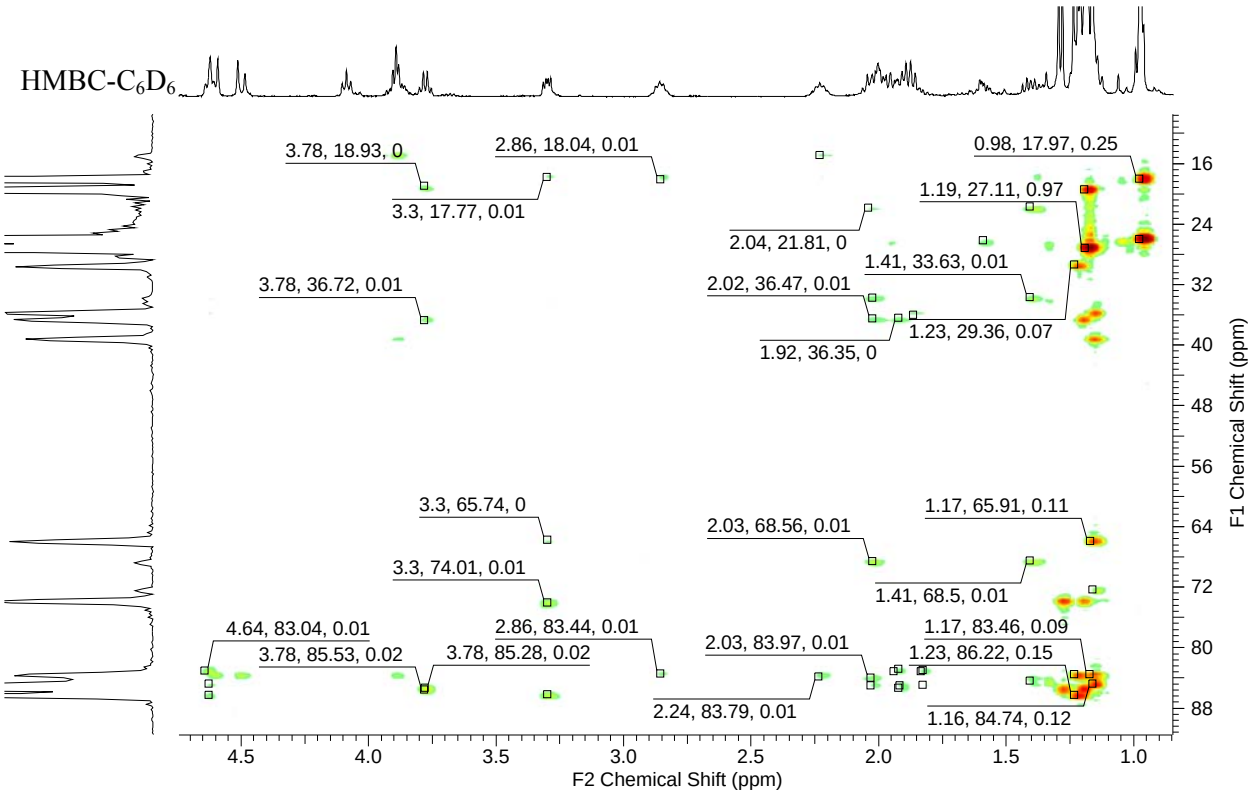
HMBC-C6D6
3.78, 18.93, 0
2.86, 18.04, 0.01
3.3, 17.77, 0.01
0.98, 17.97, 0.25
1.19, 27.11, 0.97
2.04, 21.81, 0
1.41, 33.63, 0.01
3.78, 36.72, 0.01
2.02, 36.47, 0.01
1.23, 29.36, 0.07
1.92, 36.35, 0
3.3, 65.74, 0
1.17, 65.91, 0.11
2.03, 68.56, 0.01
3.3, 74.01, 0.01
1.41, 68.5, 0.01
4.64, 83.04, 0.01
2.86, 83.44, 0.01
1.17, 83.46, 0.09
3.78, 85.53, 0.02
3.78, 85.28, 0.02
2.03, 83.97, 0.01
1.23, 86.22, 0.15
2.24, 83.79, 0.01
1.16, 84.74, 0.12
F2 Chemical Shift (ppm)
F1 Chemical Shift (ppm)

ROESY-C_6D_6

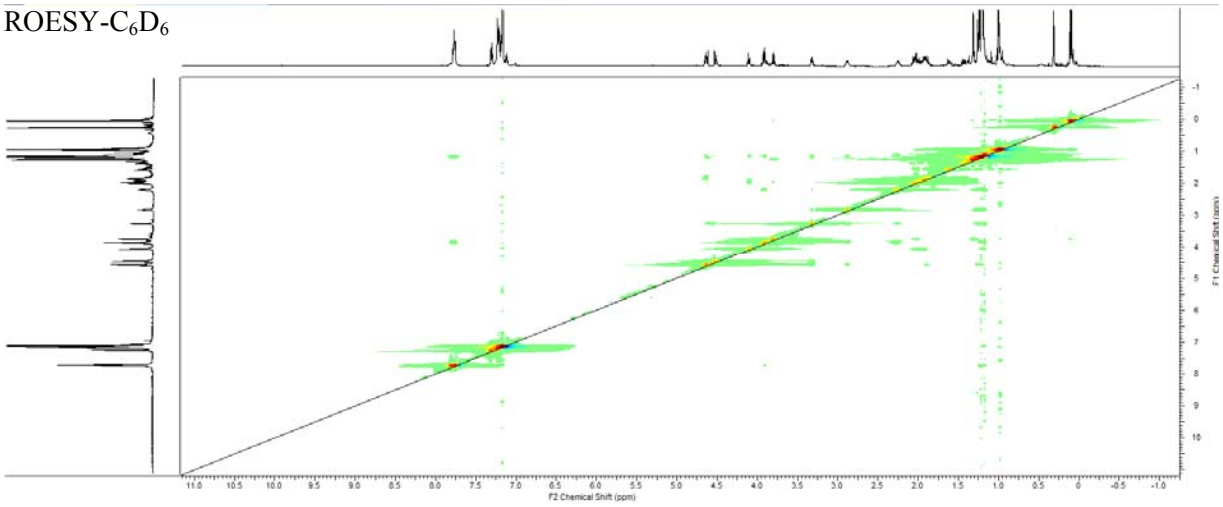
F2 Chemical Shift (ppm)
F1 Chemical Shift (ppm)

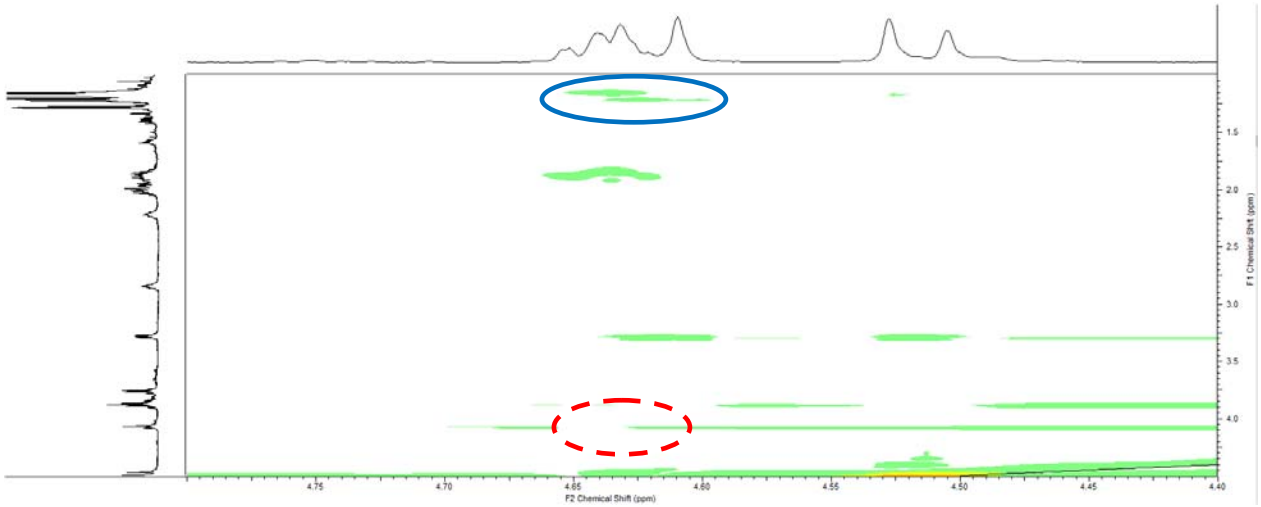
F2 Chemical Shift (ppm)
F1 Chemical Shift (ppm)

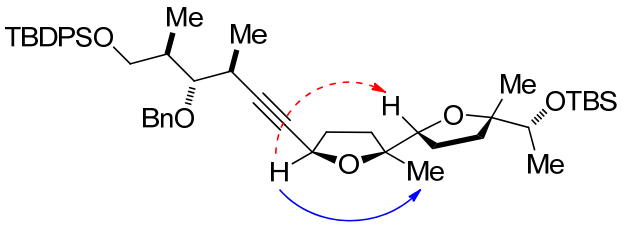
TBDPSO
Me
Me
BnO
H
O
Me
OTBS
Me
H
O
Me

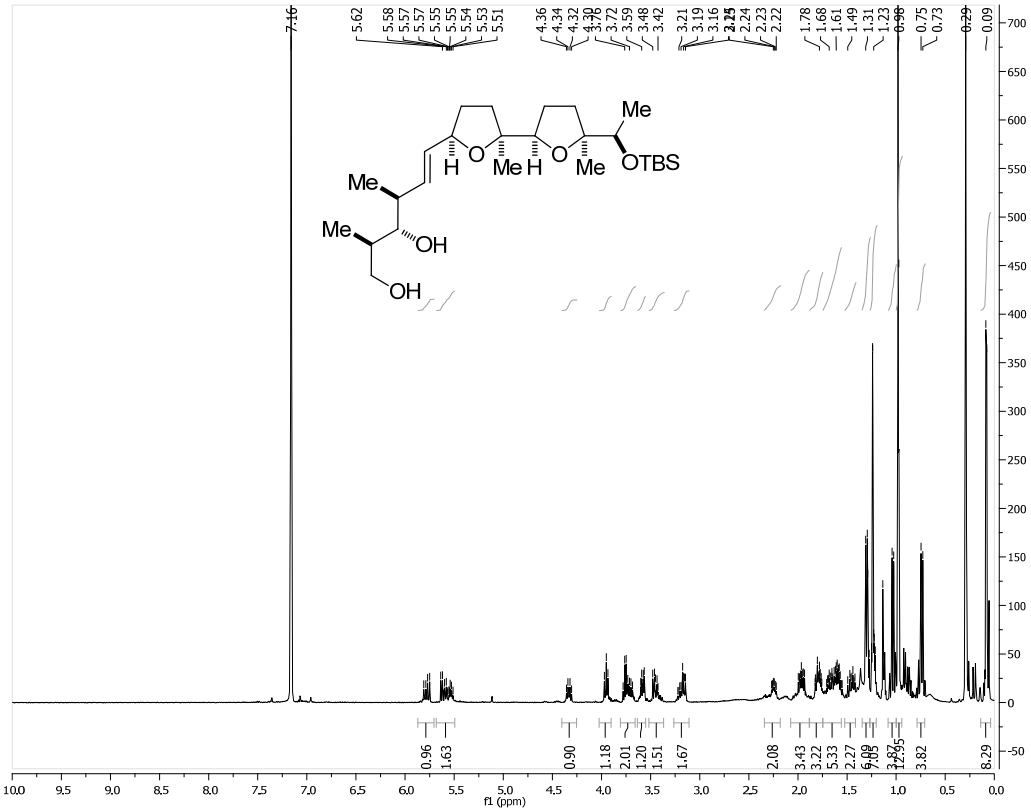
Me
H
O
Me H
O
Me
OTBS
Me
Me
OH
OH
f1 (ppm)

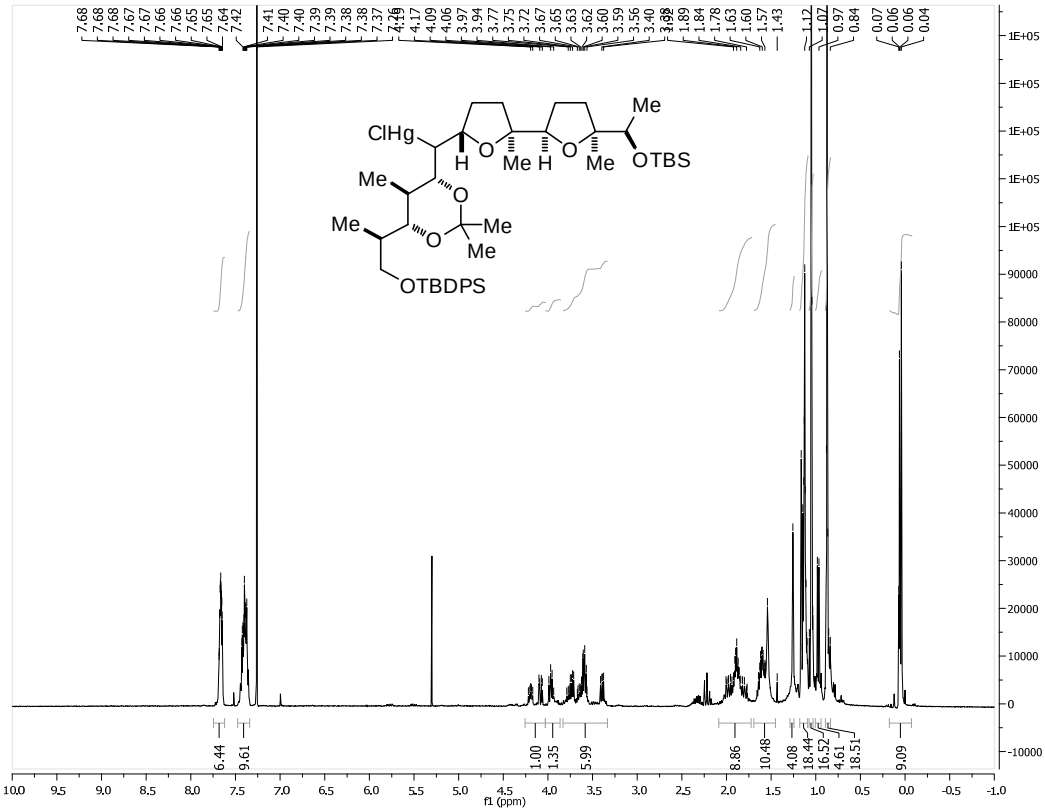
ClHg
Me
H
O
Me H
O
Me
OTBS
Me
O
Me
O
Me
Me
OTBDPS
f1 (ppm)

Crystal Structure Tables and Figures.

Table A.4.1. Crystal data and structure refinement for **1**.

Identification code	rovis176_0m	
Empirical formula	$C_7H_{10}O_3$	
Formula weight	142.15	
Temperature	120(2) K	
Wavelength	0.71073 Å	
Crystal system	Monoclinic	
Space group	$P2_1/c$	
Unit cell dimensions	a = 6.5932(3) Å	α= 90°.
	b = 7.5104(4) Å	β= 91.980(3)°.
	c = 14.0654(7) Å	γ = 90°.
Volume	696.07(6) Å^3	
Z	4	
Density (calculated)	1.356 Mg/m^3	
Absorption coefficient	0.106 mm^{-1}	
F(000)	304	
Crystal size	0.18 x 0.17 x 0.15 mm^3	
Theta range for data collection	2.90 to 28.70°.	
Index ranges	-8<=h<=8, -10<=k<=10, -18<=l<=18	
Reflections collected	16401	
Independent reflections	1801 [R(int) = 0.0392]	
Completeness to theta = 28.70°	100.0 %	
Absorption correction	Semi-empirical from equivalents	
Max. and min. transmission	0.9843 and 0.9810	
Refinement method	Full-matrix least-squares on F^2	
Data / restraints / parameters	1801 / 0 / 93	
Goodness-of-fit on F^2	1.034	
Final R indices [I>2sigma(I)]	R1 = 0.0367, wR2 = 0.0871	
R indices (all data)	R1 = 0.0507, wR2 = 0.0946	
Largest diff. peak and hole	0.329 and -0.228 e.Å^{-3}	

Table A.4.2. Atomic coordinates (x 10^4) and equivalent isotropic displacement parameters ($Å^2$x 10^3) for **1**. U(eq) is defined as one third of the trace of the orthogonalized U^{ij} tensor.

	x	y	z	U(eq)
C(1)	9703(2)	323(2)	3162(1)	20(1)
C(2)	7443(2)	581(2)	3072(1)	17(1)
C(3)	6554(2)	1056(2)	4025(1)	17(1)
C(4)	7658(2)	2643(2)	4480(1)	18(1)
C(5)	9895(2)	2252(2)	4588(1)	19(1)
C(6)	6428(2)	-1042(2)	2609(1)	25(1)
C(7)	6819(2)	3164(2)	5437(1)	25(1)
O(1)	10755(1)	1141(1)	3917(1)	22(1)
O(2)	10706(1)	-525(1)	2634(1)	30(1)
O(3)	11032(1)	2800(1)	5200(1)	30(1)

Table A.4.3. Bond lengths [Å] and angles [°] for **1**.

C(1)-O(2)	1.1949(14)	C(2)-C(3)-C(4)	111.08(9)
C(1)-O(1)	1.3917(14)	C(5)-C(4)-C(7)	110.13(9)
C(1)-C(2)	1.5036(15)	C(5)-C(4)-C(3)	109.94(9)
C(2)-C(3)	1.5225(15)	C(7)-C(4)-C(3)	112.89(9)
C(2)-C(6)	1.5257(16)	O(3)-C(5)-O(1)	115.69(10)
C(3)-C(4)	1.5259(15)	O(3)-C(5)-C(4)	126.43(11)
C(4)-C(5)	1.5064(15)	O(1)-C(5)-C(4)	117.88(9)
C(4)-C(7)	1.5242(16)	C(1)-O(1)-C(5)	125.25(9)
C(5)-O(3)	1.1950(14)		
C(5)-O(1)	1.3952(14)		

O(2)-C(1)-O(1)	115.97(10)
O(2)-C(1)-C(2)	125.78(11)
O(1)-C(1)-C(2)	118.24(9)
C(1)-C(2)-C(3)	111.54(9)
C(1)-C(2)-C(6)	110.59(9)
C(3)-C(2)-C(6)	112.72(9)

Symmetry transformations used to generate equivalent atoms:

Table A.4.4. Anisotropic displacement parameters ($Å^2 x\ 10^3$) for **1**. The anisotropic displacement factor exponent takes the form: $-2\pi^2[\ h^2\ a^{*2}U^{11} + ... + 2\ h\ k\ a^*\ b^*\ U^{12}\ ]$

	U^{11}	U^{22}	U^{33}	U^{23}	U^{13}	U^{12}
C(1)	20(1)	18(1)	21(1)	3(1)	4(1)	0(1)
C(2)	16(1)	18(1)	18(1)	1(1)	2(1)	0(1)
C(3)	13(1)	20(1)	18(1)	2(1)	2(1)	0(1)
C(4)	17(1)	17(1)	18(1)	2(1)	2(1)	1(1)
C(5)	19(1)	16(1)	22(1)	4(1)	1(1)	-2(1)
C(6)	26(1)	25(1)	24(1)	-4(1)	3(1)	-5(1)
C(7)	30(1)	24(1)	21(1)	-2(1)	6(1)	0(1)
O(1)	13(1)	25(1)	27(1)	0(1)	2(1)	0(1)
O(2)	26(1)	34(1)	31(1)	-3(1)	10(1)	7(1)
O(3)	27(1)	29(1)	34(1)	-2(1)	-9(1)	-4(1)

Table A.4.5. Hydrogen coordinates ($x\ 10^4$) and isotropic displacement parameters ($Å^2 x\ 10^3$) for **1**.

	x	y	z	U(eq)
H(2)	7188	1614	2636	20
H(3A)	6669	18	4457	21
H(3B)	5097	1344	3928	21
H(4)	7481	3683	4040	21
H(6A)	7020	-1265	1991	38
H(6B)	4969	-821	2519	38
H(6C)	6643	-2084	3020	38
H(7A)	7029	2183	5889	37
H(7B)	5364	3415	5358	37

H(7C)	7525	4229	5679	37

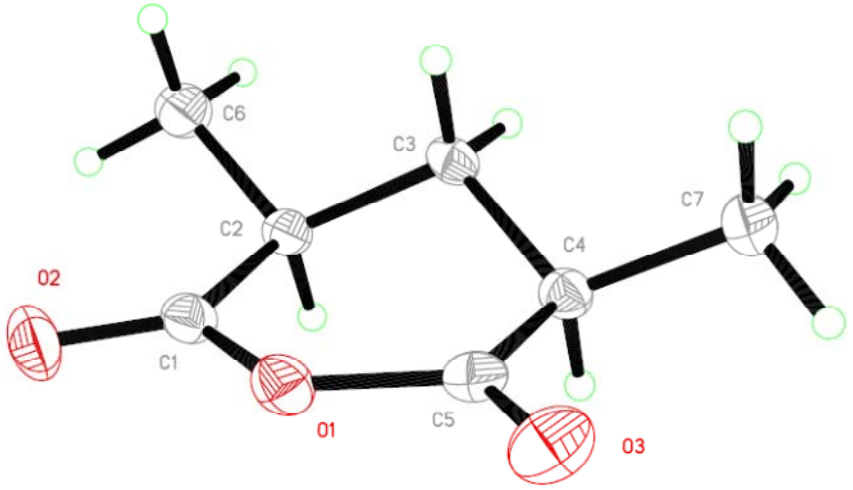

Table A.4.6. Crystal data and structure refinement for **170**.

Identification code	rovis163_0m	
Empirical formula	$C_{16}H_{20}BrN_3O$	
Formula weight	350.26	
Temperature	100(2) K	
Wavelength	0.71073 Å	
Crystal system	Orthorhombic	
Space group	$P2_12_12_1$	
Unit cell dimensions	a = 5.5460(5) Å	α= 90°.
	b = 14.5824(13) Å	β= 90°.
	c = 20.209(2) Å	γ = 90°.
Volume	1634.4(3) Å^3	
Z	4	
Density (calculated)	1.423 Mg/m^3	
Absorption coefficient	2.518 mm^{-1}	
F(000)	720	
Crystal size	0.27 x 0.11 x 0.09 mm^3	
Theta range for data collection	1.72 to 26.75°.	
Index ranges	-7<=h<=7, -18<=k<=18, -24<=l<=25	
Reflections collected	30081	
Independent reflections	3464 [R(int) = 0.1170]	
Completeness to theta = 26.75°	100.0 %	
Absorption correction	Semi-empirical from equivalents	
Max. and min. transmission	0.8145 and 0.5551	
Refinement method	Full-matrix least-squares on F^2	
Data / restraints / parameters	3464 / 0 / 194	
Goodness-of-fit on F^2	1.032	
Final R indices [I>2sigma(I)]	R1 = 0.0424, wR2 = 0.0577	
R indices (all data)	R1 = 0.0836, wR2 = 0.0682	
Absolute structure parameter	-0.001(11)	
Largest diff. peak and hole	0.479 and -0.641 e.Å^{-3}	

Table A.4.7. Atomic coordinates (x 10^4) and equivalent isotropic displacement parameters ($Å^2$x 10^3) for **170**. U(eq) is defined as one third of the trace of the orthogonalized U^{ij} tensor.

	x	y	z	U(eq)
Br(1)	11527(1)	4720(1)	-602(1)	26(1)
C(1)	11284(7)	5683(2)	27(2)	15(1)
C(2)	13107(7)	6314(3)	79(2)	16(1)
C(3)	12909(6)	7021(2)	537(2)	15(1)
C(4)	10900(6)	7096(3)	950(2)	14(1)
C(5)	9091(6)	6437(3)	892(2)	15(1)
C(6)	9257(6)	5734(3)	431(2)	19(1)
C(7)	10671(7)	7850(3)	1421(2)	15(1)
C(8)	8645(8)	8252(2)	1686(2)	15(1)
C(9)	8097(7)	9566(3)	2494(2)	20(1)
C(10)	6768(7)	9050(3)	3047(2)	20(1)
C(11)	8495(8)	8526(3)	3508(2)	23(1)
C(12)	7273(7)	7764(3)	3905(2)	26(1)
C(13)	6326(9)	7038(3)	3441(2)	26(1)
C(14)	8047(8)	6440(3)	3079(2)	38(1)
C(15)	5228(6)	9737(3)	3427(2)	27(1)
C(16)	9033(7)	7367(3)	4412(2)	37(1)
N(1)	12623(5)	8328(2)	1646(2)	21(1)
N(2)	11903(6)	8989(2)	2045(2)	23(1)
N(3)	9453(5)	8940(2)	2067(2)	18(1)
O(1)	4165(5)	6922(2)	3369(2)	41(1)

Table A.4.8. Bond lengths [Å] and angles [°] for **170**.

Br(1)-C(1)	1.899(4)	C(4)-C(7)	1.460(5)
C(1)-C(2)	1.371(5)	C(5)-C(6)	1.389(5)
C(1)-C(6)	1.391(5)	C(7)-N(1)	1.366(5)
C(2)-C(3)	1.392(5)	C(7)-C(8)	1.376(5)
C(3)-C(4)	1.396(5)	C(8)-N(3)	1.342(5)
C(4)-C(5)	1.393(5)	C(9)-N(3)	1.464(5)

C(9)-C(10)	1.536(5)	N(2)-N(1)-C(7)	109.7(3)
C(10)-C(15)	1.524(5)	N(1)-N(2)-N(3)	106.5(3)
C(10)-C(11)	1.539(5)	C(8)-N(3)-N(2)	110.7(3)
C(11)-C(12)	1.529(5)	C(8)-N(3)-C(9)	129.3(3)
C(12)-C(13)	1.509(6)	N(2)-N(3)-C(9)	120.0(3)
C(12)-C(16)	1.529(6)		
C(13)-O(1)	1.219(5)		
C(13)-C(14)	1.486(6)		
N(1)-N(2)	1.319(4)		
N(2)-N(3)	1.361(4)		

C(2)-C(1)-C(6)	121.1(3)
C(2)-C(1)-Br(1)	119.6(3)
C(6)-C(1)-Br(1)	119.3(3)
C(1)-C(2)-C(3)	119.3(3)
C(2)-C(3)-C(4)	121.2(3)
C(5)-C(4)-C(3)	118.1(4)
C(5)-C(4)-C(7)	120.8(3)
C(3)-C(4)-C(7)	121.1(3)
C(6)-C(5)-C(4)	121.2(4)
C(5)-C(6)-C(1)	119.1(4)
N(1)-C(7)-C(8)	107.4(3)
N(1)-C(7)-C(4)	122.2(3)
C(8)-C(7)-C(4)	130.2(4)
N(3)-C(8)-C(7)	105.6(3)
N(3)-C(9)-C(10)	111.7(3)
C(15)-C(10)-C(9)	108.3(3)
C(15)-C(10)-C(11)	111.7(3)
C(9)-C(10)-C(11)	112.7(3)
C(12)-C(11)-C(10)	113.8(3)
C(13)-C(12)-C(16)	111.9(4)
C(13)-C(12)-C(11)	109.8(3)
C(16)-C(12)-C(11)	110.1(3)
O(1)-C(13)-C(14)	119.4(4)
O(1)-C(13)-C(12)	120.9(4)
C(14)-C(13)-C(12)	119.7(4)

Symmetry transformations used to generate equivalent atoms:

Table A.4.9. Anisotropic displacement parameters ($Å^2 x\ 10^3$) for **170**. The anisotropic displacement factor exponent takes the form: $-2\pi^2[\ h^2\ a^{*2}U^{11} + ...\ + 2\ h\ k\ a^*\ b^*\ U^{12}\ ]$

	U^{11}	U^{22}	U^{33}	U^{23}	U^{13}	U^{12}
Br(1)	31(1)	22(1)	26(1)	-5(1)	5(1)	0(1)
C(1)	19(2)	14(2)	12(2)	4(2)	-2(2)	3(2)
C(2)	10(2)	22(2)	16(2)	3(2)	8(2)	4(2)
C(3)	8(2)	16(2)	22(2)	2(2)	-2(2)	1(2)
C(4)	10(2)	19(2)	14(2)	2(2)	-2(2)	2(2)
C(5)	9(2)	20(2)	17(2)	3(2)	4(2)	2(2)
C(6)	15(2)	22(2)	21(3)	5(2)	0(2)	-3(2)
C(7)	12(2)	21(2)	11(2)	3(2)	-1(2)	-2(2)
C(8)	12(2)	18(2)	14(2)	-2(2)	0(2)	-3(2)
C(9)	18(2)	20(2)	22(2)	-2(2)	2(2)	2(2)
C(10)	13(2)	31(2)	15(2)	-5(2)	1(2)	3(2)
C(11)	19(2)	30(2)	19(2)	-6(2)	2(2)	3(2)
C(12)	26(3)	29(3)	24(3)	6(2)	5(2)	8(2)
C(13)	22(2)	32(3)	24(3)	11(2)	-4(2)	-3(2)
C(14)	32(3)	34(3)	48(4)	-14(3)	5(3)	0(3)
C(15)	27(2)	34(3)	20(2)	-4(3)	-2(2)	8(2)
C(16)	36(3)	44(3)	30(3)	-4(3)	-8(3)	11(2)
N(1)	13(2)	27(2)	22(2)	-5(2)	-1(2)	0(2)
N(2)	16(2)	31(2)	22(2)	-7(2)	2(2)	-2(2)
N(3)	14(2)	23(2)	16(2)	1(2)	2(2)	0(2)
O(1)	19(2)	43(2)	61(3)	6(2)	-3(2)	-7(2)

Table A.4.10. Hydrogen coordinates (x 10^4) and isotropic displacement parameters ($Å^2$x 10^3) for **170**.

	x	y	z	U(eq)
H(2)	14492	6268	-196	19
H(3)	14165	7462	570	18
H(5)	7720	6470	1173	19
H(6)	8003	5293	392	23
H(8)	7015	8079	1614	18
H(9A)	6911	9908	2223	25
H(9B)	9218	10017	2693	25
H(10)	5664	8594	2836	24
H(11A)	9805	8255	3239	27
H(11B)	9238	8967	3820	27
H(12)	5876	8036	4149	32
H(14A)	8028	5824	3273	57
H(14B)	9675	6697	3112	57
H(14C)	7573	6403	2612	57
H(15A)	4397	9422	3790	41
H(15B)	4035	10009	3128	41
H(15C)	6262	10221	3608	41
H(16A)	8330	6816	4612	55
H(16B)	9348	7823	4757	55
H(16C)	10548	7206	4191	55

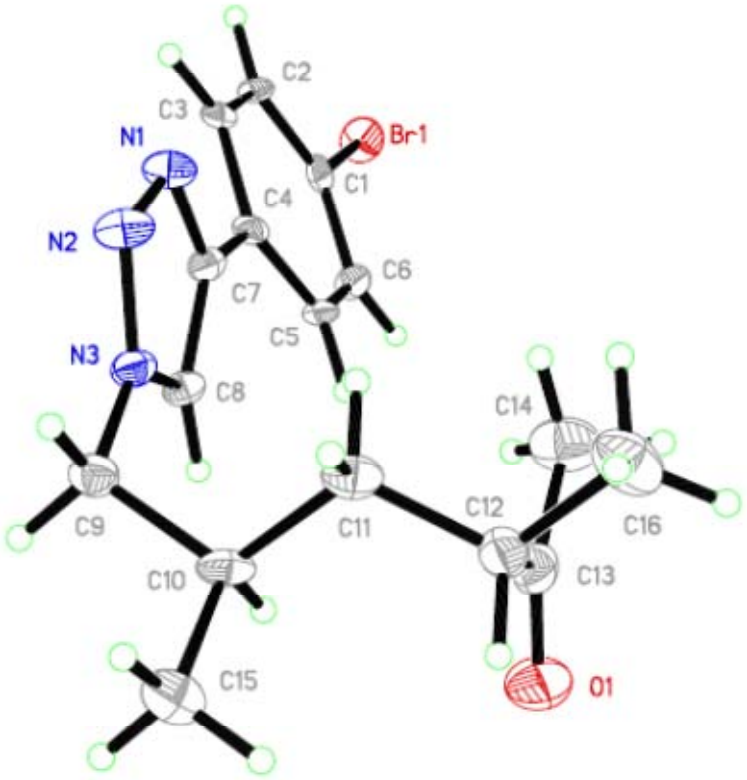
C2
C3
Br1
N1
C1
C4
N2
C6
C7
C5
N3
C8
C14
C9
C11
C12
C16
C10
C13
C15
O1

Table A.4.11. Crystal data and structure refinement for **3b**.

Identification code	rovis172	
Empirical formula	$C_{14}H_{16}O_4$	
Formula weight	248.27	
Temperature	100(2) K	
Wavelength	0.71073 Å	
Crystal system	Monoclinic	
Space group	$P2_1/n$	
Unit cell dimensions	a = 14.1305(16) Å	α= 90°.
	b = 5.0351(6) Å	β= 104.566(6)°.
	c = 18.5891(18) Å	γ = 90°.
Volume	1280.1(2) Å^3	
Z	4	
Density (calculated)	1.288 Mg/m^3	
Absorption coefficient	0.094 mm^{-1}	
F(000)	528	
Crystal size	0.47 x 0.32 x 0.12 mm^3	
Theta range for data collection	1.63 to 26.37°.	
Index ranges	-17<=h<=17, -6<=k<=6, -23<=l<=23	
Reflections collected	17179	
Independent reflections	2605 [R(int) = 0.0492]	
Completeness to theta = 26.37°	99.4 %	
Absorption correction	Semi-empirical from equivalents	
Max. and min. transmission	0.9885 and 0.9572	
Refinement method	Full-matrix least-squares on F^2	
Data / restraints / parameters	2605 / 0 / 165	
Goodness-of-fit on F^2	1.123	
Final R indices [I>2sigma(I)]	R1 = 0.0408, wR2 = 0.1059	
R indices (all data)	R1 = 0.0605, wR2 = 0.1277	
Largest diff. peak and hole	0.267 and -0.224 e.Å^{-3}	

Table A.4.12. Atomic coordinates (x 10^4) and equivalent isotropic displacement parameters ($Å^2$x 10^3) for **3b**. U(eq) is defined as one third of the trace of the orthogonalized U^{ij} tensor.

	x	y	z	U(eq)
C(1)	2217(1)	2961(3)	1709(1)	20(1)
C(2)	2100(1)	346(3)	1306(1)	20(1)
C(3)	2881(1)	65(3)	878(1)	18(1)
C(4)	3893(1)	307(3)	1406(1)	20(1)
C(5)	3986(1)	2946(3)	1791(1)	23(1)
C(6)	1063(1)	5(4)	832(1)	33(1)
C(7)	4730(1)	-120(4)	1037(1)	34(1)
C(8)	2678(1)	1248(4)	-407(1)	29(1)
C(9)	2307(1)	3467(3)	-944(1)	22(1)
C(10)	1318(1)	4086(4)	-1139(1)	29(1)
C(11)	958(1)	6065(4)	-1655(1)	29(1)
C(12)	1588(1)	7447(3)	-1978(1)	24(1)
C(13)	2574(1)	6851(3)	-1790(1)	23(1)
C(14)	2931(1)	4870(3)	-1272(1)	21(1)
O(1)	1580(1)	4227(2)	1865(1)	30(1)
O(2)	3149(1)	4034(2)	1943(1)	22(1)
O(3)	4714(1)	4232(3)	1982(1)	40(1)
O(4)	2742(1)	2157(2)	338(1)	20(1)

Table A.4.13. Bond lengths [Å] and angles [°] for **3b**.

C(1)-O(1)	1.1962(19)	C(5)-O(3)	1.191(2)
C(1)-O(2)	1.389(2)	C(5)-O(2)	1.395(2)
C(1)-C(2)	1.503(2)	C(8)-O(4)	1.4393(18)
C(2)-C(6)	1.518(2)	C(8)-C(9)	1.501(2)
C(2)-C(3)	1.520(2)	C(9)-C(14)	1.385(2)
C(3)-O(4)	1.4351(17)	C(9)-C(10)	1.388(2)
C(3)-C(4)	1.522(2)	C(10)-C(11)	1.388(2)
C(4)-C(5)	1.499(2)	C(11)-C(12)	1.380(2)
C(4)-C(7)	1.525(2)	C(12)-C(13)	1.382(2)

C(13)-C(14)	1.390(2)	O(3)-C(5)-O(2)	116.01(15)
		O(3)-C(5)-C(4)	126.07(16)
O(1)-C(1)-O(2)	115.40(15)	O(2)-C(5)-C(4)	117.92(14)
O(1)-C(1)-C(2)	126.35(15)	O(4)-C(8)-C(9)	109.26(13)
O(2)-C(1)-C(2)	118.23(14)	C(14)-C(9)-C(10)	118.70(15)
C(1)-C(2)-C(6)	110.90(14)	C(14)-C(9)-C(8)	121.19(15)
C(1)-C(2)-C(3)	109.85(13)	C(10)-C(9)-C(8)	120.07(15)
C(6)-C(2)-C(3)	114.10(13)	C(11)-C(10)-C(9)	120.77(16)
O(4)-C(3)-C(2)	107.96(12)	C(12)-C(11)-C(10)	119.92(16)
O(4)-C(3)-C(4)	109.48(12)	C(11)-C(12)-C(13)	119.98(16)
C(2)-C(3)-C(4)	110.08(12)	C(12)-C(13)-C(14)	119.86(15)
C(5)-C(4)-C(3)	109.49(13)	C(9)-C(14)-C(13)	120.76(15)
C(5)-C(4)-C(7)	110.82(14)	C(1)-O(2)-C(5)	124.71(13)
C(3)-C(4)-C(7)	114.08(13)	C(3)-O(4)-C(8)	113.89(12)

Symmetry transformations used to generate equivalent atoms:

Table A.4.14. Anisotropic displacement parameters ($Å^2 x\ 10^3$) for **3b**. The anisotropic displacement factor exponent takes the form: $-2\pi^2[\ h^2\ a^{*2}U^{11} + ...\ + 2\ h\ k\ a^*\ b^*\ U^{12}\ ]$

	U^{11}	U^{22}	U^{33}	U^{23}	U^{13}	U^{12}
C(1)	26(1)	17(1)	17(1)	4(1)	6(1)	-1(1)
C(2)	25(1)	15(1)	19(1)	0(1)	5(1)	-3(1)
C(3)	25(1)	12(1)	16(1)	1(1)	4(1)	0(1)
C(4)	24(1)	16(1)	21(1)	2(1)	5(1)	1(1)
C(5)	22(1)	19(1)	24(1)	3(1)	0(1)	1(1)
C(6)	26(1)	35(1)	36(1)	-6(1)	6(1)	-8(1)
C(7)	27(1)	38(1)	37(1)	0(1)	10(1)	5(1)
C(8)	48(1)	22(1)	18(1)	-1(1)	10(1)	6(1)
C(9)	32(1)	17(1)	15(1)	-3(1)	5(1)	2(1)
C(10)	31(1)	31(1)	25(1)	0(1)	9(1)	-6(1)
C(11)	22(1)	37(1)	26(1)	-4(1)	3(1)	3(1)
C(12)	33(1)	23(1)	15(1)	0(1)	2(1)	6(1)
C(13)	30(1)	21(1)	20(1)	-2(1)	8(1)	-1(1)
C(14)	23(1)	22(1)	19(1)	-4(1)	4(1)	4(1)

O(1)	36(1)	22(1)	38(1)	-1(1)	18(1)	4(1)
O(2)	28(1)	16(1)	23(1)	-4(1)	4(1)	-1(1)
O(3)	26(1)	25(1)	62(1)	-6(1)	-4(1)	-6(1)
O(4)	33(1)	13(1)	15(1)	1(1)	5(1)	1(1)

Table A.4.5. Hydrogen coordinates (x 10^4) and isotropic displacement parameters ($Å^2$x 10^{3}) for **3b**.

	x	y	z	U(eq)
H(2)	2218	-1085	1691	23
H(3)	2815	-1698	623	22
H(4)	3948	-1095	1795	24
H(6A)	604	109	1149	49
H(6B)	1000	-1729	585	49
H(6C)	914	1414	457	49
H(7A)	4731	1313	680	50
H(7B)	4645	-1829	776	50
H(7C)	5353	-118	1417	50
H(8A)	2228	-288	-523	35
H(8B)	3331	672	-452	35
H(10)	882	3145	-917	34
H(11)	280	6469	-1785	35
H(12)	1343	8807	-2330	29
H(13)	3007	7793	-2014	28
H(14)	3610	4473	-1142	26

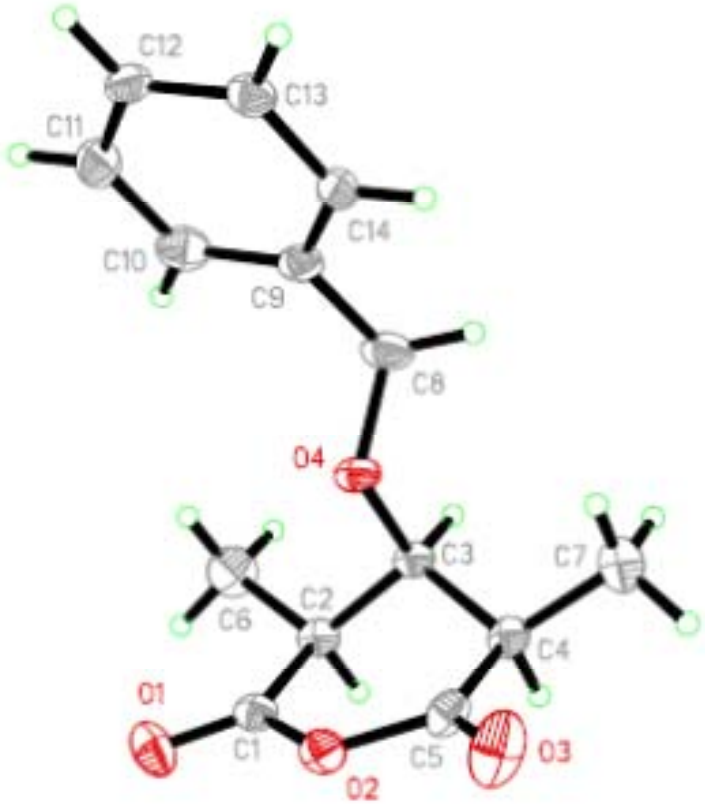
C12
C13
C11
C14
C10
C9
C8
O4
C3
C7
C6
C2
C4
O1
C1
C5
O3
O2

Table A.4.16. Crystal data and structure refinement for **137b**.

Identification code	rovis162	
Empirical formula	$C_{22}H_{25}NO_4S_2$	
Formula weight	431.55	
Temperature	115 K	
Wavelength	0.71073 Å	
Crystal system	Monoclinic	
Space group	$P2_1$	
Unit cell dimensions	a = 12.0202(10) Å	α= 90°.
	b = 8.2839(7) Å	β= 117.662(5)°.
	c = 12.0687(10) Å	γ = 90°.
Volume	1064.37(15) $Å^3$	
Z	2	
Density (calculated)	1.347 Mg/m^3	
Absorption coefficient	0.279 mm^{-1}	
F(000)	456	
Crystal size	0.17 x 0.10 x 0.06 mm^3	
Theta range for data collection	1.91 to 26.76°.	
Index ranges	-15<=h<=15, -10<=k<=10, -14<=l<=15	
Reflections collected	20567	
Independent reflections	4461 [R(int) = 0.0774]	
Completeness to theta = 26.76°	99.2 %	
Absorption correction	Semi-empirical from equivalents	
Max. and min. transmission	0.9824 and 0.9547	
Refinement method	Full-matrix least-squares on F^2	
Data / restraints / parameters	4461 / 1 / 266	
Goodness-of-fit on F^2	1.001	
Final R indices [I>2sigma(I)]	R1 = 0.0464, wR2 = 0.0781	
R indices (all data)	R1 = 0.0799, wR2 = 0.0900	
Absolute structure parameter	0.03(7)	
Largest diff. peak and hole	0.279 and -0.360 $e.Å^{-3}$	

Table A.4.17. Atomic coordinates (x 10^4) and equivalent isotropic displacement parameters ($Å^2$x 10^3) for **137b**. U(eq) is defined as one third of the trace of the orthogonalized U^{ij} tensor.

	x	y	z	U(eq)
C(1)	9753(3)	2667(4)	7275(3)	27(1)
C(2)	10890(3)	1640(4)	8033(3)	19(1)
C(3)	12042(3)	2357(4)	8783(3)	22(1)
C(4)	13092(3)	1430(4)	9460(3)	25(1)
C(5)	13022(3)	-235(4)	9411(3)	26(1)
C(6)	11873(3)	-958(4)	8664(3)	26(1)
C(7)	10814(3)	-33(4)	7979(3)	19(1)
C(8)	7678(3)	3179(4)	7031(3)	18(1)
C(9)	7433(3)	4799(4)	7503(3)	22(1)
C(10)	8490(3)	5970(4)	7698(3)	24(1)
C(11)	9248(4)	6617(6)	9000(3)	68(2)
C(12)	6776(3)	1817(4)	6956(3)	17(1)
C(13)	6912(3)	350(4)	6260(3)	26(1)
C(14)	6999(3)	1385(4)	8287(3)	20(1)
C(15)	3366(3)	4015(4)	7099(3)	18(1)
C(16)	2484(3)	3014(3)	6174(3)	15(1)
C(17)	1302(3)	3571(4)	5327(3)	20(1)
C(18)	1007(3)	5152(4)	5441(3)	23(1)
C(19)	1882(3)	6177(4)	6353(3)	24(1)
C(20)	3063(3)	5624(4)	7184(3)	24(1)
C(21)	6177(3)	5540(4)	6598(3)	31(1)
C(22)	4449(3)	1774(4)	7574(3)	15(1)
N(1)	4495(2)	3271(3)	7894(2)	18(1)
O(1)	8932(2)	2645(2)	7843(2)	19(1)
O(2)	8700(2)	6363(3)	6856(2)	30(1)
O(3)	6027(2)	435(3)	9695(2)	25(1)
O(4)	5372(2)	-1049(3)	7697(2)	27(1)
S(1)	5728(1)	436(1)	8396(1)	20(1)
S(2)	3102(1)	1086(1)	6303(1)	20(1)

Table A.4.18. Bond lengths [Å] and angles [°] for **137b**.

C(1)-O(1)	1.440(4)	C(3)-C(2)-C(1)	120.2(3)
C(1)-C(2)	1.506(4)	C(7)-C(2)-C(1)	120.9(3)
C(2)-C(3)	1.388(4)	C(4)-C(3)-C(2)	120.7(3)
C(2)-C(7)	1.388(4)	C(3)-C(4)-C(5)	120.7(3)
C(3)-C(4)	1.377(4)	C(4)-C(5)-C(6)	118.8(3)
C(4)-C(5)	1.382(5)	C(7)-C(6)-C(5)	120.8(3)
C(5)-C(6)	1.387(5)	C(6)-C(7)-C(2)	120.2(3)
C(6)-C(7)	1.383(4)	O(1)-C(8)-C(12)	107.6(2)
C(8)-O(1)	1.434(3)	O(1)-C(8)-C(9)	109.7(2)
C(8)-C(12)	1.538(4)	C(12)-C(8)-C(9)	114.3(2)
C(8)-C(9)	1.538(4)	C(21)-C(9)-C(10)	109.3(3)
C(9)-C(21)	1.523(4)	C(21)-C(9)-C(8)	112.5(3)
C(9)-C(10)	1.527(4)	C(10)-C(9)-C(8)	108.9(3)
C(10)-O(2)	1.201(3)	O(2)-C(10)-C(11)	121.6(3)
C(10)-C(11)	1.502(4)	O(2)-C(10)-C(9)	121.9(3)
C(12)-C(13)	1.528(4)	C(11)-C(10)-C(9)	116.5(3)
C(12)-C(14)	1.544(4)	C(13)-C(12)-C(8)	111.3(2)
C(14)-S(1)	1.776(3)	C(13)-C(12)-C(14)	112.1(2)
C(15)-N(1)	1.390(4)	C(8)-C(12)-C(14)	109.4(2)
C(15)-C(20)	1.398(4)	C(12)-C(14)-S(1)	116.1(2)
C(15)-C(16)	1.400(4)	N(1)-C(15)-C(20)	125.2(3)
C(16)-C(17)	1.389(4)	N(1)-C(15)-C(16)	115.0(3)
C(16)-S(2)	1.737(3)	C(20)-C(15)-C(16)	119.8(3)
C(17)-C(18)	1.380(4)	C(17)-C(16)-C(15)	121.8(3)
C(18)-C(19)	1.401(4)	C(17)-C(16)-S(2)	128.3(2)
C(19)-C(20)	1.382(4)	C(15)-C(16)-S(2)	109.9(2)
C(22)-N(1)	1.292(4)	C(18)-C(17)-C(16)	117.7(3)
C(22)-S(2)	1.730(3)	C(17)-C(18)-C(19)	121.3(3)
C(22)-S(1)	1.778(3)	C(20)-C(19)-C(18)	120.9(3)
O(3)-S(1)	1.437(2)	C(19)-C(20)-C(15)	118.5(3)
O(4)-S(1)	1.439(2)	N(1)-C(22)-S(2)	118.3(2)
		N(1)-C(22)-S(1)	121.7(2)
O(1)-C(1)-C(2)	109.4(2)	S(2)-C(22)-S(1)	119.99(18)
C(3)-C(2)-C(7)	118.8(3)	C(22)-N(1)-C(15)	109.0(2)

C(8)-O(1)-C(1)	114.0(2)	O(3)-S(1)-C(22)	108.81(13)
O(3)-S(1)-O(4)	119.67(13)	O(4)-S(1)-C(22)	105.15(13)
O(3)-S(1)-C(14)	107.03(14)	C(14)-S(1)-C(22)	103.48(14)
O(4)-S(1)-C(14)	111.51(14)	C(22)-S(2)-C(16)	87.79(14)

Symmetry transformations used to generate equivalent atoms:

Table A.4.19. Anisotropic displacement parameters ($Å^2 x\ 10^3$) for **137b**. The anisotropic displacement factor exponent takes the form: $-2\pi^2[\ h^2\ a^{*2}U^{11} + ...\ + 2\ h\ k\ a^*\ b^*\ U^{12}\ ]$

	U^{11}	U^{22}	U^{33}	U^{23}	U^{13}	U^{12}
C(1)	22(2)	31(2)	32(2)	6(2)	17(2)	3(2)
C(2)	18(2)	24(2)	18(2)	2(1)	12(2)	1(1)
C(3)	29(2)	21(2)	24(2)	-3(1)	18(2)	-3(2)
C(4)	16(2)	37(3)	22(2)	-7(2)	10(2)	-9(2)
C(5)	25(2)	34(2)	21(2)	8(2)	13(2)	7(2)
C(6)	35(2)	23(2)	26(2)	2(2)	20(2)	4(2)
C(7)	18(2)	23(2)	18(2)	-1(1)	9(1)	-3(1)
C(8)	18(2)	19(2)	16(2)	1(1)	8(1)	2(1)
C(9)	31(2)	15(2)	26(2)	1(1)	19(2)	1(1)
C(10)	29(2)	19(2)	25(2)	-2(2)	14(2)	2(2)
C(11)	84(4)	92(4)	37(2)	-26(2)	35(3)	-56(3)
C(12)	18(2)	14(2)	19(2)	0(1)	8(1)	1(1)
C(13)	30(2)	22(2)	29(2)	-7(2)	18(2)	-2(2)
C(14)	18(2)	18(2)	24(2)	4(1)	9(1)	5(1)
C(15)	19(2)	20(2)	16(2)	3(1)	10(2)	2(1)
C(16)	21(2)	10(2)	18(2)	0(1)	13(2)	-1(1)
C(17)	20(2)	23(2)	21(2)	-2(1)	12(2)	-4(1)
C(18)	21(2)	25(2)	23(2)	6(2)	10(2)	8(2)
C(19)	29(2)	19(2)	24(2)	2(2)	11(2)	8(2)
C(20)	26(2)	20(2)	20(2)	-4(1)	8(2)	0(2)
C(21)	25(2)	20(2)	53(2)	7(2)	21(2)	6(2)
C(22)	15(2)	15(2)	18(2)	2(1)	10(1)	1(1)
N(1)	21(2)	16(2)	18(1)	2(1)	10(1)	2(1)
O(1)	15(1)	26(1)	17(1)	1(1)	9(1)	2(1)

O(2)	39(1)	29(2)	29(1)	2(1)	21(1)	-8(1)
O(3)	25(1)	27(1)	24(1)	10(1)	13(1)	7(1)
O(4)	33(1)	13(1)	38(1)	1(1)	19(1)	0(1)
S(1)	19(1)	14(1)	27(1)	5(1)	12(1)	3(1)
S(2)	20(1)	14(1)	24(1)	-2(1)	9(1)	0(1)

Table A.4.20. Hydrogen coordinates (x 10^4) and isotropic displacement parameters ($Å^2$x 10^3) for **137b**.

	x	y	z	U(eq)
H(1A)	10012	3767	7238	32
H(1B)	9313	2254	6427	32
H(3)	12105	3477	8829	27
H(4)	13858	1930	9956	30
H(5)	13733	-860	9871	31
H(6)	11813	-2078	8624	31
H(7)	10049	-532	7480	23
H(8)	7600	3346	6194	21
H(9)	7439	4620	8308	26
H(11A)	9865	7361	9011	102
H(11B)	9661	5741	9563	102
H(11C)	8702	7163	9258	102
H(12)	5915	2223	6486	21
H(13A)	7748	-75	6708	39
H(13B)	6756	666	5435	39
H(13C)	6318	-463	6201	39
H(14A)	7207	2369	8780	24
H(14B)	7724	678	8665	24
H(17)	729	2902	4705	24
H(18)	212	5545	4901	27
H(19)	1665	7243	6400	29
H(20)	3643	6307	7787	28
H(21A)	6080	6563	6916	47

H(21B)	5509	4832	6509	47
H(21C)	6151	5693	5797	47